NON-EMPIRICAL CALCULATIONS ON THE ELECTRONIC STRUCTURE OF OLEFINS AND AROMATICS

by

Robert H. Findlay, B.Sc.

Thesis presented for the Degree of Doctor of Philosophy
University of Edinburgh December 1973

ACKNOWLEDGEMENTS

I wish to express my gratitude to Dr. M.H. Palmer for his advice and encouragement during this period of study. I should also like to thank Professor J.I.G. Cadogan and Professor N. Campbell for the provision of facilities, and the Carnegie Institute for the Universities of Scotland for a Research Scholarship.

SUMMARY

Non-empirical, self-consistent field, molecular orbital calculations, with the atomic orbitals represented by linear combinations of Gaussian-type functions have been carried out on the ground state electronic structures of some nitrogen-, oxygen-, sulphur- and phosphorus-containing heterocycles. Some olefins and olefin derivatives have also been studied.

Calculated values of properties have been compared with the appropriate experimental quantities, and in most cases the agreement is good, with linear relationships being established; these are found to have very small standard deviations. Extensions to molecules for which there is no experimental data have been made. In many cases it has been found possible to relate the molecular orbitals to the simplest member of a series, or to the hydrocarbon analogue. Predictions of the preferred geometry of selected molecules have been made; these have been used to predict inversion barriers and reaction mechanisms.

The extent of d-orbital participation in molecules containing second row atoms has been investigated and found to be of trivial importance except in molecules containing high valence states of the second row atoms.

CONTENTS

Page

CHAPTER ONE: Theory

The Necessity of Quantum Theory 1
The Schroedinger Wave Equation 2
The Hydrogen Atom 4
The Hydrogen Molecule 7
The Triplet State of the Hydrogen Molecule 12
Koopmans' Theorem 13
The Variational Method 14
The Hartree-Fock Method 15
The Hartree-Fock Procedure Applied to the LCAO Approximation 18
Matrix Diagonalisation 21
The Self-Consistent Field 23
Electron Density Distribution 24
Molecular and Atomic Properties 26
The Nature of the Atomic Orbitals 32
Minimising Computer Time 35

CHAPTER TWO: Results and Discussion

I. Ozonolysis

Introduction 45
Geometries and Calculation Data 47
The Ozone + Ethylene System 48
Formation and Structure of 1,2,4-Trioxolane 51
The Structure of $C_2H_4O_2$ 56
Orbital Energies and Ionisation Potentials 60
One-Electron Properties of Ethylene Oxide and 1,2,4-Trioxolane 65

II. The Azoles

Introduction 69
Total Energies 71
Orbital Energies and Ionisation Potentials 72
Correlation of Molecular Orbitals of Azoles 86
One-Electron Properties of the Azoles 90
Dipole Moments and Population Analysis 94
Tautomerism in the Triazoles and Tetrazole 102
Protonation of the Triazoles and Tetrazole 106

III. The Azines

Introduction 116
Total Energies 118
Correlation of the Calculated Energy Levels 124
Correlation of Theoretical and Experimental Energy Levels 139
Dipole Moments and Charge Distributions 145
One-Electron Properties of the Azines 150

Page

IV. Norbornadiene and Its Cations

Introduction 155
Norbornadiene 156
Scaled Norbornadiene 161
The Nature of the Norbornadiene Valency Shell Orbitals 166
Inversion Barrier of the 7-Norbornadienyl Cation 169
The 1-Norbornadienyl Cation 174
The Norbornadiene Cations 175

V. Cationic Heterocycles

Introduction 183
Calculations on the Pyrylium Cation 184
Thiopyrylium Cation 194
The Dithiolium Cations 201
d-Orbitals and their Participation in Bonding 207

VI. Phosphorous Heterocycles

Introduction 218
Phosphorin 219
Phosphole 228
Phosphole:- Inversion Barrier and Diels-Alder Reactivity 233
Orbitals and Orbital Energies 237

VII. Thiophene and Its S-Oxides

Introduction 248
Thiophene 249
Thiophene-S-Oxide 258
Thiophene-S-Dioxide 265

VIII. Thiathiophthen and Its Isosteres

Introduction 275
The Bonding in Thiathiophthen 279
Isosteres of Thiathiophthen 287

CHAPTER THREE: Appendices

1. Gaussian Basis Sets 305
2. Tables of Gaussian Basis Sets 318
3. Geometric Parameters and Symmetry Orbitals 328
4. Integrals over Gaussian Type Functions 353

PUBLICATIONS

CHAPTER ONE : Theory

The Necessity of Quantum Theory

In classical mechanics the energy E of a system of interacting particles is the sum of the kinetic energy (T_o) and potential energy (V_o)

$$E = T_o + V_o \qquad (1)$$

In this approach both the energy terms are infinitely variable resulting in an inability to explain the spectrum of atomic hydrogen. The classical concept would give rise to a continuous spectrum, while the allowed spectrum was found to consist of a series of lines. In 1885, J.J. Balmer discovered a regular relationship between the frequencies of those lines found in the visible region of the spectrum; this was

$$\nu = R\left(\frac{1}{2^2} - \frac{1}{n^2}\right) \qquad (2)$$

where ν is the frequency in wave numbers (cm^{-1}), R is a constant called the Rydberg constant and n takes the values 3,4,5.... i.e., integers greater than 2.

The problem of the interpretation of atomic spectra was solved by Neils Bohr[1] who postulated that the angular momentum (p) of an electron was quantised, i.e., that n in the expression below could only take integral values $\geq$ 1.

$$p = n\,(h/2\pi) \qquad (3)$$

where $\underline{h}$ is Planck's constant. This integer $\underline{n}$ is called the principal quantum number. The angular momentum of an electron of mass $\underline{m}$ moving in a circular path of radius $\underline{r}$ with a velocity $\underline{v}$ has an angular momentum below:-

$$p = mvr = n(h/2\pi) \qquad (4)$$

Bohr was then able to evaluate both the radius and the energy of the electron moving round a nucleus of charge Ze; these were

$$r = \frac{h^2}{4\pi^2 e^2 Z} \cdot n^2 \qquad (5)$$

$$E = - \frac{2\pi^2 me^2}{h^2} \cdot \frac{Z^2}{n^2} \qquad (6)$$

In the case of the hydrogen atom Z = 1 and the smallest orbit is that with n = 1. Insertion of these values and those of the constants into Equation 5 gives a value of 0.529Å; this is usually given the identifier a_o and is called the Bohr radius. The Bohr theory was able to predict the Balmer series, these being the result of the movement of an electron in an orbit with n = 2 to orbits with n > 2. Further it predicted the existence of other series similar to the Balmer series, this being the first example found of the series.

$$\nu = R \left(\frac{1}{n_1^2} - \frac{1}{n_2^2} \right) \quad n_2 > n_1 \qquad (7)$$

The Schrodinger Wave Equation

The Bohr Theory of atoms assumed that electrons were particles. However a beam of electrons directed at a sufficiently narrow slit, as well as going straight through, is diffracted to the sides (below)

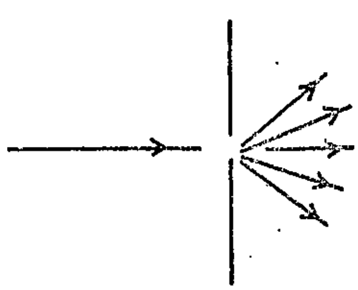

This behaviour is characteristic of waves rather than particles and exhibits the wave/particle duality of electrons. Schroedinger suggested[3] that the proper way to describe the wave character of electrons was to replace the classical kinetic and potential energy functions T_o and V_o with linear operators T and V. These were used to set up an equation of the form

$$(T + V)\Psi = E\Psi \qquad (8)$$

where Ψ is a wave function describing the movement of electrons.

In the hydrogen atom the potential energy operator is identical to the classical potential energy $(-e^2/r)$, while the classical kinetic energy $(T = p^2/2m)$ is replaced by the linear differential operator

$$T = -\frac{h^2}{8\pi^2 m}\nabla^2 \qquad (9)$$

where $$\nabla^2 = \frac{\partial^2}{\partial x^2} + \frac{\partial^2}{\partial y^2} + \frac{\partial^2}{\partial z^2} \qquad (10)$$

The Schroedinger equation for the hydrogen atom takes the form

$$\left\{-\frac{h^2}{8\pi^2 m}\nabla^2 - \frac{e^2}{r}\right\}\Psi = E\Psi \qquad (11)$$

There is considerable advantage if one works in atomic units, which take as fundamental quantities

the mass of the electron m as the unit of mass

the charge of the electron e as the unit of charge

the Bohr radius a_o as the unit of length

e^2/a_o e_o as the unit of energy

Equation (11) now becomes

$$(-\tfrac{1}{2}\nabla^2 - \tfrac{1}{r})\,\Psi = E\,\Psi \qquad (12)$$

The Hydrogen Atom

The wave function Ψ is a mathematical function just like any other. To be physically meaningful it must be restricted in several ways:- (1) it must be quadratically integrable (i.e., it must be possible to integrate Ψ twice); (2) it must be single-valued at all points in space; (3) it must go to zero at infinity; (4) Any wave function which is a solution of equation (12) would still be a valid solution if it was multiplied by c where c is any number. To fix the value of c a normalisation condition is imposed, i.e.

$$\int \Psi^* \Psi \, d\tau = 1 \qquad (13)$$

$$\int \Psi^2 \, d\tau = 1 \qquad (14)$$

where the superscript asterisk refers to the complex conjugate of Ψ. If Ψ is real then the superscript is redundant, giving Equation (14).

For the hydrogen atom equation (12) is more conveniently written in spherical polar co-ordinates. When this is done, the solutions can be written in the form

$$(r, \theta, \phi) = R_{nl}(r)\, Y_{lm}(\theta, \phi) \qquad (15)$$

where l, m, n are integers, and r, θ, ϕ are the spherical polar co-ordinates centred on the atom. The angular parts $Y_{lm}(\theta, 0)$ are called spherical harmoni s and are defined as

$$Y_{lm}(\theta, \phi) = A_{lm}(\theta)\, B_m(\phi) \qquad (16)$$

where $\quad \mathrm{Alm}(\Theta) = \left[\frac{(2\ell+1)(\ell-m)!}{2(\ell+m)!}\right]^{\frac{1}{2}} P_\ell^m (\cos\Theta) \qquad (17)$

$$B_m(\phi) = (2\pi)^{-\frac{1}{2}} \cos m\phi \,, \quad m = 0 \qquad (18a)$$

$$= (\pi)^{-\frac{1}{2}} \cos m\phi \,, \quad m \neq 0 \qquad (18b)$$

$$B_{\bar{m}}(\phi) = (\pi^{-\frac{1}{2}}) \quad \sin m\phi \qquad (18c)$$

with P_ℓ^m being associated Legendre Polynomials.[4] Some examples of these are shown in Table 1.

TABLE 1

Angular Parts of Hydrogen-Like Functions

$\ell = 0(s)$	$\ell = 1(p)$	$\ell = 2(d)$
$(\frac{1}{4\pi})^{\frac{1}{2}}$	$p_x = (\frac{3}{4\pi})^{\frac{1}{2}} \cos\Theta$	$d_{3z^2-r^2} = (\frac{5}{16\pi})^{\frac{1}{2}}(3\cos^2\Theta - 1)$
	$p_y = (\frac{3}{4\pi})^{\frac{1}{2}} \sin\Theta\cos\phi$	$d_{xz} = (\frac{15}{4\pi})^{\frac{1}{2}} \sin\Theta\cos\Theta\cos\phi$
	$p_z = (\frac{3}{4\pi})^{\frac{1}{2}} \sin\Theta\sin\phi$	$d_{yz} = (\frac{15}{4\pi})^{\frac{1}{2}} \sin\Theta\cos\Theta\sin\phi$
		$d_{x^2-y^2} = (\frac{15}{16\pi})^{\frac{1}{2}} \sin^2\Theta\cos 2\phi$
		$d_{xy} = (\frac{15}{16\pi})^{\frac{1}{2}} \sin^2\Theta\sin 2\phi$

The radial part of the atomic functions are polynomials in $\underline{r}$ multiplied by an exponential term $\exp(-\alpha r)$ where α is known as the orbital exponent; some of these are shown in Table 2. This exponent is 1 for the hydrogen atom 1s orbital and for the general case is given by Z/n where $\underline{Z}$ is the nuclear charge and $\underline{n}$ is the principal quantum number. This is identical in use to that postulated by Bohr, but arises from the boundary conditions (1)-(4) above, and is not an intrinsic assumption. The possible values of n are 1,2,3... with $\underline{\ell}$ and $\underline{m}$ being restricted to the values they

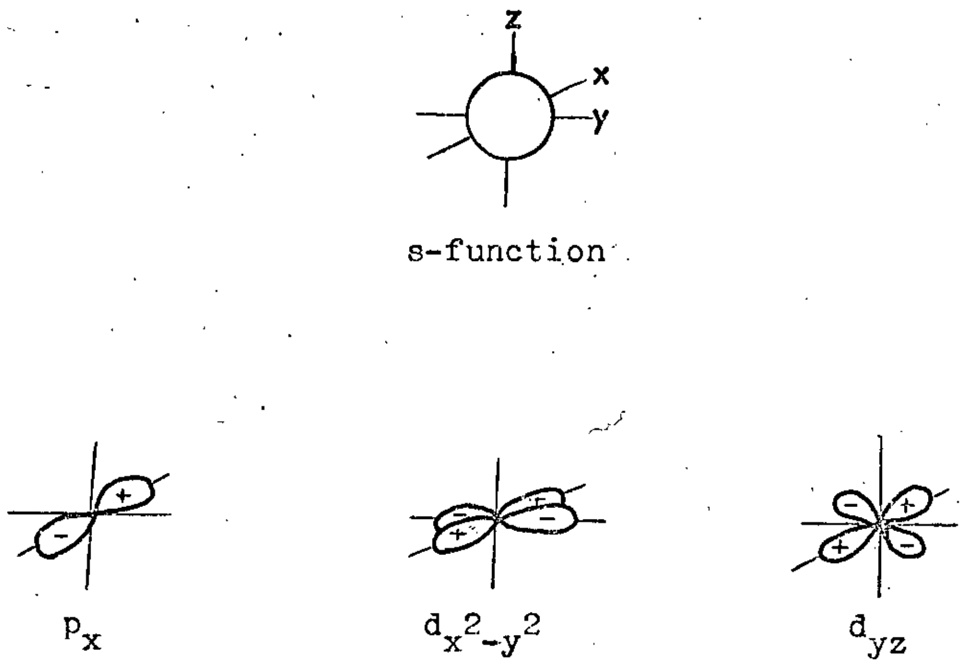

Figure 1 Angular Distribution of s, p and d Functions

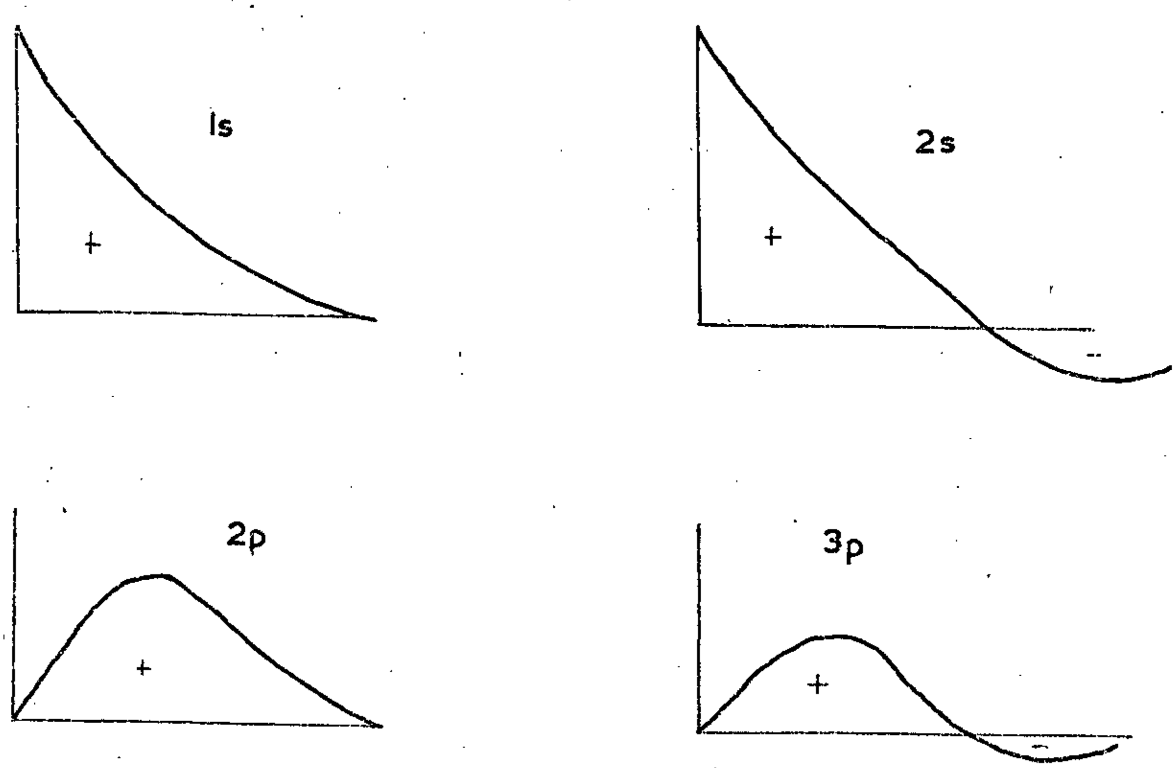

Figure 2 Radial Distribution of s and p Functions

can take; ℓ can have the values 0,1,2...n-1, and m ℓ, ℓ-1, ℓ-2,....,-(ℓ-1), -ℓ. The orbitals are labelled by letters according to the value of ℓ; s,p,d and f are used for ℓ = 0,1,2,3.

TABLE 2

Radial Parts of Hydrogen-Like Functions

n	ℓ	$R_{n\ell}(r)$
1	0	$2\alpha^{3/2} \exp(-\alpha r)$
2	0	$2\alpha^{3/2}(1-\alpha r)\exp(-\alpha r)$
	1	$(\frac{4}{3})^{\frac{1}{2}}\alpha^{5/2} r \exp(-\alpha r)$
3	0	$(\frac{2}{3})\alpha^{3/2}(3-6\alpha r + 2\alpha^2 r^2)\exp(-\alpha r)$
	1	$(\frac{8}{9})^{\frac{1}{2}}\alpha^{5/2}(2-\alpha r)r\exp(-\alpha r)$
	2	$(\frac{8}{45})^{\frac{1}{2}}\alpha^{\frac{1}{2}} r^2 \exp(-\alpha r)$

The s function is independent of angle; the three p functions have the same angular dependence as the x, y, z co-ordinates and are known as the p_x, p_y and p_z functions. d-Orbitals have the same angular dependence as quadratic expressions in x, y and z; the labels for these can be seen in Table 1. Figures 1 and 2 show angular and radial nature of the orbitals.

A fourth quantum number can be used to describe the electron completely in hydrogen and other one electron atoms. This is the spin quantum number m_s, which can have the values $+\frac{1}{2}$ and $-\frac{1}{2}$; these are often described as α and β. The use of this quantum number in hydrogen-like atoms is redundant but is necessary when such hydrogen-like functions are used to describe the electronic structure of poly-electron atoms. Thus helium (two electrons) is often described as having the electronic structure $1s^2$ where the two electrons, one of spin α and one β are placed in the 1s hydrogen-like orbital. This could be more fully written as

$$(\mathrm{He}) = 1s(1)\alpha(1)\ 1s(2)\alpha(2) \qquad (19a)$$

$$= 1s(1)\ 1\bar{s}(2) \qquad (19b)$$

where the bar implies β spin.

The Hydrogen Molecule

The hydrogen atom, and other one-electron atoms are very much a special case. Far more typical is the neutral molecule, H_2

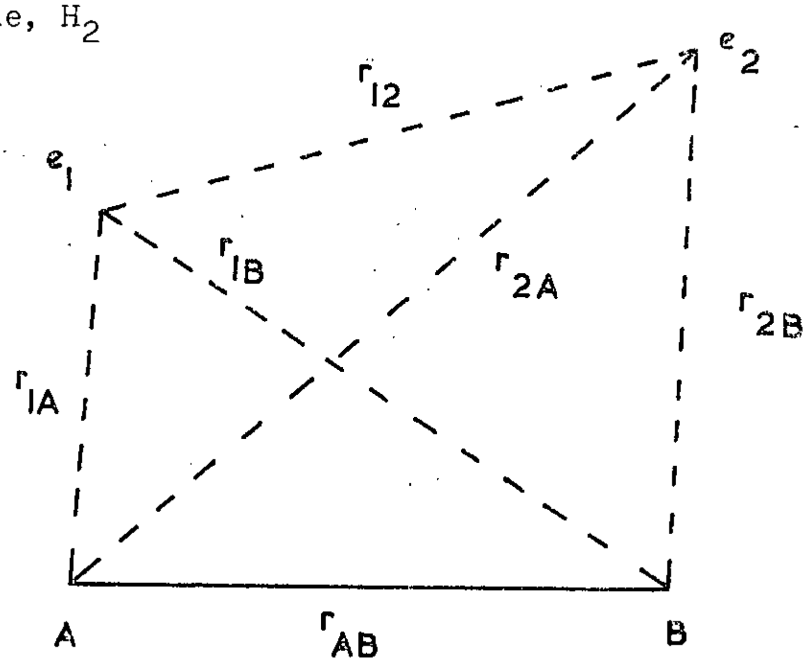

Fig. 3. The Hydrogen Molecule.

In atomic units the wave equation for this system is

$$\left(-\tfrac{1}{2}\nabla_1^2 - \tfrac{1}{2}\nabla_2^2 - \frac{1}{r_{1A}} - \frac{1}{r_{1B}} - \frac{1}{r_{2A}} - \frac{1}{r_{2B}} + \frac{1}{r_{AB}} + \frac{1}{r_{12}}\right)\Psi(1,2) = E\,\Psi(1,2) \tag{20}$$

where $-\frac{1}{2}\nabla_1^2$ = kinetic energy of electron (1)

$\frac{1}{r_{1A}}$ = coulomb attraction between nucleus A and electron (1)

$\frac{1}{r_{12}}$ = coulombic repulsion between the electrons

$\frac{1}{r_{AB}}$ = coulombic repulsion between the nuclei

In practice, rather than attempt to find a wave-function describing both electronic and nuclear motion together it is usual to break the problem down into two parts and consider first the motion of the electrons in the field of the stationary nuclei, resulting in there being a separate purely electronic problem for each set of nuclear positions. This is a reasonable procedure because the masses of the nuclei are several thousand times larger than the electron mass and the electrons will adjust themselves to new nuclear positions so rapidly that at any one instant their motion is just as it would be if the nuclei were stationary. This is the Born-Oppenheimer approximation and allows the generation of a modified, electron-only, Schroedinger equation, Equation 20a.

$$\left(-\tfrac{1}{2}\nabla_1^2 - \tfrac{1}{2}\nabla_2^2 - \frac{1}{r_{1A}} - \frac{1}{r_{1B}} - \frac{1}{r_{2A}} - \frac{1}{r_{2B}} + \frac{1}{r_{12}}\right)\Psi(1,2) = E\,\Psi(1,2) \tag{20a}$$

This is often contracted to the form

$$\left(H_1 + H_2 + \frac{1}{r_{12}}\right)\Psi(1,2) = E\,\Psi(1,2) \tag{20b}$$

where $$H_1 = -\tfrac{1}{2}\nabla_1^2 - \frac{1}{r_{1A}} - \frac{1}{r_{1B}} \tag{21}$$

If the electron repulsion was neglected and the Hamiltonian operator was the sum, $H_1 + H_2$ then we could replace Ψ (1,2) by a product of two one-electron functions, say O_1 and O_2. This idea of building up wave-functions as one-electron products corresponds with the concept of saying that the electronic structure of helium is $1s^2$(above). Continuing with this analogy one would expect to place the two electrons in the same orbital, one of which would have α spin and the other β spin. The product function would then be

$$\Psi(1,2) = A(1).\bar{A}(2) \qquad (22)$$

where Ψ describes all the electrons simultaneously and A(1), A(2) describes electrons 1 and 2 respectively.

However the idea of the wave function being a simple produce ignores the Pauli Principle which states that the total wave function should be anti-symmetric with respect to electron permutation. Thus interchanging the electrons in Equation 22 would lead to

$$\Psi'(1,2) = A(2).\bar{A}(1) \neq -\Psi(1,2) \qquad (23)$$

Only the combination $\Psi(1,2) - \Psi'(1,2)$ would be antisymmetric for exchange of electrons 1 and 2. Thus a new expression for Ψ (1,2) will now appear

$$\Psi(1,2) = \frac{1}{\sqrt{2}}\left(A(1).\bar{A}(2) - A(2).\bar{A}(1)\right) \qquad (24)$$

where $\frac{1}{\sqrt{2}}$ is a normalising factor. This is what would be obtained if the functions were placed as the elements of a two by two determinant

$$\Psi(1,2) = \frac{1}{\sqrt{2}} \begin{vmatrix} A(1) & \bar{A}(1) \\ A(2) & \bar{A}(2) \end{vmatrix} \qquad (25)$$

This determinant is known as the Slater determinant[5] and can be generalised

$$\Psi(1,2\ldots\ldots n) = \frac{1}{\sqrt{n!}} \begin{vmatrix} A(1) & \bar{A}(1) & B(1) \;\ldots\; & \bar{\Phi}(1) \\ A(2) & \bar{A}(2) \;\ldots & & \\ \vdots & & & \\ A(n) & & & \bar{\Phi}(n) \end{vmatrix} \qquad (26)$$

The antisymmetry property follows directly from the theorem that the interchange of two rows changes the sign of the determinant; another property of determinants is that the value is zero if two of the columns are identical, so that two electrons cannot be assigned the same spin orbital (the Pauli Exclusion Principle).[6]

Returning now to Equation 24(or 25) it is possible to evaluate the total energy of the system. Writing $H = H_1 + H_2 + \frac{1}{r_{12}}$ the equation becomes

$$H\,\Psi(1,2) = E\,\Psi(1,2) \qquad (27)$$

Multiplying each side by $\Psi(1,2)$ and integrating over all space (τ) one obtains

$$\langle \Psi(1,2) | H | \Psi(1,2) \rangle = E \langle \Psi(1,2) | \Psi(1,2) \rangle \qquad (28)$$

$$= E \quad \text{since } \Psi(1,2) \text{ is normalised.}$$

Substituting Equation (24) into (28) one obtains

$$E = \tfrac{1}{2} \langle \{A(1).\bar{A}(2) - A(2)\bar{A}(1)\} \,\Big|\, H_1 + H_2 + \frac{1}{r_{12}} \,\Big|\, \{A(1)\,\bar{A}(2) - A(2)\,\bar{A}(1)\} \rangle \qquad (29)$$

The first term (T_1) in the above expression will be

$$T_1 = < A(1)\ A(2) \mid H_1 \mid A(1)\ \bar{A}(2) > \quad (30a)$$

$$= \int A(1) \mid H_1 \mid A(1)\ d\tau_1 \int \bar{A}(2)\ \bar{A}(2)\ d\tau_2 \quad (30b)$$

since H_1 only operates on electron 1. On further separation into spin and space parts this becomes

$$T_1 = \int A_1 \mid H_1 \mid A_1\ dv_1 \int \alpha_1\alpha_1 ds_1 \int A_2A_2 dv_2 \int \beta_2\beta_2 ds_2 \quad (30c)$$

$$= h_{11} \times 1 \times 1 \times 1 = h_{11} \quad (30d)$$

The H_1 operator acting on $\bar{A}(1)$ will produce another such term, with H_2 producing another $2h_{22}$ terms. Since one cannot distinguish between electrons h_{11} must equal h_{22}. Each of these terms represents the energy the electron would have if it was the only electron present in the molecule.

Turning now to the electron repulsion terms, the first of these is

$$< A(1)\ \bar{A}(2) \left| \frac{1}{r_{12}} \right| A(1)\ \bar{A}(2) > \quad (31a)$$

$$= \iint A_1A_2 \left| \frac{1}{r_{12}} \right| A_1A_2\ dv_1\ dv_2 \int \alpha_1\alpha_1 ds_1 \int \beta_2\beta_2 ds_2 \quad (31b)$$

$$= J_{AA} \times 1 \times 1 \quad (31c)$$

There will be another term identical to this resulting from the operator acting on the two negative parts of $\Psi(1,2)$. This only leaves the cross term,

$$< A(1)\ \bar{A}(2) \left| \frac{1}{r_{12}} \right| A(2)\ \bar{A}(1) > \quad (32a)$$

$$= \iint A_1A_2 \left| \frac{1}{r_{12}} \right| A_2A_1 \int dv_1 dv_2 \int \alpha_1\beta_1 ds_1 \int \alpha_2\beta_2 ds_2 \quad (32b)$$

$$= 0, \text{ because of spin orthogonality} \quad (32c)$$

$$\therefore\ E(H_2) = \tfrac{1}{2}(4h_{11} + 2J_{AA}) = 2h_{11} + J_{AA} \quad (33)$$

Physically the J_{AA} term represents the electron repulsion between the charge clouds of electrons (1) and (2), and is known as the coulomb integral.

The Triplet State of the Hydrogen Molecule

The ground state of hydrogen molecule has the configuration A^2. If one of these electrons is excited into an unfilled orbital, denoted by B, and both electrons have the same spin, say α, the resulting state is a triplet of configuration A^1B^1. The wave function $\Psi(1,2) = |A\ B|$ in the shorthand notation of the Slater determinant, i.e.

$$\Psi(1,2) = \frac{1}{\sqrt{2}} \begin{vmatrix} A(1) & B(1) \\ A(2) & B(2) \end{vmatrix} \qquad (34a)$$

$$= \frac{1}{\sqrt{2}} \left(A(1)\ B(2) - B(1)\ A(2)\right) \qquad (34b)$$

The energy is then given by

$$E = \tfrac{1}{2} \left< \{A(1)B(2) - B(1)A(2)\} \middle| H_1 + H_2 + \frac{1}{r_{12}} \middle| \{A(1)B(2) - B(1)A(2)\} \right> \qquad (35)$$

Here, the only difference is that the cross term will not disappear because of spin orthogonality, i.e.

$$- \left< A(1)B(2) \middle| \frac{1}{r_{12}} \middle| A(2)B(1) \right> \qquad (36a)$$

$$= -\iint A_1B_2 \left| \frac{1}{r_{12}} \right| B_1A_2\, dv_1 dv_2 \int \alpha_1\alpha_1 ds_1 \int \alpha_2\alpha_2 ds_2 \qquad (36b)$$

$$= -K_{AB} \qquad (36c)$$

The energy then is

$$E = h_{11} + h_{22} + J_{AB} - K_{AB} \qquad (37)$$

The integral K is known as the exchange integral and results from exchange of electrons (1) and (2) between two different orbitals, so that it is not just a simple electrostatic repulsion. It arises from the necessity for antisymmetrisation.

The two energy expressions obtained for the two states of the hydrogen atom illustrate the quite general form of the energy expression for molecules:- The total energy is the sum of the one-electron energies (the energy each electron would have if it were the only electron in the molecule) plus a coulomb integral for every pair of electrons, minus an exchange integral for every pair of electrons in the molecule which have the same spin, i.e.

$$E = \sum_{i}^{n} h_{ii} + \sum_{i}^{n/2} J_{ii} + \sum_{i}^{n/2} \sum_{j(\neq i)}^{n/2} (2J_{ij} - K_{ij}) \qquad (37)$$

$$= \sum_{i}^{n} h_{ii} + \sum_{i}^{n/2} \sum_{j}^{n/2} (2J_{ij} - K_{ij}) \qquad (38a)$$

since $J_{ii} = K_{ii}$

Equation (38) refers to an n electron system, but is more often written in terms of a 2n system, which of course implies doubly occupied orbitals, i.e.

$$E = 2\sum_{i}^{n} h_{ii} + \sum_{i}^{n} \sum_{j}^{n} (2J_{ij} - K_{ij}) \qquad (38b)$$

Koopmans' Theorem

If one defines a set of energies, e_i such that

$$e_i = h_{ii} + \sum_{i}^{n} (2J_{ij} - K_{ij}) \qquad (39)$$

then this is essentially the energy of an electron in orbital Ψ_i interacting with the other 2n-1 electrons.

With the assumption that there is no reorganisation of the other 2n-1 electrons upon ionisation, $-e_i$ can be associated with the ionisation potential of an electron in orbital Ψ_i. This is called Koopmans' theorem[7] and finds very common usage in comparisons with experimentally determined ionisation potentials.

The Variational Method

The complete treatment of a quantum-mechanical problem involving electronic structure is equivalent to the complete solution of the Schroedinger equation appropriate to the system under consideration. Mathematical analysis of this partial differential equation is only possible for one-electron systems, and for many-electron systems solutions are generally found by the variational method. Solutions of the Schroedinger equation give stationary values of the energy, i.e., if Ψ is a solution then for any small change $\delta\Psi$,

$$\delta E = \delta\langle\Psi|H|\Psi\rangle = 0 \qquad (40)$$

Now, if the wave function is allowed to be flexible in that a finite number of parameters can be varied i.e., $\Psi = \Psi(c_1, c_2, c_3 \ldots c_n)$ then the energy E will be a function of those same parameters and the stationary values of E will satisfy.

$$\delta E(c_1, c_2, c_3 \ldots c_n) = \frac{\partial E}{\partial c_1}\delta c_1 = \frac{\partial E}{\partial c_2}\delta c_2 = \cdots = 0 \quad (41)$$

Solution of these algebraic equations will then lead to approximates to the energies E_i and the wave functions Ψ_i for the stationary states. As the flexibility of the variation function Ψ increases, by increasing the number of parameters, the calculated energies and wave-functions will become closer and closer to the correct values.

A very common use of the variational method is with a linear combination of fixed functions, for example atomic orbitals; ϕ_i

$$\Psi(C_1, C_2, C_3 \ldots) = C_1\phi_1 + C_2\phi_2 + C_3\phi_3 + \ldots \quad (42)$$

This last equation is the Linear Combination of Atomic Orbitals or LCAO approach.

The Hartree-Fock Method[8]

According to the variational principle, if an approximate many-electron wave function such as Equation (26) is adjusted in order to lower the energy then the accurate solution of the many electron wave equation will be approached. The best molecular orbitals are obtained by varying all the contributing one-electron functions $\Psi_1, \Psi_2 \ldots \Psi_n$ in the determinant until the energy achieves its minimum value. This does not give the correct many electron function for a closed shell system, but rather the closest possible approach by a single determinant of orbitals. Such orbitals are referred to as self consistent, or Hartree-Fock orbitals. Thus the central mathematical problem is the determination of the orbitals which give a stationary value of $\langle \Psi | H | \Psi \rangle$. In addition a constraint is placed upon the one-electron orbitals, namely that they shall be orthonormal, i.e.,

$$\int \Psi_i \Psi_j \, d\tau = \delta_{ij} \quad \text{where } \delta_{ij} = 0 \text{ if } i \neq j \quad \text{and} \quad = 1 \text{ if } i = j \quad (43)$$

Constrained variational problems of this type are handled mathematically by the calculus of variations.[9] The function G has to be minimised:-

$$G = E - 2\sum_i\sum_j e_{ji}S_{ij} = 2\sum_i h_{ii} + \sum_i\sum_j(2J_{ij} - K_{ij}) - 2\sum_i\sum_j e_{ij}S_{ij} \tag{44}$$

where the energy expression is Equation 38b above and e_{ij} are as yet undetermined constants. A stationary point of the function G is such that the variation in G, (δG), is zero to the first order, i.e., $\delta G = 0$ (45)

The variation in G caused by changing all orbitals $_i$ by an infinitesimal amount to $\Psi_i + \delta\Psi_i$ is in full

$$\delta G = 2\sum_i \delta h_{ii} + \sum_i\sum_j 2(\delta J_{ij} - \delta K_{ij}) - 2\sum_i\sum_j e_{ij}\,\delta S_{ij} \tag{46}$$

where $\delta h_{ii} = \int \delta\Psi_i^*(1)\ \underline{H_1}\ \Psi_i(1)$ + complex conjugate (47)

$$\delta J_{ij} = \int \delta\Psi_i^*(1)\ \underline{J_j}(1)\ \Psi_i(1)d\tau_1 + \int \delta\Psi_j^*(1)\ \underline{J_i}(1)\ \Psi_j(1)\ d\tau_1 + \text{complex conjugate} \tag{48}$$

$$\delta K_{ij} = \int \delta\Psi_i^*(1)\ \underline{K_j}(1)\ \Psi_i(1)\ d\tau_1 + \int \delta\Psi_j^*(1)\ \underline{K_i}(1)\ \Psi_j(1)\ d\tau_1 + \text{complex conjugate} \tag{49}$$

$$\delta S_{ij} = \int \delta\Psi_i(1)\ \Psi_j(1)\ d\tau_1 + \text{complex conjugate} \tag{50}$$

Here the coulomb <u>operator</u> $\underline{J_j}$ is defined by

$$\underline{J_j}(1) = \int \Psi_j^*(2)\,\frac{1}{r_{12}}\,\Psi_j(2)\ d\tau_2 \tag{51}$$

The exchange operator K_j cannot be written as a simple function but has the property that

$$K_j(1)\ \Psi_j(1) = [\int \Psi_j^*(2)\,\frac{1}{r_{12}}\,\Psi_i(2)\ d\tau_2] \tag{52}$$

Since the orbitals and their complex conjugates can be varied independently exactly the same equations follow if one restricts oneself to real functions and real variations. The condition for a stationary point is thus

$$\delta G = 0 = 2\sum_i \int \delta\Psi_j^*[\underline{H_1}\ \Psi_i + \sum_j(2\underline{J_j} - K_j)\Psi_i - \Sigma e_{ij}\Psi_j]d\tau \tag{53}$$

Now since $\delta\Psi$ is arbitrary this is satisfied only if the quantity in square brackets is equal to zero for each and every i.

This leads directly to the differential equations

$$[\underline{H_1} + \sum_{i}(2\underline{J_j} - \underline{K_j})]\ \Psi_i = \sum_{j} e_{ij}\ \Psi_j \quad i = 1, \ldots n \qquad (54)$$

There are thus $\underline{n}$ one-electron wave equations for the orbitals $_1 \ldots\ _n$. The quantity in square brackets is known as the Fock hamiltonian operator $\underline{F}$ and the wave equations may be written in the form

$$\underline{F}\ \Psi_i = \sum_{j} e_{ij}\ \Psi_j \qquad (55)$$

The differential equations have a whole set of values e_{ij} on the right hand side instead of the usual case of a single eigenvalue; this arises because the solutions to the set of wave equations are not unique. This is caused by one property of determinants which states that any multiple of one column may be added to another without altering the value of the determinant. This is a special case of a more general property which states that any orthogonal transformation leaves the value of the determinant unchanged. Thus the orbitals Ψ_i may be replaced by a new set $\Psi_i{}'$ where

$$\Psi_i{}' = \sum_{j} T_{ij}\ \Psi_j \qquad (56)$$

provided that $\sum_{k} T_{ik}T_{kj} = \delta_{ij}$ (57)

Substitution of Equation (57) into (55) makes a significant difference only in that the constants e_{ij} are replaced by a new set $e'_{k\ell}$ given by

$$e'_{k\ell} = \sum_{ij} T_{ki}\ e_{ij}\ T_{j\ell} \qquad (58)$$

It is clearly desirable to remove this indeterminacy from the problem and to fix the molecular orbitals uniquely. The matrix e_{ij} is hermitian resulting in there being an orthogonal transformation such that the matrix is brought to diagonal form, i.e., $e_{ij} = 0$ unless $i = j$. Applying that transformation to the orbitals, the standard eigenvalue problem is obtained:-

$$F\,\Psi_i = e_i\,\Psi_i \tag{59}$$

These are known as the Hartree-Fock equations.

The Hartree-Fock Procedure Applied to the LCAO Approximation

In the LCAO approximation each molecular orbital is considered to be of the form

$$\Psi_i = \sum_p C_{pi}\,\Phi_p \tag{60}$$

where the Φ_p are real atomic functions (Subscripts p,q,r,s will be used for atomic orbitals). The molecular orbitals Ψ_i have to form an orthonormal set and for this to be possible it is necessary that the number of atomic orbitals be greater than or equal to the number of occupied molecular orbitals. The requirement that the molecular orbitals be orthonormal in the LCAO approximation demands that

$$\sum_{pq} C_{pi}\,C_{qj}\,S_{pq} = S_{ij} \tag{61}$$

where S_{pq} is the overlap integral between atomic functions Φ_p and Φ_q, i.e.,

$$S_{pq} = \int \Phi_p(1)\,\Phi_q(1)\,d\tau_1 \tag{62}$$

The total electronic energy can also be written in terms of integrals over atomic orbitals if one substitutes the linear expansion, Equation (60), into the molecular orbital integrals. Thus

$$h_{ii} = \sum_{pq} C_{pi}^{*}\,C_{qi}\,H_{pq} \tag{63}$$

where H_{pq} is the matrix of the hamiltonian with respect to the atomic orbitals,

$$H_{pq} = \int \phi_p \; H_1 \phi_q \; d\tau_1 \qquad (64)$$

Similarly

$$J_{ij} = \sum_{pqrs} C^*_{pi} \; C^*_{qj} \; C_{ri} \; C_{sj} \langle pq/rs \rangle \qquad (65)$$

$$K_{ij} = \sum_{pqrs} C^*_{pi} \; C^*_{qj} \; C_{ri} \; C_{sj} \langle pr/qs \rangle \qquad (66)$$

where $\langle pq/rs \rangle$ is a general two-electron integral over atomic orbitals

$$\langle pq/rs \rangle = \int\int \phi_p(1) \, \phi_q(1) \, \frac{1}{r_{12}} \phi_p(2) \, \phi_q(2) \; d\tau_1 d\tau_2 \qquad (67)$$

Equation (39) then becomes

$$E = \Sigma P_{pq} H_{pq} + \tfrac{1}{2} \sum_{pqrs} P_{pq} P_{rs} [\langle pq/rs \rangle - \tfrac{1}{2} \langle pr/qs \rangle] \qquad (68)$$

where $P_{pq} = 2 \sum_{i}^{occ} C^*_{pi} \; C_{ri}$

The next step is to find the optimum values of the coefficients C_{pi} which lead to a set of molecular orbitals. This is done by reverting to the variation procedure with the small variation in Ψ_i now given by

$$\delta \Psi_i = \sum_p \delta C_{pi} \phi_p \qquad (69)$$

The condition for a stationary point in the function G, Equation (44), becomes:-

$$\delta G = 2 \sum_{i}^{occ} \delta C^*_{pi} C_{qi} H_{pq} + \sum_{ij}^{occ} \sum_{pqrs} (\delta C^*_{pi} C^*_{qj} C_{ri} C_{sj} + C^*_{pi} \delta C_{\,j} C_{ri} C_{sj})$$
$$\times \; [2\langle pq/rs \rangle - \langle pr/qs \rangle]$$

$$- \; 2 \sum_{ij} \sum_{pq} e_{ij} \delta C^*_{pi} C_{qj} S_{pq} + \text{complex conjugate} = 0 \qquad (70)$$

Since the δC^*_{pi} terms are arbitrary, the complete coefficient of each δC^*_{pi} must be zero, leading to

$$\sum_q \Big\{ C_{qi} H_{pq} + \sum_{i}^{occ} \sum_{qrs} C^*_{qj} C_{qi} C_{pj} [2\langle pq/rs \rangle - \langle pr/qs \rangle]$$

$$= \sum_i e_{ij} \sum_q C_{qj} S_{pq} \qquad (71)$$

Once again the off-diagonal elements of e_{ij} can be chosen as zero thus assuring unique specification of the molecular orbitals. The equations then take the form

$$\sum_q (F_{pq} - e_i S_{pq}) C_{pq} = 0 \tag{72}$$

where the elements of the matrix representation of the Hartree-Fock hamiltonian operator F are

$$F_{pq} = H_{pq} + \sum_{rs} P_{rs} \left[\langle pq/rs\rangle - \tfrac{1}{2}\langle pr/qs\rangle\right] \tag{73}$$

These algebraic equations were set forth by Hall and Roothaan (independently)[10] and are now generally known as the Roothaan equations.

The set of algebraic equations i.e. Equation (72) can be written in matrix form

$$\underline{\underline{F}}\,\underline{\underline{C}} = \underline{\underline{S}}\,\underline{\underline{C}}\,\underline{\underline{E}} \tag{74}$$

where $\underline{\underline{E}}$ is the diagonal matrix of the e_i terms. Solving this matrix equation is difficult but a formal solution may be obtained by defining a matrix, $\underline{\underline{S}}^{\frac{1}{2}}$, by the equation

$$\underline{\underline{S}}^{\frac{1}{2}}\,\underline{\underline{S}}^{\frac{1}{2}} = \underline{\underline{S}} \tag{75}$$

Equation (74) can be converted to a standard eigenvalue problem in the following manner:-

$$\text{Define}\quad \underline{\underline{F}}' = \underline{\underline{S}}^{-\frac{1}{2}}\,\underline{\underline{F}}\,\underline{\underline{S}}^{-\frac{1}{2}} \tag{76a}$$

$$\text{and}\quad \underline{\underline{C}}' = \underline{\underline{S}}^{\frac{1}{2}}\,\underline{\underline{C}} \tag{76b}$$

Then Equation (74) becomes

$$\underline{\underline{F}}'\underline{\underline{C}}' = \underline{\underline{C}}'E \tag{77}$$

Premultiplication of Equation (77) by $(\underline{\underline{C}}')^{-1}$, the inverse of $\underline{\underline{C}}'$ one obtains

$$(\underline{\underline{C}}')^{-1}\,\underline{\underline{F}}'\underline{\underline{C}}' = (\underline{\underline{C}}')^{-1}\,\underline{\underline{C}}'\,\underline{\underline{E}} \tag{78a}$$

$$= \underline{\underline{E}} \tag{78b}$$

Thus the problem has been reduced to determining the matrix $\underline{\underline{C}}'$ which, together with its inverse, diagonalises $\underline{\underline{F}}$. Once the matrix $\underline{\underline{E}}$ has been found, it is possible to obtain $\underline{\underline{C}}$ since, by the very process of diagonalisation, the matrix $\underline{\underline{C}}'$ has been obtained.

This formal proof has only one drawback however, and that is the determination of the matrix $\underline{\underline{S}}^{\frac{1}{2}}$. Fortunately this can be obtained by another diagonalisation procedure. Let $\underline{\underline{U}}$ be the matrix which diagonalises $\underline{\underline{S}}$ and $\underline{\underline{d}}$ be the diagonal matrix so obtained, i.e.,

$$\underline{\underline{U}}^{-1}\ \underline{\underline{S}}\ \underline{\underline{U}} = \underline{\underline{d}} \tag{79}$$

$$\text{Now } d = d^{\frac{1}{2}}d^{\frac{1}{2}} = \underline{\underline{U}}^{-1}\underline{\underline{S}}\ \underline{\underline{U}} = \underline{\underline{U}}^{-1}\underline{\underline{S}}^{\frac{1}{2}}\underline{\underline{S}}^{\frac{1}{2}}\underline{\underline{U}}$$

$$= \underline{\underline{U}}^{-1}\underline{\underline{S}}^{\frac{1}{2}}\underline{\underline{U}}\ \underline{\underline{U}}^{-1}\underline{\underline{S}}^{\frac{1}{2}}\underline{\underline{U}} \tag{80}$$

$$\text{so } d^{\frac{1}{2}} = \underline{\underline{U}}^{-1}\underline{\underline{S}}^{\frac{1}{2}}\underline{\underline{U}} \tag{81}$$

$$\text{or } S^{-\frac{1}{2}} = \underline{\underline{U}}\ d^{-\frac{1}{2}}\underline{\underline{U}}^{-1} \tag{82}$$

Thus, in order to determine $S^{\frac{1}{2}}$ it is only necessary to find the matrix which diagonalises $\underline{\underline{S}}$. The solutions to Equation (74) can thus be readily obtained by diagonalisation techniques.

Matrix Diagonalisation

Matrix diagonalisation is carried out by the Jacobi method. This method constructs the diagonal matrix $\underline{\underline{D}}$ as the limit of a sequence of transformations of the form

$$\underline{\underline{A}}_{k+1} = \underline{\underline{V}}_k\ \underline{\underline{A}}_k\ \underline{\underline{V}}_k^{-1} \tag{83}$$

$$\text{i.e., } \underline{\underline{D}} = \underline{\underline{V}}_1\ \underline{\underline{V}}_2 \cdots \underline{\underline{V}}_n\ \ \underline{\underline{A}}_0\ \underline{\underline{V}}_1^{-1}\ \underline{\underline{V}}_2^{-1}\ \underline{\underline{V}}_3^{-1} \cdots V_n^{-1} \tag{84}$$

In the Jacobi method, the matrix $\underline{\underline{A}}_k$ is searched for the largest off-diagonal element ($a^k_{ij} = a^k_{ji}$) and the rotation angle θ_k chosen such that in the matrix $\underline{\underline{A}}_{k+1}$ the ij and ji elements are zero. The elements of the rotation matrix are given by

$$V^k_{mm} = 1 \qquad (m \neq i,\ j) \tag{85a}$$
$$V^k_{ii} = V^k_{ji} = \cos\theta_k \tag{85b}$$
$$V^k_{ij} = -V^k_{ji} = \sin\theta_k \tag{85c}$$
$$V^k_{mn} = 0 \qquad (m,\ n \neq i, j) \tag{85d}$$

Matrix multiplication gives the following set of equations

$$\begin{aligned}
a^{k+1}_{im} &= a^{k+1}_{mi} = a^k_{im}\cos\theta_k + a^k_{jm}\sin\theta_k \\
a^{k+1}_{jm} &= a^{k+1}_{mj} = a^k_{jm}\cos\theta_k - a^k_{im}\sin\theta_k \\
a^{k+1}_{ii} &= a^k_{ii}\cos^2\theta_k + a^k_{jj}\sin^2\theta_k + 2a^k_{ij}\sin\theta_k\cos\theta_k \\
a^{k+1}_{jj} &= a^k_{jj}\cos^2\theta_k + a^k_{ii}\sin^2\theta_k - 2a^k_{ij}\sin\theta_k\cos\theta_k \\
a^{k+1}_{ij} &= a^{k+1}_{ji} = \tfrac{1}{2}(a^k_{jj} - a^k_{ii})\sin 2\theta_k + a^k_{ij}\cos 2\theta_k \\
a^{k+1}_{mn} &= a^k_{mn}
\end{aligned} \tag{86}$$

If the element a^{k+1}_{ij} is to become zero, then θ_k must have the value

$$\theta_k = \tfrac{1}{2}\arctan\frac{a^k_{ij}}{\tfrac{1}{2}(a^k_{ii} - a^k_{jj})} \tag{87}$$

An example[11] of this is

$$\underline{A}_k = \begin{bmatrix} 0 & 1 & 0 & 0 \\ 1 & 0 & 1 & 1 \\ 0 & 1 & 0 & 1 \\ 0 & 1 & 1 & 0 \end{bmatrix}$$

$$\tan 2\theta = \tfrac{1}{2}\,\frac{1}{(0-0)} = \infty$$

$$\therefore\ 2\theta = 90 \quad \text{and} \quad \theta = 45$$

$$\therefore \quad \underset{=}{A}_{k+1} = \begin{bmatrix} 1 & 0 & 0.707 & 0.707 \\ 0 & -1 & -0.707 & -0.707 \\ 0.707 & -0.707 & 0 & 1 \\ 0.707 & -0.707 & 1 & 0 \end{bmatrix}$$

Repeated diagonalisations are carried out in this manner until all the off-diagonal elements are zero within a given accuracy, usually of the region of 10^{-10}. This would lead to an accuracy of 10^{-5} in the total electronic energy, as defined by Equation (68).

The Self Consistent Field

The matrix elements of the Hartree-Fock operator are dependent on the orbitals through the elements P_{pq} i.e., they are defined in terms of themselves. The general procedure for solving the Roothaan equations is essentially a trial-and-error process by first assuming a trial set of molecular orbitals which allows the calculation of another, hopefully better, set. This iterative procedure is carried out until the molecular orbitals no longer change upon further iteration. These are then said to be self-consistent with the potential field that they create, and the whole procedure is called the Self Consistent Field method (SCF).

There are several methods for obtaining the trial set of molecular orbitals.

a) Diagonalisation of the H_{pq} matrix: this is equivalent to completely neglecting the field of the other electrons as a zero level of approximation. This method works reasonably well for molecules which do not have unusual structures; in other cases divergence occurs instead of convergence

b) Trial Vectors: in this method the eigenvectors themselves are given to the programme. Such eigenvectors are either obtained from semi-empirical calculations or from non-empirical calculations of very closely related molecules. Thus for the thiophene-S-oxide molecules the output eigen-vectors for the calculation with tilt angle of 20.0 degrees were used as input for the other three isomers.

c) Input of the Fock Matrix: the diagonal elements of the SCF Fock matrix are reasonably independent of the geometry of a molecule, and of the environment of a given atom. Thus a calculation of the electronic structure of methane will lead to diagonal elements reasonably accurate for a calculation on, say, benzene. Thus the diagonal elements are given to the programme as input data, whereupon the programme creates the off-diagonal elements taking into account the molecular environment as determined by the potential and kinetic energy integrals.[12]

Electron Density Distribution

For a determinantal wave function such as is used in the Hartree-Fock theory the density function is given by

$$P(r) = N_i \sum_i^{occ} \Psi_i \Psi_i \qquad (88a)$$

$$= 2 \sum_i^{occ} \Psi_i \Psi_i \qquad (88b)$$

where N_i is the orbital occupancy of the ith molecular orbital; hence Equation (88b) applies to closed shells. The integral of P(r) over all r should be equivalent to the total number of electrons in the system, i.e.,

$$2n = \int P(r)\ dr = \int \Psi_i \Psi_i dr \tag{89a}$$

$$= \sum_{pq} P_{pq} \int \phi_p \phi_q dr \text{ (using equation 60)} \tag{89b}$$

$$= \sum_{pq} P_{pq} S_{pq} \tag{89c}$$

Using this equation the electronic charge distribution may be decomposed into contributions associated with various atomic orbitals in the LCAO expansion. This detailed analysis is often called a population analysis, and was developed by Mulliken.[13] He suggested that the electron density function P(r) should be analysed in terms of the individual contribitions from each atom plus an additional contribution from both intra- and inter-atomic overlap terms. The one-electron density function can be written as

$$P(r) = \sum_R \sum_p P^R_{pp}\ P^R_{pp}(r) + \sum_R \sum_{pq}{}^{1} P^R_{pq} S^R_{pq} P^R_{pq}(r)$$
$$+ \sum \sum P^{RS}_{pq}\ S^{RS}_{pq}\ P^{RS}_{pq}\ (r) \tag{90}$$

where R, S refer to atoms and the normalised orbital and overlap densities respectively as defined below.

$$P^R_{pq}(r) = \phi^R_p(1)\ \phi^R_q(1)\ /\ S^R_{pq} \tag{91a}$$

$$P^{RS}_{pq}(r) = \phi^R_p(1)\ \phi^S_q(1)\ /\ S^{RS}_{pq} \tag{91b}$$

(In these equations the summations involving p and q are over the subset of orbitals belonging to atoms R and S).

Mulliken characterised the charge distribution by extracting three quantities from Equation (90). These are (1) Y^R, the net atomic population of atom R; (2) X^{RS}, the overlap population between atoms R and S; (3) Z^R, the gross atomic population of atom R. These quantities are defined by

$$Y^R = \sum_p P^R_{pp} + \sum_{pq}^{1} S^R_{pq}\, P^R_{pq} \tag{92a}$$

$$X^{RS} = 2 \sum_{pq} S^{RS}_{pq}\, P^{RS}_{pq} \tag{92b}$$

$$Z^R = Y^R + \sum_{R>S}^{1} X^{RS} \tag{92c}$$

In the evaluation of the gross atomic populations the overlap population X^{RS} is arbitrarily apportioned equally between atoms R and S. Such equality may be, in some cases, the cause of atomic populations having values different from those predicted by classical methods. Using the electronegativities of atoms R and S would be an alternative, i.e.

$$Z^R = Y^R + \sum_{R>S}^{1} \sum_{pq} 2. \frac{E^R}{E^R + E^S} S^{RS}_{pq}\, P^{RS}_{pq} \tag{93}$$

where E^R is the electronegativity of atom R.

An alternative method of displaying the electron density distribution is to evaluate the function P(r) or its individual orbital contributions at a grid of points in two dimensions. Such electron density contour maps yield a viausl display of the electron density distribution.

A computer program was written which evaluated such electron density distributions, with the resulting contour diagrams being plotted on a Calcomp Graph Plotter. Several contour diagrams are incorporated in this thesis.

Molecular and Atomic Properties

In this part, properties other than energy which are obtainable from SCF wave-functions are studied.

a) Multipole moments: Consider a distribution of charges e_i at points (x_i, y_i, z_i) represented by the vectors $\underline{r}_i$ from the origin 0 to e_i; the scalar quantities r_i are associated with vectors $\underline{r}_i$. If such a distribution is in an external field the energy of interaction (u) of the charge distribution with the external field is given[14] by

$$u = \sum_i e_i \phi_i \tag{94}$$

where ϕ_i is the potential of the external field at $\underline{r}_i$. This potential can be expanded in terms of the potential and to derivative at 0:-

$$u = \sum_i e_i \Big[\phi_0 + \Big\{ \left(\frac{\partial\phi}{\partial x}\right)_0 x_i + \left(\frac{\partial\phi}{\partial y}\right)_0 y_i + \left(\frac{\partial\phi}{\partial z}\right)_0 z_i \Big\} + \frac{1}{2}\Big\{ \left(\frac{\partial^2\phi}{\partial x^2}\right)_0 x_i^2 + \left(\frac{\partial^2\phi}{\partial y^2}\right)_0 y_i^2 + \left(\frac{\partial^2\phi}{\partial z^2}\right)_0 z_i^2 + 2\left(\frac{\partial^2\phi}{\partial x \partial y}\right)_0 x_i y_i + 2\left(\frac{\partial^2\phi}{\partial y \partial z}\right)_0 y_i z_i + 2\left(\frac{\partial^2\phi}{\partial x \partial z}\right)_0 z_i x_i \Big\} + \cdots\cdots \Big] \tag{95}$$

with the subscript 0 denoting a value at the origin. This can be placed in tensor notation

$$u = \sum_i e_i \Big[\phi_0 + \left(\frac{\partial\phi}{\partial r_a}\right)_0 r_{ia} + \frac{1}{2}\left(\frac{\partial^2\phi}{\partial r_a \partial r_b}\right)_0 r_{ia} r_{ib} + \frac{1}{6}\left(\frac{\partial^3\phi}{\partial r_a \partial r_b \partial r_c}\right)_0 r_{ia} r_{ib} r_{ic} + \cdots\cdots \Big] \tag{96}$$

Here a, b, c denote tensor components (with r_{ia} being x_i, y_i or z_i) and repeated suffixes imply a summation over all components; thus $r_{ia} r_{ia} = r_i^2 = x_i^2 + y_i^2 + z_i^2$. Introduction of the parameters

$$\begin{gathered} q = \sum_i e_i \quad ; \quad \mu_\alpha = \Sigma\, e_i\, r_{ia} \\ Q'_{ab} = \sum_i e_i\, r_{ia}\, r_{ib}; \quad R'_{abc} = \sum_i e_i r_{ia} r_{ib} r_{ie} \\ F_\alpha = -\left(\frac{\partial\phi}{\partial r_a}\right)_0 \quad ; \quad F'_{ab} = \left(-\frac{\partial^2\phi}{\partial r_a \partial r_b}\right)_0 \\ F''_{abc} = -\left(\frac{\partial^3\phi}{\partial r_a \partial r_b \partial r_c}\right)_0 \end{gathered} \tag{97}$$

leads to Equation (96) becoming

$$u = q.\phi_0 - \mu_a F_a - \tfrac{1}{2}Q'_{ab}\, F'_{ab} - \tfrac{1}{6}R'_{abc}\, F''_{abc} + \cdots\cdots \qquad (98)$$

It is possible to transform this by introducing new tensors.

$$Q_{ab} = \tfrac{1}{2}(3Q'_{ab} - \sum_c Q'_{cc}\, S_{ab}) = \tfrac{1}{2}\Sigma e_i(3r_{ia}r_{ib} - r_i^2\, S_{ab})$$

$$R_{abc} = \tfrac{1}{2}(5R'_{abc} - \sum_d{}' {}_{add}\, S_{bc} - \sum_d R'_{bdd}S_{ac} - \sum_d R'_{cdd}S_{ab}) \qquad (99)$$

where $S_{ab} = 0$ if $a \neq b$ and 1 if $a = b$.

The energy of interaction now becomes

$$u = q\phi_0 - \mu_\alpha F_\alpha - \tfrac{1}{3}Q_{ab}F'_{ab} - \frac{1}{15}R_{abc}F''_{abc} + \cdots\cdots (100)$$

with q being the charge of the distribution, μ its dipole-moment, Q its quadrupole moment, R its octopole moment. The quantities ϕ_0, F, F' are the potential, electric field and electric field gradient. The tensor components of these multipole moments are shown in Table 3.

Table 3

Multipole Moment Operators

Dipole Moment	$\mu_x = x,\ \ \mu_y = y,\ \ \mu_z = z$	
Quadrupole Moment	$Q_{xx} = \frac{1}{2}(3x^2 - r^2)$;	similarly for y and z
	$Q_{xy} = \frac{3}{2}\,xy$;	similarly for xz and yz
Octopole Moment	$R_{xxx} = \frac{1}{2}(5x^3 - 3xr^2)$ "	" R_{yyy} and R_{zzz}
	$Q_{xyz} = \frac{5}{2}\cdot xyz$	
	$Q_{xyy} = \frac{1}{2}(5xy^2 - xr^2)$ "	" R_{xzz}, R_{xxy} R_{xxz}, R_{yzz} R_{yyz}
Hexadecapole Moment	$H_{xxxx} = \frac{1}{8}(35x^4 - 30x^2r^2 + 3r^4)$	similarly for y,z
	$H = r^4,\ xyr^2, xzr^2,\ yzr^2$	
	$H = x^2r^2$	

Within the LCAO approximation it is possible to replace the summation with an integration, and insert the SCF eigenvectors to give, for the dipole moment say

$$\mu_x = 2 \sum_{k}^{occ} \sum_{ij} C_{ik} C_{jk} \int \phi_i \,|\, x \,|\, \phi_j \; d\tau \qquad (101)$$

The nuclear component of the dipole moment is similarly defined

$$\mu_x^{nuclear} = \sum_{i=1}^{NON} Z_i x_i \qquad (102)$$

where Z_i is the charge of one of the NON nuclei. Equations (101) and (102) are special cases of the following general expressions:-

$$E^{e\ell} = 2 \sum_{k=1}^{occ} \sum_{ij} C_{ik} C_{ij} < \phi_i \,|\, OP \left\{ (x-x_1), (y-y_1), (z-z_1) \right\} |\, \phi_j > \qquad (103)$$

$$E^{n} = \sum_{k=1}^{NON} Z_i \; OP \left\{ (x-x_1), (y-y_1), (z-z_1) \right\} \qquad (104)$$

where $E^{e\ell}$ is the electronic expectation value of the operator OP, evaluated at the point x_1, y_1, z_1 and E^n is the corresponding nuclear component. For example the operator for the Q_{xy} component of the quadrupole moment is $\frac{3}{2}(x-x_1).(y-y_1)$. All operators have to be evaluated at some point in space; now the first non-zero multipole moment (charge, dipole, quadrupole....) is origin independent, i.e., it has the same value no matter where it is evaluated. For all neutral molecules the dipole moment (if any) is thus origin independent, with Equations (101) and (102) assuming that it is being evaluated at the origin. It is however conventional to evaluate the multipole moments at the centre of the mass of the molecule; thus Q_{xy} would become

$$Q_{xy} = \frac{3}{2}(x-x_{cm})(y-y_{cm}) \tag{105}$$

The quadrupole moment possesses a useful property; it is a traceless tensor and as such the matrix of Q_{ab} values can be diagonalised. This allows one to use a single value to represent the quadrupole moment in special cases; e.g. for an axially symmetric molecule such as methylsilane, $Q_{xx} = Q_{yy} = -\frac{1}{2}Q_{zz}$ (if z is the main symmetry axis) and it is necessary only to report Q_{zz}.

b) Potential, Electric Field and Electric Field Gradient:

The potential operator has the form 1/r and is a single component operator. As shown above the electric field and the electric field gradient components can be obtained by appropriate partial differentiation. The operators so obtained are consistent with Equations (103) and (104) and are displayed in Table 4, where evaluation at the origin is assumed for the sake of clarity. These operators are functions of the atoms rather than the molecule as a whole and are thus usually evaluated at all the atoms. Electric field gradient is a trace-less second rank tensor and behaves similarly to the quadrupole moment.

Table 4
Potential, Electric Field, Electric Field Gradient

Potential	$1/r$
Electric Field	$-x/r^3$ and similarly for y, z
Electric Field Gradient	$-(3x^2-r^2)/r^5$ and similarly for y,z $-3xy/r^5$ and similarly for xz, yz.

c) Second and Higher Moments: Dipole Moment can be considered to be the first moment of the charge distribution, and can be given by OP_a where a = x, y, z. The second moment has components of the type OP_{ab}; a similar definition holds for third (OP_{abc}) and fourth (OP_{abcd}) moments. In addition there are operators derived from these, which involve r^n e.g.

$$xr^2 = xx^2 + xy^2 + xz^2 = OP_{xxx} + OP_{xyy} + OP_{xzz} \qquad (1.06)$$

These operators, shown in Table 5, are molecular (like the multipole moments) rather than atomic.

Table 5

Second and Higher Moments

Second Moment	x^2, y^2, z^2, xy, xz, yz and r^2
Third Moment	x^3, y^3, z^3, xy^2, xz^2, x^2y, x^2z, y^2z, yz^2, xyz and (combined) xr^2, $2r^2$, yr^2
Fourth Moment	x^4, y^4, z^4, x^2y^2, x^2z^2, y^2z^2, x^2r^2, y^2r^2, z^2r^2, r^4, x^3y, xy^3, xyz^2, x^3z, xy^2, xz^3, x^2yz, y^3z, yz^3

d) Diamagnetic Susceptibility and Shielding: The diamagnetic susceptibility is very closely related to the second moment as the terms in Table 6 reveal. Similarly the diamagnetic shielding shows resemblances to electric field and electric field gradient. It is not then surprising to find that susceptibility is a molecular property (centre of mass evaluation) and shielding an atomic property.

Table 6

Diamagnetic Shielding and Susceptibility

Shielding	$3/2\,(r^2 - x^2)/r^3$	and similarly for y and z
	$-3/2\ x\,y/r^3$	" " " xz and yz
Susceptibility	$3/2(r^2-x^2)$	" " " y and z
	$-3/2\ xy$	" " " xz and yz

c) Experimental Data: The dipole moments of many molecules are known, both in solution and gas phases.[15] As such it is possible to provide direct comparison with the calculated values; fewer quadrupole,[16] even less octopole[17] and only one or two hexadecapole[17] moments are known but again direct comparison is possible. Lately, second moments[16] and diamagnetic susceptibilities[16] have been evaluated. The electric field gradient has been used to predict nuclear quadrupole coupling constants[18] and correlation of diamagnetic shielding with NMR chemical shifts is very good for hydrogen atoms.[19] Finally attempts have been made to interpret core level binding energies using the potential operator.[20]

The Nature of the Atomic Orbitals, ϕ_i

It is now necessary to consider the nature of the atomic orbitals, ϕ_i, which are used in the LCAO expansion of the molecular orbitals. The first choice one would naturally tend to make would be to pick the hydrogen-like orbitals of Tables 1 and 2. However evaluation of electron-repulsion integrals could not be carried out because of the polynomial factor in the radial term. To circumvent this Slater[21] proposed that the radial part have the form

$$R_{n\ell}(r) = (2a)^{n+\frac{1}{2}}(2n!)^{-\frac{1}{2}}r^{n-1}\exp(-\alpha r) \qquad (107)$$

The orbital exponent α is given by

$$\alpha = \frac{Z-s}{n^*} \qquad (108)$$

where Z is the nuclear charge, s is a screening constant and n^* is an effective principal quantum number. These last two parameters could be chosen to give good value for energy levels, atomic radii and other properties. Slater formulated a set of rules to give good approximations to the best atomic orbitals of the atoms. Exponents are readily available for all the atoms up to and including krypton.[9]

This method has been used extensively for diatomic molecules but could not be extended readily for triatomics and polyatomics. Again four-centre integrals could not be evaluated due to an inability to obtain them in analytical form. Lately however numerical integration has become available.

The major break-through in LCAO-MO calculations came with the introduction of gaussian type functions[22] i.e., $\exp(-\alpha r^2)$ instead of $\exp(-\alpha r)$. In addition the spherical harmonics are replaced by powers of x, y and z which gave orbitals the same shape as the spherical harmonics; the general formulation for a gaussian type orbital is

$$G(r) = x^{\ell}y^{m}z^{n}\exp(-\alpha r^2) \qquad (109)$$

$$\text{e.g., } d_{xy} = xy\exp(-\alpha r^2) \qquad (109a)$$

The usefulness of these is that a generalised four centre integral can readily be replaced by a two-centre integral in the following manner.

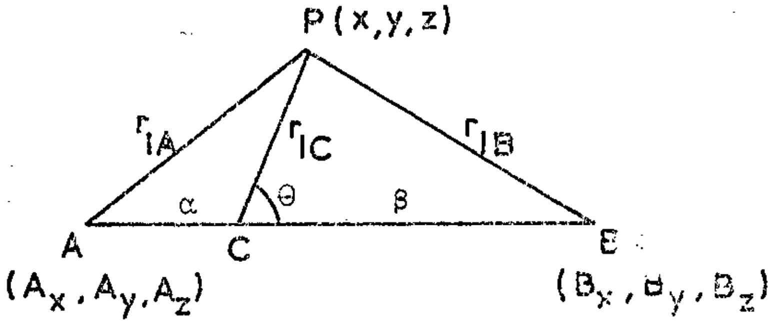

If the exponents on atoms A and B are a and b respectively then the lengths α and β can be given by

$$\alpha = \frac{b}{a+b} R_{AB} \qquad \text{and} \qquad \beta = \frac{a}{a+b} R_{AB} \tag{110}$$

Application of the cosine rule to the triangles ACP, BCP give

$$r_{1A}^2 = \alpha^2 + r_{1C}^2 + 2\alpha\, r_{1C} \cos\theta \tag{111a}$$

$$r_{1B}^2 = \beta^2 + r_{1C}^2 - 2\beta\, r_{1C} \cos\theta \tag{111b}$$

$$\therefore \quad \beta\, r_{1A}^2 + \alpha\, r_{1B}^2 = (\alpha\beta + r_{1C}^2)\, R_{AB} \tag{112}$$

$$\text{i.e.} \quad \frac{a}{a+b} R_{AB}\, r_{1A}^2 + \frac{b}{a+b} R_{AB}\, r_{1B}^2 = \frac{ab}{(a+b)^2} R_{AB}^3 + r_{1C}^2\, R_{AB} \tag{112a}$$

$$\therefore \quad a r_{1A}^2 + b\, r_{1B}^2 = \frac{ab}{a+b} R_{AB}^2 + (a+b)\, r_{1C}^2 \tag{113}$$

$$\therefore \quad \exp(-a r_{1A}^2) \exp(-b r_{1B}^2) = \exp(-a r_{1A}^2 - b r_{1B}^2)$$

$$= \exp\left\{-\frac{ab}{a+b} R^2\right\} \exp -(a+b) r_{1C}^2 \tag{114}$$

Unhappily it was found that the total electronic energy of a molecule or atom was very much less negative when a single Slater function was replaced by a single gaussian function. However, a string of gaussians was found to produce almost as good results. It has been found relatively easy to expand Slater functions in terms of gaussian functions; expansions of all orbital types up to 4p in up to six gaussians for an (arbitrary) unit exponent have been published.[23] The method of expansion is such that the unit exponent can readily be replaced by one of any magnitude, using the same gaussian expansion.

Of course expansions of Slater exponents are not absolutely necessary; it is quite possible just to optimise a string of gaussians for an atom or molecule (see Appendix 1 for further discussion). Many gaussian sets are available in the literature with those of Roos and Siegbahn[24] being used in this thesis.

One small drawback in using the gaussian type functions is that integrals which are non-s in character take a comparatively long time to perform. In order to get round this the method of floating spherical gaussians was evolved.[25] Here the only functions used are s-type and higher orbitals are represented by linear combinations of s-type orbitals at ghost centres, e.g.

S1 carbon S2

$$P = \exp(-\alpha_{s1} r^2) - \exp(-\alpha_{s2} r^2)$$

This method preserves the speed of s-type integration while retaining the electron-repulsion integrals. The total energies obtained are not too good but do reproduce experimental geometries quite well.

Minimising Computer Time

If a molecule has m atomic functions then the total number of electron repulsion integrals to be evaluated is given by $\frac{1}{8}(m^4 + 2m^3 + 3m^2 + 2m)$. There are several ways of reducing the number of integrals to be evaluated.

a) <u>The "NO-DO" method</u>: Consider the electron repulsion integral for the linear system represented below, between three S and one P type functions.

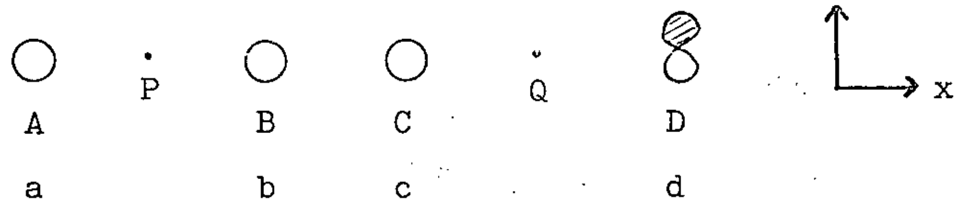

A-D are the centres with associated exponents a-d. The general electron-repulsion integral is given by

$$2\left\{\frac{(a+b)(c+d)}{\pi(a+b+c+d)}\right\}^{\frac{1}{2}} \left\{-\frac{b}{a+b}(A_i-B_i)\, S_{ab}S_{cd}\, F_0(t) + S_{ab}S_{cd}\, \frac{a+b}{c+d}(P_i-Q_i)F_1(t)\right\} \qquad (115)$$

where S_{ab} is the overlap integral between s-functions with exponents a and b, the subscript <u>i</u> implies x, y or z and $t = (a+b)(c+a)/(a+b+c+d).R^2_{PQ}$. For the illustration above both terms are zero because the z co-ordinates of A, B, P, Q are all identical. If any one of these four atoms was out of the plane of the remainder then this would not be true; similarly if the p-orbital was x the integral would be non-zero. The IBMOL-4 package recognised 64 combinations of p and s functions of which 42 were identically zero for linear systems on ground similar to those above. For a planar molecule 24 could be ignored. There was thus a considerable saving of computing time by leaving such integrals unevaluated.

b) <u>Thresholds</u>: Two thresholds were commonly used to avoid excess calculation. The first of these applied to the exponential term present in the S_{ab} (or S_{cd}) part; if this was less than the threshold value then the whole integral was set to zero; the input value was 1×10^{-7} for the calculations in this thesis. The second threshold was also an input parameter but was adjusted within the programme by using the largest gaussian exponent. If an evaluated integral was found to be less than this adjusted threshold then the whole integral was set to zero. Obviously this did not save computer time in evaluating integrals but use of zeros in the SCF section would obviously be faster. These two thresholds are common to the IBMOL and ATMOL programme packages.

c) Symmetry in Integral Evaluation: Consider the arrangement of atoms below, a distorted, square-planar form of methane.

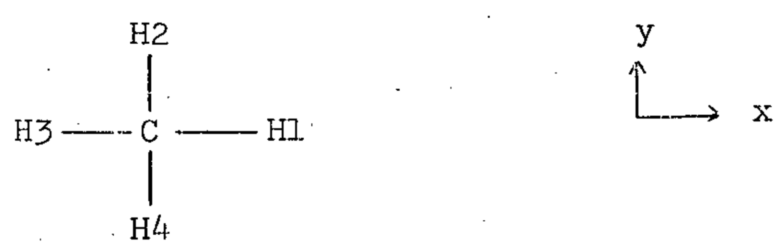

Any integral between the carbon x and H1 will be identical to that with H3 or y/H2 or y/H4 apart from a multiplying integer (± 1 in this case). Obviously setting two integrals equal is much faster than evaluating both directly. The ATMOL suite of programmes uses such equalities.

d) Symmetry of the Wave Function: Symmetry is also used in the SCF section to save time. It has already been shown that the SCF procedure requires diagonalisation of matrices. Consider now the simple atomic system, Argon, having the electronic structure $1s^2\ 2s^2\ 2p_x^{\ 2}\ 2p_y^{\ 2}\ 2p_z^{\ 2}\ 3s^2\ 3p_x^{\ 2}\ 3p_y^{\ 2}\ 3p_z^{\ 2}$. The s, p_x, p_y, p_z functions all belong to different irreducible representations. The Fock matrix obtained at SCF convergence has the form

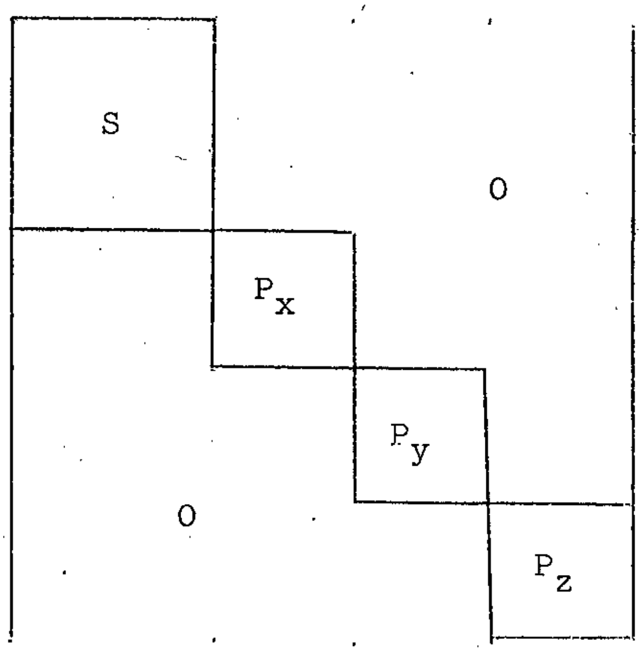

It can be seen that the Fock matrix consists of four regions, each one involving only orbitals of the same irreducible representations. Thus the matrix is partially diagonalised, by symmetry; the saving of computer time occurs because it is only necessary to diagonalise each of the sub-matrices.

In molecules the s, p_x, p_y and p_z functions do not block the Fock matrix into sub-matrices. However it is possible to take linear combinations of atomic functions which do block the matrix. The possible linear combinations are obtainable from Group Theory treatments,[26] and each irreducible representation of the molecular point group gives a sub-matrix. Consider H_2O as an example. This belongs to the point group C_{2v} which has the character table below

C_{2v}	E	$C_2(y)$	$\sigma(yz)$	$\sigma(xz)$
A_1	1	1	1	1
A_2	1	1	-1	-1
B_1	1	-1	1	-1
B_2	1	-1	-1	1

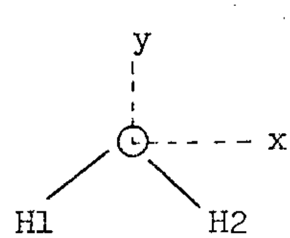

The effect of the symmetry operators on the atomic orbitals is shown below.

A.O.	E	C_2	$\sigma(yz)$	$\sigma(xz)$	Sym Orbs
O 1s	O 1s	O 1s	O 1s	O 1s	A_1
O 2s	O 2s	O 2s	O 2s	O 2s	A_1
O $2p_x$	O $2p_x$	-O $2p_x$	-O $2p_x$	O $2p_x$	B_2
O $2p_y$	O $2p_y$	O $2p_y$	O $2p_y$	O $2p_y$	A_1
O $2p_z$	O $2p_z$	-O $2p_z$	O $2p_z$	-O $2p_z$	B_1
H_1 1s	H_1 1s	H_2 1s	H_2 1s	H_1 1s	$A_1 + B_2$

To obtain the symmetry adapted orbitals (SAO) it is then necessary to multiply the character by the effect the corresponding operation has on a particular function. Thus

S.A.O.(A_1) = 1 x O 1s + 1 x O 1s + 1 x O 1s + 1 x O 1s = 4 O 1s

and the S.A.O. for the oxygen 1s is the same orbital (the multiplicative constant 4 being dropped, with normalisation procedures taking care of such constants within the programme). For the oxygen 1s orbital the A_1 representation is the only one possible, with other representations being zero, e.g.

S.A.O. (A_2) = 1 x O 1s + 1 x O 1s - 1 x O 1s - 1 x O 1s = O.

For the hydrogen atoms two S.A.O.'s are non-zero, i.e.,

S.A.O. (A_1) = 1 x H_1 1s + 1 x H_2 1s + 1 x H_2 1s + 1 x H_1 1s = $2(H_1+H_2)$1s

S.A.O. (B_2) = 1 x H_1 1s - 1 x H_2 1s - 1 x H_2 1s + 1 x H_1 1s = $2(H_1-H_2)$1s

The Fock matrix is then blocked into three submatrices, as below

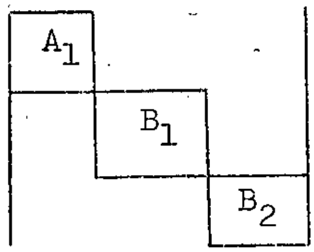

e) <u>SCF Convergence</u>: It has already been shown that the SCF procedure is iterative in nature. As each iteration uses quite a large amount of computer time it would obviously be advantageous to have some sort of extrapolation procedure. If one numbers the same matrix element of eigenvectors consecutively as C_0, C_1, C_2 ... for successive iterations it is possible to compute the ratio R given by

$$R = \frac{C_0 - C_1}{2C_1 - C_0 - C_2} \tag{116}$$

If the absolute value of R is less than 2.0 no extrapolation is done. Otherwise the extrapolated value is

$$C_3 = C_0 + R(C_1 - C_2) \tag{117}$$

This is used in the IBMOL-4 package as an optional procedure.

References

1. N. Bohr, Phil. Mag., 1913, 26, 476.

2. L. de Broglie, "Matter and Light", 1946 (W.W. Norton Co.)

3. E. Schroedinger, Ann. Physik, 1926, 79, 361.

4. B.C. Kahan, "Mathematical Techniques for Engineers and Scientists", 1966, (International Textbook Co.Ltd.)

5. J.C. Slater, Phys. Rev. 1930, 35, 509.

6. W. Pauli, Z. Physik, 1925, 31, 765.

7. T.A. Koopmans, Physica, 1933, 1, 104.

8. (a) V. Fock, Z. Physik, 1930, 61, 126; (b) D.R. Hartree, Proc. Camb. Phil. Soc. 1928, 24, 89.

9. J.A. Pople, D.L. Beveridge, "Approximate Molecular Orbital Theory", 1970 (McGraw-Hill Book Company)

10. (a) G.G. Hall, Proc. Roy. Soc. (London), 1951, A205, 541; (b) C.C.J. Roothaan, Rev. Mod. Phys. 1951, 23, 69.

11. R.L. Flurry, "Molecular Orbital Theories of Bonding in Organic Molecules" 1968 (Edward Arnold Ltd.)

12. V.R. Saunders, "Atmol-2, User Notice 4"

13. R.S. Mulliken, J. Chem. Phys., 1955, 23, (a) 1833, (b) 1841.

14. A.D. Buckingham, Quart. Rev., 1959, 13, 183.

15. A.D. McLellan, "Tables of Dipole Moments".

16. D.H. Sutler, W.H. Flygare, J.A.C.S., 1969, 91, 4063.

17. D.E. Stogryn, A.P. Stogryn, Mol. Phys., 1966, 11, 371.

18. U. Gelius, B. Roos, P. Siegbahn, Theor. Chim. Acta (Berl.), 1972, 27, 171.

19. D.S. Marynick, W.N. Lipscomb, J.A.C.S., 1972, 94, 8699.

20. H. Basch, Chem. Phys. Lett., 1970, 5, 337.

21. J.C. Slater, Phys. Rev., 1930, 36, 57.

22. S.F. Boys, Proc. Roy. Soc. (London), 1950, A200, 542.

23. R.F. Stewart, J. Chem. Phys., 1970, 52, 431.

24. B. Roos, P. Siegbahn, Theor. Chim. Acta (Berl.), 1970, 17, 209.

25. J.L. Whitten, J. Chem. Phys., 1963, 39, 349.

26. F.A. Cotton, "Chemical Applications of Group Theory," 1971, Interscience, New York.

CHAPTER TWO : Results and Discussion

General Introduction

The calculations in this thesis have been carried out using the Linear Combination of Atomic Orbitals-Molecular Orbital Self-Consistent Field method, with the atomic orbitals being linear combinations of Gaussian type orbitals; ground states of molecules have been studied.

Integral evaluations were carried out by the IBMOL-4 and ATMOL-2 suites of programmes on I.B.M. 360/50, 360/195 and 370/155 computers. Population analyses and dipole moments were obtained by satellite programmes of the above programme suites. One-electron properties were obtained by a slightly modified version of the appropriate POLYATOM-2 routines, using an I.C.L. 4-75 computer.

The calculations were carried out with a view to investigating the reactions and properties of organic systems. This has resulted in the molecules falling into various classes, which are treated separately. There are of course points common to several classes; comparisons and correlations have been drawn whenever they seemed appropriate. A major example of this is in the extent of d-orbital participation in the ground state of molecules containing second row elements. Encompassing the division into molecular types is a broad partitioning on grounds of the basis sets employed in the calculations. The first three sections used best atom basis sets with the second involving scaled basis sets. Some cross-over is provided by the molecules norbornadiene and pyrylium ion.

Turning now to the use of the calculations, SCF convergence immediately makes three properties available for predictive or comparative purposes. The first of these is total energy; it will be found in the molecular section that total energy is used to predict geometries, estimate inversion barriers, predict reaction pathways and analyse the role d-orbitals play in bonding. Closely related is the binding energy which, besides being directly comparable with experimental values, has been used to estimate relative stabilities of molecules of similar type, e.g. iso-electronic series. The second available property is the eigenvalues or orbital energies. These can of course be related directly to ionisation potentials obtained by x-ray or ultra-violet methods. As well as direct comparison use of orbital energies has been extended to predicting a possible analytical method for identifying reaction intermediates. The eigen-vectors, the third property, have been used to relate orbitals of similar molecules to one another and to examine the nature of the orbitals in terms of chemical bonding.

As a second stage the eigenvectors, plus the molecular geometry and basis set, are used to evaluate atomic and orbital populations, and hence reactivity. This reactivity includes acidity and nucleophilic substitution, and an attempt has been made to extend this to Diels Alder reactivity. Attempts have also been made to interpret core orbital energies in terms of the atomic charges.

Also obtainable from the SCF eigenvectors are the one-electron properties derived in Chapter One. Direct comparison of many such properties, especially dipole moments have been carried out. For molecules which are not yet known it is of course possible to predict some values which are likely to be of use to future experimentalists. The one-electron property, diamagnetic susceptibility, has been used in an attempt to determine aromaticity.

I. OZONOLYSIS

Introduction

The ozonolysis of olefins was interpreted for several years by the Criegee zwitterion mechanism.[1] This involved the formation of a primary ozonide, having a 1,2,3-trioxolane structure (1), which rearranged via a zwitterion intermediate to give a 1,2,4-trioxolane (2).

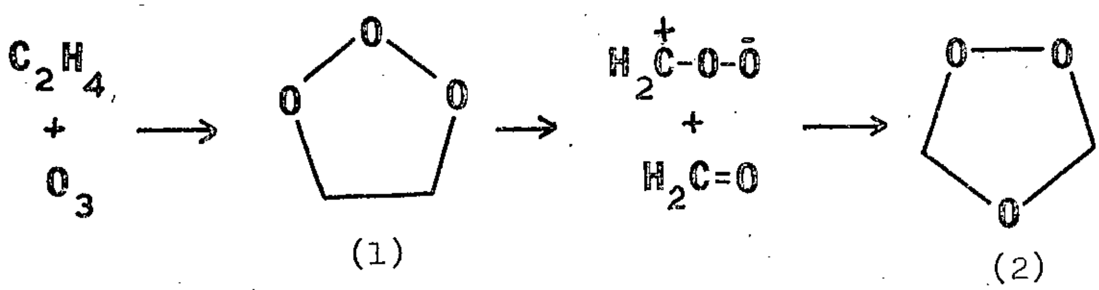

In the case of the olefin being ethylene the parent heterocycle, 1,2,4-trioxolane, was isolated; it was the formation of such 1,2,4-trioxolanes which necessitated Criegee postulating the zwitterion intermediate.

This mechanism was subsequently amended by Story and his co-workers[2] to allow for the formation of cross-ozonides (3) by an aldehyde exchange.

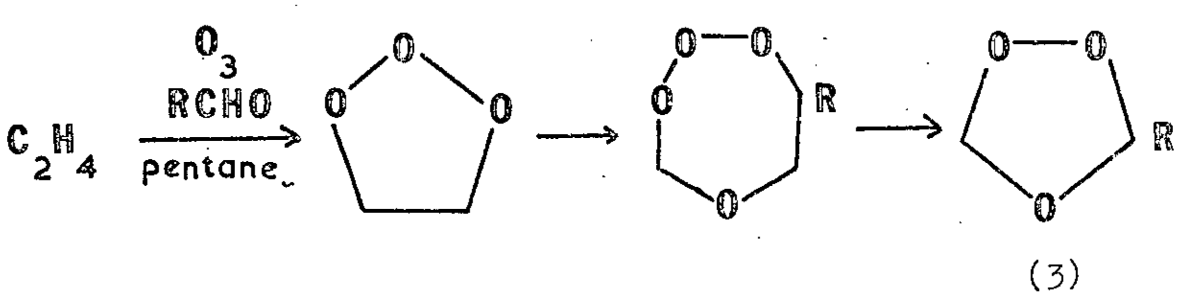

The formation of such cross ozonides is of course possible by the Criegee mechanism; however, the use of ^{18}O-enriched RCHO in the solvent gave rise to

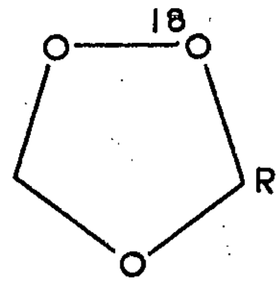

This is consistent with the aldehyde exchange mechanism but not the zwitterion mechanism which would predict the ^{18}O to occur as $C-^{18}O-C$.

It was further found that, as the concentration of propionaldehyde ($R = CH_3CH_2$) increased relative to the amount of solvent hydrocarbon, the nature of the products changed until, at 100% propionaldehyde no 1,2,4-trioxolanes were isolated, but only cyclohexanone, acetaldehyde and propionic acid. These were thought to be formed by the following reaction scheme.[3]

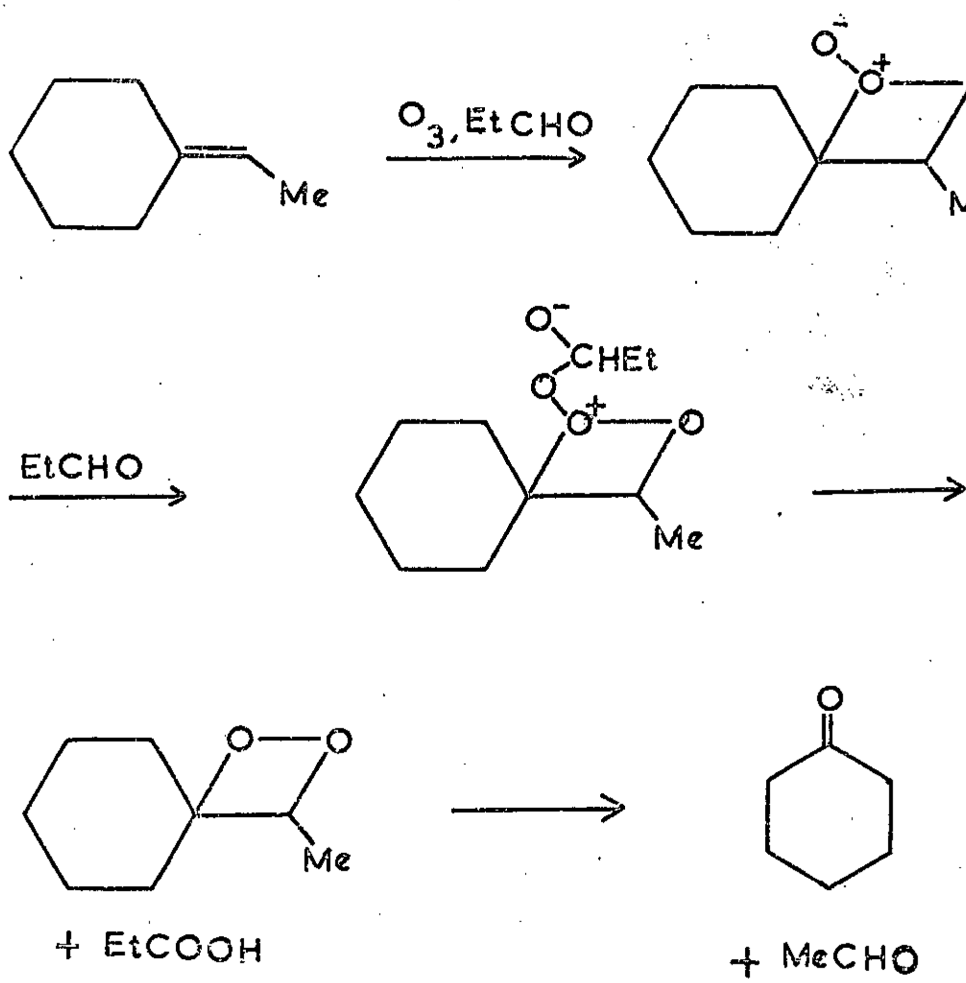

When this reaction was extended to more hindered olefins it was found that substantial quantities of epoxide were formed. Story and his co-workers abandoned the aldehyde exchange mechanism in favour of a scheme[3] in which there were several competing intermediates involved in ozonolysis reactions:-

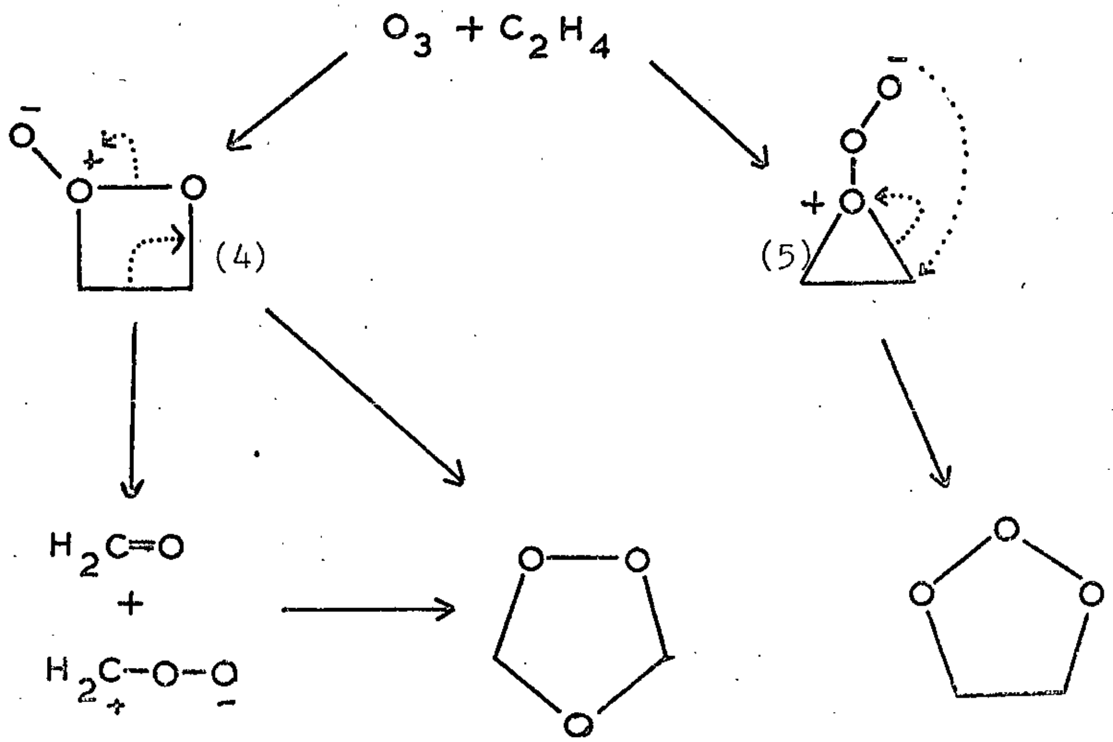

The most likely intermediates for this mechanism would be the peroxy-epoxide (5) and the Staudinger molozonide (4); the former being the intermediate for formation of epoxides.

Geometries and Calculation Data

Using ethylene as a model olefin, calculations have been carried out to determine which of the isomeric intermediates (1,2,4 or 5) is the most likely to occur. Such a determination could only be completely valid after optimisation of all the length and angle parameters in each

TABLE 1

Total Energies[a] for 1,2,3-trioxolane, molozonide and peroxy-epoxide structures

	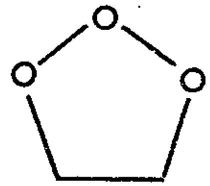	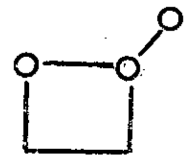	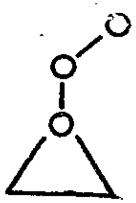
T.E.(au)	-301.28606	-301.24981	-301.10778
1-El.(au)	-811.10232	-783.67734	-784.35889
2-El.(au)	307.82776	294.84067	295.10044
N.R.(au)	201.98850	187.58686	188.15068
B.E.(au)	-0.23986	-0.20361	-0.06158
B.E.(kcal/mole)	-150.50	-127.8	-38.6
ΔE (kcal/mole)[b]	-7.79	+ 14.96	+104.1

Footnotes: a) 1-El = 1-Electron <u>or</u> Nuclear-Electron Attraction Energy
2-El = 2-Electron <u>or</u> Electron-Electron Repulsion Energy
N.R. = Nuclear Repulsion Energy
T.E. = Total Energy = 1-El + 2-El + N.R.
B.E. = Binding Energy = Total Energy - Σ Atom Total Energies.

This nomenclature will hold for all Tables of this type.

b) ΔE = Energy of intermediate - (Energy of O_3 + Energy of C_2H_4)

of the three molecules. Obtaining a multi-dimensional energy "surface" in this manner is too expensive in computer time and resources for molecules of such low symmetry. Since the geometries of these molecules are of course unknown they had to be constructed from similar known molecules. In order to minimise the errors caused by not carrying out a full geometry optimisation, the same "known" molecules were used for each of the intermediates.

From ethylene oxide C-C, C-H and C-O lengths, as well as H-C-H[4] angles were used; ozone supplied the O-O length and O-O-O angle.[5] Using these parameters the 3-membered ring in the peroxy-epoxide structure (5) is identical with that of ethylene oxide. Full details of geometries and symmetry orbitals are to be found in Appendix 2. The calculations were carried out with minimal basis sets, the same exponents and contraction coefficients being used for each molecule. The exact values of these, together with the energies of the atoms are tabulated in Appendix 2, Tables 1, 2 and 4 for H, C and O respectively.

The Ozone + Ethylene System

The energies of the three intermediates under consideration are shown in Table 1, and are represented graphically below. Also included in this figure is the sum of O_3 and C_2H_4 energies. All three intermediates have a negative binding energy, i.e. they are all thermodynamically stable with respect to dissociation into the constituent atoms. Only 1,2,3-trioxolane, however, is stable with respect to decomposition to ozone + ethylene. Thus the

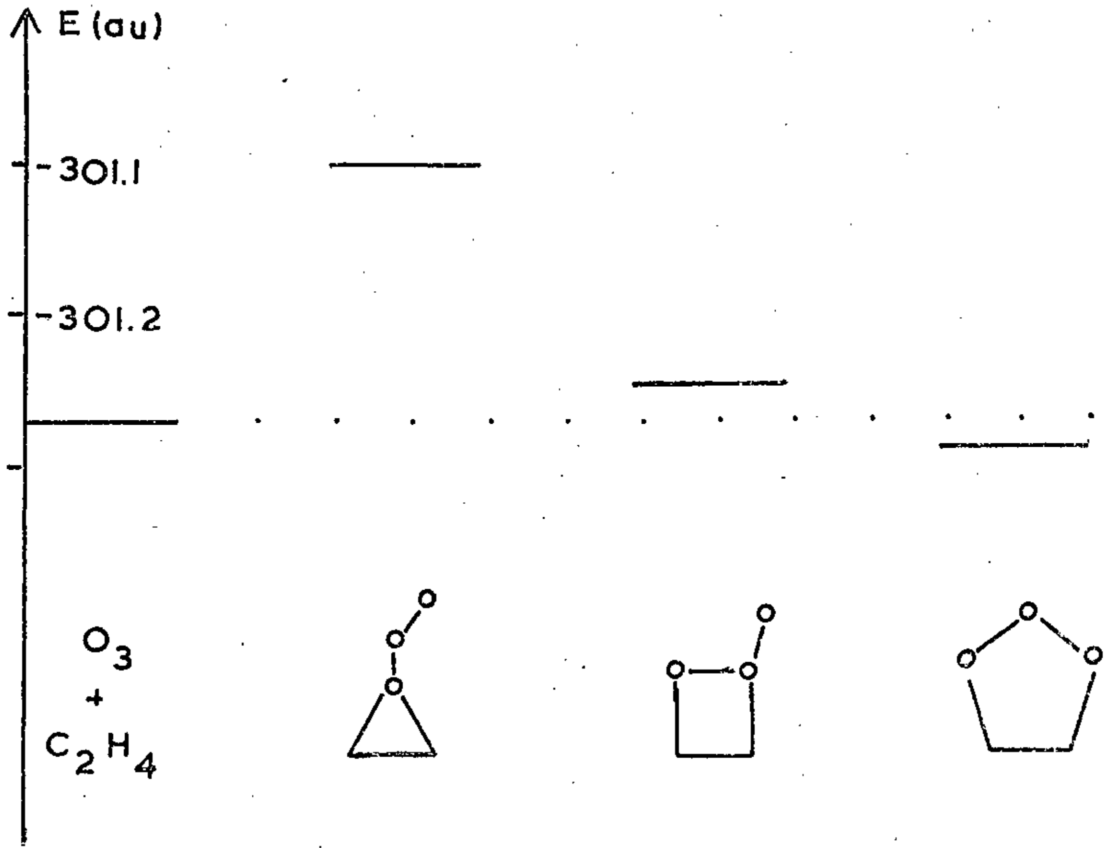

Figure 1. Total Energies of Ozonolysis Intermediates

most likely reaction pathway for the ozonolysis of ethylene is via 1,2,3-trioxolane. The most feasible alternative is for reaction to occur by means of the Staudinger molozonide, while the peroxy-epoxide is very unlikely to form. While this disagrees with Story's reaction scheme, the energy of activation for formation of the peroxy-epoxide (104.1 kcal/mole) is sufficiently large to be prohibitive for ethylene + ozone. However it is not so large as to preclude peroxy-epoxide formation in other more suitable cases.

The charge distributions, as determined by a Mulliken population analysis[6] and the dipole moment of these molecules are shown below.

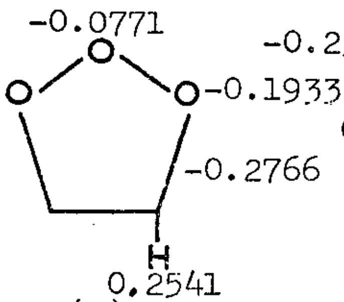

(1)

μ = 2.86D

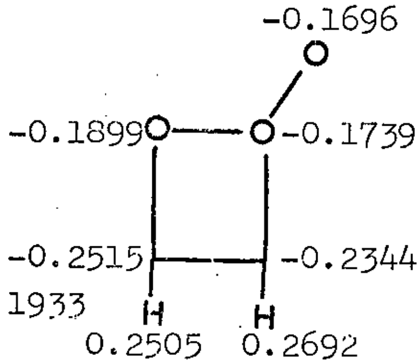

(4)

4.36D

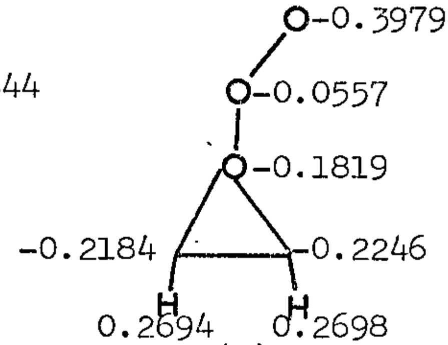

(5)

7.74D

The most obvious feature of these charge distributions is that there is no $>O^{+}-O^{-}$ or $>O^{+}-O-O^{-}$ nature in (4) or (5). While the Mulliken method of obtaining such distributions is not perfect, it is not so badly in error that it would give these distributions if the correct representation were the $>O^{+}-O^{-}$ type. This latter classical charge distribution is obtained by saying that the new bond is formed by the divalent oxygen atom sharing one of its lone pairs with the new approaching atom. Thus the divalent (ring) oxygen has a formal charge of +1 (a lone pair replaced by ½ of the electrons in a bond) and the extra-annular oxygen has a charge of -1 (electron "hole" replaced by ½ of the electrons in a bond). It is at this point that the "chemical" distribution stops. However since there are other electrons in the molecule it is not likely that they will tolerate such a distribution, and there is a general σ-electron movement towards the nominally positive oxygen. Comparing (4) with (1) the hydrogens lose electrons, becoming more positive; the carbons and oxygens also lose electrons and become less negative. It is thus hardly surprising that there is an increase in the dipole moment. A similar situation occurs in (5), with the exception that the central oxygen atom acts as a buffer between the formal positive and negative charges. This results in the monovalent oxygen being very negative and hence a very large dipole moment is calculated for (5).

Such a delocalisation is applied in some cases to formal chemical charges. For example, pyridine-N-oxide is usually written as the structure on the left below, but the remaining structures[7] (resonance forms) among others are used to explain reactions of this molecule.

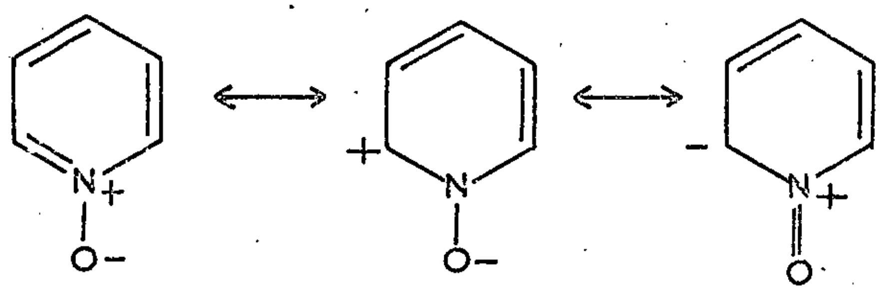

Formation and Structure of 1,2,4-trioxolane

The exact structure of 1,2,4-trioxolane has long been in doubt. An electron diffraction study[8] found that molecular models of C_2 (half-chair) and C_s (envelope) symmetry gave equally good fits to experimental intensity and radial distribution curves. In an attempt to clarify the structure Groth carried out an X-ray diffraction study[9] of the 3-carboxy-5-anisyl derivative; this however was found to have structural disorder associated with the

1,2,4-trioxolane ring. Accordingly calculations have now been done to decide which isomer is the more likely to occur. The Gaussian basis sets were identical to those above and again the exact geometries used are shown in Appendix 2, with the results of these calculations in Table 2 where (2a) represents the C_s and (2b) the C_2 structure.

TABLE 2

Total Energies for geometries of 1,2,4-trioxolane

	2a	2b	2c
	C_s (envelope)	C_2 ($\frac{1}{2}$-chair)	C_2 ($\frac{1}{2}$-chair)
T.E.(au)	-301.36915	-301.42250	-301.46323
1-El.(au)	-800.83834	-808.44889	-800.19200
2-El.(au)	301.17640	307.05080	302.70930
N.R. (au)	196.29279	199.97559	196.01948
B.E. (au)	-0.32351	-0.37686	-0.41759
B.E. (kcal/mole)	-203.1	-236.7	-262.9
Dipole Moment (D)[a]	2.63 D	0.70	0.92

a) Experimental value = 1.09 D, see Ref. 10.

It can be seen from this table that the C_2 structure is preferred by 33.6 kcal/mole. Comparison of the nuclear repulsion energy shows that this is greater in 2b than 2a, that is the atoms are closer together in 2b; this would lead one to expect an increase in the magnitude of the 1-Electron and 2-Electron energies. Evidently the gain in nuclear attraction energy (1-electron), a stabilising effect, offsets the increase in the other two destabilising terms, resulting in a preference for structure (2b).

Subsequent to carrying out these calculations, a C_2 structure was reported by Gillies and Kuczowski,[10] the determination being carried out by microwave spectroscopy. Since the structure found was slightly different from calculation 2b (mainly in the O-O length) a further calculation has been carried out using this new geometry, the results of which appear in the column (2c). This geometry was found to be more stable than the other C_2 structure by 26.2 kcal/mole, making it 59.8 kcal/mole more stable than the C_s isomer. Any further reference to 1,2,4-trioxolane applies to structure (2c).

The two most likely precursors of the Criegee zwitterion + formaldehyde are 1,2,3-trioxolane and the molozonide. Cleavage occurs along the dotted lines below. These also show the total overlap populations between the centres which split apart to form the intermediate.

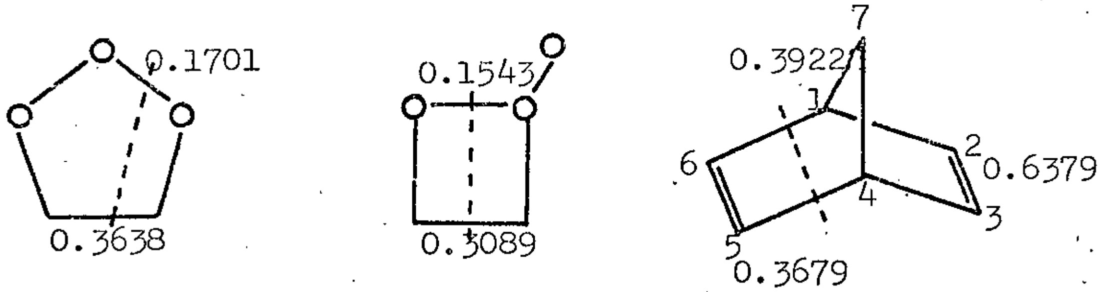

The overlap population between centres can be taken as a measure of bond strength. Norbornadiene, the third figure above, is known to cleave readily under mass spectrometry conditions to two ions of mass P^+ and $(P-26)^+$. This represents loss of acetylene from the molecule by splitting along the dotted line. The calculations on norbornadiene

TABLE 3

Total Energies for formaldehyde and the Criegee zwitterion.

	$H_2C = O$	H_2CO_2
T.E.(au)	-113.41306	-187.73977
1-El.(au)	-215.67187	-403.52559
2-El.(au)	70.86911	141.52590
N.R.(au)	31.38969	74.25992
B.E.(au)	-0.19604	+0.08932
B.E.(kcal/mole)	-123.0	+56.0

Figure 2 Total Energies for Formation of 1,2,4-Trioxolane

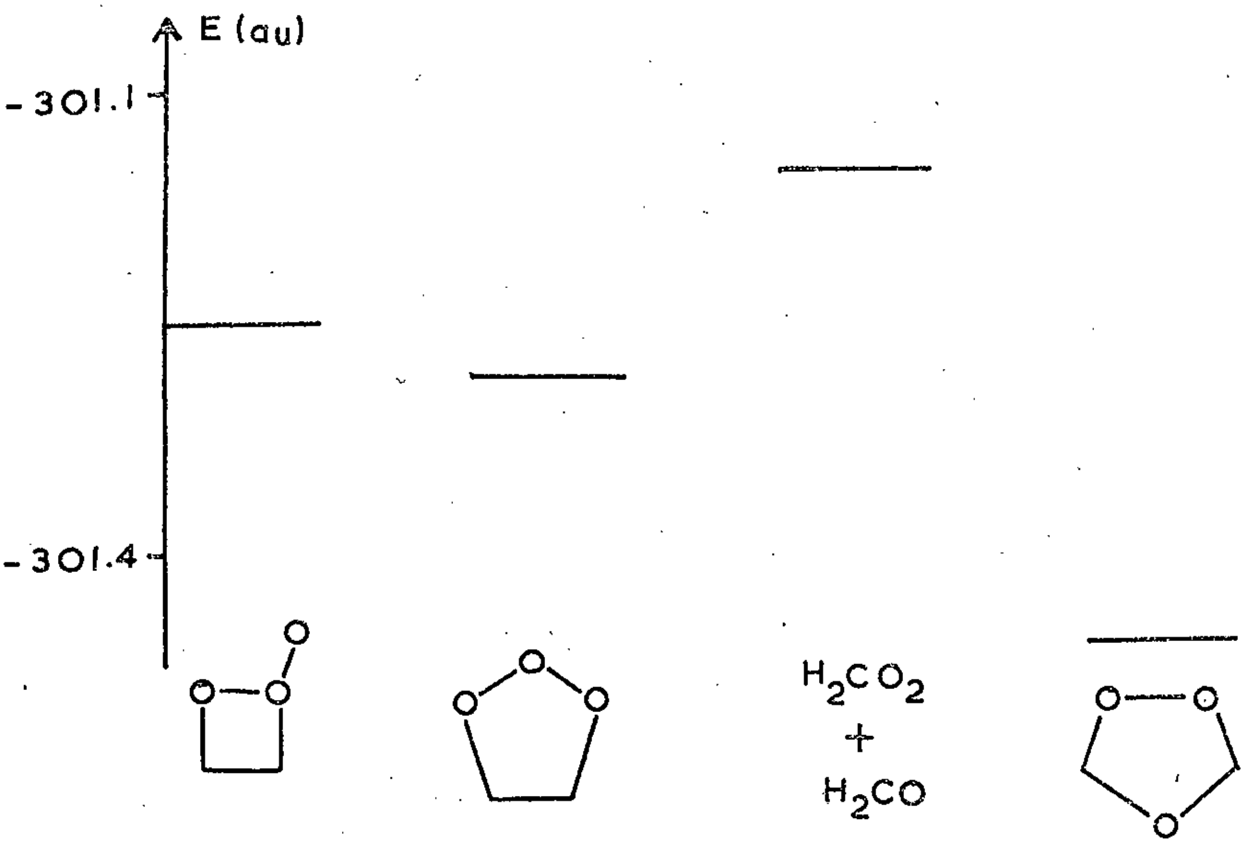

using the same basis set (see Section IV) gave the overlap populations above; these predict the correct order of bond strength and the bond through which splitting occurs has a population greater than that of the ozonolysis compounds. Thus fusion of the ozonolysis compounds is quite reasonable. 1,2,3-Trioxolane would appear to be less easily split, which is consistent with the energy differences between the precursors and the H_2CO_2+ H_2CO system (Figure 2). These energies are 83.6 and 60.6 kcal/mole for 1,2,3-trioxolane and molozonide respectively. (The calculations on formaldehyde were based on the experimental geometry,[11] with the zwitterion created by adding an oxygen atom to formaldehyde. The same exponents and contraction coefficients were used as for the rest of the molecules in this Section. The energies are shown in Table 3 while exact geometries are to be found in Appendix 3).

Since 1,2,4-trioxolane is formed at very low temperatures[10] ($-95^{\circ}C$), such large activation energies would appear to prohibit H_2CO_2 + H_2CO being formed. However recombination to give 1,2,4-trioxolane releases 191.4 kcal/mole. Thus, equating total energy differences to heats of reaction, the rearrangement of both 1,2,3-trioxolane and molozonide to 1,2,4-trioxolane is exothermic to the extent of 107.8 and 130.8 kcal/mole respectively. Thus only one molecule of 1,2,3-trioxolane needs to rearrange to supply more than enough energy to send another to the H_2CO_2 + H_2CO transition state. Therefore, as 1,2,3-trioxolane is the more likely isomer on energy grounds, at low temperatures rearrangement will occur in a smooth manner. In the case of the molozonide intermediate one rearrangement would supply sufficient energy to activate two more molecules of molozonide to the transition state. Thus a chain-reaction would be possible and will become increasingly more probable as the temperature rises since the formation of molozonide will become more likely.

This presupposes that recombination occurs to give 1,2,4-trioxolane and not the starting materials. An important factor in controlling the orientation of recombination will be the electrostatic interaction between the atoms. Below are the net charges for the intermediates H_2CO_2 + H_2CO.

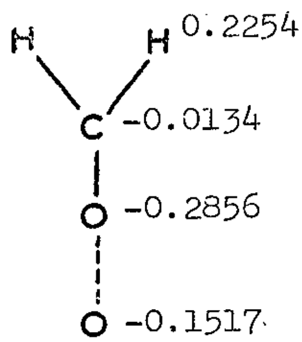

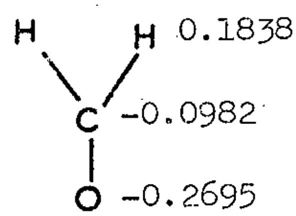

In both molecules only the hydrogen atoms have a positive charge. There is then no direct coulombic attraction between the big (non-hydrogen) atoms to control the orientation. However the orientation which leads to the least coulombic repulsion is that which gives rise to 1,2,4-trioxolane. This orientation will also minimise hydrogen-hydrogen repulsion and maximise hydrogen-big atom attraction. Thus one would predict on electrostatic grounds that recombination will give 1,2,4-trioxolane and not the starting materials.

TABLE 4

Total Energies for 1,2-dioxetane, epoxide-O-oxide structure, singlet oxygen and ethylene

	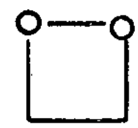	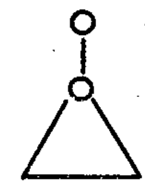
T.E.(au)	-226.74946	-226.64070
1-El.(au)	-573.68613	-558.69458
2-El.(au)	212.84046	205.64228
N.R. (au)	134.09621	126.41160
B.E. (au)	-0.31548	-0.20672
B.E. (kcal/mole)	-197.9	-129.7

	O_2	C_2H_4
T.E.(au)	-149.08755	-77.68925
1-El.(au)	-260.55097	-167.66885
2-El (au)	83.41784	56.73247
N.R. (au)	28.04557	33.24713
B.E. (au)	+0.13665	-0.47947
B.E. (kcal/mole)	+85.7	-300.9

The Structure of $C_2H_4O_2$

Loss of an oxygen atom from the molozonide and the perepoxide gives 1,2-dioxetane (6) and the epoxide-O-oxide of ethylene (7); these are the products of parallel and perpendicular addition of (singlet) oxygen to ethylene, i.e.

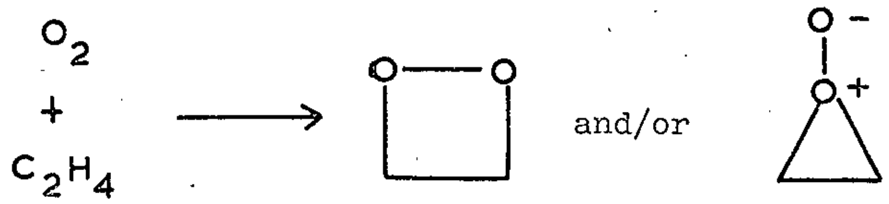

(6) (7)

Calculations have been carried out on these molecules using an option in the IBMOL-4 suite of programmes which allows the deletion of atoms from molecules whose integrals have already been obtained. The only restrictions are that the co-ordinates, Gaussian exponents and contraction co-efficients of the un-deleted atoms must stay the same as in the original calculation. Besides the molecules discussed here, ethylene oxide was obtained in this manner. The detailed geometries and symmetry orbitals are to be found in Appendix 2.

The energies of these molecules appear in Table 4, together with those of ethylene and singlet molecular oxygen. Figure 3 represents graphically the total energies of (6), (7) and the systems 2 x formaldehyde and ethylene + singlet oxygen molecule. The figure shows that both (6)and (7) are thermodynamically unstable with respect to formation of C_2H_4 + singlet oxygen, the respective energy differences

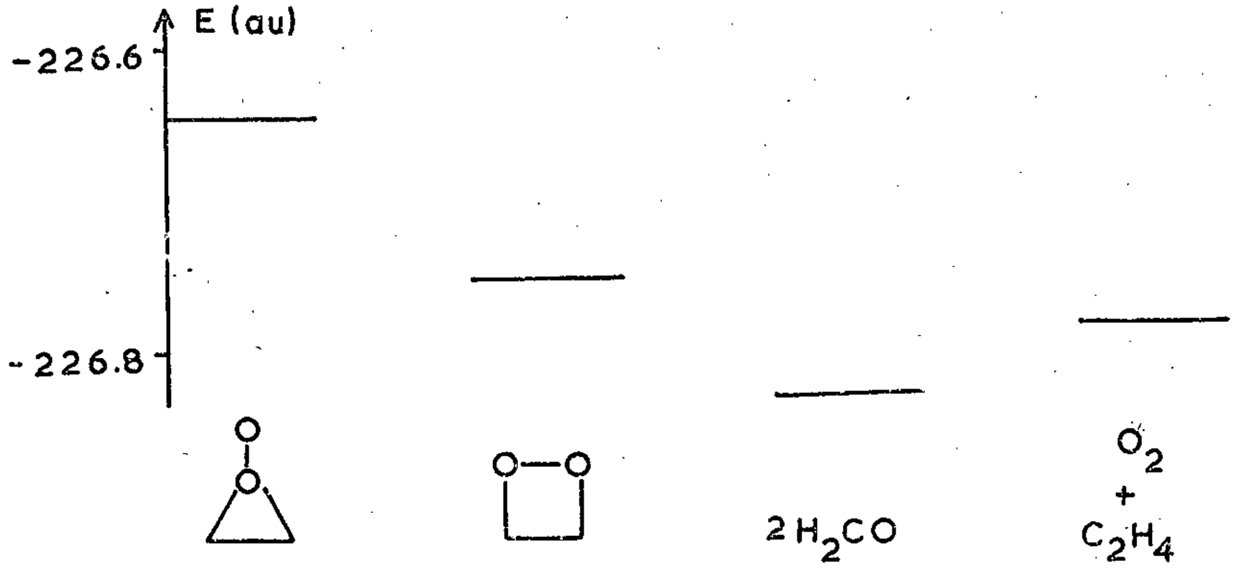

Fig. 3. The $C_2H_4O_2$ System

being 70 and 16 kcal/mole respectively. For 1,2-dioxetane there is a more favourable decomposition pathway - decomposition to two molecules of formaldehyde. (The epoxy-O-oxide would have to rearrange to 1,2-dioxetane before forming formaldehyde). A reaction scheme consistent with these observations is

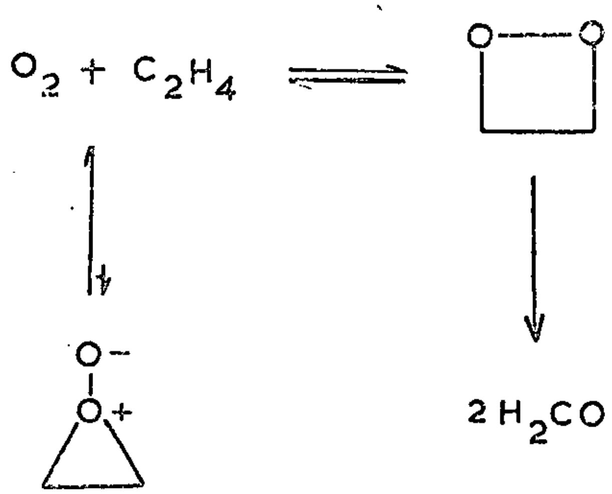

Any epoxide-O-oxide formed would revert to starting materials with the principal reaction being formation of formaldehyde via a 1,2-dioxetane intermediate.

Experimentally compounds derived from both epoxide-O-oxides and 1,2-dioxetanes have been isolated, when the reacting olefin is 1,2-diphenylcyclobutene.[12]

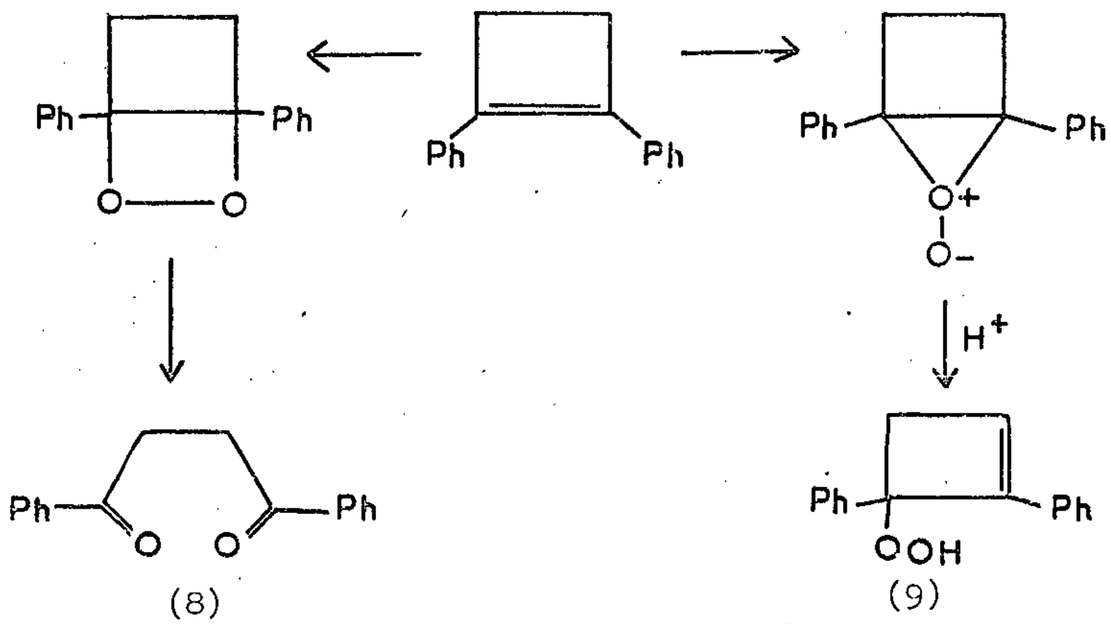

The diketone (8) is formed in non-polar solvents such as benzene or methylene chloride, while the hydroperoxide (9) is isolated from reactions in methanol or acetone. In the case of a simpler olefin, tetramethoxyethylene the sole product in non-polar solvents is the 1,2-dioxetane[13] (below)

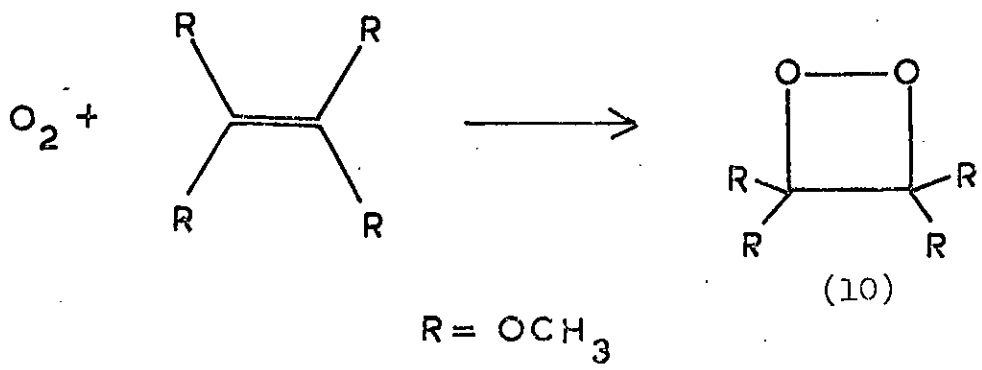

The structure of (10) was determined by spectroscopic methods. Decomposition gave the corresponding ester, dimethylcarbonate. Carbonyl compounds are also the products from 1,2-dioxetanes produced by the action of base on halogenated hydroperoxides.[14]

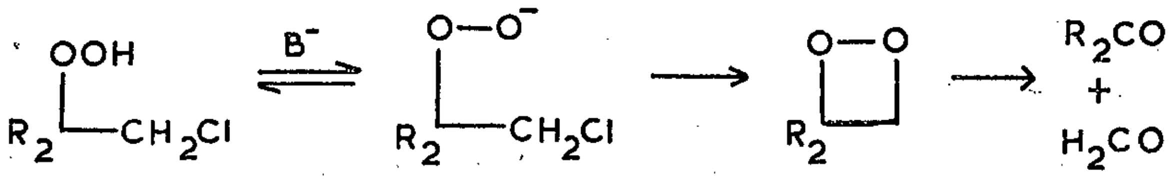

(11)

$R = CH_3$

The kinetics of the decomposition of 3,3-dimethyl-1,2-dioxetane (11) have been studied[15] with the activation energy for decomposition being 23.0 kcal/mole in carbon tetrachloride. The existence of 1,2-dioxetanes in ozonalysis reactions has also been inferred by Story and his co-workers,[16] who postulated the existence of 3-spiro-cyclohexyl-4,4-dimethyl -1,2-dioxetane (12) when the corresponding 1,2-diol was isolated after reacting the crude ozonolysis product with $LiAlH_4$.

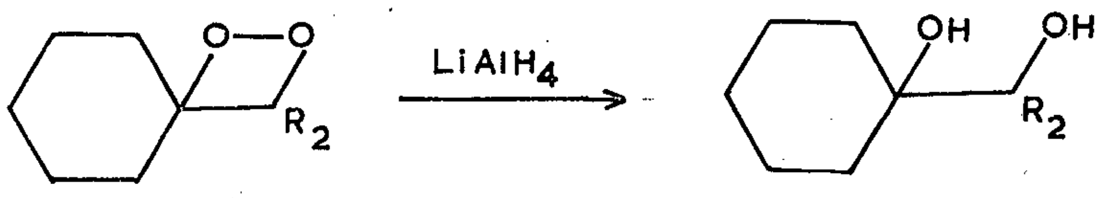

(12)

$R = CH_3$

Thus experimentally, the evidence definitely favours the formation of 1,2-dioxetanes in non-polar solvents. Since, with the exception of gas-phase reactions, this system is

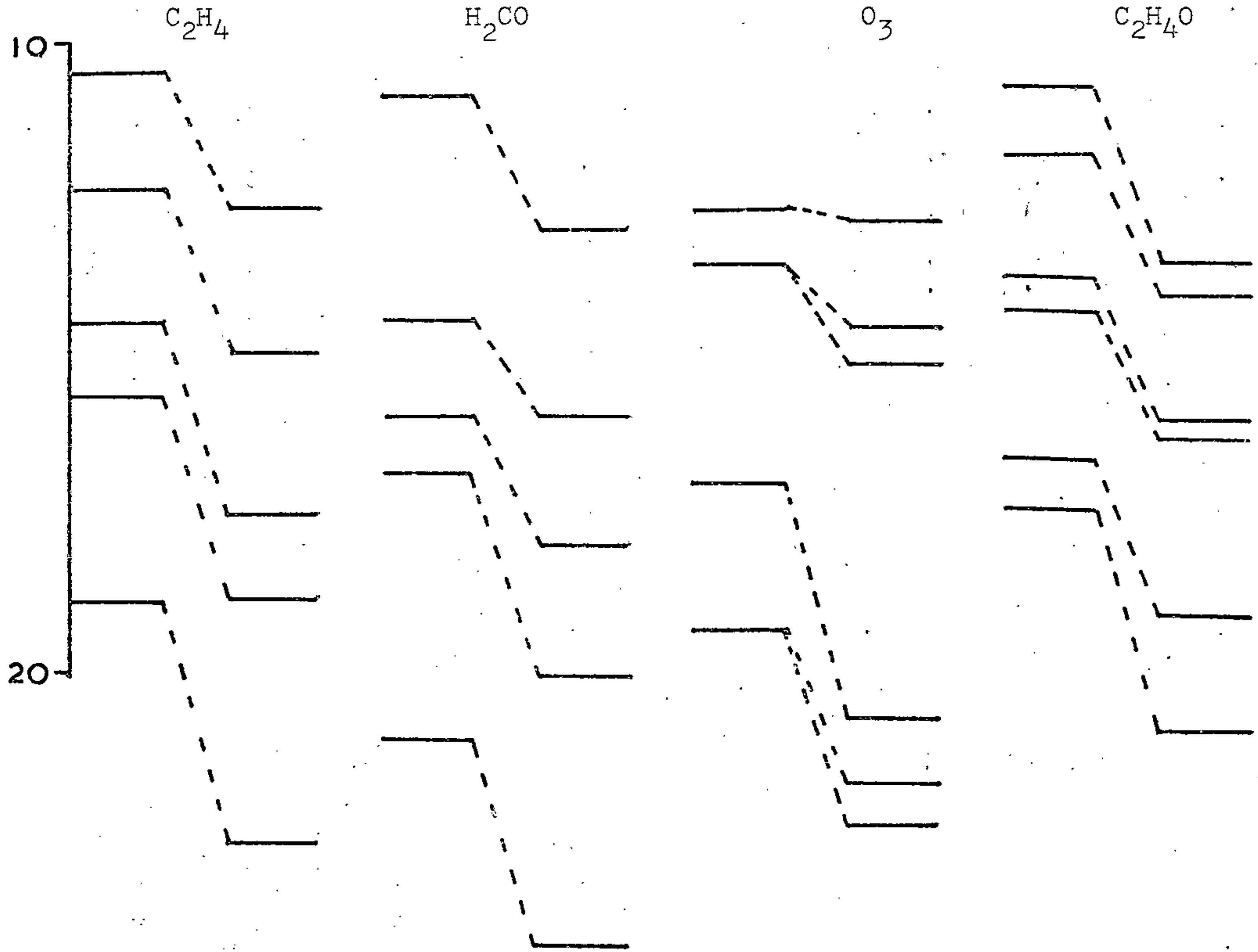

Fig. 4. Calculated and Observed Ionisation Potentials

the best for comparison with calculated results; there is fair agreement between the calculated predictions and experimental results. The charge distributions and dipole moments of (6) and (7) are shown below.

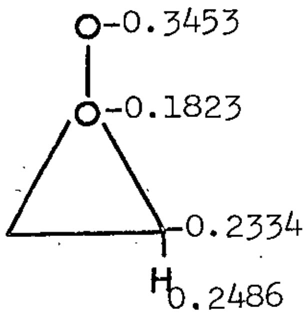

4.97D

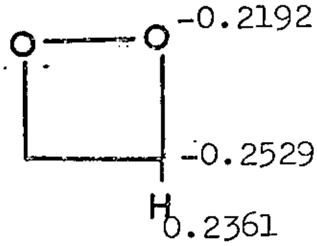

2.61D

Again, the charge distribution in the epoxide-O-oxide does not reflect the O^+-O^- as is usually written, the reason for this being the same as for the molozonide and peroxy-epoxide molecules. However the formally O^- atom has a very negative charge at the expense of the rest of the atoms in the molecule and gives rise to the high dipole moment. Indeed this is almost twice as large as that of 1,2-dioxetane.

Orbital Energies and Ionisation Potentials

The photo-electron spectra of formaldehyde,[16] ethylene[17] and ethylene oxide[18] have been reported in the literature. Figure 4 shows how the calculated orbital energies compare with the experimental ionisation potentials for these molecules. Included also is the correlation for ozone; due to contamination by O_2, the observed spectrum[19] of O_3 is in some doubt.

TABLE 6

Orbital Energies and Ionisation Potentials (in brackets)

$H_2C = O$		C_2H_4	O_3
A_1	A_1	A_g	A_1
-561.5	-559.89	-310.59	-570.31
-313.59	-312.19	-29.79	-562.33
-39.85	-40.31	-17.50(14.47)	-47.88
-24.16(~21.0)	-26.58	B_{3u}	-28.98
-17.95(16.0)	-19.03(16.6)	-310.56	-22.28(19.3)
B_2	-14.00(11.7)	-22.58(18.87)	-14.54(13.5)
-20.31(16.9)	B_2	B_{2u}	B_2
-12.96(10.86)	-312.19	-18.81(15.68)	-562.34
B_1	-24.82	B_{1g}	-38.54
-15.92(14.40)	-16.02(13.7)	-14.96(12.38)	-20.72(17.0)
	B_1	B_{1u}	-15.08(13.5)
	-20.88(17.4)	-12.66(10.51)	B_1
	-13.46(10.57)		-21.70(19.3)
	A_2		A_2
	-16.27(14.20)		-12.80(12.52)

TABLE 5

Total Energies of O_3 and Ethylene Oxide

	O_3	
T.E.(au)	-223.58435	-152.24769
1-El.(au)	-443.34573	-353.58644
2-El.(au)	151.20407	126.23665
N.R. (au)	68.55731	75.10210
B.E. (au)	+0.25195	-0.42578
B.E.(kcal/mole)	+158.1	-267.2

Table 5 shows the total energies of ethylene oxide and ozone, while Table 6 contains the experimental ionisation potentials and calculated orbital energies for the four molecules mentioned above. Excluding the values for ozone because of the experimental uncertainty, the remaining 16 points yield a least squares evaluated line of equation IP(expt) = 0.877 IP(calc) - 0.502 with a standard deviation of 0.036 and 0.642 in the slope and intercept respectively; the overall standard deviation is 0.486. This best straight line and the points for it are shown in Figure 5.

Taking this best straight line it is possible to obtain a set of predicted experimental ionisation potentials. Table 7 contains the calculated and predicted experimental IP's for the three ozonolysis intermediates (1), (4) and (5). The predicted experimental values are those obtained from the calculated orbital energies of less than 26eV since the calculated data used to obtain the best straight line did not extend beyond this value. Table 8 contains similar

TABLE 7

Calculated IP's and Predicted Experimental IP's – Ozonolysis Intermediates

	(1)			(4)			(5)	
	Calc.	Pred. Exp.		Calc.	Pred. Exp.		Calc.	Pred. Exp.
A_1	562.74		A'	562.86		A'	565.30	
	561.51			561.67			561.25	
	312.77			555.14			551.94	
	46.79			313.47			314.81	
	33.92			313.29			314.49	
	26.65	22.87		46.23			45.63	
	21.52	18.37		34.52			39.58	
	17.41	14.76		31.38			31.74	
	15.33	12.94		29.69			27.19	23.34
B_2	561.51			23.38	19.99		25.80	22.12
	312.78			21.24	18.12		21.20	18.08
	39.50			20.60	17.56		19.71	16.78
	26.33	22.58		16.58	14.03		17.53	14.86
	18.55	15.76		15.16	12.79		13.74	11.54
	15.81	13.36		11.32	9.42		8.66	7.09
B_1	22.81	19.50	A"	23.05	19.71	A"	21.95	20.41
	18.87	16.06		18.25	15.50		19.11	16.25
	11.02	9.16		17.83	15.08		18.07	15.34
A_2	19.06	16.23		12.84	10.75		14.44	12.16
	14.14	11.89		10.77	8.94		7.47	6.05

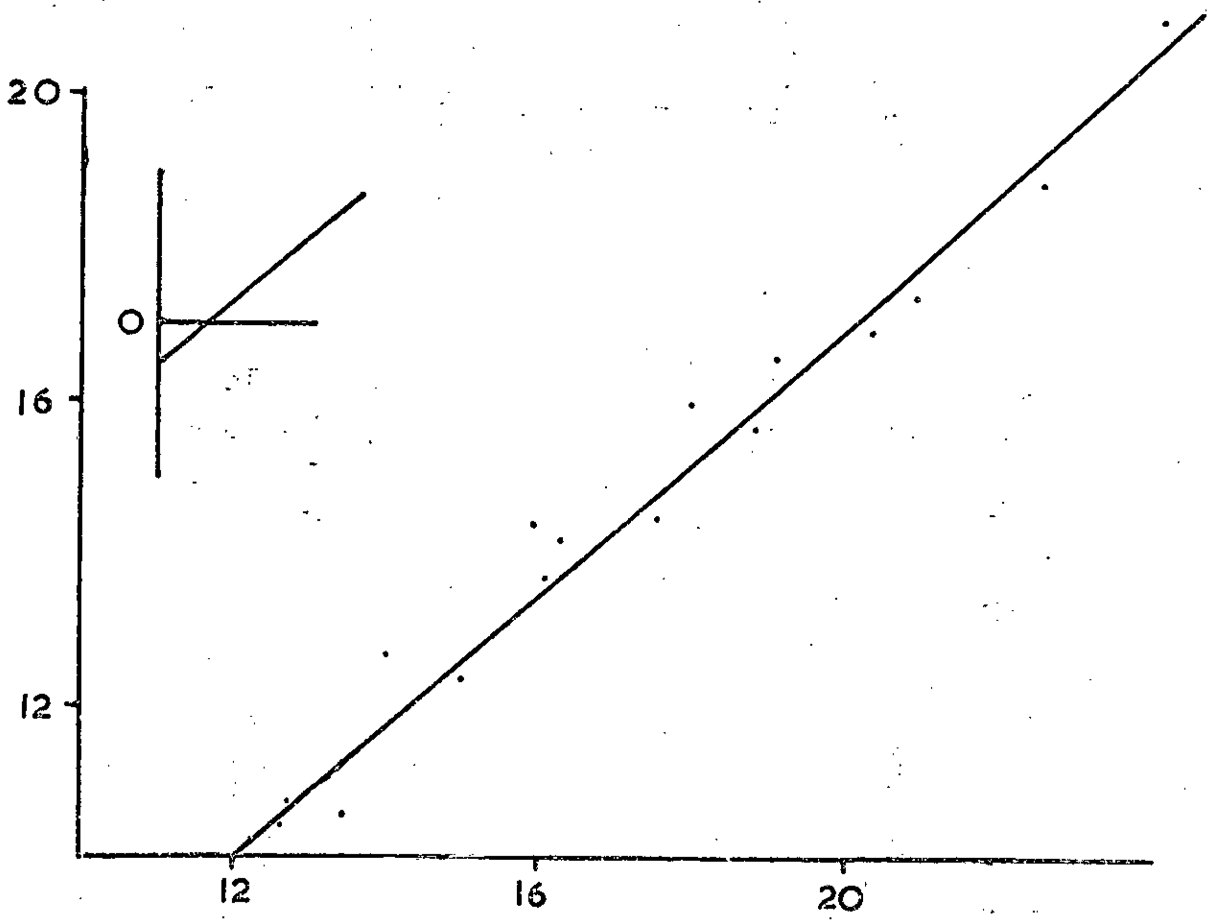

Fig. 5. Calculated v. Experimental Ionisation Potentials.

values for other species likely to occur during ozonolysis.

From these tables it can be seen that all the compounds which contain the formal O^+-O^- charge distribution are characterised by two ionisation potentials of less than 10eV. Indeed, of the molecules which do not have this structure, only 1,2,3-trioxolane has any IP below 10eV. Such low ionisation potentials are characteristic of very highly localised molecular orbitals; for example in the spectra of tertiary amines and amine-N-oxides, the first experimental ionisation potential of pyridine-N-oxide being 8.4eV.[20] As an example of how localised these orbitals can be the eigenvector for the out-

TABLE 8

Calculated IP's and Predicted Experimental IP's - Other Molecules

H_2CO_2

	Calc.	Pred. Exp.
A'	562.15	
	559.17	
	315.12	
	45.17	
	32.95	
	25.32	21.70
	20.33	17.32
	17.95	15.24
	11.00	9.13
A"	22.25	19.00
	16.28	13.77
	11.39	9.48

(6)

	Calc.	Pred. Exp.
A_1	560.39	
	312.54	
	45.05	
	30.26	
	20.55	17.52
	19.47	16.57
	15.46	13.05
B_2	560.46	
	312.55	
	32.73	
	22.74	18.44
	13.95	11.73
B_1	22.08	18.86
	16.80	14.23
A_2	17.45	14.80
	11.14	9.26

(7)

	Calc.	Pred. Exp.
A_1	564.79	
	552.90	
	313.65	
	43.72	
	34.74	
	25.78	22.10
	19.34	16.46
	15.82	13.37
B_2	313.64	
	26.29	22.54
	19.31	16.43
	9.30	7.65
B_1	17.72	14.60
	8,83	7.24
A_2	17.34	14.70

(2c)

	Calc.	Pred. Exp.
A	561.48	
	559.75	
	313.79	
	43.22	
	38.18	
	25.08	21.49
	21.00	17.91
	19.46	16.56
	16.43	13.90
	15.16	12.79
	13.42	11.26
B	561.52	
	313.81	
	35.71	
	26.34	22.59
	21.71	18.53
	18.36	15.59
	17.32	14.68
	15.25	12.87
	13.00	10.90

of-plane atomic orbital in the molecular orbital of lowest IP for the molozonide structure is 0.891.

Since these orbitals are heavily localised they will not be greatly affected by replacement of hydrogen atoms by other substituents, provided that such substituents do not themselves have localised orbitals. Thus, monitoring of an ozonolysis reaction by photo-electron spectroscopy would give valuable insight into the species which were present if the spectrometer could scan fast enough. Similarly for the reactions of singlet oxygen with ethylene, detection of epoxide-O-oxide would be possible. (In this case the measurement of the dipole moment would serve as confirmation of what the end product was, since that of the epoxide-O-oxide is very large and almost double that of 1,2-dioxetane).

There is one major drawback to attempting to detect the presence of ozonolysis and related intermediates. Since ozonolysis is by necessity carried out at very low temperatures it may not be possible to obtain a high-enough concentration of intermediates in the gas phase. The technique of ESCA spectroscopy circumvents this problem. The orbital energies of approximately 560eV correspond to molecular orbitals which are largely localised on the oxygen 1s levels and may thus be assigned to a particular atom. The orbital energies can be found in Tables 7 and 8 and are assigned to the atoms (below), where the carbon 1s levels are also included.

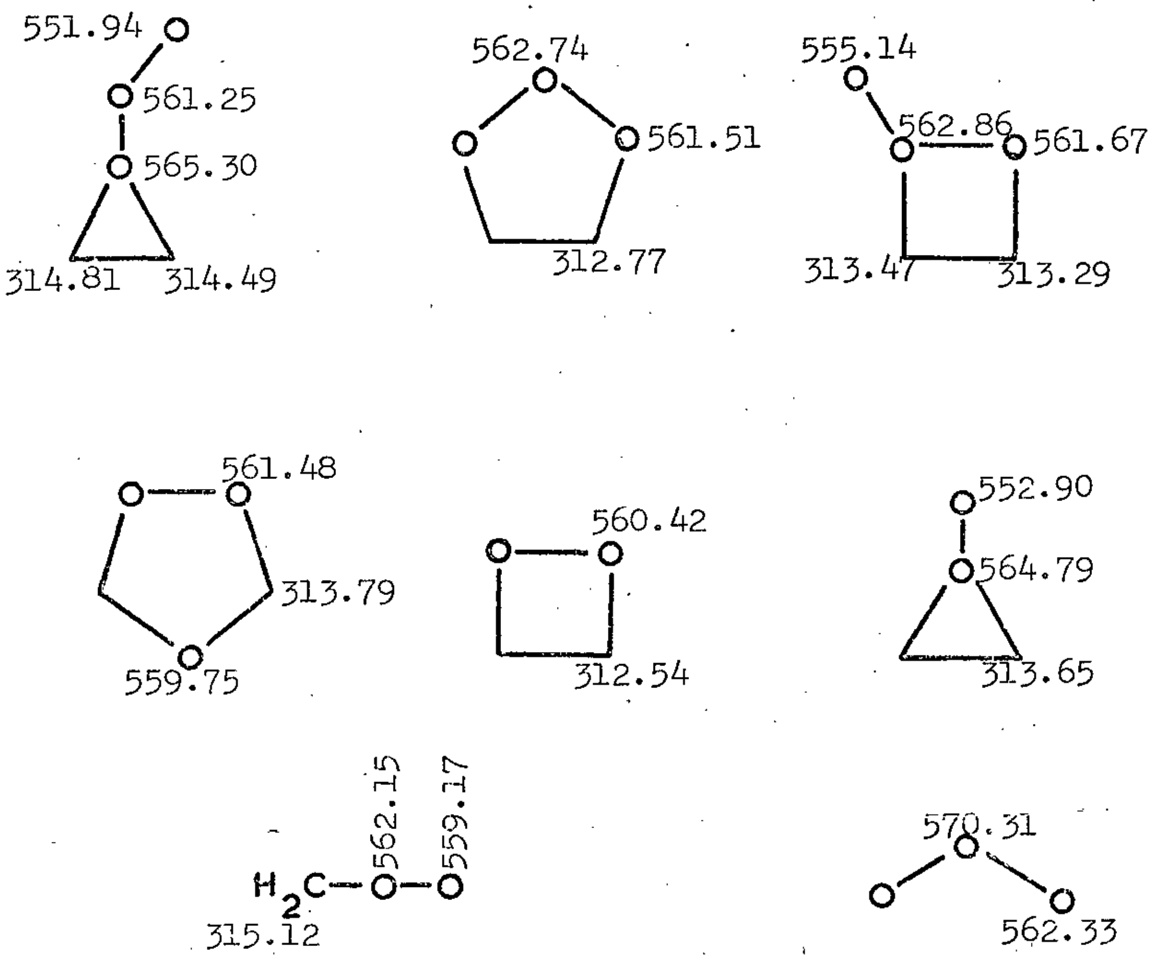

The molecules with oxygen atoms which are formally written with a negative charge have very low oxygen 1s ionisation potentials. Although the population analysis does not suggest a unit negative charge on these atoms they are always the most negative in the molecule. It would thus be expected that they would be the easiest atoms from which to remove an electron, i.e. they would have the lowest ionisation potential. The formally +1 atoms would be expected by the same argument to have high ionisation potentials, as indeed they do have. The carbon 1s levels are virtually unaffected with the sole exception of the Criegee zwitterion, where the ionisation potential is ~2eV

TABLE 9

One-Electron Properties of Ethylene Oxide and 1,2,4-Trioxolane

Property	Components	C_2H_4O Calc.	C_2H_4O Expt.	$C_2H_4O_3$ Calc.	Units.
Dipole Moment	μ	1.57	1.88	0.92	Debye
Quadrupole Moment	Q_{xx}	1.64	2.5 ± 0.4	7.97	10^{-26} esu.cm²
	Q_{yy}	-3.64	-4.3 ± 0.5	-8.01	
	Q_{zz}	2.00	1.8 ± 0.8	0.04	
2nd Moment (electronic)	g_{xx}	17.17	16.3 ± 0.4	39.31	10^{-16} cm²
	g_{yy}	14.02	13.3 ± 0.4	35.64	
	g_{zz}	7.58	6.8 ± 0.4	11.63	
	g_{xz}	-	-	0.67	
Diamagnetic Susceptibility (electronic)	X_{xx}	-91.64	-85.4 ± 0.9	-200.52	10^{-6} erg/(G².mole)
	X_{yy}	-105.01	-97.7 ± 1.1	-216.11	
	X_{zz}	-132.30	-125.4 ± 2.0	-317.97	
	X_{xz}	-	-	2.85	
	$zz-\frac{1}{2}(xx + yy)$	-33.98	-33.85	-109.66	

higher than the rest of the carbon atoms. It would appear from this that, of the two possible structures for the zwitterion, resonance form (a) would appear to predominate.

$$H_2C^+ - O - O^- \longleftrightarrow H_2C = O^+ - O^-$$
$$\text{(a)} \qquad\qquad\qquad \text{(b)}$$

While calculations using minimal basis sets tend to overestimate core ionisation potentials, and differences between core levels, the differences in these molecules are sufficiently large to enable one to detect the presence of molecules with formal O^+–O^- charges.

<u>One-electron Properties of Ethylene Oxide and 1,2,4-Trioxolane</u>

Using the SCF eigenvectors, together with information regarding the co-ordinates, Gaussian exponents and contraction coefficients it is possible to calculate many one-electron properties of molecules. Several of these have been experimentally obtained for ethylene oxide,[21] and are presented in Table 9, together with the corresponding properties for 1,2,4-trioxolane. All the properties have been evaluated at the centre of mass, using the carbon-12 scale ($^{12}C = 12.00000$). The orientation of the molecules is such that the C_2 axis is the y-axis, the z-axis is perpendicular to the mean ring plane, with the x-axis perpendicular to these two.

Overall there is reasonably good agreement with experiment. Where the experimental data refers to electronic properties only, the calculated values are greater than experimental. The situation is reversed when the experimental quantity consists of both nuclear and electronic terms i.e. in this case the calculated value is less than the experimental. With the exception of quadrupole moment the calculated values have the correct relative component magnitudes. In the case of quadrupole moment the experimental error is sufficiently large to allow the reversing of the Q_{xx} and Q_{yy} terms, thus bringing them into agreement with the calculated values.

The experimental method used for determining the properties (except dipole moment) allows the possibility of two sets of values.[21] For example the quadrupole moment alternatives for the xx, yy and zz components are -22.9, 3.4 and 19.5 x 10^{-26}esu.cm^2 respectively. The figures in Table 9 represent those that Flyare and his co-workers thought most likely; the calculated values endorse his choice.

Since the agreement for the properties is good for ethylene oxide, the predicted values for 1,2,4-trioxolane should be in reasonable agreement with experimental data.

Summary

Using ethylene as a model the ozonolysis of olefins has been investigated. Of the three proposed reaction intermediates 1,2,3-trioxolane is the preferred initial product, with the Staudinger molozonide slightly inferior in energy. The rearrangement of these via the Criegee zwitterion to 1,2,4-trioxolane has been investigated as has the geometry of this last compound. Simultaneous calculations on the ethylene-singlet oxygen yields a reaction scheme consistent with experimental observations. The

ionisation potentials and one-electron properties have been favourably compared with experimental data. Such comparisons have been used to predict further experimental information.

References

1. R. Criegee, Rec. Chem. Progr., 1957, 18, 111.

2. P.R. Story, J.A. Alford, J.R. Burgess, W.C. Ray, J.A.C.S., 1971, 93, 3042.

3. P.R. Story, J.A. Alford, J.R. Burgess, W.C. Ray, J.A.C.S., 1971, 93, 3044.

4. T.E. Turner, J.A. Howe, J. Chem. Phys., 1956, 24, 924.

5. R.H. Hughes, J. Chem. Phys., 1956, 24, 131.

6. R.S. Mulliken, J. Chem. Phys., 1955, 23 (a) 1833, "overlap populations give quantitative figures which may be taken as a measure of bonding and anti-bonding strengths", (b) 1841, (c) 2338.

7. M.H. Palmer, "Structure and Reactions of Heterocyclic Compounds" Edward Arnold Ltd., London, 1967.

8. A. Almenning, P. Kolsaker, H.M. Seip, T. Willadson. Acta Chem. Scand., 1969, 23, 3398.

9. P. Groth, Acta Chem. Scand., 1970, 24, 2137.

10. C.W. Gillies, R.L. Kuczkowski, J.A.C.S., 1972, 94, 6337.

11. G. Herzberg, "Electronic Spectra of Polyatomic Molecules", Vol. III, p.612 (Publ., Van Nostrand Reinhold, 1966).

12. A.G. Schultz, R.H. Schlessinger, Tet. Lett., 1970, 2731.

13. S. Mazur, C.S. Foote, J.A.C.S., 1970, 92, 3225.

14. W.H. Richardson, J.W. Peters, W.P. Konika. Tet. Lett., 1966, 45, 5531.

15. W.H. Richardson, M.B. Yelvington, H. Edward O'Neal, J.A.C.S., 1972, 94, 1619.

16. C.R. Brundle, D.W. Turner. Chem. Comm., 1967, 314.

17. D.W. Turner, C. Baker, A.D. Baker, C.R. Brundle, "Molecular Photoelectron Spectroscopy", Wiley-interscience, London, 1970.

18. H. Basch, M.B. Robin, N.A. Keubler, C. Baker, D.W. Turner. J. Chem. Phys., 1969, 51, 52.

19. T.N. Radwan, D.W. Turner. J.C.S.(A), 1966, 85.

20. S.M.F. Kennedy, M.H. Palmer, private communication.

21. D.H. Sutter, W. Huttner, W.H. Flygare. J. Chem. Phys., 1969, 50, 2869.

II. AZOLES

Introduction

There has been much work done on the electronic structure of the five-membered nitrogen heterocycles, the azoles (below)

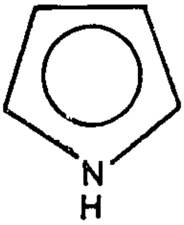

Pyrrole

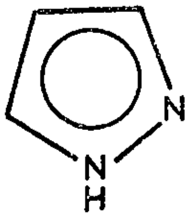

Pyrazole

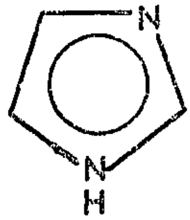

Imidazole

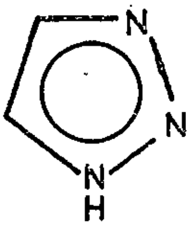

1,2,3-Triazole

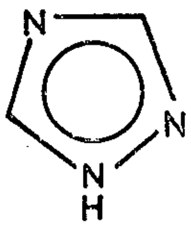

1,2,4-Triazole

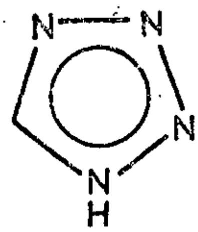

Tetrazole

The electronic structure calculations have ranged from empirical[1] through semi-empirical[2-6] to non-empirical[7,8] calculations. Various ground state properties such as dipoles moments[1,3,5-8] ionisation potentials[2,3,5,7,8] charge distributions[1-8] and tautomerism[4-6] have been investigated; ultra-violet transitions have also been studied.[2,6] In general the agreement between experimental and calculated values is reasonable for all methods, but of course in many of the empirical and semi-empirical methods such experimental data is used for calibration. Of the non-empirical calculations, that of Clementi on pyrrole[7] was based on a geometry[9] which has since been superseded by a microwave determination.[10] Berthier's calculations on pyrazole[8] and imidazole[8] used geometries based upon averages from data on other molecules, and hence enforced a standardised situation which allowed no special exceptions for these molecules; he also used a different basis set from reference 7. There is thus no consistent set of non-empirical calculations on the azoles. Calculations have therefore been carried out on all of the azoles with the same basis set, using experimental geometries where possible.

Minimal basis sets were used with the carbon and nitrogen being represented by seven s-type and 3 x three p-type functions. Hydrogen was represented by three s-type functions. Full data of Gaussian exponents and contraction coefficients are to be found in Appendix 2, Tables 1, 2 and 3 for hydrogen, carbon and nitrogen respectively.

The recent microwave structure for pyrrole[10] was used, while imidazole,[11] pyrazole,[12] 1,2,4-triazole[13] and tetrazole[14] were taken from crystal structures (in the case of tetrazole the 5-amino derivative was used). The geometry of 1,2,3-triazole was based on the remaining azoles. For calculations on isolated molecules the ideal structure is one determined by gas phase methods, i.e., microwave or electron-diffraction spectroscopy. While the rotational constants of pyrazole,[15] imidazole[16] and 1,2,4-triazole[17] have been reported some years ago, the full details of geometries have never appeared.

Full details of the geometries used are given in Appendix 2 along with the symmetry orbitals. For all molecules the out of plane axis is the z-axis so that $p_z \equiv p_\pi$.

TABLE 1

Total Energies for the Azoles

	Pyrrole	Pyrrole[7]	Pyrazole
T.E. (eu)	-208.04264	-207.93135	-223.73266
1 El. (eu)	-595.83665	-	-628.84177
2 El. (eu)	266.69231	-	238.04159
N.R. (eu)	161.10170	160.78558	167.06752
B.E. (eu)	-0.84039	-0.83779	-0.36163
B.E. (kcal/mole)	-526.6	-525.7	-226.9

	Pyrazole[8]	Imidazole	Imidazole[8]
T.E. (eu)	-223.823	-223.93474	-223.849
1 El. (eu)	-	-624.87695	-
2 El. (eu)	-	236.44661	-
N.R. (eu)	-	164.49560	-
B.E. (eu)	-0.568	-0.56367	-0.594
B.E. (kcal/mole)	-356.4	-353.7	-372.7

	1,2,3-Triazole	1,2,4-Triazole	Tetrazole
T.E. (eu)	-239.84985	-239.80328	-255.80079
1 El. (eu)	-655.29297	-653.40207	-675.71377
2 El. (eu)	246.76871	245.81027	252.31150
N.R. (eu)	168.67440	167.78851	167.60148
B.E. (eu)	-0.31110	-0.26453	-0.09435
B.E. (kcal/mole)	-195.2	-166.0	-59.22

Total Energies

The total energies of molecules (1)-(6) are recorded in Table 1, together with Clementi's results for pyrrole and Berthier's for pyrazole and imidazole. In the case of pyrrole the present total energy is better than that of Clementi by 0.11 au. This can largely be explained by the difference in the basis sets used, since the improvement in binding energy is very much smaller (0.003 au.). Berthier's calculation on pyrazole is better than that reported here, both in terms of total energy and of binding energy. By comparing the binding energies of the two calculations the effects of differing basis sets are minimised, leaving only geometry as the difference between the calculations. It would thus appear that Berthier's standard geometry is a better approximation to a gas-phase structure than the crystal structure of reference 12; such a result is not too unexpected since pyrazole exists as a hydrogen bonded polymer[12] and the geometry used was one unit of this polymer.

The situation is different in imidazole in that the total energy from Berthier's calculation is considerably worse than the present one while his binding energy is marginally better. It would thus appear that his geometry is slightly nearer that which will be found from a gas-phase determination. Thus neither of these molecules have strongly unique geometric factors.

As the number of nitrogen atoms in the ring increases the binding energy decreases. There are two factors contributing to this:- 1) a C-H bond which contributes considerably to the bonding in the molecule is replaced by an almost non-bonding nitrogen lone pair orbital; 2) the π-system becomes increasingly more localised on the nitrogen atoms because of their considerably greater electronegativity. The decrease in magnitude of the binding energy from pyrrole to the average of the diazoles (Berthier's calculations) is 162.6 kcal/mole; from there to the average triazole figure and thence to tetrazole the values are 153.4 and 94.2 kcal/mole respectively. On this basis it is likely that N_5H should exist as atoms rather than as the molecule pentazole. Using thermochemical data from the "JANAF Thermochemical Tables" for atoms and "Thermochemistry of Organic and Organometallic Compounds" (by J.D. Cox and G. Pilcher, Academic Press, 1970) for pyrrole, imidazole and pyrazole the experimental binding energies are -1.640, -1.465 and -1.445 au. respectively. The relationship between experimental and calculated binding energies is then given by B.E.(exp) = 0.733 B.E.(calc) -641 kcal/mole. It is then possible that the intercept would be sufficiently large for pentazole to exist (see pentazine and hexazine in Section III). Decomposition to HN_3 and N_2 is another possibility, the likelihood of which cannot be estimated without calculations on these molecules.

Orbital Energies and Ionisation Potentials

The photo-electron spectrum of pyrrole has been reported by several authors;[19,20,21] while there is general agreement that the two lowest ionisation potentials should

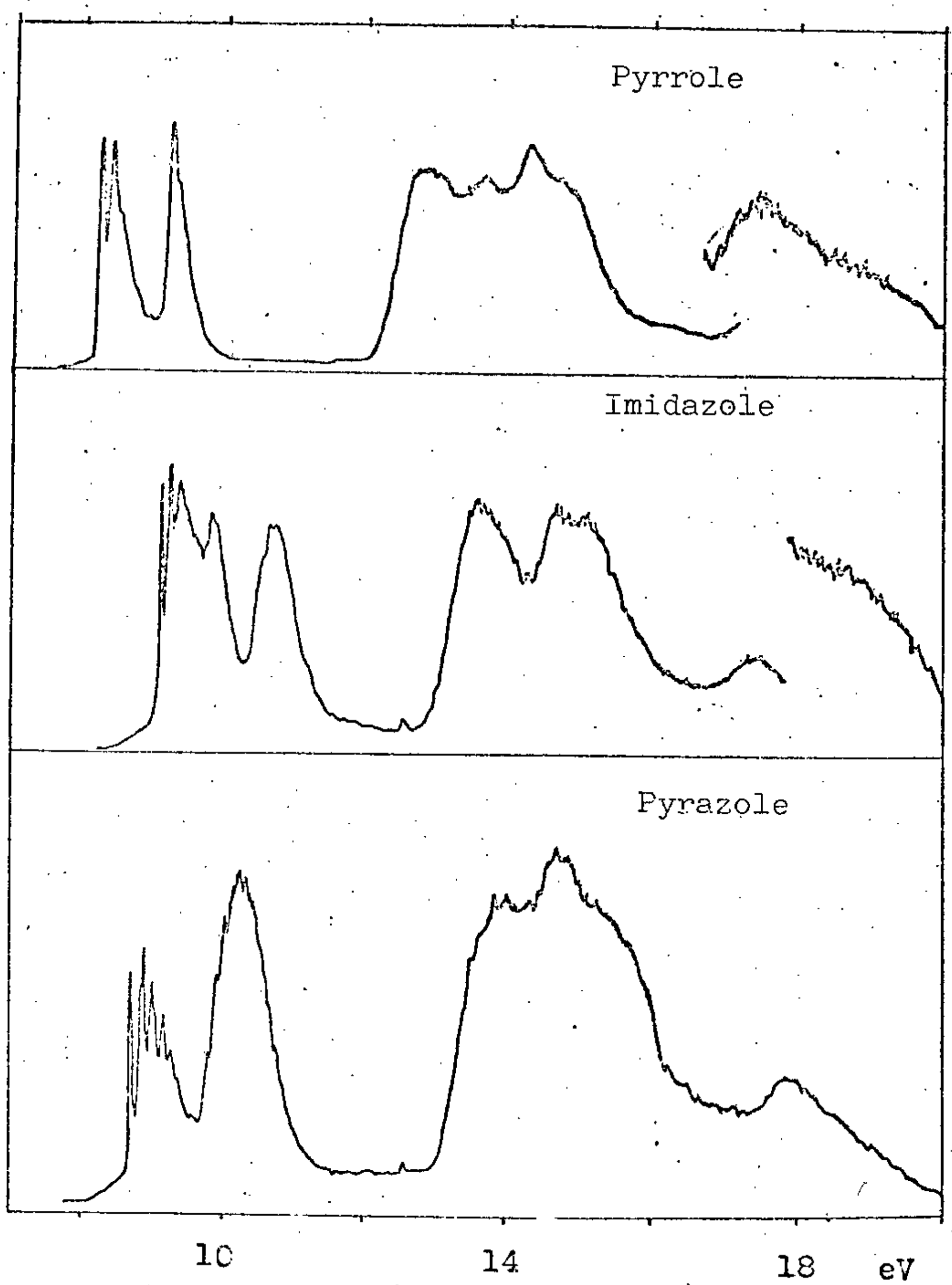

Figure 1. Photo-electron Spectrum of Pyrrole, Imidazole and Pyrazole

be assigned to the two top π-levels, there has been no completely convincing assignment of either the third π-level or the σ-levels. Lindholm, using his spectroscopically parameterised version of the INDO program[21] (SPINDO), predicts a set of energy levels for pyrrole which fits the observed spectrum very well. However such success depends on the accuracy with which the parameters were obtained, and if based on wrong assumptions (say regarding the ordering of the molecular orbitals) may be entirely fortuitous. The spectra for all the azoles have been recorded; those for pyrrole and pyrazole agree with those previously published, while there is no data on the remaining azoles to date.

The spectra of the azoles appear in Figures 1 and 2. They were recorded on a Perkin Elmer PS16 spectrometer which had a resolution of 30m eV for bands in the region of 10 eV. Commercial samples of pyrrole, pyrazole, imidazole and 1,2,4-triazole were used, while standard synthetic methods were used to prepare 1,2,3-triazole[22] and tetrazole.[23] Pyrrole, purified by distillation and low temperature crystallisation, was admitted to the spectrometer via a volatile sample manifold inlet. The remaining azoles were introduced via a direct insertion probe in the temperature range 25-75°C, the lowest temperature giving a satisfactory spectrum being used.

To facilitate the correlation of orbital energies with experimental ionisation potentials the original (delocalised) molecular orbitals were transformed into hybrid orbitals using Coulson's method.[24] This allows one to take linear

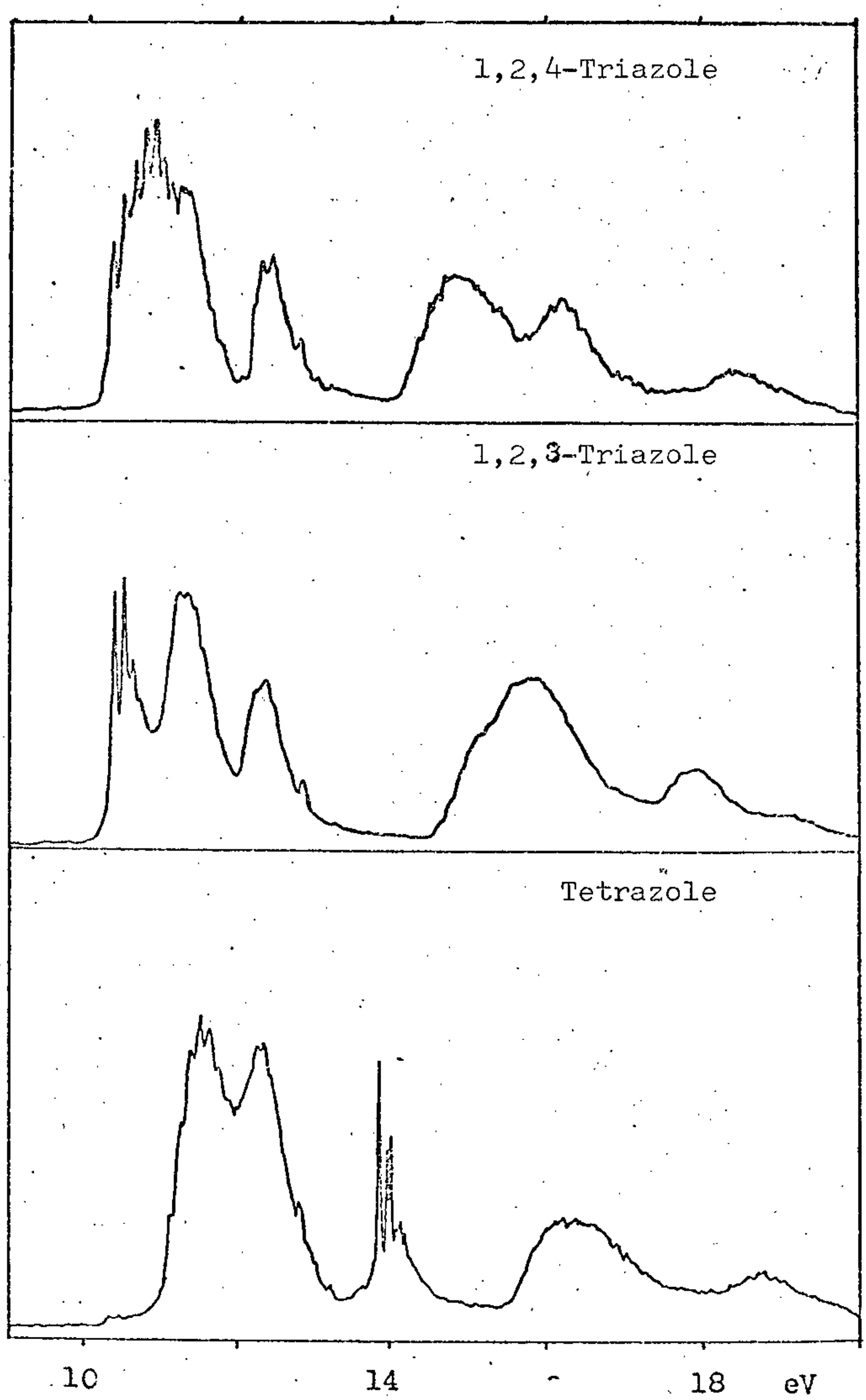

Figure 2. Photo-electron Spectrum of 1,2,4-Triazole, 1,2,3-Triazole and Tetrazole

combinations of s and p orbitals on the same centre and to generate hybrid orbitals pointing in any direction provided that the angle between any pair of hybrid orbitals is greater than 90°. For the azoles the 2s, $2p_x$ and $2p_y$ were formed into hybrids of pseudo-sp^2 type, the directions being chosen such that they pointed directly to neighbouring atoms (in the case of >C-H and >N-H); for lone-pair type nitrogens (>N:) the lone pair was assumed to be along the bisector of the external angle. Figure 3 shows the direction of some of the hybrid orbitals of 1,2,3-triazole; the relative amounts of 2s, $2p_x$, $2p_y$ for these hybrids are shown in Table 2. This Table also shows the overlap integral between hybrid orbitals on the same centre; Coulson's method depends on these overlaps being zero - as can be seen they are sufficiently small to be considered zero.

TABLE 2

Analytical Form of the Hybrid Orbitals of Figure 3, with Overlap Integrals between Hybrids on the Same Centre

Orbital	s	x	y		Overlap
Ψ_1	1.0	-0.00280	1.06815	$\Psi_1\Psi_2$	-0.10×10^{-11}
Ψ_2	1.0	-1.36738	-0.93978	$\Psi_1\Psi_3$	-0.15×10^{-13}
Ψ_3	1.0	1.37228	-0.93260	$\Psi_2\Psi_3$	0.34×10^{-10}
Ψ_4	1.0	1.46304	1.00552	$\Psi_4\Psi_5$	-0.15×10^{-11}
Ψ_5	1.0	-0.90742	0.32580	$\Psi_4\Psi_6$	-0.80×10^{-11}
Ψ_6	1.0	0.48933	-1.70649	$\Psi_5\Psi_6$	-0.64×10^{-11}

As a second stage the hybrid orbitals were combined into bond orbitals. For example, from Figure 3, two bond

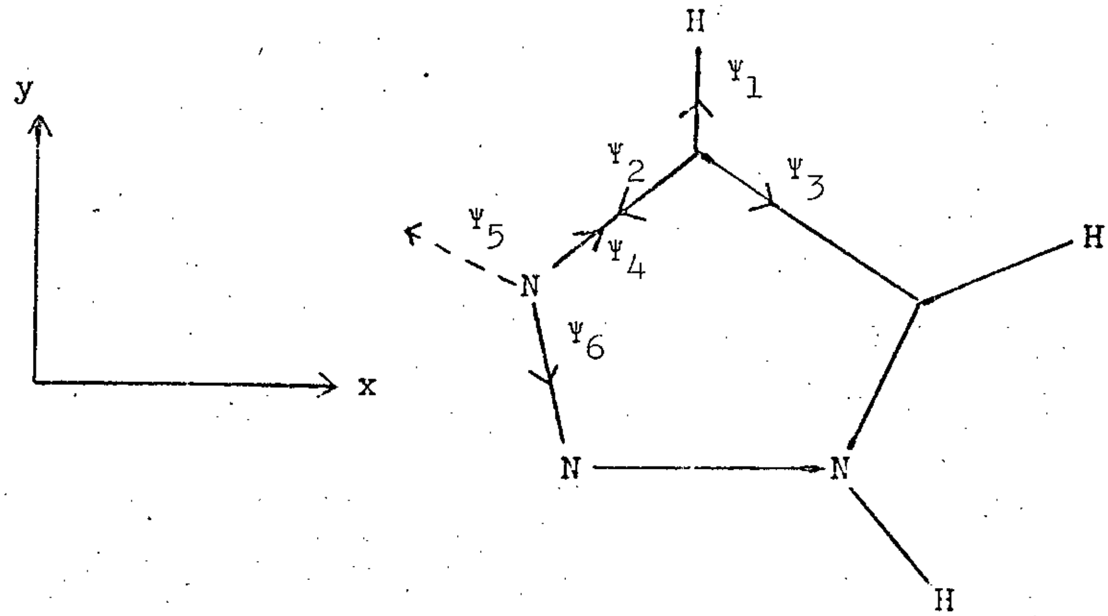

Figure 3 Some Hybrid Orbitals of 1,2,3-Triazole

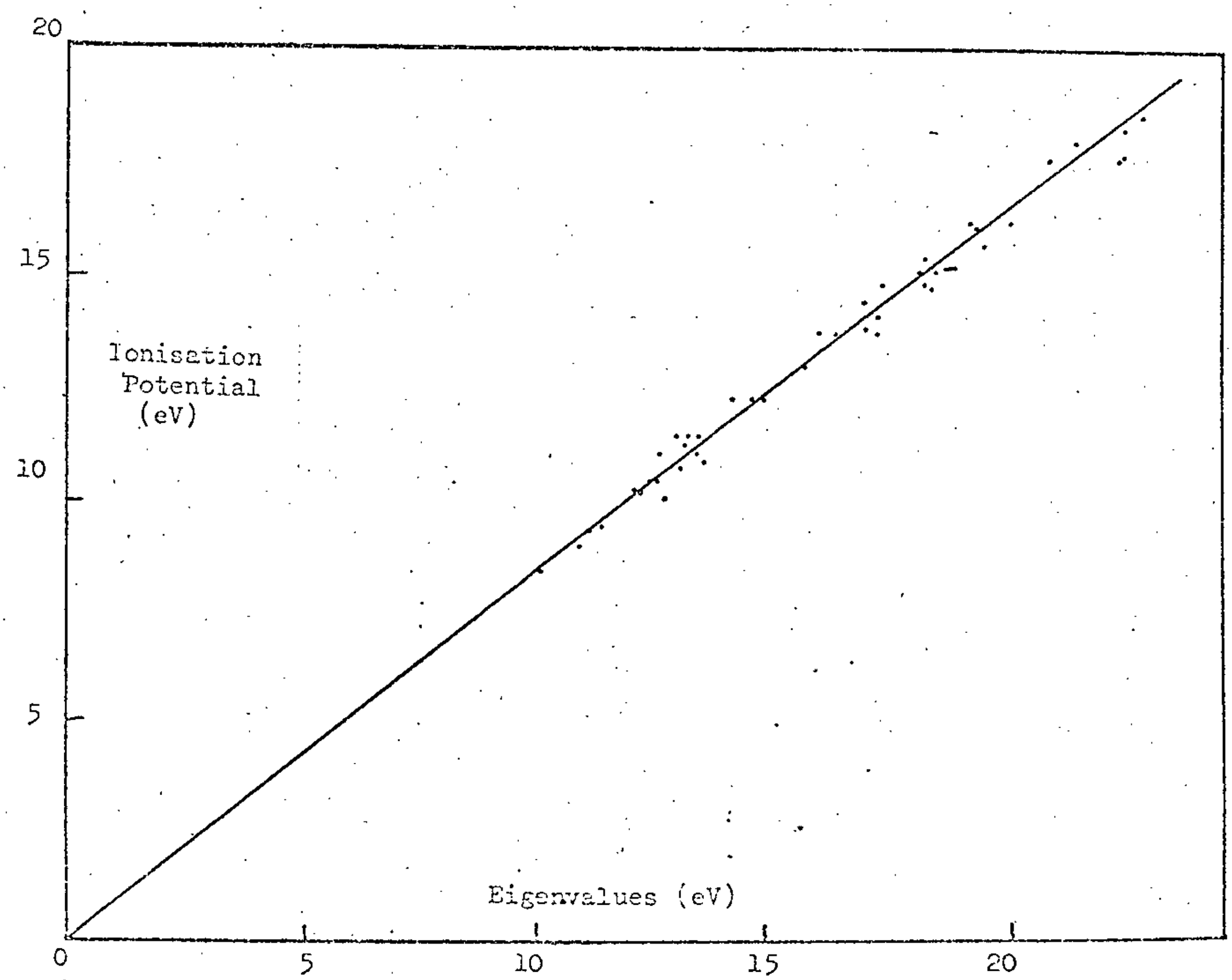

Figure 4 Correlation of Observed Ionisation Potentials and Calculated Eigenvalues

orbitals are $\Psi_2 + \Psi_4$ and Ψ_1 + H; there were of course the corresponding antibonding pairs. As is to be expected these transformations had no effect on the total energies nor on orbital energies. Using all 3 sets of SCF solutions (delocalised, hybrid and bond orbital) it is possible to obtain the principal character of each orbital. These characters have been listed, together with orbital energies in Tables 3.1-3.6 inclusive. The results are presented by irreducible representation; except in the case of pyrrole, the azoles are of C_s symmetry giving A' and A" representations, with A' being sigma- and A" being pi-type. The sigma representations in pyrrole are A_1 and B_2 and pi are B_1 and A_2; for simplicity the orbitals have been assigned to σ and π types with A', A_1 and B_2 being σ and A", B_1 and A_2 being π. Only in the case of pyrrole is there likely to be confusion, so the orbital energies have been labelled 1σ - 15σ and 1π - 3π in Table 3.1.

The orbital energies fall into several regions, the first of which is the core-level region. This comprises the orbitals 1σ - 5σ which are highly localised 1s levels, having eigenvectors of approximately 0.98-0.99. The nitrogen atom to which a hydrogen atom is attached (N_1 in all cases) has the highest binding energy (most negative orbital energy) while a nitrogen atom in the α-(2,5)-position is more strongly bound than one in the β-(3,4)-positions. The carbon 1s levels move smoothly to higher binding energy as more nitrogen atoms are incorporated into the rings. On electronegativity grounds the nitrogen will

TABLE 3.1

Orbital Energies and Principal Character of Pyrrole

Eigenvalue (eV)	Principal Character	Centres/Bond Orbitals
A_1		
-427.9 (1σ)	1s	N
-311.0 (2σ)	1s	C_{α}^{+}
-309.8 (4σ)	1s	C_{β}^{+}
-36.95 (6σ)	2s	$N^{+}, (C_{\alpha} + C_{\beta})^{+}$
-30.01 (7σ)	2s	$C_{\beta}^{+}, -N$
-22.93 (9σ)	2s	$C_{\alpha}N^{+}$
-21.29 (11σ)	$2p_{C\alpha\beta}$, $1s_H$	$C_{\alpha}H^{+}$, $C_{\beta}C_{\beta}$
-17.68 (12σ)	$2p_{C\alpha\beta}$, $2p_N$, $1s_H$	NH, $C_{\alpha}C_{\beta}{}^{+}$
-16.02 (15σ)	$2p_{C\beta}$, $1s_H$	$C_{\beta}H^{+}$, $C_{\beta}C_{\beta}$
B_2		
-311.0 (3σ)	1s	C_{α}^{+}
-309.8 (5σ)	1s	C_{β}^{-}
-28.27 (8σ)	$2s_{C\alpha\beta}$, $2p_N$	$C_{\alpha}C_{\beta}^{-} + C_{\alpha}N^{-}$
-22.23 (10σ)	$2s_{C\beta}$, $2p_{yC\alpha}$, $2p_{xN}$	$C_{\alpha}C_{\beta}^{-} - C_{\alpha}N^{-}$
-17.31 (13σ)	$2p_{xC}$, $1s_H$	$C_{\alpha}H^{-}$
-16.37 (14σ)	$2p_{xC}$, $2p_{yC\beta}$, $1s_H$	$C_{\beta}H^{-}$, $C_{\alpha}C_{\beta}^{-}$
B_1		
-17.69 (1π)	$2p_{zCN}$ ("A")	$N{+}C_{\alpha}C_{\beta}^{+}$
-11.65 (2π)	$2p_{zCN}$ ("E")	$-N$, $C_{\beta}C_{\beta}$
A_2		
-10.34 (3π)	$2p_{zC}$ ("E")	$C_{\alpha}C_{\beta}^{-}$

TABLE 3.2

Orbital Energies and Principal Character of Pyrazole

Eigenvalue (eV)	Principal Character	Centres/Bond Orbitals
A'		
-429.7	1s	N_1
-426.9	1s	N_2
-312.2	1s	C_5
-311.5	1s	C_3
-310.6	1s	C_4
-39.95	2s ("A")	N, C
-32.32	2s ("E")	$N_1C_5 - N_2C_3$
-30.81	2s ("E")	$C_3C_4C_5 - N_1N_2$
-24.77	2p, $1s_H$	$NH + C_3H$
-24.07	2p, $1s_H$	$C_3H + C_5H - C_4H$
-22.79	2p, $1s_H$	C_5N_1, $C_4H + C_5H$
-19.24	2p, $1s_H$	$NH - C_3H$
-18.59	2p, $1s_H$	$C_4H - C_5H$
-17.58	2p, $1s_H$	$C_4C_5 - C_3C_4$
-13.84	sp^2	N_2
A"		
-19.15	$2p_z$ ("A")	N_1, C
-13.01	$2p_z$ ("E")	$N_2C_3C_4 - N_1C_5$
-11.32	$2p_z$ ("E")	$N_1N_2 - C_2C_3$

TABLE 3.3

Orbital Energies and Principal Character of Imidazole

Eigenvalue (eV)	Principal Character	Centres/Bond Orbitals
A'		
-428.3	1s	N_1
-425.5	1s	N_3
-312.1	1s	C_2
-311.5	1s	C_5
-310.9	1s	C_4
-38.69	$2s_{N,C}$ ("A")	N, C
-33.31	$2s_{N,C}$ ("E")	$C_5N_1 - C_4N_3$
-29.39	$2s_{N,C}$ ("E")	C_4C_5, $N_3C_2N_1H$
-23.79	$2s_{N,C}$, $2p_{N,C}$, $1s_H$	NH, CN
-23.71	" " "	$C_4H - C_5H$
-21.84	" " "	$C_2H + C_5H$
-18.59	$2p_{N,C}$, $1s_H$	C_4C_5, NH
-17.60	$2p_{N,C}$, $1s_H$	$C_2N_1C_5$, C_2H-C_5H
-17.33	sp^2, $1s_H$	C_2H-C_4H, $C_2N_3C_4$
-12.83	sp^2	N_3
A"		
-18.57	$2p_z$ ("A")	N,C
-12.71	$2p_z$ ("E")	CN^-
-11.17	$2p_z$ ("E")	CC, NCN

TABLE 3.4

Orbital Energies and Principal Character of 1,2,3-Triazole

Eigenvalue (eV)	Principal Character	Centres/Bond Orbitals
A'		
-429.4	1s	N_1
-428.2	1s	N_2
-427.0	1s	N_3
-312.5	1s	C_5
-311.5	1s	C_4
-42.03	2s ("A")	$N_1 + N_2 + N_3$
-34.69	2s	$N_1 - N_3$
-31.98	2s	$N_2 - (C_4 + C_5)$
-25.18	2s 2p $1s_H$	NH, N_3C_4, C_4C_5
-24.09	2s 2p $1s_H$	NN + CN, $C_4H - C_5H$
-22.85	2p $1s_H$	CN, $C_4H + C_5H$
-18.85	2p $1s_H$	C_4C_5, NH - C_5H
-18.47	2p $1s_H$	C_4H, CN
-15.16	sp^2	$N_3 + N_2$
-12.81	sp^2	$N_3 - N_2$
A"		
-19.90	$2p_z$	$N_1 + N_2 + N_3 + C_4 + C_5$
-13.71	$2p_z$	$N_3C_4 - N_1C_5$
-12.35	$2p_z$	$(N_1+N_2+N_3)-(C_4+C_5)$

TABLE 3.5

Orbital Energies and Principal Character of 1,2,4-Triazole

Eigenvalue (eV)	Principal Character	Centres/Bond Orbitals
A'		
-429.5	1s	N_1
-427.5	1s	N_2
-426.2	1s	N_4
-313.1	1s	C_5
-312.1	1s	C_3
-41.13	2s ("A")	$N_1+N_2+N_3$, C_3+C_5
-34.40	2s ("E")	N_1N_2 - $C_5N_4C_3$
-32.73	2s ("E")	C_5N_1 - C_3N_2
-25.07	2s 2p $1s_H$	$C_5H + N_1N_2 + C_3N_4$
-24.68	2s 2p $1s_H$	C_3H + NH
-22.90	2s 2p $1s_H$	C_5H + $N_1C_5N_4$
-19.02	2p	$N_2C_3N_4$
-18.76	2p	C_3H + CN
-14.92	sp^2	N_2 + N_4
-13.34	sp^2	N_2 - N_4
A"		
-19.72	$2p_z$ ("A")	$N_1+N_2+N_4+C_3+C_5$
-13.42	$2p_z$ ("E")	N_1 - C_3N_4
-12.50	$2p_z$ ("E")	C_3N_2 - N_4C_5

TABLE 3.6

Orbital Energies and Principal Character of Tetrazole

Eigenvalue (eV)	Principal Character	Centres/Bond Orbitals
A'		
-429.7	1s	N_1
-429.0	1s	N_2
-428.0	1s	N_3
-427.0	1s	N_4
-313.8	1s	C_5
-43.09	2s ("A")	$N_1+N_2+N_3+N_4$, C_5
-35.80	2s ("E")	$N_2+N_3 -2N_4$
-34.55	2s ("E")	$N_1+N_2 - (N_3+C_5)$
-26.08	2s 2p $1s_H$	NH
-25.35	2s 2p $1s_H$	$N_1N_2 + C_5H$
-23.26	2s 2p $1s_H$	C_5H + CN
-19.56	2p	$N_1N_2N_3N_4$
-16.70	sp^2 ("A")	$N_2+N_3+N_4$
-13.73	sp^2 ("E")	$N_2 - N_4$
-13.50	sp^2 ("E")	$2N_3 - N_2 - N_4$
A"		
-20.46	$2p_z$ ("A")	$N_1+N_2+N_3+N_4+C_5$
-14.47	$2p_z$ ("E")	$N_1C_5 - N_2N_3N_4$
-13.24	$2p_z$ ("E")	$N_1N_2 - C_5N_4$

require more of the electrons than did the carbon it replaced; consequently the remaining carbons will have a smaller share of the electrons, thus becoming more positive, resulting in a higher binding energy. The separation of the energy levels for each element is quite large (1-2 eV) but is likely to be larger than that found experimentally. In any case gas phase measurements would be necessary for comparison purposes as the molecules form hydrogen bonded polymers in the solid state.

The next region consists largely of 2s orbitals of nitrogen and carbon. These correspond to the A_1 + E orbitals of the cyclopentadienyl anion. The orbital lowest in energy (6σ) is a positive combination of all the 2s levels with nitrogen predominating. It is therefore to be expected that 6σ will become more and more binding as the number of nitrogen atoms in the ring increases. The E representations have one nodal plane in the cyclopentadienyl anion; the site of this nodal plane in the azoles' pseudo-E orbitals (7σ, 8σ) is controlled in most cases by the nitrogen atoms.

TABLE 4

2s Levels in Pyrazole

$6\sigma(A_1)$	$0.500N_1 + 0.358N_2 + 0.132C_3 + 0.096C_4 + 0.168C_5$
7σ("E")	$0.424N_1 - 0.369N_2 - 0.353C_3 + 0.245C_5$
8σ ("E")	$0.213N_1 + 0.331N_2 - 0.165C_3 - 0.398C_4 - 0.305C_5$

Thus for pyrazole (Table 4) the nodal plane is either parallel (8σ) or perpendicular (7σ) to the N-N bond. A similar situation exists for 1,2,4-triazole. The only example where the nodal position is not determined purely by symmetry with respect to the siting of the nitrogen atoms is in 1,2,3-triazole, where the division is into bonding regions with CC + NN (8σ) and CN + CNN (7σ) character rather than 2CN (8σ) and CC + NNN (7σ). The two separately strongly bonding NN regions obtained are evidently more favourable than the NNN system. The split in the pseudo degenerate energy levels is much larger for 1,2,3-triazole (2.71 eV) and imidazole (3.92 eV) than for the other compounds (1.6 eV).

For molecules with one or two nitrogen atoms the comparatively small amount of delocalisation of nitrogen 2s with carbon 2s, 2p and nitrogen 2p can be understood in terms of the free atom orbital energies which are,[18] in the Hartree-Fock limit:- N, 2s, 25.72eV; N, 2p, 15.44 eV; C, 2s, 19.20 eV; C, 2p, 11.79 eV. For molecules containing three nitrogen atoms, the splitting of the atomic 2s nitrogen levels on molecular formation leads to the overlap of nitrogen and carbon 2s levels, in turn giving rise to very delocalised orbitals. This is evidently what occurs in the 6σ-8σ orbitals in 1,2,3-triazole.

The He II photo electron spectrum of pyrrole[25] covers this region of orbital energies. Some of these are also accessible to He I and it is found that the He I is less intense than the corresponding He II spectrum. Since, for He I excitation the cross-section of an s-orbital is less than that for a p-orbital (the reverse holds for He II excitation) it is plausible on this basis to assign the five σ orbitals (6σ-10σ) to the 2s orbitals in this region. This is consistent with the principal character of the

TABLE 5

Vertical Ionisation Potentials (eV) and Assigned Energy Levels

Pyrrole	Imidazole	Pyrazole	1,2,4-Triazole	1,2,3-Triazole	Tetrazole	Regions
8.23 $1A_2$ 9.22 $2B_1$	8.78 3A" 10.3 (2A", 15A')	9.15 3A" 9.88 2A" 10.7 15A'	10.0 3A" 10.56 15A' 11.1 2A" 12.15 14A'	10.06 3A" 10.9 (15A', 2A") 12.1 14A'	11.3 (3A", 15A', 14A') 12.1 2A" 13.63 13A'	A
12.85 $9A_1$ 13.65 $6B_2$ 14.3 $5B_2$ 14.7 ($8A_1$, $1B_1$)	13.7 14A' 14.0 13A' 14.7 1A" 15.3 12A'	13.6 (14A', 13A') 14.7 1A" 15.1 12A'	14.6 13A' 15.1 12A' 16.0 1A"	15.0 (13A', 12A') 15.6 1A'	16.1 (12A', 1A")	B
17.5 $7A_1$	17.9 11A'	17.5 11A'	18.2 11A'	17.6 11A'	18.5 11A'	C

orbitals 6σ-10σ for pyrrole.

Of the eighteen molecular orbitals, ten have so far been accounted for; there are thus eight (five σ and three π) still to be assigned, all of which are accessible to He I excitation. The observed spectra up to 20 eV may be separated into three distinct regions (Table 5). Region A, which extends from 8-10 eV in pyrrole, moves to higher binding energy as nitrogen atoms are substituted for C-H groups, and is at 10-14 eV in tetrazole. It contains two or three more or less separated bands, some or all of which show resolved fine structure. Region B begins some 2 eV to higher binding energy than region A for each molecule and contains a set of strong overlapping bands with no resolvable vibrational structure. It extends over about 3 eV for pyrrole reducing gradually to about 1.5 eV for tetrazole. Region C consists of a single band of moderate intensity and no vibrational structure with vertical IP 17.5-18 eV and with a downward trend from pyrrole to tetrazole.

Substitution of CH by N in the ring will transform one σ- level from largely $>$C-H to $\geq$N: lone pair. The binding energy of the orbital in this substitution will thus be markedly decreased, while the reverse tendency should occur with the other orbitals owing to the general effect that an increase in nuclear attraction leads to a lowering of the eigenvalues. These effects are found to occur; while pyrrole has two clearly separated bands in Region A, pyrazole has three and 1,2,4-triazole has four (two of which are considerably overlapping). For imidazole, 1,2,3-triazole and tetrazole there are two, three and three observed bands respectively, where the calculations predict three, four and five; there must again be considerable overlapping.

The "promotion" of bands of Region B to Region A results in Region B shrinking in width and overall intensity. Region C is unaffected except for the expected shift to higher binding energy. This single level in Region C is well separated from the other bands, has moderately high intensity resulting from largely p-orbital character. The calculations show that the 11σ level is well separated from those of lower binding energy and derives largely from p-orbital components from the ring atoms towards hydrogen atom(s) of the α-positions with respect to the N-H group. Accordingly Region C is assigned to orbital 11σ. The seven outstanding bands of regions A and B can then be divided on experimental intensity and calculated groupings to be in the following ratios (A:B):- pyrrole 2:5; diazoles 3:4; triazoles 4:3; tetrazole 5:2. Region A contained $2\pi + (n-1)\sigma$ levels where n is the number of nitrogen atoms. The calculations suggest that in all the compounds the third π level is at lowest binding energy; assigning the first band in each spectrum to this level and the band near 18 eV to 11σ suggested that the ratio of observed IP to calculated eigenvalue was consistently about 0.81. The whole set of 48 points were then plotted as a graph of observed IP versus Calculated Eigenvalue, Figure 4, using where appropriate the intensity ratios of regions A and B and assuming that the calculated orbital ordering was correct. The two sets of data correlate well, the best straight line having a slope of 0.799 ± 0.023 while the maximum deviation from the line is 0.6 eV and the standard deviation is 0.4 eV. Bearing in mind the uncertainties in the geometries used for some of the molecules and the limited size of the basis set, this correlation is very good and justifies the assumption that the ordering of the energy levels is correctly calculated.

Correlation of Molecular Orbitals of Azoles

The azoles are aza-analogues of the cyclopentadienyl anion (D_{5h} symmetry) but of lower symmetry (C_{2v} for pyrrole, C_s for the remainder). It has already been shown that the first three ion-core levels (6σ-8σ) fall into, in most cases, the $A_1 + E$ combinations of $C_5H_5^-$. The only other orbitals which can be directly fitted to an A + E combination are the three π-orbitals. The most strongly bound is the A representation, being a symmetric combination of all p_z orbitals, with the largest eigenvector being that of N_1 in all cases (N_1 is the nitrogen to which hydrogen is bonded). The other two orbitals have a single node each, passing through or perpendicular to the N-H direction.

The control of nodal positions by the N-H bond extends to the centre group of valency shell orbitals which contain the main X-H (X = C, N) bonding levels together with CN and CC ring bonding, i.e. the orbitals in this region 9σ-13σ are very strongly influenced by the N-H position. Thus, if one assumes that the N-H bond lies along the y-axis, the orbitals fall into two main types

a) those which have longitudinal polarisation with orbitals largely given by $(2p_y \pm 2s)_{N,C} \pm 1s_H$

b) transverse polarisation with $(2p_x \pm 2s)_{N,C} \pm 1s_H$.

(This classification does not imply polarisation in the dipole moment sense since transverse polarisation in pyrrole (e.g. 11σ) leads to a zero dipole moment perpendicular to the N-H bond (Figure 5.)

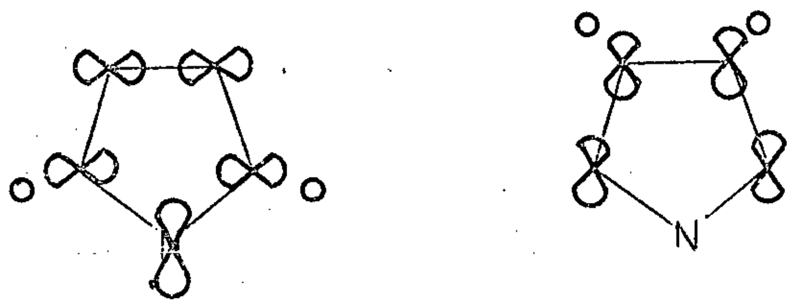

Fig. 5. Transverse (11σ) and Longitudinal (12σ) Polarisation.

There is a slight tendency to form A_1 + E arrangements in this range of molecules. The E orbitals of $C_5H_5^-$ are of radial and tangential character, which, in the case of pyrrole, appears to a small extent in the 11σ and 12σ orbitals. It is however still less evident in the other azoles, such that these can be best regarded (in pyrrole) as $C_\beta C_\beta^+ + C_\alpha H^+$ and $C_\alpha C_\beta^+ + C_\beta H^+$ bonding respectively. All the orbitals in this region contain $1s_H$ together with s and p character from the ring atoms. Using longitudinal and transverse polarisation it is possible to correlate the orbitals in this region. Thus the 9σ orbital in pyrrole ($C_\beta H^+$ + NH) correlates with 9σ in the other azoles, except for 1,2,4-triazole where it is 10σ. These are all longitudinally polarised and consist of NH + C_3H in pyrazole and

Figure 6 Correlation of Orbitals 9σ-11σ
(T = Transverse Polarisation;
L = Longitudinal Polarisation)

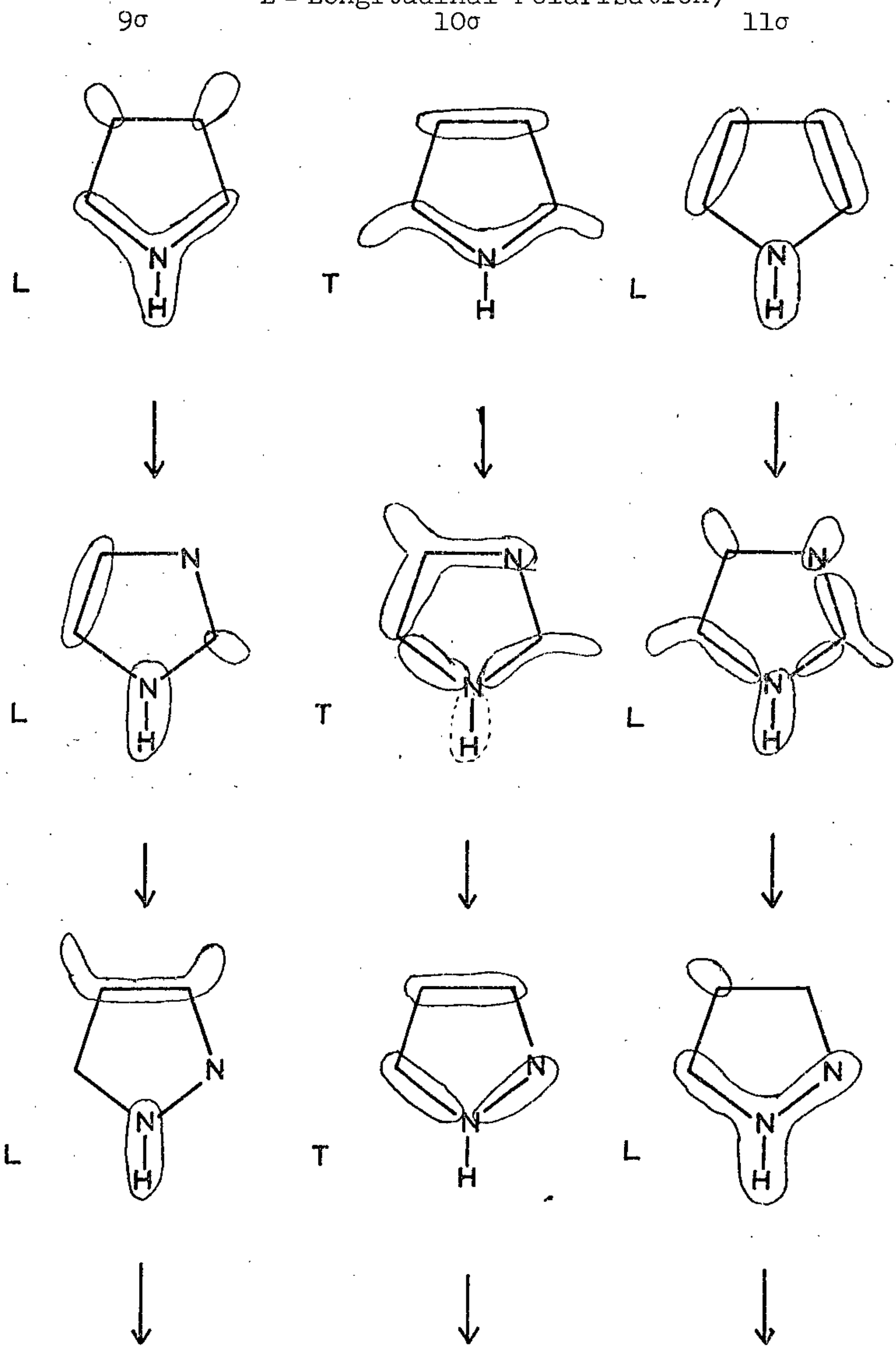

Figure 6 (continued)

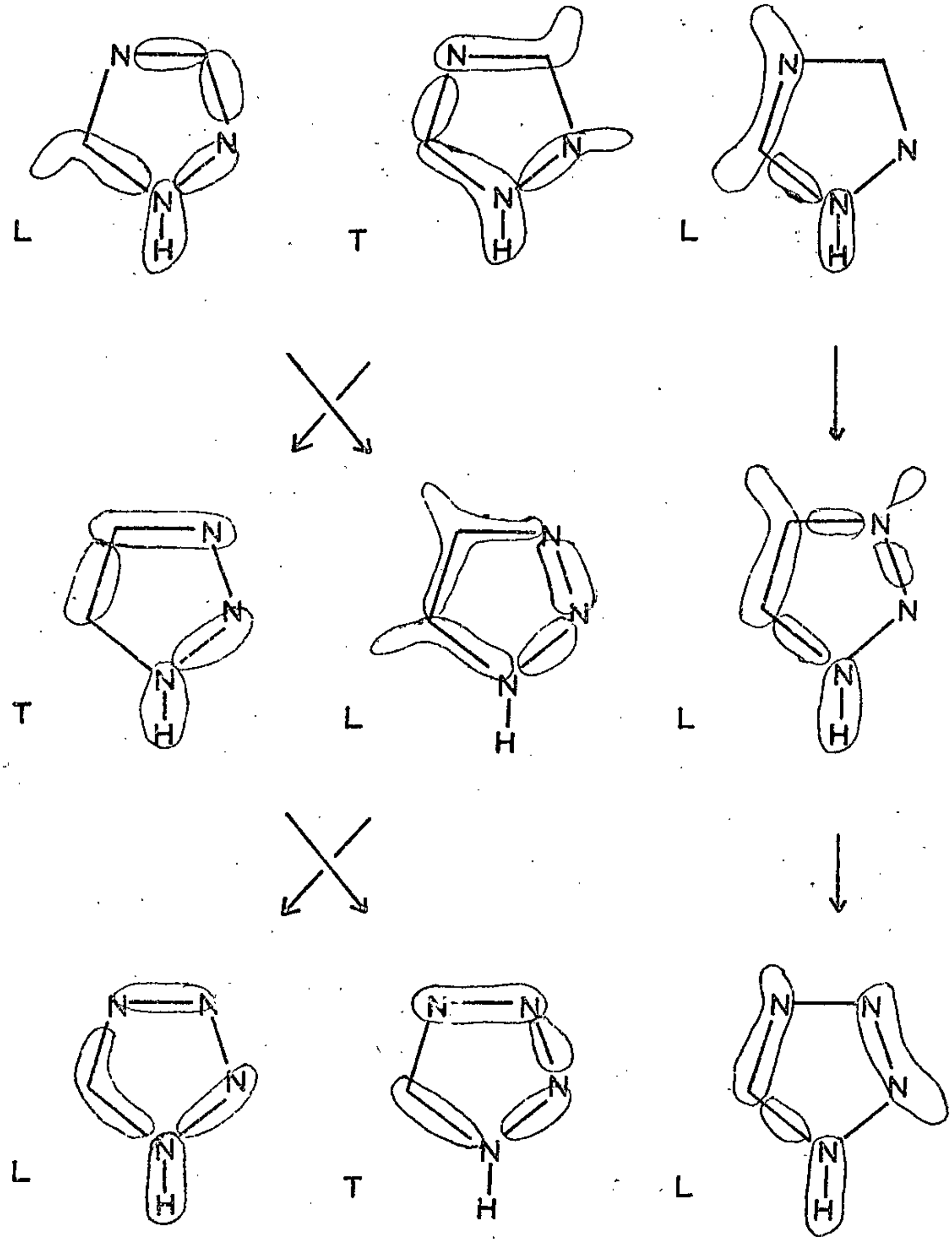

Figure 7   Correlation of Orbitals 6σ–8σ
(S = Nodeless Orbital)

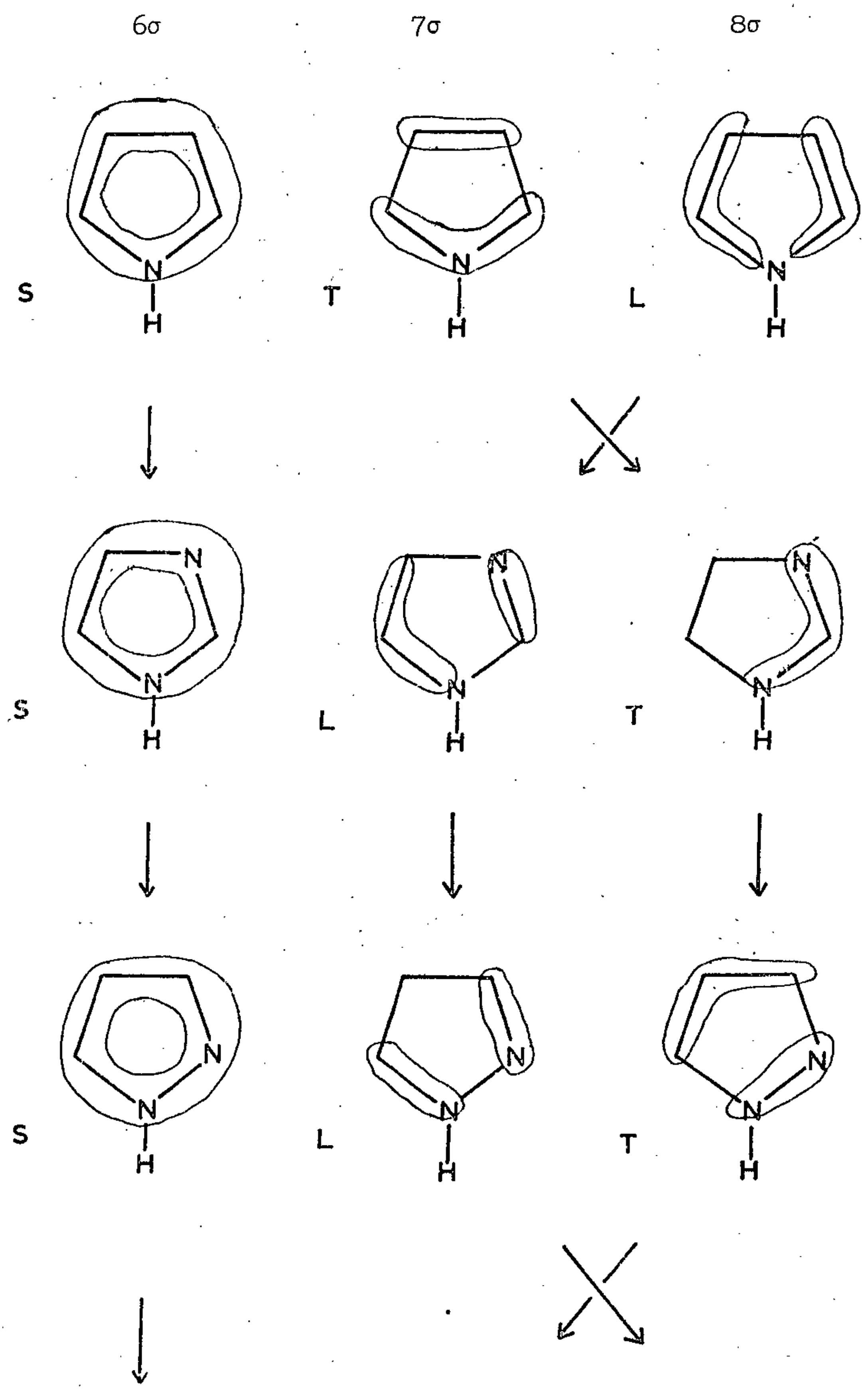

Figure 7 (continued)

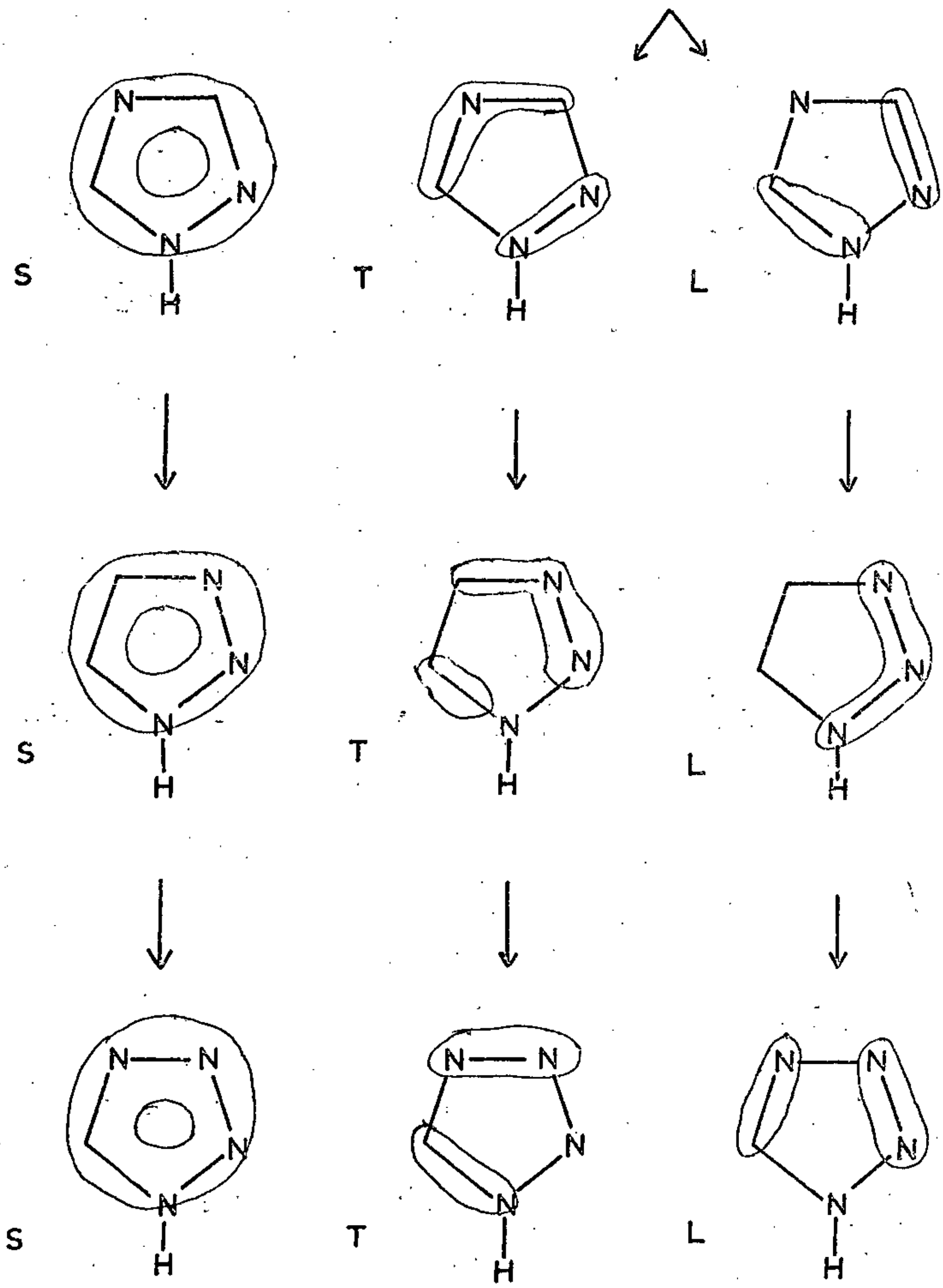

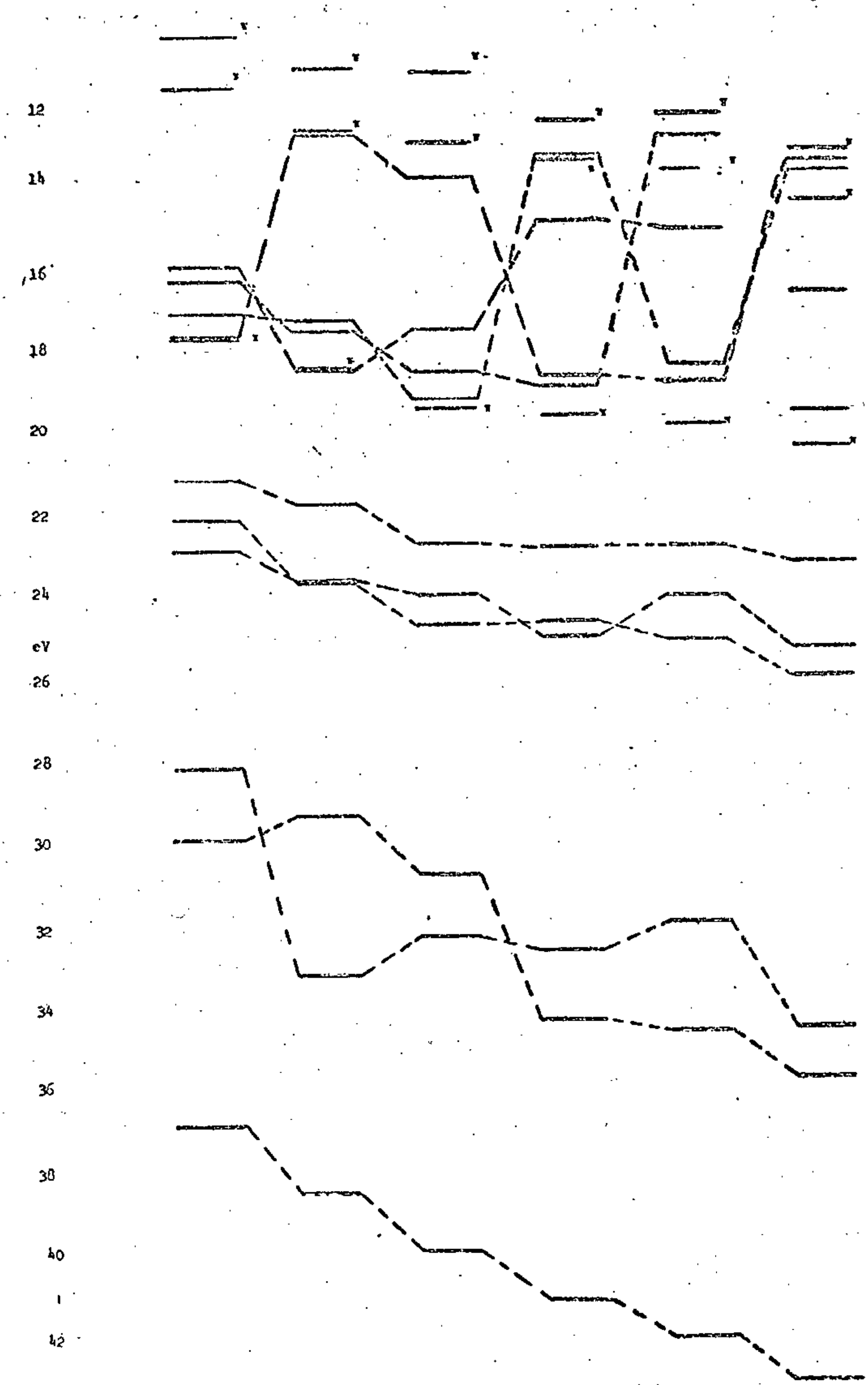

Figure 8. Correlation of Azole Molecular Orbitals, in order, from left to right, Pyrrole, Imidazole, Pyrazole, 1,2,4-Triazole, 1,2,3-Triazole and Tetrazole.

1,2,4-triazole. Similarly, 11σ in pyrrole correlates with the other 11σ orbitals which have largely transverse C-H components (C_5H with a little less C_4H in pyrazole and 1,2,3-triazole, C_2H + C_5H in imidazole and C_5H in 1,2,4-triazole and tetrazole). The use of this correlation by polarisation is shown in Figure 6 for the 9σ-11σ orbitals. The only complication in this method of correlation lies in the (accidental) near degeneracy in the energies of the orbital pairs 9σ/10σ and 13σ/14σ in imidazole and 12σ/13σ in 1,2,3-triazole. This leads to the orbitals having mixed transverse and longitudinal polarisation character.

In the orbitals 6σ-8σ there is again the pseudo C_2-axis, as was found in the 9σ-13σ region. However in this case it is controlled not by the N-H bond but by the siting of the nitrogen atoms, whether they be >N: or $\gt$NH. This leads to a slightly more arbitrary analysis than in the 9σ-13σ range since the transverse and longitudinal polarisations tend to be more difficult to define. However, combining this with the symmetry of the wave function in bond orbitals it is possible to obtain a reasonable correlation (see Figure 7). The symmetry of the bond orbital wave function is only in the sign of the eigenvectors and not their absolute magnitude. Such correlations are summarised in Figure 8.

The orbitals 15σ in the diazoles, 14σ, 15σ in the triazoles and 13-15σ in tetrazole are lone pair orbitals. The eigenvectors for the hybrid orbitals in the lone pair direction are shown in Table 6. These orbitals are highly

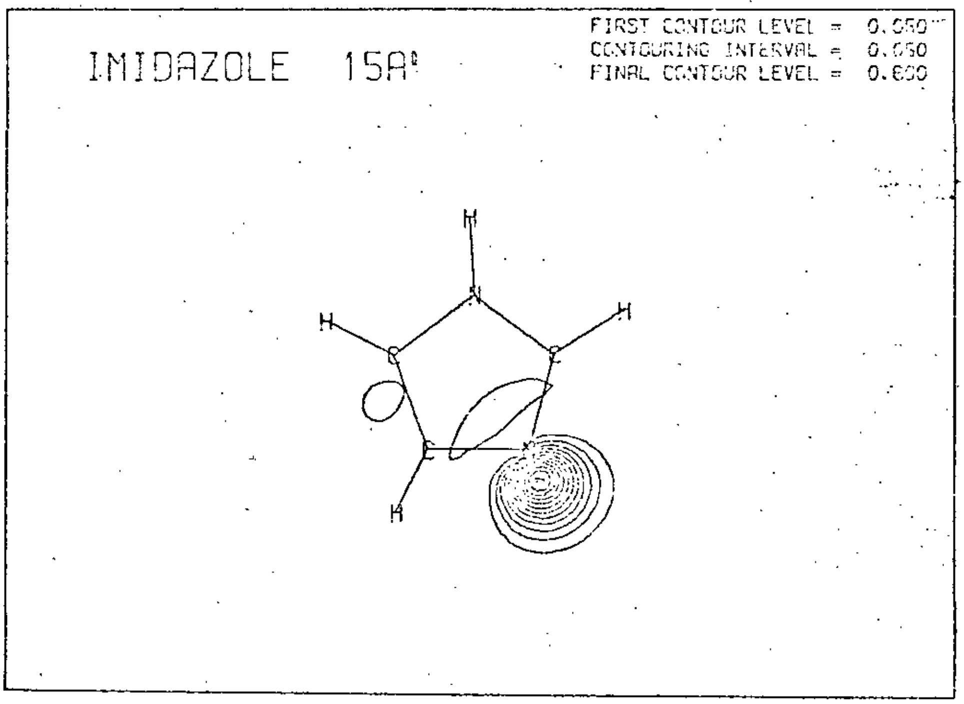

Figure 9a (above) Lone Pair Orbital of Imidazole

Figure 9b (below) Symmetric Combination of Lone Pair Orbitals in 1,2,4-Triazole

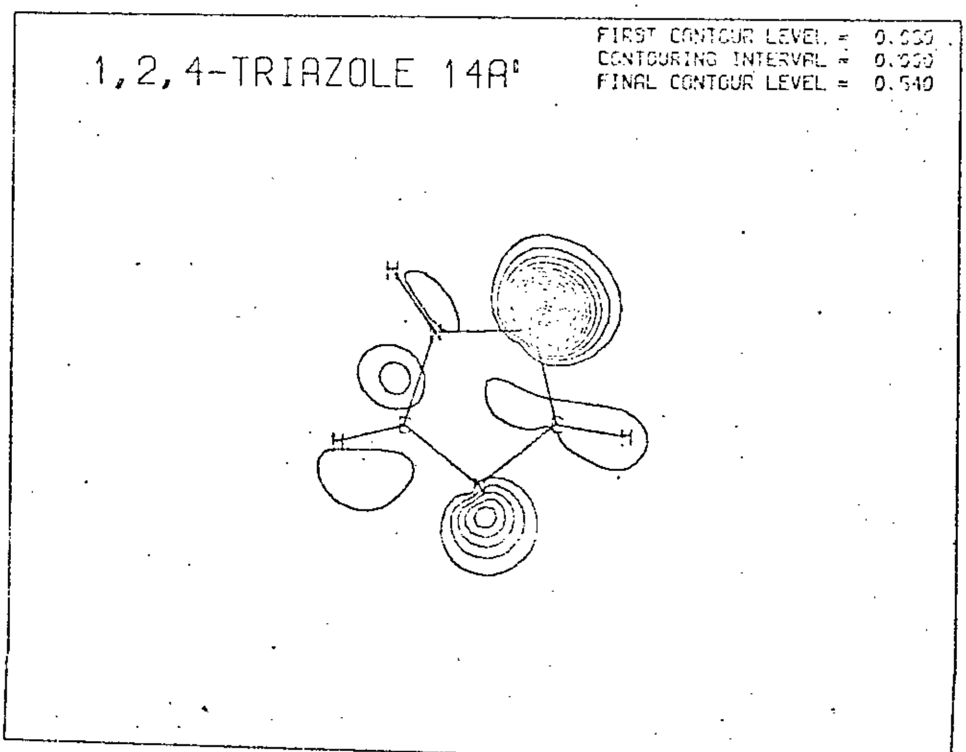

TABLE 6

Lone Pair Levels

Pyrazole	-0.927 N_2						15σ
Imidazole	-0.936 N_3						15σ
1,2,3-Triazole	0.815 N_2	-0.606	N_3				15σ
	-0.492 N_2	-0.707	N_3				14σ
1,2,4-Triazole	-0.828 N_2	+0.409	N_4				15σ
	-0.833 N_4	-0.438	N_2				14σ
Tetrazole	-0.822 N_3	+0.444	N_4	+0.424	N_2		15σ
		-0.763	N_4	+0.576	N_2		14σ
	-0.455 N_3	-0.382	N_4	-0.629	N_2		13σ

localised in the diazoles, but in the triazoles they form reasonably localised linear combinations of the form $(LP_A \pm LP_B)$ with the symmetric combination being at a more bonding level than the antisymmetric combinations. It is not therefore surprising to find that the three lone pair orbitals of tetrazole form an A_1 + E set, with combinations of the type $LP_A + LP_B + LP_C$ (A, 13σ), $LP_B - LP_C$ (E, 14σ) and $2LP_A - LP_B - LP_C$ (E, 15σ). The energy difference in 1,2,3-triazole (2.3 eV) is greater than that of 1,2,4-triazole (1.6 eV) owing to the closer proximity in the former case of the nitrogen atoms. Electron density plots of some representative lone pair orbitals occur in Figures 9a - 9f.

Such lone pair levels are usually thought to be virtually non-bonding, i.e. to have a binding energy less than or equal to that in the free atom (which would have to be taken

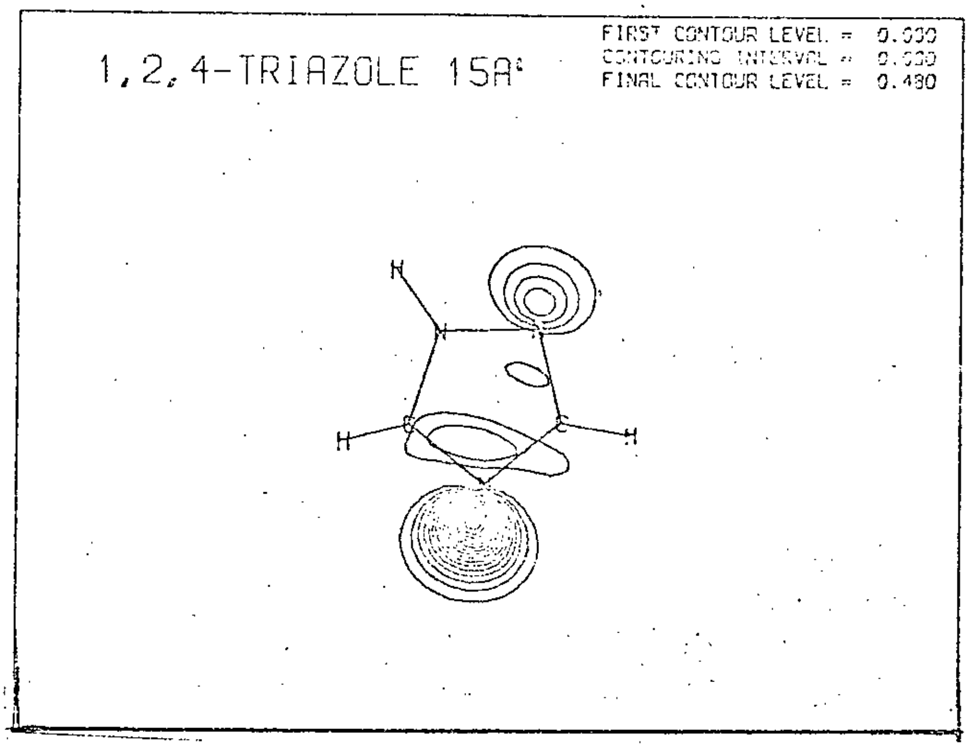

Figure 9c (above) Anti-symmetric Combination of Lone Pair Orbitals in 1,2,4-Triazole

Figure 9d (below) Totally Symmetric (LP_A+LP_B+LP_C) Lone Pair Combination

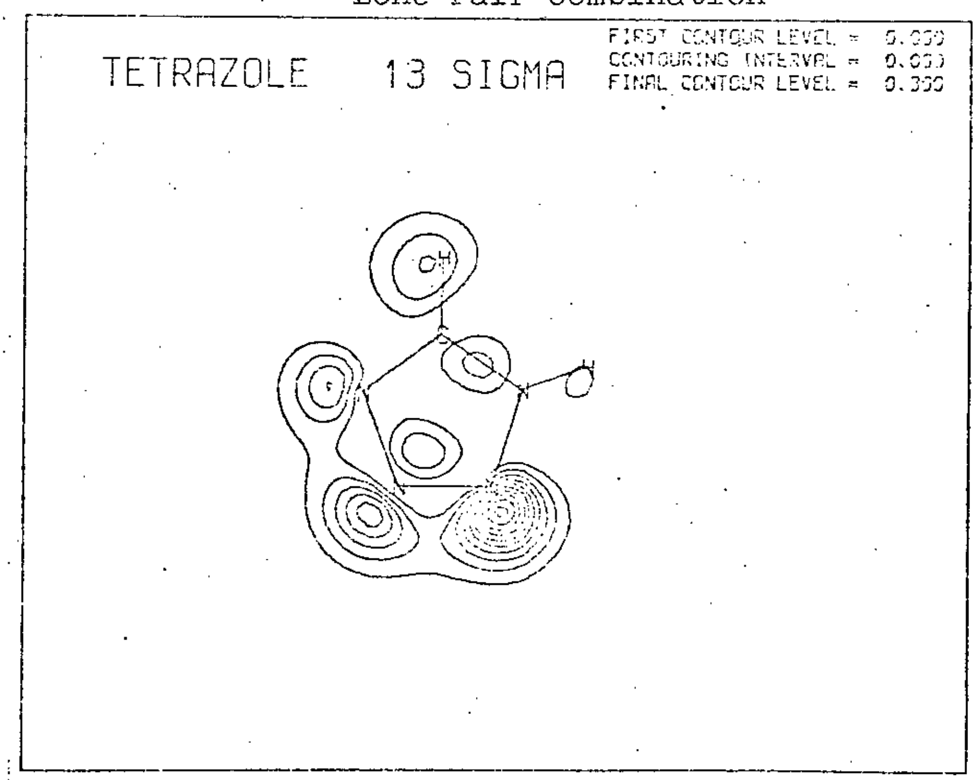

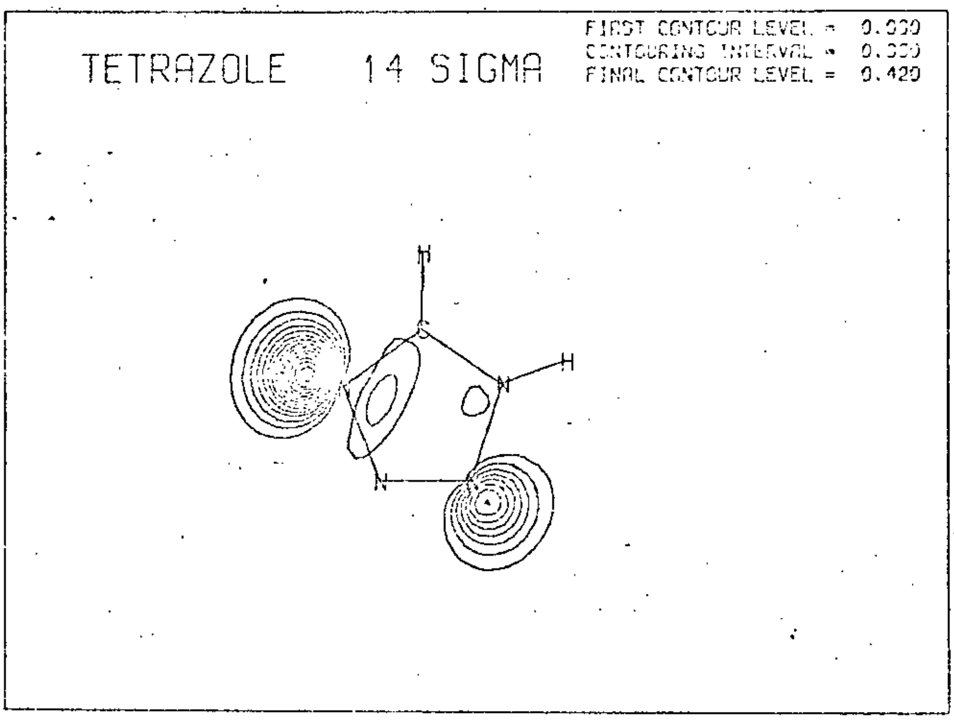

Figure 9e (above) "E" Combination (LP_A-LP_C) of Lone Pair Orbitals

Figure 9f (below) "E" Combination ($2LP_B$-LP_A-LP_C) of Lone Pair Orbitals

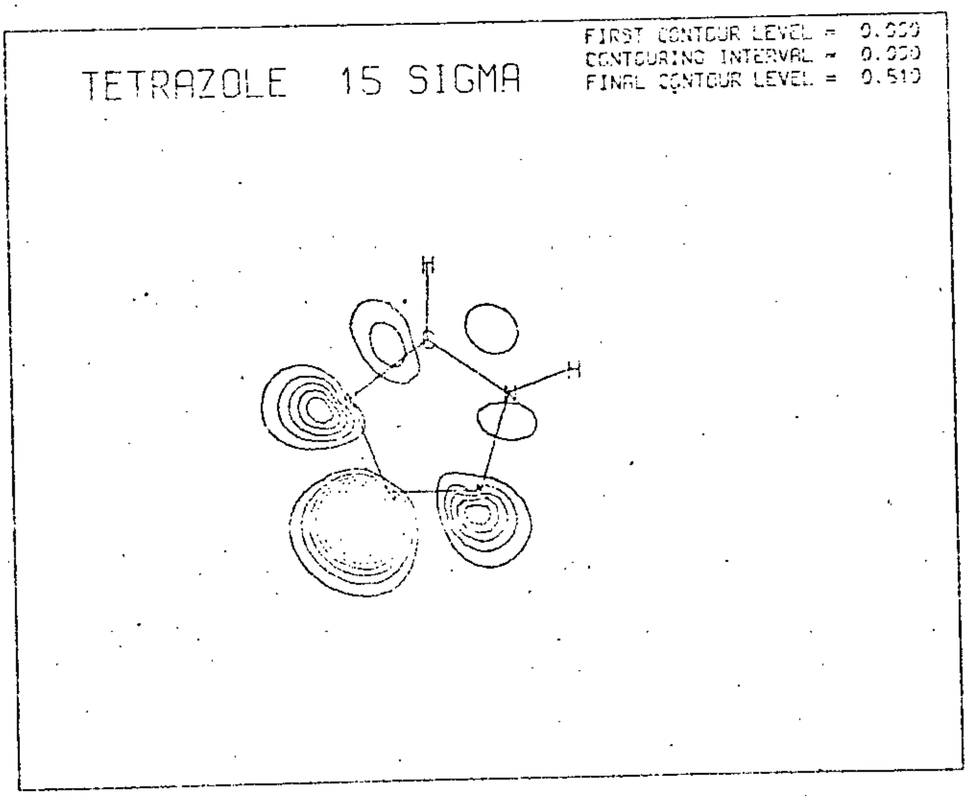

as sp^2 hybridised with a weighted average energy.) That this is not true can be seen from the magnitudes of the orbital energies and ionisation potentials. Further, lone pair levels are assumed to be less binding than π-orbitals. Again the results do not support this view.

One-Electron Properties of the Azoles

Several one-electron properties of the azoles are presented in Table 7 together with the experimental values for pyrrole.[26] This allows an estimate of how accurately the wave function for these molecules can predict experimental values.

The quadrupole moment tensors are obviously not very well represented. This can be explained on the grounds that such tensor components result from small differences in large numbers, and the values could be much improved by the use of a larger basis set. In the case of the diamagnetic susceptibility and second moment tensors the experimental measurements refer to the electronic contribution to the property only and would be expected to be nearer the experimental values. This is indeed found to be true with the calculations tending to over-estimate the experimental values by 4-5% for both properties. The experimental method used to determine the properties listed in Table 7 lead to two values for the properties; Flygare chose the set of values which seemed to be most reasonable. As was found for ethylene oxide, the results for pyrrole endorse his choice.

TABLE 7

Some 1-Electron Properties of the Azoles

Molecule / Property		Pyrrole	Pyrrole(expt)[a]	Pyrazole	Imidazole	1,2,3-Triaz.	1,2,4-Triaz.	Tetrazole
Quad. Mom[b]	xx	6.31	6.60 ± 1.2	12.64	7.60	4.83	8.54	5.06
	yy	0.91	5.8 ± 1.6	-8.83	-3.49	-2.92	-7.42	-6.08
	zz	-7.22	-12.4 ± 2.3	-3.81	-4.11	-1.91	-1.12	1.02
Diamag Sus[c]	xx	-205.5	-195.7 ± 1.1	-183.64	-190.61	-172.58	-172.83	-168.13
	yy	-204.7	-197.6 ± 1.3	-187.77	-187.21	-174.40	-175.86	-163.67
	zz	-342.8	-329.8 ± 0.2	-308.84	-315.32	-288.8	-290.84	-278.08
	xy	-	-	3.66	-1.36	1.29	-0.37	-1.43
$zz-\frac{1}{2}(xx + yy)$		-137.7	-133.2	-123.13	-126.41	-115.29	-116.49	-112.18
2nd Moment[d]	xx	40.50	39.1 ± 0.6	+36.91	+36.76	+34.3	+34.64	32.25
	yy	40.31	38.6 ± 0.6	+35.90	+37.56	+33.8	+33.92	33.30
	zz	+7.95	7.4 ± 0.6	+7.37	+7.37	+6.86	+6.82	6.33
	xy	-	-	+0.86	-0.32	-0.30	0.09	-0.34

a) From reference 26

b) In units of 10^{-26} esu cm^2

c) Electronic contribution only, in units of 10^{-6} erg/(G^2 mol)

d) " " " " " " 10^{-16} cm^2

In this same publication Flygare and Sutter have suggested that the term xx-½(xx + yy) can be considered as a measure of the aromaticity of a ring system in that it represents how different the out-of-plane magnetic susceptibility is when compared to the average of the in-plane components. The values reported are however for the total magnetic anisotropy, i.e. the sum of paramagnetic and diamagnetic terms:

$$\chi_{ij} = \chi^{p}_{ij} + \chi^{d}_{ij} \qquad i,j = x,y,z \qquad (1)$$

$$\chi^{d}_{ij} = -\frac{e^2N}{4mc^2} < 0 \mid \sum_n (y_n^2 + z_n^2) \mid 0 > \qquad (2)$$

$$\chi^{p}_{ij} = -\frac{e^2N}{4mc^2}\left[\frac{hg_{ij}}{8\pi G_{ij}M} - \frac{1}{2}\sum_{\ell} Z_{\ell}(y_{\ell}^2 + z_{\ell}^2)\right] \qquad (3)$$

Equation (2) is the electronic term, while the first term in equation (3) cannot be evaluated by a ground state wavefunction. Therefore the only comparison that can be made is with the diamagnetic susceptibility term; fortunately however the trends apparent in total magnetic susceptibility are also found to occur in the diamagnetic contribution. These values for a sample of molecules, taken from work by Flygare[26,27] appear in Table 8. From this it can be seen on chemical grounds that the more negative is the zz-½ (xx + yy) term the more aromatic is the molecule.

The diamagnetic anisotropy term for the azoles shows that the aromaticity of these molecules decreases as the number of nitrogen atoms in the molecules increases. Further, where there are identical numbers of nitrogen atoms in the molecules, e.g. the diazoles and triazoles, the more aromatic

TABLE 8

Total and Diamagnetic Susceptibilities

Total	Benzene	Pyridine	Pyrrole	Furan
xx	-34.9	-28.3	-31.9	-30.5
yy	-34.9	-30.4	-37.0	-33.3
zz	-94.6	-86.8	-76.8	-70.6
$zz-\frac{1}{2}(xx + yy)$	-59.7	-57.45	-42.35	-38.7
Diamagnetic				
xx	-286	-271.9	-195.7	-189.5
yy	-286	-275.7	-197.6	-182.5
zz	-508	-480.6	-329.8	-313.9
$zz-\frac{1}{2}(xx + yy)$	-222	-206.8	-133.15	-127.9

molecule is the isomer in which there are fewer N-N bonds, i.e. imidazole is more aromatic than pyrazole and 1,2,4-triazole than 1,2,3-triazole. This trend is similar to that found for binding energy and is a symptom of the same underlying cause, i.e. that the more nitrogen atoms present in a molecule the less stable is that molecule.

The second moments are, like the diamagnetic susceptibility terms, in reasonable agreement with experiment. They decrease as the number of nitrogen atoms increase, showing that the electron distribution is much more compact. This is indicative of the higher degree of localisation of the electrons when nitrogen replaces C-H. Considering only the zz component, this shows that as the number of nitrogen atoms increases the average height above the plane gets less, i.e. there is more localisation of the electrons, presumably in nitrogen.

Dipole Moments and Population Analysis

The dipole moments and vector components of the azoles are shown in Table 9, where the directions have been rotated such that the components lie either parallel (μ_{11}) or perpendicular ($\mu_{\perp}$) to the N-H bond, which itself points in a negative y-direction. The convention used for signs of dipole moment vector components is that a positive dipole has its negative end in the positive cartesian direction.

TABLE 9

Dipole Moment Components in the Azoles (in Debye units)

	Exp.	Calc.	μ_{11}	$\mu_{\perp}$	μ_{σ}	μ_{π}
Pyrrole	1.80	2.01	2.01	0.0	-0.53	2.54
Pyrazole	2.21	2.85	2.23	1.77	1.65 (-30.1)	3.07 (+83.0)
Imidazole	3.8	4.41	4.31	0.96	1.46 (+52.4)	3.15 (+95.3)
1,2,3-Triazole		4.50	3.26	3.10	2.79 (81.7)	2.87 (83.0)
1,2,4-Triazole	3.20	3.56	3.50	0.65	1.14 (54.0)	2.91 (86.6)
Tetrazole	5.15	5.17	4.72	2.11	2.53 (47.0)	2.92 (82.5)

TABLE 10

Population Analyses of the Azoles

Pyrrole

	N1	C2,C5	C3,C4
1s + 2s	3.398	3.025	3.050
$2p_\sigma$	2.454	1.917	2.064
$2p_\pi$	1.628	1.096	1.090
H	0.670	0.836	0.847

Pyrazole

	N1	N2	C3	C4	C5
1s + 2s	3.365	3.588	3.009	3.033	3.005
$2p_\sigma$	2.408	2.391	2.139	2.133	2.085
$2p_\pi$	1.531	1.146	1.116	1.114	1.092
H	0.615	-	0.723	0.770	0.736

Imidazole

	N1	N3	C2	C4	C5
1s + 2s	3.380	3.552	3.009	3.024	3.028
$2p_\sigma$	2.457	2.621	1.882	2.057	2.004
$2p_\pi$	1.585	1.101	1.088	1.133	1.094
H	0.644	-	0.794	0.764	0.784

1,2,3-Triazole

	N1	N2	N3	C4	C5
1s + 2s	3.365	3.586	3.534	3.001	3.013
$2p_\sigma$	2.384	2.209	2.544	2.060	2.067
$2p_\pi$	1.586	1.131	1.092	1.132	1.058
H	0.616	-	-	0.766	0.756

1,2,4-Triazole

	N1	N2	N4	C3	C5
1s + 2s	3.366	3.587	3.552	3.003	2.992
$2p_\sigma$	2.389	2.442	2.623	1.986	1.975
$2p_\pi$	1.582	1.103	1.096	1.130	1.088
H	0.613	-	-	0.739	0.737

Tetrazole

	N1	N2	N3	N4	C5
1s + 2s	3.369	3.581	3.571	3.587	3.012
$2p_\sigma$	2.414	2.322	2.398	2.461	1.961
$2p_\pi$	1.626	1.117	1.091	1.137	1.028
H	0.583	-	-	-	0.740

The values for the total moment are in reasonable agreement with experiment, there being a tendency to predict a higher dipole moment than that found. Except in the case of pyrrole, where there is only one non-zero component, it would seem reasonable that part of the error will come from each non-zero component, resulting in an error in the angle that the total dipole moment will make with the N-H bond. Unfortunately the available microwave data does not contain the individual components, so that no estimate of the accuracy of the individual components can be made. (A study of experimental results in McLellan's "Tables of Dipole Moments" shows that no reliable increment can be made for an N-methyl group).

The populations of the atoms in the azoles are given in Table 10. There are several striking trends in the populations. The hydrogen which is attached to nitrogen has a much lower population than those attached to carbon (i.e. it has a higher positive charge.) This is what would be expected on acidity grounds; the order of charges would thus give the following order of acid strengths (weakest first):- pyrrole < imidazole < 1,2,3-triazole $\simeq$ pyrazole $\simeq$ 1,2,4-triazole < tetrazole. An alternative method of assessing relative acid strengths is to examine the overlap populations between centres, which gives a measure of relative bond strengths. The values for X-H (X = C, N) are shown in Table 11. It can be seen that the N-H bond has a smaller overlap population in all cases showing that, as expected, N-H is weaker than C-H. On the basis of data

TABLE 11

X-H Overlap Populations

	N1-H	C2-H	C3-H	C4-H	C5-H
Pyrrole	0.3795	0.4291	0.4356	0.4356	0.4291
Pyrazole	0.3526	-	0.4318	0.4401	0.4349
Imidazole	0.3637	0.4158	-	0.4311	0.4287
1,2,3-Triazole	0.3553	-	-	0.4288	0.4276
1,2,4-Triazole	0.3552	-	0.4222	-	0.4248
Tetrazole	0.3623	-	-	-	0.4184

in this Table the order of acidities is (weakest acid first) pyrrole < imidazole < tetrazole < 1,2,3-triazole ≃ 1,2,4-triazole < pyrazole. The pKa for 1,2,4-triazole is not known; the values for the remaining azoles are as follows:- tetrazole (~5), 1,2,3-triazole (9.42), pyrazole (14.0), imidazole (14.2) and pyrrole (16.5). While this order is not in agreement with that predicted by the charge or overlap population methods, it is important to note that pKa is the thermodynamic quantity, while charge and overlap population relate to kinetic acidity.

Another trend of the population analysis appears in the populations of the $2p_\pi$ functions of the nitrogens and carbons. In classical terms the atomic species ⩾N: and ⩾C-H each contribute one electron to the π-system while ⩾N-H contributes two. The former, one π-electron type, have a $2p_\pi$ population of slightly greater than 1.0 showing that they are π-acceptors, while the latter, ⩾N-H type are very much π-donors to the extent of ~0.3 electrons. They are very heavy σ-acceptors to counter-balance this, while ⩾CH, ⩾N: are σ-donors. The delocalisation of the two π electrons could be considered to be a measure of the aromaticity of the system with the smaller the population the more aromatic the molecule. The order of decreasing aromaticity would then be pyrazole, 1,2,4-triazole, imidazole, 1,2,3-triazole, tetrazole and pyrrole. This does not agree with the order predicted by diamagnetic anisotropy; however, since population analysis is a somewhat arbitrary procedure, it is more likely that the diamagnetic anisotropy will predict the correct order.

A trend that is not immediately apparent from Table 10 is the virtually constant effect on the population of an atom when the adjacent carbon atoms are replaced by nitrogens. This data is shown in Table 12, from which it can be seen that substitution of N for C-H leads to a drop in population by approximately 0.10 electrons, with very little variation. Similar results were also found for the azines, and for nitrogen-oxygen heterocycles.

TABLE 12

Total Population as a Function of Neighbouring Atoms

	C - X - C	C - X - N	N - X - N
X = NH	7.451 ± 0.030	7.344 ± 0.050	7.217 ± 0.070
X = N_α	-	7.145 ± 0.035	6.996 ± 0.030
X = N_β	7.272 ± 0.001	7.178	7.061
X = $C_\alpha H$	-	6.149 ± 0.030	6.011 ± 0.030
X = $C_\beta H$	6.244 ± 0.030	6.180 ± 0.100	6.095 ± 0.020

Using the population analysis data and assuming a classical structure for sigma and pi systems it is possible to compare the bond polarisation relative to the unpolarised classical structure with a complete separation of σ and π systems. For example, consider the σ system of pyrrole:- the H_N has a net charge of 0.3298e which must be balanced by -0.3298e at the nitrogen. Thus the N-H bond has a moment of 0.3298. The remaining -0.4260e of the σ population of N gives rise to a C-N moment of 0.2130. The C_α-H moment is 0.1636, and since the total charge from the moments must equal the total charge from the population the C_α-C_β moment is 0.0396 (C_β at positive end). The remaining moments can be obtained by a similar inspection method for C_{2v} (or higher symmetry) molecules. For C_s symmetry the method is more complex, and is exemplified by the π-moments of pyrazole (below).

The first part is to set up (arbitrarily) the various bond moment vectors, i.e.

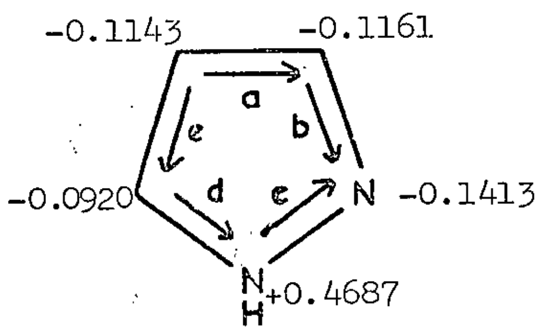

$-c-d = 0.4687$	$a = 0.0116$
$+c-b = -0.1463$	$b = -0.1045$
$+b-a = -0.1161$	$c = -0.2508$
$+a+e = -0.1143$	$d = -0.2179$
$-e+d = -0.0920$	$e = -0.1259$
$a+b+c-d-e = 0.0$	

The negative end of the moment is the arrow-head, with the π-charges given outside the molecule. The first 5 equations are then set up in the following manner; the -ve end of b and the +ve end of c must equal the charge on N2,

TABLE 13

Bond Moments in the Azoles

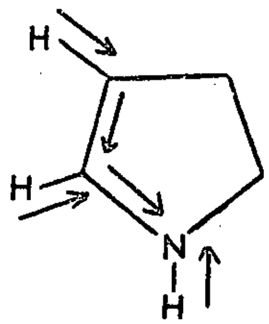

	N-H	C2-H	C3-H
	0.3298	0.1636	0.1535

	N-C2	C2-C3
σ	0.2611	0.0396
π	-0.1860	-0.0900

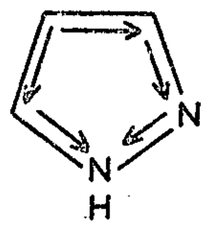

	N-H	C3-H	C4-H	C5-H	
	0.3850	0.2773	0.2298	0.2643	
	N1-N2	N2-C3	C3-C4	C4-C5	C5-N1
σ	0.1547	0.1336	0.0044	0.0586	0.2325
π	-0.2508	-0.1045	0.0116	-0.1259	-0.2179

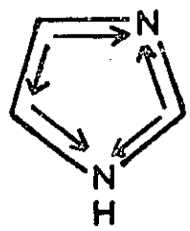

	N-H	C2-H	C4-H	C5-H	
	0.3559	0.2059	0.2360	0.2158	
	N1-C2	C2-N3	N3-C4	C4-C5	C5-N1
σ	0.2471	0.0679	0.1045	0.0502	0.2337
π	-0.2026	+0.1145	-0.0140	-0.1186	-0.2126

Table 13 (contd.)

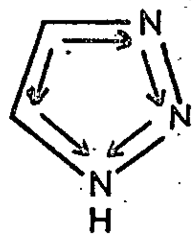

N-H	C4-H	C5-H
0.3845	0.2339	0.2445

	N1-N2	N2-N3	N3-C4	C4-C5	C5-N1
σ	0.1395	0.0346	0.1125	0.0013	0.2253
π	-0.2249	-0.0936	-0.0012	-0.1308	-0.1890

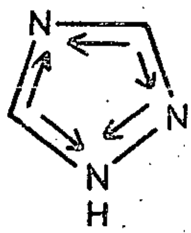

N-H	C3-H	C5-H
0.3870	0.2611	0.2632

	N1-N2	N2-C3	C3-N4	N4-C5	C5-N1
σ	0.1289	0.1578	0.1138	0.0618	0.2350
π	-0.2168	-0.1136	-0.0164	+0.1129	-0.2011

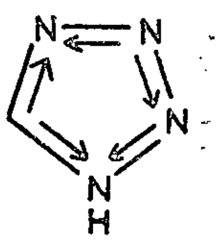

N-H	C5-H
0.4170	0.2597

	N1-N2	N2-N3	N3-N4	N4-C5	C5-N1
σ	0.1143	0.0169	0.0135	0.0343	0.2523
π	-0.2092	-0.0918	0.0005	0.1368	-0.1645

i.e. $-b+c = -0.1463$. These 5 equations are not independant and a sixth is necessary for determining a-e. This is obtained by the algebraic sum of the vectors, in a clockwise or anti-clockwise direction, equalling 0.0 and is the sixth equation above. The values obtained from these equations are shown above, with the minus sign indicating that the initial guess set the vector in the wrong direction.

This method is equally applicable to the sigma and pi systems and the results are shown in Table 13, where 1) the sigma moments point in the direction of the arrows, 2) the pi moments are given a sign relative to the sigma system, 3) the H atoms are always at the positive end of the dipole.

The resulting bond moments are very reproducible from molecule to molecule. The sigma set shows that the C-N bond is polarised in the direction expected from electro-negativity considerations. Hydrogen-carbon and hydrogen-nitrogen are very heavily polarised while C-C and N-N bonds are very little polarised, as one would expect. In contrast to this the N-NH system is quite heavily polarised towards the N(H) nitrogen. There is in fact a general polarisation towards the NH position in the sigma system, which leads to a clear difference in the $C_\alpha N_\beta$ and $C_\beta N_\alpha$ polarisations (average values 0.070 and 0.159 respectively). This heavy flow of electrons is partially offset by the π-system, where the bond moments, with very few exceptions are polarised in the opposite direction to the σ-system, i.e. there is a π flow from position one to the β position.

The splitting of dipole moments into sigma and pi contributions has long been a favoured method of analysis

While it is a simple matter to arrive at average positions of the sigma and pi electrons (by addition of the components of orbitals of sigma and pi symmetry), partitioning the nuclear contribution is a somewhat arbitrary procedure, there being several ways in which this could be done:-
a) the pi contribution is 6/36 of the total nuclear and the sigma share is 30/36 - this is based on there being 6π electrons and 30σ electrons; b) a refinement of the first method where the σ share consists of all the hydrogen atoms plus (30-n)/(36-n) of the C-N atoms (n is the number of hydrogens) and the π gets the remaining 6/(36-n) parts, e.g. for pyrazole the σ contribution is $4 \times H + \frac{26}{32}$ N,C and the π 6/32 N,C; c) the assumption of a classical structure with the following sharing:- $>$C-H has $\frac{5}{6}\sigma$ and $\frac{1}{6}\pi$, $>$N-H has $\frac{5}{7}\sigma$ and $\frac{2}{7}\pi$ and $\geqslant$N: has $\frac{6}{7}\sigma$ and $\frac{1}{7}\pi$. This last method of partitioning has been used in other cases and the results are to be found in Table 9, together with the angle that μ_σ and μ_π make with respect to the $\mu_\perp$ direction.

The first important feature is the constancy of the direction of the π dipole moment which, to within a few degrees, is in all cases in the direction of μ_{11}. In contract μ_σ changes direction quite markedly and in a seemingly arbitrary manner. However much of this can be explained by considering changes in σ <u>bond</u> moments.

In pyrrole $\mu\sigma$ is in the direction of $-\mu_{11}$; addition of a nitrogen alpha to the N-H (giving pyrazole) replaces a very polar C-NH with a less polar N-NH and creates a fairly polar C-N. The net effect of these changes is to cause a σ bond moment rotation anti-clockwise, resulting in μ_σ for pyrazole being anti-clockwise of its position in pyrrole. Similarly in creating imidazole from pyrrole the C-NH terms nearly cancel resulting in the control of μ_σ coming from the C2-N3 and C4-N3 bond moments. It is not then surprising that μ_σ points between these two directions. Obtaining 1,2,4-triazole from pyrazole generates two new C-N dipoles which has the effect of rotating μ_σ of pyrazole in an anti-clockwise direction. From 1,2,4-triazole to tetrazole some of this rotation is lost due to the formation of less polar N-N bonds and μ_σ of tetrazole is clockwise of 1,2,4-triazole. The only azole which cannot be at least qualitatively rationalised in this manner is 1,2,3-triazole with its very high degree of rotation.

Tautomerism in the Triazoles and Tetrazoles

1,2,3-Triazole, 1,2,4-triazole and tetrazole can exist in other forms than those described above. These tautomeric forms are obtained by moving hydrogen atoms from one nitrogen to another, giving compounds 4a-6a.

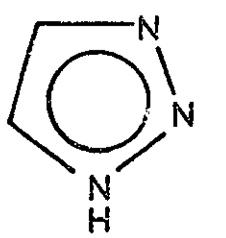

(4)
1H-1,2,3-triazole

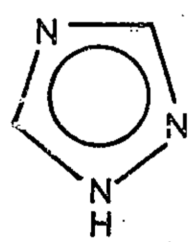

(5)
1H-1,2,4-triazole

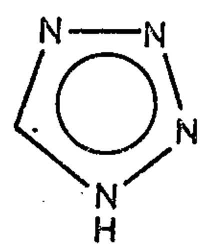

(6)
1H-tetrazole

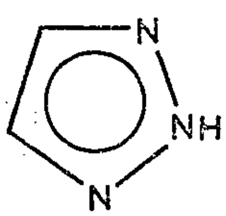

(4a)
2H-1,2,3-triazole

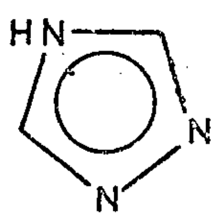

(5a)
4H-1,2,4-triazole

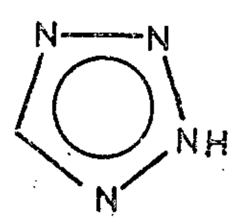

(6a)
2H-tetrazole

The nomenclature for these molecules is based on the nitrogen atoms position first of all (i.e. 1,2,3 or 1,2,4) and then the prefix 1H, 2H or whatever identifies the nitrogen to which the hydrogen is attached. It is however conventional to omit the position of the hydrogen when it is in the 1H position, i.e. in 4-6. Calculations have accordingly been carried out on the compounds 4a-6a with a view to determining which is the more stable structure, i.e. which is most likely to be found in the gas phase. The same basis sets were used as for molecules (1)-(6); with the exception of 2H tetrazole the geometries were constructed by averaging the lengths of the 1H-tautomers since the molecules increase in symmetry to C_{2v}. 2H-Tetrazole was based on the 2-methyl-5-amino derivative with the N-CH3 being replaced by a N-H with the same bond length as for the 1H-tautomer. Full details of the geometries are to be found in Appendix 3.

TABLE 14

Total Energies for the Triazole and Tetrazole Tautomers

	4a	5a	6a
T.E. (au)	-239.89881	-239.79188	-255.79094
1-El (au)	-645.60138	-653.53090	-677.79389
2-El (au)	242.25262		253.27476
NR (au)	163.44995	167.87007	168.72820
B.E. (au)	-0.36010	-0.25448	-0.08450
B.E. (kcal/mole)	-225.9	-159.7	-53.0
B.E. (1H)	-195.2	-166.0	-59.2

The total energies for the molecules 4a-6a are in Table 14, where for reference are included the binding energies of the 1H tautomers. In the case of 1,2,3-triazole it is predicted that the more stable tautomer is that with

C_{2v} structure. The energy difference is fairly large being 30.7 kcal/mole, but gas-phase microwave data shows that the molecule exists as the C_s isomer. On the other hand 1,2,4-triazole is predicted to exist as the C_s isomer (energy in its favour by 6.3 kcal/mole) while tetrazole should be in the 1H form by 6.2 kcal/mole. These are both in agreement with the experimental findings, where gas-phase microwave measurements predict the 1H tautomer for 1,2,4-triazole and ultraviolet spectroscopy indicates that 1H tetrazole should be the stable isomer. Indeed the agreement with experimental dipole moments for both tetrazole tautomers is excellent (tetrazole 5.11D; 1-ethyltetrazole 5.22D; 2-ethyltetrazole 2.65D) since the calculated values are 5.18D (1H) and 2.55D (2H). It would therefore appear that 1,2,3-triazole suffers somewhat from both isomers being of a constructed geometry, which is not true in the case of tetrazole (both tautomers based on experimental data) and 1,2,4-triazole (1H based on experimental data). Even so, this represents a considerable improvement on the semi-empirical methods which either 1) predict the relative energies of the tautomers correctly only after an extrapolation procedure[6] or 2) get only 1,2,4-triazole the correct way round.[4] In non-empirical calculations the only work is that by Berthier on 4H-1,2,4-triazole where an energy of -239.782 au was obtained, which is slightly worse (by 6.2 kcal/mole) than that obtained here.

Like the 1H tautomers those under consideration here have certain trends in common both among themselves and with the 1H tautomers. For example the three occupied π

TABLE 15

Orbital Energies of the Triazole and Tetrazole Tautomers

2H-1,2,3-Triazole	4H-1,2,4-Triazole	2H-Tetrazole
A_1	A_1	A'
-429.18 (1σ)	-429.39 (1σ)	-430.91
-427.47 (3σ)	-426.57 (3σ)	-429.10
-311.53 (5σ)	-312.81 (5σ)	-428.23
-40.49 (6σ)	-40.91 (6σ)	-427.32
-31.71 (8σ)	-35.45 (7σ)	-312.73
-24.67 (9σ)	-25.08 (9σ)	-43.68
-21.55 (11σ)	-23.86 (11σ)	-36.10
-18.74 (12σ)	-18.87 (13σ)	-34.56
-14.44 (14σ)	-14.55 (14σ)	-26.82
		-25.17
B_2	B_2	-22.67
-427.48 (2σ)	-426.60 (2σ)	-19.46
-311.54 (4σ)	-312.82 (4σ)	-16.35
-33.72 (7σ)	-31.82 (8σ)	-14.63
-23.43 (10σ)	-24.67 (10σ)	-13.68
-17.92 (13σ)	-19.56 (12σ)	
-13.53 (15σ)	-12.66 (15σ)	
B_1	B_1	A"
-19.08 (1π)	-19.74 (1π)	-21.47
-12.80 (2π)	-13.73 (2π)	-14.17
		-13.28
A_2	A_2	
-12.47 (3π)	-12.21 (3π)	

orbitals have the following features: a) the first π orbital has a totally symmetric orbital with the largest eigenvector being that associated with the NH nitrogen. b) the remaining two π orbitals either have a node perpendicular (2π orbital) or parallel (3π) to the N-H direction. These three orbitals thus confirm with the A+E set which was found with the 1H tautomers. The energy difference between the pseudo-E levels (Table 15) is 0.33, 1.52 and 0.89eV for 4a, 5a, and 6a respectively; the values for the 1H tautomers are 1.36, 0.92 and 1.23eV. Thus the closer the $\geqslant$N: type of nitrogen atoms are together the greater is the interaction between them and the greater the difference between the pseudo-E pair.

This same effect is to be found in the lone pair levels of the triazoles. Thus 4a has a difference of 0.91eV as against 2.36eV in 4; in the latter the lone pairs are on adjacent nitrogen atoms while they are separated by an N-H in the former case. This reasoning leads to the prediction that the split for 4H-1,2,4-triazole (2 adjacent) should be greater than that for the 1H-tautomer (separated by a C-H group); the energy differences are 4H, 1.89eV and 1H 1.58eV. The lone pair levels are very much the same in character as for the 1H-tautomers, showing a symmetric combination at a lower energy than the anti-symmetric lone pair combination. These were the top two occupied σ levels. Similarly the top three σ orbitals in 2H-tetrazole are lone pair levels of a very similar nature to the 1H-tautomer, with the lowest of the form $LP_1+LP_3+LP_4$, then a pseudo-E pair LP_1-LP_3 (14σ) and $2LP_4-LP_1-LP_3$ (15σ).

Figure 10a Correlation of Tautomeric Azoles with Pyrrole Orbitals (6σ–8σ). Pyrrole Orbitals are shown at top of Figure.

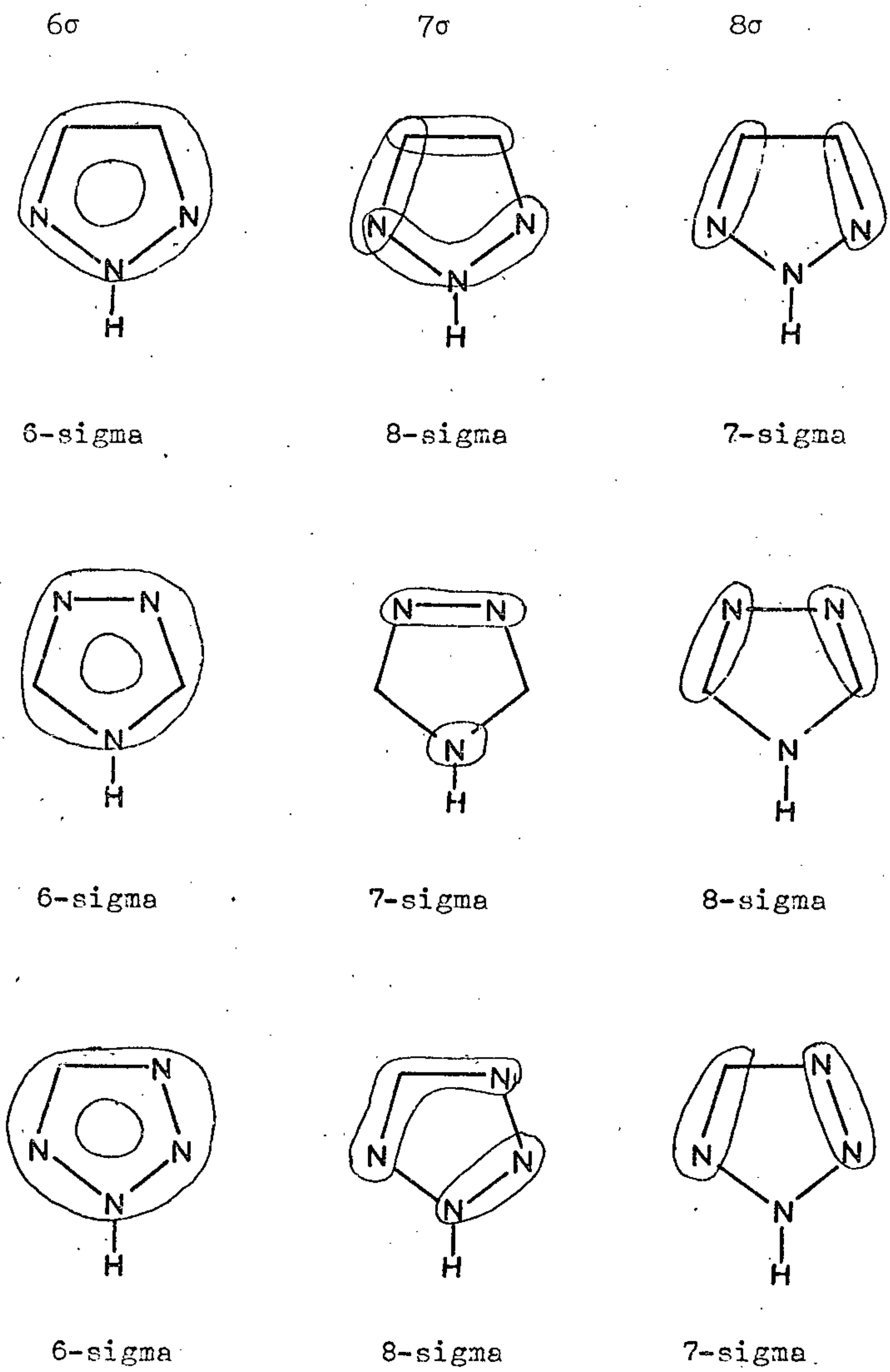

Figure 10b Correlation of Orbitals 9σ–11σ with those of Pyrrole

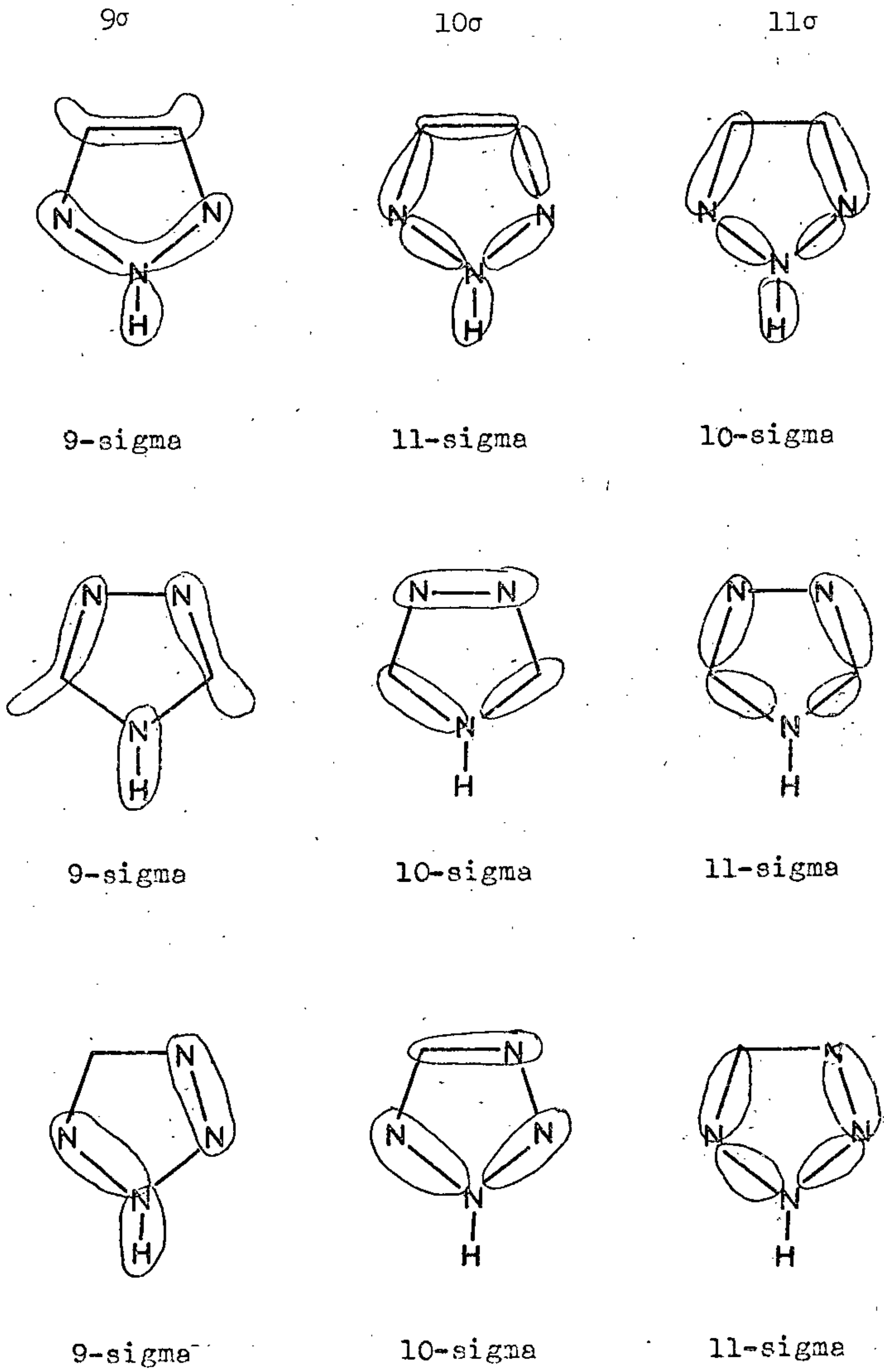

The core levels show the same trends as the 1H-tautomers did, with the level of highest binding energy that of the N-H type of nitrogen. The nitrogens alpha (adjacent) to the N-H are at higher binding energy (2H-1,2,3-triazole) than those beta (4H-1,2,4-triazole); the same trend applies to the carbon 1s levels in the triazoles. In 2H-tetrazole there is the expected general increase in carbon 1s binding energy due to the extra nitrogen atom. Once this has been taken into account the carbon has almost the same ionisation potential as 2H-1,2,3-triazole which is to be expected since the carbon is beta to the N-H in 2H-tetrazole.

In the orbitals 6σ-8σ the correlation with the pyrrole orbitals is easily made. The first of these is a totally symmetric 2s level with nitrogen having the largest eigenvectors; this then conforms to the A type found in pyrrole. It is not surprising then that 7σ and 8σ form the E pair; there is however some cross-over in the order of these two functions, as can be seen in Figure 10a. The correlation of the remaining orbitals is reasonably straightforward with the exception of the 12σ and 13σ orbitals of tetrazole where, as was found for the 1H-tautomer the orbitals 12σ-15σ do not correlate at all well. Figure 10b shows the correlation of 9σ-11σ with pyrrole.

Protonation of the Triazoles and Tetrazole

The triazoles and tetrazoles can all be protonated in positions which give rise to the tautomeric forms below.

TABLE 16

Total Energies of Protonated Triazoles and Tetrazoles

	7a	7b	8a	8b
T.E.	-240.10542	-240.12711	-240.09559	-240.07064
1-El	-664.48869	-666.34287	-662.24372	-662.89045
2-El	246.10329	246.87091	244.93853	245.25601
NR	178.27998	179.34485	177.20960	177.56380
B.E. (au)	-0.46611	-0.48780	-0.45628	-0.43133
B.E. (kcal/mole)	-292.5	-306.1	-286.3	-270.7
	9a	9b	9c	9d
	-256.01666	-256.04417	-256.04554	-255.99839
	-682.23785	-683.38948	-685.16980	-686.97405
	250.13375	250.59051	251.42776	252.22089
	176.08745	176.75480	177.69651	178.75477
	-0.20965	-0.23716	-0.23853	-0.19138
	-131.6	-148.8	-149.7	-120.1

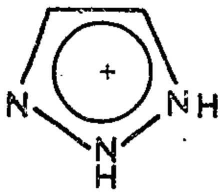

(7a)

1H,2H-1,2,3-triazole

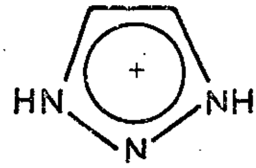

(7b)

1H,3H-1,2,3-triazole

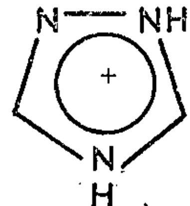

(8a)

1H,4H-1,2,4-triazole

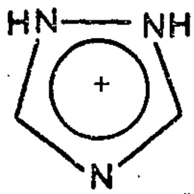

(8b)

1H,2H-1,2,4-triazole

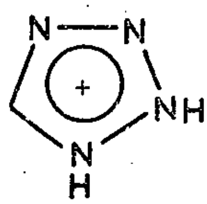

(9a)

1H,2H-tetrazole

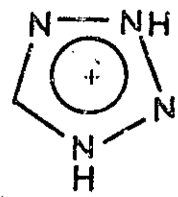

(9b)

1H,3H-tetrazole

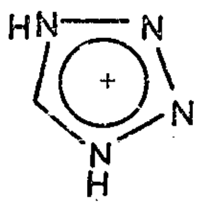

(9c)

1H,4H-tetrazole

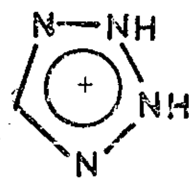

(9d)

2H,4H-tetrazole

Calculations have therefore been carried out on these ions in order to determine which of the protonated species is likely to exist. The basis sets used were identical to those of the neutral species; with the exception of 9b, constructed geometries were used. (The geometry of 9b was based on that of 5-amino-1,3-dimethyl tetrazolium chloride). Full geometries can be found in Appendix 3.

The total energies of the protonated triazoles and tetrazoles are presented in Table 16. In the case of charged molecules the definition of binding energy presents a problem. Consider the pathways available for the decomposition of 7a into its constituent atoms:-

1) 7a $\longrightarrow$ $2xC + 3xN + 3xH + H^+$

2) 7a $\longrightarrow$ $2xC + 2xN + N^+ + 4xH$

3) 7a $\longrightarrow$ $1xC + 1xC^+ + 3xN + 4xH$.

The preferred set of atoms will be that in which the most stable cation is formed (or rather the least unstable). Leaving out H^+ as a possible product on the grounds that it is unlikely to be formed when there are carbon and nitrogen available, the most suitable criterion for determining which of 2) or 3) is the more likely is the atomic ionisation potential. The experimental ionisation potentials for carbon and nitrogen are 11.3 and 14.5eV respectively, showing that the least unstable atomic arrangements is pathway 3). However before this can be used to find binding energies, it is necessary to show that the basis sets used for carbon and nitrogen predict the same order of ionisation potentials. The calculated values are nitrogen 14.65eV, and carbon 10.79eV which is in good agreement with the experimental values; accordingly decomposition pathway 3) has been used to evaluate the binding energies of Table 16.

The binding energies of the protonated species are considerably greater than the corresponding neutral compounds. Thus, since binding energy is the only means of comparing the relative stabilities of molecules of different atomic composition, protonation of an azole is a thermo-dynamically favourable process, i.e. it is more favourable to exist as HA^+ than as H^++A (A = Azole)

In the 1,2,3-triazole system the favoured structure is the most symmetric one, i.e. molecule 7b; similarly one of the C_{2v} tautomers of the protonated tetrazoles is most favoured (9c) but is at only slightly better (more negative) energy than one of the C_s tautomers (9b). In contrast to this, the preferred isomer for the 1,2,4-triazole system is the C_s symmetry molecule, (8a). There is however one feature common to all of these four compounds, namely that the preferred isomer is the one which does not have adjacent N-H groups in the ion. Since these bonds have very high dipole separations, N-H dipole interactions are the principal factor in determining the relative stabilities of protonated species. This criterion explains the relative energies of 9b and 9c, where the N atoms are further apart in 9c, thus making it more stable than 9b. The use of constructed geometries is not without its dangers as was shown with the prediction of the wrong isomer being preferred for the neutral 1,2,3-triazole tautomers. However, as the structures of the predicted isomers show a coherent pattern, it would seem probable that the predictions are this time correct.

Accordingly it is possible to calculate the proton affinities of the three neutral azoles, where proton affinity is defined as the change in binding energy upon protonation of a neutral molecule (here the geometries are the experimentally correct tautomers for the neutral species, and "best-energy" for the protonated species). In this manner the proton affinities for 1,2,3-triazole, 1,2,4-triazole and tetrazole are -110.9, -120.3 and -90.5 kcal/mole respectively. In other words the calculations predict that 1,2,4-triazole is a stronger base than 1,2,3-triazole, which is in agreement with the experimental pKa values for gain of a proton (1,2,3-triazole, 1.17; 1,2,4-triazole, 2.30).

Addition of a proton to the neutral molecule generates a positively charged heterocycle; this environment would make it more difficult to remove an electron resulting in ionisation potentials becoming greater in magnitude. Such a pattern ought then to be found in the calculated orbital energies; that this does occur can be seen from the orbital energies of the protonated species (Table 17). For example, the 15σ orbital energy of the protonated 1,2,3-triazole system is 20.95 or 21.91eV (depending on the tautomer), compared to 13.34eV in the neutral molecule. This lowering of orbital energy by approximately 7eV applies not only to valence-shell σ orbitals, but also to core and pi levels. This is not then simply a replacement of a relatively non-bonding lone-pair by a lower orbital energy N-H bond, but is a systematic lowering of the eigenvalues due to the positive charge on the molecule.

The question of where this positive charge lies in the molecule again shows a deficiency in the classical approach, where the charge is thought firstly to reside in the nitrogen to which the new hydrogen is bonded, with resonance forms allowing delocalisation via the pi system to the other ring atoms i.e.

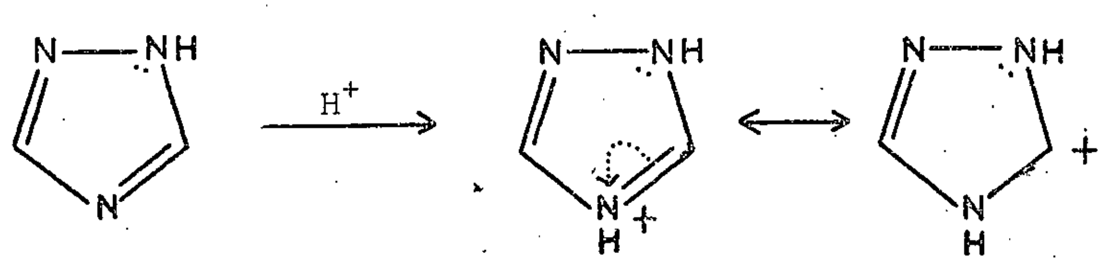

TABLE 17

Orbital Energies (eV) of Protonated Azoles

	7a	7b	8a	8b
σ	438.41	437.51	436.91	437.42
	437.08	437.51	436.71	437.40
	436.00	437.39	434.91	433.70
	319.99	319.19	321.67	320.72
	318.40	319.18	319.75	320.71
	49.76	50.24	48.51	48.97
	42.20	42.76	42.78	41.96
	39.81	39.57	39.71	40.46
	32.84	33.75	32.77	32.68
	31.63	31.95	31.99	32.01
	31.01	29.88	30.95	31.51
	27.13	28.07	27.68	26.90
	25.71	25.31	26.45	26.89
	24.65	25.25	25.26	25.60
	20.95	21.91	20.96	20.10
π	27.53	27.51	26.87	27.43
	21.07	22.15	21.86	20.58
	19.73	19.11	19.30	20.19

	9a	9b	9c	9d
σ	439.30	439.06	437.67	439.38
	438.20	438.53	437.67	439.36
	437.48	437.77	436.99	437.01
	434.73	435.94	436.96	437.01
	321.79	320.76	322.83	320.17
	50.98	51.09	50.84	51.69
	43.70	44.08	43.77	44.24
	41.82	41.91	42.82	42.72
	34.20	35.19	34.09	35.18
	33.26	33.23	33.70	33.11
	32.74	30.17	31.55	32.92
	27.65	29.03	29.16	27.98
	26.81	26.46	26.95	26.08
	22.41	23.25	22.93	23.04
	20.41	21.45	20.72	21.63
π	28.55	28.15	27.95	28.94
	21.49	22.88	22.70	21.88
	20.58	19.91	21.08	21.02

This predicts two possibilities which are borne out by calculations:- 1) although protonation occurs via the σ system, it effects the pi system as well. 2) the new $\geq$N-H atom formed by protonation of $\geq$N: behaves in a similar manner to the original $\geq$N-H atom. The population analysis of Table 18 reveals both effects, while the effect on the π-orbital energies is sufficiently large that the virtual (unoccupied) π-orbitals are of negative energy.

The classical approach does not however allow one feature which the population analysis shows to be very important:- on protonation the population of the hydrogen atoms decreases from ~0.82 to ~0.62 (C-H) or from ~0.62 to ~0.42 (N-H). In other words a large part of the new positive charge appears on the peripheral hydrogen atoms, <u>not</u> on the ring atoms. This will of course minimise the electrostatic repulsion between the fractional positive charges by placing them as far apart as possible, while at the same time leaving the ring atoms not very much different from what they were in the neutral species.

Protonation also reduces the X-H (X = C,N) overlap populations, resulting in the X-H bonds being more readily broken (Table 18).

TABLE 18

Population Analyses of Protonated Azoles

		N1	N2	N3	C4	C5
7a	σ	5.737	5.624	6.077	5.062	5.161
	π	1.547	1.536	0.930	1.100	0.888
	H	0.4901	0.527	–	0.652	0.670

		N1,N3	N2	C4,C5
7b	σ	5.819	5.881	5.081
	π	1.483	0.992	1.021
	H	0.498	–	0.661

		N1,N2	N4	C3,C5
8b	σ	5.744	6.128	5.034
	π	1.541	1.083	0.918
	H	0.519	–	0.643

		N1	N2	C3	N4	C5
8a	σ	5.814	5.981	4.982	5.914	5.009
	π	1.491	1.069	1.035	1.502	0.903
	H	0.514	–	0.641	0.515	0.632

		N1	N2	N3	N4	C5
9a	σ	5.781	5.690	5.933	5.989	5.014
	π	1.554	1.526	0.941	1.091	0.888
	H	0.496	0.466	–	–	0.629
9b	σ	5.840	5.869	5.764	5.983	4.962
	π	1.507	0.979	1.473	1.062	0.978
	H	0.487	–	0.456	–	0.640

		N1,N4	N2,N3	C5
9c	σ	5.828	5.861	5.023
	π	1.540	1.059	0.801
	H	0.485	–	0.620

		N1,N4	N2,N3	C5
9d	σ	6.045	5.694	4.952
	π	0.944	1.520	1.072
		–	0.467	0.636

	X1–H	X2–H	X3–H	X4–H	X5–H
7a	0.334	0.324	–	0.412	0.407
7b	0.332	–	0.332	0.409	0.409
8a	0.338	–	0.406	0.335	0.406
8b	0.336	0.336	0.407	–	0.407
9a	0.338	0.327	–	–	0.395
9b	0.334	–	0.323	–	0.399
9c	0.338	–	–	0.338	0.395
9d	–	0.327	0.327	–	0.397

References

1. A.J. Owen, Tet., 1961, 14, 237.

2. R.L. Flurry, E.W. Stout, J.J. Bell, Theor. Chim. Acta (Berl) 1967, 8, 203.

3. W. Woznicki, B. Zurawski, Acta Phys. Pol., 1967, 31, 95.

4. M. Roche, L. Pujol, J. Chim. Phys., 1971, 68, 465.

5. R. Cabo, S. Fraga, Anal. Fis., 1970, 66, 401.

6. M. Roche, L. Pujol, Bull. Soc. Chim. Fr. 1969, 1097.

7. G. Berthier, L. Proud, J. Serre, "Quantum Aspects of Heterocyclic Compounds in Chemistry and Bio-Chemistry," Edited by E.D. Bergman and B. Pullman. The Israel Academy of Sciences and Humanities, Jerusalem 1970 (Distributed by Academic Press)

8. E. Clementi, H. Clementi, D.R. Davis, J. Chem. Phys., 1967, 46, 4725.

9. B. Bak, D. Christerisen, W.B. Dixon, L. Hanser-Nygaard, J. Rastrup-Andersen, J. Chem. Phys., 1956, 24, 720.

10. B. Bak, D. Christerisen, L. Hansen-Nygaard, J. Rastrup-Andersen, M. Schottlaender, J. Mol. Spec., 1962, 9, 124.

11. S. Martinez-Carrera, Acta Cryst., 1966, B20, 783.

12. H.W.W. Ehrlich, Acta Cryst., 1960, B13, 946.

13. P. Goldstein, J. Ladell, G. Abowitz, Acta Cryst., 1969, B25, 135.

14. K. Britts, I.L. Karle, Acta Cryst., 1967, B22, 308.

15. W.H. Kirchoff, J.A.C.S., 1967, 89, 1312.

16. J.H. Griffiths, A. Wardley, V.E. Williams, N.L. Owen, J. Sheridan, Nature, 1967, 216, 1301.

17. K. Bolton, R.D. Brown, F.R. Burden, A. Mishra, J. Chem. Soc. (D) 1971, 873.

18. E. Clementi, Supplement, "Tables of Atomic Functions", IBM J. of Res. and Development, 1965, 9, 2.

19. A.D. Baher, D. Beteridge, N.R. Kemp, R.E. Kirby, J. Chem. Soc. (D), 1970, 286.

20. M.H. Palmer, A.J. Gaskell. Theor. Chim. Acta (Berl.) 1971, 23, 51.

21. P.J. Derrick, L. Åsbrink, O. Edqvist, B.-Ö. Jonsson, E. Landholm, Int. J. Maes. Spec. Ion Phys., 1971, 6, 191.

22. C. Pedersen, Acta Chem. Scand. 1959, 13, 888.

23. a) J.S. Minihina, R.M. Herbst, J. Org. Chem., 1950, 15, 1082.

b) R.A. Henny, W.G. Finnegan, J.A.C.S. 1954, 76, 290.

24. C.A. Coulson, "Valence", Oxford Univ. Press, 1961, p.203.

25. P.J. Derrick, L. Åsbrink, O. Edqvist, E. Lindholm, Spectrochim. Acta. 1971, 27A, 2525.

26. D.H. Sutter, W.H.Flygare, J.A.C.S. 1969, 91, 6895.

27. (a) R.L. Shoemaker, W.H. Flygare, J. Chem. Phys., 1969, 51, 2988.

(b) J.H.S. Wang, W.H. Flygare, J. Chem. Phys., 1970, 52, 5636.

(c) D.H. Sutter, W.H. Flygare, J.A.C.S., 1969, 91, 4063.

III. AZINES

Introduction

The azines are six-membered rings containing at least one nitrogen atom:-

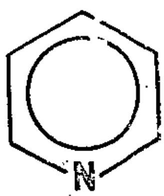

(1)

Pyridine

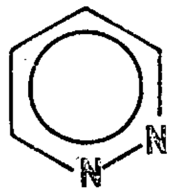

(2)

Pyridazine

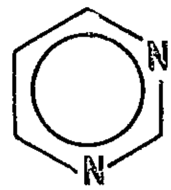

(3)

Pyrimidine

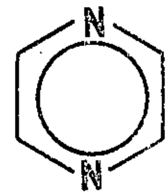

(4)

Pyrazine

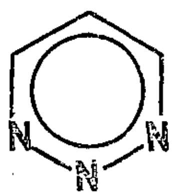

(5)

1,2,3-Triazine

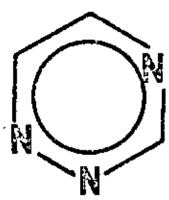

(6)

1,2,4-Triazine

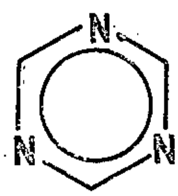

(7)

1,3,5-Triazine

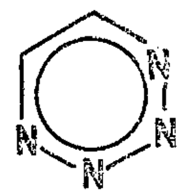

(8)

1,2,3,4-Tetrazine

(9)

1,2,3,5-Tetrazine

(10)

1,2,4,5-Tetrazine .

(11)

Pentazine

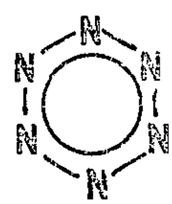

(12)

Hexazine

There have been non-empirical calculations[1-3] on two of the azines carried out using experimental geometries. Clementi has carried out calculations on pyridine[1a] and pyrazine[1b] using basis sets rather similar to those employed for the azoles; pyrazine has also been investigated using somewhat larger basis sets.[2,3] In the semi-empirical field, Lindholm[4,5] and his co-workers have used the Extended Huckel method for comparison with the observed photo-electron ionisation potentials. Heilbronner has also interpreted[6-8] the photo-electron spectra in terms of another Huckel procedure. Other properties investigated include heats of formation,[9] ultra-violet spectra,[10,11,12] lone pair orbitals,[13,14] geometries and bond lengths,[11,12] dipole moments[11,12] and ionisation potentials.[11,15]

Non-empirical calculations have therefore been carried out on all the azines with the exception of pyrazine. After the results for pyridine were obtained, and found to be so similar to those of Clementi, pyrazine was omitted on the grounds that another calculation would be a waste of computer resources, since Clementi's calculation could be employed. Further, the larger basis sets on pyrazine would be considerably better in energy than the minimal basis sets, but probably show few other advantages since the orbital energies, for example, are very similar in both cases.

Minimal basis sets were employed, the exponents and contraction coefficients being identical to those used for the azoles. The exponents and contraction coefficients can be found in Appendix 2, Tables 1, 2 and 3 for hydrogen, carbon and nitrogen respectively. Of the azines, pyridine, the diazines, 1,3,5-triazine and 1,2,4,5-tetrazine have been known for many years; 1,2,4-triazine has only recently been synthesized.[16] The geometries of all the known azines except 1,2,4-triazine have been determined[17-22] by microwave spectroscopy (pyridine, pyridazine) or X-ray crystallography (pyrimidine, pyrazine, 1,3,5-triazine, 1,2,4,5-tetrazine).

With the exception of hexazine, the geometric parameters of the remainder were chosen by analogy with the geometries of the known azines. Because of its high symmetry, the bond length of hexazine was optimised by the CNDO-2 procedure yielding a length of 1.284Å; for the non-empirical calculation this was increased to 1.292Å because the C-C length of benzene predicted as being optimal by the CNDO-2 procedure was 0.008Å less than that found experimentally. Full details of geometries can be found in Appendix 3, together with the symmetry orbitals.

Total Energies of the Azines

In Table 1 are shown the total energies for all the azines which have been investigated, together with the results obtained by Clementi for pyridine and pyrazine. The total energy of pyridine is 89.7 kcal/mole better than that found by Clementi, but comparison of the binding energies indicates that this improvement is largely due to basis set differences. The similarity between these results is great enough to justify the omission of pyrazine from the investigation.

As was found for the azoles, there is a reasonably steady decrease in the binding energy as the number of nitrogen atoms in the molecule increases. The cross-over point at which a molecule becomes less stable than the constituent atoms appears between the tetrazines and pentazine. Thus both pentazine and hexazine are not predicted to exist on the grounds that they have a positive binding energy. However comparison of experimental[23] and

TABLE 1

Total Energies of the Azines

	Pyridine	Pyridine[1a]	Pyridazine
T.E. (au)	-245.76489	-245.62194	-261.68003
1-El (au)	-733.73373	-	-760.94102
2-El (au)	282.47203	-	+291.29111
N.R. (au)	205.49681	-	207.96989
B.E. (au)	-0.95219	-0.9383	-0.69939
B.E. (kcal/mole)	-597.5	-588.8	-438.9

	Pyrimidine	Pyrazine[1b]	1,2,3-Triazine	1,2,4-Triazine
T.E. (au)	-261.67872	-261.55432	-277.59443	-277.61161
1-El (au)	-762.26596	-	-787.26331	-787.75888
2-El (au)	291.87855	-	299.68565	299.96951
N.R. (au)	208.70869	-	209.98323	210.17776
B.E. (au)	-0.69808	-0.7092	-0.44585	-0.46303
B.E. (kcal/mole)	-438.0	-445.0	-279.8	-290.6

	1,3,5-Triazine	1,2,3,4-Tetrazine	1,2,3,5-Tetrazine
T.E. (au)	-277.54134	-293.51233	-293.54386
1-El (au)	-797.80361	-813.03726	-810.64642
2-El (au)	304.56137	307.72164	306.70101
N.R. (au)	215.70090	211.80329	210.40155
B.E. (au)	-0.39276	-0.19536	-0.22693
B.E. (kcal/mole)	-246.5	-122.6	-142.4

	1,2,4,5-Tetrazine	Pentazine	Hexazine
T.E. (au)	-293.47477	-309.39321	-325.28963
1-El (au)	-817.03802	-846.00741	-872.51195
2-El (au)	309.52232	319.13923	327.18347
N.R. (au)	214.04093	217.47497	220.03885
B.E. (au)	-0.15827	0.09142	0.36270
B.E. (kcal/mole)	-99.31	+57.4	227.6

calculated binding energies (Table 2) for pyridine and the diazines (using thermochemical data from Reference 23a for the molecules and from Reference 23b for the atoms) gives a linear plot of equation B.E. (exp) = 0.814 B.E.(calc) − 708 kcal/mole (very similar to that found for the azoles).

TABLE 2

Experimental and Calculated Binding Energies (kcal/mole)

Molecule	$\Delta H_f^o(g)$	B.E. (exp)	B.E. (calc)
Pyridine	+34.55	-1193.5	-597.5
Pyridazine	+66.52	-1051.64	-438.9
Pyrimidine	+46.99	-1071.17	-438.0
Pyrazine	+46.86	-1071.30	-445.0

Once this equation has been applied to pentazine and hexazine, the binding energies become -660.3 and -521.7 kcal/mole respectively, i.e. they are predicted to be thermodynamically more stable than as atoms. However a more valid comparison for chemical purposes is their stability with respect to decomposition into the small fragment molecules, HC ≡ CH, HCN and N_2. Calculations have been carried out on these molecules using their experimental geometries; the energy comparisons of the azines with all possible decomposition pathways to these fragment molecules is shown in Table 3. From this table it can be seen that pentazine and hexazine are thermodynamically unstable with respect to decomposition into the appropriate small fragment molecules.

Pyridine and all the diazines are very much more stable than their fragment molecules; further the triazines,

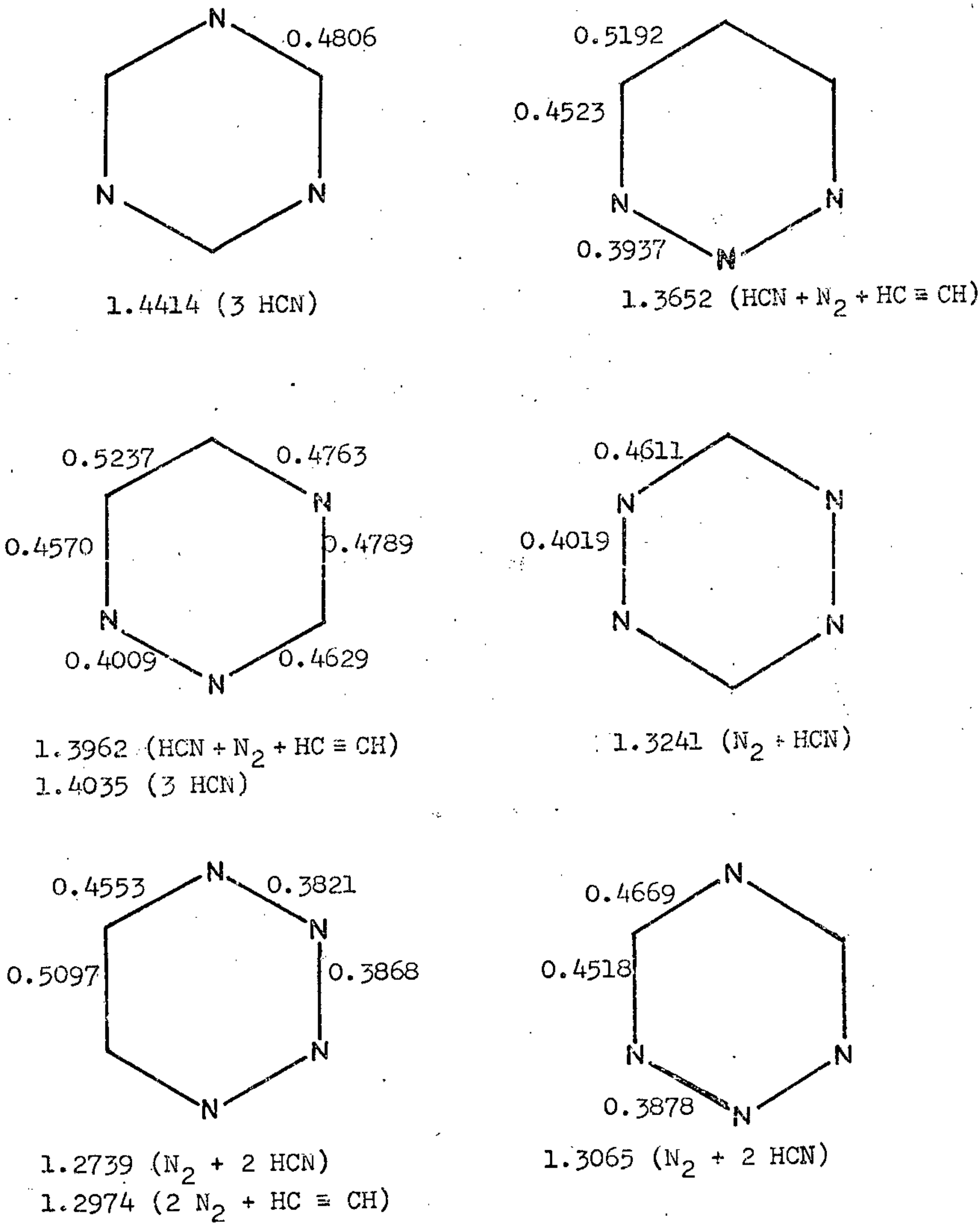

Fig. 1. Overlap Populations of the Azines

with the exception of 1,3,5-triazine, should all be stable molecules. Finding that the longest known triazine should decompose to fragment molecules is somewhat surprising; it is however consistent with the binding energy values of Table 2. (The preparation of 1,3,5-triazines from nitriles often requires the use of high temperatures and pressures; this is compatible with the nitriles being more stable than the azines with the high temperature and pressure being needed to force them to combine.) In a similar fashion, the only known tetrazine, 1,2,4,5-tetrazine is the least stable with respect to decomposition to atoms or fragment molecules.

Figure 1 shows some of the results obtained from a population analysis on the triazines and tetrazines; beside each unique bond is the total overlap population between the centre constituting that bond. Below each molecule is the sum of the overlap population of the bonds which would have to be broken to form the fragment molecules. Thus the smaller this number is the easier it would be to break the bonds involved. For the triazines, the largest value of this number is found in 1,3,5-triazine, which is closely followed by the more recently synthesised 1,2,4-triazine. This of course has two possible decomposition pathways, of which the formation of 3HCN molecules is thermodynamically preferred (Table 3). Such a decomposition pathway has a larger sum of overlap populations and hence the alternative route (to N_2 + HCN + HC ≡ CH) is kinetically preferred. The remaining triazine, 1,2,3-triazine has the

TABLE 3

Fragmentary Decomposition Stabilities (kcal/mole)

Molecule	No. of $HC\equiv CH^a$	No. of HCN^b	No. of N_2^c	$E_{mol}-E_{frag}$
Pyridine	2	1	0	-215.1
Pyridazine	2	0	1	-162.6
"	1	2	0	-112.1
Pyrimidine	1	2	0	-111.3
Pyrazine[d]	1	2	0	-33.2
1,2,3-Triazine	1	1	1	-59.1
1,2,4- "	1	1	1	-69.9
"	0	3	0	-19.41
1,3,5- "	0	3	0	+24.69
1,2,3,4-Tetrazine	1	0	2	-8.3
"	0	2	1	+42.22
1,2,3,5- "	0	2	1	+22.43
1,2,4,5- "	0	2	1	+65.78
Pentazine	0	1	2	+116.29
Hexazine	0	0	3	+180.61

a) T.Energy = -76.447566
b) T.Energy = -92.526893
c) T.Energy = -108.52582
d) Clementi's Pyrazine and above fragments.

lowest overlap population sum of the triazines, but is still higher than the known tetrazine; thus it is quite possible that 1,2,3-triazine will be synthesized. In contrast to this, the as yet unknown tetrazines will prove much more difficult to isolate. In summary, since one can relate overlap population to bond strength, 1,3,5-triazine and 1,2,4,5-tetrazine are kinetically more stable than their isomers, and 1,2,3-triazine is the most kinetically stable of those not yet known.

All three diazine isomers are known, with the stability order on the basis of binding energy being pyrazine > pyridazine ≥ pyrimidine. Thus pyridazine and pyrimidine are thermodynamically less stable than pyrazine, and should rearrange to it under appropriate conditions. This phenomenon has been investigated experimentally[24] with the perfluoro aromatics below.

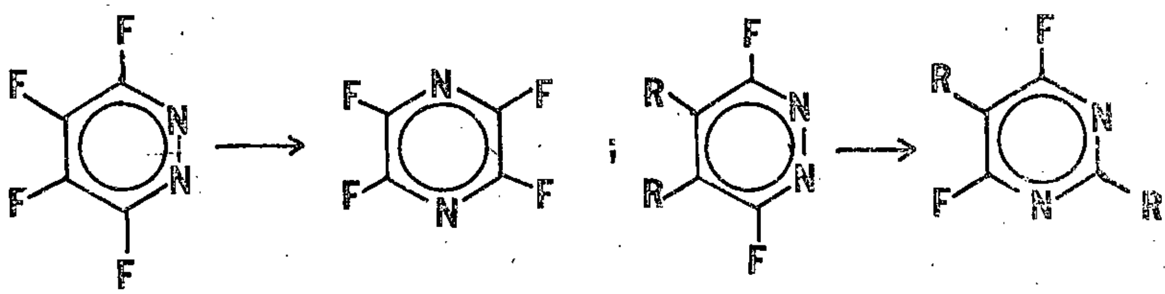

R = C_3F_7

This evidence indicates that the rearrangements are possible but does not agree with the predicted changes based on the binding energies of the parent heterocycles (the pyridazine nucleus rearranges to the pyrazine nucleus less readily than to the pyrimidine nucleus, while the opposite is predicted by binding energies). This does not cast doubt on the validity of the calculations since (a) perfluoro-compounds do not necessarily reflect the behaviour of the parent heterocycle, (b) experimental technique consisted of a brief exposure to 580°C, so that the perfluoro compounds may not be thermodynamically at equilibrium.

Correlation of the Calculated Energy Levels

The azines vary in molecular point group such that the only common feature of the molecules is a σ/π separation of the orbitals. Thus the symmetry in decreasing order is D_{6h} (benzene; hexazine); D_{3h} (1,3,5-triazine), D_{2h} (pyrazine; 1,2,4,5-tetrazine), C_{2v} type A (pyridine; pyrimidine; 1,2,3-triazine; 1,2,3,5-tetrazine; pentazine), C_{2v} type B (pyridazine; 1,2,3,4-tetrazine) and C_3 (1,2,4-triazine). It is necessary to divide the C_{2v} species into two types, the first of which (A) has the C_2-axis passing through an atom and a σ orbital occupation of $1\text{-}11a_1$, $1\text{-}7b_2$. In type B the C_2-axis passes through a bond resulting in an occupation of $1\text{-}10a_1$, $1\text{-}8b_2$. While it is conventional in group theory to make the highest rotation axis the z-axis, it is more convenient to make the z-axis the out of plane axis in all molecules.

Despite the varying nature of the molecular point groups it is possible, from a study of the eigenvectors to show that all of the orbitals are perturbations of the benzene system. The molecules thus show an <u>approximate</u> D_{6h} symmetry in that the wave functions show nodal planes in the same position as benzene, although the wave functions are less smooth. A result of this is that the position of the symmetry axes in the various point groups becomes less important since it is no longer the symmetry of the wave function but siting of the nodal planes which is under consideration. The allowed combinations of atomic orbitals in D_{6h} symmetry are shown in Figure 2. There $\pm$ represents the sign of the atomic orbital in the symmetry orbital, where the atomic orbital is 1s, 2s, or $2p_z$ type; the arrow represents the linear combination of $2p_x$ and $2p_y$ orbitals which transform according to D_{6h}, namely the radial (R) and tangential (T) orbitals. The arrowhead will be taken conventially to be the positive end of R and T orbitals.

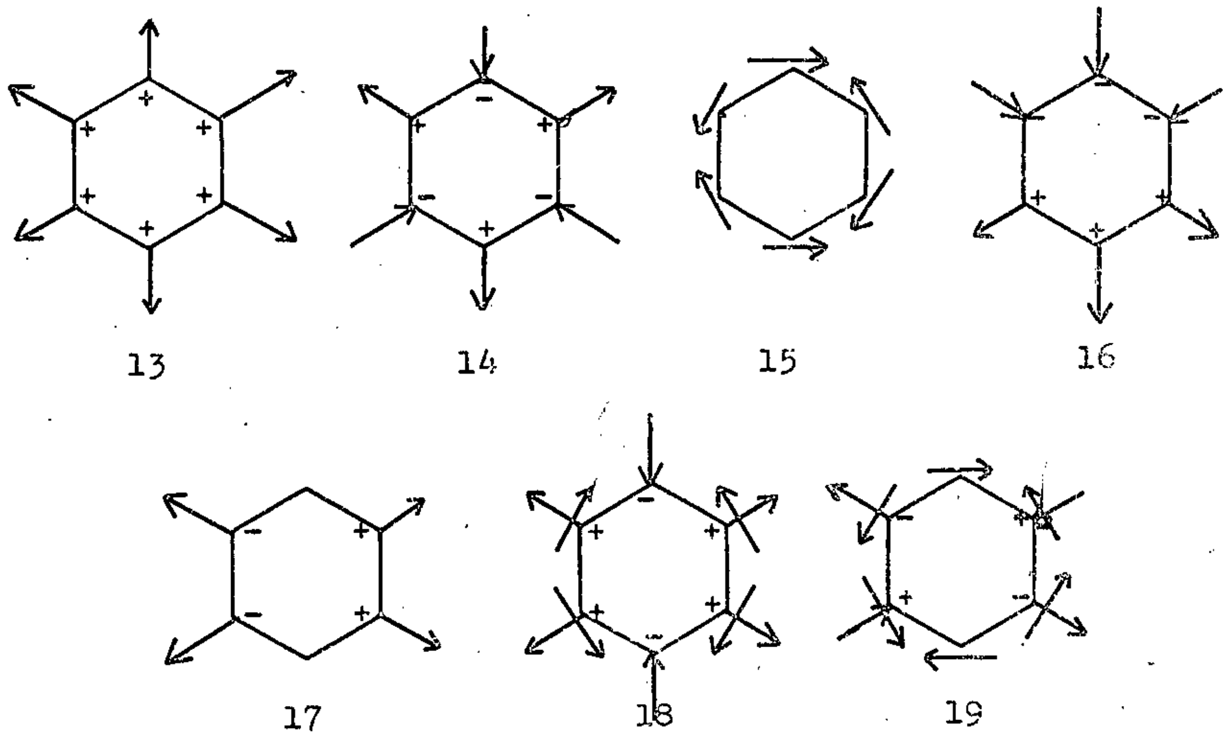

Fig. 2. The Symmetry Orbitals of Benzene in the Ground State.

The two types of C_{2v} orbitals have orbitals of a_1 and b_2 type which correlate differently with the e_{1uA}, e_{1uB}, b_{1u} and b_{2u} orbitals; some examples are shown below.

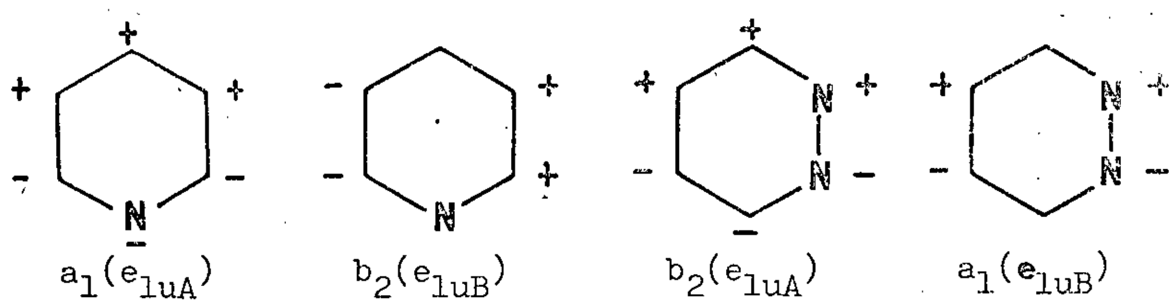

It is not necessary that the a_1 orbitals of the C_{2v} correlate with a_1 nor do all of the b_2 correlate with b_2. In Table 4 the definition of non-D_{6h} groups in terms of the benzene symmetry orbitals is listed.

TABLE 4

The Orbital Correlation

		13	14	15	16	17	18	19
D_{6h}	σ	a_{1g}	b_{1u}	b_{2u}	e_{1uA}	e_{1uB}	e_{2gA}	e_{2gB}
	π	a_{2u}			e_{1gA}	e_{1gB}		
D_{3h}	σ	a_1'	a_1'	a_2'	e'	e'	e'	e'
	π	a_2''			e''	e''		
D_{2h}	σ	a_g	b_{2u}	b_{3u}	b_{2u}	b_{3u}	a_g	b_{1g}
	π	b_{1u}			b_{3g}	b_{2g}		
C_{2vA}	σ	a_1	a_1	a_1	a_1	b_2	a_1	b_2
	π	b_1			b_1	a_2		
C_{2vB}	σ	a_1	b_2	b_2	b_2	a_1	a_1	b_2
	π	b_1			a_2	b_1		
C_s	σ	a'	a'	a'	a'	a'	a'	a'
	π	a''			a''	a''		

Analysis of the effect of aza-substitution on the orbital energies leads to the conclusion that, although there is a shift to higher binding energy as the number of nitrogen atoms increases, the effect is not purely additive with respect to the number of nitrogen atoms. It can however be explained in terms of orbital symmetry, with the introduction of a nitrogen atom having a large, medium or small effect upon orbital energies. These will be called the first, second and third order perturbations respectively.

TABLE 5

First, Second and Third Order Effects on Orbital Energies

Third Order		Second Order		First Order	
Molecule	Energy	Molecule	Energy	Molecule	Energy
Benzene	29.5	Benzene	29.5	Benzene	24.0
Pyridine	30.1	Pyrimidine	31.5	Pyridine	25.0
Pyrazine	30.8	Pyridazine	32.1	Pyrazine	26.0
Pyrimidine	34.5	1,2,4,5-Tetrazine	34.7	Pyrimidine	25.7
1,2,3-Triazine	35.2			1,2,3-Triazine	27.0
1,3,5-Triazine	35.7			1,2,3,5-Tetrazine	28.4
1,2,3,5-Tetrazine	35.2				
Benzene	24.0			Pyridazine	31.5
Pyridine	24.5			1,3,5-Triazine	35.7
Pyrazine	25.35			1,2,3-Triazine	33.2
Pyrimidine	26.1			1,2,3,5-Tetrazine	36.5
1,2,3-Triazine	26.65				
1,2,3,5-Tetrazine	27.25				

Third order perturbation occurs when a nitrogen atom is introduced in a nodal plane in the molecule. At first sight it might appear that a nodal nitrogen atom should have no effect on the orbital energy. This would be true if the nitrogen contained only 2s or R type orbitals, since they <u>must</u> have zero eigenvectors in the nodal planes. There is in general a non-zero T component which can interact with anti-symmetric 2s or 2p orbitals on the adjacent centres, and lead to an energy perturbation. Some typical examples of this can be found in Table 5a for the e_{1u} and e_{2g} type of orbitals. For the inner valency shell orbitals of largely $2s_N$ or $2s_C$ character the tangential (T) component is small so that the third order effect is particularly small, being about 0.6eV per nitrogen atom introduced in the $2e_{1u}$ and $2e_{2g}$ orbitals. The first and second order perturbations occur when the nitrogen atom is introduced in non-nodal positions either at the centre of the wave (Table 5b) or adjacent to the nodal position (Table 5c). Consider an orbital of e_{1u} type (below) where the figures inside the ring are an arbitrary numbering system and those outside represent the eigenvector nature at the various positions.

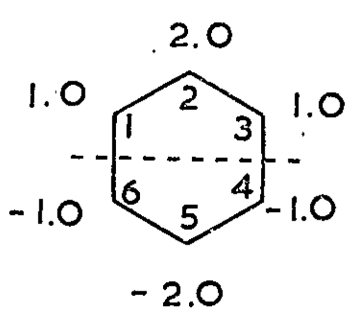

e_{1uA}

For this ring numbering the wave function has maximum amplitude at C2 and C5; introduction of a nitrogen atom at either of these two positions leads to a first order effect, with the electron attracting property of the nitrogen atom supporting the waves' natural tendency. This first order effect is quite large being often 2.5eV or more per nitrogen atom introduced, e.g. benzene to pyridine (2.0eV) and pyridine to pyrazine (3.2eV).

Introduction of nitrogen atoms at positions 1, 3, 4 and 6 leads to a second order effect. For example, benzene to pyridazine ($2e_{1uA}$ to $4b_2$, 2.6eV) and benzene to pyrimidine ($2e_{1uA}$ to $6a_1$, 2.0eV); the second order effect is smaller than the first order per nitrogen atom. For the other benzeneoid orbitals e_{1uB}, e_{2gA}, e_{2gB} and b_{1u} all the eigenvectors are equal so that only a second order effect is observed on the addition of a nitrogen atom.

i) Core Levels. The first six levels in all the azines are heavily localised (with eigenvectors greater than 0.98) and shift fairly constantly to higher binding energy as the number of nitrogen atoms increase. The separation of core levels of a particular type of atom (N or C) within a molecule is fairly small, the largest nitrogen separation being 1.4eV in 1,2,3,5-tetrazine (see Table 6). A similar separation occurs in the pyrimidine carbon 1s energies; pyrimidine is 1,2,3,5-tetrazine with the CH and N atoms reversed. Other pairs of molecules related in the same way and showing the same splits of carbon 1s and nitrogen 1s levels are:- pyridazine and 1,2,3,4-tetrazine (0.4eV); 1,2,3-triazine (0.7eV); 1,2,4-triazine (0.4eV). Such a

TABLE 6

Calculated Molecular Orbital Energies (eV)

Pyridine		Pyridazine		Pyrimidine		Pyrazine		1,3,5-Triazine		1,2,4-Triazine	
A_1	-426.37	A_1	-427.70	A_1	-427.07	A_1	-427.07	E'	-427.79	A'	-428.36
	-311.96		-312.35		-313.04		-427.07		-313.90		-428.09
	-311.40		-311.95		-312.60		-312.27		-35.8		-427.59
	-311.27		-38.8		-311.72		-312.25		-27.4		-313.48
	-35.85		-32.5		-38.0		-37.45		-19.05		-313.12
	-31.51		-25.4		-31.5		-34.64		-13.50		-312.78
	-24.95		-21.9		-25.7		-26.04	A_1'	-427.73		-39.74
	-21.04		-20.9		-21.8		-21.21		-313.88		-36.00
	-19.11		-17.9		-19.5		-19.67		-40.3		-32.89
	-17.21		-14.7		-17.8		-14.50		-23.0		-27.42
	-12.46	B_2	-427.73		-14.2		-12.01		-16.9		-26.27
B_2	-311.96		-312.36	B_2	-427.07	B_2	-312.28	A_2'	-22.2		-21.78
	-311.28		-311.94		-312.60		-312.25	A_2"	-19.3		-21.38
	-30.18		-32.1		-34.5		-30.82	E"	-14.4		-19.77
	-24.61		-26.2		-26.1		-25.33				-18.51
	-19.70		-19.3		-20.7		-20.55				-15.41
	-18.24		-18.1		-18.05		-18.60				-14.58
	-15.91		-12.1		-12.75		-16.62				-12.00
B_1	-16.79	B_1	-17.8	B_1	-17.9	B_1	-17.67			A"	-18.61
	-12.42		-13.25		-12.9		-13.43				-14.13
A_2	-12.12	A_2	-12.85	A_2	-13.4	A_2	-12.56				-13.45

TABLE 6 (Contd.)

1,2,3-Triazine		1,2,4,5-Tetrazine		1,2,3,4-Tetrazine		1,2,3,5-Tetrazine		Pentazine		Hexazine	
A_1	-428.84	A_{1g}	-429.23	A_1	-429.46	A_1	-429.50	A_1	-430.67	A_{1g}	-431.69
	-428.21		-314.15		-429.13		-428.66		-430.49		-46.60
	-313.15		-41.8		-313.72		-428.04		-429.60		-22.57
	-312.40		-27.7		-41.99		-314.17		-315.35	E_{2g}	-431.75
	-40.46		-22.3		-34.81		-41.26		-44.47		-31.65
	-33.14		-15.45		-28.36		-36.47		-37.80		-13.62
	-27.00	B_{2u}	-429.25		-22.39		-28.32		-29.40	E_{1u}	-431.72
	-21.88		-314.16		-22.02		-22.17		-22.72		-41.09
	-19.18		-34.7		-17.67		-17.95		-19.70		-18.29
	-16.91		-21.1		-12.68		-15.81		-16.19	B_{1u}	-431.76
	-12.46		-15.7	B_2	-429.49		-12.35		-13.96		-17.32
B_2	-429.25	B_{3u}	-429.23		-429.13	B_2	-428.69	B_2	-430.68	B_{2u}	-25.12
	-313.16		-38.7		-313.72		-314.22		-429.60	A_{2u}	-22.34
	-35.13		-22.7		-37.54		-35.70		-39.52	E_{1g}	-17.14
	-26.70		-16.9		-27.82		-27.29		-30.08		
	-21.44	B_{1g}	-29.5		-19.85		-22.02		-23.73		
	-18.65		-12.35		-16.25		-19.02		-17.30		
	-13.14	B_{1u}	-19.8		-13.36		-13.71		-12.25		
B_1	-18.67	B_{3g}	-14.45	B_1	-19.58	B_1	-19.29	B_1	-21.02		
	-13.73	B_{2g}	-15.35		-14.41		-14.37		-15.64		
A_2	-13.89			A_2	-14.93	A_2	-14.57	A_2	-16.05		

correlation, if it could be extended to other series of molecules would enable quite accurate predictions of the theoretical separation energies of core electrons to be made. The experimental separations are likely to be smaller than those calculated, but gas phase spectra, which are not readily obtainable with present instrumentation would be necessary for significant comparisons. Correlation with solid phase spectra would be better than for the azoles, since there are no N-H bonds in the azines to generate hydrogen bonded polymers.

ii) π-Electron Energy Levels. The occupied π-orbitals of benzene are a_{2u} and e_{1g}. Although the e_{1g} benzenoid levels are split in all the azines except hexazine and 1,3,5-triazine, the energy separation is less than 2eV in all cases; if an average value of the pairs is taken then the e_{1g} behaves in a similar fashion to the $1a_{2u}$ orbital. Furthermore these π-levels vary in an almost superimposable manner with the azine σ-analogues of the $3a_{1g}$, $2e_{2g}$ and $1b_{2u}$ orbitals. In all of these cases there is a largely monotonic shift to higher binding energy as the number of nitrogen atoms in the ring increases; this is to be expected since the geometric differences are small, the molecules have a constant number of electrons, which are being attracted to an increasingly positive environment with an associated increase in binding energy.

iii) The Inner Valency Shell Orbitals. These orbitals, of similar character to the benzene $2a_{1g}$, $2e_{1u}$ and $2e_{2g}$ orbitals, cover the range 7σ to 11σ and are largely 2s(N) and 2s(C) in nature; there are no nodes in 7σ ($2a_{1g}$) so that this is stabilised by all the atoms in the ring. Although the eigenvectors are larger at N than C in this series they cannot be considered as solely 2s(N) levels. Thus, although there is a progressive energy shift to hexazine from benzene, and although the largest change (2.8eV) lies between benzene and pyridine, the separation of the free atom 2s orbital energies is 6.52 in the Hartree-Fock limit. Thus considerable delocalisation is implied on energetic as well as eigenvector grounds.

The energetic shifts of the pseudo $2e_{1u}$ orbitals are very similar to the $2a_{1g}$ changes, especially if the mean value of the orbital energies are taken (except in 1,3,5-triazine and hexazine this formerly degenerate pair are separated). The one exception to this general trend is pyridazine where there is an increase in energy going from pyrimidine to pyridazine in the average of the pseudo $2e_{1u}$ pair while $2a_{1g}$ drops steadily. This, together with the apparently capricious separation of the energies of the two pseudo-degenerate orbitals (0.4eV is pyridazine, 4.0eV in 1,2,4,5-tetrazine) can be explained by the effect of the nodal positions in the two orbitals. The first order effect leads to an increase in binding energy of about ~2.5eV for each nitrogen atom introduced; thus orbital $3b_{2u}$ in pyrazine which has two nitrogens placed correctly for a first order effect resulting in a lowering of energy by ~5.0eV compared to benzene. In contrast the other half of the pyrazine degenerate pair, orbital $2b_{3u}$, has the nitrogens placed correctly for two third order effects only. This orbital is not lowered terribly much therefore, and results in a large separation of the formerly degenerate levels. On this basis it would be expected that 1,2,3,5-tetrazine should show a large separation. There are however two effects opposing this, 1) the first order lowering by N2 is partially offset by second order tendencies of N1 and N3, 2) there is some second order effect on e_{1uB} orbital due to there being nitrogen atoms off-axis, which did not apply to pyrazine. It is having nitrogen atoms off-axis which causes the large separation in 1,2,4,5-tetrazine's pseudo-e_{1u} pair. Thus, the e_{1uA} orbital has lowering by four second-order effects as has the e_{1uB} orbital. However the second order effect on the e_{1uA} is about 1.2eV (Table 5b) per nitrogen atom while it is about 2.5eV in e_{1uB}; this results in the split for 1,2,4,5-tetrazine being large. (The uneven distribution of electron density in e_{1uB} does not conflict with the wave's natural intensity distribution, which is in contrast to the e_{1uA} type where the natural tendency is to have the wave at its most intense away from the second order nitrogen.)

Pyridazine having a higher average value than that expected from the $2a_{1g}$ orbital for the pseudo $2e_{1u}$ pair is caused by the orbital $5a_1$ being at an unexpectedly high level; examination of the eigenvectors shows that, while the orbital $5a_1$ is of e_{1uA} character, the largest eigenvectors involve the carbon atoms so that the expected second order perturbation is less than usual. In addition, the gap between the energy levels is small because this molecule has two nitrogen atoms off the e_{1uB} axis.

The second degenerate pair in this region, the benzenoid $2e_{2g}$ and $1b_{2u}$ orbitals show similar effects to the other two

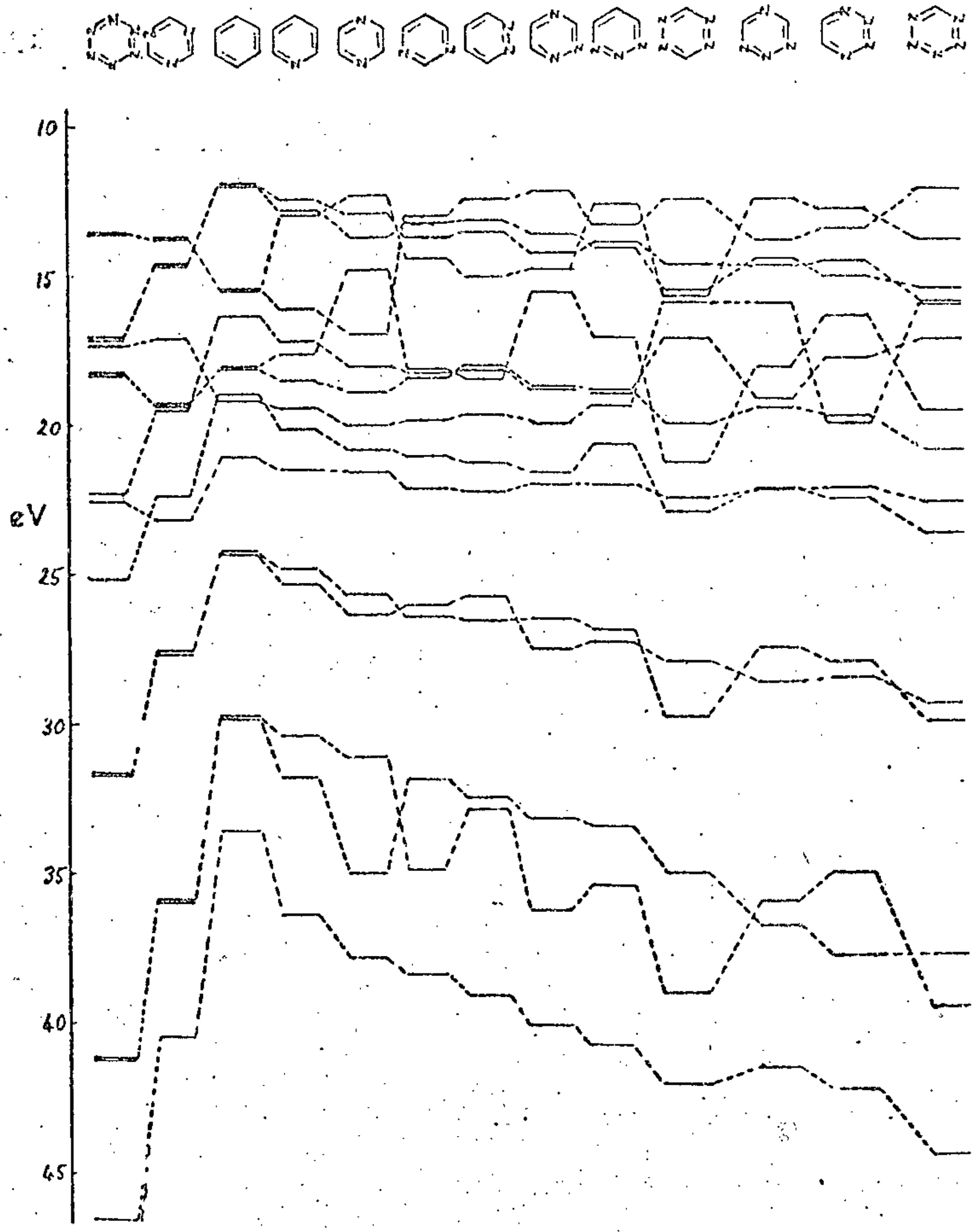

Figure 3 Overall Correlation Diagram of Ionisation Potentials

Figure 4 Least Squares Correlation Diagram

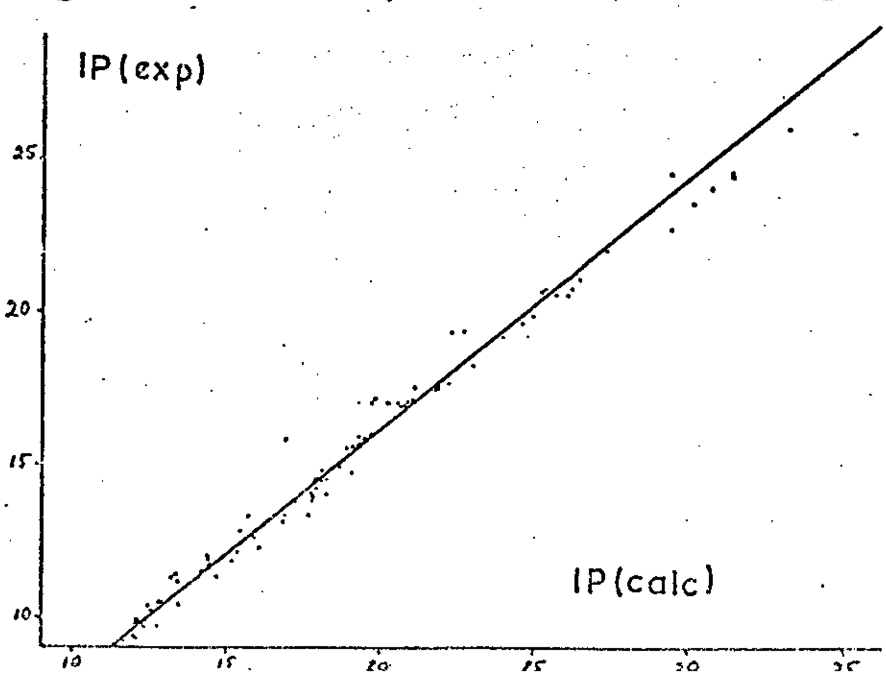

orbital types. In $2e_{2g}$ the second order effect of the nitrogen atom is about 1.2 ± 0.3eV, and the third order effect is about 0.6eV in $2e_{2gB}$. The entirely tangential orbitals of pseudo $1b_{2u}$ character vary in energy to a lesser extent than the others. This is a natural consequence of the difference in orbital energies between 2s(N) and 2s(C) while that for 2pN and 2pC is 3.6eV.

iv) Outer Valency Shell Orbitals. Replacement of $\geq$ CH in benzene by $\geq$N: removes a C-H bonding level and introduces a "lone pair" level, characterised by very high coefficients of 2s(N) and nitrogen radial functions in the molecular orbital. The first ionisation potential from any of the azines is greater than 9eV, so that these lone pair orbitals cannot be termed non-bonding. The total populations of the nitrogen atoms shows that they are overall effectively sp^2 hybridised, but the "lone pair" orbitals have sharply varying proportions of 2s and 2p. For n nitrogen atoms n lone pair orbitals would be excepted, and would be non-degenerate in most cases. Since they contain a high electron density outside the internuclear regions they are expected to be the lowest binding energy σ-species within a molecule. Complications arise from the lone pair orbitals having the same symmetry (radial) as the C-H bonding levels; namely that mixing of these two types can occur provided that the lone pair orbital has an energy comparatively near the appropriate CH level. The principal CH bonding levels in benzene are, in increasing binding energy, $3e_{2g}$, $3e_{1u}$, $2b_{1u}$ and $3a_{1g}$, although $3e_{2g}$ has about 50% tangential orbital

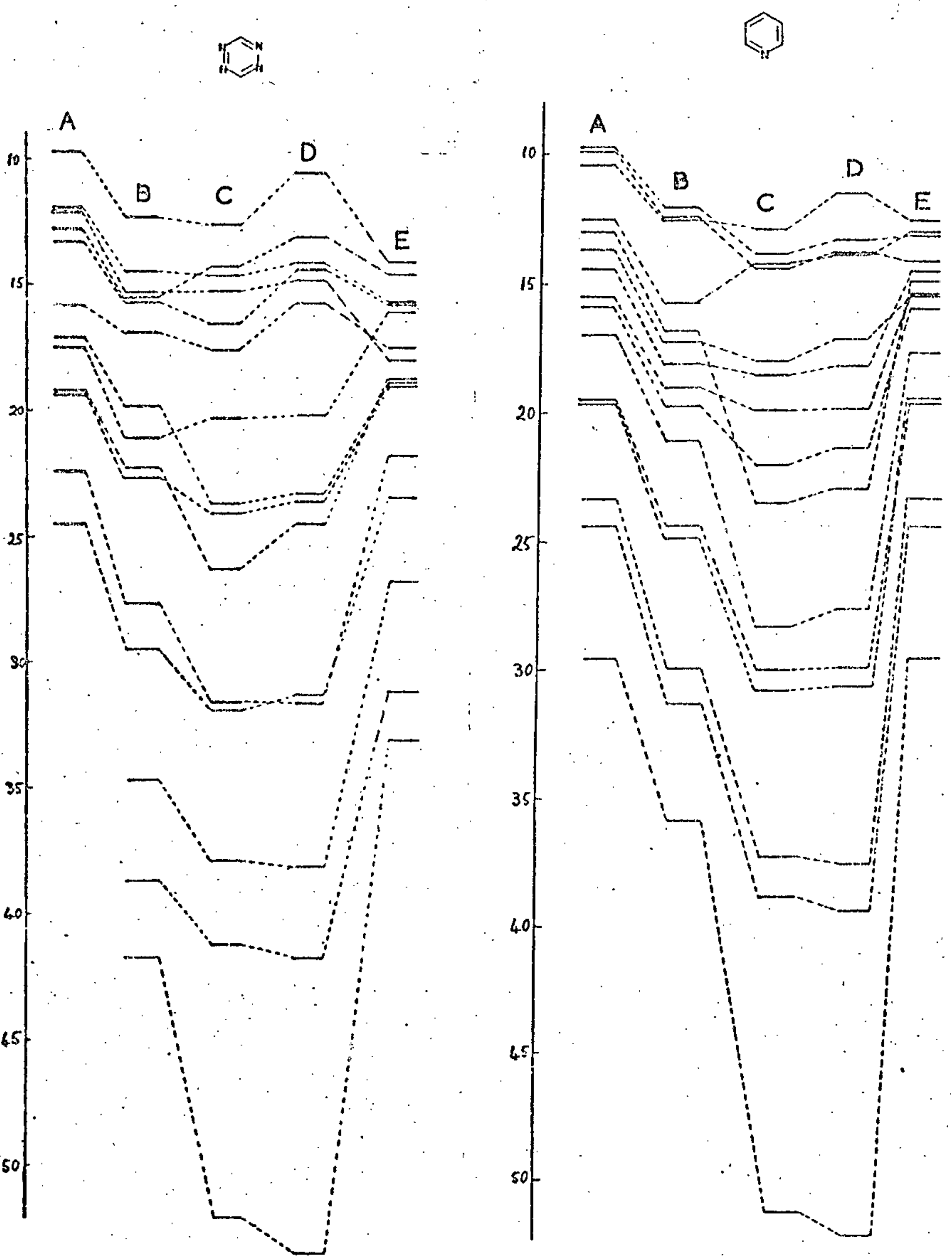

Figure 5. Correlation of Experimental Ionisation Potentials (A) with those predicted by the LCGO(B), CNDO-2(C), INDO(D) and EHM(E) methods.

character in benzene itself. If the lone pair orbitals were strictly localised on nitrogen then the distinction between $3e_{2g}$ and $3e_{1u}$ would disappear in several cases; for example $3e_{2gA}$ and $3e_{1uA}$ would both be symmetric lone pair combinations in pyrimidine, similarly $2b_{1u}$ and $3a_{1g}$ would be the symmetric lone pair combination (a_1') in 1,3,5-triazine. Thus residual amounts of C-H bonding character have enabled the completion of the overall correlation diagram (Figure 3), which shows how the occupied orbitals of the azines correlate to those of benzene, without loss of distinction between the symmetry species.

In the diazines there are two lone pair orbitals evident, which can be described as ($N_i \pm N_j$) where N_i and N_j are the lone pair orbitals of nitrogen atoms i and j. In pyrimidine and pyridazine the symmetric combination lies to higher binding energy than the anti-symmetric combination; for pyrazine the opposite is true. For pyrazine the $3e_{2gB}$ and $3e_{1uB}$ orbitals are nodal at the nitrogen atoms, and hence cannot be lone pair orbitals; however the lone pair combinations are satisfied by $3e_{2gA}$ and $3e_{1uA}$ and, since $3e_{2g}$ lies to lower binding energy than $3e_{1u}$ in benzene, with aza-substitution likely to have a similar effect in the two cases, the order of the lone-pair orbitals is interpretable. For both pyrimidine and pyridazine the lowest binding energy benzenoid molecular orbitals available for the lone pairs are e_{2gA} and e_{2gB}; a degenerate pair. In both molecules e_{2gB} has a node between the nitrogen atoms; since they are then unlikely to perturb the e_{2gB} level as much as in the e_{2gA} series, the

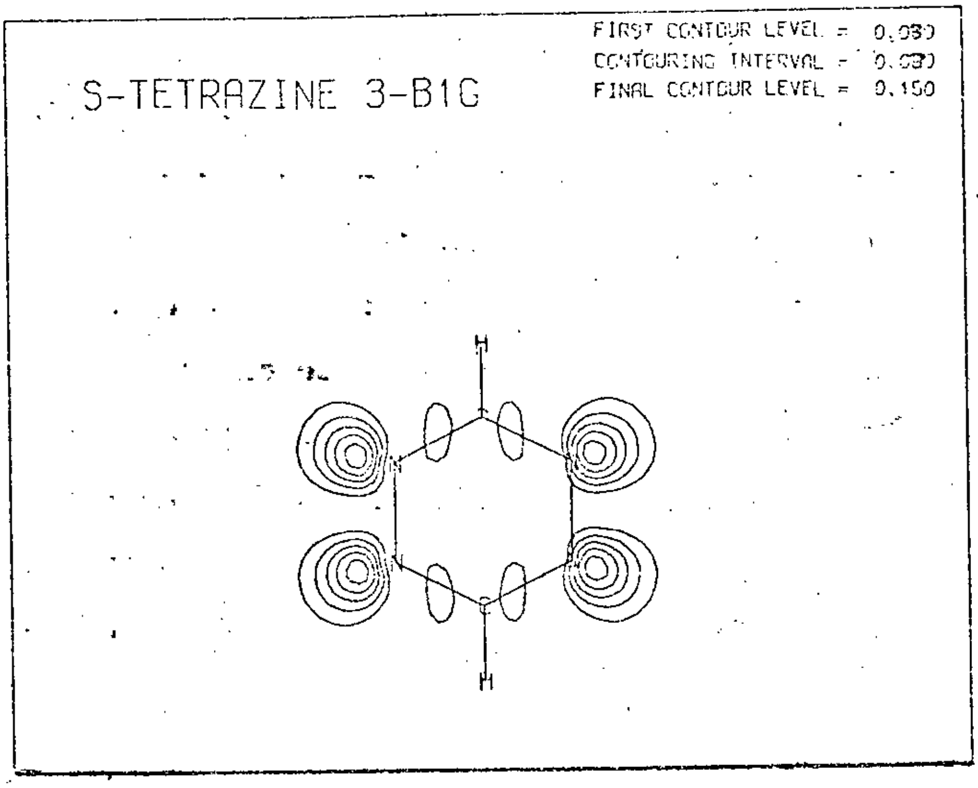

Figure 6a (above) Lowest IP combination of lone pair orbitals for 1,2,4,5-tetrazine

Figure 6b (below) Second lone pair combination

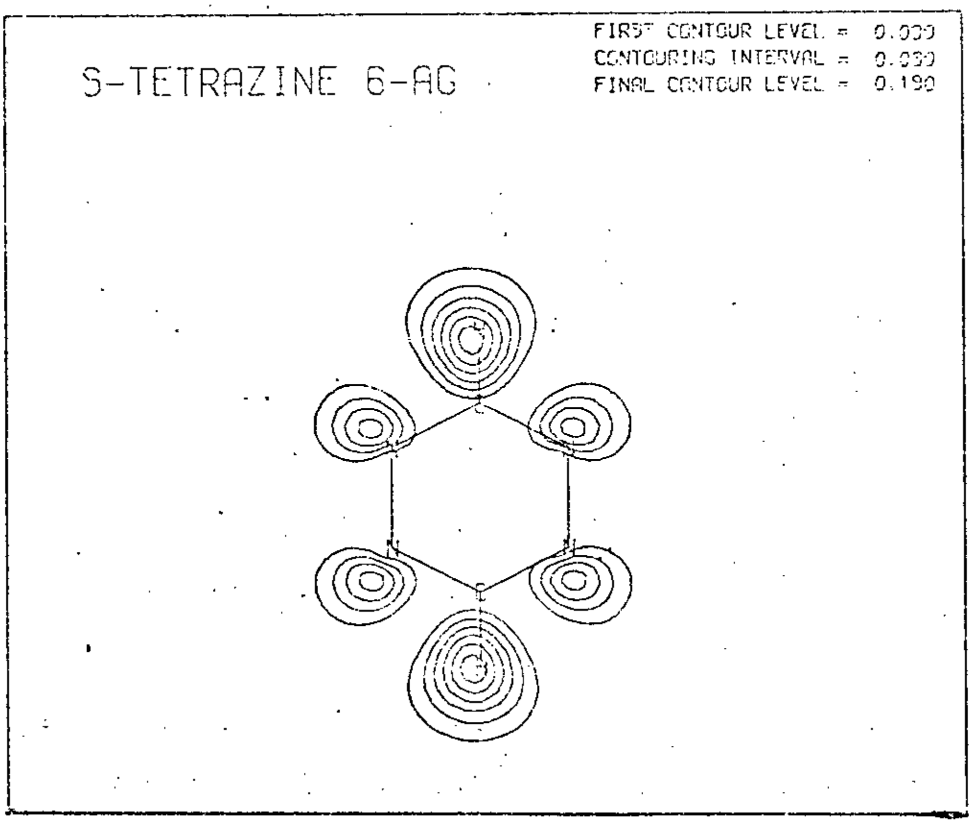

e_{2gB} will occur at lower binding energy.

Several apparently anomalous lone pair combinations are explained similarly: thus in 1,2,4-triazine no orientation of nodal planes can lead to the symmetric $(N_1 + N_2 + N_3)$ combination, which can only arise with $3a_{1g}$ whose binding energy is too high to be capable of supporting a lone pair combination of three nitrogen atoms. A similar argument applied to 1,2,3,5-tetrazine shows that $N_1 + N_2 + N_3 + N_5$ would again be of $3a_{1g}$ type, resulting in the totally symmetric combination being replaced by an orbital of lower binding energy - a $2b_{1u}$ type.

Since the nitrogen lone pair levels occur at low binding energy, it is unlikely that there will be a significant interaction with CH levels unless there are several nitrogen atoms such that one of the linear combinations is of high enough binding energy to appear in the CH region. Such an interaction does occur in 1,2,4,5-tetrazine where there are five levels high in lone pair character; of these $5a_g$ and $6a_g$, separated by 6.8eV are the symmetric and anti-symmetric combinations of $(N_1 + N_2 + N_4 + N_5)$ with $(C_3H + C_6H)$. Although the effect is less marked, the symmetric lone pair combination, $(N_1 + N_3 + N_5)$ of 1,3,5-triazine shows similar evidence of interaction with the symmetric CH levels since the two orbitals $5a_1'$ (largely lone pair) and $4a_1'$ (largely CH) are separated by some 6eV. This and the $5a_g/6a_g$ separation of 1,2,4,5-tetrazine are the largest single separations of orbitals of the same symmetry in the outer valency shell of the azines. This can be attributed to mixing of the form shown below.

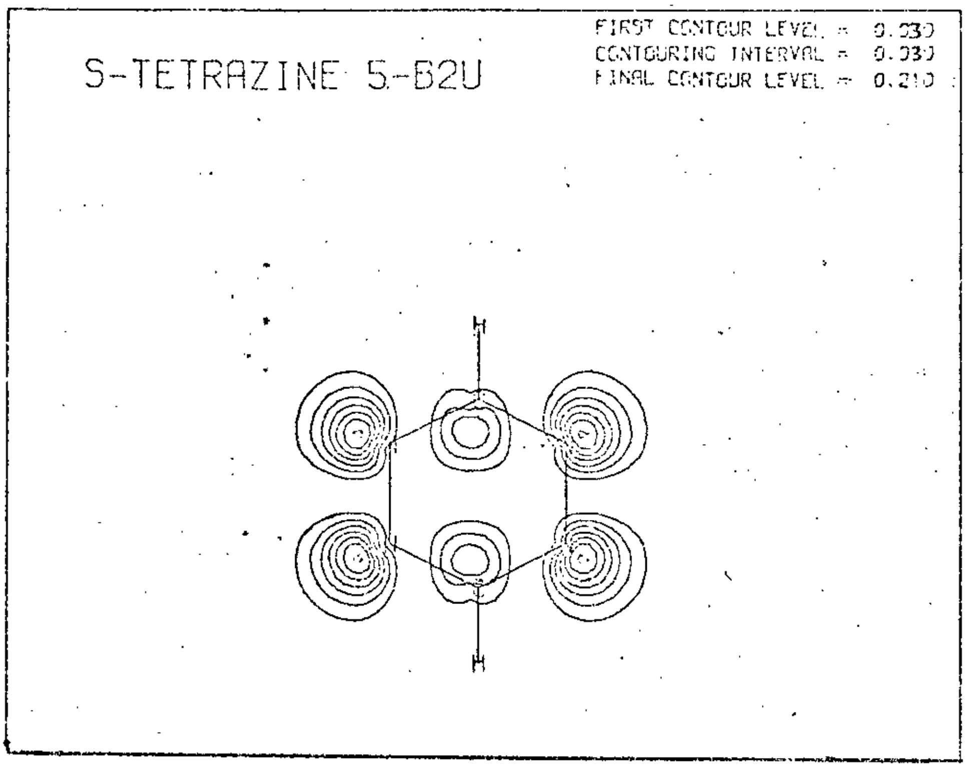

Figure 6c (above) Third lone pair combination

Figure 6d (below) Fourth lone pair combination

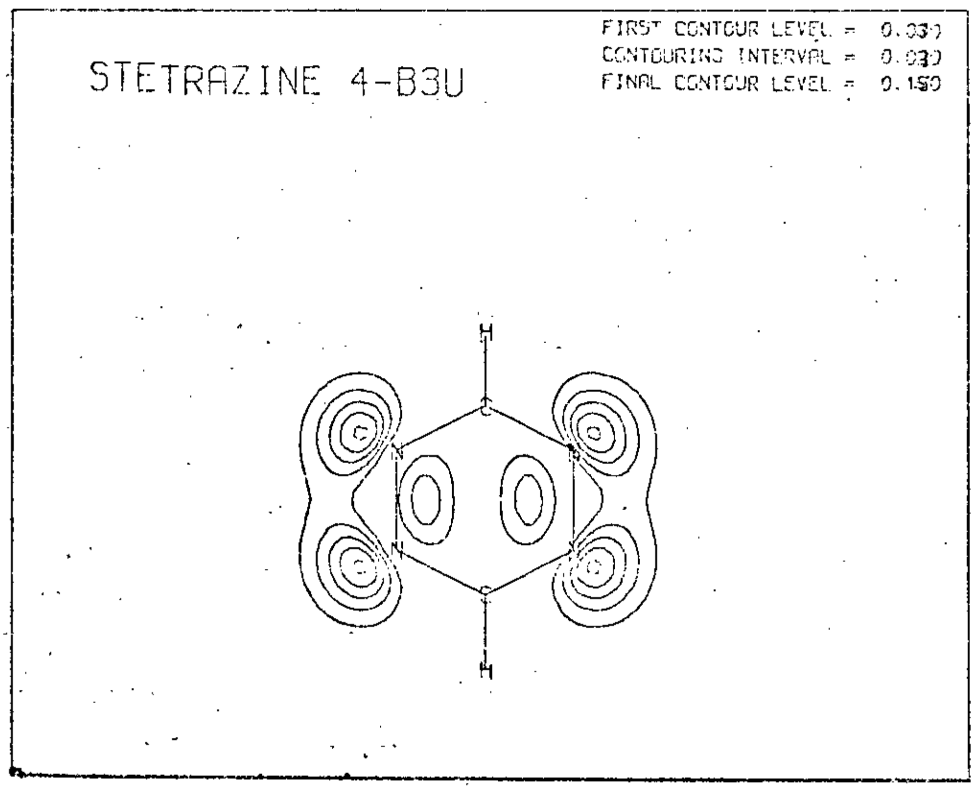

TABLE 7

Azine Lone Pair Orbitals and their Correlation with Benzene

Molecule	S.O.	B.S.O.	Nature
Pyridine	$11a_1$	$3e_{2gA}$	N_1
Pyridazine	$8b_2$	$3e_{2gB}$	N_1-N_2
	$10a_1$	$3e_{2gA}$	N_1+N_2
Pyrimidine	$7b_2$	$3e_{2gA}$	N_1-N_3
	$11a_1$	$3e_{2gB}$	N_1+N_3
Pyrazine	a_g	$3e_{2gA}$	N_1+N_4
	b_{2u}	$3e_{1uA}$	N_1+N_4
1,2,3-Triazine	$11a_1$		$N_1-N_2+N_3$
	$7b_2$	e_{2gB}	N_1-N_3
	$10a_1$	e_{2gA}	$N_1+N_2+N_3$
1,2,4-Triazine	$18a'$	e_{2gB}	$N_1-N_2+N_4$
	$17a'$	e_{2gA}	N_2+N_4
	$16a'$	e_{1uB}	N_1-N_4
1,3,5-Triazine	$6e'$	e_{2g}	$2N_1-N_3-N_5$
			N_3-N_5
	$5a_1'$	$2b_{1u}$	$N_1+N_3+N_5$
1,2,3,4-Tetrazine	$10a_1$	e_{2gA}	N_2+N_3
	$8b_2$	e_{2gB}	N_2-N_3
	$7b_2$	e_{1uA}	N_1-N_4
	$9a_1$	e_{1uB}	N_2+N_3
1,2,3,5-Tetrazine	$11a_1$	e_{2gA}	$N_1+N_3-N_2-N_5$
	$7b_2$	e_{2gB}	N_1-N_3
	$10a_1$	b_{1u}	N_2-N_5
	$9a_1$	e_{1uA}	$N_1+N_2+N_3-N_5$
1,2,4,5-Tetrazine	$3b_{1g}$	e_{2gB}	$N_1+N_4-N_2-N_5$
	$6a_g$	e_{2gA}	$N_1+N_2+N_4+N_5-$ (C_3H+C_6H)
	$5b_{2u}$	e_{1uA}	$N_1+N_5-N_2-N_4$
	$4b_{3u}$	e_{1uB}	$N_1+N_2-N_4+N_5$
	$5a_g$	a_{1g}	$N_1+N_2+N_3+N_4+C_3H+C_6H$.
Pentazine	$11a_1$	e_{2gA}	N_3
	$10a_1$	b_{1u}	$N_1+N_5-N_2-N_4$
	$7b_2$	e_{2gB}	$N_1-N_2+N_4-N_5$
	$6b_2$	e_{1uB}	$N_1+N_2-N_4-N_5$

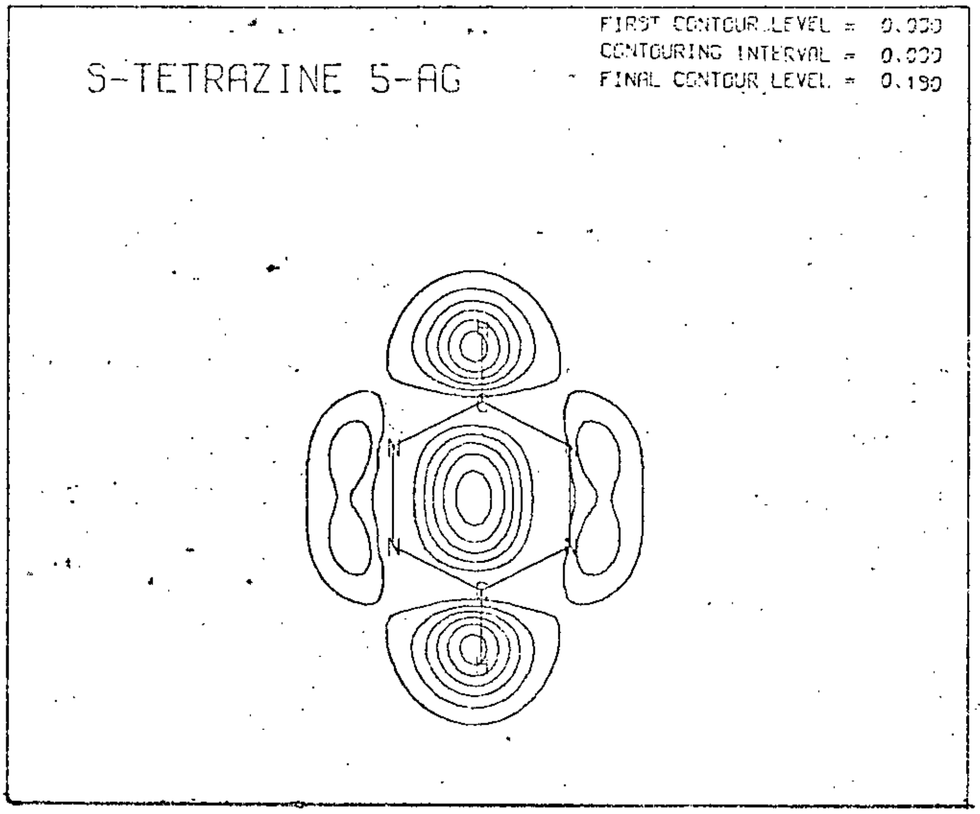

Figure 6e (above) Fifth lone pair combination

Figure 7a (below) C-H bonding level in pyridine

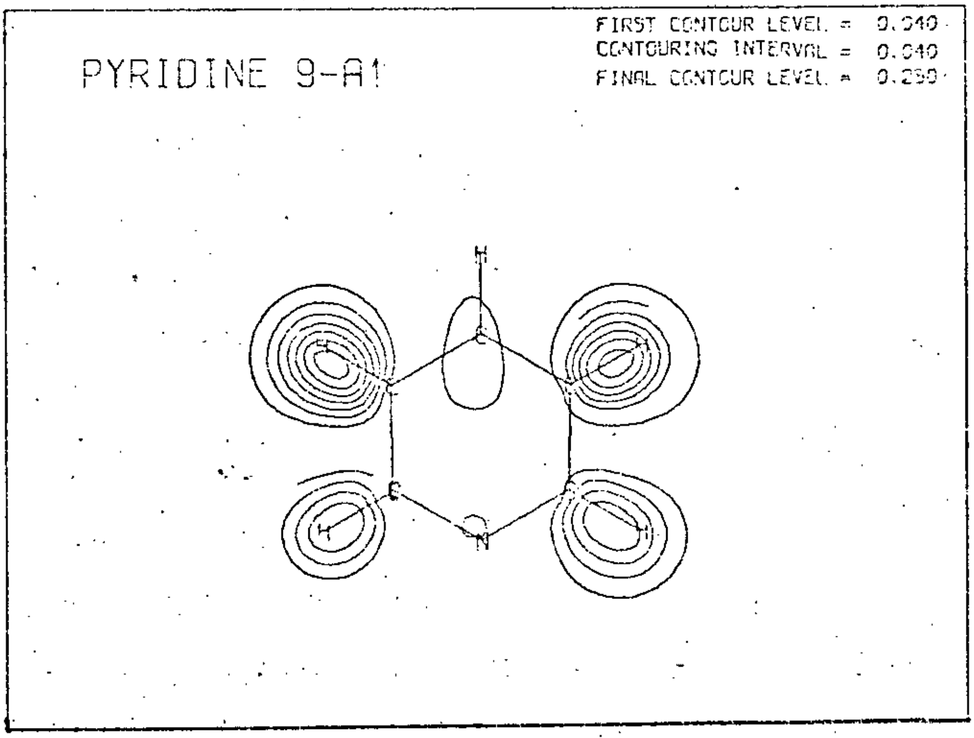

$$0.45(N_1+N_3+N_5) - 0.18(C_2H+C_4H+C_6H)$$

$N_1+N_2+N_3$

$C_2H+C_4H+C_6H$

$$0.16(N_1+N_3+N_5) + 0.2(C_2H+C_4H+C_6H).$$

In Table 7 the calculated lone pair combinations together with their assignment in terms of benzene-like orbitals are recorded. In all cases it is clear that the orbitals have been filled in the order $3e_{2g}>3e_{1u}>2b_{1u}>3a_{1g}$ i.e. in a reverse aufbau principle. This is consistent with their energies in benzene.

Correlation of Theoretical and Experimental Energy Levels

Various workers have studied the photo-electron spectra of benzene and the azines, but of these Lindholm et al. have studied the widest range of binding energy by the use of He(I) and He(II) radiation. Figure 4 shows the correlation of the theoretical and experimental energy levels based upon Koopman's theorem and the data of Table 6. In correlating the two series line for line it has been implicitly assumed that the ordering of the orbitals is correctly given by the calculations. This is supported by comparing the grouping of the experimental and calculated levels (Table 8). In all cases, except for pyrazine the number of lines within the theoretical groups is in agreement with experiment. Further support comes from the observation that in each diazine spectrum there is at least one peak near 16eV (experimental) that has a much lower intensity than adjacent peaks. The cross-section of 2s electrons to He(I) irradiation is much

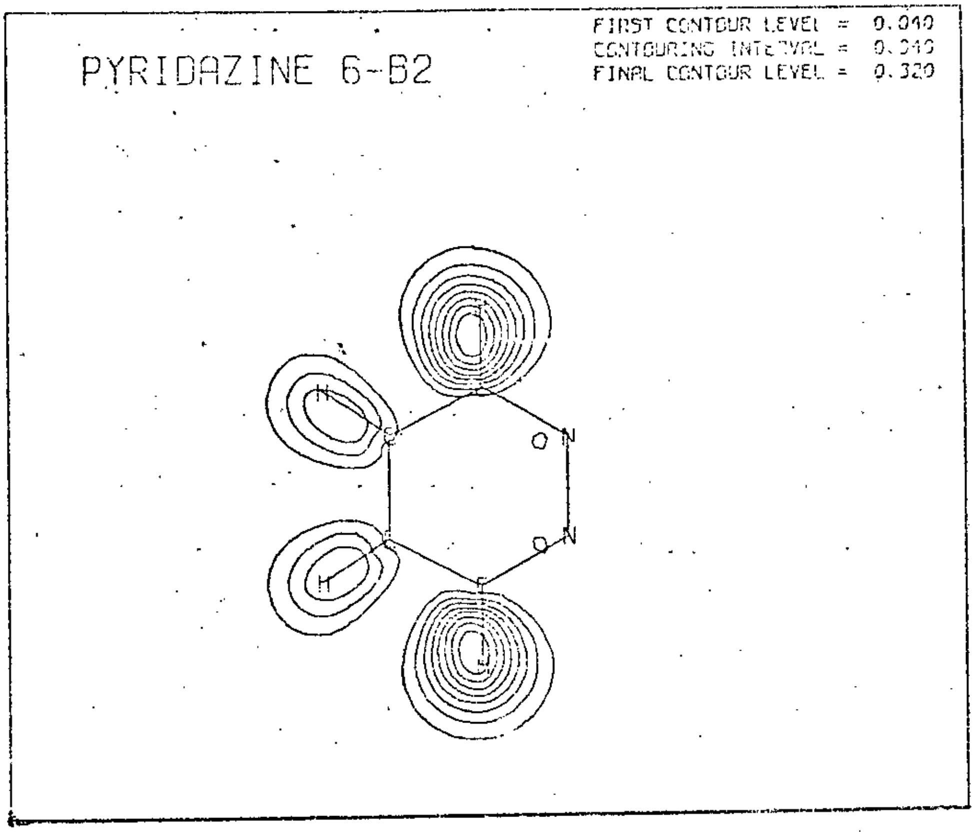

Figure 7b (above) C-H bonding level in pyridazine

Figure 7c (below) C-H bonding level in 1,3,5-triazine

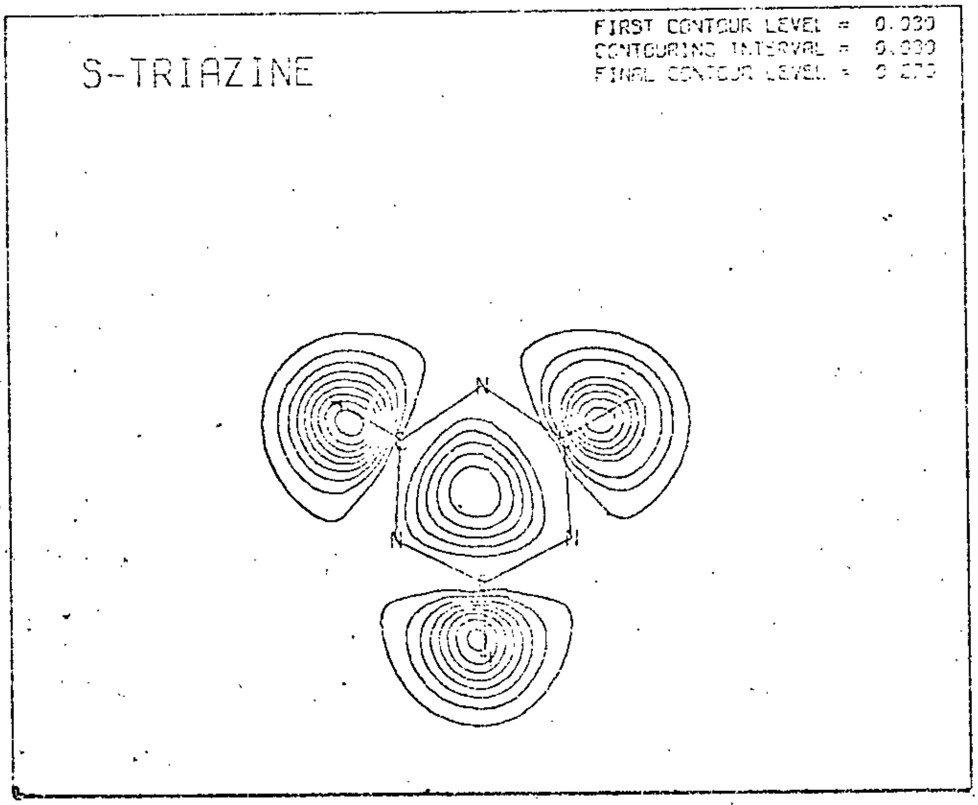

lower than that of 2p electrons, so the low intensity of this peak is therefore consistent with high 2s character. This peak and the corresponding benzene peak to $2b_{1u}$ which has a carbon contribution almost equally split between $2s_C$ and R_C orbitals.

Assuming then that, since the calculations predict the correct groupings, the orbital ordering within a group is correct, the experimental data was plotted against the calculated energies. (Figure 5). If energy levels beyond an observed ionisation potential of 22eV (i.e. He(I) only used), the points yield a least squares fit of the form IP(exp) = 0.81 IP(calc)-0.1eV, with a standard deviation of 0.2eV; if all 92 points are included the relationship is IP(exp) = 0.785 IP(calc) + 0.33eV with a standard deviation in the slope and intercept of 0.01 and 0.20eV respectively, while the overall standard deviation is 0.540. This line is very similar to that found for the azoles, and effectively passes through the origin.

Table 8 also contains the major groupings of the energy levels as determined by the INDO, CNDO-2 and Extended Huckel Methods (EHM) procedures; the data for the EHM was obtained from Lindholm's work. It is clear that none of these semi-empirical methods give as good a prediction of the groupings as the non-empirical results do. Further, even when the semi-empirical energies are treated in the best possible manner the least squares fits of the experimental and calculated energies is very much poorer (the best possible treatment is to assume that each semi-empirical method gives the correct ordering although of

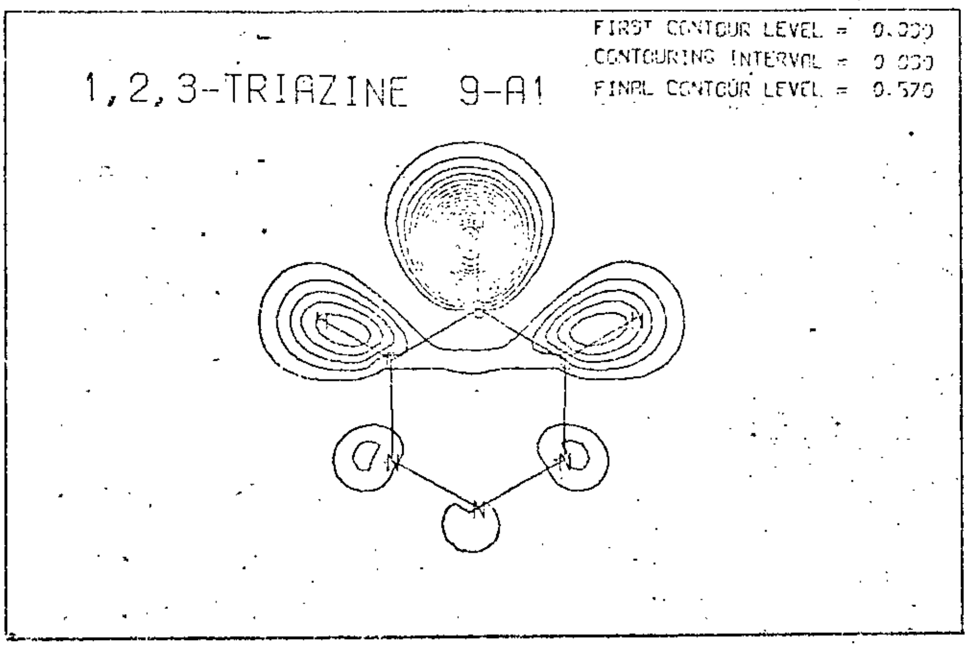

Figure 7d (above) C-H bonding level in 1,2,3-triazine

Figure 7e (below) C-H bonding level in 1,2,3,4-tetrazine

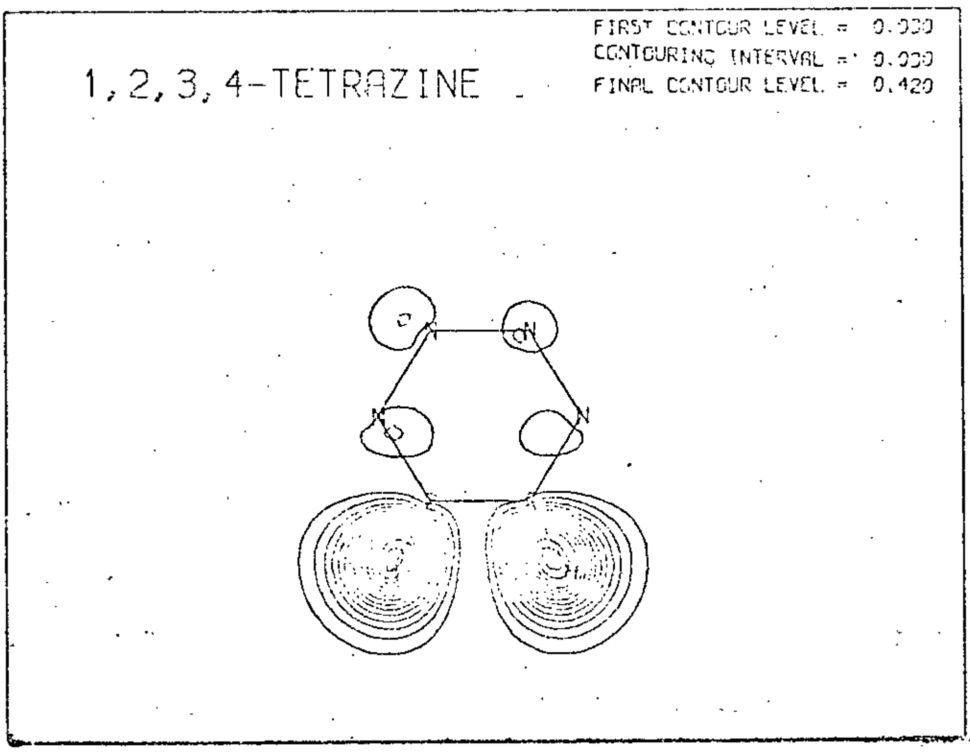

TABLE 8

Comparison of Experimental and Calculated Orbital Energy Groupings

	C_6H_6	Pyridine	Pyridazine
Expt.	2:3:5:2:2:1	3:7:2:2:1	4:6:2:(?)*
LCGO	2:3:4:1:2:2:1	3:7:2:2:1	4:6:2:2:1
INDO-2	4:3:1:1:3:2:1	4:5:3:2:1	4:2:1:2:1:2
INDO	4:3:1:1:3:2:1	4:5:3:2:1	4:2:1:2:1:2
EHT	4:5:1:2:2:1	3:6:1:2:2:1	10:2:2:1

Pyrimidine	Pyrazine	1,3,5-Triazine
4:3:3:2:1:(?)*	2:2:3:(2+1):2:1	2:2:1:4:1:2
4:3:3:2:1:1:1	4:6:2:1:1:1	4:1:3:2:2:2:1
4:2:1:2:1:2:2:1	4:2:1:2:1:2:1:1:1	2:2:3:2:1:2:2:1
4:2:1:2:1:2:2:1	1:4:1:3:1:2:1:1:1	2:2:3:2:1:2:2:1
3:1:3:3:2:1:1:1	2:2:6:2:1:2	2:5:3:2:2:1

* Experimental He(II) spectra not yet reported

course not all calculations can be correct simultaneously. Any attempt to force experimental groupings on the semi-empirical methods would only worsen their least squares fit.) Thus the least squares fits for 77 points (benzene was omitted from these calculations) are:- (1) CNDO-2; IP(exp) = 0.546 IP(calc) + 3.71eV with the standard deviation in slope and intercept being 0.015 and 0.342eV; (2) INDO; IP(exp) = 0.504 IP(calc) + 4.987eV, with standard deviations in the slope and intercept of 0.022 and 0.542eV; (3) EHM, IP(exp) = 1.359 IP(calc) - 7.485eV, with the standard deviations being 0.037 and 0.651eV. From this it is evident that, even when used in the best possible way, the semi-empirical methods are very much poorer in predicting experimental ionisation potentials. This is very much emphasized when the overall standard deviation, or scatter, is directly used; the figures are:- non-empirical, 0.540; CNDO-2, 1.026; INDO, 1.69 and EHM, 1.05eV.

The major problem in interpreting photo-electron spectra is the identification of the symmetry of the orbital from which the electron is ejected. To circumvent this problem the experimental spectra are often calibrated by the results of semi-empirical or non-empirical quantum chemical calculations. Before this calibration can be reliable two criteria must be met (a) the major groupings must be reproduced by the calculated energy levels, (b) the calculated levels must not be too dependent on input parameters. Consider first the EHM method:- the orbital energies cover roughly the experimental range, but are very severely cramped in the outer valency shell. Assignments are thus more uncertain and even the primary groupings are different to define in some cases. As far as a choice of parameters is concerned, that made by Lindholm gives results that are numerically similar to experiment in the 12-16eV region, but which differ considerably at both ends of the observed spectrum, thus accounting for a differing slope from the remaining least squares fits.

The CNDO-2 and INDO methods reproduce the groupings better then EHM but grossly exaggerate the spread of the energy levels. For example the lowest σ and lowest π energy levels (highest binding energy) are shifted to very high binding energy compared to the experimental values. It seems likely that this effect is due to the omission of the core levels and the reduction of the nuclear charge, so that the innermost σ and π levels become pseudo core-levels. Both these methods give identical orbital ordering in most cases. The parameters used in CNDO-2 and INDO are those originally programmed by Pople; Lindholm has however reparameterised the INDO procedure to give a better fit of experimental and calculated data. This SPINDO procedure has improved results for hydro-carbons but has not yet been extended to heterocycles.

As has already been pointed out the non-empirical calculations fit the experimental groupings quite well, although there is a tendency to over-estimate the value of the ionisation potential. The only parameter for L.C.G.O. calculations is the length of the basis set which does not seem important for furan and pyrrole, thiophene, pyrazine or benzene.

It would therefore appear that the semi-empirical methods are not sufficiently accurate to predict correctly the experimental ionisation potentials. This is despite it being possible to establish linear relationships between observed and calculated values, these are probably of little use owing to slope and intercept variations; Thus only the L.C.G.O. series have significance.

Since there are quite marked differences between the assignments of Lindholm & Heilbronner it is appropriate to compare their assignments with those obtained with the present non-empirical calculations.

In pyridine, the closely spaced group at lowest binding energy is generally agreed to consist of the lone pair orbital ($11a_1$) and the two π-levels ($1a_2$ and $2b_1$), the non-empirical calculations all place the ionisation potential order as $1a_2 < 2b_1 < 11a_1$ while both Lindholm and Heilbronner place the first ionisation potential as $11a_1$ with the π-levels in either order. Given the closeness of the levels, it seems unlikely that any single calculation can assign the orbitals unequivocally, although the consistency of the non-empirical results with different basis sets seems likely to make them correct. The next seven orbital energies to higher binding energy are assigned very similarly to those of Lindholm, except that, within each of the pairs $9a_1/5b_2$ and $11a_1/6b_2$, the a_1 orbital is predicted to appear at lower binding energy.

In pyrimidine, pyridazine, 1,3,5-triazine and 1,2,4,5-tetrazine the assignments agree very closely with those of Lindholm for almost all of the observed lines, the sole exceptions being trios of closely spaced lines near 14eV in the diazine spectra, and a single reversal of the innermost π-level ($1a_{2''}$) in 1,3,5-triazine with the symmetric lone pair level ($5a_1'$). Heilbronner's assignments differ from those of the non-empirical calculations and Lindholm's in the interchange of individual pairs of lines for each molecule. In the case of 1,2,4,5-tetrazine, the agreement with Lindholm is good, with an interchange of $4b_{3u}$ and $4b_{1u}$ and the raising of the $5a_g$ orbital being sufficient to bring the calculations into identical order with the non-empirical results. The second and third π-levels appear at a much higher binding energy in Heilbronner's calculations.

Thus, in summary then, there is considerably better agreement between the results obtained by Lindholm and the non-empirical calculations than between the latter and

Heilbronner's Huckel calculations. The non-empirical calculations thus favour Lindholm's assignments with the differences occurring within groups of closely spaced lines.

Dipole Moments and Charge Distributions

The dipole moments and charge distributions of the azines are listed in Tables 9 and 10 respectively. Only

TABLE 9

Dipole Moments and Vector Components in 6-Membered Rings

Molecules	μ(exp)	μ(calc)	μ_{11}	μ	μ_{σ}	μ_{π}
Pyridine	2.15	1.82	-1.82	0.0	-1.65	-0.17
Pyridazine	4.22	3.65	-3.65	0.0	-3.16	-0.49
Pyrimidine	2.44	2.15	-2.15	0.0	-1.83	-0.32
1,2,4-Triazine	-	2.16	1.21	-1.79	-1.93 (-124.8°)	-0.24 (-118.0°)
1,2,3-Triazine	-	4.41	-4.41	0.0	-3.87	-0.54
1,2,3,4-Tetrazine	-	4.01	-4.01	0.0	-3.51	-0.51
1,2,3,5-Tetrazine	-	2.48	-2.48	0.0	-2.16	-0.32
Pentazine	-	2.84	-2.84	0.0	-2.35	-0.49

three of the known azines which possess dipole moments have had them reported. The agreement with the experiment values[25] is quite good with the calculated value being some 86% of the experimental; it would be reasonable to expect that the calculations similarly underestimate the values which will be found once the ring systems are available. The position of the nitrogen atoms would appear to dominate the magnitude of the dipole moment. When the nitrogen atoms are all at one end of a molecule the dipole moment is high (for example,

TABLE 10

Population Analysis of the Azines

<u>Pyridine</u>	N	C2,C6	C3,C5	C4
1s + 2s	3.5116	3.0526	3.0632	3.0563
2pσ	2.7303	2.0325	2.1636	2.1695
2pπ	0.9933	1.0094	0.9984	0.9911
Total	7.2352	6.0945	6.2252	6.2169
H	–	0.7813	0.7821	0.7818

<u>Pyridazine</u>	J1,N2	C3,C6	C4,C5
1s + 2s	3.5392	3.0444	3.0642
2pσ	2.5787	2.0541	2.1782
2pπ	1.0109	1.0074	0.9817
Total	7.1288	6.1059	6.2241
H	–	0.7722	0.7692

<u>Pyrimidine</u>	N1,N3	C2	C4,C6	C5
1s + 2s	3.5339	3.0162	3.0526	3.0689
2pσ	2.6942	1.9766	2.0704	2.1676
2pπ	1.0156	1.0060	0.9760	1.0107
Total	7.2442	5.9988	6.0990	6.2472
H	–	0.7622	0.7676	0.7701

<u>Pyrazine</u>	N	C
1s + 2s	3.4902	3.0550
2pσ	2.7382	2.1144
2pπ	0.9951	1.0025
Total	7.2235	6.1719
H	–	0.7739

<u>1,2,3-Triazine</u>	N1,N3	N2	C4,C6	C5
1s + 2s	3.5444	3.5584	3.0489	3.0565
2pσ	2.5754	2.4379	2.0700	2.1978
2pπ	1.0093	1.0221	0.9862	0.9869
Total	7.1291	7.0184	6.1046	6.2412
H	–	–	0.7550	0.7628

<u>1,2,4-Triazine</u>	N1	N2	N4	C3	C5	C6
1s + 2s	3.5516	3.5437	3.5085	3.0354	3.0444	3.0449
2pσ	2.5691	2.5874	2.7443	1.9443	2.0729	2.0746
2pπ	0.9953	1.0040	0.9848	1.0181	0.9930	1.0049
Total	7.1160	7.1351	7.2376	6.0158	6.1103	6.1244
H	–	–	–	0.7548	0.7614	0.7626

<u>1,3,5-Triazine</u>	N	C
1s + 2s	3.5271	3.0080
2pσ	2.7080	2.0220
2pπ	1.0158	0.9841
Total	7.2509	6.0141
H	–	0.7344

<u>1,2,4,5-Tetrazine</u>	N	C
1s + 2s	3.5465	3.0187
2pσ	2.5814	2.0052
2pπ	0.9875	1.0251
Total	7.1154	6.0491
H	–	0.7205

<u>1,2,3,4-Tetrazine</u>	N1,N4	N2,N3	C5,C6
1s + 2s	3.5526	3.5661	3.0439
2pσ	2.5735	2.4307	2.0880
2pπ	0.9903	1.0218	0.9880
Total	7.1164	7.0186	6.1198
H	–	–	0.7450

TABLE 10 (Contd.)

1,2,3,5-Tetrazine	N1,N3	N2	N4	C4,C6
1s + 2s	3.5561	3.5650	3.5346	3.0457
2pσ	2.5610	2.4492	2.7123	1.9533
2pπ	1.0222	0.9923	0.9942	0.9844
Total	7.1393	7.0065	7.2411	5.9834
H	-	-	-	0.7431

Pentazine	N1,N5	N2,N4	N3	C6
1s + 2s	3.4933	3.5352	3.5333	3.0386
2pσ	2.6622	2.4524	2.4717	1.9565
2pπ	0.9774	1.0216	1.0110	0.9909
Total	7.1329	7.0092	7.0160	5.9860
H	-	-	-	0.7140

pyridazine with two nitrogen atoms adjacent has a higher dipole moment than pyridine with its single nitrogen). When pyridazine is converted to pyrimidine, the nitrogen atoms have more C-N dipoles surrounding them than they do in pyridazine, but now they oppose one another resulting in a reduction of the dipole moment. In a similar fashion 1,2,3-triazine has all the nitrogen atoms together in the molecule, and hence a high dipole moment; when one nitrogen is (a) moved round the ring (generating 1,2,4-triazine) there are once again C-N dipoles in opposed directions and the value decreases; (b) a nitrogen replaces the C5-H5 group (generating 1,2,3,5-tetrazine) there are again opposing C-N dipoles created and the value drops (c) a nitrogen replaces C4-H4 (generating 1,2,3,4-tetrazine) the two almost parallel C-N dipoles become considerably less parallel (the angle between them is ~ 60°) and the dipole moment decreases. When the C5-H5 group is replaced by yet another nitrogen, pentazine is formed with the expected dipole moment being less as the C-N dipoles are at an angle of ~120°; the smaller dipole is found.

Included in Table 9 are the dipole moment vector components parallel (μ_{11}) and perpendicular (μ) to the C2-axis (in 1,2,4-triazine the μ_{11} direction is defined as the perpendicular bisector of the exterior angle at N1); the sense of the vector components is shown below, with a positive dipole moment having its negative end in the positive cartesian direction.

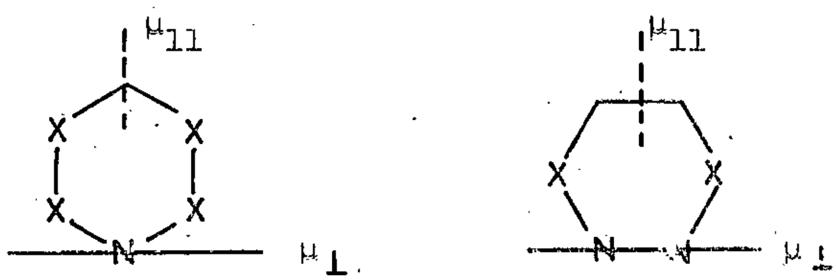

X = CH, N

For all these molecules the value of μ_{11} is negative, i.e. the nitrogen is at the negative end of the molecule. This is consistent with nitrogen being more electronegative than carbon.

As was done for the azoles the dipole moment was partitioned into σ and π moments. The partitioning of the nuclear component into σ and π parts was accomplished in the same manner as the azoles, i.e. $\frac{1}{7}$ of the N and $\frac{1}{6}$ of C terms were assigned to the pi system; there are of course no complications of >NH type to be found in the azines. The value of the σ-moment is of approximately the same magnitude as that found in the azoles; on the other hand the π-moments are very much smaller and in all cases point

TABLE 11.

Bond Population-Moments ($X^{\delta+} - Y^{\delta-}$) in the Azines

Sigma System

X-Y	H-C	C-N	N-N	C-C
	0.241	0.121	0.004	0.007
No. of points	29	30	7	11
Maximum Deviation	0.023	0.015	0.003	0.003

Pi System

X-Y	C-N	C-C	N-N
	0.004	0.008	0.012
No. of points	30	11	7
Maximum Deviation	0.003	0.010	0.010

in the same direction as the σ-moment (even in the C_s symmetry 1,2,4-triazine). This can be explained by each atom donating only one electron to the π-system, whereas in the azoles the >NH group donates two.

In support of this the p_π populations of Table 10 are all very close to unity. This in turn results in the bond moments (determined in the same manner as the azoles) being much smaller than the π-bond moments of the azoles, by a factor of 3 or 4. Accordingly only the average values and deviations of the π-bond moments are recorded in Table 11. Since the π-bond moments (and π-populations) are small there is no need for a large counter moment in the σ-system and the values are again considerably less than the azoles. The only exception to this is the C-H value which is virtually the same as found in the azoles.

Nitrogen atoms are generally π-acceptors and carbon generally π-donors with there being occasional variations from this arrangement. Nitrogen is a σ-acceptor in all cases and sufficiently so to more than counterbalance the cases where it is a π-donor, i.e. in all cases the nitrogen atoms are negative. Similarly the carbon atoms are σ-acceptors, but this does not outweigh the π-donation in all cases. This results in the carbon atoms having a positive charge (but only just) in some cases; these cases all have a nitrogen on each side of the carbon in question.

The negative charge in (almost) all the C/N atoms occurs at the expense of the hydrogen atoms, which are in all cases positively charged. Indeed as the number of nitrogen atoms increases the population of the hydrogen diminishes since the smaller number of hydrogen atoms tries to satisfy the demands of the same number of larger atoms. These demands cannot be completely met and the total population declines and the charge separations decrease. The average atomic populations - Table 12 - show this.

TABLE 12

Average Atomic Populations in the Azines

	H	C	N
Mono-azine	0.7817	6.1713	7.2352
Diazines	0.7705	6.1498	7.1988
Triazines	0.7505	6.0826	7.1687
Tetrazines	0.7362	6.0508	7.1048
Pentazine	0.7140	5.9860	7.0600

Table 10 also shows that the nitrogen 2s functions are more localised than carbon, since the population of nitrogen is typically 1.52 while that for carbon is 1.05. Substitution of C-H by N has a similar effect to that found for the azoles, i.e. the population of a group X drops by approximately 0.11 electrons when the adjacent C-H group is replaced by N (below).

	C-X-C	N-X-C	N-X-N
X = N	7.240 ± 0.02	7.130 ± 0.02	7.015 ± 0.020
X = CH	6.240	6.130 ± 0.02	7.015

One-Electron Properties of the Azines

Some one-electron properties of the azines are reported in Table 13. The values of the quadrupole moment tensor components for pyridine are in reasonable agreement with the experimental data, with correct signs being obtained and the correct order for each component in magnitude. However the xx and yy components are in error by 2.4 and 2.9 units; it would seem likely that the quadrupole moments for the other azines could also be considerably in error, especially for those components which are calculated to be low in magnitude.

The second moments of pyridine are in considerably better agreement with experimental data although the xx and yy terms are reversed in order. The errors in the experimental data are sufficiently large to enable these two terms to be interchanged. There is a general tendency for the values to decrease in magnitude as the number of nitrogen atoms increases, if one allows 1,3,5-triazine and 1,2,4,5-tetrazine to be considered as being abnormally low. A similar trend was found in the azoles, where it was attributed to increasing localisation of the electrons by the more electronegative nitrogen atoms. This also can be applied to the azines; the value for the azine is higher than the value for the azole with the same number of nitrogen atoms, supporting the view that this can be related to delocalisation of the electrons since six-membered rings must be larger than five-membered.

The diamagnetic susceptibility components are also in good agreement with the experimental values; this is

TABLE 13

Some 1-Electron Properties of the Azines
(Experimental values in brackets)[a]

a) Quadrupole Moment (in 10^{-26} esu.cm^2)

	xx	yy	zz
Pyridine	7.30(9.7±1.1)	-3.39(-3.5±0.9)	-3.31(-6.2±1.5)
Pyridazine	-4.84	5.77	-0.93
Pyrimidine	-4.61	4.81	-0.20
1,2,3-Triazine	-0.22	-1.52	1.74
1,2,4- "	10.45	-12.64	2.18
1,3,5- "	-0.97	-2.12	3.09
1,2,3,4-Tetrazine	-8.09	2.98	5.11
1,2,3,5- "	5.91	-11.03	5.13
1,2,4,5- "	-12.65	6.55	6.09

b) Second Moment (in 10^{-16} cm^2)

	xx	yy	zz
Pyridine	-59.68(-56.2±0.8)	-57.47(-57.1±0.8)	-9.05(-7.9±0.8)
Pyridazine	-55.84	-55.22	-8.52
Pyrimidine	-54.93	-55.45	-8.48
1,2,3-Triazine	-53.23	-52.25	-8.01
1,2,4- "	-52.98	-52.19	-7.98
1,3,5- "	-50.23	-50.39	-7.91
1,2,3,4-Tetrazine	-50.35	-50.05	-7.50
1,2,3,5- "	-51.09	-50.24	-7.47
1,2,4,5- "	-50.10	-48.52	-7.45

c) Diamagnetic Susceptibility (in 10^{-6} erg/G^2 mole)

	xx	yy	zz	zz-$\frac{1}{2}$(xx+yy)
Pyridine	-282.19	-291.55	-496.98	-210.11
	(-275.7±2.0)	(-271.9±1.6)	(-480.6±2.2)	(-206.8)
Pyridazine	-270.41	-273.07	-471.17	-199.42
Pyrimidine	-271.19	-269.01	-468.27	-198.17
1,2,3-Triazine	-255.65	-259.81	-447.50	-189.77
1,2,4- "	-255.27	-258.62	-446.21	-189.70
1,3,5- "	-247.33	-246.65	-426.88	-179.9
1,2,3,4-Tetrazine	-244.13	-245.41	-425.95	-181.2
1,2,3,5- "	-244.85	-248.43	-429.90	-183.3
1,2,4,5- "	-237.43	-244.12	-418.36	-177.6

a) Experimental Values taken from Reference 26 especially true of the aromaticity term, $zz-\frac{1}{2}(xx+yy)$ although the agreement may be fortuitously good due to a cancellation of the large errors in the individual components. However the figures are sufficiently good for one to feel reasonably confident that the experimental data, once obtained, will be similar to the values of Table 13. The aromaticity term behaves in a similar manner to what was found for the azoles, i.e. it decreases as the number of nitrogen atoms increases with 1,3,5-triazine and 1,2,4,5-tetrazine being abnormally low; this mirrors the trend found in the binding energies. As was found for the second moments the aromaticity term (and the individual components) start at a higher value than the azoles. It would therefore seem that the aromaticity starts at a different origin for the azines; comparison would then only be valid betweeniso-electronic ($\sigma + \pi$) species.

It should be noted that the experimental method of determining these properties gives rise to two different sets of values for the properties. Choice between them is made on grounds of "reasonableness", or "intuition"; the values of Table 13 endorse this choice, and will be useful in making such a choice for the remaining azines.

References

1. E. Clementi, J. Chem. Phys., 1967, 46, (a) 4731, (b) 4737.

2. M. Hackmeyer, J.L. Whitten, J. Chem. Phys., 1971, 54, 3739.

3. J.D. Potke, J.L. Whitten, J.A. Ryan, J. Chem. Phys., 1968, 48, 953.

4. B.O. Jonsson, E. Lindholm, Int. J. Mass Spectrom. Ion Phys., 1969, 3, 385.

5. C. Fridh, L. Åsbrink, B.O. Jonsson, E. Lindholm, Int. J. Mass. Spectrom, Ion Phys., 1972, 8, (a) 85; (b) 101, (c) 215, (d) 229, (e) 485.

6. R. Gleiter, E. Heilbronner, V. Hornung, Helv. Chim. Acta, 1972, 55, 255.

7. F. Brogli, E. Heilbronner, T. Kobayoshi, Helv.Chim. Acta, 1972, 55, 274.

8. E. Heilbronner, V. Hornung, F.H. Pinkerton, S.F. Thames, Helv. Chim. Acta, 1972, 55, 289.

9. M.J.S. Dewar, T. Marita, J.A.C.S., 1969, 91, 796.

10. D.R. Kearns, M.A. El-Bagomin, J. Chem. Phys., 1963, 38, 1508.

11. L. Pujol, Tet., 1968, 24, 3635.

12. I. Fischer-Hjalmors, M. Sindborn, Acta Chem. Scand., 1968, 607.

13. R. Holtmann, J. Chem. Phys., 1964, 40, 2745.

14. T. Yonezawa, H. Yamabe, H. Kato, Bull. Soc. Chim. Japan, 1969, 42, 76.

15. M.J.S. Dewar, S.D. Worley, J. Chem. Phys., 1969, 51, 263.

16. W.W. Paudler, J.M. Barton, J. Org. Chem., 1966, 31, 1770.

17. B. Bak, L. Hamon, J. Rastrup-Anderson, J. Chem. Phys., 1954, 22, 2013.

18. P.J. Wheatley, Acta Cryst., 1960, 13, 80.

19. P.J. Wheatley, Acta Cryst., 1957, 10, 182.

20. (a) W. Werner, H. Dreizler, H.D. Rudolph, Z. Naturforsch, 1967, 22a, 531; (b) K.K. Innes, J. Mol. Spec. 1967, 24, 247.

21. P.J. Wheatley, Acta Cryst., 1955, 8, 224.

22. F. Bertinotti, G. Giacomello, A.M. Liquori, Acta Cryst., 1956, 9, 510.

23. (a) "JANAF Thermochemical Tables", 2nd Ed., 1971, Published by the American National Bureau of Standards, (b) J.D. Cox, G. Pilcher, "Thermochemistry of Organic and Organometallic Compounds", Academic Press, 1970.

24. R.D. Chambers, J.A.H. McBride, W.K.R. Musgrave, J.C.S.(c), 1971, 3384.

25. A.L. McClellan, "Tables of Experimental Dipole Moments", W.H. Freeman, London, 1963.

26. J.H.S. Wang, W.H. Flygare, J. Chem. Phys., 1970, 52, 5636.

IV. NORBORNADIENE AND ITS CATIONS

Introduction

Bicyclo-(2,2,1)-hepta-2,5-diene or norbornadiene (1) as it is more commonly called is the parent hydrocarbon of the 7-norbornadienyl cation (2).

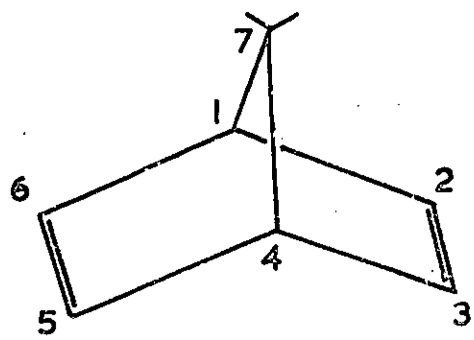

(1)

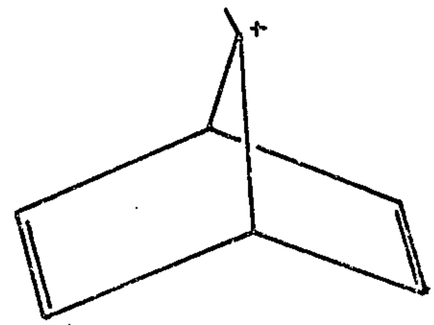

(2)

The structure of this cation has been the subject of a considerable amount of speculation and controversy,[1] both from an experimental[1,2,3] and from a theoretical[4,5,6,7] point of view. The classical approach to the structure of the cation leads to the assumption that the 7-CH group should rearrange until the molecule is of C_{2v} symmetry. However the low temperature NMR studies of Winstein and his co-workers[2] showed that the C_{2v} structure could not be the correct one since the olefinic protons were not all equivalent at low temperatures. There must therefore be some form of "flipping" of the 7-CH group, and these workers were able to place a lower estimate on the energy barrier to this inversion of 19.55 kcal/mole. At this time they could only provide an estimate of the barrier since the ion underwent side reactions on heating before inversion became fast on the NMR time scale. However Winstein has subsequently[3] amended the inversion barrier to 16.7 kcal/mole.

There have been several estimates made of this energy barrier by semi-empirical procedures.[4-7] Hoffmann, using the extended Huckel method[4] obtained a value of 8 kcal/mole, while Winstein,[7] performing a partial geometry optimisation with the CNDO/2 procedure obtained a value of 184 kcal/mole, which is obviously incorrect by an order of magnitude. The best of the semi-empirical calculations was that of Dewar,[6] using the MINDO/2 procedure with full geometry optimisation, who obtained a value of 26 kcal/mole; however the author (of this paper and this program) has subsequently[8] reported that there were several features of the MINDO/2 program which were not optimal for non-classical carbonium ions.

Norbornadiene

As a preliminary to the determination of the above energy barrier for the inversion about the 7 C-H group, an investigation of the parent hydrocarbon was undertaken. The geometry of this was based on the complex[9] "nor Pd Cl_2", in which the norbornadiene group was almost of C_{2v} geometry. Electron diffraction data[10] showed that the molecule was of C_{2v} symmetry, but was not used because a) there was insufficient data for a full set of co-ordinates to be obtained, b) only the average C-H length was reported. Accordingly the complex with $PdCl_2$ was slightly modified to generate a structure with C_{2v} symmetry. Full details of this geometry, together with its symmetry orbitals are to be found in Appendix 2. A minimal basis set was used for both carbon and hydrogen; details of the exponents and contraction coefficients can be obtained from Appendix 2, Tables 1 and 3 for hydrogen and carbon respectively.

The total energies and orbital energies of norbornadiene are given in Table 1. As can be seen, the binding energy of norbornadiene is not particularly large,

TABLE 1

Calculated Energies for Norbornadiene

Total Energy (au)	-267.70658
1-Electron Energy (au)	-941.59191
2-Electron Energy (au)	376.49740
N. Repulsion Energy (au)	297.38793
Binding Energy (au)	-0.45714
Binding Energy (kcal/mold)	-286.9

Orbital Energies (eV)

A1	B2	B1	A2
-311.96	-310.75	-311.96	-310.73
-311.37	-33.60	-310.73	-22.35
-310.74	-22.33	-29.20	-16.91
-36.30	-17.54	-21.35	
-31.28	-15.26(π)	-17.70	
-25.99	-11.94(π)	-17.15	
-22.42			
-18.23			
-14.84			
-13.21(π)			

being only 286.9 kcal/mole. This is somewhat smaller than pyrrole (526 kcal/mole) and pyridine (598 kcal/mole). Indeed since the addition of a carbon atom in going from pyrrole to pyridine leads to an increase in binding energy, the further addition of a C-H group to pyridine (which would give a compound iso-electronic with norbornadiene) would be expected also to lead to an increase in binding energy compared to pyridine. Thus the binding energy of norbornadiene is abnormally low and can be considered as an indication of the instability of the molecule.

As usual the orbitals of lowest energy are very localised on the 1s functions, and can be considered core functions. The four olefinic carbons appear at lowest ionisation potential thus reflecting the greater electron density around the olefinic carbon atoms. The apex carbon appears next at slightly less than 0.6 eV higher ionisation potential than the olefinic carbons; the energy difference between the apex (C-7) and the junction carbons (C1, C4) is similar to this value.

In three-dimensional molecules such as norbornadiene there is no clear separation of sigma and pi orbitals on symmetry grounds as there was in the azoles and azines. However the orbitals 10a, $6b_2$ and to a considerably lesser extent $5b_2$ are largely π-orbitals, with the predominant eigenvectors being C-p_z of approximate magnitude 0.75, where C-p_z is that which is most appropriate for the π-direction. The He(I) photo-electron spectrum[11] has two very narrow lines at the low ionisation potential end, which have been assigned to electrons from the pi orbitals; the calculations support this assignment. Correlation of the observed and calculated ionisation potentials leads to a least squares line of equation IP(exp) = 1.309 IP(calc) - 7.619, with standard deviations in slope and intercept being

0.151 and 0.420 respectively and the overall standard deviation is 0.937. This line is markedly different from, and not so good as that found for the azines or azoles.

The dipole moment of 0.58D is oriented such that the negative end is at the electron rich olefinic end of the molecule. The result of a Mulliken population analysis are presented in Table 2. The atomic populations indicate that the olefinic carbons are least negative which would place them at the highest ionisation potential end of the core orbital photo-electron spectrum. This is in direct opposition to the eigenvalue order and is a result of the arbitrary equipartition of the overlap population which is employed in determining atomic populations. This charge distribution also disagrees with the direction of the dipole moment.

TABLE 2

Mulliken Analysis of Norbornadiene

a) Atomic Populations

C1, C4	6.2753	H1, H2	0.7264
C2, C3, C5, C6	6.2631	H3, H4, H5, H6	0.7568
C7	6.4015	H7, H7	0.7579

b) Overlap Populations

C-C (Olefinic)	0.6379	C-H (Olefinic)	0.4912
C-C (Junction-Olefin)	0.3679	C-H (Junction)	0.4245
C-C (Apex-Junction)	0.3922	C-H (Apex)	0.4209

However the populations of the hydrogen atoms show that the apex hydrogens are the most negative; this is in agreement with which hydrogen atom is the most likely to be removed to generate a norbornadienyl cation (this would entail removal of a hydride ion). On the other hand, the hydrogen atom next most likely is not H1/H4 but the olefinic hydrogens; this is of course impossible in the presence of saturated centres. Besides, all the hydrogen atoms are positively charged.

A better and more consistent method is to investigate the total overlap populations between centres, which give a measure of the kinetic strength of bonds. First let us consider the breaking of the carbon skeleton; in a mass spectrometer the largest non parent ion is at P-26, which is caused by loss of acetylene from the molecular ion by breaking bonds C1-C2 and C3-C4 (or C4-C5 and C6-C1). The overlap populations would predict such a skeletal breakdown as the most likely since these bonds have the smallest overlap population. (Strictly speaking, the populations of the radical cation should be used for comparison with the mass spectrum, but since this involves the loss of only one electron out of fifty it has been assumed that the overlap populations of the radical cation will be practically identical to that of the parent molecule). This prediction leads one to assume with some confidence that the reactivities of the C-H bonds will be placed in the correct order. Thus the apex bond is most likely to break followed closely by the other saturated centres, with the olefinic C-H bond being strongest, i.e. the correct order since it is the 7-norbornadienyl cation which will be investigated later.

Despite such encouraging predictions, there are two points which are not as good as would be expected on grounds of the results for the azines and the azoles. These are the low binding energy and the fairly poor agreement of calculated and experimental ionisation potentials. Both these figures can be improved upon.

Scaled Norbornadiene

Using the scale functions from methane and ethylene the calculation on norbornadiene was repeated, yielding the results of Table 3. The energy has improved considerably

TABLE 3

Calculated Energies for Scaled Norbornadiene

Total Energy (au)	-268.18036
1-El Energy (au)	-947.24069
2-El Energy (au)	381.67300
N.R. Energy (au)	297.38793
Binding Energy (au)	-0.93092
Binding Energy (kcal/mole)	-584.2

Orbital Energies (eV)

A1	B2	B1	A2
-308.00	-306.04	-308.01	-306.02
-307.57	-31.49	-306.02	-20.69
-306.03	-20.67	-27.31	-14.81
-34.12	-16.06	-19.76	
-29.36	-13.27(π)	-16.02	
-24.41	-9.62(π)	-15.22	
-21.17			
-16.53			
-12.78			
-11.00(π)			

with the introduction of scaled functions, to the extent of 297.3 kcal/mole. This improvement is in line with that predicted from the methane and ethylene improvements, i.e.

somewhat less than sum of twice the improvement in ethylene and thrice the improvement in methane. As expected from the magnitude of the scale factors, both the one-electron and two-electron energy terms have increased in magnitude, with the attractive energy increase outweighing the repulsive energy increase. The definition of binding energy creates a problem reminiscent of that encountered in the protonated azoles. Here the problem is whether scaled or "Best Atom" gaussian sets should be used for evaluating bind energies; the binding energy in Table 3 was based on a "Best Atom" set. This was used as 1) it is a better representation of the atoms (as "best atom" implies) and 2) the retention of scaled functions would imply that atoms formed by dissociation of a molecule still retained some of the characteristics of the molecule.

The ordering of the orbital energies remains virtually unchanged in the two calculations, with the only two orbitals which cross in energy being the $4b_2$ and $5b_1$ orbitals, which were the two closest together in energy terms in the unscaled calculation (the separation was 0.16eV). The scaled levels show the same changes as the model systems, methane and ethylene; the valence shell orbitals are approximately 2eV less negative in the scaled calculation which brings them nearer the experimental values.[11] This improvement in magnitude is paralleled by an overall improvement in the least squares fit; the best straight line for the scaled calculation is given by IP(exp) = 1.197 IP(calc) - 3.513 with standard deviations in slope and intercept and the overall standard deviation being

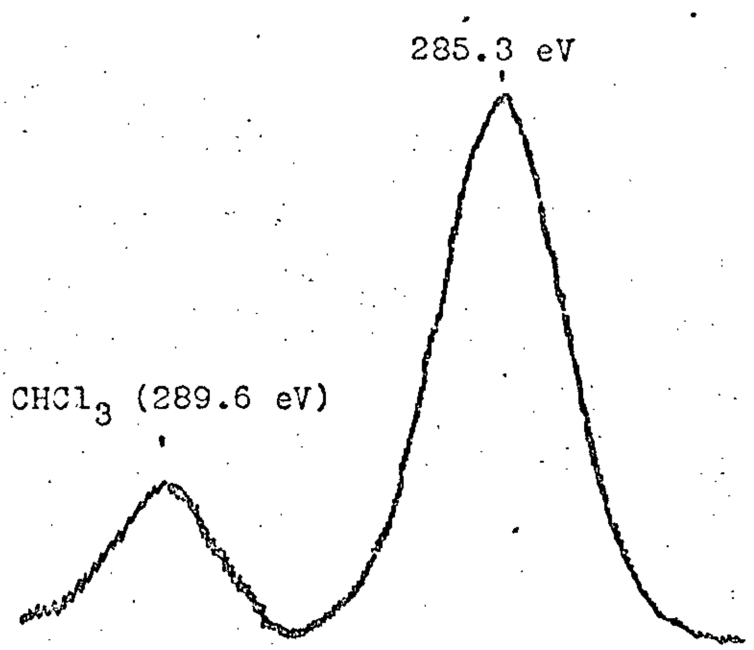

Fig. 1 Core Levels of Norbornadiene on AEI ES100

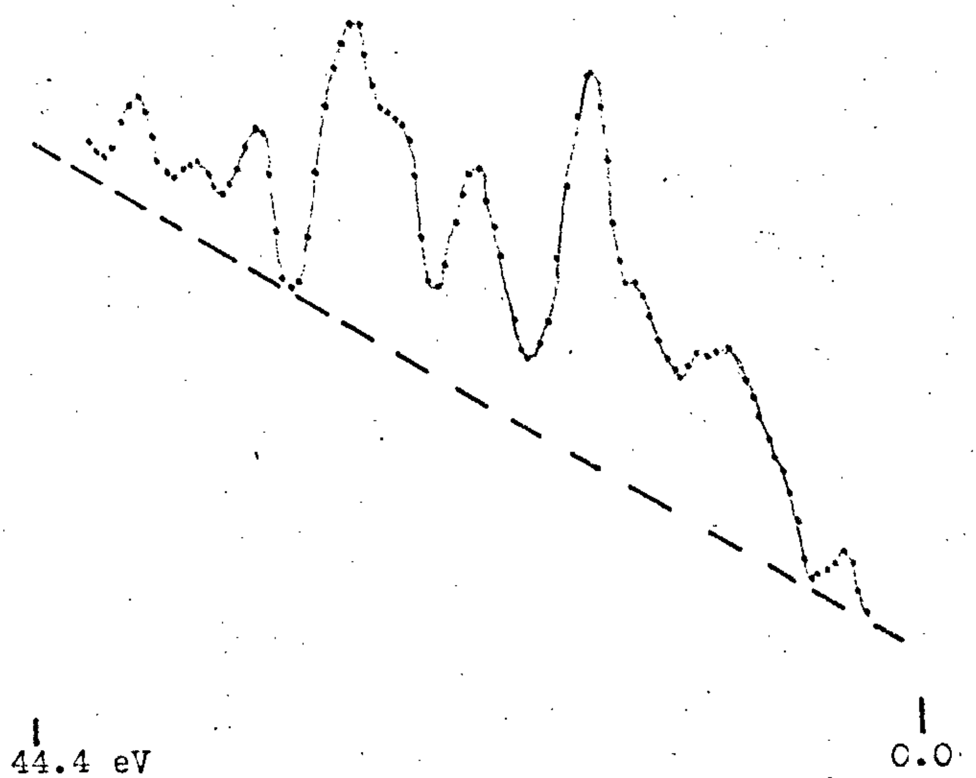

Fig. 2 Valency Shell Levels of Norbornadiene on HP 5950A

0.118, 1.664 and 0.809 respectively. These standard deviations are considerably less than those of the unscaled ("best atom") calculations, while the slope and intercept tend more to the values they ought to have if Koopmanns' Theorem is strictly followed (i.e. 1.0 and 0.0 respectively).

The core levels are affected somewhat more than the valency shell orbitals, with the ionisation potential reduced by approximately 4eV. The order is the same as the unscaled set (junction, apex, olefinic) but the energy gap is reduced to 0.43eV between the junction and the apex, while it is increased to 1.54eV between the olefinic and apex carbons. This region of the photo-electron spectrum has been examined by X-ray photo-electron spectroscopy, using an AEI ES100 spectrometer. The 1s electron binding energy, a broad singlet at 285.3eV (Figure 1) was determined using chloroform (289.6eV, Figure 1) and n-hexane (285.0eV) as internal standards. This procedure involves only the measurements of well-resolved doublets close together on the energy scale, thus overcoming any possible errors arising from charging or non-linearity of the energy scale. At half-height the broad carbon 1s line has a peak width of 1.9eV, to be compared with the usual width for single peaks of approximately 1.4eV. The peak which should have a 2:1:4 weighting has a rather smaller splitting than that calculated, i.e. the difference between the highest and lowest carbon 1s level is experimentally about 0.6eV (from width at half-height) whereas the calculations make the difference 1.9eV. Such an overestimate of core level separations is fairly common in such calculations;[15] similarly the calculations place the core levels approximately 20-30eV to higher binding energy than those found experimentally.

Using the experimental value it is possible to arrive at some estimate of the strain involved in the norbornadiene system. The only figures available for comparison are the soft X-ray emission spectra of Mattsen and Ehlert,[13] who obtain 276.5, 279.6 and 277.7eV for methane, ethylene and cyclohexane respectively. After allowing 7.3eV (based on cyclohexane) for the differences in experimental technique the solid state ESCA binding energy in an unstrained olefinic system is probably near 286.9eV. (Since there are four olefinic carbons in norbornadiene, the experimental 1s level will be characterised mainly by these carbons). The value for norbornadiene (285.3eV) suggests that there may be up to 1.6eV of strain evident here; thermochemical estimates of 1.07[14] and 1.28eV[16] have been given.

The valency shell was also examined on the ES100 spectrometer, using both the Al K_α and He(I) irradiation. The resolution on this machine with X-ray bombardment revealing only four broad bands which were centred on 8.0, 13.0, 17.2 and 26.6eV and which had integrated areas of 1:5:9:3 respectively. Using He(I) irradiation the resolution was considerably better and is similar to that of Heilbronner, having peaks and shoulders (sh) at 8.6, 9.4, 11.1(sh), 12.17, 13.64 and 15.03eV. Since the ES100 had not revealed any peaks at higher ionisation potential than the work of Heilbronner, a further sample was examined on the Hewlett-Packard 5950A spectrometer which, unlike the AEI instrument, is fitted with a monochromator. This improved

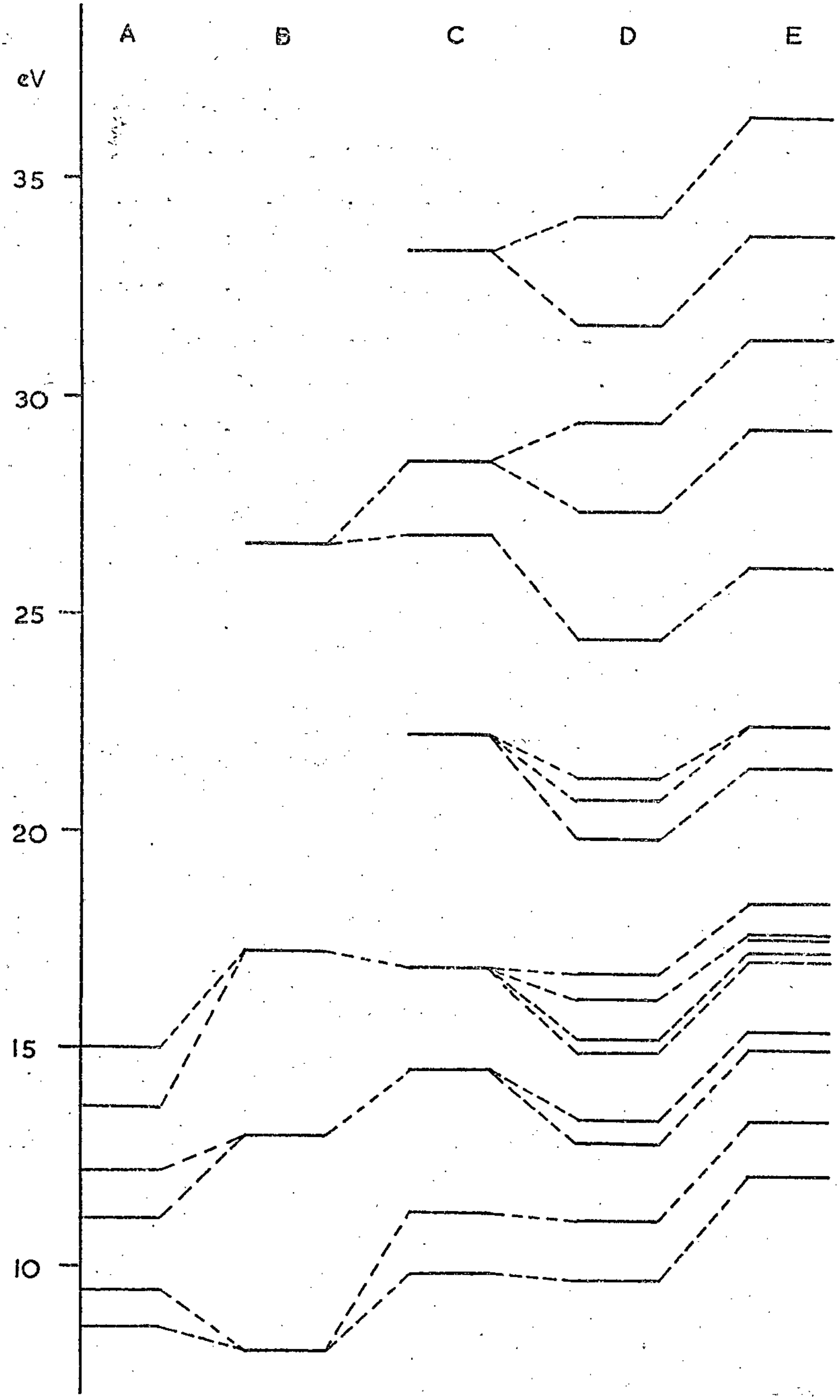

Fig. 3. Correlation Diagram of Ionisation Potentials and Orbital Energies; A. He(I) on ES100; B. Al K_α on ES100; C. HP5950A; D. Scaled gaussian set; E. Unscaled gaussian set.

the resolution immensely and the spectrum is reproduced in Figure 2. The main peaks and associated shoulders (sh) are at 9.8, 11.2(sh), 14.5(sh), 16.8, 22.2, 26.8(sh), 28.5 and 33.4eV. The approximate areas are in the ratios 1:1:1:3:2:2:3:2 with at least one further peak probable between those at 11.2 and 14.5eV where the counts per second do not fall too near the base line. Direct comparison of the higher ionisation potentials is difficult since there is not sufficient resolution, even on the HP5950A, to assign the theoretical lines; however, the theoretical lines can be grouped together with centroids at 9.62, 11.0, 13.03, 15.8, 20.8, 24.41, 28.33 and 32.8eV. The linear least squares fit of those centroids to the experimental data gives IP(exp) = 1.010 IP(calc) - 0.713eV, with standard errors in slope and intercept of 0.038 and 0.805 respectively. The correlation of the three sets of experimental ionisation potentials and the two sets of calculated energy levels is fairly straightforward, and is shown in Figure 3.

Table 4 shows the population analysis of scaled norbornadiene. The data is very little different from that of the unscaled run, and the predictions made there still hold true. The change in the dipole moment is similarly small, the value for the scaled calculation being 0.76 D.

TABLE 4.

Population Analysis for Scaled Norbornadiene

C1,C4	6.1808	H1,H4	0.8205
C2, C3,C5,C6	6.1566	H2,H3,H5,H6	0.8650
C7	6.2635	2 x H7	0.8237
C1-H1	0.4285	C1-C2	0.3661
C2-H2	0.4693	C2-C3	0.5724
C7-H7	0.4126	C4-C7	0.3837

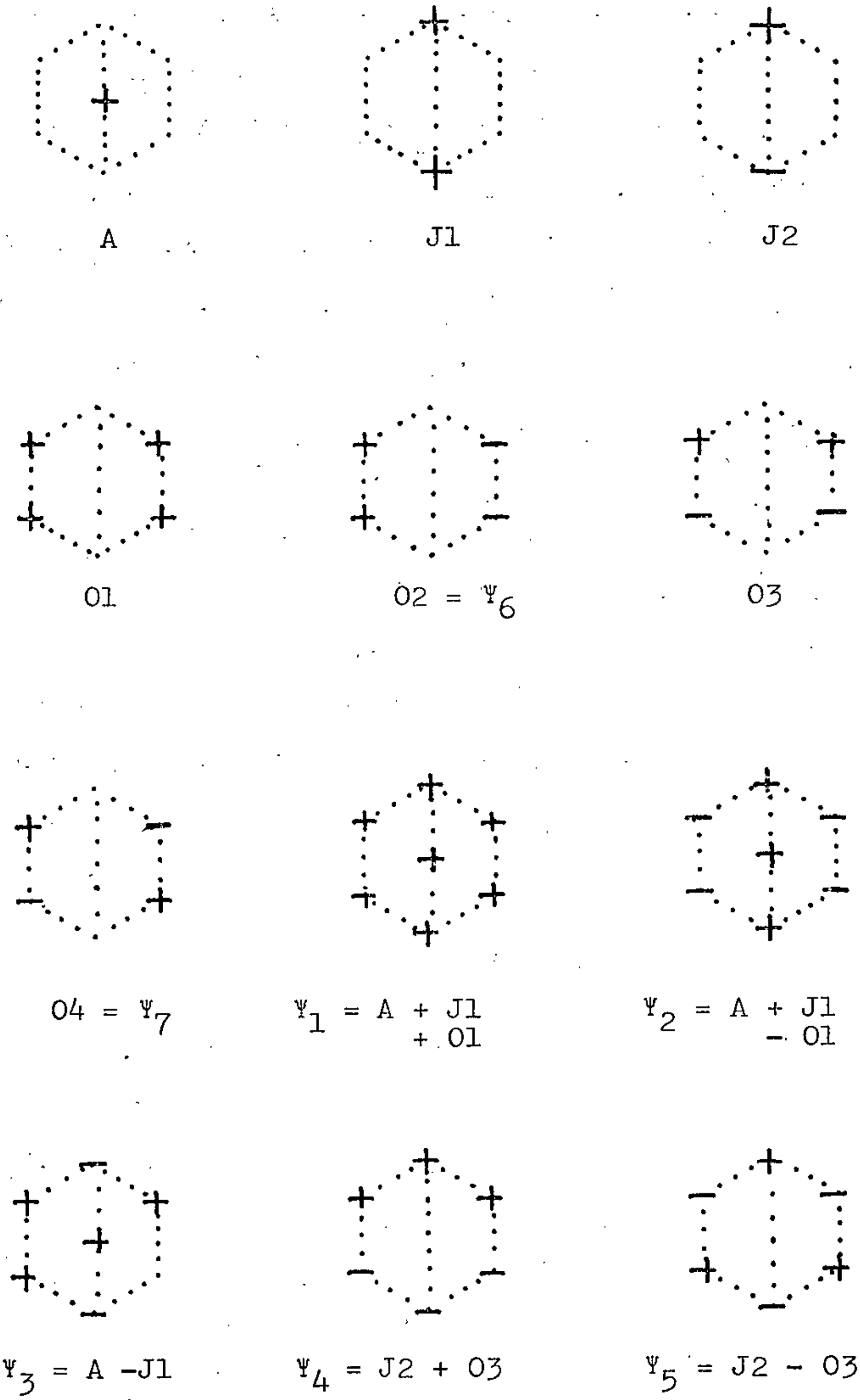

Fig. 4. 2s-Symmetry Orbitals (A, J1, J2, 01–04) and their Combinations (Ψ_1–Ψ_7)

The Nature of the Norbornadiene Valency Shell Orbitals

Scaling alters the eigenvectors by only a small amount compared to the unscaled set. The discussion which follows is therefore equally applicable to both scaled and unscaled calculations. In the azines and azoles it has been shown that the low lying valency shell orbitals tend to be of predominantly 2s character. Figure 4 shows the carbon 2s symmetry orbitals as well as the possible combination of these symmetry orbitals. It is possible to place the orbitals Ψ_1-Ψ_7 in order by the number of nodes present, i.e. Ψ_1 (0 nodes); Ψ_2 (1 node parallel to olefinic plane); Ψ_4 (1 node bisecting the olefinic bonds); Ψ_6 (1 node passing through C1-C4-C7); Ψ_3 (2 nodes parallel to olefinic plane); Ψ_7 (2 nodes, one bisecting the olefinic bonds and one passing through C1-C4-C7) and finally Ψ_5 (3 nodes, as indicated in Figure 4). As the energy of the allowed combinations increases it becomes more and more likely that the predominantly 2s character will become increasingly "contaminated" by carbon 2p and hydrogen 1s functions. Another possibility for molecular orbitals Ψ_1-Ψ_5 is that combination of symmetry orbitals does not occur and the molecular orbitals will be localised in only one of the contributing symmetry orbitals.

The lowest energy (most negative) orbital is $4a_1$ and hence could be any one of the combination orbitals Ψ_1-Ψ_3. It is hardly surprising however that $4a_1$ turns out to be the nodeless combination Ψ_1. The eigenvectors decrease in magnitude in the order olefin, junction, apex, showing that the olefinic centres tend to predominate at high ionisation potentials (the first valence ionisation potential in ethylene is greater than that in methane). It is not then surprising that of the one node functions, the purely olefinic combination orbital, Ψ_6 occurs next in the table of orbital energies (orbital $2b_2$). The next molecular orbital is $5a_1$ which has combination orbital Ψ_2 as its predominant feature. Again, this is a single node orbital where the node, parallel to the olefinic carbon plane, passes through the olefin carbon - bridge carbon bonds. Orbitals $4a_1$ and $5a_1$ can be considered as the symmetric and antisymmetric combinations of saturated and unsaturated carbon 2s levels, with the symmetric combination occurring at highest ionisation potential.

Orbital $3b_1$ is of type Ψ_4, the remaining single node combination orbital. In contrast to $4a_1$, the olefinic 2s levels have smaller eigenvectors than the junction 2s orbitals, showing that one is passing from an unsaturated to a saturated region of 2s orbitals. There is besides some evidence of weak C-H bonding, of C_{2s}-H_{1s} character, involving the junction atoms. This orbital is the last that can be truly considered as a localised 2s orbital, although the 2s functions still play an important role, but not the predominant one.

Orbital $6a_1$ is the next occupied orbital and has a considerable amount of 2s character, namely in the apex carbon; however since this has a significant amount of apex p_z and apex hydrogen 1s its primary characteristic is C7-H bonding. In a similar fashion $7a_1$ is predominantly junction C-H bonding, having large contributions of p-orbitals

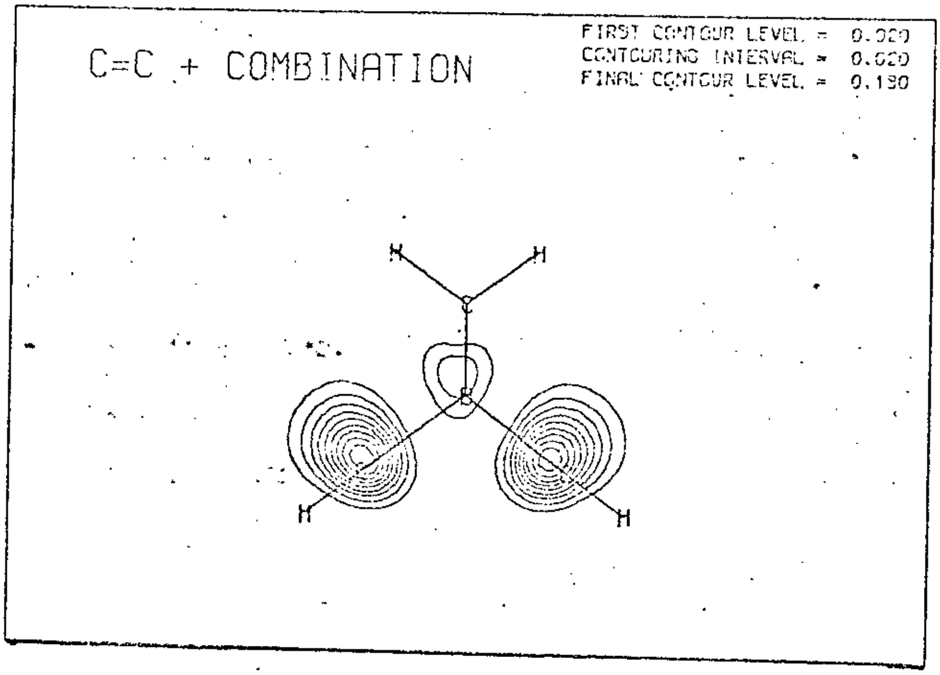

Figure 5a (above) Symmetric Combination of Olefinic σ-Orbitals

Figure 5b (below) Anti-symmetric Combination of Olefinic σ-Orbitals

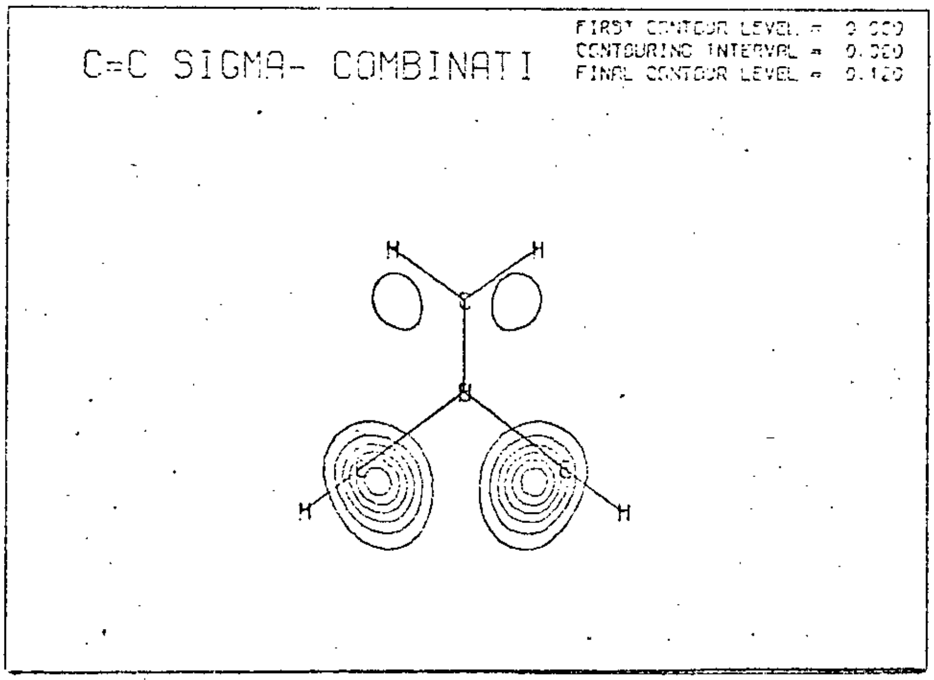

in the direction C-H. Since these are the symmetric combinations of C-H bonds one would expect to find two more orbitals which have the antisymmetric combinations of saturated C-H bonds. The $4b_2$ orbital contains this combination for the apex C-H pair, although there is also some olefinic carbon-hydrogen bonding present. The antisymmetric combination of junction C-H bonds appears in orbital $5b_1$. The olefinic C-H bonds are not so localised as the saturated C-H bonds, and occur in most orbitals and are the main contributing bonds only in orbitals $2a_2$ and $4b_1$.

The first of the predominantly ring bonding orbitals is $3b_2$, where the bonding occurs along the saturated type of bonds, but not along the σ olefinic bonds (There is no reason on grounds of symmetry why this should be so since there is a symmetry orbital pointing directly along the olefinic C-C direction which is not nodal in the middle of this bond). The eigenvector for this σ-olefinic bond is very low, being 0.07. There is however some pseudo π-overlap across the olefinic centres. In contrast to this is orbital $5b_2$ where there is a very large eigenvector for olefinic σ bonding (0.87) although there is sufficient olefinic π-type and apex p type bonding to make this a pseudo π-type of orbital.

A similar situation to the $3b_2/5b_2$ one exists in the $8a_1/9a_1$ pair where the upper of these is mainly olefinic σ-bonding (eigenvector = 0.82) and the lower is bonding along saturated C-C bonds (In $8a_1$ there is also a small amount of apex C-H bonding). In fact $9a_1$ and $5b_2$ are the main symmetric and antisymmetric olefinic σ bonds. The

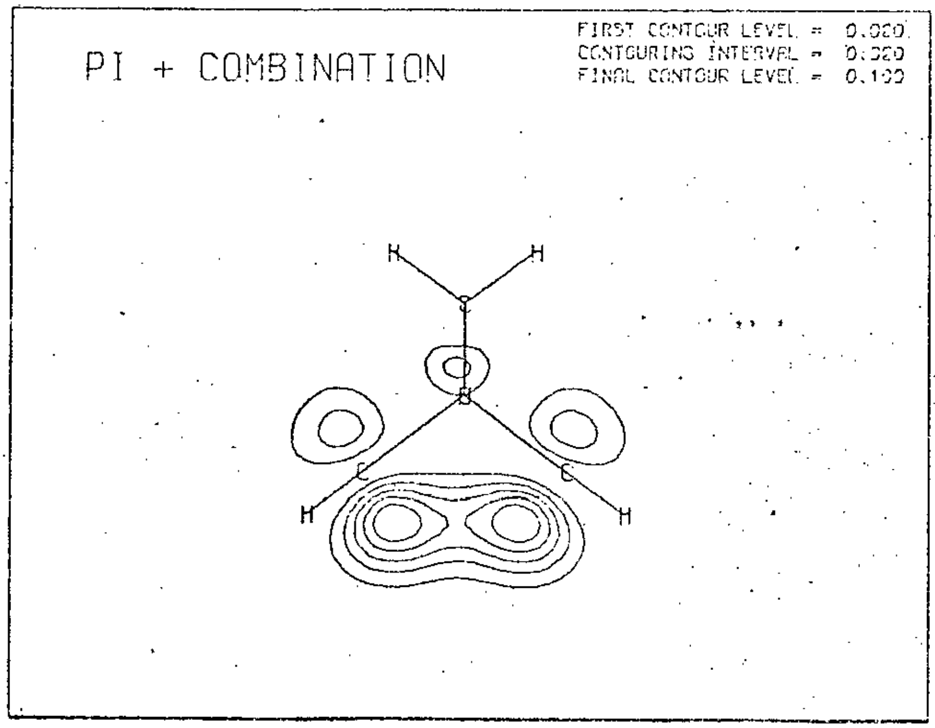

Figure 5c (above) Symmetric Combination of
π-Orbitals

Figure 5d (below) Anti-symmetric Combination
of π-Orbitals

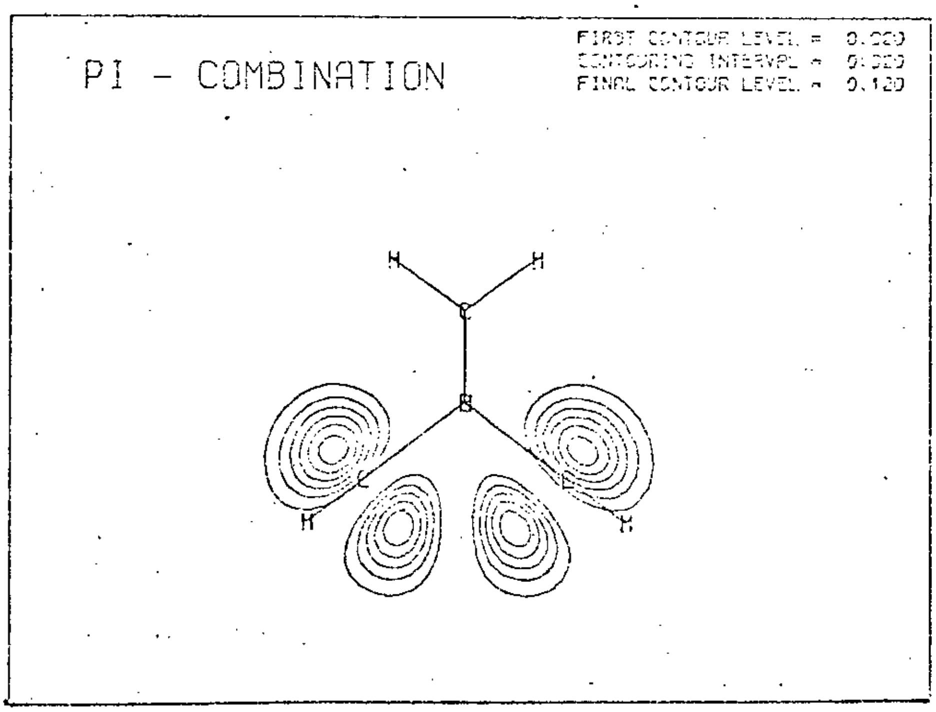

two other orbitals which contribute to the bonding along saturated C-C bonds are $6b_1$ and $3a_2$.

The orbitals of lowest ionisation potential ($10a_1$, $6b_2$) are of π-type symmetry as already mentioned. It is possible to take linear combinations of the two contributing p orbitals at the olefinic centres so that one obtains two new p orbitals, one of which is perpendicular to the plane and one parallel to the plane of the olefinic systems, i.e. P_π and P_σ bonds. The eigenvectors for the P_π are 0.85 in $10a_1$ and 0.99 in $6b_2$. These correspond to the symmetric ($10a_1$) and anti-symmetric ($6b_2$) olefinic π orbitals, with the antisymmetric at lower IP than the symmetric orbital.

The splitting between the two pi-levels is predicted to be larger than that found experimentally (1.38eV against 0.85eV). This could in part be due to using the geometry of a palladium complex where the olefinic bonds are drawn closer together thus increasing their interaction.

Some of the key orbitals are given in Figs. 5a-5d.

The Inversion Barrier of the 7-Norbornadienyl Cation

Since the scaled basis set gave a much improved total energy, and since the calculated ionisation potentials were in better agreement with the experimental data, the scaled basis set was used for the cation.

In order to determine any inversion barrier it is necessary to obtain the total energies of two different states of the molecule. These can be regarded as the transition and ground state geometries. Consider as an example PH_3; the transition state would be a planar molecule

Fig. 6. Plot of Total Energy (E) against Angle (Θ)

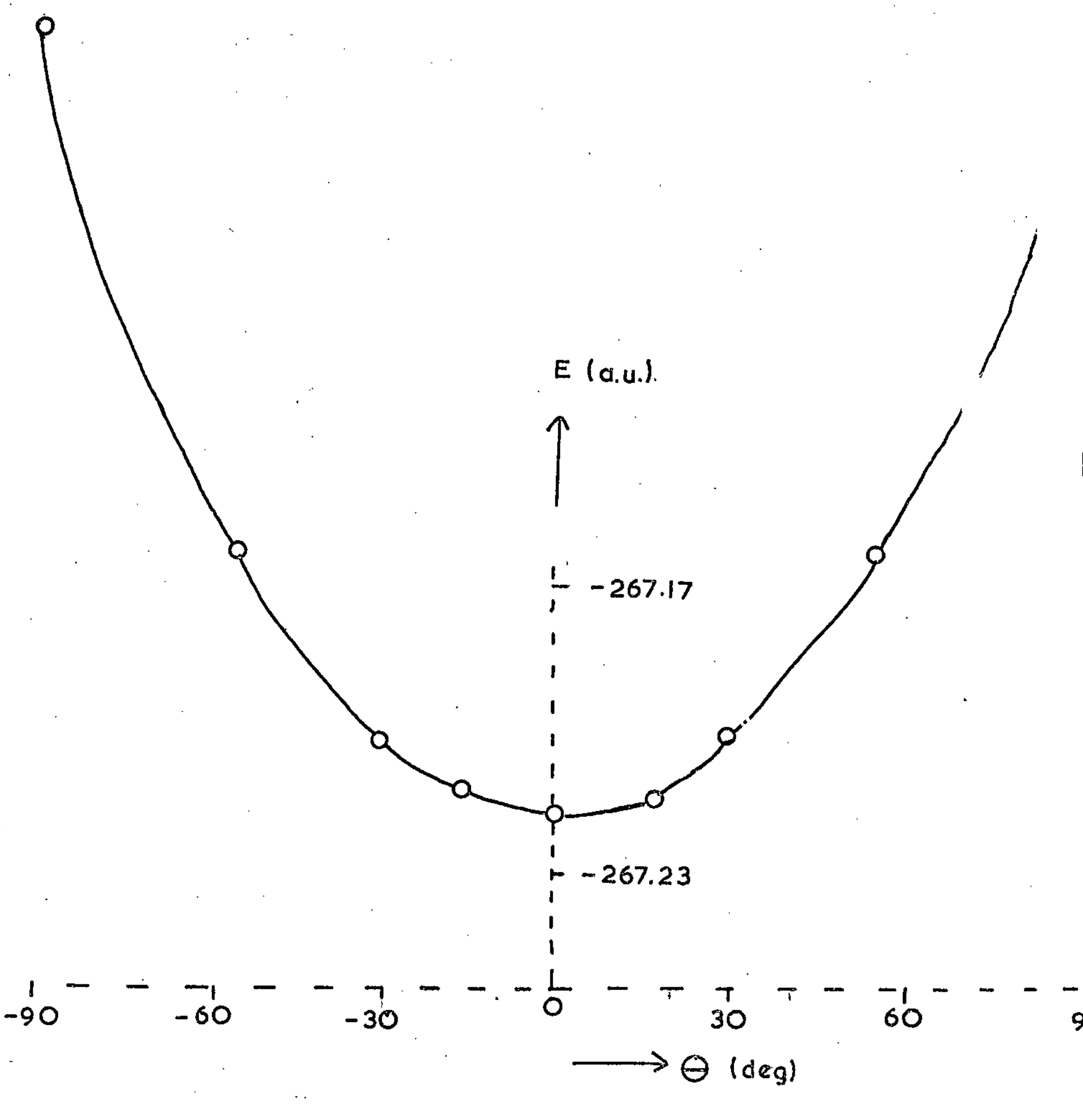

while the ground state would be pyramidal in form.

The transition state for the flipping of the 7-norbornadienyl cation could be one of the two possible structures below. Structure (3) is a symmetric one: structure (4) allows for the hydrogen at the 7 position failing to flip until C7 has passed through the symmetric arrangement of the carbon skeleton.

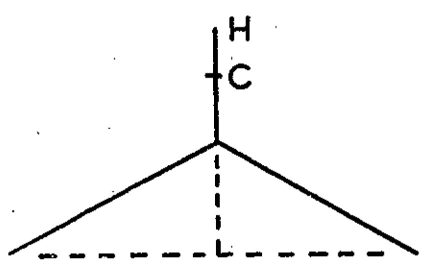

(3)

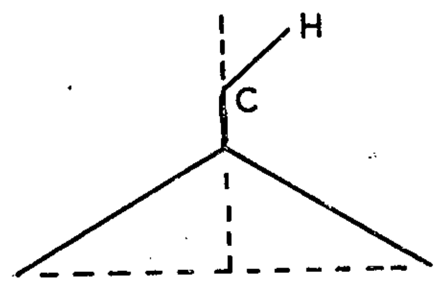

(4)

Which of these two possibilities actually occurs can be found by determining the total energy of the cation as a function of the angle θ in structure (4). This data is shown in Table 5 and graphically in Figure 6. From these it is

TABLE 5

Total Energy of the 7-Norbornadienyl Cation, as a Function of the Angle θ

θ	E_{tot}
0.0°	-267.21008
15.0°	.20669
30.0°	.19651
54.75°	.16450
90.0°	.07309

immediately obvious that the symmetric structure (3) is considerably favoured over the unsymmetrical structure (4);

thus the possibility suggested previously[17] that there were two mirror image transition states is eliminated. One further alternative is that the carbon is not symmetrically placed in the transition state, giving structure (5), another mirror image form.

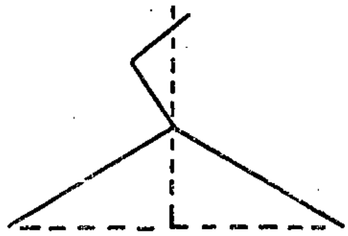

(5)

This possibility has not been investigated for several reasons:- 1) too much computer time would be used in determining the transition state; 2) the semi-empirical method used by Dewar has indicated it does not exist; 3) the curve of Figure 5, by reason of its smoothness indicates that such a structure is unlikely. (Each of the structures of type (4) are special cases of structure (5). There would then be some indication in Figure 5 of a double maximum, instead of the almost parabolic curve that has been obtained. While this is not conclusive, taken together with Dewar's semi-empirical calculations it seems unlikely that an investigation of this nature would be fruitful.) The transition state for inversion of the 7-norbornadienyl cation has accordingly been assigned as having structure (3), with a total energy of -267.21008 au.

It is now possible to turn one's attention to the geometry of the ground state. Since a full geometry optimisation (as was carried out by Dewar) is not feasible

Fig. 7. Total Energy (in au) against Angle (deg) the C4-C7-Cl Plane makes with Vertical Direction. (O, calculated points; □, parabolic minima; △, "minimum of minima").

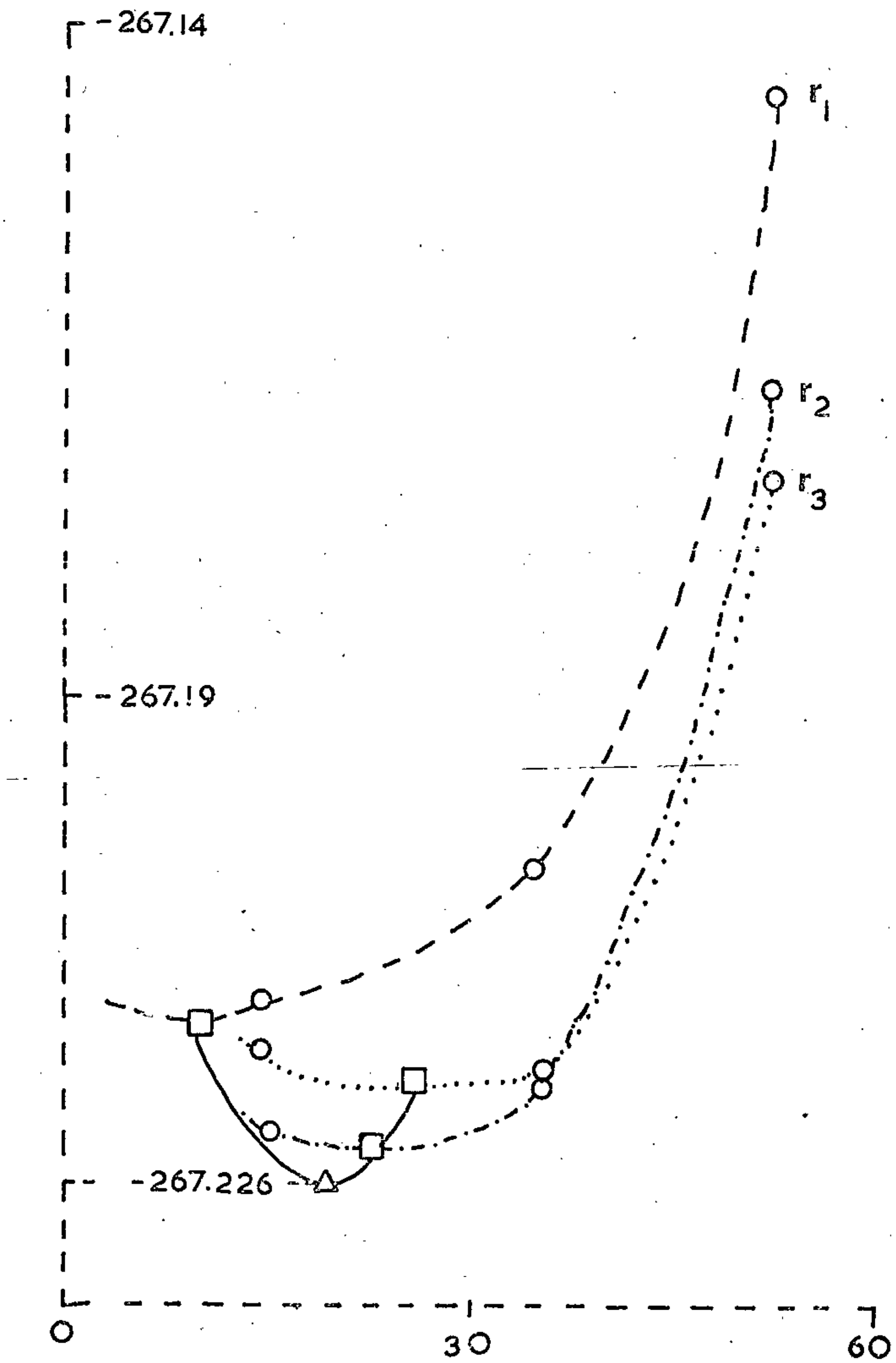

with non-empirical calculations, two parameters were chosen as being the key ones in determining the geometry of the ground state; they are shown below.

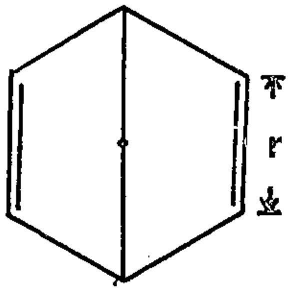

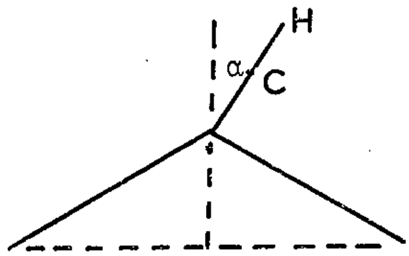

The angle α is the angle which the C1-C7(H7)-C4 plane makes with the vertical (horizontal being defined as the plane of the olefinic carbons). The angles chosen were 18, 36 and 54 degrees and were based on those obtained by Dewar (38.8) and Winstein (55°) with their respective semi-empirical methods. The distance r is the length of the C-C olefinic bond towards which the C7-H7 group is tilted. Again 3 distances were chosen; the shortest, r_1, was the original C-C olefinic length, while the longest, r_3, was the C-C length from cyclopropane since this would be the largest possible bond if C7 was to move within a single bond distance of C2 and C3. The final length, r_2, was based on the average of these two lengths. Calculations were carried out at all possible combinations of r and α. The nine points so obtained are shown in Table 6.

TABLE 6

Total Energy of the 7-Norbornadienyl Cation, as a Function of α and r.

	α = 18°	36°	54°
r = 1.366	-267.21310	.20370	.14509
= 1.453	.22261	.21896	.16776
= 1.540	.21727	.21862	.17424

Fig. 8. Total Energy (in au) against Olefinic Bond Length (in Å); symbols have same meaning as previous figure.

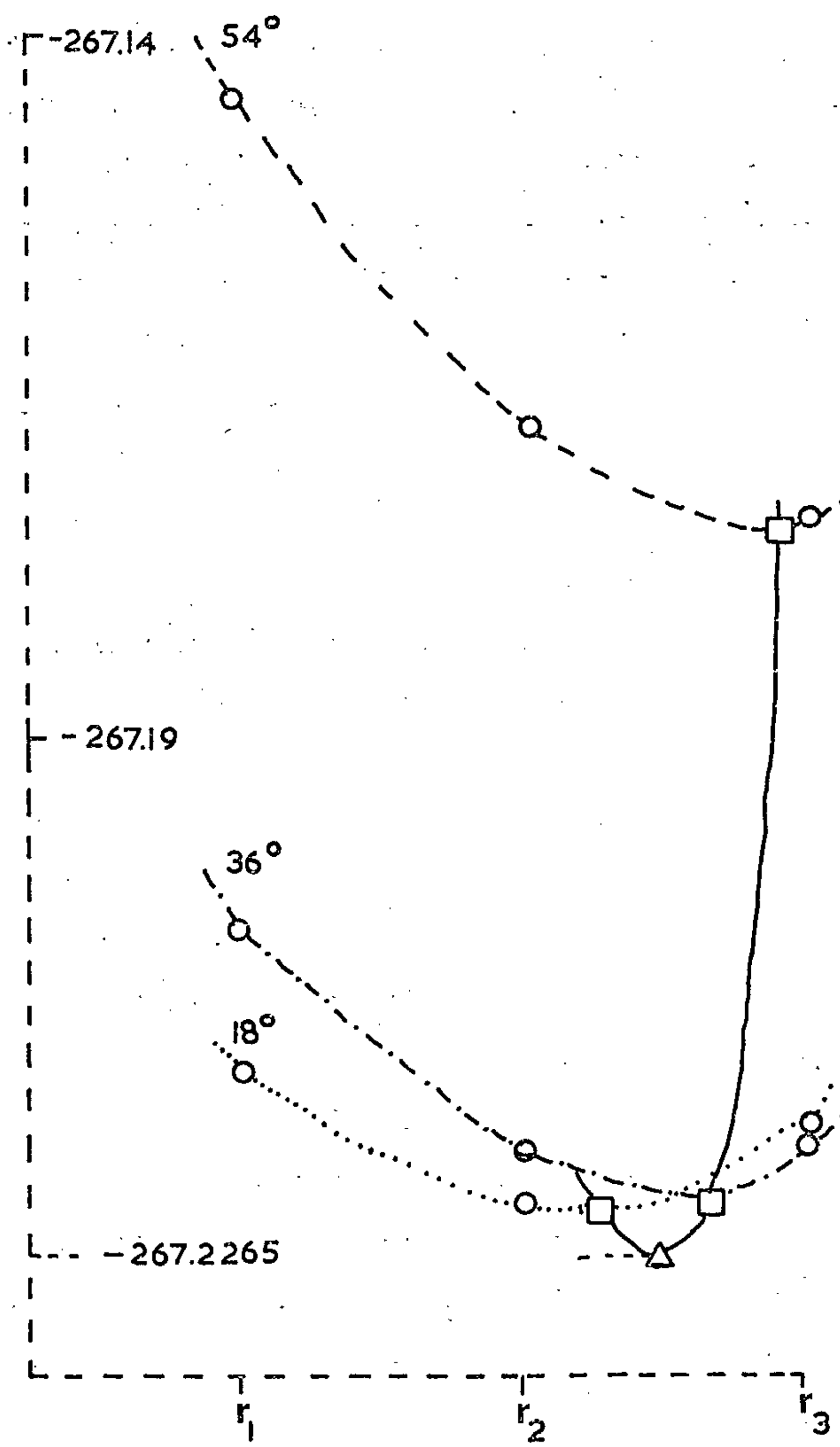

Figure 7 shows how the total energy varies with the angle at each of the r values. Figure 8 shows the variation of energy with r at each of the angles α. It then only remains to determine from this grid of points an optimal geometry representing the ground state of the cation. For each of the six curves in Figures 7 and 8 parabolic interpolation gave the minimum for each curve; these minima are enclosed in squares (for $r = r_1$, $\alpha = 0, 18, 36$ degrees were used in the parabola since $\alpha = 18, 36, 54$ gave a maximum not a minimum; all other cases gave minima). The values for the parabolic minima for the E versus α were further treated in a parabolic manner giving a "minimum of minima" to be used as the optimal value of α. (While this last parabolic treatment is of doubtful mathematical validity, it is at least as good as, and probably much better than a minimum obtained by a free-hand curve drawing method). The optimal value for r was found in a like manner. While still holding the reservations about the mathematical validity it should be noted that a) the energy predicted for each of the optimal parameters is better than any value shown in Table 6 and b) the energies for optimal r and α are almost identical (Figures 7 and 8). The values of r and α for the ground state geometry are 1.475Å and 26.12° respectively. A calculation was therefore carried out using this optimal geometry, the results of which are presented in Table 7, together with the corresponding values for the transition state. From these two calculations the barrier to inversion is 8.5 kcal/mole.

TABLE 7

Total Energies of Transition and Ground States of the 7-Norbornadienyl Cation

	Ground	Transition
T.E.(au)	-267.22370	-267.21008
1-El (au)	-908.13339	-908.93220
2-El (au)	+356.20673	356.68681
N.R. (au)	284.70296	285.03531
Binding (au)	-0.86651	-0.85259
Binding (kcal/mole)	-543.7	-535.2

The 1-Norbornadienyl Cation

It has already been shown that the weakest C-H bond in the norbornadiene molecule is C7-H, resulting in the prediction that the kinetically favoured cation is the 7-cation. By removal of a hydrogen from one of the bridge carbon atoms one generates the 1-cation and it is then possible to compare the thermodynamic stabilities of these two cations. (The C1-H bond is almost as weak as the C7-H). From chemical concepts it is difficult to predict which is the more stable form of the cation; the 7-cation is secondary making it less stable than the tertiary 1-cation. On the other hand, the generation of the 1-cation involves the most rigid part of the molecule and is reminiscent of 9-bromotriptycene which is very reluctant to form carbonium ions of the type of the 1-cation.

A calculation of the 1-cation has been carried out where the junction hydrogen has been removed leaving the rest of the molecule at the same geometry. The results of this can be found in Table 8, which shows that the 7-norbornadienyl cation is more stable (by 3.3 kcal/mole) than the Cl-cation. This energy difference is small however and the conclusion could easily be reversed by a geometry optimisation of the Cl-cation. Such an optimisation was not carried out as this calculation was carried out for comparison purposes only.

TABLE 8

Total Energies of the 1-Norbornadienyl Cation

Total Energy	-267.21836
1-El Energy	-909.28085
2-El Energy	356.74825
N.R. Energy	285.31424
Binding Energy	-0.86117
Binding (kcal/mole)	-540.4

<u>The Norbornadiene Cations</u>

Tables 7 and 8 show the total energies of the cations of principal interest, i.e. the 1-norbornadienyl cation, and the 7-norbornadienyl cation (transition and ground states). Using the sum of the atom energies as $6 \times C + 7 \times H + 1 \times C^{+}$ the binding energies of these Tables were obtained. All the cations are considerably less stable than the parent hydrocarbon (the opposite of what was found in the azoles/protonated azoles). Thus they will be more reactive than the parent hydrocarbon; there is some evidence of this in the side reactions which occurred with the 7-cation in Winsteins' original estimation of the inversion barrier.

The population analysis in Table 9 shows the effect on

TABLE 9

Population Analysis of Norbornadiene Cations

	Transition State	Ground State	C4-cation
C1	6.1811	6.1651	6.1506
C2	6.0902	6.0303	6.0476
C3	6.0902	6.0303	6.1188
C4	6.1811	6.1651	5.7214
C5	6.0902	6.1031	6.1188
C6	6.0902	6.1031	6.0476
C7	5.7832	5.9110	6.2634
H1	0.7530	0.7517	0.7634
H2	0.8208	0.8175	0.8174
H3	0.8208	0.8175	0.8046
H4	0.7530	0.7517	-
H5	0.8208	0.8218	0.8046
H6	0.8208	0.8218	0.8174
H7	0.7045	0.7102	0.7622
C1-H1	0.4165	0.4167	0.4180
C2-H2	0.4670	0.4611	0.4701
C3-H3	0.4770	0.4611	0.4653
C4-H4	0.4165	0.4167	-
C5-H5	0.4770	0.4659	0.4653
C6-H6	0.4770	0.4659	0.4701
C7-H7	0.3913	0.3946	0.4064
C1-C2	0.3635	0.3452	0.3647
C2-C3	0.5553	0.4759	0.5573
C3-C4	0.3635	0.3452	0.3937
C4-C5	0.3635	0.3782	0.3937
C5-C6	0.4759	0.5608	0.5573
C1-C7	0.3911	0.3878	0.3690
C4-C7	0.3911	0.3878	0.3794

the charge distribution. Considering first the carbon which classically carries the positive charge, the centre with lowest population is the C1-cation. It would be expected that, with olefinic centres adjacent, it would be possible to delocalise some of the charge onto these centres. Such a delocalisation cannot occur via the π-system of the olefinic centres, since the orbital which is electron deficient on C1 is in the nodal plane of the π-system. Any delocalisation therefore has to occur through the sigma-system. That it does occur is evident from the populations of the olefinic carbons with those farthest from the classical charged atom being most affected; thus the greater the charge dispersal the better it appears to be. This delocalisation of the charge by means of the olefinic centres shows up in the overlap populations also, with the olefinic bonds becoming weaker and the saturated bonds from the cationic centre to the adjacent olefinic centre becoming stronger, i.e. there is an averaging out of bond strengths across an allylic type system. Besides this through-bond dispersal of the positive charge, a through-space mechanism also operates, with the C4 atom being lowered in population by 0.03 electrons (almost as much as the adjacent olefinic centre).

The largest drop in population of the cationic centres occurs for C7, especially in the transition state (~0.48 electrons). Even in this case there is by no means a complete charge on the cationic centre; all the remaining atoms, including hydrogen help to disperse the charge

TABLE 10

Orbital Energies of Norbonadiene Cations

Transition State	Ground State	Cl-Cation
-319.61	-318.41	-319.26
-315.71	-315.85	-315.38
-315.70	-315.85	-314.84
-313.37	-315.07	314.27
-313.36	-315.06	314.27
-313.35	-312.79	314.26
-313.35	-312.78	314.26
-41.48	-41.82	-41.76
-37.99	-37.77	-38.57
-36.27	-35.90	-36.43
-34.35	-34.80	-34.05
-31.32	-30.97	-31.09
-28.20	-28.20	-28.19
-27.08	-28.00	-27.34
-26.89	-26.99	-26.72
-26.08	-26.31	-25.76
-25.37	-24.91	-23.74
-23.61	-23.76	-22.85
-22.50	-22.47	-22.41
-21.70	-21.58	-22.36
-20.10	-20.24	-20.41
-19.38	-19.31	-20.07
-17.51	-17.82	-18.61
-16.28	-16.21	-16.75

round the molecule. In the (unsymmetrical) ground state it is the atoms towards which the C7-H group is tilted that are most affected by the charge dispersion. In the ground state cation the bond between these olefinic centres is lengthened and there is a considerable drop in the overlap population between the carbons; the other olefinic centres have their overlap population virtually unaffected. Similarly there is very little change in population when the transition state is generated. Despite the fact that there is no positive population between C7 and C2 and C3 (the olefinic centres to which it is tilted) it would appear that the reason for the ground state being unsymmetrical lies in the more efficient delocalisation of the positive charge.

It is possible to estimate further the extent of delocalisation of the positive charge by considering the 1s orbital energies. Olah has shown[18] that in a pure sp^2 hybridised carbonium ion such as the tertiary butyl cation the charge is effectively localised on the classical cationic centre, since the centre atom here occurs at approximately 3.9eV higher binding energy than the outer methyl-type carbon atoms. Where delocalisation occurs, as in the tropylium ion, while there is a shift to higher binding energy because of the positive charge, the 1s levels all occur at the same position. The orbital energies of the three cations are shown in Table 10. The binding energy difference between the saturated carbon 1s levels in the C1-cation and the transition state cation is 3.9eV, exactly that which was found by Olah for $(CH_3)_3C^+$. Bearing in mind

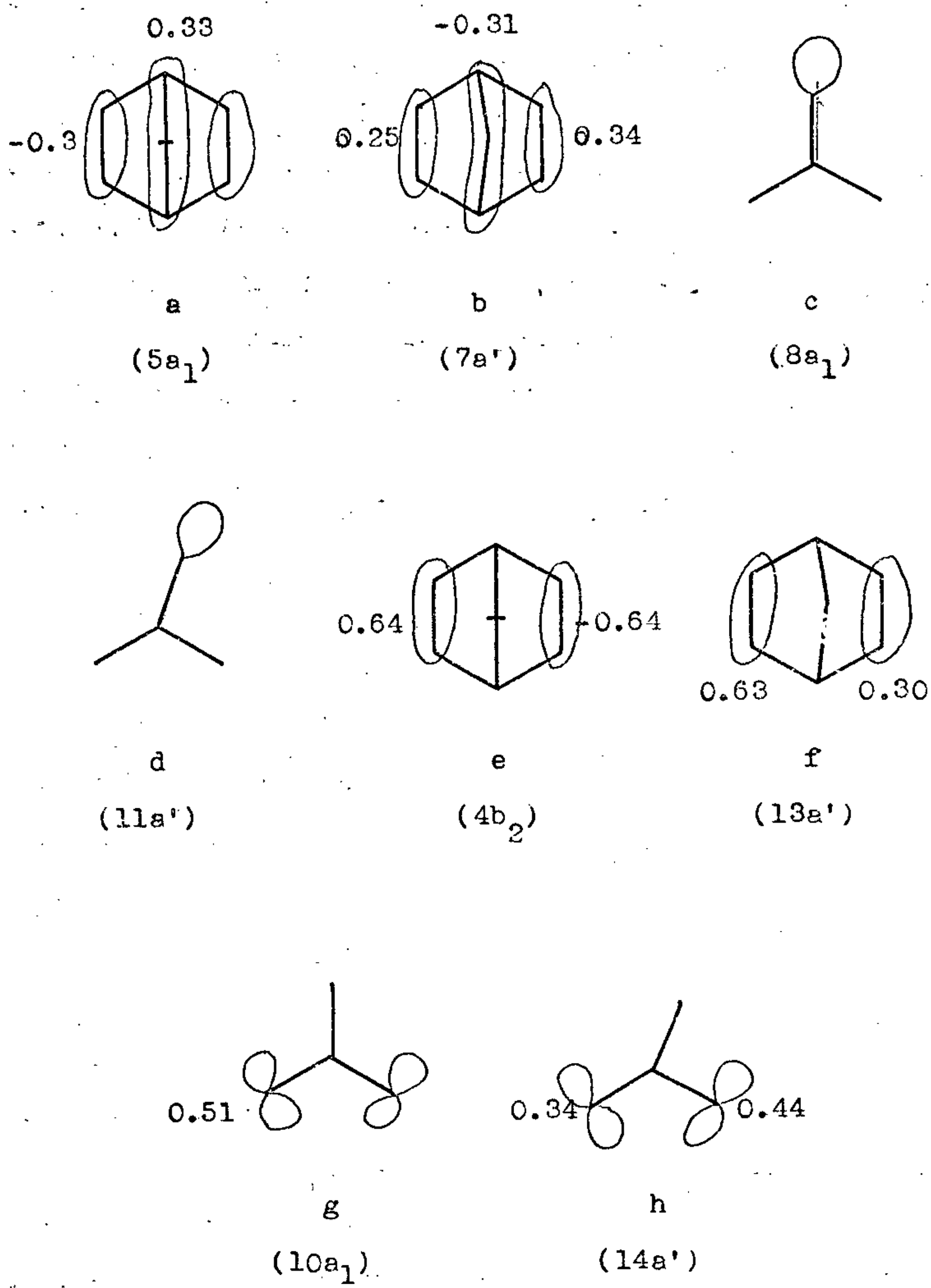

Figure 9 Some Orbitals of the 1-Norbornadienyl Cation (Transition and Ground States): (a) and (b), 2s-levels; (c) and (d), apex C-H level; (e) and (f), olefinic sigma bonds; (g) and (h), pi-orbitals

that there is a tendency for gaussian calculations to over-estimate energy differences between 1s levels, it would appear that there is a small delocalisation of the positive charge in these two species. When attention is turned to the ground state cation, this binding energy difference is considerably less, being 2.6eV implying that there is a large amount of delocalisation of the charge.

The effect on the orbital energies when the cation is generated is to lower them by approximately 7.4eV in the valency shell region (in the core region it is a more variable lowering but always greater than 8eV). This lowering of the eigenvalues affects the virtual orbitals also, resulting in there being some virtual orbitals of negative energy (this was also found in the azoles when protonation occurred).

Generation of the cation has very little effect on the nature of the orbitals. Thus there are orbitals of primarily 2s character, two orbitals (in a symmetric and anti-symmetric pair) of π-type, two olefinic σ-type and so on; i.e. almost identical with the neutral parent molecule. The only significant difference is the loss of a C-H level, as one would expect. Thus in the ground state and transition state 7-cations there is only one apex C-H bond but two junction C-H orbitals; this situation is reversed in the 1-cation. Some examples of the orbitals for the cations are shown in Figures 9a-9h.

Summary

The electronic structure of norbornadiene has been investigated using two different basis sets. The results of each calculation have been compared with experimental data and found to give a reasonable fit. The nature of the orbitals has been demonstrated and data from the population analysis used to predict which of the saturated cations is most likely to be formed. The transition and ground state geometries of the 7-cation have been obtained, yielding an inversion barrier of 8.5 kcal/mole (a lower limit since the transition state is likely to be nearer optimal than the ground state). This barrier is the closest to experimental yet obtained. Finally the effect of the positive charge is discussed together with experimental data on the 1s ionisation potentials.

References

1. P.D. Bartlett, "Non-classical Ions", W.A. Benjamin, New York, NY (1965).

2. M. Brookhardt, R.K. Lustgarten, and S. Winstein, J.A.C.S., 1967, 89, 6352.

3. M. Brookhardt, R.K. Lustgarten and S. Winstein, J.A.C.S., 1972, 94, 2347.

4. R. Hoffmann, J.A.C.S., 1964, 86, 1259.

5. H. Konishi, H. Kato, T. Yonezwana, Bull. Chem. Soc. Japan, 1970, 43, 1676.

6. M.J.S. Dewar, W.W. Schoeller. Tetrahedron, 1961, 27, 4401.

7. S. Yoneda, Z. Yoshida, S. Winstein. Tetrahedron, 1972, 28, 2395.

8. N. Bodor, M.J.S. Dewar, Donald H. Lo, J.A.C.S., 1972, 94, 5303.

9. N.C. Baenziger, G.F. Richards, and J.R. Doyle. Acta Cryst., 1965, 18, 924.

10. T.W. Muecke, M.I. Davis, Trans. Amer. Cryst. Ass., 1966, 2, 173.

11. P. Bischof, J.A. Hashmall, E. Heilbronner and V. Hornung, Helv. Chim. Acta 1969, 52, 1745.

13. R.A. Mattsen, R.C. Ehlert. J. Chem. Phys., 1968, 48, 5465 (Soft X-ray emission spectrum of acetylene, ethylene and methane).

14. R.B. Turner, P. Goebel, B.J. Malliou, W.E. von Doering, J.F. Coburn, M. Pomerantz, J.A.C.S., 1968, 90, 4315.

15. Michael H. Palmer, Antony J. Gaskell and M.S. Barber. Theor. Chem. Acta (Berl.) 1972, 26, 357.

16. P. von R. Schleyer, J.E. Williams, and K.R. Blanchard, J.A.C.S., 1968, 90, 4315.

17. L. Salem, J. Durup, G. Bergeron, D. Cazes, X. Chapuisat, H. Kagan, J.A.C.S., 1970, 92, 4472.

18. G.A. Olah, G.D. Mattescu, J.L. Riemenschneider, J.A.C.S., 1972, 94, 2529.

V. CATIONIC HETEROCYCLES

Introduction

The heterocycles of Group VI elements which are analogous to pyridine necessarily have a positively charged framework. The oxygen analogue is the pyrylium ion (1), while the sulphur analogue is called thiopyrylium (2). These may formally be regarded as being formed by the replacement of a -CH=CH- group in the tropylium cation by O and S respectively. Replacement of two such -CH=CH- groups by S leads to the 1,2-dithiolium (3) and 1,3-dithiolium (4) cations. Since the replacement of two 1π electron donors by one 2π electron donor does not affect the number of π-electrons, these molecules all have 6π electrons and are potential aromatic systems.

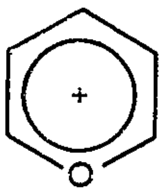

(1)

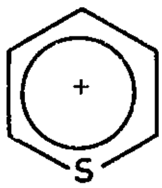

(2)

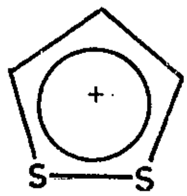

(3)

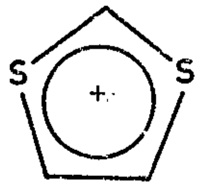

(4)

The largest amount of quantum-mechanical information reported[1-15] on these molecules has been concerned with the ultra-violet spectra,[2-4,10-12,14,15] often of very highly substituted derivatives, and benzo-derivatives;[8,11] other phenomena investigated include bond lengths,[4,12b,13] charge distributions,[5,8,12] NMR chemical shifts[5] and aromaticity.[1,5]

There is a shortage of data on the systems (1)-(4) and the following were used in the calculations. For the 1,2-dithiolium salt the simplest structure reported,[16] that of the 4-phenyl compound, was used. Pyrylium was based on the structure of the pyridinium cation, thiopyrylium on phosphorin and the 1,3-dithiolium cation on the analogous molecule bis-(1,3-dithiole)[17]. Full details of lengths and angles can be found in Appendix 3. Basis sets will be described at the point appropriate for each molecule.

Calculations on the Pyrylium Cation

Non-empirical calculations have been carried out on the pyrylium ion using two different minimal basis sets. For the first calculation the standard best atom set was employed, with the functions described in Appendix 2, Tables 1, 2 and 4 for H, C and O respectively. When this was complete the results of several scaled runs were available and, since these gave improved molecular energies, the standard basis sets were replaced by the appropriate scaled functions. This left the pyrylium ion somewhat misplaced since it could not be directly compared with the analogous thiopyrylium ion. Accordingly the calculation was repeated using a scaled set for each atom; the scaling factors for hydrogen and carbon were taken from scaled ethylene (Tables 8 and 9 in Appendix 2 respectively) while those for oxygen were taken from scaled vinyl alcohol. Such scaled functions were found to be suitable in hetero-aromatics such as furan[18] and can be found in Table 12 of Appendix 2. The repetition of such a calculation was useful on two grounds (1) it enabled a direct comparison to be made with the thiopyrylium cation (2) more generally it supplied a "cross-over" molecule for six-membered rings, as the azines had been studied with best atom bases.

TABLE 1

Total Energies of Pyrylium Ion (1a) and Scaled Pyrylium Ion (1b)

	1a	1b
T.E. (au)	-265.77082	-266.06431
1-El. (au)	-774.65270	-777.43618
2-El. (au)	291.71601	-294.20601
N.R. (au)	217.16586	217.16586
B.E. (au)	-1.01687	-1.31056
B.E. (kcal/mole)	-638.1	-822.2

Table 1 shows the total energies of the pyrylium ion using both basis sets. Binding energy is defined here as being the difference in energy between the molecule and the atomic species 5 x H + 4 x C + 1 x C^+ + 1 x O; carbon was assumed to form the ionic atom since it has the lower calculated (O = 13.26eV, C = 10.80eV) and experimental (13.61 and 11.3eV) ionisation potential (cf. protonated azoles, Section 2); best atom basis sets were used for all atoms, on the same grounds as was discussed for norbornadiene (Section 4). The binding energy of the "best-atom" pyrylium ion is some 40 kcal/mole more negative than was found for pyridine using a best atom calculation; this then implies that the oxygen heterocycle is more thermodynamically stable than the nitrogen one. A possible cause of this is the net positive charge on the molecule drawing the electrons more closely together. If this were true it would be expected that both the electron-nuclear attraction and electron-electron repulsion energies would be greater for the pyrylium ion; comparison of the energies with those of Table 3.1 shows that the expected variations do occur. This table also shows that there is a considerable increase in nuclear repulsion energy; since this implies the atoms are closer together, the expected energy change could comprise effects from the nuclei being closer together, as well as the electrons being drawn in by the positive charge. The scaled calculation is considerably better in terms of energy, by 184.1 kcal/mole; while this is not such a large improvement as was found for norbornadiene, it is of course a considerably smaller molecule. Since the majority of scale factors are greater than unity the one- and two-electron energies show the expected increase in magnitude.

The orbital energies of pyridine, unscaled and scaled pyrylium ion are shown in Table 2. In all cases the orbital of highest energy is that localised on the heteroatom 1s orbital with the oxygen 1s orbital being at considerably greater binding energy than in either furan[19] 562.7eV) or than that of 1,2,5-oxadiazole[19] (564.2eV) where it is in a more electron deficient environment. In the scaled calculation there is the expected shift to lower binding energy (by analogy with norbornadiene); the shift is very much smaller in magnitude than the carbon 1s changes on scaling but is of the same approximate magnitude as was found for furan and 1,2,5-oxadiazole.[18,19] The increase in binding energy from furan to 1a shows how the positive charge, a valence shell phenomenon can effect the core orbitals. The carbon 1s orbitals occur in the same

TABLE 2

Orbital Energies (eV) of Pyridine, Pyrylium and Scaled Pyrylium

	Pyridine	1a	1b		Pyridine	1a	1b
A_1	-426.37	-572.06	-571.94	B_2	-311.96	-320.70	-317.83
	-311.96	-320.69	-317.83		-311.28	-317.85	-314.55
	-311.40	-318.76	-315.59		-30.18	-37.79	-36.58
	-311.27	-317.85	-314.55		-24.61	-32.83	-31.81
	-35.85	-50.04	-49.05		-19.70	-27.49	-26.52
	-31.51	-40.21	-37.91		-18.24	-24.93	-24.08
	-24.95	-32.24	-31.20		-15.91	-22.60	-21.61
	-21.04	-28.85	-28.13				
	-19.11	-25.51	-24.72	B_1	-16.79	-26.54	-25.85
	-17.21	-25.21	-24.47		-12.42	-20.27	-19.29
	-12.46	-21.59	-20.73				
				A_2	-12.12	-18.62	-17.44

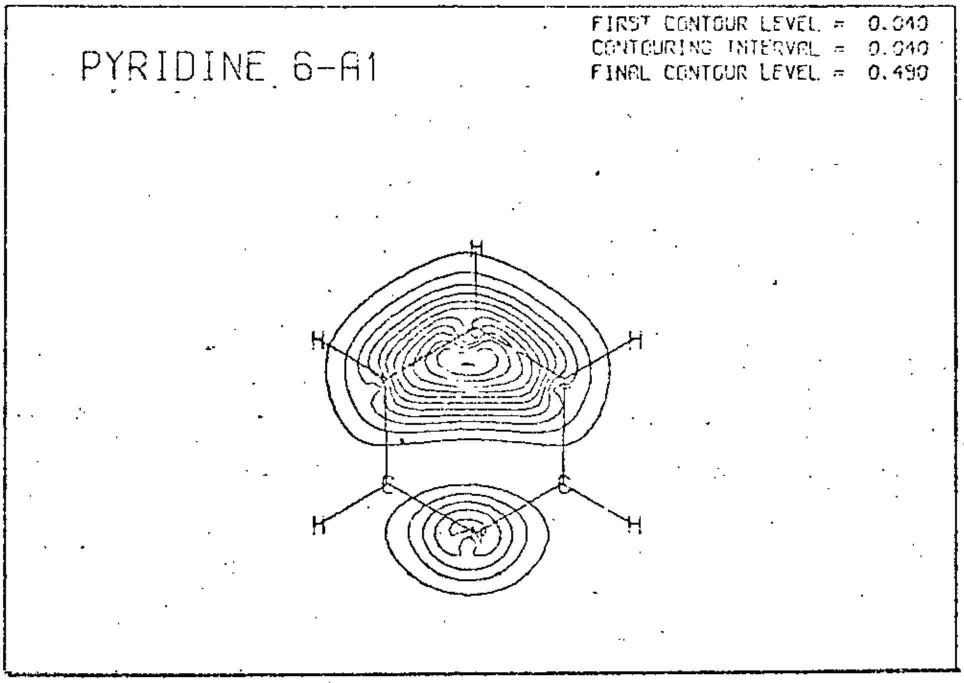

Figure 1 Comparison of the $6a_1$ orbitals of pyridine and the pyrylium ion showing the different position of the nodal planes (see text)

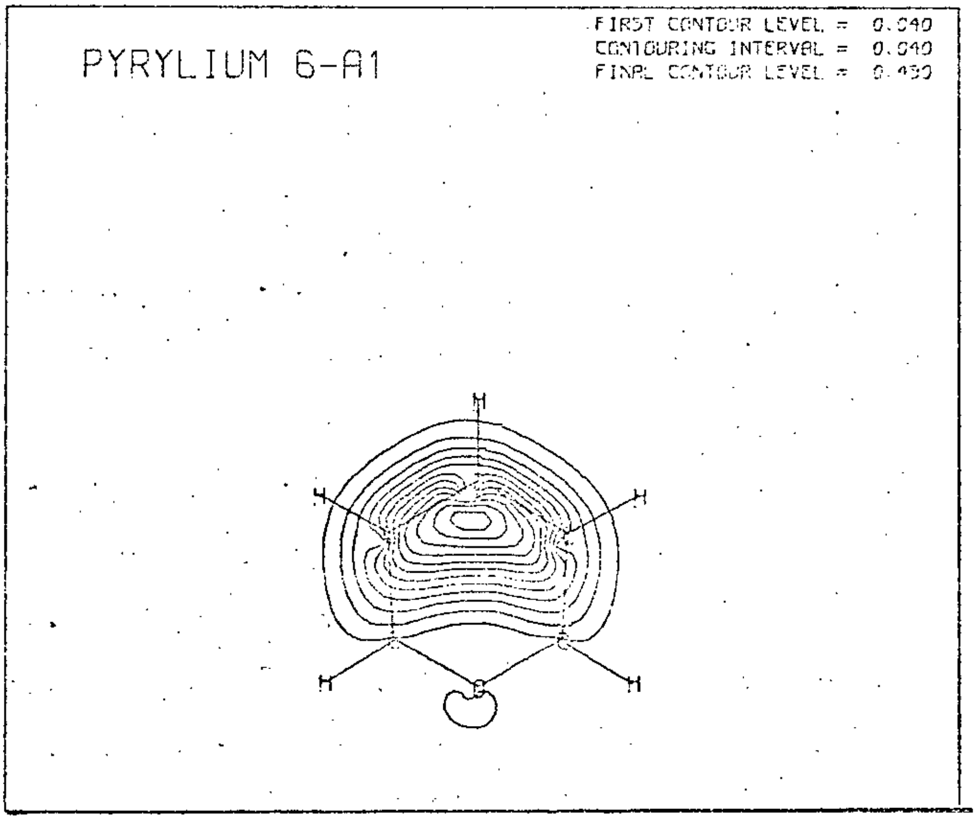

(decreasing) order of binding energies in all three molecules, namely C2(=C6), C4, C3(=C5). The span of energies in pyridine is 0.7eV, but in the (unscaled) pyrylium ion the spread is 2.8eV; this is increased in the scaled calculation to 3.3eV. It is possible then that the difference in energy levels may be detectable using x-ray photo-electron spectroscopy. The decrease in orbital energy on replacement of N by O^+ is greatest for the carbon next to the hetero-atom (8.7eV); it does not however decrease with decreasing distance from the hetero-atom since the C4 1s orbital has its energy made more binding than the C3/C5 value (7.3eV as opposed to 6.6eV).

Orbital $5a_1$, the first orbital after the core orbitals is very highly localised on the oxygen 2s function. This orbital shows the greatest increase in binding energy when comparison is made with the corresponding pyridine orbital. The extent of localisation can be judged from (1) the eigenvector of the 2s orbital being 0.76 in this orbital (2) the population analysis which credits the oxygen 2s function in orbital $5a_1$ with a population of 1.33 out of a total 2s population of 1.68 (79%), the remaining being spread fairly evenly through the remaining a_1 orbitals. (similar figures, 1.40e in $5a_1$ being 80% of the total, hold for the scaled calculation). This localisation is also true of pyridine but is much less marked; the tendency for localisation due to the 2s orbital energy of the oxygen atom is reinforced by the nominal unit charge on the oxygen atom. This can be shown by examination of the corresponding orbital in furan[18,19] ($4a_1$) where the eigenvector of the 2s orbital is 0.72, giving a population of 1.24 which is 73% of the total.

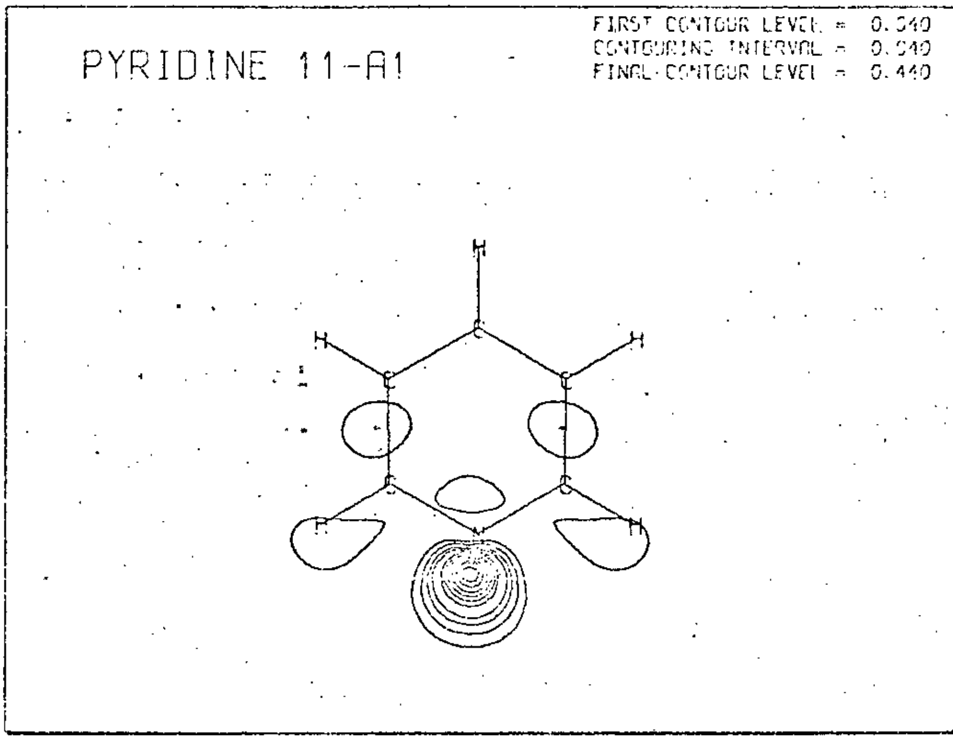

Figure 2 Lone pair orbital in pyridine and the corresponding orbital of the pyrylium ion, which has no lone pair character

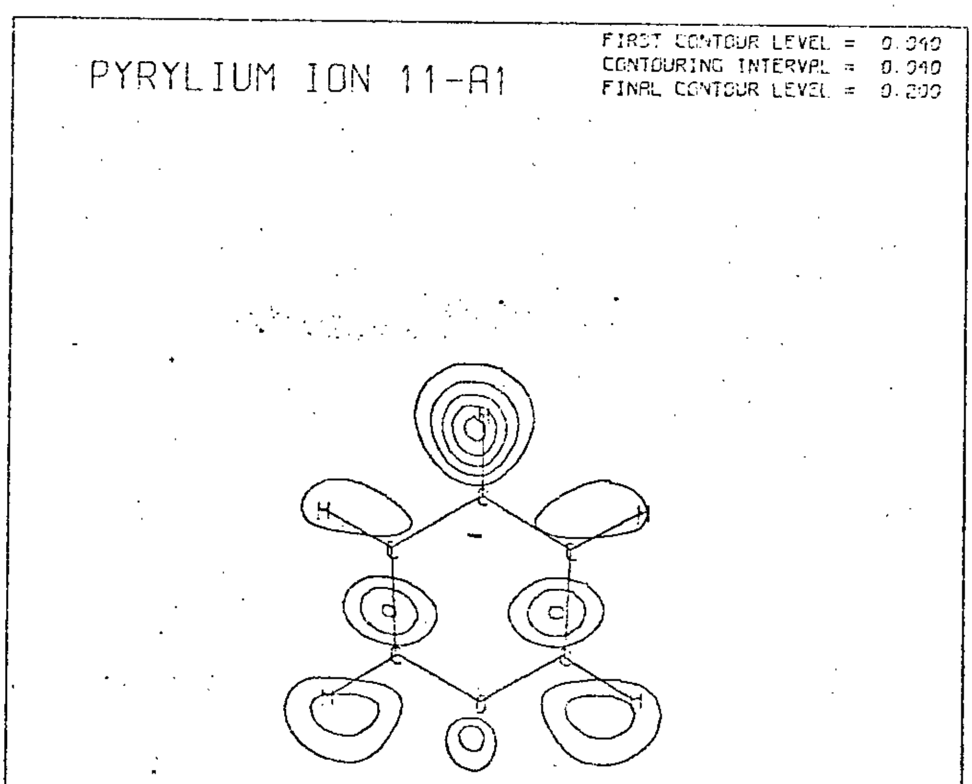

The energies of the remaining orbitals do not in general show such a marked increase in binding energy; the typical increase in binding energy is approximately 7eV upon the introduction of O^+ with the main exception being $1b_1$, where the orbital is very heavily localised on oxygen $2p_\pi$, to such an extent that there is virtually no contribution from the C5 $2p_\pi$ function. This is a further indication of the effect of the orbital energies of oxygen i.e. where the orbital is virtually localised on an oxygen function (e.g. in $5a_1$ and $1b_1$) by virtue of its free atom orbital energy being so much lower than the other atoms, then that orbital is at abnormally high binding energy. The introduction of scaled functions has the same effect as in norbornadiene, i.e. a general decrease in binding energy; the ordering of the orbitals is identical in both calculations.

TABLE 3

Character of the Valency Shell Orbitals in the Pyrylium Ion

Orbital	Nature
$5a_1$	Highly localised oxygen 2s level
$6a_1$	Predominantly 2s, but with O value of opposite sign to carbon 2s functions. C4 is highest eigenvector, decreasing to C2/C6.
$7a_1$	Large amount of 2s present, but no longer predominant. Mainly ring C2-C3/C5-C6 bonding.
$8a_1$	Totally symmetric C-H bonding level, plus a little ring bonding.
$9a_1$	More C-H bonding of the form (C2-H)-(C3-H)-(C4-H) + (C5-H).
$10a_1$	Very delocalised orbital with main bonding being O-C2/O-C6.
$11a_1$	Some lone pair characteristic but not particularly marked.

(Contd.

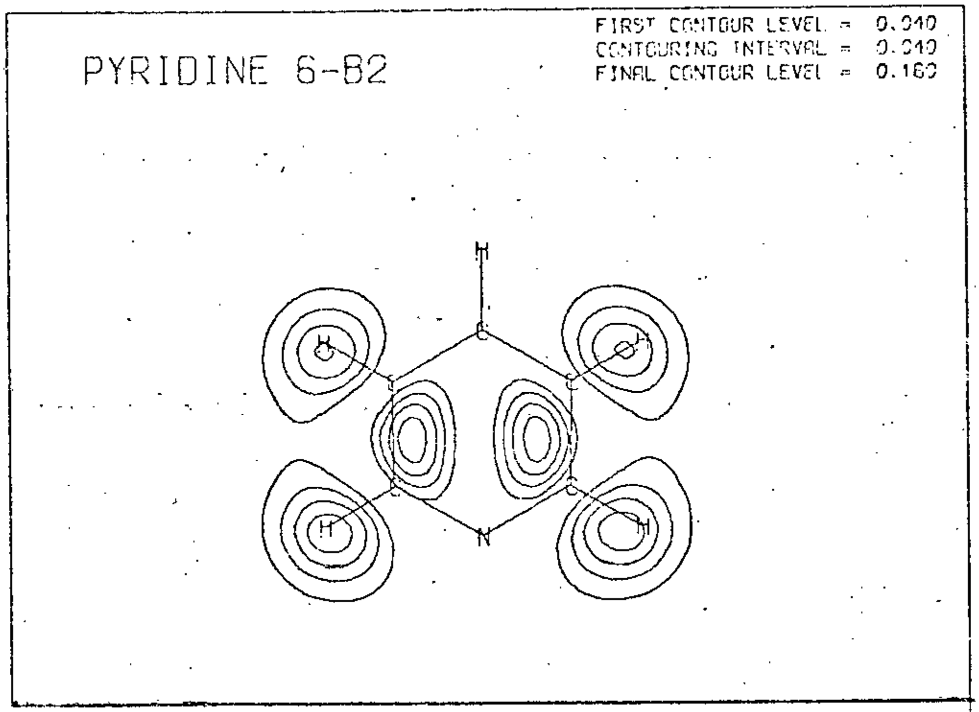

Figure 3 Orbital $6b_2$, showing a greater electron density around the C_α positions

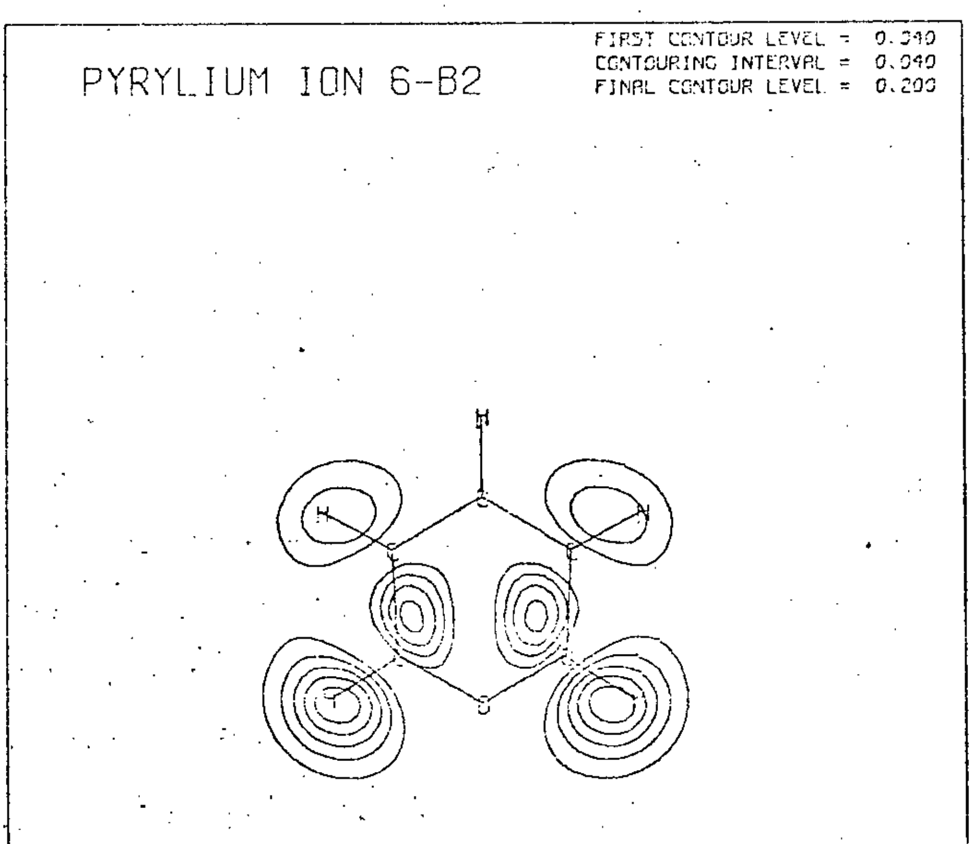

Table 3 (Contd.)

Orbital	Nature
$3b_2$	Extensive ring bonding from O to C4. C2-C3 bond is exclusively 2s in nature.
$4b_2$	General ring bonding with oxygen somewhat isolated from remainder of molecule.
$5b_2$	p-Bonding in pairs round ring, with a node passing through each atom.
$6b_2$	C-H Bonding of type (C2-H) + (C3-H)-(C4-H)-(C5-H)
$7b_2$	Similar to $5b_2$, but has an additional node perpendicular to C3-C4 bond. Significant amount of C-H bonding giving a double W shaped orbital.
$1b_1$	Heavily localised on O $2p_\pi$ orbital. C4 effectively non-existent.
$2b_1$	Split into two parts 1) oxygen 2) carbon with C2/C6 of zero eigenvector.
$1a_2$	C2-C3 bond with C2 slightly greater.

The overall nature of the orbitals in pyrylium, whether one considers the scaled or unscaled sets, is similar in many respects to that of pyridine, as one would expect. These differences consist of differences in degree rather than in nature; thus orbital $6a_1$, which in= pyridine is nodal across the C2-C3 and C5-C6 bonds, is nodal between the O and the C2, C6 atoms. This node occurs just on the oxygen side of the α-carbons so that it has shifted by approximately half a C-C bond length. Similarly the lone pair character of the top σ-orbital ($11a_1$) is very much reduced with the appropriate p eigenvector being reduced from 0.81 (pyridine) to 0.55 (pyrylium ion). Such differences are by no means confined to the A_1 symmetry type. For example, $6b_2$, a predominantly C_α-H/C_β-H bonding level in both molecules has a greater amount of C_α-H than C_β-H in

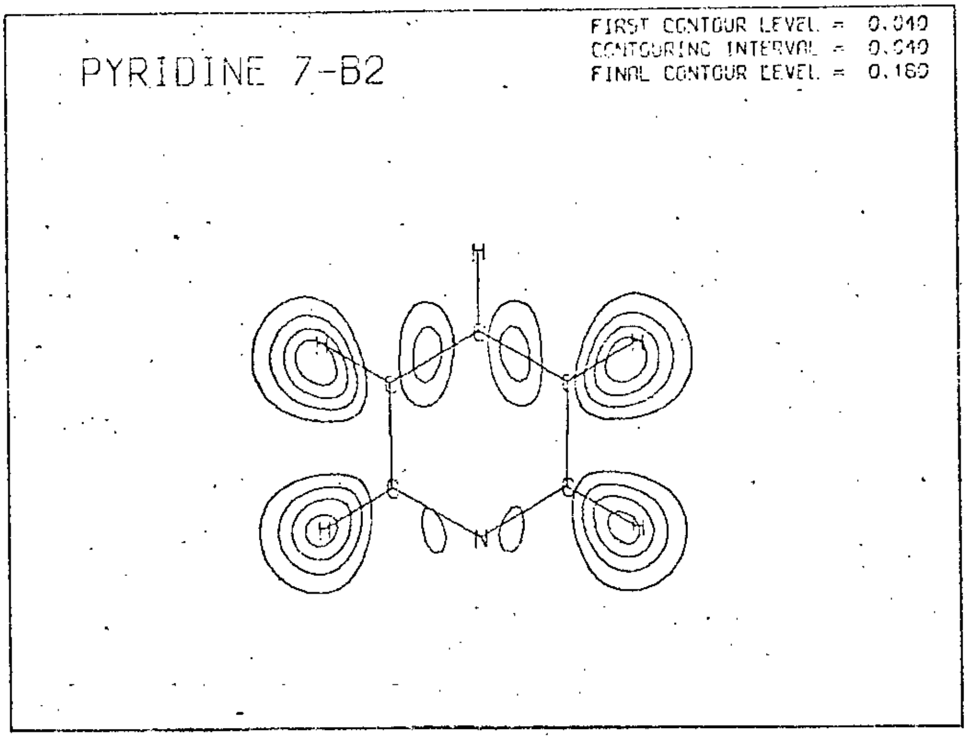

Figure 4 Electron density is moved away from the oxygen atom, the opposite of preceding Figure

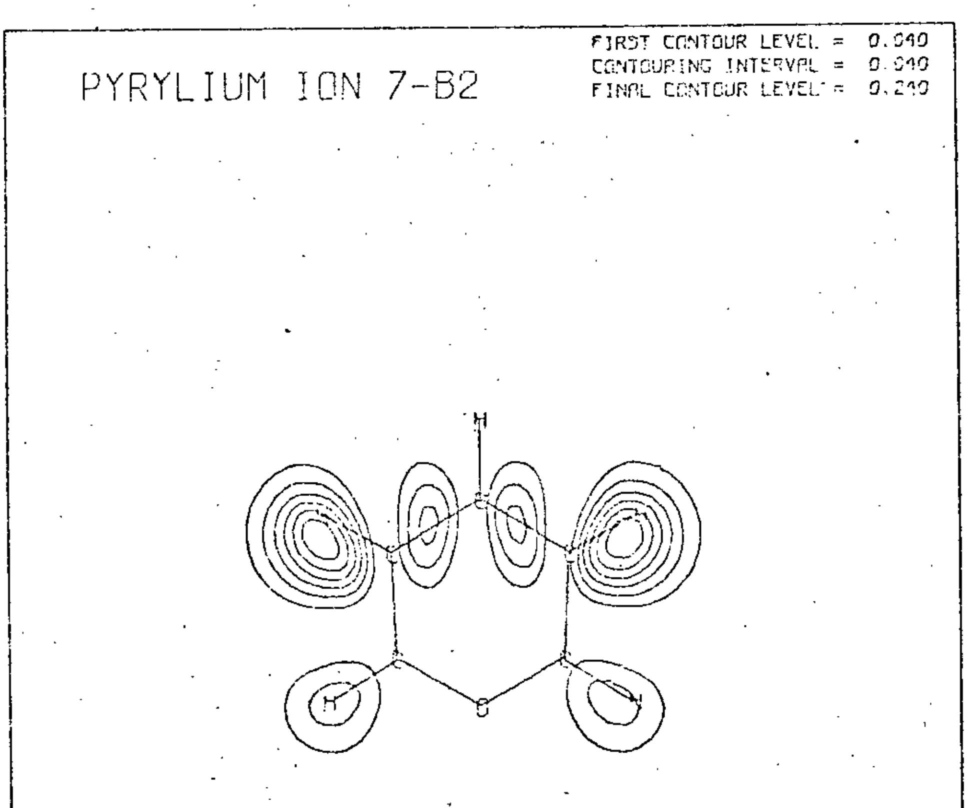

the pyrylium ion, while in pyridine they are almost equal. In the π-system orbital $1b_1$ has already been mentioned; orbital $2b_1$ behaves in a similar fashion to $6a_1$ in that the nodal plane lies between C_α-O instead of C_α-C_β. There is thus an overall effect of the molecule splitting into two entities; in the pyrylium ion the first part is O, the second part is the carbon atoms. In pyridine the split is into C2-N-C6 and C3-C4-C5 moieties. (The nature of the orbitals is recorded in Table 3). This in general leads to an increase in eigenvector when compared to pyridine, if there was no node between the nitrogen and its adjacent carbons; similarly, where there was a node the eigenvectors in general show a movement away from the hetero-atom. This type of push-pull mechanism explains results for orbitals such as $7b_2$ where the C_α-C_β bond is more prominent in pyrylium than in pyridine.

TABLE 4

Population Analysis of Pyrylium and Scaled Pyrylium.

a) Best Atom Calculation.

	O	2,C6	C3,C5	C4
1s + 2s	3.6769	3.0694	3.0738	3.1078
$2p_\sigma$	3.0407	1.9734	2.1585	2.2513
$2p_\pi$	1.5606	0.8433	0.9955	0.7617
Total	8.2772	5.8852	6.2280	6.1208
H	-	0.6563	0.6912	0.6807

b) 'Scaled' Calculation

1s + 2s	3.7471	3.0330	3.0523	3.0924
$2p_\sigma$	3.0777	1.8869	2.0926	2.1890
$2p_\pi$	1.6120	0.8311	0.9889	0.7479
Total	8.4368	5.7510	6.1339	6.0292
H	-	0.7368	0.7663	0.7594

Table 4 shows the results of a Mulliken population analysis on both pyrylium calculations; although the numbers are different in magnitude in the two calculations trends are the same, and as such can be discussed together. The oxygen atom has a net negative charge which is in direct opposition to the classical structure drawn for (1) above, where it is implicitly assumed that the positive charge is localised on the oxygen atom. The population is somewhat less than that found for furan[18,19] but greater than for 1,2,5-oxadiazole[18,19] (using the appropriate basis sets for comparison). This is in keeping with the different electronegativities of C, N and O.

The alternative classical representation is that the oxygen replaces two carbon atoms in the tropylium ion, giving a two-electron donor to the π-system (if pyridine-like the oxygen would give only one-electron to the π-system). The $2p_{\pi}$ population of 1.56 and 1.61 for the unscaled and scaled sets respectively is very much more reminiscent of the situation in pyrrole ($2p_{\pi}$ = 1.63) than that in pyridine ($2p_{\pi}$ = 0.99). This then suggests that the better classical representation is the one where oxygen is a 2 electron π-donor. However this requires that the oxygen atom accepts 1.04e from the p-σ system, a rather large transfer. The classical one π-electron arrangement does not require re-arrangements of such magnitude (+0.33e from oxygen 2s, -0.04e from p-σ and -0.56e from p-π).

It is possible to use the population analysis of Table 4 to predict the relative preference of the carbon atoms for nucleophilic attack. Total population predicts that only carbon atoms C2 and C5 should be attacked, as these are the only ring atoms with a net positive charge. Nucleophilic attack on 2,4,6-trisubstituted pyrylium salts does occur at the C2(C6) position;[20,21] however the effect on the total population of the substituents cannot be predicted. As nucleophilic attack on the ring carbons must occur from a direction perpendicular to the plane of the ring (in plane attack is prevented by the hydrogen atoms) it is likely that the $2p_{\pi}$ populations may be a more correct criterion for predictions regarding nucleophilic attack. This then predicts that the most active position would be the C4 position, closely followed by the C2/C6 positions. This would appear to contradict the experimental evidence of the 2,4,6-trisubstituted compounds (above); however, when the C4 position is free from substituents nucleophilic attack occurs at this position.[22]

TABLE 5

Second Moments[a] and Diamagnetic Susceptibilities[b]

		Pyridine	1a	1b
2nd Moment	xx	-59.7	-55.8	-55.1
	yy	-57.5	-57.0	-56.4
	zz	-9.1	-8.5	-7.6
Diamag. Sus	xx	-282.2	-277.8	-271.84
	yy	-291.5	-272.7	-266.03
	zz	-497.0	-478.2	-473.07
$zz-\frac{1}{2}(xx+yy)$		-210.1	-202.9	-204.13

a) Electronic term only, in units of $10^{-16}cm^2$
b) " " " " " " $10^{-6}erg.G^2/mole$.

The tensor components of the second moment and diamagnetic susceptibility properties are shown in Table 5, along with those of pyridine. The second moment values for pyrylium ion are smaller than those for pyridine, indicating that the charge pulls the electrons in towards the nuclei. The aromaticity factor, $zz-\frac{1}{2}(xx+yy)$ as defined by Flygare[23] from the diamagnetic susceptibility tensors indicates that the pyrylium ion is slightly less aromatic than pyridine. Translation of this aromaticity charge into chemical shift differences is not possible because of the effect of the molecular charge (counter ion and solvent do not appear to affect the NMR spectrum significantly)[24]. If one assumes that the hydrogen populations give an indication how the nuclei are shielded from the applied field, then the lower the population of a hydrogen atom then the farther downfield (lower τ values) will the hydrogen resonate. The predicted order is then (high to low field) C3/C5, C4, C2/C6 which is in qualitative agreement with the observed data (C3/C5, 1.5τ; C4, 0.7τ; C2/C6 0.4τ).

Thiopyrylium Cation

Scaled minimal basis sets were used for this molecule. The scale factors used for carbon and hydrogen were those obtained by scaling ethylene; those for sulphur came from scaling of thio-formaldehyde. The exponents and contraction coefficients can be found in Appendix 2, Tables 8, 9 and 13 for H, C and S respectively.

TABLE 6

Total Energies (au) and Orbital Energies (eV) for the Thiopyrylium Cation

T.E.	-588.14487
1-El.	-1319.4685
2-El.	465.88060
N.R.	265.44302
B.E. (au)	-0.99593
B.E. (kcal/mole)	-624.9

A_1	-2501.8	B_2	-315.4
	-315.4		-314.3
	-314.9		-188.7
	-314.3		-35.09
	-246.3		-29.75
	-188.6		-24.60
	-39.25		-23.54
	-35.74		-20.38
	-29.79		
	-26.40	B_1	-188.55
	-24.11		-21.72
	-22.27		-17.79
	-19.37		
		A_2	-17.12

The total energy terms obtained for thiopyrylium are shown in Table 6; evaluation of the first ionisation potential for sulphur gave a value of 9.5eV against 10.8eV for carbon. This is in reasonable agreement with the experimental values of 10.36(S) and 11.3(C); accordingly the atom species used in determining the binding energy were 5 x C + 5 x H + 1 x S^+ with unscaled basis sets being used for atomic calculations. The binding energy thus evaluated is slightly less than the unscaled pyrylium ion and considerably less in magnitude than that of scaled pyrylium, with which comparison should be made. This then predicts that the thiopyrylium cation is less stable with respect to decomposition to the atoms than is the pyrylium ion.

Starting at highest binding energy the first ten orbitals are localised and can be regarded as core orbitals. The first of these is the sulphur 1s orbital; it is followed by the carbon 1s orbitals where the order (in decreasing binding energy) is C2/C6, C4, C5/C3. This is the same order as was found for pyridine and both calculations on the pyrylium ion; the span of carbon 1s energies in thiopyrylium is only 1.0eV which is much less than that found for the pyrylium ion. Since a span of 1.9eV was not resolvable using ESCA techniques on norbornadiene (Section 4) it is unlikely that it will be possible to separate these peaks. The small span of carbon 1s energies is consistent with the electronegativities of sulphur and oxygen. Thus when oxygen is present it is a very electron withdrawing group and this makes great lowering of the C2/C6 and C4 core orbital energies take place. In contrast the sulphur atom is very much less electro-negative resulting in the carbon atoms receiving a somewhat greater share of the electrons. This is shown by the average of the carbon energies being 1.2eV to lower ionisation potential than the pyrylium ion. The remaining core orbitals are the hetero-atom 2s and 2p orbitals; the three 2p orbitals occur at some 58eV less negative binding energy than does the 2s level (cf. 63eV in the free atom). There are very slight energy differences in the three 2p functions.

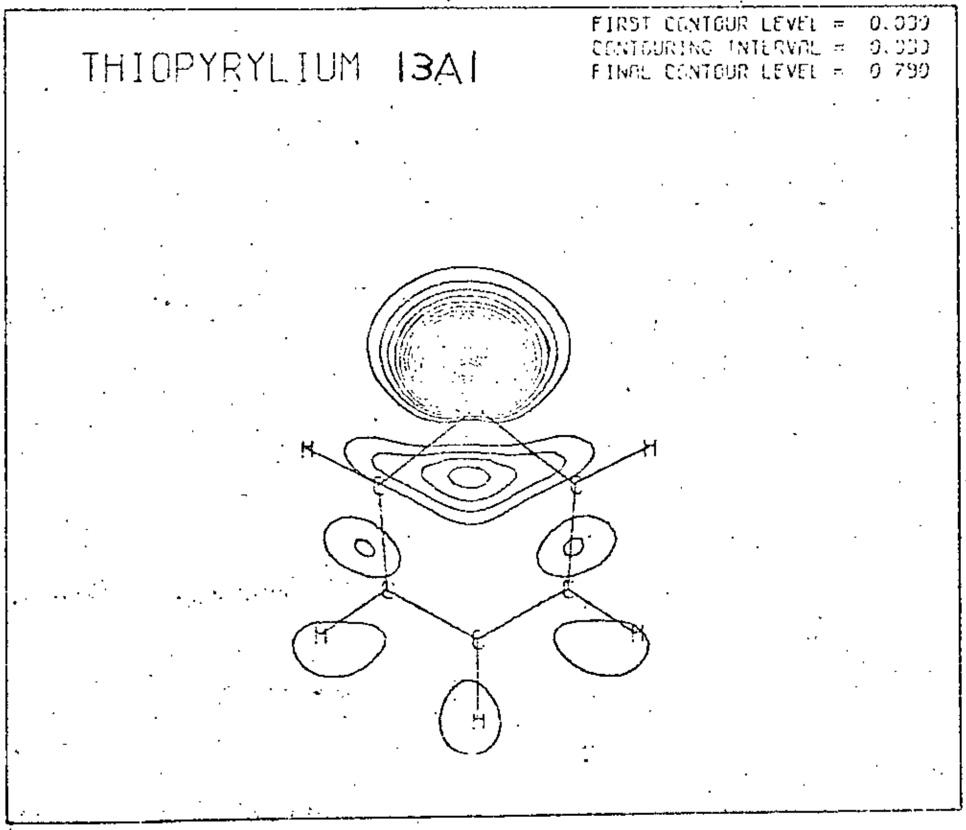

Figures 5a and 5b. Some valence shell orbitals for thiopyrylium

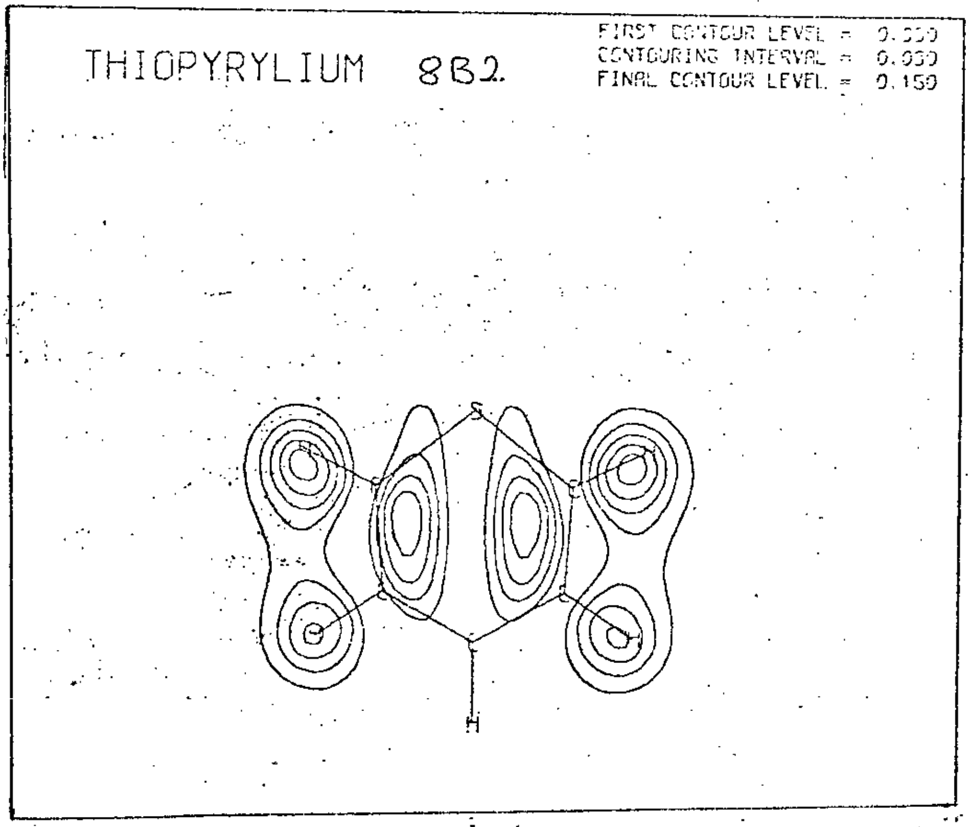

TABLE 7

Nature of Thiopyrylium Valence Shell Orbitals, and Assignment in Terms of Benzene Orbitals

Orbital	Benzene Type	Nature
$7a_1$	A_{1g}	Symmetric valency shell S orbital
$8a_1$	E_{1u}	Valency shell S with nodal plane passing through C2-C3 and C5-C6 bonds
$4b_2$	E_{1u}	Valency shell S with node through S and C4 (Other "half" of pseudo-degenerate pair)
$9a_1$	E_{2g}	Valency shell S:- S1+C4-C2-C3-C5-C6 in nature
$5b_2$	E_{2g}	Valency shell S (C2-C3 C5-C6) with C4 and S1 x orbitals
$10a_1$	A_{1g}	Symmetric C-H level
$11a_1$	B_{1u}	C-H level of (C2-H)+(C6-H)-(C3-H)-(C5-H) type
$12a_1$	E_{1u}	S1 lone pair + (C2-H) + (C6-H) - C3-H)-(C4-H)-(C5-H)
$7b_2$	E_{1u}	(C2-H) + (C3-H) - (C5-H) - (C6-H)
$13a_1$	E_{2g}	Sulphur lone pair
$8b_2$	E_{2g}	Mixed C-H and ring bonding
$6b_2$	B_{2u}	Ring bonding
$2b_1$	A_{2u}	Symmetric valency shell z combination
$3b_1$	E_{1g}	(C3 + C4 + C5) - (S1 + C2 + C6) z combination with C2, C6 small
$1a_2$	E_{1g}	C2 + C3 - C5 - C6 combination.

In the pyrylium ion it was found that the first non-core orbital was very localised on the oxygen 2s orbital. This was attributed to the 2s function being of much lower energy in the free atom and hence not interacting strongly with the carbon functions. Calculations on the sulphur atom using the unscaled basis set showed that the 3s orbital energy was very similar to that of carbon 2s (22.07eV and 24.65eV respectively); the values for the 3p and 2pvalues are almost identical (12.19eV and 11.78eV). The sulphur

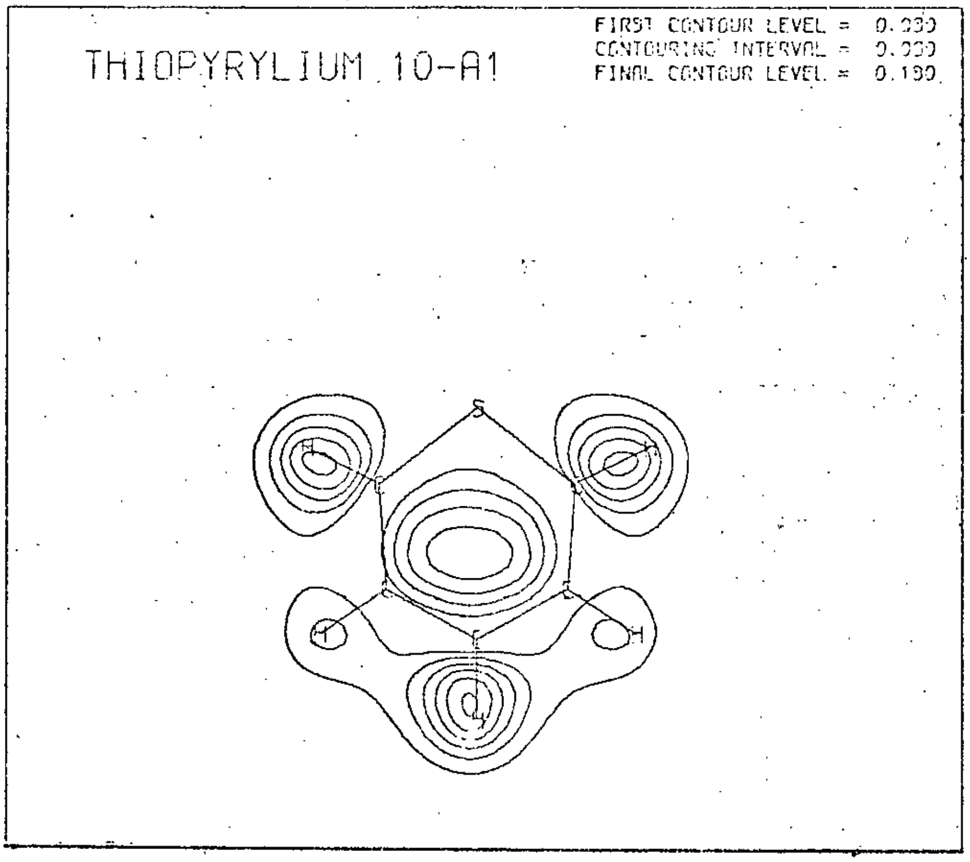

Figures 5c and 5d. Some valence shell orbitals for thiopyrylium

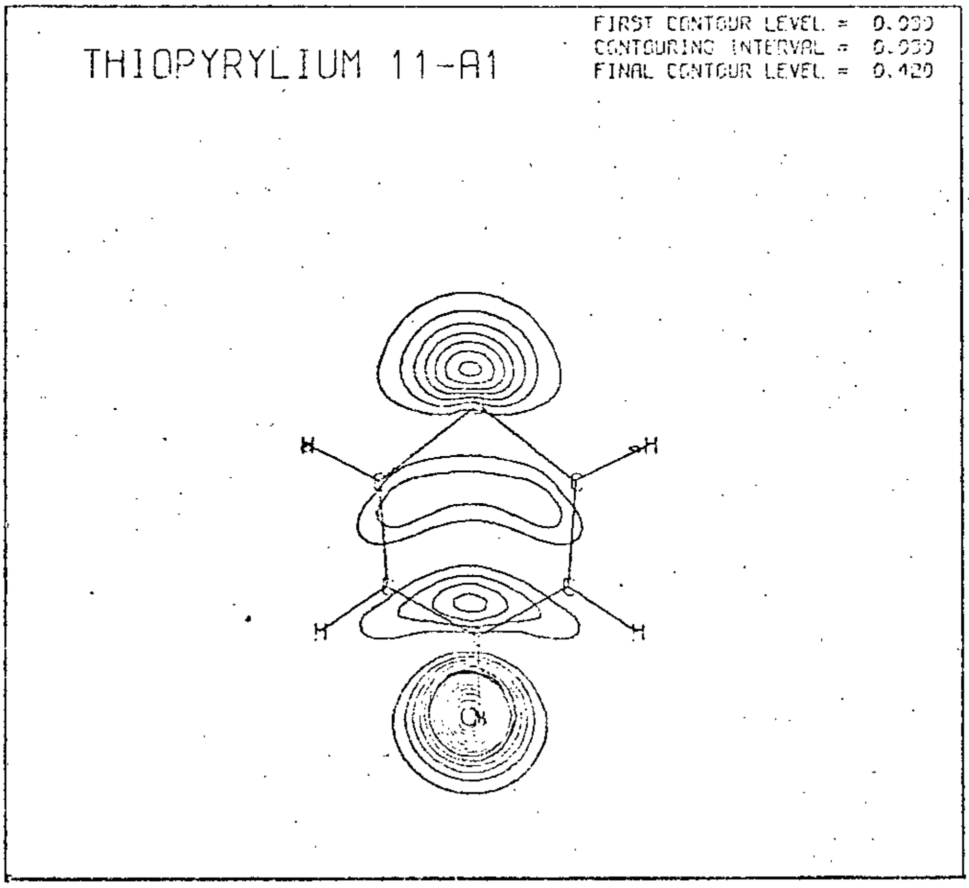

atom would then be likely to behave much more as a carbon atom than did the oxygen in pyrylium ion or even the nitrogen in pyridine, i.e. there is much less distortion of the benzene molecule in thiopyrylium than in pyrylium. Assignments could then be made of the valence shell orbitals to pseudo-benzene type orbitals (D_{6h}) with more ease then was found for pyridine (the differences in degree found in the pyrylium ion were sufficiently marked to cause changes in the positions of nodes and hence disallow the benzene type of analysis). The nature of the valency shell orbitals is recorded in Table 7, together with the assignments in terms of benzene orbitals. The occupation order is the same as for benzene but, since this is also true of pyridine, this does not show how alike the thiopyrylium cation and benzene are; the gap between the pseudo-degenerate levels shows this in a striking manner (Table 8). In most cases the thiopyrylium orbitals have an overall tendency to be closer together in energy when they are pseudo-generate.

TABLE 8

Separation of Pseudo-degenerate levels in Thiopyrylium and Pyridine (in eV)

Pseudo-Degenerate Pair	Pyridine	Separation in Thio-pyrylium
$8a_1/4b_2$	1.4	0.69
$9a_1/5b_2$	0.5	0.04
$12a_1/7b_2$	0.9	1.27
$13a_1/8b_2$	3.2	1.00
$3b_1/1a_2$	0.4	0.67

In view of the near equality of the electronegativities of carbon and sulphur it is not surprising that the orbital energies are somewhat similar. This has several important consequences on the electronic structure:- (i) the orbitals corresponding to those which were largely localised on oxygen will decrease their ionisation potential quite sharply. The observed energy change is 9.8eV for $7a_1$ and 4.1eV for $2b_1$ ($5a_1$ and $1b_1$ in pyrylium) which can be contrasted with a decrease of approximately 2eV for the other orbitals (ii) the sulphur 3s population of 1.74 electrons comes from orbitals 7-$9a_1$ and 11-$13a_1$ not predominantly from one orbital, (iii) the sulphur atoms has a net positive charge of 0.4234 (from Table 9) since the carbon atoms are able to get a larger share of the electron than they could in the pyrylium ion, (iv) because of (iii) the carbon atoms have a higher population and become more alike in charge, which is of course compatible with the lesser span of the 1s orbital energies. A further result of (iii) is that the hydrogen atoms become somewhat less positively charged (population increases).

TABLE 9

Population Analysis of Thiopyrylium Ion

	S	C2/C6	C3/C5	C4
Core + Valence s	11.6940	3.1360	3.0509	3.0764
Valence p_σ	2.3764	2.1351	2.1041	2.1785
Valence p_π	1.5063	0.8942	0.9592	0.7979
Total	15.5766	6.1653	6.1143	6.0528
H	-	0.7469	0.7742	0.7689

The total population of the carbon atoms is greater than six for all carbons; on this basis none should be activated towards nucleophilic attack. However the $2p_{\pi}$ carbon populations show that the preferred order is C4 > C2/C6 > C3/C5, i.e. the same order as was found for the pyrylium ion. Extending this to take in both molecules, the reactivity order would be C4(O), C4(S), C2/C6 (O), C2/C6(S), C3/C5(O), C3/C5(S). The hydrogen populations predict the H2/H6 protons to be at lowest field in the NMR spectrum, then H4 and finally H3/H5; this is the correct predicted order but comparison with the pyrylium populations shows that the thiopyrylium resonances should be upfield of the corresponding pyrylium resonances. This is not in fact observed and emphasizes that the population analysis is only a qualitative guide to experimental data. It may be that the lower electronegativity of S allows greater delocalisation.

TABLE 10

1-Electron Properties of Thiopyrylium Cation.[a]

	xx	yy	zz	$zz-\frac{1}{2}(xx+yy)$
Second Moment	-64.55	-84.33	-9.34	-
Diamag. Sus.	-397.42	-313.48	-631.65	-276.20

a) For units see Table 5.

Some 1-electron properties of the thiopyrylium cation are shown in Table 10; the second moment components are somewhat greater than those found with the scaled pyrylium calculation. This is to be expected since the sulphur

TABLE 11

Total Energies (au) and Orbital Energies (eV) of the Dithiolium Cations

	1,2-Dithiolium	1,3-Dithiolium
T.E.	-908.01639	-908.02141
1-El.	-1783.4320	-1766.4419
2-El.	600.15072	-591.94399
N.R.	275.26486	266.47650
B.E.	-0.64531	-0.65033
B.E. (kcal/mole)	-404.9	-408.1

A_1	-2502.01	B_2	-2502.03	A_1	-2501.98	B_2	-2501.98
	-317.00		-317.01		-317.52		-315.71
	-315.65		-247.01		-315.73		-246.71
	-246.90		-189.32		-246.70		-189.06
	-189.26		-189.24		-189.06		-189.01
	-189.19		-36.29		-188.99		-35.32
	-41.37		-29.72		-40.41		-28.78
	-35.88		-24.66		-35.76		-22.81
	-29.58		-21.44		-30.18		-19.86
	-27.82				-26.97		
	-23.39	B_1	-189.11		-24.59	B_1	-188.95
	-20.40		-23.22		-21.67		-22.64
			-18.32				-18.06
		A_2	-189.16			A_2	-188.95
			-18.71				-18.44

orbitals are more diffuse than the oxygen. The aromaticity parameter is very much larger than that found for the pyrylium ion; this is reminiscent of the difference between the azoles and the azines and can similarly be described as a change in origin of the aromaticity parameter, i.e. the aromaticity term can only be applied to iso-electronic species.

The Dithiolium Cations

The basis sets used were identical to the thiopyrylium cation case, and the results of these calculations are shown in Table 11, where the atomic species used to determine the binding energies were 3 x H + 3 x C + 1 x S + 1 x S^+. The binding energies are almost identical, but considerably smaller than those found for the thiopyrylium cation. It would seem therefore that, as the number of hetero-atoms substituted for -HC=CH- groups in the tropylium cation increases, the stability of the molecules decrease.

The core orbital ionisation potentials occur at higher binding energy than was found for the thiopyrylium cation. This is consistent with the same charge being present in a smaller nuclear framework; the sulphur 2p orbital energies for several substituted 1,2-dithiolium cations has been reported;[25] the values found here show the same trend as first row 1s levels, i.e. the calculations overestimate by some 25eV. In the 1,2-dithiolium cation the carbon atoms adjacent to sulphur have 1s orbital energies more negative, by 1.3eV than the unique carbon. This would lead one to expect that unique carbon in the 1,3-dithiolium case to be

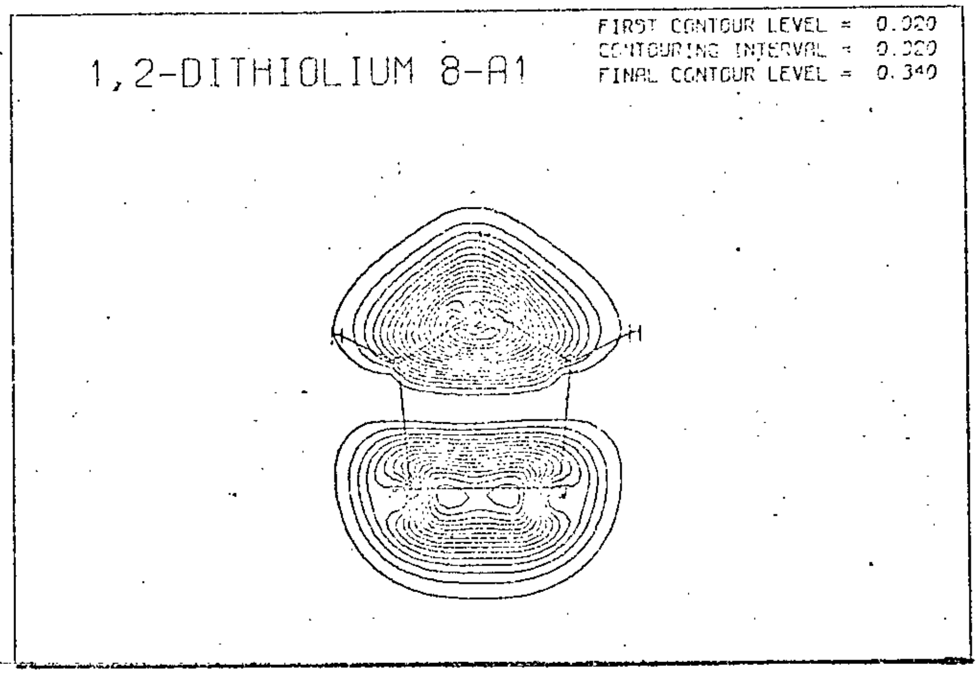

Figure 6a (above) Separation into S-S and allyl parts

Figure 6b (below) Separation into C-C and C-S-C parts

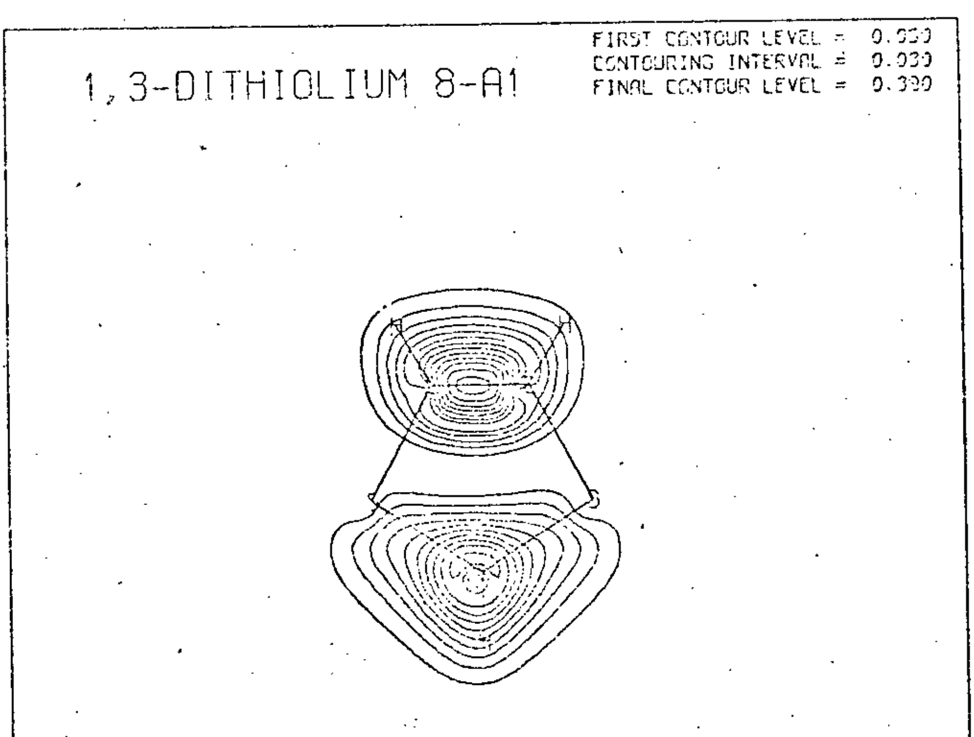

at higher ionisation potential still, since it is adjacent to two sulphur stoms, and the C4/C5 atoms to be at the same value as C3/C5 of the 1,2 isomer. That this is not so can be seen from Table 11. The observed carbon 1s values can be explained by the following two classical representations:-

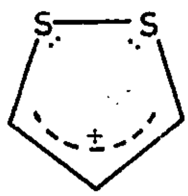

(5)

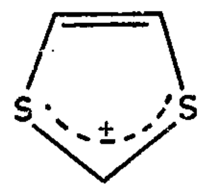

(6)

where in each case the positive charge is delocalised over three atoms. Representation (5) is an alkyl carbonium ion with a di-sulphide bridge; a calculation on the allyl positive ion using the same carbon-hydrogen skeleton as in the 1,2-dithiolium cation gave the centre carbon a 1s orbital energy of -316.33 and the terminal carbons -318.52eV, similar to what was found for the 1,2-dithiolium cation. The two "olefinic" carbons C4/C5 of structure (6) are at lower ionisation potential because the positive charge is not delocalised over them. The remaining atom, C3 of 6, does not show the allyl characteristic because it is in the centre of a 4-electron 2-centre bond, involving the π-orbitals of S1-C2-C3. If these structures are to be considered realistic there are clearly several characteristics which must also occur:- (a) the overlap population and π-populations for the carbon part of (5) must be similar to those found for the carbonium ion; (b) the p_{π} populations of the sulphur

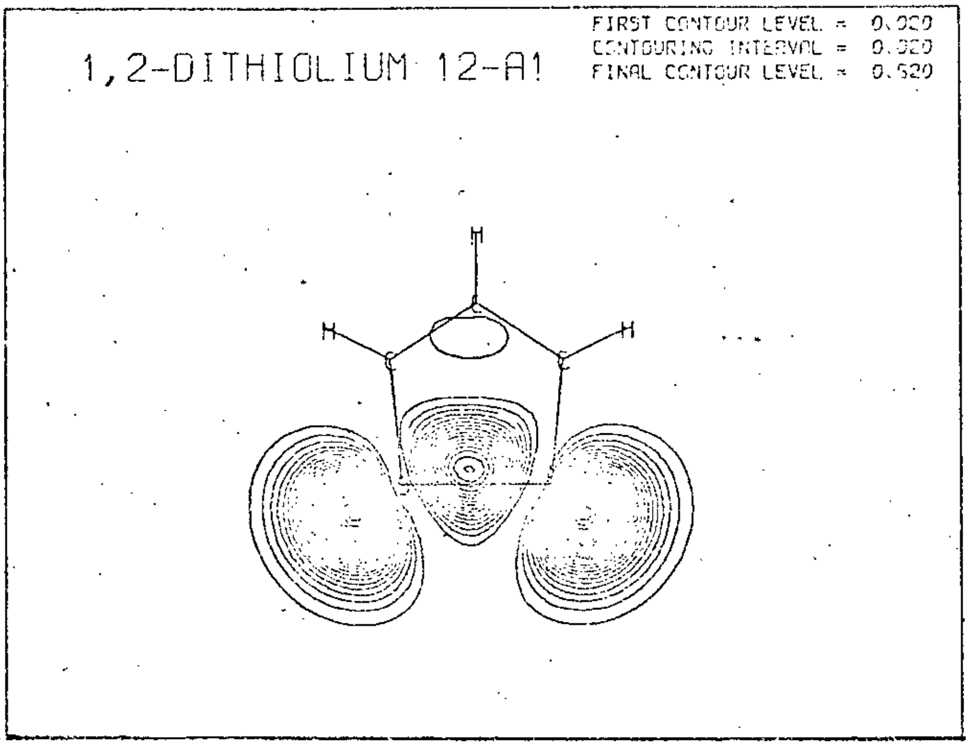

Figures 7a and 7b   Symmetric lone pair orbitals in the dithiolium cations

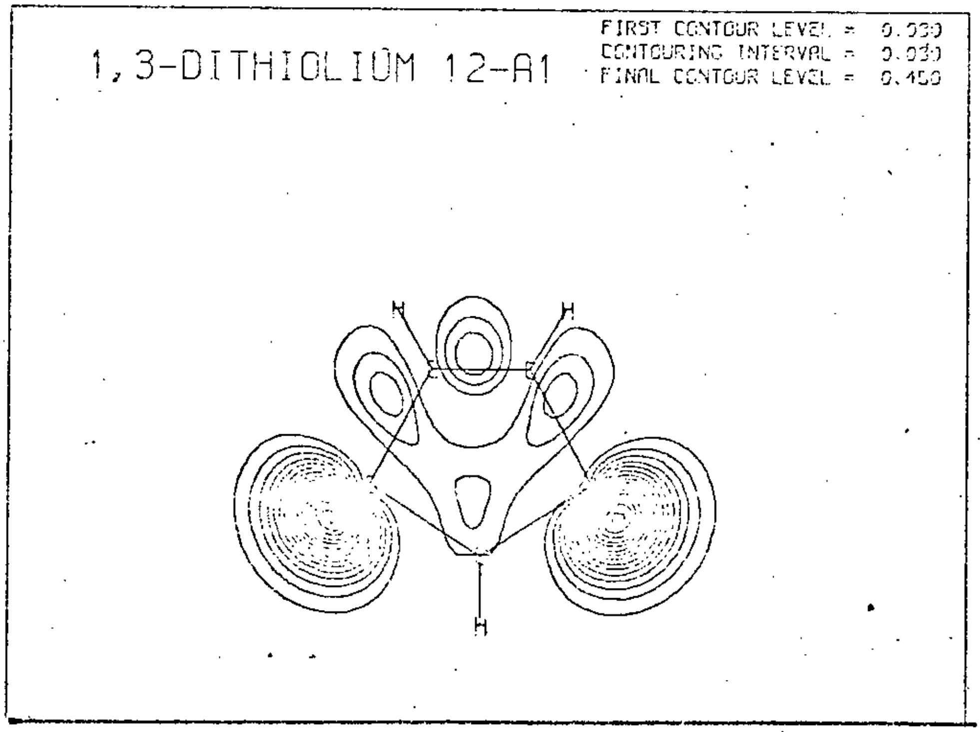

atoms in (5) must be greater than in (6) because in the latter case they have the positive charge associated with them; (c) the C4-S3/C5-S1 overlap π-population should be higher than the C3-S1/C2-S3 values, and probably higher than sulphur-carbon π overlaps in other molecules, because of the 4-electron 2-centre system; (d) the π-overlap population between C4 and C5 in (6) should be high (tending to be more olefinic). That most of these criteria are met can be seen in Tables 12a-12c where the appropriate results are listed together.

TABLE 12

The Dithiolium Cations and the Allyl Cation

a) C-C Overlap and π-Populations

		S	C_a^*	C_b^*
(5)	0.5305	1.6339	0.8537	1.0356
Allyl	0.5037	-	0.4743	1.0513
(6)	0.6146	1.5743	1.0288	0.8063

b) C-S π-Overlap Populations

(5)		0.0970
(6)	C4-S3	0.0415
	C2-S3	0.1030
(2)		0.0873

c) C-C π-Overlap Populations

(5)	C4-C3	0.1395
(6)	C5-C4	0.2136

* C_a is the symmetry-related pair of carbons, C_b the unique atom.

Since the carbon 2s/2p orbital energies are very similar to the sulphur 3s/3p values it is very likely that the orbital nature will be the same in both dithiolium species.

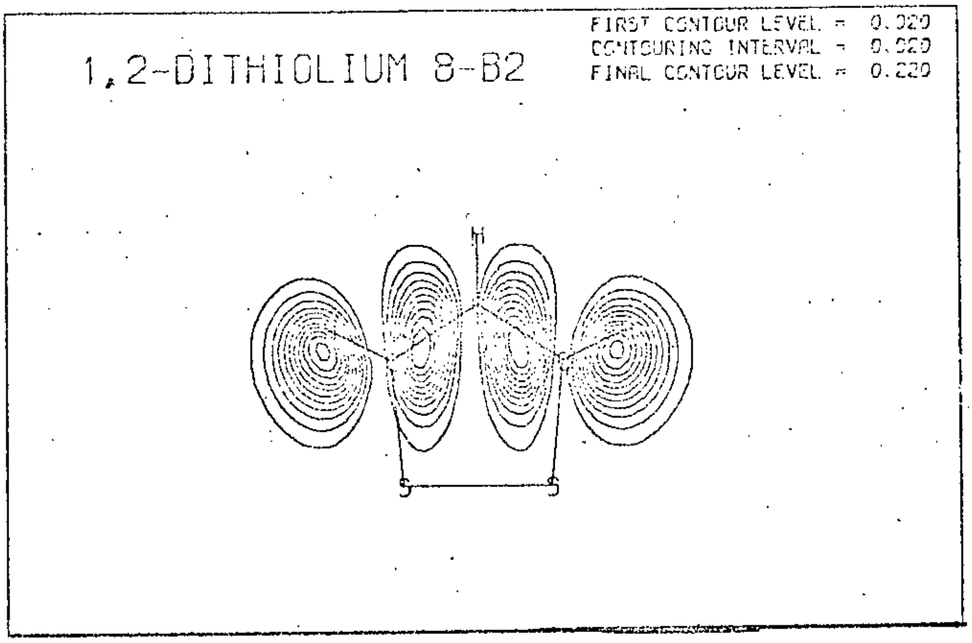

Figure 8a (above) Carbon ring bonding, with sulphur not participating

Figure 8b (below) Large amount of ring bonding, with sulphur taking an active part

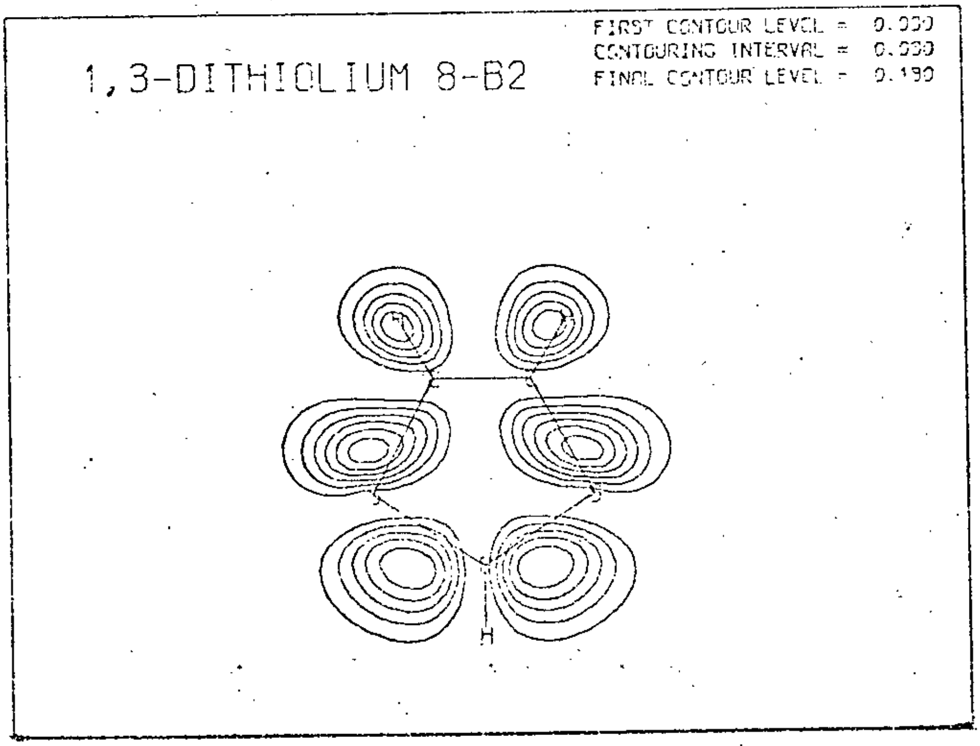

That this is found to be true can be seen from Table 13, where (a) represents the 1,2-dithiolium ion and (b) the 1,3-dithiolium ion. The lowest in energy are predominantly sulphur and carbon valence S in nature, as was found for thiopyrylium. In contrast however the C-H levels are

TABLE 13

Nature of Dithiolium Orbitals

Orbital	Nature
$7a_1$	(a) and (b). Totally symmetric 2s level with sulphur slightly larger than carbon.
$8a_1$	(a) and (b). Nodal plane perpendicular to C2 axis splitting into (a) S1 + S2 - C3-C4-C5 and (b) S1 + C2 + C3 - C4-C5.
$9a_1$	(a) and (b). Mixture of ring bonding and C-H bonding.
$10a_1$	(a) and (b). " " " "
$11a_1$	(a) and (b). Largely ring bonding through the p orbitals.
$12a_1$	(a) and (b). Symmetric lone-pair combination.
$6b_2$	Valency shell S level for both (a) and (b).
$7b_2$	(a) and (b). Antisymmetric C-H bonding with carbon p/sulphur S ring bonding fairly important.
$8b_2$	(a) Inter-carbon ring 2p-bonding with some C-H evident, (b) C-H level with some C5-S1/C4-S3 2p-3p bonding.
$9b_2$	Antisymmetric lone pair level in both molecules.
$2b_1$	(a) Very much sulphur 3z orbital with carbon eigenvectors of same sign (b) Much more even distribution but sulphur still predominates.
$3b_1$	Split of π-orbitals into structures (5) and (6).
$2a_2$	(a) Sulphur eigenvector slightly greater than carbon. (b) Sulphur eigenvector 5 times greater than carbon.

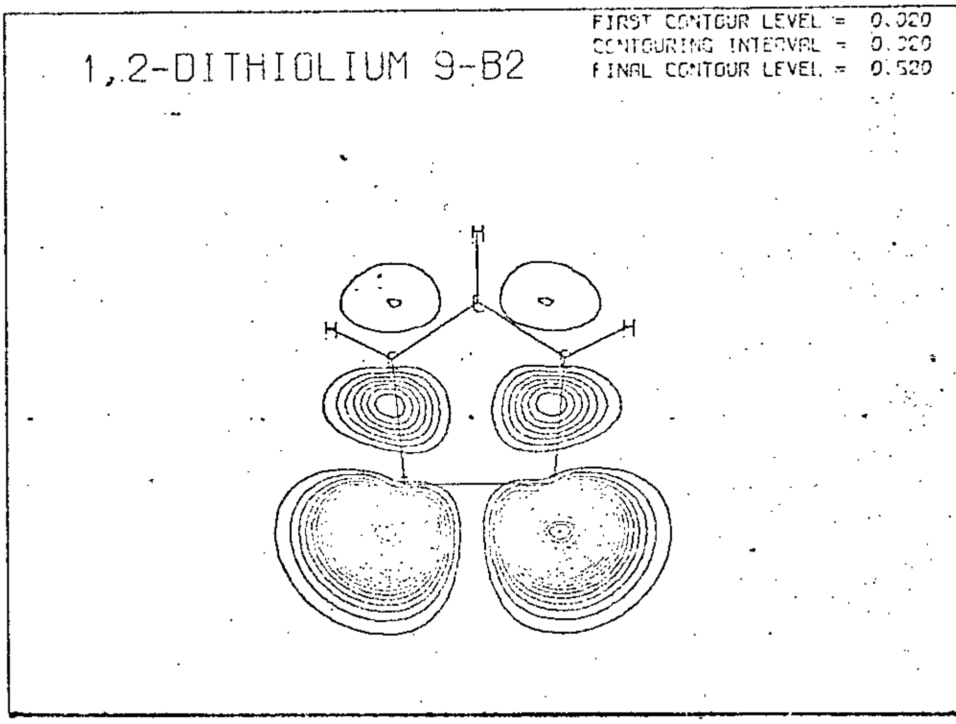

Figure 9 Lone pair anti-symmetric combinations

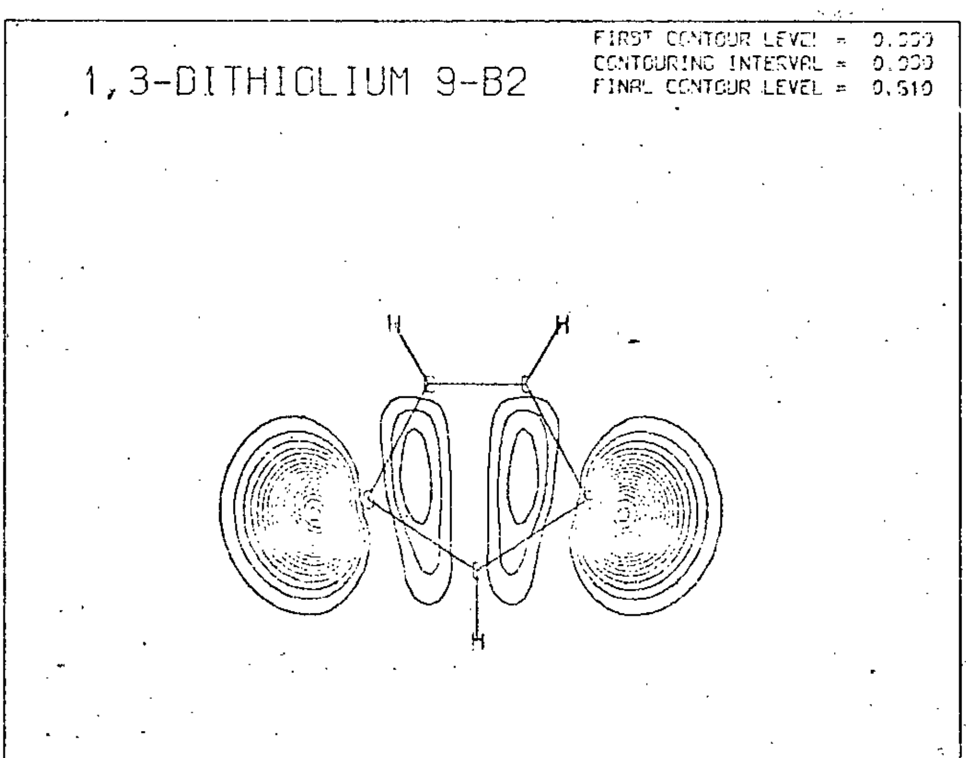

often associated with ring bonding (all types), in $10a_1$ and $7b_2$ for example, although the former orbital could be regarded as a totally symmetric radial orbital with radial being C-H or sulphur lone pair orbital. The sulphur lone pair orbitals appear predominantly in the $12a_1/9b_2$ orbitals, these being the symmetric and anti-symmetric combinations respectively. Since the sulphur atoms are further apart in the 1,3-isomer it is somewhat surprising that the lone pair orbitals are split by a larger value than in the 1,2 case. Orbital $3b_1$ shows the tendency of the pi system to split into representations (5) and (6), with the nodal plane splitting the 1,2-dithiolium cation into S-S and allylic parts and the 1,3-dithiolium into olefinic and S-C-S parts.

A common feature of cationic molecules is the presence of virtual orbitals of negative energy. Table 14 represents this type of orbital for the molecules 1a, 1b, 2-4.

TABLE 14

Lowest Unoccupied Molecular Orbitals of Hetero-aromatics

1a	1b	2	3	4
$-6.45(B_1)$	$-5.07(B_1)$	$-5.35(B_1)$	$-3.87(B_2)$	$-1.47(A_1)$
$-4.62(A_2)$	$-2.88(A_2)$	$-2.66(A_2)$	$-0.99(B_1)$	$-6.33(B_1)$
			$-6.59(A_2)$	$-1.89(A_2)$

Polarographic reduction of 3 and 4 has recently been reported[26] with the ½-wave potentials being -0.69v and -0.12v respectively. The orbital energies of Table 14 can be compared with this data. Using an aufbau principle with the additional electron going into the lowest unoccupied orbital the agreement is not too good. However if one takes the highest negative energy orbital (i.e. those of -0.99 and -1.47eV energy) the agreement is much improved. It is possible then that the figures for (scaled) pyrylium and thio-pyrylium (-2.88 and -2.66eV) would be in equally good agreement. Calculations on "one-electron added" species would of course be more exact.

TABLE 15

Population Analysis of the Dithiolium Cations

(a), 1,2-dithiolium

	S1,S2	C3, C5	C4
Core + Valence S	11.7886	3.1133	3.0114
Valence p_σ	2.2204	2.1872	2.0827
Valence p_π	1.6340	0.8537	1.0356
Total	15.6430	6.1541	6.1296
H	-	0.7516	0.7728

(b) 1,3-dithiolium

	S1,S3	C2	C3,C5
Core + Valence S	11.7542	3.2158	3.0718
Valence p_σ	2.2421	2.1590	2.1001
Valence p_π	1.5743	0.8063	1.0288
Total	15.5706	6.1810	6.2007
H	-	0.7488	0.7638

The population analysis in Table 15 shows that the sulphur atom is positively charged in each molecule, with the carbon atoms negatively charged. Again using the $2p_\pi$ population of the carbon as a measure of reactivity towards nucleophiles, only the atoms C3/C5 in (3) and C4 in (4) are available for attack. The majority of experimental data has been gathered from reactions with substituted 1,2-dithiolium species and benzo derivatives of the 1,3-dithiolium cation. The reactions below[27,28] show that the predictions based on $2p_\pi$ population are correct.

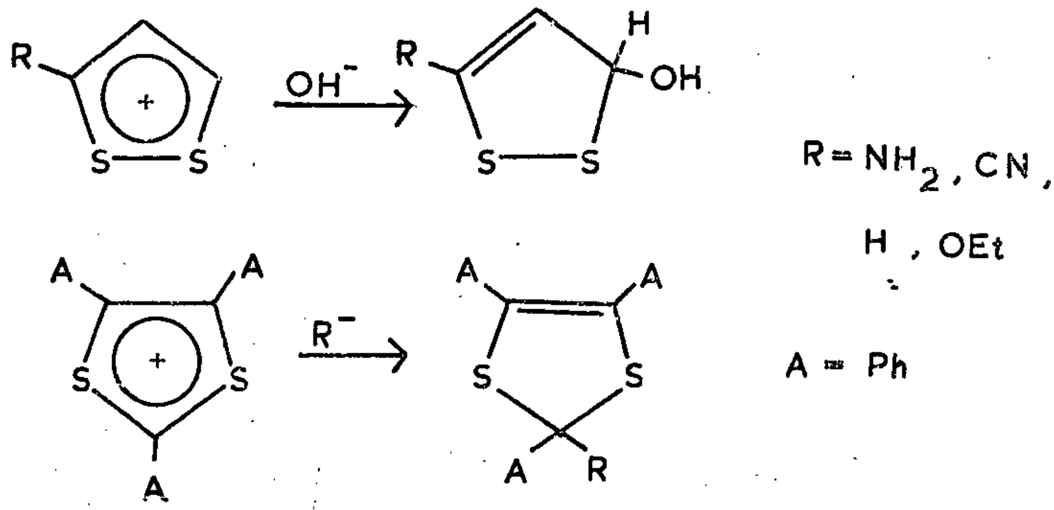

Some 1-electron properties are recorded in Table 16. The aromaticity term for the 1,3-isomer is considerably higher than for the 1,2-dithiolium cation.

TABLE 16

Second Moment and Diamagnetic Susceptibility Components

		xx	yy	zz	zz-½(xx + yy)
2nd Moment of	(3)	-64.63	-63.23	-9.41	-
	(4)	-86.31	-50.95	-9.40	-
Dia.Sus. of	(3)	-308.22	-313.27	-541.62	-230.88
	(4)	-256.00	-406.04	-582.31	-251.29

d-Orbitals and their Participation in Bonding

The second row elements (Al-Ar) all have 3d orbitals which are unoccupied but which lie only slightly above the ground state. The use of these orbitals to explain the ground state bonding was first suggested by Longuet-Higgins for thiophene[29] where the sulphur $3p_z$, $3d_{yz}$ and $3d_{xz}$ are hybridised to form two occupied and one unoccupied π-orbital; this of course can be extended to the species being considered here. An alternative analysis[30] without involving d-orbitals is to form three sp^2 hybridised orbitals from the sulphur 3s, $3p_x$, $3p_y$ functions two of which contain 1 electron (for σ-bonds to the adjacent atoms) and one containing 2 electrons of lone pair nature. This would leave the $3p_z$ of sulphur with 2_π electrons, one of which is lost to form the 6_π system in the sulphur cations investigated here. Thus, since one of these theories of bonding requires the use of d-orbitals, calculations were carried out on the molecules 2-4 with d-orbitals included in order to estimate to what extent the d-orbitals are involved.

TABLE 17

d-Orbitals in Gaussian Type Functions

l	m	n	Type
0	0	0	s
1	0	0	p_x
0	1	0	p_y
0	0	1	p_z
2	0	0	d_{x^2}
0	2	0	d_{y^2}
0	0	2	d_{z^2}
1	1	0	d_{xy}
1	0	1	d_{xz}
0	1	1	d_{yz}

The general form of a Gaussian type function is $x^l y^m z^n \exp(-ar^2)$ where l, m, n are zero or positive integers. The nature of s, p and d functions are shown above (Table 17). There are thus 6 d-type functions in Gaussian basis sets, in contrast to the chemical five functions. Further, Gaussian type d's are not an ortho-normal set. The overlap integral between d_{x^2} and d_{y^2}, d_{x^2} and d_{z^2} and d_{y^2} and d_{z^2} is 0.3333 (from the calculation on thiopyrylium). Since neither of these defects is particularly appealing, it is fortunate that suitable linear combinations, suggested by Rank & Csizmadia[31] enable one to circumvent both these problems. The d_{xy}, d_{xz}, d_{yz} offer no problems as they are ortho-normal and identical with the usual chemical functions; the $d_{x^2-y^2}$ chemical function is formed by simply taking a linear combination of x^2 and y^2; chemical d_{z^2} becomes $3d_{z^2-r^2}$ ($= 2d_{z^2-x^2-y^2}$). The remaining combination is $x^2+y^2+z^2$ ($=r^2$) which thus has the same symmetry as another s function. It is called the 3s' function hereafter, and can best be regarded as one member of a double zeta 3s function. The Gaussian exponent used was that suggested by Csizmadia[36] (0.541).

Two calculations have been carried out on each molecule; the first of these was an spd set where the five "chemical" d-orbitals were included. In the second set the 3s' function was added, giving an spd + 3s' set. The total energies of the molecules 2-4 are given in Table 18, where the ΔE term is the change in energy referred to the corresponding sp

TABLE 18

Total Energies of Sulphur Cationic Aromatics, with Additional d-Functions.

	2, spd	2, spd + 3s'
T.E.	-588.23031	-588.27773
1-El.	-1320.2027	-1319.7654
2-El.	466.52935	466.04462
N.R.	265.44302	215.44302
B.E.(au)	-1.08137	-1.12879
B.E. (kcal/mole)	-678.6	-708.3
ΔE	-53.6	-83.4
	3, spd	3, spd + 3s'
	-908.17655	-908.27342
	-1784.9200	-1784.0006
	601.47856	600.46228
	275.26486	275.26486
	-0.80547	-0.90234
	-505.4	-566.2
	-100.5	-161.3
	4, spd	4, spd + 3s'
	-908.16769	-908.26285
	-1767.9060	-1767.0120
	593.26178	592.27260
	266.47650	266.47650
	-0.79661	-0.89177
	-499.9	-559.6
	-91.8	-151.5

basis set calculation, with negative implying that there is an improvement in energy. Addition of the five d-functions leads to an improvement of approximately 50 kcal/mole for each sulphur atom in the molecule. As this is a fairly large value it would seem likely that the d-orbitals do play a significant part in the bonding of these molecules. However, when the 3s' is added to the spd set there is a further improvement of some 30 kcal/mole (per sulphur atom), and this with only one new function, compared to the five d-functions. It would seem therefore that the d-functions represent only a gain in variational flexibility and not a better representation of the ground state bonding. The d-orbitals are thus acting as polarisation functions since the energy improvement is similar to that obtained for furan (30 kcal/mole) and 1,2,5-oxadiazole (46 kcal/mole),[18] where d-orbitals can only exist as polarisation functions.

TABLE 19

d-Orbital Populations and Eigenvectors

	2	3	4
Largest eigenvector (spd)	0.069	-0.109	0.101
" " (spd + 3s')	0.120	-0.152	0.186
Total d population (spd)	0.1757	0.1456	0.1441
" " " (spd + 3s')	0.5313	0.4951	0.4950

Further evidence of the small amount of d-orbital participation comes from the eigenvectors and populations of these orbitals. This data is presented in Table 19, from which it can be seen that the additional 3s' function has more effect on the population than the five d-orbitals together. Further, in all cases, where the 3s' function is added the largest eigenvector immediately switches to it from any other d-orbital. It must therefore be concluded that the d-orbitals participate in the ground state only to a trivial extent.

TABLE 20

	2, spd	2, spd + 3s'		3, spd
S	15.7072	15.7174	S1, S2	15.7162
C2, C6	6.0859	6.0778	C3, C5	6.0604
C3, C5	6.1074	6.1094	C4	6.1286
C4	6.0577	6.0575	H1, H5	0.7676
H2, H6	0.7590	0.7598	H4	0.7830
H3, H5	0.7785	0.7787		
H4	0.7733	0.7735		

3, spd + 3s'		4, spd	4, spd + 3s'
15.7211	S1, S3	15.6870	15.6939
6.0528	C2	6.1310	6.1275
6.1319	C4, C5	6.0430	6.0337
0.7685	H2	0.7778	0.7787
0.7832	H4, H5	0.7650	0.7662

The effect of the addition of the 5 d-orbitals and the 3s' orbital on the populations of the atoms is quite dramatic as Table 20 shows. There is a net flow of electrons towards the sulphur atom, at the expense of all the other atoms. This can be explained in two ways:- (a) the sp basis set calculations was unbalanced with the sulphur being less well represented than carbon and hydrogen (b) the addition of polarisation functions to sulphur alone has unbalanced the basis set. It is somewhat difficult to decide which of these is the more likely since (1) the great effect of the 3s' function indicates that the sulphur basis set can be improved upon, (2) the p_π populations with d-orbitals predict the reactions with nucleophiles less well (Table 21).

TABLE 21

Valence Shell π-Populations

	2, spd	2, spd + 3s'		3, spd	3, spd + 3s'
S	1.5257	1.5262	S1,S2	1.6436	1.6447
C2,C6	0.8892	0.8872	C3,C5	0.8484	0.8458
C3,C5	0.9447	0.9468	C4	1.0278	1.0306
C4	0.8142	0.8135			

	4, spd	4, spd + 3s'
S1,S3	1.5938	1.5951
C2	0.8020	0.7974
C4,C5	1.0116	1.0119

The orbital energies are largely unaffected by the inclusion of d-orbitals (Table 22), with the major changes occurring in the sulphur 1s and 2s orbital energies when the 3s' function is included. There is a change of 3eV to higher binding energy, which, since this takes it further away from experimental values (by analogy carbon 1s, sulphur 2p values), is indicative that the d-orbitals and 3s'

TABLE 22

Orbital Energies (eV), with d-Orbitals

	2, spd	2, spd + 3s'	3, spd
A_1	-2501.12	-2503.97	-2501.55
	-315.15	-315.17	-316.46
	-314.59	-314.59	-315.02
	-314.11	-314.09	-246.08
	-245.63	-246.57	-188.48
	-187.99	-189.14	-188.46
	-38.63	-38.69	-40.06
	-35.27	-35.33	-35.00
	-29.54	-29.59	-29.11
	-26.12	-26.10	-27.30
	-23.95	-23.96	-23.16
	-22.09	-22.08	-20.57
	-19.54	-19.53	
B_2			-2501.57
	-315.15	-315.18	-316.46
	-314.11	-314.09	-246.19
	-188.05	-189.20	-188.56
	-34.82	-34.81	-188.52
	-29.61	-29.59	-35.42
	-24.44	-24.42	-29.13
	-23.29	-23.28	-23.93
	-20.29	-20.28	-21.56
B_1	-187.96	-189.10	-188.40
	-21.41	-21.38	-22.58
	-17.49	-17.47	-17.70
A_2	-16.86	-16.85	-188.45
			-18.08

TABLE 22 (Contd.)

	3, spd + 3s'		4, spd		4, spd + 3s'
A_1	-2504.50	A_1	-2501.24	A_1	-2504.13
	-316.47		-317.24		-317.27
	-314.99		-315.30		-315.30
	-247.02		-245.80		-246.74
	-189.68		-188.19		-189.36
	-189.65		-188.16		-189.32
	-40.12		-39.25		-39.32
	-35.09		-35.17		-35.17
	-29.08		-29.68		-29.72
	-27.28		-26.44		-26.43
	-23.13		-24.17		-24.13
	-20.52		-21.67		-21.66
B_2	-2504.57	B_2	-2501.24	B_2	-2504.15
	-316.48		-315.28		-315.29
	-247.23		-245.81		-246.79
	-189.76		-188.20		-189.36
	-189.71		-188.17		-189.34
	-35.47		-34.36		-34.53
	-29.22		-28.41		-28.41
	-23.92		-22.59		-22.56
	-21.56		-19.92		-19.88
B_1	-189.60	B_1	-188.12	B_1	-189.28
	-22.52		-22.03		-21.98
	-17.67		-17.46		-17.43
A_2	-189.64	A_2	-188.12	A_2	-189.28
	-18.04		-17.86		-17.82

TABLE 23a

1-Electron Properties, with Added d-Orbitals

		xx	yy	zz	zz-$\frac{1}{2}$(xx + yy)
2nd Moment					
(2)	spd	-64.49	-83.89	-9.30	-
(2)	spd + 3s'	-64.47	-83.86	-9.27	-
(3)	spd	-63.87	-62.67	-9.33	-
(3)	spd + 3s'	-63.82	-62.62	-9.28	-
(4)	spd	-85.19	-50.79	-9.33	-
(4)	spd + 3s'	-85.14	-50.74	-9.29	-
Diamagnetic Suscept.					
(2)	spd	-395.32	-313.04	-629.49	-275.31
(2)	spd + 3s'	-395.12	-312.84	-629.28	-275.31
(3)	spd	-305.46	-310.55	-536.87	-228.81
(3)	spd + 3s'	-305.04	-310.13	-536.43	-228.85
(4)	spd	-255.06	-401.01	-576.88	-248.84
(4)	spd + 3s'	-254.64	-400.59	-576.44	-248.82

TABLE 23b

Diamagnetic Shielding (1/r in ppm) in Scaled Pyrylium and Thiopyrylium

	(1)	(2)	(2)	(2)
		sp	spd	spd + 3s'
H2	187.21	211.48	211.75	211.75
H3	183.98	202.78	202.82	202.83
H4	182.85	200.51	200.63	200.63

function are unbalancing the basis set. Table 23a shows the effect of the d-orbitals on the one-electron properties, second moment and diamagnetic susceptibility; comparison with previous Tables shows that the effect is very slight. In the case of the diamagnetic shielding this is of some importance; Lipscomb has shown that the 1/r term of this operator is very useful in predicting NMR spectra. This operator also shows little effect of the addition of d-orbitals which is in contrast to the conclusions of Yoshida et al., who could only get reasonable agreement with the NMR spectrum by involving d-orbitals (These workers were using extended Huckel methods, hence they correlated NMR chemical shifts with the population of the adjacent carbon atoms). It should be noted that Lipscomb only found correlations within a molecule, i.e. it is thus not possible to predict the relative NMR spectra of pyrylium and thiopyrylium.

References

1. A.T. Balaban, and Z. Simon, Tet., 1962, 18, 315.

2. G.V. Boyd, N. Singer, Tet., 1965, 21, 1263.

3. Z. Simon, A.T. Balaban, Rev. Rouamine Chem., 1964, 9, 339.

4. K. Nishimoto, L.S. Forster, Theor. Chim. Acta (Berl.) 1964, 4, 155.

5. C.C. Rentio, A.T. Balaban, Z. Simon, Rev. Rouamine Chem., 1966, 11, 1193.

6. J. Fabian, A. Mehlhorn, R. Zahradnik, Theor. Chim. Acta (Berl.), 1968, 12, 247.

7. G. Karlsson, O. Martensson, Theor. Chim. Acta, (Berl.) 1969, 13, 195.

8. O. Martensson, C.H. Warren, Acta Chem. Scand. 1970, 24, 2745.

9. O. Martensson, Acta Chem. Scand., 1970, 24, 3417.

10. J. Fabian, A. Mehlhorn, R. Zahradnik, J. Phys. Chem. 1968, 72, 3975.

11. J.E. Young, J.C. Ohnmacht, J. Org. Chem. 1967, 32, 444.

12. R. Zahradnik, C. Parkanyi, Coll. Czech Chem. Comm. (a) 1965, 30, 3016; (b) 1963, 28, 1117.

13. G. Bergion, Arkiv. Kemi., 1964, 19, 181.

14. Z. Yoshida, T. Kobayashi, Theor. Chim. Acta (Berl.) 1971, 20, 216.

15. Z. Yoshida, H. Sugimoto, S. Yoneda, Tet., 1972, 28, 5873.

16. F. Grundvvig, A. Hordvik, Acta Chem. Scand., 1971, 25, 1567.

17. W.F. Cooper, N.C. Kenny, J.W. Edmonds, A. Nagel, F. Wudl, P. Coppens, J.C.S., 1971, 889.

18. M.H. Palmer, A.J. Gaskell, M.S. Barber, Theor. Chim. Acta (Berl.), 1972, 26, 357.

19. M.H. Palmer, A.J. Gaskell, Theor. Chim. Acta (Berl.) 1971, 23, 52.

20. A.T. Balaban, G. Mihai, C.D. Nenitzescu, 1962, 18, 257.

21. G. Kobrich, D. Wunder, Annalen, 1962, 654, 131.

22. K. Dimroth, K.H. Wolf, Angew. Chem. 1960, 72, 777.

23. R.C. Benson, W.H. Flygare, J.A.C.S., 1970, 92, 7523.

24. S. Yonoda, T. Sugimoto, Z. Yoshida, Tet., 1973, 29, 2009.

25. B.J. Lindberg, S. Hogberg, G. Malmsten, J.-E. Bergmark, O. Nilsson, S.-E. Karlsson, A. Fahlman, U. Gelius, Chem. Scripta, 1971, 1, 183.

26. K. Fabian, H. Hartmann, J. Fabian, R. Mayer, Tet., 1971, 27, 4705.

27. Advances in Heterocyclic Chemistry, 1966, 7, 63.

28. D. Leaver, D.M. McKinnon, W.A.H. Robertson, J.C.S., 1965, 32.

29. H.C. Longuet-Higgins, Trans. Faraday Soc., 1949, 45, 173.

30. Advances in Heterocyclic Chemistry, 1965, 5, 1.

31. A. Rank, I.G. Csizmadia, Canad. J. Chem. 1968, 46, 1205.

VI. PHOSPHORUS HETEROCYCLES

Introduction

The second row analogues of pyridine and pyrrole, namely phosphorin (phospha-benzene) (1) and phosphole (2), have been the subject of much interest both from the synthetic[1-6] and theoretical[7-11] points of view.

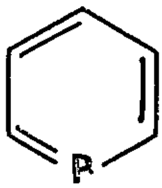

(1)

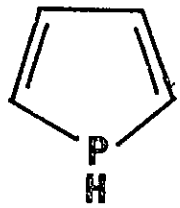

(2)

Isolation of the parent heterocyclic system, phosphorin, has been accomplished[11] and many benzo and heavily substituted derivatives are known; phosphole itself has not been isolated, the simplest compound to date being 1-methylphosphole,[12,13] although several heavily substituted derivatives are known. Semi-empirical calculations have been carried out on phosphorin[7] and several derivatives[14] with a view to estimating the extent of d-orbital participation[10] and predicting experimental ionisation potentials. Phosphole has also been under investigation to determine whether or not it is planar.[10]

The simplest known geometries of these two molecules are 2,6-dimethyl-4-phenylphosphorin[15] (microwave spectroscopy on phosphorin has been reported[16] but is incomplete) and 1-benzylphosphole.[17] The phosphole derivative does not have a planar ring, with the phosphorus group out of the plane of the four ring carbons. Accordingly calculations have been carried out on both the planar and pyramidal forms since the puckering of the ring away from planarity could be caused by crystal packing forces. This is especially worth considering as the analogous compound, pyrrole, is planar.

Minimal basis sets were used for all atoms; carbon and hydrogen attached to carbon were represented by scaled ethylene sets (Appendix 2, Tables 8 and 9); phosphorus and the hydrogen attached to it in phosphole were obtained by scaling of the Roos and Seigbahn[18] set in the model molecule $H_2C{=}P{-}H$. These basis sets are to be found in Tables 14 and 15 of Appendix 2. The minimal basis sets were augmented by a single d-function, also obtained from $H_2C{=}P{-}H$; this resulted in the calculations being carried out in four basis sets sp, sp+3s', sp+3d, sp+3d+3s'. Definition of the 3s' function may be obtained from the previous section.

Phosphorin

The total energy of phosphorin for each of the four basis sets are listed in Table 1. The binding energy is considerably higher than that found for the thiapyrylium ion; comparison with pyridine is somewhat more difficult since the calculations there used unscaled basis sets. However, if one assumes that the change for the pyrylium ion can be transferred to pyridine then the predicted binding energy for scaled pyridine would be in the region of -780 kcal/mole; phosphorin would then be somewhat less stable than pyridine.

TABLE 1

Total Energies of Phosphorin

	sp	spd	sp + 3s'	spd + 3s'
T.E.	-531.79672	-531.86186	-531.84046	-531.90524
1-El.	-1232.7286	-1233.3179	-1232.0395	-1232.6434
2-El.	447.46599	477.99009	446.73316	447.27227
N.R.	253.46590	253.46590	253.46590	253.46590
B.E.	-1.19549	-1.26063	-1.23923	-1.30401
" (kcal/ mole)	-750.2	-791.0	-777.6	-818.3
ΔE	-	-40.8	-27.4	-68.1

The addition of the 3s' function improves the energy by 27.4 kcal/mole; the one-electron and two electron energies both decrease in magnitude implying that the electrons are more delocalised. This is consistent with the slope of the 3s' function, which would allow the in-plane electrons to spread away from the carbons since one lobe points directly away from the ring and two lobes allow delocalisation above and below the ring. Further, the 3s' is a very diffuse orbital, having a low exponent. When the 3s' function is replaced by the five standard d-functions there is once again an improvement in energy of 40.8 kcal/mole compared to the sp basis set. This is greater in magnitude than that observed for the addition of the 3s' function, but is hardly surprising considering that there are five times as many variational parameters being added. However the improvement is not that much greater than the 3s' improvement; it must then be concluded that, as in the sulphur cationic hetero-aromatics, the d-orbitals are very little involved in the bonding of ground state phosphorin, but rather that they introduce more variational flexibility.

Further evidence of this comes from the population of the d-functions in each basis set:- sp(0.0), sp+3s' (0.255), spd (0.207), spd+3s' (0.473). These figures compare with the occupation of a single d_{xy} function in O, N, C in 1,2,5-oxadiazole, where the respective values are 0.017, 0.024 and 0.033; the population in phosphorin of the d_{xy} function is 0.111. The population of this orbital in phosphorin is considerably larger than the 1,2,5-oxadiazole case; it could conceivably be held that this showed there was some d-orbital participation in phosphorin. However, in 1,2,5-oxadiazole all the atoms contain the polarisation functions, while in phosphorin the phosphorus is the only atom with a d-orbital included, i.e., the basis set is unbalanced with respect to phosphorus when the d-orbitals are added.

The 5 x 3d orbitals improve the energy of the molecule in the opposite way to the 3s' improvement, i.e., the 3d functions increase the magnitude of both the one-electron and two-electron energy terms. This implies that the electrons are more localised than in the sp basis set. The d_{xy} and d_{yz} functions occur in the same symmetry representations as the phosphorous $3p_x$ and $3p_z$ functions; combinations of these would lead to p-d hybridisation (below).

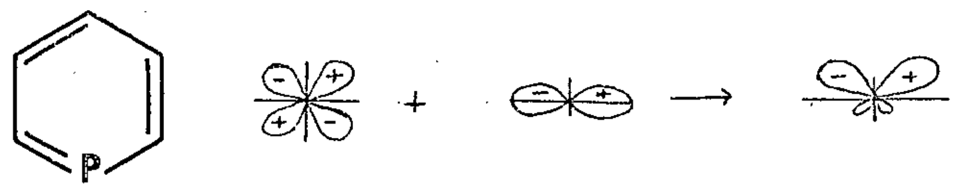

This combination of d and p orbitals has strongly directed lobes into the ring and will cause a localisation of the electrons within the ring. The p-d combination of orbitals would lead to a pd hybrid outside the ring. Such a combination could only occur if there was a nodal plane between the phosphorus and the adjacent atoms. Otherwise the tendency to improve bonding would be too great and p+d is the favoured combination for that to occur. Examination of the eigenvectors shows that there is no B_2 orbital with such a nodal plane. This is also true of p_z, d_{yz} hybridisation in the B_1 representation with p+d hybrids being formed.

The other π- symmetry type has no component atomic orbital from the phosphorus in the sp basis; the d_{xz} introduced with an spd set results in bonding to the phosphorus being possible. This symmetry representation will then cause a delocalisation of electrons. The two remaining d-functions $d_{x^2-y^2}$ and d_{z^2} (to use the standard nomenclature) both occur in the same symmetry representation. The $d_{x^2-y^2}$ function has nodal planes at 45^o to the principal C_2 axis, and hence they point more or less directly to the C_2-H_α atoms. Thus introduction of the $d_{x^2-y^2}$ function is likely to cause localisation of the electrons in the manner below (using orbital 8a as an example).

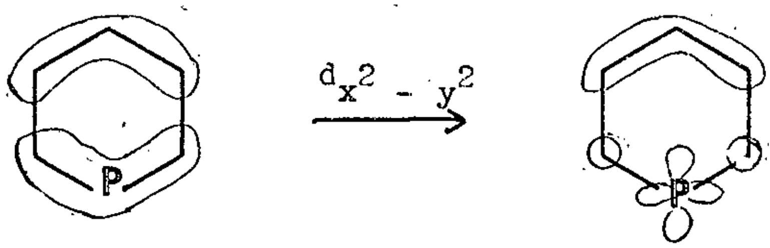

The remaining d_{z^2} function is likely to cause delocalisation of the electrons in a similar fashion to the 3s' function. It is likely to be less however due to the nodal plane passing through the phosphorus.

Thus the localisation of the electrons observed upon the addition of 5xd-functions is caused by pd hybridisation and the nodal planes of the $d_{x^2-y^2}$ function, partially offset by the delocalisation of electrons into the d_{xz} and d_{z^2} functions.

When the full basis set is used (i.e. spd + 3s') the 3s' delocalisation and d localisation effects occur independently, the binding energy improvements being additive. Thus the spd + 3s' basis set has the best energy.

TABLE 2

Population Analyses and Dipole Moments of Phosphorin

	sp	sp + 3s'	spd	spd + 3s'
P	14.6722	14.7115	14.8693	14.9131
C2, C6	6.3278	6.3111	6.2193	6.2008
C3, C5	6.1438	6.1441	6.1366	6.1369
C4	6.1539	6.1513	6.1557	6.1536
H2, H6	0.8445	0.8487	0.8542	0.8525
H3, H5	0.8477	0.8427	0.8521	0.8515
H4	0.8463	0.8455	0.8504	0.8403
μ(D)	1.87	2.01	0.99	1.11

Table 2 shows the population of each atom for all four basis sets. In the minimal basis set the phosphorous carries a fairly heavy positive charge and the carbon atoms a negative one. In contrast to the thia-pyrylium cation the C2/C6 atoms are most negative, followed by the C4 atom. The reason for the difference between phosphorus and pyridine/pyrylium ion/thiapyrylium ion is that phosphorus is less electronegative than carbon (the other hetero-atoms are more electronegative). Thus C2/C6 have a larger share of the electrons, and as usual this alternates round the ring resulting in C4 being more negative than C3/C5. Similarly the p_{π} populations alternate with C2/C6 (1.0012) greater than C4 (0.9998) and C3/C5 (0.9846). Thus carbon atoms adjacent to the hetero-atom should be reactive towards electrophilic attack, those beta towards nucleophilic attack and the gamma carbon as in benzene. The phosphorus atom has itself a high p_{π} population (1.0287) and would appear to be the predominant feature in controlling the reaction with benzyne.[19] Benzyne gives the 1,4 cyclo-addition product and not the other possible one, that from 2,5(or 3,6) cyclo-addition; 1,4-cyclo-addition involves one π-electron rich centre (P) and one neutral (C4) while the other orientation involves one π-electron rich (C2) and one π-electron deficient centre (C5). This of course assumes that benzyne is electrophilic in nature, which would seem to be true since it reacts with such species as alcohols, amines and thiols.[20]

Addition of the 3s' function increases the phosphorus population somewhat, at the expense of the C2/C6 atoms; the C4-H4 system also shows a drop in populations, but the C3-H3/C5-H5 actually show an increase in population. There must then be a net flow of electrons from the C4-H4 system towards the hetero-atom, allowing the beta carbons to gain electrons. This movement of electrons towards the phosphorus causes an increase in the dipole moment since the hetero-atom is at the negative end of the dipole (shown figuratively below).

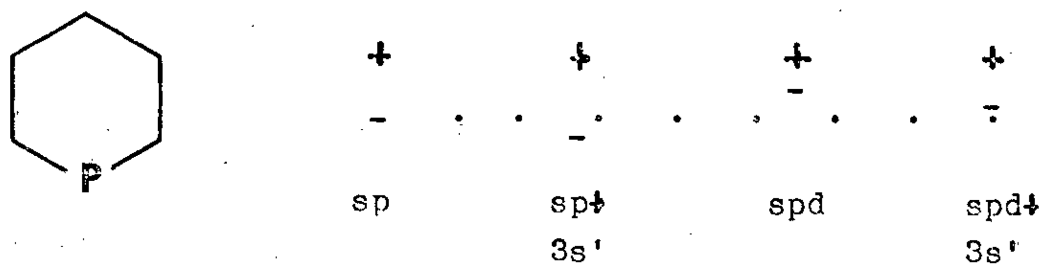

Replacement of the 3s' function by the 3d set again causes the population of the phosphorus atom to increase, but to a much greater extent than in the 3s' case. The pattern of flow is somewhat different, with both the C2/C6 and C3/C5 decreasing in population; the C4-H4 system is virtually unchanged as a whole but there is a reduction in the hydrogen population and an increase in the carbon population. Thus once again there is a net flow towards the phosphorus end of the molecule. As the d_{xy} function points most directly towards neighbouring atoms, it is not surprising to find that it is the predominantly filled d-orbital, with a population of 0.111 electrons. Since the total gain on P is 0.175e (in the sigma system), this accounts for 63% of the movement of electrons. In the π-system there is a gain of 0.023e. The total d-orbital population is 0.207e while the gain in electrons is 0.199e; there must be some slight back-donation of electrons through s and p functions. In contrast the 3s' leads to a total population of 0.255e for the d-orbitals; as the charge on P increases by only 0.049e there must be a considerable amount of back-donation.

The addition of the 3d functions, despite a rise in the phosphorus population, leads to an unexpected and drastic reduction in the dipole moment. Examination of the orbital contributions shows that the great majority of orbitals undergo very little change in the dipole moment contribution (< 0.01 au). In the A_1 representation, 5 orbitals are significantly changed. The $d_{x^2-y^2}$ function is likely to push electrons away from the phosphorus (decreasing dipole moments) while the d_{z^2} is likely to increase the dipole moment (as the 3s' function did). Thus it is not surprising to find that three of the five significant orbitals increase the moment and two decrease it. The magnitudes are such that the changes virtually cancel.

In the B_2 orbitals only three of the eight are significantly different. pd-Hybridisation already encountered above will lead to a hybrid orbital whose centre of charge (x) will lie away from the atom upon which the orbitals exist (below).

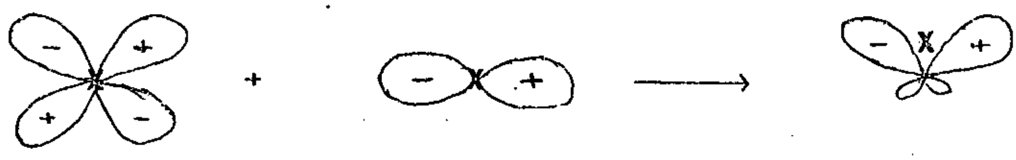

Thus the average position of electrons will be moved (a) away from the ring for a p-d hybridisation, (b) towards the centre of the ring for p+d hybrids. As already mentioned p+d is the only kind found and this will result in a decreased dipole moment contribution, which will partly be offset by increased atomic orbital populations. Two of the three orbitals show such a decrease, in sufficient magnitude to offset the only increase which was found to be caused by electron rearrangement within the carbon/hydrogen framework (C3, C4 and C5 with the associated hydrogens lost electrons relative to the C2/C6 area). In a similar fashion p+d-hybridisation accounts for the decrease in dipole moment contributions from the two (out of three) numerically significant orbitals. Conversely the sole A_2 orbital now has access to the phosphorus via the d_{xz} orbital and it introduces an increased contribution. The calculated dipole moments with the varying basis sets straddle the experimental[16] value of 1.540.

When both 3s' and d functions are included the effect on population and dipole moment is virtually additive.

TABLE 3

Total Energies of Planar Phosphole

	sp	sp + 3s'	spd	spd + 3s'
T.E.	-493.95638	-493.99832	-494.00970	-494.05158
1-El.	-1081.0112	-1080.4543	-1081.3250	-1080.7873
2-El.	384.39632	383.79751	384.6568	384.07724
N.R.	202.65847	202.65847	202.65847	202.65847
B.E.	-0.96564	-1.00758	-1.01896	-1.06084
B.E.(kcal/mole)	-605.9	-632.3	-639.4	-665.7
ΔE	-	-26.4	-33.5	-59.8

TABLE 4

Total Energies of Puckered Phosphole

	sp	sp + 3s'	spd	spd + 3s'
T.E.	-493.98113	-494.02371	-494.05651	-494.09921
1-El.	-1082.3376	-1081.7276	-1082.9210	-1082.3173
2-El.	384.93835	384.28571	385.44636	384.79993
N.R.	203.41816	203.41816	203.41816	203.41816
B.E.	-0.99039	-1.03297	-1.06577	-1.10847
B.E.(kcal/mole)	-621.5	-648.2	-668.8	-695.6
ΔE	-	-26.7	-47.3	-74.1

Phospholes

The total energies of planar and puckered phosphole are shown in Tables 3 and 4 respectively. Planar phosphole was generated from the puckered isomer by rotating the C2-P-C5 plane about the C2-C5 axis; this allows the C2-P/C5-P bonds to retain the same length as in the puckered configuration.

The binding energies are quite high but not as high as was found for phosphorin. They are also somewhat less than the value obtained by a scaled basis set calculation on pyrrole (-665.4), when minimal basis sets are compared. Thus phosphole is a less stable molecule than either its six-membered or nitrogen analogues.

Addition of the 3s' function improves the energy in both isomers with the same change (reduction) in magnitude of both one-electron and two electron energies, as was found in phosphorin. In planar phosphole there is a hydrogen atom where there was none in phosphorin; thus the values of the changes in magnitude in either of these energy terms is smaller than those found in phosphorin as delocalisation cannot be so complete. On the other hand, in puckered phosphole the atoms bonded to the phosphorus atom lie between the lobes so that the delocalisation will be more complete than in the planar case, but not so complete as in phosphorin, where the bonded atoms are one fewer as well as being between lobes.

Addition of the 3d functions shows the same effect on the electron energy terms as it did in phosphorin - both these terms increase in magnitude In puckered phosphole the change in each term is greater than in phosphorin; this can be attributed to 1) all five d-functions have at least two of their lobes pointing more or less directly towards neighbouring atoms (this is not true of phosphorin), 2) d_{z^2} is more remote from the C2/C5 carbon atoms and will be less efficient in delocalising, 3) d_{xz} exerted its delocalising effect because it allowed electrons to spread to the phosphorus atom in planar phosphole by introducing a phosphorus function where previously there was none; by virtue of the lower symmetry this is not true of the puckered isomer. Planar phosphole belongs to the C_{2v} point group and hence the d_{xy}, d_{xz} and d_{yz} functions would be expected to have similar effects to those in phosphorin, i.e. the one-electron and two-electron energy term changes will be smaller than in puckered phosphole. However examination of these terms in Tables 1 and 3 shows that the drop is to below the phosphorin values, thus the $d_{x^2-y^2}$ and d_{z^2} functions must be playing a vastly different role. The only difference between the phosphorus in phosphorin and planar phosphole is in the latter having a P-H bond. The $d_{x^2-y^2}$ function has one lobe pointing directly towards the hydrogen atom and so opens up more regions of space for the electrons in this bond. This will also hold true for the d_{z^2} with a more efficient delocalisation being possible due to the out of plane lobes. Thus the delocalisation effects of d_{z^2} are enhanced while the localisation effects of $d_{x^2-y^2}$ are somewhat offset. (This does <u>not</u> contradict the discussion on the effect of the 3s' function; there delocalisation of the ring carbons was reduced by the presence of the hydrogen, while here the hydrogen is responsible for some delocalisation which could not occur except in its presence).

The dipole moments and population analysis of the various calculations on the phosphole isomers are shown in Tables 5 and 6. With phosphorin it was possible to rationalise the change in dipole moment and the changes in basis set; the same can be done for the phosphole molecule in both configurations. The dipole moment changes in planar phosphole are shown below in a diagramatic form.

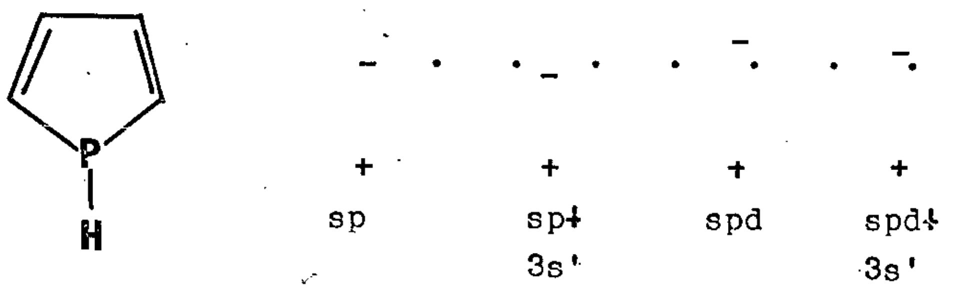

In phosphole the dipole moment is oriented in the opposite direction to phosphorin, so the changes in dipole moment would also be reversed. Addition of the 3s' function increases the population on phosphorus (Table 5); this movement of electrons will lead to a reduction in the dipole moment if it is primarily at the expense of carbon atoms (plus their associated hydrogens) and to an increase if at the expense of H(P). The population analysis shows that there is a loss of electrons at H(P) but not sufficient to make this the dominant term; there will thus be a decrease in the dipole moment on addition of the 3s' function. It is not surprising, however, to find that the magnitude of the

TABLE 5

Population Analysis and Dipole Moment of Planar Phosphole

	sp	sp + 3s'	spd	spd + 3s'
P	14.7980	14.8518	14.9591	15.0202
C2, C5	6.2856	6.2696	6.2223	6.2046
C3, C4	6.1702	6.1688	6.1694	6.1680
H(P)	0.8913	0.8765	0.8451	0.8259
H2, H5	0.8491	0.8480	0.8539	0.8530
H3, H4	0.8505	0.8494	0.8522	0.8515
μ(D)	1.39	1.32	1.58	1.53

TABLE 6

Population Analysis and Dipole Moment Components of Puckered Phosphole

	sp	sp + 3s'	spd	spd + 3s'
P	14.7067	14.7598	14.9363	14.9896
C2, C5	6.3195	6.3040	6.2302	6.2143
C3, C4	6.1543	6.1529	6.1499	6.1485
H(P)	0.9560	0.9410	0.8932	0.8780
H2, H5	0.8479	0.8467	0.8544	0.8534
H3, H4	0.8470	0.8460	0.8508	0.8500
μ_a(D)	0.54	0.64	0.21	0.29
μ_b(D)	1.00	1.07	0.41	0.47
μ(D)	1.14	1.25	0.46	0.55

change is less than in phosphorin. The 3d functions which allow hybridisation will serve to increase the dipole moment since it is oriented in the opposite direction; the increase will be less in magnitude than the decrease in phosphorin because the d_{z^2}, d_{xz}, $d_{x^2-y^2}$ allow some movement towards the phosphorus. This is found to be true. By analogy with phosphorin one would expect the d-orbitals to behave independently of the 3s' function with the change on going to the full basis set being the sum of the 3s' and d changes; this again is found to be true.

In puckered phosphole there are two dipole moment vectors to be considered (below).

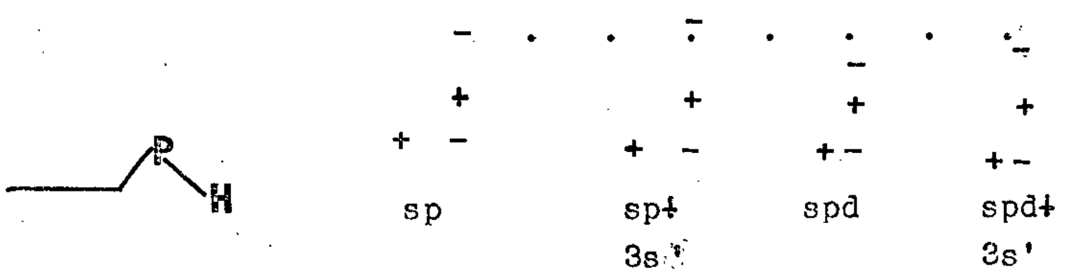

Here the dipole moment vectors are oriented with the negative ends towards the phosphorus atom; behaviour of the magnitudes of the components is expected to be the same as for phosphorin rather than planar phosphole and this is shown to be the case.

The addition of the 3s' function improves the energy by approximately 26 kcal/mole in each configuration, showing that the 3s' is non-directional in nature, i.e. a true s-orbital. Replacing the 3s' function with the 3d function again improves the energy over the sp set. The energy improvement is greater for the puckered isomer; since the

TABLE 7

Total Energies of Phosphine

a) Pyramidal

	sp	sp + 3s'	spd	spd + 3s'
T.E.	-341.77271	-341.81632	-341.83356	-341.87733
1-El.	-508.97731	-508.37400	-509.42604	-508.82387
2-El.	149.67981	149.03290	150.06770	149.42175
N.R.	17.52478	17.52478	17.52478	17.52478
B.E.	-0.21833	-0.26194	-0.27918	-0.32295
B.E. (kcal/mole)	-137.0	-164.4	-175.2	-202.7
ΔE	-	-27.4	-38.2	-65.7

b) Planar

	sp	sp + 3s'	spd	spd + 3s'
T.E.	-341.73082	-341.77320	-341.76815	-341.81059
1-El.	-509.10551	-508.59047	-509.32701	-508.82103
2-El.	149.9721	149.41470	150.15628	149.60786
N.R.	17.40258	17.40258	17.40258	17.40258
B.E.	-0.17644	-0.21882	-0.21377	-0.25621
B.E. (kcal/mole)	-110.7	-137.3	-134.1	-160.8
ΔE	-	-26.6	-23.4	-50.1

d-functions are more directed than the 3s' function, one would expect different improvements for the different configurations. The greater energy improvement for the puckered isomer is caused by the low symmetry of the molecule; this allows the d_{xy}, d_{x^2}, d_{y^2} functions to interact with more s and p functions than in the planar isomer. Also the $d_{x^2-y^2}$ and d_{z^2} have atoms between more lobes and thus they can interact more than in the planar form. When the 3s' and d sets are both added then the effect is the usual additive one.

Phosphole; Inversion Barrier and Diels-Alder Reactivity

For all basis sets the puckered geometry of phosphole is preferred to the planar molecule; thus in contrast to pyrrole, the preferred configuration about the hetero-atom is pyramidal. 1-Benzylphosphole is not then distorted from planarity by crystal packing forces alone.

The energy difference between the puckered and planar forms is the barrier to inversion about the phosphorus atom; the values for this inversion barrier are (in order sp, sp + 3s', spd, spd + 3s') 15.6, 15.9, 29.4, 29.9 kcal/mole respectively. In order to estimate the accuracy of the basis set in predicting such quantities, calculations have been carried out on the inversion barrier of phosphine for which a large basis set calculation is available. The results for the present basis set are to be found in Table 7, the inversion barriers being 26.3, 27.1, 41.0, 41.9 kcal/mole (for the same basis set order as above). The large calculation gave 30.9 and 37.2 kcal/mole for minimal and spd sets. Thus the sp basis set used here would appear to be somewhat inadequate, but that the addition of d-functions would appear to over-compensate for the inadequacy. The inversion barrier for phosphine has been estimated[21] to be either 27.4 or 31.8 kcal/mole from the vibrational frequencies of the pyramidal molecule, which is in good agreement with the calculated value. From this same method[21] the barrier for trimethylphosphine is 22.0 kcal/mole; since the value for 1-iso-propyl-2-phenyl-5-methylphosphole is found[22a] to be ~16 kcal/mole, the value for unsubstituted phosphole (2) is also likely to be in good agreement with the experimental value once this has been determined. Another estimate of the barrier to inversion at a phosphole-type centre is 23.7 kcal/mole for a heavily substituted benzo-phosphole derivative.[22b]

The inversion barrier calculated for phosphole is lower than that predicted for phosphine. The angle through which the phosphorus atom is tilted may not correspond to the one for which a minimum could be found, i.e. the calculated value for phosphole represents only a lower limit to the experimental value. However the error introduced by this approximation is likely to be very small since an experimental geometry was used for phosphole. The other likely cause of a low inversion barrier is that the transition state in phosphole is more stable (i.e. more negative in energy) than that of phosphine. In phosphole the planar form is reminiscent of pyrrole, an aromatic molecule. It is conceivable then that phosphole could show some aromatic character, which is of course impossible for phosphine. This would then serve to lower the inversion barrier by stabilisation of the transition state.

The possibility of aromaticity brings up the question of the stability of phosphole. It is somewhat strange that the parent phosphole species has not yet been isolated although phosphorin, only slightly more stable on binding energy grounds, is known. However decomposition to the atoms is not the reaction that is likely to inhibit the isolation of phosphole, with one very likely possibility being a Diels-Alder addition or even a dimerisation. To estimate the likelihood of such a reaction it is necessary to know something about the diene character of the C5-C4 (= C2-C3) and C3-C4 bonds, where aromatic species have even bond orders and overlap populations, and dienes alternating overlap populations. This information can be obtained from the overlap populations between the centres forming these bonds; the higher the population the more olefinic and the lower the population the more like a single bond. This information is presented in Table 8 where benzene is included as an aromatic standard with cyclopentadiene and cis-butadiene as olefinic standards; included also are some other 5-membered beterocyclic compounds.

In benzene the populations are identical, as they must be on symmetry grounds, resulting in the Diels-Alder reactivity index (R) being unity. Benzene does not undergo Diels-Alder additions. In phosphorin the value does not differ markedly from unity. At the other end of the scale

TABLE 8

Diels-Alder Reactivity Indices

Molecule	Overlap C2-C3	Populations C3-C4	R(= C2-C3 ÷ C3-C4)
Benzene	0.52055	0.52055	1.000
Phosphorin	0.51975	0.516441	1.006
Pyrrole	0.57771	0.49169	1.175
Thiophene	0.595037	0.477387	1.246
Furan	0.6837	0.5329	1.283
Planar Phosphole	0.605796	0.468373	1.293
Thiophene-S-oxide	0.602121	0.461132	1.306
Puckered Phosphole	0.612439	0.445881	1.374
Cyclo-pentadiene	0.621512	0.428813	1.449
cis-Butadiene	0.607642	0.403400	1.506

are the two olefinic species cyclo-pentadiene and butadiene with R = 1.449 and 1.506 respectively; it is evident from Table 8 that the C2-C3 and C3-C4 are quite different from one another at high R values. That this R value is a true index of Diels-Alder reactivity can be seen from cyclo-pentadiene, which is commercially available as the Diels-Alder dimeric adduct. Pyrrole does not react in a Diels-Alder fashion with maleic anhydride;[23] thiophene forms Diels-Alder adducts with acetylenes;[23] thiophene-S-oxide dimerises in the same way as cyclo-pentadiene.[23]

Thus for phosphole, the preferred configuration lies in the middle of the Diels-Alder reactive molecules. It is then extremely likely that it will first be isolated as a

TABLE 9

Orbital Energies of Phosphorin (eV) for all Basis Sets

sp		sp + 3s'		spd		spd + 3s'	
A_1	B_2	A_1	B_2	A_1	B_2	A_1	B_2
-2163.87	-307.26	-2167.33	-307.31	-2163.50	-307.12	-2166.91	-307.15
-307.26	-306.35	-307.30	-306.47	-307.11	-306.31	-307.15	-306.44
-307.21	-143.37	-307.28	-144.91	-306.93	-142.84	-306.99	-144.35
-306.35	-27.85	-306.47	-27.90	-306.31	-27.63	-306.44	-27.68
-196.49	-22.34	-197.80	-22.38	-195.93	-22.20	-197.21	-22.23
-143.30	-16.91	-144.84	-16.95	-142.8	-16.70	-144.30	-16.74
-31.02	-16.52	-31.07	-16.57	-30.67	-16.32	-30.72	-16.36
-26.56	-12.87	-26.63	-12.93	-26.15	-12.83	-26.22	-12.89
-21.65		-21.72		-21.32		-21.40	
-19.44	B_1	-19.47	B_1	-19.17	B_1	-19.21	B_1
-17.10	-143.32	-17.17	-144.85	-16.89	-142.80	-16.96	-144.31
-15.08	-14.25	-15.13	-14.29	-14.85	-13.99	-14.89	-14.02
-9.92	-9.23	-10.00	-9.29	-10.16	-8.99	-10.24	-9.04
	A_2		A_2		A_2		A_2
	-10.30		-10.34		-10.06		-10.09

dimer. Planar phosphole comes considerably nearer the aromatic end of the series, thus supporting the reason (above) for the low inversion barrier compared to phosphine. Experimentally, the phosphole system shows both aromatic and diene character. The ultra-violet and N.M.R. spectra of the 1-methyl derivative are very likely 1-methylpyrrole,[13] while the 1,2,5-triphenyl[24] and pentaphenyl[24] derivatives undergo reactions with maleic anhydride and methyl acetylene-dicarboxylate to give either the Diels-Alder adduct[25] or species derived from this.[24,25] It has also been suggested on photoelectron spectroscopy data[26] that phospholes (and arsoles) are diene-like in nature.

Orbitals and Orbital Energies

The orbital of greatest ionisation potential (Tables 9, 10 and 11) is localised on the phosphorus 1s orbital. The orbital energy is approximately 1.5eV more negative in the phosphole isomers, parallelling the effects found in the azoles. These effects also occur in the phosphorus 2s and 2p levels but to a slightly lesser extent, the differences being 1.1 and 1.3 eV respectively. Addition of the d-functions has very little effect on the phosphorus core levels, the largest change being for puckered phosphole 1s level whose orbital energy becomes 0.56eV less negative. In contrast to this the 3s' function alters the core levels by ~3eV in the 1s level and the 2s and 2p levels by ~1.3eV, the change being towards higher ionisation potential in all cases.

TABLE 10

Orbital Energies of Planar Phosphole (eV) for all Basis Sets

	sp	sp + 3s'	spd	spd + 3s'
A_1	-2165.37	-2168.45	-2165.20	-2168.23
	-306.15	-306.26	-306.18	-306.28
	-305.93	-305.98	-305.90	-305.93
	-197.58	-198.65	-197.20	-198.25
	-144.69	-145.97	-144.27	-145.53
	-30.71	-30.74	-30.54	-30.56
	-24.05	-24.12	-23.85	-23.92
	-20.14	-20.19	-20.11	-20.16
	-18.63	-18.66	-18.52	-18.54
	-15.46	-15.48	-15.51	-15.53
	-13.64	-13.67	-13.54	-13.57
B_2	-306.15	-306.26	-306.18	-306.28
	-305.94	-305.98	-305.90	-305.94
	-144.62	-145.90	-144.24	-145.50
	-26.17	-26.20	-26.13	-26.15
	-18.84	-18.86	-18.79	-18.81
	-15.19	-15.23	-15.13	-15.15
	-12.81	-12.84	-12.86	-12.88
B_1	-144.55	-145.82	-144.22	-145.47
	-13.90	-13.92	-13.78	-13.80
	-8.22	-8.26	-7.93	-7.96
A_2	-9.10	-9.12	-9.02	-9.04

TABLE 11

Orbital Energies of Puckered Phosphole (eV) for all Basis Sets.

	sp	sp + 3s'	spd	spd + 3s'
A'	-2165.16	-2168.40	-2164.60	-2167.83
	-306.58	-306.62	-306.49	-306.53
	-305.92	-306.02	-305.94	-306.04
	-197.49	-198.67	-196.71	-197.89
	-144.43	-145.85	-143.69	-145.09
	-144.35	-145.75	-143.64	-145.04
	-31.24	-31.73	-30.91	-30.94
	-24.51	-24.60	-24.04	-24.13
	-20.26	-20.32	-20.04	-20.10
	-18.72	-18.76	-18.51	-18.55
	-15.26	-15.28	-15.16	-15.19
	-14.33	-14.37	-14.19	-14.22
	-13.00	-13.03	-12.91	-12.94
	-9.43	-9.48	-9.35	-9.40
A"	-306.58	-306.63	-306.50	-306.54
	-305.92	-306.02	-305.94	-306.04
	-144.41	-145.81	-143.67	-145.07
	-26.49	-26.53	-26.37	-26.39
	-19.08	-19.11	-18.98	-19.01
	-15.53	-15.57	-15.37	-15.40
	-13.05	-13.09	-13.05	-13.09
	-9.38	-9.41	-9.18	-9.21

The carbon 1s levels are virtually unaffected by the addition of either the 3s' or 3d functions, the maximum change being 0.1eV. In phosphorin the order of (decreasing) ionisation potential is C3/C5, C4, C2/C6, quite different from what is found in pyridine. This can be rationalised on the grounds of the differences in electronegativity of nitrogen and phosphorus (3.0 and 2.1 respectively, on the Pauling scale). This replacement of a C-H group of benzene by nitrogen will introduce a movement of electrons towards the hetero-atom (carbon has electronegativity of 2.5). The adjacent carbons would become more positive resulting in a higher binding energy; by analogy with pyrylium and thia-pyrylium ions the carbon of the 4-position will feel the hetero-atom effect next most strongly and carbons 3 and 5 last. Introducing phosphorus, with a lower electronegativity than carbon, will produce the opposite effect; thus C2/C6 will gain electrons at the expense of the hetero-atom and will thus appear at <u>low</u> ionisation potential. Again the C4 carbon will be affected next and finally the C3/C5 pair, resulting in the observed ionisation potential order. The same effect would be expected to operate in the pyrrole/phosphole pair with the carbons adjacent to the phosphorus expected to be at lower ionisation potential. This is, however, only found with puckered phosphole; the atoms occur at virtually the same ionisation potential (0.22eV different). The energy difference which had to be reversed in pyrrole (1.45eV)[27] is much larger than that for pyridine (0.71eV). The difference in binding energies of the carbon 1s levels is unlikely to be sufficiently large to be resolvable with ESCA techniques.

Closely related to the electronegativities of the atoms are the valence orbital energies, shown in Table 12 for the unscaled basis sets.

TABLE 12

Valency Shell Orbital Energies (eV)

	N	C	P
Valency s	24.64	18.42	17.45
Valency p	14.65	11.24	10.17

The first valency shell orbital of planar phosphole has an ionisation potential of 30.7eV while that of pyrrole is some 4eV greater. This lowering of ionisation potential in the phosphorus heterocycle is to be expected in the valency shell s orbital energies of Table 12, i.e. the low atomic 3s energy leads to an orbital energy less negative than the highly localised nitrogen 2s orbital required. In support of this are the P-3s and N-2s populations in this orbital:- N, 1.01, 71.8% of total; P, 0.15, 11.5%.

Since both phosphorus and nitrogen are involved to some extent in the bonding in all the orbitals except those of A_2 symmetry it would be expected that the orbital energies of planar phosphole should occur at lower ionisation potential than the corresponding orbital in pyrrole. Comparing the data of Table 10 with reference 27 this is found to be true for all orbitals except $4b_2$ ($3b_2$ in pyrrole). This sole exception is nodal at the hetero-atom and consists of carbon 2s levels in both molecules. Further, since the difference of phosphorus and nitrogen p-orbital energies is less than the s-orbital difference, and the p functions predominate at lower ionisation potentials, then the difference in molecular orbital energies will be less at the low energy end of the spectrum. The simplest example of this is the $2b_1/1b_1$ phosphole/pyrrole pair (p-orbitals only) whose energy difference is 1.97eV compared to the $6a_1/4a_1$ pair (mainly s functions) which has a 4.02eV change. The $3b_1$ orbital is affected in the same way and turns out to be at lower ionisation potential than the $1a_2$ orbital. This is also found in semi-empirical calculations.[10]

The only orbital which does not have any N/P character (on symmetry grounds) is the $1a_2$ orbital in both molecules. This is the only one which has a significant increase in ionisation potential. This can be explained on the grounds that planar phosphole is bigger than pyrrole. Thus, as two independent olefinic bonds (at infinite separation) are brought together, they will split into symmetric (S) and anti-symmetric (A) pairs, with the separation being greater as they move closer, giving the diagram below.

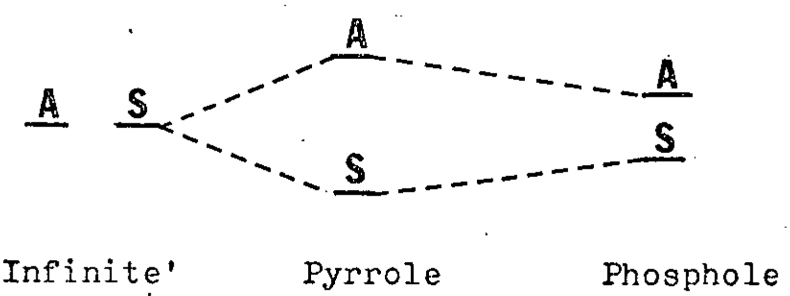

Thus in the bigger molecule the antisymmetric combination will be at more negative energy and the ionisation potential will be greater.

The orbital energies of puckered phosphole are very similar to the planar isomer as can be seen from Tables 10 and 11. The two lowest ionisation potentials are almost identical in magnitude, and arise from an antisymmetric olefinic π-combination (8a") and a lone pair orbital on phosphorus (0.48 3s + 0.66 3p). Photo-electron spectroscopy[26] of 1-phenyl phosphole gives two bands at the low ionisation potential end of the spectrum; saturation of the cis-butadiene segment, giving 1-phenylphospholane, left the first band virtually unchanged. From this it was deduced that the conformation consists of a butadiene system and a hetero-atom with no conjugation of the hetero-atom into the ring system. The total energies, orbital energies and overlap populations of Tables 3, 4, 8, 10 support this view.

Comparison of phosphorin and pyridine is hampered by the differing basis sets for these molecules - scaled for phosphorin and unscaled for pyridine. Ideally, the calculation on pyridine should be repeated using a scaled basis set; since the use of such a repetition would be confined to the present discussion, it would be a waste of computer resources. As the next best approximation the orbital energies of pyridine have been adjusted by the changes produced going from unscaled to scaled pyrylium. These have been recorded in Table 13.

TABLE 13

"Amended" Pyridine Valency Shell Orbital Energies

	Difference	New Value		Difference	New Value
A_1	-0.99	-34.86	B_2	-1.21	-28.97
	-2.30	-29.21		-1.02	-23.59
	-1.04	-23.91		-0.97	-18.73
	-0.72	-20.32		-0.85	-17.39
	-0.79	-18.32		-0.99	-14.92
	-0.74	-16.47	B_1	-0.69	-16.10
	-0.86	-11.60		-0.98	-11.44
			A_2	-1.18	-10.94

The "corrected" energies of pyridine are all greater in magnitude than phosphorin, as was to be expected by analogy with the pyrrole/phosphole pair; the sole exception to this is the A_2 representation which showed an increase in the case of phosphole. In other respects this a_2 orbital behaves very much like phosphole in that it occurs at higher binding energy than tha $3b_1$ orbital. This phenomenon was first reported[7] as a result of semi-empirical calculations where it was supposed to offer proof of d-orbital partici-pation. Since this arrangement occurs with the sp basis set it obviously cannot offer such proof; instead it is caused by substituting a low ionisation potential p-orbital ($3p_z$ of phosphorus) for a high ionisation potential p-orbital ($2p_z$ of nitrogen) thus allowing the molecular ionisation potential to decrease. That this decrease is sufficiently large to place $3b_1$ at lower ionisation potential than $1a_2$ is purely accidental. It has further been suggested that the highest B_1 orbital ($3b_1$) will be raised in energy due to 3p-2p π conjugation being less efficient than 2p-2p; on the basis of the atomic orbital energies, interaction between carbon and phosphorus is likely to be better than nitrogen-carbon interaction.

As was found for pyridine the orbital order of the first three orbitals is predicted differently by non- and semi-empirical methods; LCGO predict $3b_1 < 13a_1 < 1a_2$ while CNDO/2 predict $3b_1 < 1a_2 < 13a_1$. In both methods orbital $13a_1$ is predominantly a phosphorus lone pair orbital (0.65 3s + 0.73 3p). Extrapolation of 2,4,6-tri-t-butylphosphorin to phosphorin,[14] using the corresponding pyridine analogues predicts that the "experimental" values for phosphorin should be 6.85, 7.45 and 8.85eV which are in reasonable agreement with those of Table 9.

REFERENCES

1. G. Markl, Angew. Chem. (Int. Ed.), 1966, 5, 846.

2. G. Markl, F. Lieb., A. Merz, Angew. Chem. (Int. Ed.) 1967, 6, (a) 458, (b) 944.

3. P. deKoe, F. Bickelhaupt, Angew. Chem. (Int. Ed.) 1967, 6, 567.

4. P. deKoe, R. Van Voen, F. Bickelhaupt, Angew. Chem. (Int. Ed.) 1968, 1, 465.

5. K. Dimroth, W. Mach, Angew. Chem. (Int. Ed.) 1968, 1, 460.

6. G. Markl, A. Merz, Tet. Lett. 1969, 1231.

7. H. Oehling, A. Schweig, Tet. Lett. 1970, 4941.

8. Z. Simon, M. Mracec, Rev. Roum. Chim., 1971, 16, 449.

9. D.A. Brown, J.C.S., 1962, 929.

10. H.L. Hase, A. Schweig, H. Hahn, J. Radlett, Tet., 1973, 29, 469.

11. A.J. Ashe, J.A.C.S. 1971, 93, 3293.

12. L.D. Quin, J.G. Byson, J.A.C.S., 1967, 89, 5984.

13. L.D. Quin, J.G. Byson, G.C. Moreland, J.A.C.S., 1969, 91, 3308,

14. H. Oehling, W. Schafer, A. Schweig, Angew. Chem. (Int. Ed.) 1971, 10, 656.

15. J.C.J. Bart, J.J. Daly, Angew. Chem. (Int. Ed.) 1968, 1, 811.

16. R.L. Kuczkowski, A.J. Ashe, J. Mol. Spec., 1972, 42, 457.

17. P. Coggon, J.F. Engel, A.T. McPhail, L.D. Quin, J.A.C.S., 1970, 92, 5779.

18. B. Roos, P. Siegbahn, "Proceedings of the Seminar on Computational Problems in Quantum Chemistry" Strassburg, 1969.

19. G. Markl, F. Lub, C. Martin, Tet. Lett., 1971, 1249.

20. T.L. Gilchrist, C.W. Rees, "Carbenes, Nitrenes and Arynes", p.108, Thomas Nelson & Sons Ltd., 1969.

21. R.E. Watson, J.A.C.S., 1954, 76, 2645.

22. W. Egan, R. Tang, G. Zon, K. Mislow, J.A.C.S. (a) 1970, 92, 1442. (b) 1971, 93, 6205.

23. M.H. Palmer, "The Structure and Reaction of Heterocyclic Compounds", Edward Arnold Ltd., London, 1967.

24. A.N. Hughes, S. Uaboonkul, Tet., 1968, 24, 3437.

25. E.H. Braye, W. Hubel, I. Caplier, J.A.C.S., 1961, 83, 4406.

26. W. Schafer, A. Schweig, G. Markl, H. Hauptmann, F. Matley, Angew. Chem. (Int. Ed.) 1973, 12, 145.

27. M.H. Palmer, A.J. Gaskell, M.S. Barber, Theor. Chim. Acta (Berl.), 1972, 26, 357.

VII. THIOPHENE and ITS S-OXIDES

Introduction

Thiophene (1) has been the subject of many theoretical treatments;[1-18] both empirical and semi-empirical calculations have been carried out on electronic spectra[3,4,6-11,13,15,16], dipole moment,[2,4,6,13] ionisation potentials[6,7,8,12,15], charge distributions[2,12] on the parent and substituted compounds. The participation of 3d-orbitals in ground[1,5] and excited state[5] properties,[1,5] as well as 4s and 4p-orbitals[5] has been studied. Non-empirical calculations have also investigated d-orbital participation[17,18] and their effect on some molecular properties.[18]

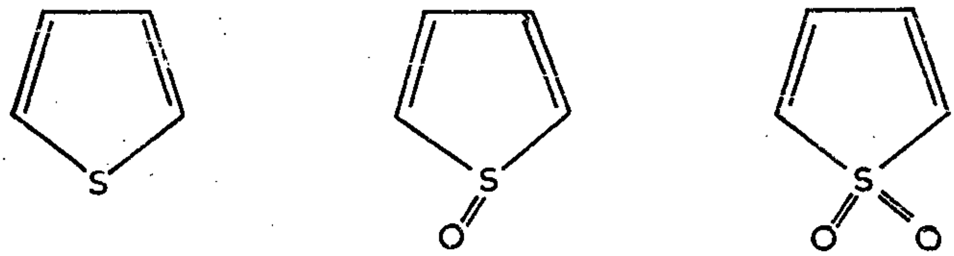

(1) (2) (3)

Oxidation of thiophene with per-acids leads to thiophene-S-oxide (2) and thiophene-S-dioxide (3). Very little is known about the structure of these species since they very readily dimerise in a Diels-Alder fashion; this Diels-Alder activity has been investigated[19] as have polarographic reduction potentials.[20] Accordingly calculations have been carried out on thiophene and both its oxides with a view to determining geometries and the electronic structure of these molecules.

Thiophene

Calculations on thiophene were carried out at the experimental equilibrium geometry,[21] as determined by microwave spectroscopy, and using scaled basis sets. The carbon and hydrogen functions were those of scaled ethylene and those of sulphur were taken from scaled thioformaldehyde (i.e. the same basis sets as for the sulphur compounds of Section 5). Full details of geometry can be found in Appendix 3 and of basis sets in Appendix 2 (Tables 8, 9, and 13). This calculation was carried out in order to (a) compare the basis set with that of Clark and Armstrong[17] (the calculation by Gelius et al.[18] was published after this calculation was completed) (b) to provide a starting point for the calculations on the mono- and di-oxides of thiophene.

As was done for the other sulphur heterocycles (Section 5) the minimal basis set was augmented by a single d-function for each of the Gaussian type d-orbitals; linear combinations of these were taken to generate the 5 chemical d-functions and an additional s-function (3s'). There are thus three calculations of sp, spd and spd + 3s' type, the results of which are shown in Table 1. The binding energy is somewhat lower than that obtained for the thiopyrylium ion but higher than the value for the dithiolium cations. Thiophene is predicted to be a less stable molecule than its first row analogue, furan (binding energy = -603.9) paralleling what was found for the Group 5 analogues, pyrrole and phosphole. The binding energy is approximately 64% of the experimental value[22] (-931.1 kcal/mole) for the minimal basis set, rising to 72% for the spd + 3s' (full) basis set; both these figures lie reasonably near the lines found for the azoles and azines.

TABLE 1

Total Energies of Thiophene in all Basis Sets

	sp	spd	spd + 3s'
T.E.	-550.07505	-550.14417	-550.19143
1-El.	-1157.6736	-1158.2968	-1157.8512
2-El.	404.64287	405.1969	404.70405
N.R.	202.95572	202.95572	202.95572
B.E.	-0.94550	-1.01462	-1.06188
B.E. (kcal/mole)	-593.3	-636.7	-666.3
ΔE	-	-43.4	-73.0

For the same type of basis set (sp or full) the total energies are 0.34 au worse (less negative) than the larger basis set calculations of Clark and Armstrong (CA hereafter) and 0.85 au worse than the double-zeta basis set calculations of Gelius et al. (GRS). Thus in terms of total energy the present basis set is worse than either the CA or GRS calculations; the binding energy of these workers is not reported but is likely to be better than that obtained here.

Addition of the d functions to the minimal basis set calculations increases the magnitude of both the 1-electron and 2-electron energy terms; as in the phosphorus heterocycles this can be explained by delocalisation into the d_{z^2} and d_{xz} functions partly compensating for the localisation caused by the remaining d-orbitals. Knowing the direction of the dipole moment in the sp set the relative magnitude of the spd dipole moment can be predicted:- the negative end is towards the sulphur atom so that p-d hybridisation will push the electrons away from the sulphur (but not in atomic population sense) and decrease the dipole moment. The dipole moment values of Table 2 show that this is correct.

TABLE 2

Population Analysis and Dipole Moment of Thiophene

	sp	spd	spd + 3s'
μ(D)	1.25	0.44	0.47
S	15.8563	15.9626	15.9725
C2,C5	6.2393	6.1722	6.1653
C3,C4	6.1654	6.1643	6.1657
H2,H5	0.8266	0.8362	0.8368
H3,H4	0.8404	0.8459	0.8451

Generation of the full basis set by addition of the 3s' function to the spd set brings about a reduction in the magnitudes of both 1-electron and 2-electron energy terms, i.e., the 3s' is having its usual effect of delocalising the electrons of the sigma system. One would then expect the dipole moment to be increased slightly compared to the spd set and this is what is found (Table 2). The value predicted by the full set is very much closer to the experimental value of 0.54D;[23] The GRS calculation is nearer still (0.61D) but on the opposite side of the experimental, while the CA calculation predicts a very small moment of 0.05D (in neither case is there any indication of direction).

Increasing the basis set by the 3d functions improves the energy by -43.4 kcal/mole with the further addition of the 3s' generating a further improvement of -29.6 kcal/mole; the 3s' function would then appear to be having a slightly less effect than all the 3d functions. It must then be concluded that the d-orbitals of sulphur are only used to a trivial extent in the ground state. In support of this the very much better GRS calculation (in terms of energy) shows that the full basis set improves the energy by only 18.5 kcal/mole, with the CA improvement being very similar to that found here. Further evidence comes from the d-orbital populations of Table 3.

TABLE 3

d-Orbital Populations

	Present	GRS	CA
d_σ	0.451	0.143	0.648
d_π	0.039	0.038	0.070
Total	0.490	0.181	0.718

Thus the nearer the Hartree-Fock limit, the less the d-orbitals contribute to the ground state electronic structure (the population of the CA calculation is probably abnormal because that calculation was "double-zeta" in the d functions).

The population analysis is recorded in Table 2, for all three of the present basis sets. The sulphur population increases as the basis set increases, mainly at the expense of the adjacent carbon atoms, with the remaining atoms being virtually unchanged. The charge on the sulphur is smaller than the values obtained for the CA and GRS sp basis calculations, but once the full set of d-orbitals is included, both the present and GRS calculations make the sulphur almost neutral. The CA calculation leaves the sulphur positively charged by 0.227 electrons. It would seem therefore that the present basis set is as good as the CA and GRS sets in estimating dipole moments and charge distributions.

The core orbital energies have been studied in both solid[24] and gas[25] phases; the results of these are presented in Table 4.

TABLE 4

Core Orbital Energies of Thiophene (eV)

	Carbon-1s	Sulphur-2s	Sulphur-2p
Solid	285.1	228.7	165.3, 164.5
Gas	290.2, 290.5	-	171.2, 169.9

In neither solid- nor gas-phase spectra were the carbon 1s lines resolved although in both cases the peak width at half-height was 0.1eV broader than benzene under identical conditions. In the solid state this was assumed to mean that the carbon 1s levels were experimentally split by 0.1eV, which was in agreement with the CA calculations published elsewhere. The gas phase spectrum was treated differently and a deconvolution technique produced a separation of 0.34eV; further this same technique was found to give a separation of 0.3eV when applied to the solid phase spectrum.

TABLE 5

Orbital Energies of Thiophene

	sp	spd	spd + 3s'
A_1	-2492.31	-2491.92	-2494.81
	-307.30	-307.11	-307.14
	-307.00	-306.73	-306.73
	-237.45	-236.89	-237.85
	-179.77	-179.26	-180.41
	-32.64	-32.04	-32.07
	-26.96	-26.51	-26.61
	-20.92	-20.71	-20.75
	-19.51	-19.26	-19.26
	-15.36	-15.12	-15.12
	-12.99	-13.19	-13.17
B_2	-307.30	-307.12	-307.14
	-307.00	-306.74	-306.73
	-179.81	-179.28	-180.43
	-27.06	-26.81	-26.80
	-20.53	-20.39	-20.37
	-16.25	-15.96	-15.95
	-14.67	-14.64	-14.62
B_1	-179.69	-179.19	-180.35
	-15.30	-14.99	-14.96
	-10.25	-9.93	-9.91
A_2	-9.82	-9.53	-9.51

It would thus seem that the carbons are separated by 0.34eV which is in good agreement with the values of Table 5 (0.30, 0.38 and 0.41eV for sp, spd and full basis sets respectively, with the C2/C5 carbons being at higher ionisation potential). This is in much better agreement than the 0.59eV of CRS and the 0.1eV of CA. The sulphur 2s level is in reasonable agreement with the experimental value and in much better agreement than the GRS figure of 244.6eV.

The sulphur 2p orbitals are split by spin-orbit coupling; the weighted average value for 164.5eV (solid phase) is considerably different from the calculated value of 179.76eV but the latter is much more in line with the gas phase value of 170.33eV. This is very pleasing since the calculations refer to an isolated molecule, i.e. in the gas phase. The 2p levels are some 0.5eV less than the values for some 1,2-dithiolium derivatives.[26] This is in agreement with the charges on the molecule (+1 for the 1,2-dithiolium cation, 0 for thiophene). The calculated energy difference between the 2p levels is very much larger (~10eV) but is in the correct order for charge differences. Since both these heterocycles are at experimental geometries and the same basis sets were used for each the reason for the discrepancy is likely to be the ignoring of the anion in evaluating the wave function for the 1,2-dithiolium cation. This would probably surrender some electrons and hence reduce the ionisation potential.

The valence shell ionisation potentials have been studied by ESCA[25] and He(II)[27] photo-electron spectroscopy techniques. The ionisation potentials are virtually identical but, since the ESCA is able to probe further into the valency energies, these were used to generate a least squares relationship. This was IP(exp) = 0.751 IP(calc) + 2.030eV, with the overall standard deviation, and standard deviations in slope and intercept being 0.444, 0.019 and 0.378 respectively. When the gas phase core levels are included the equation is:- IP(exp) = 0.952 IP(calc) - 1.612 (1.367, 0.003, 0.407). This is somewhat worse than the excellent valency shell only plot but is by no means bad when the range of energies is considered. The order of energies is identical to that obtained by the GRS calculation ($11a_1 < 7b_2 < 2b_1 < 10a_1 < 6b_2$) but is somewhat different to that obtained by semi-empirical means ($2b_1 < 11a_1 < 7b_2 < 10a_1 < 6b_2$). This is similar to what was found for pyridine and phosphorin (Sections III and VI respectively). Using the eigenvectors of each of these wave functions, the relative intensities of the lines were obtained; it was found that the non-empirical calculations gave a better fit to the observed spectrum.[25] The non-empirical calculations would therefore appear to predict the correct order.

The effect of the d functions on the orbital energies is much the same as that for the other sulphur and phosphorus heterocycles - a slight reduction in ionisation potential for most orbitals. The further addition of the 3s' function affects only the sulphur core orbitals, there being a movement to higher binding energy of 2.9, 0.96, and 1.15eV for the 1s, 2s and 2p levels respectively. Again this has been found before.

As well as the dipole moment some other one-electron properties for thiophene have been calculated from the GRS basis set. These, together with such experimental values[28] as are available are compared with those obtained using the present basis set in Table 6. The diamagnetic susceptibility and second moment components are in reasonable agreement with the experimental values, although for both properties the GRS calculation is somewhat better. The values for the second moment are somewhat greater than furan, consistent with the greater size of the molecule and the more diffuse nature of the sulphur atomic orbitals. The potential operators (1/r) for each unique centre are virtually identical for both basis sets with the sulphur slightly more different from the GRS calculation than carbon or hydrogen. Indeed the only significant discrepancies between the two basis sets are in the closely related properties, quadrupole moment and electric field gradient. The present sp set gets the sign of one component of the quadrupole moment wrong and the relative magnitudes of the remaining two terms reversed. Addition of the d-functions goes very far to improving these errors without rectifying them completely. (The d-functions had very little effect on the properties discussed above).

TABLE 6

Properties of Thiophene

Property & Component	sp	sp, GRS	spd + 3s'	spd, GRS	Experimental
Quadrupole Moment (10^{-26}esu.cm^2)					
xx	6.064	6.784	5.278	6.536	6.6 ± 1.5
yy	-1.738	0.809	-0.046	1.303	1.7 ± 1.6
zz	-4.320	-7.593	-5.23	-7.839	-8.3 ± 2.2
Diamagnetic Susceptibility (10^{-6}erg/G^{2}mole)					
xx	-288.60	-286.64	-286.59	-285.78	-284.8 ± 3.0
yy	-228.24	-226.90	-227.68	-226.38	-225.7 ± 3.0
zz	-444.78	-440.64	-442.69	-439.70	-438.1 ± 3.0
zz-$\frac{1}{2}$ (xx+yy)	-186.36	-183.87	-185.56	-183.62	-183.05 ± 3.0
2nd moment (au)					
xx	161.79	160.31	161.53	160.13	159 ± 4.3
yy	212.61	210.60	211.14	210.06	209.3 ± 4.6
zz	30.33	30.68	30.13	30.53	30.4 ± 4.3
1/r Operators (au)					
S	67.09	66.11	66.91	66.12	
C2,C5	25.68	25.66	25.68	25.67	
C3,C4	25.09	25.04	25.10	25.05	
H2,H5	11.14	11.19	11.15	11.19	
H3,H4	10.70	10.76	10.71	10.76	
Electric Field Gradient at Sulphur (au)					
xx	− 2.773	-1.930		-1.929	
yy	0.169	0.324		0.410	
zz	2.612	1.606		+1.520	
Quadrupole Coupling Constant for S^{33}, assuming $Q(S^{33})$ = -0.062 barns (MHz)					
xx	40.9	28.12		28.10	
yy	-2.45	-4.72		-5.97	
zz	-38.06	-23.40		-22.14.	

TABLE 7

Total Energies of Thiophene Sulphoxide at Varying Angles

a) Angle = 0.0°

	sp	sp + 3s'	spd	spd + 3s'
T.E.	-624.46893	-624.51956	-624.64166	-624.69087
1-El.	-1417.4021	-1416.9428	-1417.7908	-1417.3614
2-El.	510.38529	509.87534	510.60127	510.12265
N.R.	282.54786	282.54786	282.54786	282.54786
B.E.	-0.72814	-0.77427	-0.89997	-0.94918
B.E. (kcal/mole)	-456.7	-485.9	-564.7	-595.6
ΔE	-	-29.2	-108.0	-138.9

b) Angle = 20.0°

	sp	sp + 3s'	spd	spd + 3s'
T.E.	-624.47135	-624.52193	-624.64646	-624.69560
1-El.	-1418.3201	-1417.8591	-1418.7785	-1418.3460
2-El.	510.86770	510.35605	511.15096	510.66931
N.R.	282.89107	282.98107	282.98107	282.98107
B.E.	-0.72966	-0.78024	-0.90477	-0.95391
B.E. (kcal/mole)	-457.9	-489.6	-567.7	-598.6
ΔE	-	-31.7	-109.8	-140.7

c) Angle = 40.0°

	sp	sp + 3s'	spd	spd + 3s'
T.E.	-624.47452	-624.52519	-624.65472	-624.70381
1-El.	-1421.1601	-1420.6945	-1421.7514	-1421.3119
2-El.	512.35734	511.84100	512.76841	512.27983
N.R.	284.32828	284.32828	284.32828	284.32828
B.E.	-0.73283	-0.78350	-0.91303	-0.96212
B.E. (kcal/mole)	-459.9	-491.6	-572.9	-603.7
ΔE	-	-32.7	-113.0	-143.8

d) Angle = 60.0°

	sp	sp + 3s'	spd	spd + 3s'
T.E.	-624.46898	-624.51995	-624.65246	-624.70172
1-El.	-1426.2227	-1425.7496	-1426.9080	-1426.4599
2-El.	515.00942	514.48532	515.51121	515.01391
N.R.	286.74431	286.74431	286.74431	286.74431
B.E.	-0.72729	-0.77826	-0.91077	-0.96003
B.E. (kcal/mole)	-456.4	-488.4	-571.5	-602.4
ΔE	-	-32.0	-115.1	-146.0

Thiophene-S-oxide

In order to generate this molecule use was made of an option whereby an atom can be added to a molecule whose integrals have already been evaluated. Thus the heterocyclic ring is identical to thiophene; the S-O length of 1.49Å was taken from dibenzo-thiophene-S-dioxide[29] and the basis set used for the oxygen atom was scaled vinyl alcohol (Appendix 2, Table 12) i.e. the same as for the pyrylium ion. A partial geometry optimisation of the tilt angle (below) was carried out, with the angles chosen being 0, 20, 40 and 60°; this also enabled the estimation of the inversion barrier at the sulphur atom.

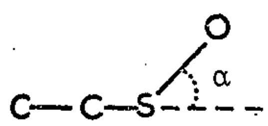

Tilt angle = α

The total energies of the four molecules thus studied are presented in Table 7. Addition of an oxygen atom to the sulphur appears to destabilise the S-oxide with respect to the parent compound, since the binding energy (for like basis sets) is less than that for thiophene. This is caused by some loss of aromaticity as the overlap populations of the C2-C3/C4-C5 and C3-C4 bonds become more diene-like in nature (thiophene, 0.5950, 0.4774; thiophene-S-oxide, 0.6021, 0.4611).

Addition of the 3s' function improves the energy by approximately the same amount for each angle and is of comparable magnitude to the improvement found in thiophene.

In contrast to this, it is found that the 3d-orbitals improve the energy by approximately $2\frac{1}{2}$ times the thiophene value. This would then appear to mean that the inclusion of d-orbitals gives a better representation of the ground state than when they are omitted. The largest eigenvectors for the d-orbitals in the spd calculation on thiophene and the dioxide are as follows:- thiophene, -0.085; thiophene-S-oxide (in order 0, 20, 40, 60 degrees), -0.199, 0.195, 0.177, -0.137. This then supports the contention that the d-orbitals are significant in the bonding of thiophene-S-oxide. Further support comes from the effect of the 3s' function on the spd calculation; in the S-oxides the largest vector changes very little (<0.001) and is associated with the same d-function. In thiophene the introduction of the 3s' function causes the largest eigenvector to become associated with the 3s' function. The total d-orbital populations in thiophene and its S-oxide are also in support of this, the values being 0.149 in the spd calculation on thiophene and 0.471 in its S-oxide.

From the data in Table 7 it is possible to estimate the barrier to inversion and the preferred tilt angle for thiophene-S-oxide. The transition state for inversion is immediately available, being the planar (tilt angle = 0) molecule; an optimal geometry has to be found for the ground state. Parabolic interpretation of the total energy against the tilt angle using the values for 20, 40 and 60 degrees gave rise to the following optimal tilt angles:- sp, 37.28; sp + 3s', 37.67; spd, 45.70; spd + 3s', 45.94.

Since the spd calculation is the better description of the molecule, the tilt angle in thiophene-S-oxide is 45.70 degrees. To strictly evaluate the inversion barrier a calculation should be carried out at each of the optimal tilt angles; however all the angles are very close to the already calculated 40 degree tilt. This was then assumed to be sufficiently near the optimal value to be satisfactory. (As a check on this the optimal sp angle was run, this being the least expensive in computer time. The total energy obtained, -624.47436 au, is identical with the 40 degree calculation to the 4th place of decimals). On this basis then, the inversion barrier is 3.4, 3.5, 5.0 and 4.9 kcal/mole for sp, sp + 3s', spd, and spd + 3s' basis sets respectively. The only experimental evidence is for the compound below where the barrier is found

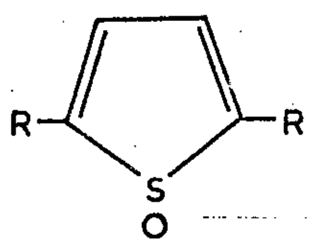

R = $-CMe_2.CH_2.Bu^t$

to be 14.8 kcal/mole by NMR studies.[30] The effect of the large groups in the 2 and 5 positions is somewhat difficult to estimate:- (a) hydrogen bonding of the $-CH_2-$ group can stabilise both ground and transition states (b) repulsion between the H of $-CH_2-$ and the oxygen atom could de-stabilise both ground and transition states. Since the non-empirical calculations on phosphole and phosphine gave reasonable agreement with experimental barriers, it is quite likely

TABLE 8

Orbital Energies of Thiophene Sulphoxide (Planar)

	sp	sp+3s'	spd	spd+3s'
A'	-2498.19 (A_1)	-2501.14	-2497.92	-2500.76
	-554.72 (A_1)	-554.79	-557.99	-558.04
	-308.09 (A_1)	-308.12	-307.95	-307.97
	-307.75 (A_1)	-307.75	-307.40	-307.39
	-242.51 (A_1)	-243.48	-241.67	-242.59
	-185.10 (A_1)	-186.28	-184.24	-185.36
	-184.84 (B_1)	-186.02	-184.14	-185.26
	-36.36 (A_1)	-36.43	-37.18	-37.22
	-33.11 (A_1)	-33.09	-32.66	-32.65
	-27.40 (A_1)	-27.46	-26.87	-26.94
	-21.51 (A_1)	-21.54	-21.23	-21.26
	-19.94 (A_1)	-19.96	-19.65	-19.67
	-17.36 (B_1)	-17.32	-17.14	-17.10
	-16.03 (A_1)	-16.03	-15.95	-15.95
	-14.74 (A_1)	-14.75	-15.53	-15.52
	-13.82 (B_1)	-13.81	-14.25	-14.23
	-9.05 (B_1)	-9.04	-9.28	-9.26
A"	-308.10 (B_2)	-308.12	-307.96	-307.98
	-307.75 (B_2)	-307.75	-307.40	-307.39
	-184.96 (B_2)	-186.14	-184.17	-185.29
	-27.90 (B_2)	-27.39	-27.61	-27.60
	-21.63 (B_2)	-21.61	-21.34	-21.32
	-17.10 (B_2)	-17.09	-16.82	-16.80
	-16.50 (B_2)	-16.49	-16.32	-16.30
	-11.24 (B_2)	-11.22	-12.76	-12.73
	-10.61 (A_2)	-10.60	-10.32	-10.30

that the value for thiophene-S-oxide is correct. The addition of an oxygen atom to thiophene introduces four more occupied orbitals. In planar thiophene-S-oxide one of these will appear as an oxygen core level and the other three as one each in the A_1, B_2 and B_1 symmetry representations. In the non-planar configurations the A_1 and B_1 combine to give the A' representation. The orbital energies of the planar and non-planar (represented by the 40 degree configuration) are shown in Tables 8 and 9.

The sulphur core orbitals are shifted to higher binding energy compared to thiophene, with the 1s level increasing by ~7eV and the 2s, 3p levels by ~5eV. In addition there is a considerable amount of splitting of the three 2p levels, especially in the planar case; the three different cartesian directions are of course very different in their chemical environment. The carbon 1s levels are only slightly affected by the addition of the oxygen atom, although there is a slight shift to higher binding energy. The oxygen atom is at very much lower binding energy than in the case of the pyrylium ion. This is to be expected on the grounds that the molecule is neutral rather than positively charged; however it also occurs at some 5eV lower binding energy than in the thiathiophthen isostere. This is consistent with a very high negative charge on the oxygen atom, this being -0.67 in the 40 degree configuration.

Of the four additional occupied orbitals, there is still one which can appear in the A_1 representation of planar thiophene-S-oxide. This orbital appears as the highest

TABLE 9

Orbital Energies of Thiophene Sulphoxide (40.0°)

	sp	sp+3s'	spd	spd+3s'
A'	-2497.92	-2500.90	-2497.29	-2500.18
	-553.85	-553.93	-556.62	-556.67
	-308.06	-308.06	-307.92	-307.91
	-307.92	-307.94	-307.74	-307.77
	-242.30	-243.29	-241.13	-242.08
	-184.82	-186.02	-183.66	-184.80
	-184.61	-185.80	-183.54	-184.69
	-36.27	-36.35	-36.51	-36.50
	-32.98	-32.96	-32.70	-32.68
	-27.32	-27.38	-26.86	-26.92
	-21.56	-21.59	-21.32	-21.36
	-20.16	-20.17	-19.93	-19.94
	-17.07	-17.04	-16.79	-16.75
	-16.18	-16.18	-16.02	-16.02
	-14.92	-14.93	-15.42	-15.41
	-13.15	-13.15	-13.55	-13.54
	-9.24	-9.24	-9.64	-9.62
A"	-308.07	-308.06	-307.93	-307.91
	-307.92	-307.94	-307.75	-307.77
	-184.71	-185.91	-183.59	-184.74
	-27.96	-27.95	-27.73	-27.71
	-21.68	-21.66	-21.45	-21.43
	-17.10	-17.09	-16.82	-16.81
	-16.55	-16.54	-16.38	-16.37
	-10.91	-10.90	-12.05	-12.03
	-10.51	-10.50	-10.29	-10.28

binding energy valency shell orbital, consisting predominantly of the oxygen 2s atomic orbital together with some sulphur 3s contribution. It does not however correspond to an oxygen addition to the totally symmetric valency S orbital of thiophene i.e. it is a new orbital. The totally symmetric ring combination of thiophene occurs as the next orbital of the A_1 representation and is nodal between sulphur and oxygen. This splitting of oxygen away from the ring is common in many of the molecular orbitals as far as the large eigenvectors are concerned although slight positive overlaps do occur in most orbitals. It would seem that in the sp calculation the structure of thiophene-S-oxide is best represented by thiophene with a loosely attached oxygen atom. The only other orbital which has strong S-O bonding is the lowest ionisation potential of the A_1 representation which in thiophene was a lone pair orbital pointing directly towards where the oxygen now lies. The correlation of thiophene and thiophene-S-oxide molecular orbitals is shown in Table 10.

In the B_2 representation there is a one-to-one correspondence between the molecular orbitals of thiophene and its S-oxide (Table 10); the additional orbital appears at the low ionisation potential end of the representation and consists of an oxygen transverse orbital. In the B_1 representation the new function appears in the middle. The $2b_1$ is a positive combination of p_π orbitals in thiophene; in its S-oxide the oxygen is in symmetric combination with the ring. Orbital $4b_1$ is $3b_1$ of thiophene (node through the

C2/C5 atoms, with oxygen antisymmetric. This leaves the middle orbital, $3b_1$ which has a diene π-system in antisymmetric combination with the S-O π level.

TABLE 10

Correlation of the Molecular Orbitals Thiophene and its Oxide (0.0 and 40.0 Isomers)

Thiophene	Thiophene-S-Oxide (Planar)	Thiophene-S-Oxide (40.0)
$6a_1$	$8a_1$	$9a'$
$7a_1$	$9a_1$	$10a'$
$8a_1$	$10a_1$	$11a'$
$9a_1$	$11a_1$	$12a'$
$10a_1$	$12a_1$	$14a'$
$11a_1$	$13a_1$	-
$4b_2$	$4b_2$	$4a''$
$5b_2$	$5b_2$	$5a''$
$6b_2$	$6b_2$	$6a''$
$7b_2$	$7b_2$	$7a''$
$2b_1$	$2b_1$	$(13a')$
$3b_1$	$4b_1$	-

In the non-planar molecules the same correlation with thiophene can be carried out (see Table 10) but to a somewhat lesser extent. The lessening in the correlation is caused by the lower symmetry of the molecule, which allows the σ and π systems to intermingle. This affects the former sulphur lone pair and the π-levels mainly, with for example, 15a' being mixed S-O and π-orbitals.

Addition of the 3s' function causes a shift to higher binding energy of the sulphur core levels of ~3eV and ~1.1eV for the 1s and 2s, 2p levels respectively, while leaving the carbon 1s levels and oxygen 1s levels almost unchanged. The 3d functions also cause their usual, very small, shift to lower binding energy for the carbon and sulphur core levels. The effect on the core level of oxygen is very different and quite dramatic, with the energy being shifted 3.2eV in a higher binding energy direction. This is consistent with better bonding between the S and O atoms, resulting in a smaller oxygen population (Table 11). The oxygen electrons which were formerly non-bonding will move into the S-O region

Table 11

Population Analyses for Thiophene Sulphoxide (60.0)

	sp	sp+3s'	spd	spd+3s'
S	15.2576	15.2817	15.4886	15.5098
O	8.7055	8.6919	8.5851	8.5724
C2,C5	6.2382	6.2311	6.1726	6.1661
C3,C4	6.1421	6.1436	6.1379	6.1395
H2,H5	0.8129	0.8133	0.8227	0.8232
H3,H4	0.8252	0.8252	0.8299	0.8300
μ_y	3.92	3.93	3.44	3.43
μ_z	2.84	2.83	2.70	2.69
μ	4.84	4.84	4.37	4.36

TABLE 12

Total Energies of Thiophene-S-Dioxides

	sp	sp+3s'	spd	spd+3s'
a) Angle = 40.0				
T.E.	-698.21067	-698.26169	-698.4885	-698.53839
1-El.	-1741.1178	-1740.6757	-1741.9010	-1741.5032
2-El.	646.6727	646.1595	647.1781	646.2590
N.R.	396.2345	396.2345	396.2345	396.2345
B.E.	+0.14316	+0.09214	-0.13467	-0.18456
B.E.(kcal/mole)	+89.8	+57.8	-84.5	-115.8
ΔE	-	-32.0	-174.3	-205.6
b) Angle = 80.0				
	-698.80815	-698.86198	-699.12422	-699.17450
	-1720.3484	-1719.8724	-1720.9682	-1720.54912
	638.1592	637.6294	638.4630	637.99356
	383.3810	383.3810	383.3810	383.3810
	-0.45432	-0.50815	-0.77039	-0.82067
	-285.1	-318.9	-483.4	-515.0
	-	-33.8	-198.3	-229.9
c) Angle = 120.0				
	-698.90399	-698.95827	-690.25519	-699.30579
	-1720.1882	-1719.7057	-1721.0171	-1720.58008
	637.6285	637.09172	638.1063	637.6186
	383.65567	383.65567	383.65567	383.65567
	-0.55016	-0.60444	-0.90136	-0.95196
	-345.2	-379.3	-565.6	-597.4
	-	-34.1	-220.4	-252.2

(the S-O total overlap population increases from 0.0689 in the sp calculation to 0.3221 in the spd calculation). Further evidence comes from the only valency shell orbital (6a") to be affected by a significant amount (>0.2eV) which moves by 1.5eV to higher binding energy and which was the oxygen lone pair orbital.

Thiophene-S-dioxide

This molecule was generated using the "add" procedure on the mono-S-oxide; the S-O bond length was maintained at 1.49Å with the new oxygen atom being placed so that C_{2v} symmetry was obtained. Three O-S-O angles were used (40, 80 and 120 degrees) in order to enable the determination of an optimal angle.

The total energies for each of the three structures and for each of the four basis sets are shown in Table 12. The destabilisation found for the addition of an oxygen to thiophene is maintained here and is indeed emphasized. In the 40 degree case the molecule has a positive binding energy with the sp and sp+3s' basis sets. The nuclear repulsion, one-electron and two-electron energies are 13, 21 and 8 au greater in magnitude than in the 80 and 120 degree case. The electron rich oxygen atoms are very close together, and this closeness would appear to make the molecule unstable. The 3s' function improves the energy of each molecule by approximately 33 kcal/mole; this is similar to what is found for other compounds containing second row atoms. Replacement of the 3s' function by the 3d functions leads to a very large improvement (>170 kcal/

mole in each molecule) in energy; this is considerably larger than that found for the mono-S-oxide and is excellent evidence for the necessity of d-orbitals in ground state bonding in thiophene-S-dioxide.

TABLE 13

d-Orbital Populations in Thiophene-S-dioxide (120 degrees)

	sp+3s'	spd	spd+3s'
3s'	0.377	-	0.349
$d_{x^2-y^2}$	-	0.037	0.036
d_{z^2}	-	0.270	0.268
d_{xy}	-	0.240	0.238
d_{xz}	-	0.162	0.160
d_{yz}	-	0.193	0.191
Total	0.377	0.902	1.242

Further corroboration comes from the d-orbital populations in Table 13 and the largest d-orbital eigenvectors in Table 14. The d-orbitals all have large populations except for the $d_{x^2-y^2}$ which does not point directly towards any of the atoms bonded to sulphur. The total population in the spd case is approximately one electron, indicating that the d-orbitals are necessary. The largest d-orbital eigenvector is by no means insignificant and its nature does not change when the 3s' function is added. This is similar to what was found for the mono-S-oxide.

TABLE 14

Largest d-Orbital Eigenvector in Thiophene-S-Dioxide

	40.0	80.0	120.0
spd, Type	0.228, d_{yz}	-0.224, d_{xy}	0.217, d_{z^2}
spd+3s', Type	0.228, d_{yz}	-0.223, d_{xy}	0.217, d_{z^2}

The three O-S-O angles are sufficient to enable a parabolic interpolation of the energy to be carried out, giving a value for the predicted experimental angle. The values obtained for the sp, sp+3s', spd and spd+3s' bases sets are 107.64, 107.65, 110.38 and 110.40 degrees. These values are similar to those found for dibenzo-thiophene-S-dioxide (120)[29] and a tetrahydro derivative of thiophene-S-dioxide (117.8).[31] It would thus seem likely that the experimental geometry will prove to have an O-S-O angle in the close proximity of 110°. This could be found soon as the iron tricarbonyl complex of thiophene-S-dioxide has recently been obtained.[32] The calculation nearest the optimal value is that with an O-S-O angle of 120 degrees; this will be used as being the structure hereafter.

The effect on the core energies (Table 15) of the addition of another oxygen atom to the S-oxide is much the same as adding one to thiophene, i.e. the sulphur 1s orbital increases in binding energy by 5.6eV going from thiophene to the mono-S-oxide and a further 5.5eV with the addition of the second oxygen atom. Indeed this places the 1s orbital energy higher than in the cationic sulphur heterocycles. Consistent with this is the extremely low population of the

TABLE 15

Orbital Energies of Thiophene-S-dioxide (120 degrees)

	sp	sp+3s'	spd	spd+3s'
A_1	-2503.47	-2506.57	-2502.52	-2505.42
	-554.37	-554.43	-557.52	-557.56
	-309.33	-309.32	-309.00	-308.98
	-308.36	-308.39	-308.21	-308.22
	-247.10	-248.13	-245.11	-246.06
	-189.59	-190.84	-187.70	-188.85
	-39.34	-39.46	-38.84	-38.94
	-33.76	-33.73	-33.31	-33.28
	-27.73	-27.76	-27.10	-27.13
	-22.23	-22.25	-21.87	-21.90
	-20.84	-20.87	-20.51	-20.54
	-17.40	-17.42	-17.70	-17.71
	-17.07	-17.07	-16.76	-16.75
	-11.33	-11.32	-13.00	-12.97
B_2	-309.33	-309.32	-309.00	-308.98
	-308.36	-308.39	-308.21	-308.23
	-189.53	-190.78	-187.69	-188.84
	-28.94	-28.92	-28.52	-28.50
	-23.08	-23.03	-22.55	-22.53
	-18.25	-18.24	-17.85	-17.84
	-17.78	-17.77	-17.40	-17.40
	-11.18	-11.16	-12.33	-12.30
B_1	-554.44	-554.50	-557.61	-557.65
	-189.62	-190.87	-187.72	-188.87
	-35.18	-35.14	-35.72	-35.67
	-17.04	-17.02	-17.13	-17.11
	-14.01	-14.01	-14.43	-14.41
	-11.20	-11.19	-12.10	-12.08
A_2	-12.51	-12.50	-13.62	-13.60
	-10.93	-10.92	-10.55	-10.54

sulphur atom (Table 16). The 2s and 2p sulphur core levels show the same trends as the 1s in going from thiophene to its S-dioxide. The addition of the 3s' function has its usual effect in a shift to higher binding energies by ~3eV for the 1s level and ~1.1eV for the 2s and 2p levels; the d-orbitals result in a small shift to lower binding energies. The carbon 1s levels are also at higher binding energy than in the mono-S-oxide and, while they occur in the same order as in the mono-S-oxide (C3/C4 at higher binding energy) the energy separation is somewhat greater. These energies are virtually unaffected by the additional d-functions. The oxygen 1s orbitals are again at very low binding energy compared to the charged (pyrylium) compound and the neutral thiathiophthen analogue; the 3s' function has no effect on the energy but the 3d functions, as in the mono-S-oxide, cause a shift of some 3eV to higher binding energy. This can again be explained by the essentially lone pair electrons on the oxygen being pulled into the S-O bonding region. Consistent with this are 1) the decrease in oxygen population on the addition of the d-functions (Table 16) 2) the increase in the S-O overlap

TABLE 16

Population Analysis and Dipole Moment of Thiophene-S-dioxide (120)

	sp	sp+3s'	spd	spd+3s'
S	14.6534	14.6909	15.0801	15.1101
O	8.6982	8.6850	8.5404	8.5288
C2,C5	6.2448	6.2368	6.1694	6.1637
C3,C4	6.1228	6.1244	6.1245	6.1261
H2,H5	0.7983	0.7981	0.8088	0.8093
H3,H4	0.8102	0.8102	0.8169	0.8170
μ(D)	6.40	6.39	5.53	5.53

populations (Table 17), 3) the change in order of the outer valency shell orbitals (sp, sp+3s':- $7b_2>13a_1>4b_1>5b_1>1a_2>14a_1>6b_1>8b_2>2a_2$; spd, spd+3s':- $12a_1>7b_2>4b_1>13a_1>5b_1>1a_2>14a_1>8b_2>6b_1>2a_2$). These changes in order are

TABLE 17

Total Overlap Populations in Thiophene-S-Oxide (120^{o})

	sp	sp+3s'	spd	spd+3s'
S-O	0.114	0.113	0.421	0.423
S-C	0.257	0.256	0.359	0.359
C_2-C_3	0.545	0.545	0.540	0.540
C2-H2	0.411	0.410	0.409	0.409
C3-H3	0.393	0.391	0.392	0.391

caused by the $7b_2/12a_1$, $13a_1/4b_1$ and $6b_1/8b_2$ orbitals reversing in order of energy. In the sp calculation the lowest ionisation potential member of these pairs had a considerable amount of oxygen lone pair character; the movement of such orbitals into the S-O bonding region meant that they were less localised and resulted in an increase in binding energy. The sp levels were so nearly (accidentally) degenerate that this caused the observed reversals. (In agreement with this the S-O overlap populations for these orbitals became more bonding, as is shown in Table 18).

TABLE 18

Orbital Overlap Populations between Sulphur and Oxygen

	$12a_1$	$4b_1$	$8b_2$	$1a_2$	$14a_1$
sp	-0.037	-0.072	-0.008	-	-0.017
spd	+0.009	-0.037	0.030	0.041	0.041

Two other orbitals ($1a_2$, $14a_1$) are predominantly lone pair and show a considerable drop in energy on the introduction of d-orbitals. The energy difference between them and the next orbital to higher binding energy is sufficiently large to prevent any change in orbital order. The S-O overlap population also becomes more binding.

The change in the eigenvectors is small in most molecular orbitals so that the nature is largely unchanged upon the addition of d-orbitals; there are two exceptions to this pattern. One is orbital $2a_2$, where the d_{xy} function is new to the representation and makes it possible for sulphur to participate in bonding to the oxygen and carbon atoms. There is thus generated a very small S-O overlap, π-type in nature. The other orbital, $5b_1$, has quite large changes in eigenvectors, as is shown in Table 19.

TABLE 19

Eigenvectors of Orbital $5b_1$

		sp	spd
S	3z	-0.41	-0.25
C2,C5	2z	0.34	0.40
C3,C4	2z	0.62	0.61
O1, O2	2s	0.42	0.32
O1, O2	2y	0.40	0.20
O1, O2	2z	0.21	0.42

The oxygen y and z orbitals reverse in relative magnitude and the S 3z decreases; the orientation of the molecules is such that this results in the S-O region going from anti-bonding to bonding (the S-O overlap increases from

-0.019 to 0.003). The very small variation in eigenvectors in most orbitals is consistent with there being no one orbital responsible for the increase in S-O population which has been found.

Unlike thiophene-S-oxide the C2-C3/C4-C5 bond is less olefinic than in thiophene (Table 17). Thus the decrease in molecular stability cannot be associated with a reduced aromaticity. It is likely to be caused by the lower S-C overlap in thiophene-S-dioxide and the high S-O overlap population; thus the molecule is potentially ready to lose SO_2. The mass spectrum of the iron-tri-carbonyl complex[32] has loss of SO_2 as the first peak involving the heterocyclic ring.

From the large positive charge on sulphur and large negative charge on oxygen it is not surprising to find the dipole moment orientation below.

The addition of the 3s' function moves electrons towards sulphur mainly at the expense of the oxygen atoms; this produces a decrease in dipole moment. The 3d functions move electrons away from the non-bonding region to the S-O region; this then gives the expected change (a reduction) in the dipole moment. At the same time it is consistent with the increase in magnitude of the one-electron and two-electron energy terms.

Summary

Calculations have been carried out on thiophene and both its S-oxides in order to estimate the contributions made by d-orbitals in ground state bonding and to predict the geometry of these molecules. In thiophene the d-orbitals are involved to a trivial extent; in the S-oxides they are very necessary to the description since they introduce substantial bonding to the oxygen atoms. Without d-orbitals the oxygen atoms are loosely bonded; the d-orbitals cause localisation of the oxygen lone pair electrons as is shown by greatly increased S-O overlap populations (this is achieved without reduction of S-C overlap populations).

References

1. H.C. Longuet-Higgins, Trans. Far. Soc., 1949, 45, 174.
2. A.J.H. Wachters, D.W. Davies, Tet., 1964, 20, 2841.
3. N. Solony, F.W. Birss, J.B. Greenshields, Can. J. Chem., 1965, 43, 1569.
4. D.S. Sappenfield, M. Keevoy, Tet., 1963, 19, 157.
5. D.T. Clark, Tet., 1968, 24, 2663-79.
6. R. Phen-Tan-Luu, L. Bouscana, E.J. Vincent, J. Metzger, Bull. Soc. Chem. Fr., 1967, 3283.
7. F.P. Billingsley, J.E. Bloor, Theor. Chim. Acta (Berl.), 1968, 11, 325.
8. J. Fabian, A. Mehlhorn, R. Zahradrik, J. Phys. Chem. 1968, 72, 3975.
9. J. Fabian, A. Mehlhorn, R. Zahradrik, Theor. Chim. Acta (Berl.), 1968, 12, 1247.
10. C.B. Chowdhury, R. Basu, J. Ind. Chem. Soc., 1969, 66, 779.
11. A. Jug, M. Bonnet, Y. Ozias, Theor. Chem. Acta (Berl.), 1970, 17, 49.
12. M.J.S. Dewar, N. Trinajstic, J.A.C.S., 1970, 92, 1453.
13. A. Skancke, P.N. Skancke, Acta Chem. Scand., 1970, 24, 23.
14. J. Devanneaux, J.F. Labarre, J. Chim. Phys. Physiochim. Biol., 1969, 66, 1780.
15. H.A. Howell, Theor. Chim. Acta (Berl.), 1970, 18, 239.
16. A. Jasiri, T. Asano, T. Nakajima, Tet. Lett., 1971, 21, 1785.
17. D.T. Clark, D.A. Armstrong, Chem. Comm., 1970, 319.
18. U. Gelius, B. Roos, P. Siegbahn, Theor. Chim. Acta (Berl.), 1972, 27, 171.
19. P.W. Lert, C. Trinelle, J.A.C.S., 1971, 93, 6391.
20. F. de Jong, M. Janssen, J.C.S. Perkin II, 1972, 572.
21. B. Bak, D. Christensen, L. Hansen-Nygaard, J. Rastrup-Andersen, J. Mol. Spec., 1961, 7, 58.
22. Reference 23 of Section 3.

23. B. Harris, R.J.W. Lefevre, E.P.A. Sullivan, J.C.S., 1953, 1672.

24. D.T. Clark, D.M.J. Lilley, Chem. Phys. Lett., 1971, 9, 234.

25. U. Gelius, C.J. Allan, G. Johansson, H. Siegbahn, D.A. Allison, K. Siegbahn, Physica Scripta, 1971, 3, 237.

26. B.J. Lindberg, S. Hogberg, G. Malmster, J-E. Bergmark, O. Nilsson, S-E. Karlsson, A. Fahlman, U. Gelius, Chem. Scripta, 1971, 1, 183.

27. P.J. Derrick, L. Asbrink, O. Edqvist, B-O, Jonsson, E. Lindholm, Int. J. Mass Spec. Ion Phys., 1971, 6, 177.

28. W.H. Flygare, D.H. Sutter, J.A.C.S., 1969, 91, 4063.

29. L. Kronfield, R.L. Sass, Acta Cryst., 1968, 24, 981.

30. W.L. Mock, J.A.C.S., 1970, 92, 7610.

31. F. Ellis, P.G. Sammes, M.B. Hurthouse, S. Neidle, J.C.S. (Perkin I), 1972, 1560.

32. Y.L. Chow, J. Fossey, R.A. Perry, Chem. Comm., 1972, 501.

VIII. THIATHIOPHTHEN and ITS ISOSTERES

Introduction

The first compound synthesized having the thiathiophthen ring system (1) was the 2,5-dimethyl derivative prepared[1] by Arndt and his co-workers in 1925. The structure they proposed (2) was corrected to the ring system (1) by x-ray crystallography.[2]

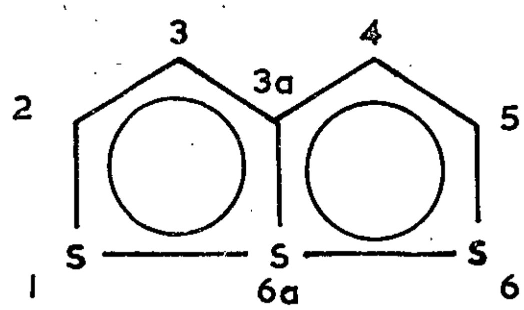

(1)

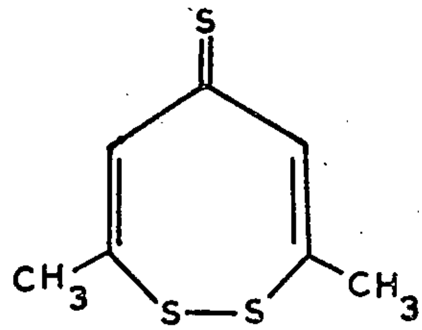

(2)

The S-S bond lengths were found to be equal, leading to the postulate of "single bond-no bond" resonance[2] (structures 3a and 3b).

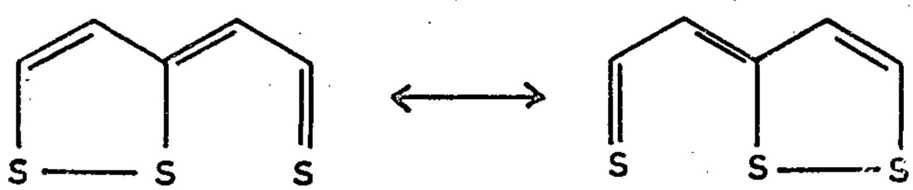

(3a) (3b)

Before examining the bonding of the sulphur atoms, it is first necessary to deal with the possibility of a rapid equilibrium between structures 3a and 3b. If such an equilibrium did exist then it would be expected that an unsymmetrical substitution would lead to the existence of molecules with unsymmetrical S-S bond lengths; this has been found for several molecules (for example the 2-methyl-4-phenyl[3] and 2,4-diphenyl[4] derivatives). Such a distortion could also be explained by crystal packing forces acting on a symmetric structure. The symmetrically substituted 2,5- and 3,4-diphenyl derivatives also have unsymmetric S-S bond lengths which are also likely to be caused by crystal packing forces, with the 2,5-diphenyl compound having the two phenyl groups at different twist angles (3.5 and 45.1 degrees) with respect to the thiathiophthen ring system.[5a] Inter-molecular forces could be the cause of this since the 2,5-diphenyl-3,4-diazathiathiophthen has twist angles of 7.0 and 2.9 degrees;[5b] semi-empirical calculations also indicate this possibility.[6]

In support of the rapid equilibrium concept are two experimental phenomena; 1) reports[7,8] that x-ray diffraction studies for the 2,5-dimethyl compound could be ambiguous (they could represent the average of a two-fold disordered arrangement having one long and one short S-S bond) led to a re-examination and refinement[9] of the x-ray analysis of this compound. The symmetric structure gave a slightly worse analysis than the unsymmetric one; however the asymmetry was excessive and regarded as unacceptable.[9] 2) Examination of this compound by the ESCA technique[10] yielded a broad peak in the sulphur 2p region. Deconvolution of this peak was better when a 1:1:1 distribution was assumed, compared to a 2:1 distribution.

On a theoretical level calculations by Gleiter and Hoffmann[11] both with and without d-orbitals predict a symmetric structure with d's and an unsymmetric without (it is necessary to point out that the energy curves and text do not appear to agree in this paper). CNDO/2 calculations by Clark and Kilcast[12] predict that the symmetric structure is 5 kcal/mole more stable than the unsymmetric (this was a Kekulé-type structure, using the 3,4-diphenyl derivative as a basis).

One very significant point has not yet been considered. In the rapid equilibrium concept, the two valence isomers 3a and 3b must have identical energies, and must therefore exist as a 50:50 mixture. Unsymmetric substitution would lead to two different isomeric compounds; x-ray crystallography has revealed only one compound in all cases. This then leads one to one of two conclusions:- a) the thiathiophthens are essentially symmetrical with distortions caused by mainly crystal packing forces; or b) substitution leads <u>in all cases</u> to a new "mixture" consisting of 100% of one isomer only. The former conclusion is much more likely than the latter; accordingly investigation has been limited to the symmetric structure alone.

The Kekulé-like structures 3a and 3b satisfy both the octet rule and the normal valencies of the atoms in the molecule. The sulphoniumylid structure[13] (4a) also conforms with these requirements.

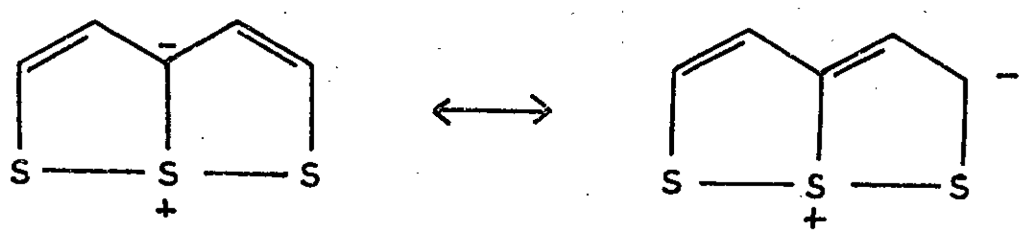

(4a) (4b)

This structure gives a satisfactory 10π electron system (the terminal sulphur atoms contribute 2 electrons each; the 3a carbon atom also contributes two and the remaining carbon atoms are each), thus explaining the stability of the molecule. (The 10π electrons are of course based on the valency shell electrons only; with there being two core electrons of π-symmetry, the total number of π-electrons is sixteen). However classical delocalisation of the charge (giving 4b) would lead to the 2 and 5 positions being negatively charged, thus contradicting the experimental evidence which shows these positions to be active towards nucleophiles but not electrophiles.

In order to overcome this difficulty it is possible to postulate a double bond between the atoms 3a and 6a, giving a quadrivalent sulphur atom (5a). In classical concepts

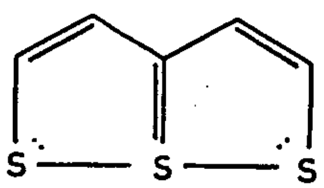

(5a)

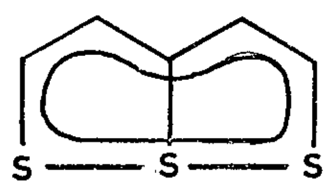

(5b)

such a valency requires the use of d-orbitals. Besides the work of Gleiter and Hoffmann,[11] and Clark and Kilcast,[12] all of whom predict the use of d-orbitals on the centre sulphur, the semi-empirical calculations of Maeda[14] show that σ-bonding between the sulphur atoms could arise from pd hybridisation. Correlation of calculated and observed ultra-violet transitions by Johnstone and Ward[15] similarly predict that d-orbitals are necessary to explain the bonding of the centre sulphur atom.

TABLE 1

Total Energies of Thiathiophthen, in All Basis Sets.

	A	B	C	D	E	F	G	H
T.E.	-1381.0944	-1381.1455	-1381.1892	-1381.1628	-1381.1883	-1381.2141	-1381.2838	-1381.4048
1-El.	-3052.4907	-3051.9422	-3051.1514	-3052.8350	-3053.6948	-3052.3000	-3052.728	-3052.5044
2-El.	1094.6816	1094.0819	1093.2474	1094.9574	1095.7917	1094.3711	1094.7294	1094.3848
N.R.	576.7148	576.7148	576.7148	576.7148	576.7148	576.7148	576.7148	576.7148
B.E.	-0.95678	-1.00788	-1.05161	-1.02518	-1.05068	-1.07648	-1.14618	-1.26718
B.E. (kcal/mole)	-600.4	-632.4	-659.9	-643.3	-659.3	-675.5	-719.2	-795.2
ΔE	-	-32.0	-59.5	-42.9	-58.9	-75.1	-118.8	-194.8

In this concept of the bonding all carbon atoms give one electron to the π-system with the terminal sulphur atoms contribute two each to the π- and two each to the σ-systems; the centre sulphur atom contributes only one electron to the π-system but three to the σ-system. All three sulphur atoms have two lone pair electrons.

The Bonding in Thiathiophthen

Calculations have been carried out on thiathiophthen at the experimental geometry,[16] as determined by x-ray crystallography, in order to investigate the bonding properties. The carbon and hydrogen exponents were those of scaled ethylene (Tables 8 and 9, Appendix 2) and the sulphur those of scaled thio-formaldehyde (Table 13, Appendix 2). These were augmented by six d-functions on each sulphur, resulting in calculations being carried out using the basis sets below:

- A sp basis set on all atoms
- B sp + 3s' on centre sulphur atom (6a)
- C sp + 3s' on terminal sulphur atoms (1, 6)
- D spd on centre sulphur atom
- E spd on terminal sulphur atoms
- F spd + 3s' on centre sulphur atoms
- G spd + 3s' on terminal sulphur atoms
- H spd + 3s' on all sulphur atoms.

The total energies for these calculations are shown in Table 1. The improvement in energy for the sp + 3s' calculations is of the same approximate magnitude as has been found for other sulphur heterocycles, i.e. about 30 kcal/mole per sulphur atom. Replacement of the 3s' by the 3d functions leads to an energy improvement somewhat greater in magnitude than that of the 3s' functions. The 6a sulphur atom 3d functions improve the energy somewhat more than does the terminal sulphur pair. In neither case is the improvement anything resembling that found for the thiophene-S-oxides (Section VII) and it must therefore be concluded that the d-orbitals do not significantly participate in the ground state bonding of thiathiophthen. (This does not, however, invalidate the work of Johnstone and Ward[15] since it is quite feasible that the d-orbitals could play a large part in the excited state electronic structure, which is of course necessary for ultra-violet spectroscopy). Further evidence of this comes from the total overlap populations of Table 2 and the d-orbital occupancies of Table 3. In the former table there are only small changes

TABLE 2

Overlap Populations in Thiathiophthen; Sulphur with Adjacent Atoms

	A	D	E	H
6a - 3a	0.3855	0.4375	0.3882	0.4345
6a - 1	0.0261	0.0691	0.0341	0.0920
1 - 2	0.3691	0.3655	0.4225	0.4345

in overlap population on introduction of the d-orbitals; again this is markedly different from the situation in the thiophene-S-oxides. Similarly the d-orbital populations, both individually and in total, are much more reminiscent of thiophene (and other heterocycles like the 1,2-dithiolium ion) than its S-oxides.

Table 3

d-Orbital Occupations in Thiathiophthen

	B	C	D	E
3s'	0.350	0.344	-	-
$d_{x^2-y^2}$	-	-	0.104	0.050
d_{z^2}	-	-	0.025	0.014
d_{xy}	-	-	0.007	0.005
d_{xz}	-	-	0.009	0.003
d_{yz}	-	-	0.017	0.017
Total	0.350	0.344	0.162	0.089

The lack of significant d-orbital participation would appear to eliminate (5a) as a possibility, since in classical usage this structure requires the involvement of d-orbitals. Supporting this elimination are two other factors:- (1) the overlap population between the atoms C2-C3 and C3-C3a are almost identical (0.5436 and 0.4989 respectively). Indeed applying the Diels-Alder reactivity index method of section VI the value of 1.09 occurs more to the aromatic end of the system; structure 5a would be olefinic/saturated in nature and show a high index value; further these populations occur just on either side of the 1,2-dithiolium value of 0.5305 (2) the overlap population (Table 2) between the C2-S1 atoms is very large, being reminiscent of the value obtained for thio-pyrylium (0.3821) and 1,2-dithiolium (0.3989). However both these objections could be overcome by delocalisation of the π-electrons into structure 5b.

TABLE 4

Population Analysis of Thiathiophthen (sp Basis Set)

	s	x	y	z	Total	H
S 6a	1.8813	0.9773	1.1759	1.7450	15.7390	-
S1, S6	1.8444	1.5348	1.0651	1.6333	16.0444	-
C 3a	1.0963	1.1009	0.9630	0.8922	6.0422	-
C2, C5	1.1104	1.1490	1.0671	0.8920	6.2081	0.8216
C3, C4	1.0044	0.9431	1.1020	1.1563	6.1946	0.8418

Turning now to the sulphoniumylid structure, there would also appear to be little evidence for the existence of this structure. The population analysis of Table 4 shows that the 3a carbon atom, far from having a complete negative charge is that with the lowest population. Further, since this charge would be expected to lie in the π-system, the 3a carbon would have the highest z population; Table 4 shows that it is very low and essentially equal lowest of all the carbon atoms. The only factor supporting the sulphoniumylid structure is the net positive charge on the 6a sulphur atom; however this is caused by a very low population of an in-plane p component (p_x) and not by the expected p_π deficiency. Thus the bonding is not well described by a sulphoniumylid structure.

This structure was rejected on chemical grounds since "classical delocalisation" would lead to the C2, C5 atoms being negative and not positive as reactivity demands. Since there is a positive sulphur atom in the classical structure with three very electron-rich centres around it, it would seem unlikely that electrons from one of these electron-rich centres (C3a) would move away from the electron-deficient centre. Thus taking the sulphoniumylid structure as starting point, there would be back-donation of the two p_{π} electrons of carbon 3a into the vacant p_{π} orbital of sulphur 6a; this latter orbital will receive donations from the terminal sulphur atoms also. These in turn will receive electrons from the adjacent carbon atoms (C2/C5); beyond this point it is difficult to predict what will be the ultimate outcome of the competing demands for electrons. The p_z populations of Table 4 show that the value for the sulphur atoms is characteristic of a 2π-electron donor (cf. the value for thiophene); there must thus be considerable movement of electrons towards the 6a sulphur atom. It is also found that the C2/C5 positions have the lowest population and would thus be most reactive towards nucleophiles; similarly the C3/C4 atoms are predicted to be very reactive to electrophiles. Both these predictions are found to be true.[17-21]

Delocalisation of the π-electrons of the sulphoniumylid structure in the above fashion will generate a molecule identical to that of 5b. It would therefore seem that structure 5b is the best overall representation of the bonding in thiathiophthen provided it is realised that there is no significant d-orbital participation in the representation. Similarly if one desires a classical structure, 5a is the nearest to the true structure, subject again to the lack of d-orbital participation.

The nature of the S-S bonds themselves are of interest. It has been suggested that they should consist of π-interaction only;[22] this has been criticised[13] on the grounds that the bond strength would be too small. The population analysis indicates that the S-S bond is made up of almost equal proportions of σ and π overlap populations (0.0136 and 0.0125 respectively). The total is much less than is usually found for S-S overlaps (0.1503 in H_2S_2 at the experimental geometry[23] and using the present basis set; 0.2145 in the 1,2-dithiolium cation). Although the value for thiathiophthen is small it is quite definitely present and indicates that there is a bond between the sulphur atoms. Presumably the sulphur atoms would prefer to move closer together in order to form better and stronger bonds, but strain within the rings would act to prevent this. Some evidence that this is so comes from 2,5-diphenyl-3,4-diazathia-thiophthen where the average S-S length is 2.32Å, slightly less than the 2.33Å of 2,5-diphenylthiathiophthen.[7] It should be noted that this is not merely a result of the differences of the sulphur atomic orbitals since the overlap population between the sulphur atoms in the 1,3-dithiolium cation is -0.073, at an S-S distance of 2.96Å.

Ring strain can also be considered as having a large effect on the distortion from unequal S-S bond lengths in unsymmetrically substituted compounds. In the symmetrically substituted compounds the centre sulphur atom experiences the same "pull" from either side, and so has no tendency to distort. Unsymmetric substitution on the other hand will make the effect uneven, resulting in the centre sulphur moving towards one of the terminal sulphur atoms. This

TABLE 5

Core Orbital Energies in Thiathiophthen

		A	B	C	D	E	H
S 6a	1s	-2493.88	-2497.15	-2493.87	-2493.48	-2493.69	-2496.69
	2s	-239.05	-240.20	-239.06	-238.48	-238.80	-239.40
	$2p_x$	-181.31	-182.69	-181.32	-180.82	-181.07	-181.94
	$2p_y$	-181.28	-182.66	-181.30	-180.76	-181.06	-181.89
	$2p_z$	-181.20	-182.57	-181.21	-180.69	-180.97	-181.83
S1, S6	1s	-2489.96	-2489.94	-2492.94	-2490.16	-2489.47	-2493.37
	2s	-235.60	-235.61	-236.64	-235.76	-235.06	-236.29
	$2p_x$	-177.85	-177.92	-179.15	-178.08	-177.40	-178.85
	$2p_y$	-177.91	-177.91	-179.14	-178.08	-177.39	-178.85
	$2p_z$	-177.81	-177.87	-179.09	-178.02	-177.35	-178.78
C 3a	1s	-310.21	-310.23	-310.20	-310.19	-309.89	-309.91
C2, C5	1s	-309.35	-309.34	-309.36	-309.26	-309.19	-309.13
C3, C4	1s	-308.04	-308.04	-308.04	-307.93	-307.64	-307.54

movement will continue until the gain in overlap population due to closer proximity to one sulphur equals the loss from the other sulphur atom. Such a balancing effect also explains why movement does not continue to a substituted dithiolium structure.

The core orbital energies are shown in Table 5 for several basis sets. All the 6a sulphur core levels occur at higher binding energy than the corresponding core orbitals of the terminal sulphur atoms. This is what one would expect on the basis of the populations of the sulphur atoms. The 2s levels are approximately as far from the experimental values[24] (Table 6) as they were in thiophene (~11eV) and

TABLE 6

Experimental Core Orbital Energies

S 2s	228.5	227.0
S 2p	164.1, 165.1	162.6, 163.6

the sp levels show a similar departure from the experimental values. The additional 3s' functions have very little effect on the core levels of adjacent atoms, although there is the usual considerable shift to higher binding energy of the core levels of the atom to which the 3s' function is added. The d-orbitals have their usual effect on binding energies - a small movement to lower ionisation potential; the addition of d-orbitals to the centre sulphur atom has virtually no effect on the terminal atoms orbital energies. This is not at all like the effect found in thiophene-S-oxides and is additional evidence that the d-orbitals are not involved in ground state bonding of this molecule. The carbon core orbital energies have not been reported, but the 3a is of highest binding energy as one would expect from the charge distribution (from Table 4). However the C3/C4 and C2/C5 are in the reverse order to the atomic populations.

The valency shell region has been investigated by He(I) spectroscopy;[25] a least squares fit of the observed and calculated data yielded the equation IP(exp) = 0.546 IP(calc) + 3.463 with the standard deviation in slope, intercept and the overall standard deviation being 0.009, 0.104 and 0.049 respectively. While this line is somewhat different from that for thiophene, it represents an excellent correlation of the observed and calculated data.

The dipole moment is also in reasonable agreement with the experimental value of 3.01D;[26] the value for each basis set is:- A, 3.87; B, 3.87; C, 3.85; D, 3.40; E, 2.57; F, 3.40; G, 2.56; H, 2.17. With the negative end of the dipole towards the sulphur atoms, the 3s' functions would be expected to increase the dipole moment by analogy with phosphorin and thiophene. This is in fact what occurs for the addition of the 3s' to the 6a atom, although the change is very small (<0.001) and is not significant in the accuracy with which dipole moments are usually reported. However the centre of gravity of the electrons happens to occur between the sulphur atoms in the sp basis set; when the 3s' function is added to the terminal sulphur atoms, the net result is a movement of electrons to the C-H end of the molecule and a reduction in dipole moment. The d-orbitals have the expected reduction effect on the dipole moment;

this is larger for the terminal sulphur atoms than the centre one and can be attributed to the formation of pd hybrids.

The population analyses of Table 7 show that the addition of the d-orbitals and/or the 3s' function causes an increase in population of the atom(s) to which they are added.

TABLE 7

Population Analysis of Thiathiophthen

	B	C	D	E	H
S1,S6	16.0431	16.0491	16.0398	16.1336	16.1318
S6a	15.7465	15.7408	15.8329	15.7260	15.8280
C2,C5	6.2077	6.2004	6.2061	6.1114	6.1023
C3,C4	6.1956	6.1961	6.1950	6.1998	6.2024
C3a	6.0356	6.0419	5.9529	6.0322	5.9381
H2,H5	0.8217	0.8222	0.8233	0.8307	0.8330
H3,H4	0.8408	0.8408	0.8428	0.8454	0.8474

Isosteres of Thiathiophthen

The atomic arrangement in thiathiophthen is not by any means unique; the terminal sulphur atoms have been replaced by oxygen,[27] nitrogen[28] and selenium[29] atoms, while the centre sulphur has only been replaced by selenium.[30] Calculations have accordingly been carried out on the three isosteres shown below.

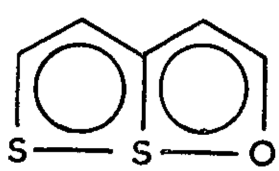

(6)

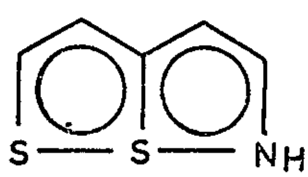

(7)

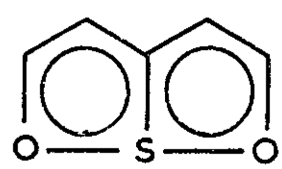

(8)

TABLE 8

Total Energies (au) of 6-Oxo-thiathiophthen

	A	B	C	D	E	F	G	H
T.E.	-1059.0073	-1059.0554	-1059.0540	-1059.0647	-1059.0579	-1059.1132	-1059.1050	-1059.2111
1-El.	-2433.6318	-2433.1315	-2433.1594	-2434.0520	-2434.2166	-2433.5585	-2433.7500	-2433.6490
2-El.	883.4819	882.9336	882.9629	883.8448	884.0162	883.3028	883.5025	883.2954
N.R.	491.1425	491.1425	491.1425	491.1425	491.1425	491.1425	491.1425	491.1425
B.E.	-0.9563	-1.0044	-1.0030	-1.0137	-1.0069	-1.0622	-1.0540	-1.16013
B.E. (kcal/mole)	-600.1	-630.3	-629.4	-636.1	-631.8	-666.5	-661.4	-728.0
ΔE	-	-30.2	-29.3	-36.0	-31.7	-66.4	-61.3	-127.9

TABLE 9

Total Energies (au) of 6-Aza-thiathiophthen

	A	B	C	D	E	F	G	H
T.E.	-1039.2279	-1039.2769	-1039.2750	-1039.2996	-1039.2739	-1039.3485	-1039.3216	-1039.4435
1-El.	-2418.8132	-2418.2841	-2418.3230	-2419.1717	-2419.3699	-2418.6618	-2418.8925	-2418.7287
2-El.	882.55467	881.9767	882.0175	882.8416	883.0655	882.2828	882.5404	882.2547
N.R.	497.0305	497.0305	497.0305	497.0305	497.0305	497.0305	497.0305	497.2547
B.E.	-1.0165	-1.0655	-1.0636	-1.0882	-1.0625	-1.1371	-1.1102	1.2321
B.E. (kcal/mole)	-637.9	-668.6	-667.4	-682.8	-666.7	-713.5	-696.6	-773.1
ΔE	-	-30.7	-29.5	-44.9	-28.8	-75.6	-58.7	-135.2

In order to minimise computing expense the geometry of the carbon, hydrogen framework and of the central sulphur is the same as in thiathiophthen; for the same reason this was extended to the terminal sulphur atom in (5) and (6). The oxygen and N-H groups are placed so that the S-O and S-N distances are as nearly as possible those found in the crystal structures.[31,29] The geometries of (6)-(8) are based on thiathiophthen although computation was actually carried out in the order (8), (6), (7), (1). Both the oxygen containing compounds have been isolated,[27,32] with the simplest aza derivative yet known in the N-phenyl.[33] The gaussian sets for oxygen were the same as for the pyrylium ion (scaled vinyl alcohol) while those for nitrogen were from scaled vinyl amine (as was the hydrogen attached to the nitrogen). These basis sets were augmented by a single d-function (of each d-type) on each of the sulphur atoms leading to calculations with sets of type A-H. In (7) there is only the central sulphur atom, with sets A, B, D & F the only ones valid.

The total energies of the molecules are shown in Tables 8-10. Using binding energies as a criterion the molecules can be seen to be almost as stable as thiathiophthen; indeed the aza-derivative is somewhat more stable (by ~37 kcal/mole) thus inferring that this molecule should be capable of being isolated. These tables reveal once again that d-orbitals play virtually no significant part in the ground-state bonding, with the energy improvement ranging from 28.8 to 44.9 kcal/mole, compared to approximately

TABLE 10

Total Energies of 1,6-Dioxo-thiathiophthen.

	sp	sp + 3s'	spd	spd + 3s'
T.E.	-736.8472	-736.8938	-736.8984	-736.9440
1-El.	-1829.7488	-1829.2788	-1830.1633	-1829.6969
2-El.	679.9638	679.4472	680.3271	679.8151
N.R.	412.9378	412.9378	412.9378	412.9378
B.E.	-0.88288	-0.92948	-0.93408	-0.97968
B.E. (kcal/mole)	-554.0	-583.2	-586.1	-614.7
D.E.	-	-29.2	-32.1	-60.7

30 kcal/mole for the 3s' function. The d-orbital populations of Table 11 support this view.

TABLE 11

d-Orbital Populations in Thiathiophthen Isosteres (spd Basis)

	(6), S6a	(6), S6	(7) S6a	(7), S6	(8) S6a
d_{xy}	0.006	0.006	0.009	0.005	0.008
d_{xz}	0.005	0.004	0.009	0.003	0.002
d_{yz}	0.013	0.016	0.015	0.016	0.012
$d_{x^2y^2}$	0.074	0.057	0.115	0.050	0.062
d_{z^2}	0.019	0.015	0.025	0.014	0.016

The dipole moment (Table 12) of 1,6-dioxothiathiophthen (7) has the negative end of the dipole moment towards the S/O end of the molecule. Addition of the 3s' function increases the dipole moment by a small movement of electrons towards the sulphur atom (Table 12); as usual p+d hybridisation moves the average position of the electrons away from

TABLE 12

Dipole Moments of Thiathiophthen Isosteres

	O,S,O	S,S,O			S,S,NH		
		μ_x	μ_y	μ	μ_x	μ_y	μ
A	3.22	-2.09,	3.78,	4.32	3.92,	1.59,	4.23
B	3.23	-2.10,	3.78,	4.32	3.81,	1.70,	4.12
C	-	-2.09,	3.77,	4.32	3.83,	1.69,	4.19
D	2.75	-1.97,	3.22,	3.78	3.65,	1.31,	3.88
E	-	-2.78,	3.11,	4.18	3.07,	1.03,	3.24
F	2.75	-1.98,	3.22,	3.78	3.65,	1.31,	3.88
G	-	-2.79,	3.11,	4.18	3.09,	1.02,	3.25
H	-	-2.65,	2.58,	3.70	2.95,	0.68,	3.02

TABLE 13

Atomic Populations in 1-Azathiathiophthen

	A	B	C	D	E
S1	16.1039	16.1095	16.0225	16.0907	16.1825
S6a	15.6786	15.6856	15.7722	15.7848	15.6747
N1	7.4502	7.4610	7.4630	7.4646	7.4665
C5	6.2185	6.2169	6.2093	6.2156	6.1224
C4	6.2028	6.2040	6.2045	6.2010	6.2054
C3a	6.0428	6.0349	6.0409	5.9514	6.0366
C3	6.2157	6.2160	6.2153	6.2190	6.2179
C2	6.0005	5.9962	5.9960	5.9917	5.9998
H5	0.8298	0.8301	0.8307	0.8312	0.8374
H4	0.8481	0.8483	0.8484	0.8498	0.8514
H3	0.8564	0.8564	0.8564	0.8589	0.8582
H2	0.8394	0.8394	0.8392	0.8395	0.8419
H(N)	0.7034	0.7016	0.7015	0.7015	0.7052

sulphur (although the population increases) and brings about a reduction in dipole moment. These effects are consistent with the change in one- and two-electron energies found in Table 10. The dipole moment of the mono-oxygen and aza-isosteres is somewhat more complex with there being two non-zero components. The component parallel to the C3a-S6a bond (μ_y in Table 12) is in the same direction as in thiathiophthen although it is considerably smaller in the case of the aza-compound. Such a change is likely to be caused by the highly polar N-H bond (see atomic populations of Table 13); this bond is polarised in the opposite direction to the dipole moment of thiathiophthen.

When the terminal S atom in thiathiophthen is replaced by O it would be expected to make the new non-zero component (μ_x) have its negative end towards the oxygen atom since oxygen is more electronegative than sulphur. With the positive dipole moment being defined in direction as below

the values in Table 12 show that this is indeed true. Replacement of S by N-H leads to the x-component of the dipole moment being of opposite sign compared to the oxygen derivative. The electronegativity of nitrogen is less than that of oxygen and this would be expected to lead to a smaller value of the x-component, but would be in the same direction. Of very great importance then must be the N-H

TABLE 14

Atomic Populations in 1-Oxothiathiophthen

	A	B	C	D	E
S6	15.9526	15.9524	15.9570	15.9412	16.0277
S6a	15.7276	15.7315	15.7281	15.8049	15.7253
O1	8.4855	8.4853	8.4858	8.5018	8.4898
C5	6.2236	6.2236	6.2159	6.2192	6.1278
C4	6.1758	6.1767	6.1774	6.1765	6.1789
C3a	6.0448	6.0390	6.0447	5.9532	6.0389
C3	6.2216	6.2267	6.2219	6.2322	6.2255
C2	5.8299	5.8298	5.8298	5.8246	5.8320
H5	0.8141	0.8142	0.8148	0.8163	0.8219
H4	0.8347	0.8347	0.8348	0.8371	0.8381
H3	0.8498	0.8499	0.8499	0.8524	0.8518
H2	0.8400	0.8401	0.8400	0.8404	0.8422

TABLE 15

Atomic Populations in 1,6-Dioxothiathiophthen

	sp	sp + 3s'	spd	spd + 3s'
S6a	15.4983	15.5008	15.5764	15.5795
O1, O6	8.5123	8.4732	8.5147	8.5149
C2, C5	5.8094	5.7513	5.8057	5.8056
C3, C4	6.2447	6.2271	6.2475	6.2487
C3a	6.0258	6.0180	5.9336	5.9277
H2, H5	0.8252	0.8259	0.8269	0.8270
H3, H4	0.8462	0.8480	0.8502	0.8502

moment, which was found to have a considerable effect on the y-component. Since the N-H moment is in the same direction as the x-component it must be the controlling factor in determining the direction. (It has already been shown that pyrrole and the other azoles have dipole moments largely controlled by an $\overset{\delta-}{N}-\overset{\delta+}{H}$ moment). Of the three isosteres the only experimental dipole moment available is that of the oxygen isostere,[26] the value being 3.78D. The minimal basis set figure is in reasonable agreement with this value, but it is obtained exactly when the d-functions are added to the centre (6a) atom. Similarly the best value obtained for thiathiophthen was obtained with the spd set on the centre sulphur. It is thus probable that experimental values for (6) and (7) will be best represented by the same basis set.

TABLE 16

Overlap Populations in Thiathiophthen Isosteres

	X=Y=O	X=O, Y=S	X=NH, Y=S
X1-C2	0.3747	0.3993	0.4655
C2-C3	0.5078	0.4603	0.5036
C3-C3a	0.5039	0.5436	0.5321
C3a-C4	0.5039	0.4633	0.4837
C4-C5	0.5078	0.5777	0.5674
C5-Y6	0.3747	0.3384	0.3562
Y6-S6a	0.0752	0.1731	0.0522
S6a-X1	0.0752	0.0077	0.0853
S6a-C3a	0.3498	0.3580	0.3819
X1-Y6	3×10^{-6}	0.0002	0.0018

The overlap populations for the minimal basis set calculations are shown in Table 16. Replacement of S in thiathiophthen by O has a marked effect on the populations with the S-S increasing by a factor of 3 for the same interatomic distance. On the other hand the S-O overlap is much smaller than that between the same atoms in thiathiophthen. This is consistent with the formation of a molecule of the following type (a).

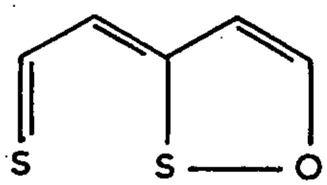

(a)

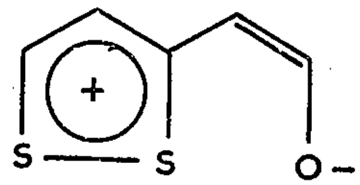

In support of this are the overlap populations between the carbon atoms, where the values indicate a greater tendency to single and double bonds than thiathiophthen did. The alternative zwitterion structure (above) since the C2-C3 overlap population is relatively small and is indeed the smallest recorded in thiathiophthen and the isosteres, where a high population would be expected. Delocalisation of the negative charge on the oxygen atom to the C3 atom would explain this low population, but in that case the total atomic population for the O-CH-CH part should be verging on 23.0; the value from Table 14 is only 22.23. However in support of the zwitterion structure the high C-S overlap populations, which are very similar to those of thiathiophthen. In that case there was no necessity to postulate a zwitterion structure; it is then unlikely that it would be required for the oxygen isostere. Indeed the bonding is very similar to thiathiophthen as the overlap populations of Table 16 show; the overlap population between the terminal atoms of the X-S-Y system is still small but indicative of some direct bonding.

In most aspects the bonding in the nitrogen isostere is very similar to that of thiathiophthen and the oxygen isostere; the single but very marked difference occurs in the S-N overlap population which is very much larger than that found in thiathiophthen. This would tend to make one think that the structure here would best be represented by 9a below; this would have to be amended to structure 9b to allow

(9a) (9b)

an aromatic π-system in the nitrogen-containing ring. The C-C overlap populations are however the opposite way round for either of structures 9a or 9b. This high S-N overlap is thus likely to be a function of the geometry around the nitrogen atom; the S-O bond is slightly longer than the S-N although in both cases the bond is actually somewhat longer than that found in crystal structures. (However the higher S-N populations, compared to S-O, is consistent with the existence of S,N compounds which have no analogous O,N compounds, e.g. tetraculphur tetranitride). Ignoring this geometric effect ultra-violet irradiation of the nitrogen isostere would give the transoid compound 10 below (the oxygen isostere is known to give 11 under ultra-violet treatment,[34] and the lower population bond in the S-S-O system is the S-O one).

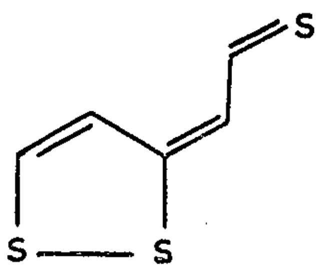

(10)

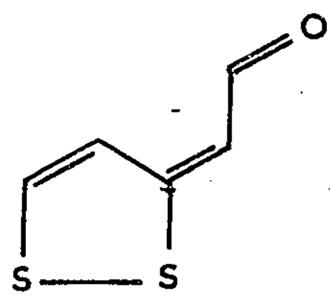

(11)

The S-O overlap populations in the di-oxygen isostere are also somewhat larger than the S-S were in thiathiophthen; thus assignment of the (almost) colinear structure to this compound rather than a transoid type, based on infra-red data,[32] is likely to be correct. The overlap population between the oxygen atoms is very small; replacement of the centre sulphur atom by an oxygen atom could be done without affecting any bond lengths in the carbon skeleton. It is possible then that the O-O-O compound could be isolated.

Replacement of the sulphur atom by an oxygen causes the population of the C2 carbon atom to be reduced by a considerable amount (~0.38e); the nitrogen atom makes for a decrease in the C2 population also but the effect is less than that of the oxygen atom. This is consistent with the different electronegativities of N, O and S atoms. In contrast the 6a sulphur atom is virtually unchanged in population on generating the oxygen isostere, with a lowering of 0.01e being found; in the di-oxygen compound the effect is much more marked, there being a drop of 0.23e. The nitrogen isostere also lowers the 6a population to a considerably greater extent than the electronegativity would predict; this is thus likely to be an effect of the close proximity of the nitrogen to the sulphur. The C3 atoms show the opposite trend to that of the C2 atoms with the magnitudes being considerably less; the remaining atoms are virtually unaffected in population.

TABLE 17

Core Orbital Energies of Thiathiophthen Isosteres (in eV)

		(8)	(6)	(7)
S 6a	1s	-2496.01	-2493.80	-2493.61
	2s	-240.88	-238.91	-238.64
	$2p_x$	-183.19	-181.21	-180.91
	$2p_y$	-183.16	-181.17	-180.91
	$2p_z$	-183.08	-181.10	-180.82
S 1	1s	-	-2491.98	-2488.94
	2s	-	-237.39	-234.64
	$2p_x$	-	-179.71	-176.95
	$2p_y$	-	-179.66	-176.90
	$2p_z$	-	-179.59	-176.85
X	1s	-559.75	-559.04	-422.30
C 2	1s	-311.44	-310.72	-309.61
C 3	1s	-307.31	-307.37	-306.86
C 3a	1s	-310.66	-310.05	-309.27
C 4	1s	-307.31	-308.48	-307.19
C 5	1s	-311.44	-309.64	-308.51

The core orbital energies of the 6a sulphur atom (Table 17) do reflect the electronegativities of the hetero-atom, which the populations did not. Thus the nitrogen containing molecule has the 6a sulphur atom core orbitals at higher binding energy than thiathiophthen itself, but somewhat lower than the value for the oxygen-containing molecule. The effect of two oxygen atoms is more than twice that of one. The C2 carbon increases in binding energy slightly in ionisation potential upon the introduction of NH for S; there is a very much greater shift when oxygen is introduced. Similar effects occur in the C3 binding energies but are reduced in magnitude compared to the C2 effects. The remaining carbon atoms are largely unaffected, showing that the effect of the hetero-atom diminishes with distance.

Experimental data is available[10] only for heavily substituted derivatives of the mono-oxygen analogue. The average value obtained for these is 531.1eV for the solid state spectra. This is quite different from the value found for furan (535.1eV),[35] also in the solid state. The calculated values for the molecules are 559.75eV and 561.55eV respectively; the error is some 30eV in evaluating the absolute values. The experimental differences are reasonably well reproduced. This is also true of the sulphur 2p levels where the average value for the 6a and 6 sulphur atoms is 163.7 and 164.5eV respectively. Again the absolute values are considerably in error but the experimental differences are fairly reasonably evaluated. No values for the carbon atoms are reported.

Table 18

Valency Shell Orbital Energies (Minimal Basis Sets)

S-S-S	O-S-O	S-S-O	S-S-NH
$\underline{A_1}$		$\underline{A'}$	
-33.66	-38.14	-37.41	-33.56
-28.94	-32.32	-33.37	-31.80
-28.16	-28.48	-30.48	-28.95
-22.87	-24.84	-28.27	-27.98
-21.15	-21.09	-27.68	-26.43
-20.21	-20.80	-23.93	-23.48
-15.59	-16.64	-23.42	-22.55
-14.04	-15.78	-21.14	-20.98
-8.49	-11.78	-20.54	-20.08
		-20.08	-19.49
$\underline{B_2}$		-17.42	-16.98
-31.67	-38.05	-16.51	-16.38
-26.32	-29.24	-15.51	-15.42
-23.40	-23.94	-15.02	-14.92
-19.90	-20.94	-13.46	-13.01
-17.23	-17.62	-11.08	-8.80
-15.79	-17.04		
-12.97	-13.54	$\underline{A''}$	
		-16.72	-16.07
$\underline{B_1}$		-15.01	-13.75
-16.63	-17.23	-12.56	-11.45
-12.05	-14.05	-11.80	-10.83
-11.23	-12.05	-9.01	-8.02
$\underline{A_2}$			
-14.03	-16.09		
-8.82	-9.16		

The nitrogen 1s value is predicted to be at higher binding energy than that for pyrrole.[35] This again is likely to be a geometrical effect, and is carried into the valency shell orbital energies (Table 18). The mono-oxygen analogue shows a lowering compared to thiathiophthen in the valency shell region; this is further emphasized upon generating the di-oxygen analogue. Both the C_{2v} isosteres have virtual orbitals of negative energy (-0.05eV and -1.51eV in thiathiophthen and its di-oxygen analogue). They should thus be readily reduced as the sulphur cationic heterocycles were.

References

1. F. Arndt, P. Nachtwes, J. Pusch, Chem. Ber., 1925, 58, 1633.

2. (a) S. Bezzi, M. Mammi, C. Garbuglio, Nature, 1958, 182, 247;
   (b) C. Garbuglio, M. Mammi, G. Traverso, Gazz. Chim. Ital., 1958, 88, 1226;
   (c) M. Mammi, R. Bardi, C. Garbuglio, Acta Cryst., 1960, 13, 1048.

3. A. Hordvik, K. Julshamn, Acta Chem. Scand., 1969, 23, 3611.

4. A. Hordvik, E. Sletten, J. Sletten, Acta Chem. Scand., (a) 1966, 20, 2001; (b) 1969, 23, 1852.

5. (a) A. Hordvik, L. Milje, Chem. Comm. 1972, 182;
   (b) A. Hordvik, Acta Chem. Scand., 1971, 25, 1583.

6. (a) L.K. Hansen, A. Hordvik, Acta Chem. Scand., 1970, 24, 2246;
   (b) L.K. Hansen, A. Hordvik, L.J. Saethre, Chem. Comm. 1972, 222.

7. A. Hordvik, Acta Chem. Scand., 1968, 22, 2397.

8. S.M. Johnson, M.G. Newton, I.C. Paul, R.J.S. Beer, D. Cartwright, Chem. Comm., 1967, 1170.

9. F. Leung, S.C. Nyburg, Chem. Comm., 1969, 137.

10. B.J. Lindberg, S. Hogberg, G. Malmston, J.-E. Bergmark, O. Nilsson, S.-E. Karlsson, A. Fahlman, U. Gelius, Chemica Sempta, 1971, 1, 183.

11. R. Gleiber, R. Hoffmann, Tet., 1968, 24, 5899.

12. D.T. Clark, D. Kilcast, Tet., 1971, 27, 4367.

13. N. Loezac'h Advances in Heterocyclic Chemistry, 1971, 13, 210.

14. K. Maeda, Bull. Soc. Chim Japan, (a) 1960, 33, 1466; (b) 1961, 34, 1166; (c) 1961, 34, 785.

15. R.A.W. Johnston, S.D. Ward. Theor. Chim. Acta, 1969, 42, 420.

16. A. Hordvik, L.J. Saethre, Acta Chem. Scand., 1970, 24, 2261.

17. R.J.S. Beer, D. Cartwright, R.J. Gast, R.A.W. Johnstone, S.D. Ward. Chem. Comm., 1968, 688.

18. R.J.S. Beer, D. Cartwright, D. Harris, Tet. Lett., 1967, 953.

19. J. Bignebat, H. Quinou, C.R. Acad. Sci., (a) 1969, 269, 1129; (b) 1968, 267, 180.

20. J.G. Dingwall, D.H. Reid, K. Wade, J. Chem. Soc. (C), 1969, 913.

21. R.J.S. Beer, R.P. Carr, D. Cartwright, D. Harris, R.A. Slater, J. Chem. Soc. (C), 1968, 2490.

22. E.M. Shustorovich. Zh. Obshch. Khim., 1959, 29, 2424.

23. G. Winnewisser, M. Winnewisser, W. Gordy, J. Chem. Phys., 1968, 49, 3645.

24. D.T. Clark, D.T. Kilcast, D.H. Reid. Chem. Comm., 1971, 638.

25. R. Gleiter, V. Hornung, B. Lindberg, S. Hogberg, N. Lozac'h, Chem. Phys. Lett., 1971, 11, 401.

26. M. Sanesi, G. Traverso, M. Lozzarone. Ann. Chim. (Rome), 1963, 53, 548.

27. D.H. Reid, R.G. Webster, J. Chem. Soc., Perkin II, 1972, 1447.

28. A. Hordvik, K. Julshamn, Acta Chem. Scand., 1972, 26, 343.

29. A. Grandin, J. Vialle, Bull. Soc. Chim. Fr., 1967, 1851.

30. A. Hordvik, T.S. Rimala, L.J. Saethre, 1972, 26, 2139.

31. A. Hordvik, E. Sletten, J. Sletten, 1969, 23, 1377.

32. D.H. Reid, R.G. Webster, J.C.S. Chem. Comm., 1972, 1283.

33. F. Leung, S.C. Nyburg, Can. J. Chem., 1972, 50, 324.

34. C.Th. Pedersen, C. Lohse, Chem. Comm., 1973, 123.

35. M.H. Palmer, A.J. Gaskell, M.S. Barber, Theoret Chim. Acta (Berl.), 1972, 26, 357.

SUGGESTIONS FOR FUTURE WORK

General Considerations and Extensions

The purpose of any theory is to make predictions. However before any validity can be attached to a theory it is necessary that it can predict, reasonably accurately, the data which is already known; for example, if the calculations predicted a value for the dipole moment of pyridine which was too large by a factor of 10, then considerable doubt would be cast on dipole moments obtained for pentazine.

The first predicted value obtained from a calculation is the total/binding energy of the molecule. For the calculations considered above, experimental data is somewhat sparse, being confined mainly to the azines and azoles. In all molecules the experimentally obtained value is considerably greater than that calculated; this is caused largely by the omission of correlation effects, with a minimal basis set adding to the discrepancy. However, linear relationships between calculated and experimental binding energies have been established (Sections II and III). One drawback of the lack of accuracy in predicting binding energies is to make it difficult to postulate the existence of molecules such as hexazine.

As far as the azines are concerned there would appear to be some hope of a correlation between diamagnetic susceptibility anisotropy and the binding energy. Plotting one against the other leads to a reasonable straight line; a line, almost parallel, exists for the azoles. Attempts have been made to relate the diamagnetic susceptibility anisotropy to the aromaticity have been made; this appears to be reasonable within an iso-electronic series. It should be pointed out that the existence of such an anisotropy does not necessarily infer aromaticity, but merely states that there is a considerable difference between the out-of-plane and in-plane components. In order to test this calculations could be carried out on Kekulé structures for the azines and benzene; it is possible that the anisotropy would not be very different from what is found for the experimental geometries.

Such calculations would also test the concept of using the overlap populations as a guide to kinetic reactivity, as was done in the Section on the azines. The overlap population have been used as a guide to the activation energy, ΔE_1, for the following decomposition scheme.

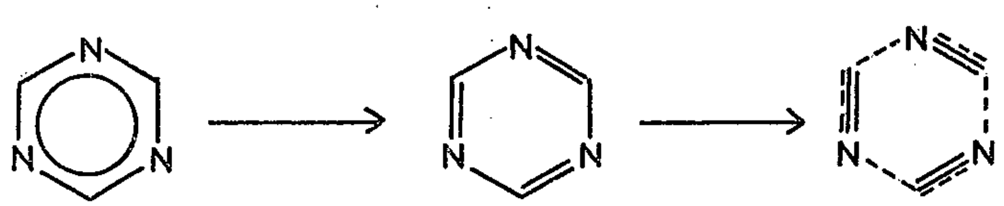

Obviously calculations on the Kekulé isomer would lead to a value for ΔE_1, which ought to show the trends predicted by overlap populations.

Turning now to eigenvalues, it has been shown that the experimental ionisation potentials are well predicted by using Koopmans' theorem, for all molecules for which experimental evidence is available. Scaled functions predict the numerical values somewhat better than best-atom functions although the improvement in least squares plotting is not very great. In the case of the azines there have been disagreements[1,2] in assignments of the peaks using semi-empirical procedures; the LCGO calculations of Section III have favoured the assignments made by Lindholm.[1]

The orbital energies of virtual orbitals have been used for comparison with the half-wave reduction potentials obtained experimentally[3] for the dithiolium cations. The results were fair and could probably be improved upon by calculations on the radical generated by the addition of an electron to the cations. Such extensions are attractive since they involve the use of pre-computed integrals, thus obtaining more efficient use of computer time. Electrochemical reduction has been carried out on the azines;[4] calculations on the radical anion would be simple to perform. Thiathiophthen and its di-oxygen isostere were both predicted to have negative energy virtual orbitals and are thus likely to be electrochemically reduced. Indeed the di-anion of thiathiophthen would be worthy of investigation since it is one precursor of the thiathiophthen system.[5] It also should be noted that excited states are formed by addition of electron(s) to ground state molecules,; so that for the sulphur containing compounds the extent of d-orbital participation could be quite marked.

Inversion barriers have been found, for phosphine and the 7-norbornadienyl cation, to be in reasonable agreement with experimental values; it is likely then that those for phosphole and thiophene-S-oxide should also be fairly accurate. 7-Hetero derivatives of the norbornadiene system are known, but which seem to be much less stable than norbornadiene itself. Decomposition to an acetylene + a five-membered heterocycle or to benzene + an atom both seem to occur. It is possible that the overlap populations of the relative bonds could be used to explain such decompositions. In the case of the phosphorus heterocycles the addition of one or more oxygen atoms to the phosphorus would give indications of the stability of phosphorin and phosphole with respect to oxidation.

Some generalisations can be made about the one-electron properties which have been evaluated:- 1) dipole moments are in fair agreement with experiment; 2) the electronic part of the second moment and diamagnetic susceptibility tensors agree with such experimental evidence as is available; 3) potential at a nucleus agrees well with calculations using a double-zeta basis set; 4) quadrupole moments are disappointingly poor compared both to experimental and calculated (double-zeta) values; 5) electric field gradient of sulphur in thiophene is somewhat between the accuracy of dipole and quadrupole moments.

d-Orbital participation has involved a considerable amount of this thesis. The results can be summarised as follows:- For molecules containing sulphur of valency 3(thiophene and the cationic sulphur compounds) or 4(thiathiophthen and itsisosteres) d-orbital participation is negligible, while it is very important for valencies higher than 4(the thiophene-S-oxides).

Indications have already been given where future work, consisting mainly of adding atoms to or altering atoms in molecules already studied, could be profitable. Further work involving molecular systems with no exact structural precursor is possible. Thus there is the transoid structure for the thiathiophthen series of molecules (molecule of Section VIII) and loosely bonded intermediates in the ozonolysis study e.g.

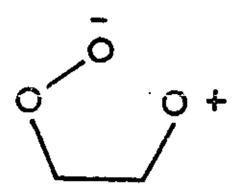

References

1. Azines, Reference 5.
2. Azines, References 6 - 8.
3. Cationic Heterocycles, Reference 26.
4. K.B. Wiberg, T.P. Lewis, J.A.C.S., 1970, 92, 7154.
5. Thiathiophthen, Reference 13.

CHAPTER THREE : Appendices

Appendix 1. Gaussian Basis Sets

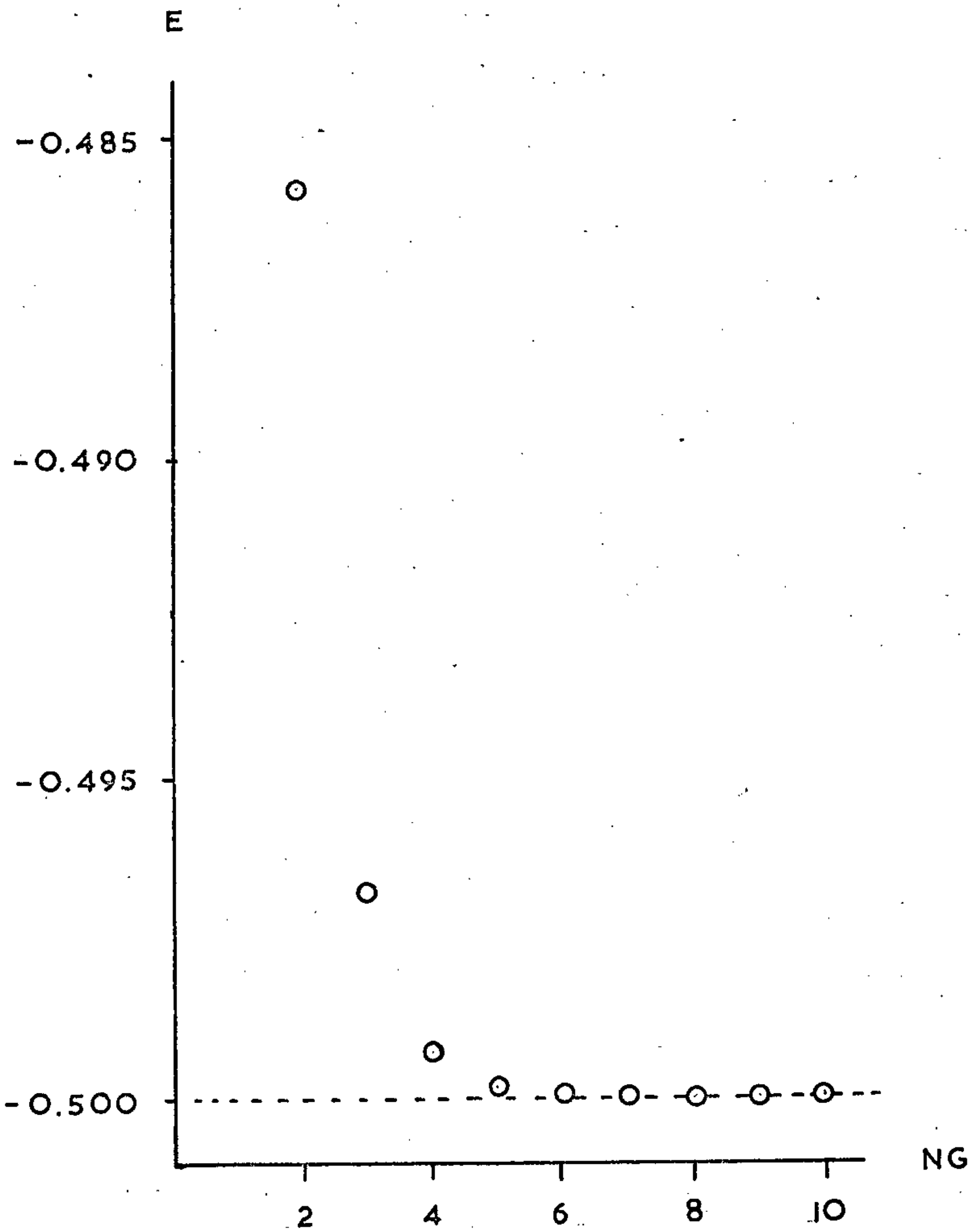

Figure 1. Total Energy (E) in au as a function of the Number of Gaussians (NG), for the Hydrogen Atom. The Hartree-Fock limit is -0.500 au.

Length of Basis Set and its Effect on Energy

The Gaussian basis sets used in calculations in molecules are obtained by optimising the exponents[1] using total energy of the particular atom as the criterion for optimal values. Many such sets have been reported in the literature (for example, references 2-5); the results of several sets for hydrogen and oxygen appear in Tables 1 and 2 respectively.

TABLE 1

Gaussian Sets for the Hydrogen Atom

Exponents	Total Energy	Exponents	Total Energy
0.201558	-0.485812	0.089859	-0.499946
1.332795		0.258165	
		0.798266	
0.151398	-0.496779	2.825682	
0.618444		12.418535	
4.50180		82.702833	
0.121964	-0.499278	0.080106	-0.499982
0.444647		0.212882	
1.962998		0.594110	
13.017085		1.324635	
		6.444576	
0.103062	-0.499810	28.311350	
0.327109		188.750157	
1.164076			
5.121509			
34.052079			

From these it can be seen the energy improves as the number of Gaussian functions increases. This is shown in diagrammatic form in Figure 1 for the hydrogen atom. It is clear from this figure that there is a limiting value of the energy,

TABLE 2

Gaussian Basis Sets for the Oxygen Atom

s-Exponents	p-Exponents	Total Energy
0.579735	0.547380	-73.975183
9.286970	3.175230	
43.120125		
286.817626		
0.321531	0.374857	-74.701079
1.070653	1.684713	
6.820784	8.142162	
22.124572		
79.622313		
350.751980		
2332.28070		
0.194145	0.152579	-74.808962
0.505047	0.429693	
1.285748	1.151066	
3.327341	3.045327	
7.624367	8.538137	
17.798687	27.578776	
43.743538	117.848357	
114.489178		
323.694699		
1011.142331		
3618.128040		
16238.09415		
109245.43772		

where additional Gaussian functions do not significantly improve the energy. This limiting value of the energy is known as the Hartree-Fock limit and is the value obtained with an infinite series of Gaussians; the Hartree-Fock limits for hydrogen and oxygen are -0.5000 au and -74.80939 au respectively.

The basis sets of Tables 1 and 2 have been used in calculations on the water molecule.[6] The total energy obtained for several combinations of these hydrogen and oxygen sets is shown in Table 3 (where an as, bp set is defined as consisting of a s-type functions with b p-type functions in each of the three cartesian directions). The Hartree-Fock limit for water has been estimated[6] as being -76.026 au. Thus if an accuracy of 0.001 au is required then a 13s,7p/6s set (for O/H) would be a good choice. If the accuracy required was 0.01 au then a 9s,5p/5s set, giving a total energy of -76.01467 au would be adequate. Thus the accuracy obtainable for a molecular calculation is virtually the same as that for an atomic calculation.

TABLE 3

Calculations on the Water Molecule, with Various Basis Sets

Oxygen Functions	Hydrogen Functions	Total	Total No. of Functions	No. of 2-El Integrals
4s,2p	2s	-75.15053	14	5,565
"	3s	-75.17413	16	9,316
	4s	-75.17890	18	14,706
7s,3p	2s	-75.86667	20	22,155
	3s	-75.88745	22	32,131
	4s	-75.89138	24	45,150
13s,7p	5s	-76.02418	44	490,545
	6s	-76.02492	46	584,821
	7s	-76.02573	48	692,076

As well as giving a good total energy the basis sets chosen must be balanced, both physically and formally. A physically balanced (molecular) basis set gives reasonable estimates of molecular properties such as dipole moment. Formal balance is more difficult to achieve since the criterion used to estimate this is that the charges on the atoms should be reasonable. The difficulty arises in defining reasonable atomic charges; however both formal and physical balance can be achieved by using atomic basis sets of similar accuracy[6] i.e. a poor H with a poor O or a good H with a good O but never a poor H with a good O.

Reducing the Size of a Basis Set

The accuracy in energy obtained in molecular calculations is only achieved at some expense. Table 3 also shows the number of electron-repulsion integrals which have to be calculated and stored. Thus the 13s, 7p/7s set, yielding the best energy, requires 692,076 integral evaluations, and this for a molecule of no real chemical interest. Taking benzene as a typically-sized molecule, a 13s,7p/7s set (for C/H) calculation would consist of 266 functions and require the evaluation of 6.3×10^8 integrals. This would require the total storage capacity of some 150 magnetic tapes. The time to read a full magnetic tape is 1-2 minutes;[6] thus something between 2½-5 hours would be spent taking the data into core without carrying out any processing. It is thus obvious that some form of compromise between accuracy and computer resources. This compromise is achieved by gathering the exponents into groups and is exemplified in Table 4 for a

TABLE 4

Carbon Basis Set

a) Exponents (α_i)

s	p
1412.29	4.18286
206.885	0.851563
45.8498	0.199206
12.3887	
3.72337	
0.524194	
0.163484	

b) Orbital Energies and Eigenvectors

1s -11.3227	2s -0.70230	2p -0.42171
0.004813	-0.001020	0.112194
0.037267	-0.008141	0.466227
0.172403	-0.038437	0.622569
0.459261	-0.126098	
0.456185	-0.190474	
0.034215	0.522342	
-0.009977	0.594186	

c) Total Energy = -37.656 au

d) $1s = 0.004813 \exp(-\alpha_1 r^2) + 0.037267 \exp(-\alpha_2 r^2) + 0.172403 \exp(-\alpha_3 r^2) + 0.459261 \exp(-\alpha_4 r^2) + 0.456185 \exp(-\alpha_5 r^2)$

$2s = 0.522342 \exp(-\alpha_6 r^2) + 0.594186 \exp(-\alpha_7 r^2)$

$2p_x = 0.112194\, x \exp(-\alpha_8 r^2) + 0.466227\, x \exp(-\alpha_9 r^2) + 0.622569\, x \exp(-\alpha_{10} r^2)$

7s,3p carbon set. This grouping or contraction procedure is often carried out by examination of the eigenvectors for the ungrouped calculation (Table 4b). The eigenvectors usually show a significant drop in magnitude (and often a change in sign) such that the exponents are "naturally" grouped; these groupings are indicated in Table 4 by dashed lines. Thus the 1s orbital of carbon is represented by the series of Gaussians in Table 4d; the 2s and 2p are similarly shown. This is then a minimal basis set, i.e. one contracted function for each atomic orbital; it is known as a "Best Atom" minimal basis set.

For the carbon atom in Table 4 the original sixteen variational parameters have been reduced to five; there is thus a deterioration in energy of the contracted set compared to the uncontracted set. This deterioration gets worse as the number of electrons increases (Table 5) but can, to a

TABLE 5

Effect of Contraction on Total Energy (au)

Atom	Uncontracted Basis	T.E. (uncont)	T.E. (cont)	ΔE
B	7s, 3p	-24.514	-24.48317	0.03083
C	"	-37.656	-37.61049	0.04551
N	"	-54.339	-54.27539	0.06361
O	"	-74.700	-74.61214	0.08786
F	"	-99.234	-99.12376	0.11024
Si	10s, 6p	-288.773	-288.28413	0.48887
P	"	-340.630	-340.06278	0.56722
S	"	-397.400	-396.69879	0.70121

certain extent, be offset by contracting to what is known as a "double-zeta" basis set, where each atomic orbital is represented by two contracted functions. Contraction of the carbon basis set of Table 4 to a double-zeta basis set has been reported[7] and is given in Table 6. For the transition metals contraction to a minimal basis results in a loss of energy of some 3.3 au compared to the uncontracted functions;[8] the double-zeta calculation is 3.1 au. better than the minimal basis set. It would therefore appear that double-zeta will be necessary for any calculations involving third-row atoms.

TABLE 6

Double-zeta Basis Set for Carbon

1s(A)	$0.004813 \exp(-\alpha_1 r^2) + 0.037267 \exp(-\alpha_2 r^2) +$ $0.172403 \exp(-\alpha_3 r^2) + 0.459261 \exp(-\alpha_4 r^2)$
1s(B)	$1.0 \exp(-\alpha_5 r^2)$
2s(A)	$1.0 \exp(-\alpha_6 r^2)$
2s(B)	$1.0 \exp(-\alpha_7 r^2)$
2p(A)	$0.112194 \exp(-\alpha_8 r^2) + 0.466227 \exp(-\alpha_9 r^2)$
2p(B)	$1.0 \exp(-\alpha_{10} r^2)$

The deterioration found for atoms upon making use of the contraction procedure is also evident in molecules. For example an uncontracted calculation on oxygen difluoride using a 7s, 3p set on all atoms yielded a total energy of -270.07863 au, with the minimal basis set (using the same contraction method as in Table 4) resulting in a value 0.30639 au worse (i.e. -270.77224 au).

The Gaussian exponents used for the calculations in this thesis were those of Roos and Siegbahn for non-hydrogen[3] atoms; the hydrogen set was that of Huzinaga[2a]. These were chosen for several reasons:- 1) it is similar to those used in several reported calculations; 2) it was possible to compare with results obtained by other workers in this group; 3) it gave a reasonable compromise between computational speed and accuracy. Contraction was to a minimal basis set, the choice being forced since computing facilities were originally very restricted. This was mainly due to the program requiring such large core storage that on the 360/50 it was necessary to run outwith HASP. Running could only take place under special arrangement at weekends. Further the program was not suitable for running remotely (on machines with large core storage) since it required direct intervention by the computer operators. This situation remained until the operator intervention routines were coded out (with, at the same time, the introduction of some automatic safety measures). However the results would seem to indicate that basis set and contraction procedure were reasonably good.

Improvement of Minimal Basis Set Calculations

There are three main methods for improving the representation of electronic structure as determined by minimal basis sets. These are:- 1) determine new contraction coefficients; 2) add polarisation functions; 3) use the concept of molecular scaling factors.

The first method does not appear to have been much used. Method 2) has a two-fold effect on the electronic structure. The first of these is to increase the variational flexibility of the calculation by introducing additional parameters. The second is to concentrate the electrons in the bonding regions of the molecule. Such polarisation functions have been used by several groups of workers, some results of which are shown in Table 7.

TABLE 7

Effect of Polarisation Functions on Total Energy

Molecule	Polarisation Functions		Improvement in Energy
Thiophene	Hydrogen	2p	-0.023(au)
Pyrrole	"	2p	-0.01470
Furan	"	2p	-0.09433
1,2,5-Oxadizaole	"	2p	-0.05540
"	" C, N, O	2p + 3d	-0.12864

As can be seen the energy does improve quite considerably but there is one drawback to these calculations. Namely, the time taken to evaluate integrals over p and d functions is greater than over s functions only. Further the number of integrals to be evaluated and stored is increasing, thus regenerating the problem which the introduction of contracted functions was designed to alleviate.

Method 3) involves the (mental) decomposition of a chemically interesting molecule into a subset of small model molecules. The exponents of the atoms in the small molecules are then optimised, against energy, to obtain new exponents.

Scaling, and the Determination of Scale Factors

It is inherent in the existence of molecules that they are different from atoms and there is no reason therefore why a "Best Atom" set should not be modified slightly to take more account of the chemical environment in which the atom exists. This procedure, known as scaling, has been suggested by several authors,[9-11] and involves replacing equation (1) by equation (2)

$$\Psi = \sum_i C_i \exp(-\alpha_i r^2) \qquad (1)$$

$$\Psi = \sum_i C_i \exp(-\alpha_i k r^2) \qquad (2)$$

where k is known as the scale factor. It has been suggested[10] that the scale factor should be an average for each atom; this, however, would only be a molecular correction factor to the "Best Atom" set, and not an environmental correction.

Taking the norbornadiene system as an example there are two environments for carbon and hydrogen. These are the saturated (C1, C4 and C7) and the olefinic (C2, C3, C5, C6) regions, with a hydrogen atom being of the same environment as the carbon to which it is bonded. The ideal way to improve the energy by scaling would be to optimise the k values in norbornadiene itself. Such an undertaking would be far too wasteful of computer time, so that model systems are optimised and thence transferred to the larger system (the assumption of transferability is likely to be largely valid since the model systems are chosen from the larger system). For the saturated and olefinic regions the models chosen were methane and ethylene, these being the smallest molecules available of the correct type.

In each of these model systems the Gaussian sets which were scaled were those representing carbon 2s, carbon 2p and hydrogen 1s orbitals. Scaling of the carbon 1s functions was omitted on the grounds that it is unlikely to be very much affected by a change in environment since it is such a highly localised orbital.

The scale factor k for any given orbital is obtained by carrying out three calculations with various k values and determining the k value which minimises E in $E = ak^2 + kb + c$, i.e., a parabolic minimisation procedure. If by chance the k values predicted the optimal value to be outside the k range used, further calculations were done until three k values were found which produce an interpolated optimal value, rather than an extrapolated one. The results for such a procedure for methane are presented in Tables 8 (k values and SCF energies) and 9 (parabolic interpolation of Table 8).

Scaling for methane was begun by assuming that k for the carbon 2s and 2p orbitals was the same as in ethylene. Runs 1, 2 and 3 provided the data for the parabolic minimisation of E versus k(H) giving the optimal k(H) value. The values for k(2s) and k(2p) were obtained in a similar manner. The scale factor for hydrogen was then re-optimised and was found not to be substantially different from the first value found; thus scaling was found to be optimal at that

TABLE 8

Scale Factors and SCF Energies for Methane

Run	k_H	k_{2s}	k_{2p}	E
1	1.40	1.1088	1.1354	-40.093761
2	1.60	"	"	-40.102461
3	1.80	"	"	-40.098166
4	1.6339	"	"	-40.102539
5	1.6339	"	1.00	-40.098810
6	1.6339	"	1.30	-40.089370
7	1.6339	"	1.11959	-40.102786
8	1.6339	1.00	1.11959	-40.102403
9	1.6339	1.20	1.11959	-40.099914
10	1.6339	1.06445	1.11959	-40.103213
11	1.40	1.06445	1.11959	-40.095035
12	1.800	1.06445	1.11959	-40.099538
13	1.63945	1.06445	1.11959	-40.103249
Unscaled	1.0	1.0	1.0	-39.985839

stage. In Table 9 where the equations of the various parabolas were shown, the coefficient of a is always positive. This indicates that the turning point obtained is a minimum (a positive second derivative at a turning point indicates a minimum; in the case of the parabola this second derivative = 2a, so that it is the sign of a which shows the nature of the turning point).

TABLE 9

Parabolic Interpolation of Methane Scaling Factors

Runs used	k_{min}	Function	a	b	c
1,2,3	1.6339	H 1s	0.16244	-0.53081	-39.66900
4,5,6	1.11959	C 2p	0.40773	-0.91297	-39.59157
7,8,9	1.06445	C 2s	0.17506	-0.37268	-39.90478
10,11,12	1.63945	H 1s	0.14274	-0.46802	-39.71968

TABLE 10

Effect of Scaling on Methane Energies

	$(1f_2)^3$	$2a_1$	$1a_1$	Total Energy
Unscaled	-16.33	-27.00	-309.60	-39.98584
Scaled	-14.85	-25.33	-305.09	-40.10325
Scaled uncontracted	-14.52	-25.59	-305.02	-40.14162
Photo-electron	13.5-14.5	23.0	275.7	-

TABLE 11

Effect of Scaling on Ethylene Energies

	$1b_{1u}$	$1b_{1g}$	3ag	$1b_{2u}$	$2b_{3u}$	2ag	$1v_{3u}$	lag	Total Energy
Unscaled	-12.66	-14.96	-17.50	-18.81	-22.58	-29.79	-310.58	-310.59	-77.6893
Scaled	-10.64	-13.57	-15.77	-17.49	-21.14	-27.84	-305.8	-305.82	-77.8314
Photo-electron	10.51	+12.38	14.4	15.6	-18.8	-	-279.6	-279.6	-

Tables 10 and 11 show how scaling affects the orbital and total energies for methane and ethylene respectively. In both cases the total energy is more negative, the improvement in methane being 73.7 kcal/mole and in ethylene 89.2 kcal/mole. Since norbornadiene has two olefinic and three saturated regions we would expect an energy improvement of approximately 400 kcal/mole on introduction of the scaled orbitals, although it will probably be somewhat less due to the lack of hydrogen atoms in norbornadiene.

All the scale factors are greater than unity, i.e., the orbitals are more diffuse. Ionisation will thus be easier since the electron-nuclear attraction will be less; this in turn will lower the ionisation potentials of ethylene and methane bringing them into better agreement with the experimental values,[12-15] Koopman's theorem being assumed.

These more diffuse orbitals will mean that both the electron-electron repulsion energy and electron-nuclear attraction will increase in magnitude, since in the former case the electrons on different centres will approach one another more closely while in the latter the electrons will approach adjacent nuclei more. This has two important consequences:- a) the two factors which change oppose one another and will thus pass through a minimum b) scaling of this nature is a molecular property since it depends on the existence of more than one atomic centre.

Although the carbon 1s orbitals were not scaled there is a significant change in the core ionisation potentials. These move to lower ionisation potential and indicate how the valence shell electrons can effect the core orbitals.

References

1. P.S. Bagus, C.C.J. Roothaan, Methods in Computational Physics, 1963, 2, 47.

2. a. S. Huzinaga, J. Chem. Phys., 1965, 42, 1293
   b. S. Huzinaga, C. Arnau, J. Chem. Phys., 1970, 52, 2224.

3. B. Roos, P. Siegbahn, Theor. Chim. Acta (Berl.), 1970, 17, 209.

4. T.H. Dunning, J. Chem. Phys., 1971, 55, 716.

5. C. Salez, A. Veillard, Theor. Chim. Acta (Berl.), 1968, 11, 441.

6. E. Clementi, J.W. Mehl, "IBMOL-5, Quantum Mechanical Concepts and Algorithms," IBM Research, 1971.

7. B. Roos, P. Siegbahn, Theor. Chim. Acta (Berl.), 1972, 27, 171.

8. B. Roos, A. Veillard, G. Vinat, Theor. Chim. Acta (Berl.), 1971, 20, 1.

9. R. Ditchfield, W.J. Mehre, J.A. Pople, J. Chem. Phys., 1971, 54, 724.

10. M. Klessinger, Theor. Chim. Acta (Berl.), 1969, 15, 353.

11. W.J. Mehre and J.A. Pople, J.A.C.S., 1971, 93, 289.

12. K. Mamrin, G. Johansson, U. Gelius, A. Fahlman, C. Nordling and K. Siegbahn, Chem. Phys. Letters, 1968, 1, 613 (Valence shell region of methane).

13. R.B. Turner, P. Goebel, B.J. Mallion, W.E. von Doering, J.F. Coburn and M. Pomerantz, J.A.C.S., 1968, 90, 4315 (Soft x-ray emission spectrum of methane)

14. A.D. Baker, C. Baker, C.R. Brundle and D.W. Turner, Int. J. Mass Spectrum. Ion Phys., 1968, 1, 285 (Valence shell region of ethylene)

15. R.A. Mattsen and R.C. Ehlert, J. Chem. Phys., 1968, 48, 5465 and 5471 (Soft x-ray emission spectrum of acetylene, ethylene and methane).

Appendix 2. Tables of Gaussian Basis Sets

The Gaussian basis sets used in the calculations discussed in Part Two are listed in this Appendix. They are arranged in two main groups; Tables 1-7 are the standard sets taken from Roos and Siegbahn's "best atom" calculations;[1] Tables 8-17 consist of scaled basis sets in the order in which they are presented in Part Two. Here only the valency shell exponents are listed since they are the only ones scaled. Atom Energies, and appropriate cationic energies are included in Tables 1-7.

Reference

1. B. Roos, P. Siegbahn, "Proceedings of the Seminar on Computational Problems in Quantum Chemistry", Strausburg, 1969.

TABLE 1

Hydrogen Basis Set (Standard)

Exponent	Contraction Coefficient	Type
4.50037	0.07048	
0.681277	0.407890	1s
0.151374	0.647670	

Total Energy = -0.4972 au.

TABLE 2

Carbon Basis Set (Standard)

Exponent	Contraction Coefficient	Type
1412.29	0.004869	
206.885	0.037702	1s
45.8498	0.17442	
12.3887	0.464630	
3.72337	0.461510	
0.524194	0.49450	2s
0.163484	0.56308	
4.18286	0.112194	
0.851563	0.466227	2p
0.199206	0.622569	

^{3}P state Total Energy = −37.61049 au

Orbital Energies = 1s −11.25443 au

2s −0.67695 au

2p −0.41311 au

Total Energy of C^+ = −37.21385

TABLE 3

Nitrogen Basis Set (Standard)

Exponent	Contraction Coefficient	Type
2038.41	0.004479	
301.689	0.034581	
66.4630	0.164263	1s
17.8081	0.453898	
5.30452	0.468979	
0.764993	0.513598	2s
0.234424	0.605721	
5.95461	0.119664	
1.23293	0.474629	2p
0.286752	0.611142	

^4S state	Total Energy	-54.27539 au
	Orbital Energies	1s -15.54489 au
		2s -0.90623 au
		2p -0.53851 au

Total Energy of N^+ = -53.73691

TABLE 4

Oxygen Basis Set (Standard)

Exponent	Contraction Coefficient	Type
2714.89	0.004324	
415.725	0.032265	
91.9805	0.156410	1s
24.4515	0.447813	
7.22296	0.481602	
1.06314	0.504708	2s
0.322679	0.616743	
7.75579	0.129373	
1.62336	0.481269	2p
0.365030	0.604484	

^3P state	Total Energy	-74.61214	
	Orbital Energies	1s	-20.56811
		2s	-1.19083
		2p	-0.58974

Total Energy of O^+ -74.12498.

TABLE 5

Silicon Standard Set

Exponent	Contraction Coefficient	Type
19237.2	0.001570	
2885.41	0.012066	
655.111	0.059960	1s
184.413	0.210054	
59.2516	0.449954	
20.4626	0.387533	
4.41116	0.450911	2s
1.61479	0.654968	
0.29139	0.247058	
0.140147	0.86997	3s
95.7865	0.027944	
21.9200	0.168160	2p
6.43988	0.458069	
1.98998	0.499275	
0.48293	0.289739	3p
0.122840	0.823106	
0.353329	1.0	3d

^3P state Total Energy = -288.28413

Orbital Energies 1s -68.24054
2s -5.81689
2p -4.03580
3s -0.48903
3p -0.27463

TABLE 6

Phosphorus Basis Set (Standard)

Exponent	Contraction Coefficient	Type
22566.5	0.001531	
3380.80	0.011793	
766.417	0.058861	1s
214.964	0.208183	
68.9703	0.447369	
23.9195	0.390968	
5.26929	0.441137	2s
1.96297	0.667165	
0.350435	0.557322	3s
0.131021	0.609385	
109.959	0.028840	2p
25.1292	0.175866	
7.51127	0.461765	
2.39583	0.490526	
0.531089	0.391025	3p
0.150160	0.729140	
0.370806	1.0	3d

^4S state Total Energy -340.06278

Orbital Energies

1s	-79.42371
2s	-7.1634
3s	-0.6414
2p	-5.2017
3p	-0.3738

TABLE 7

Sulphur Basis Set (Standard)

Exponent	Contraction Coefficient	Type
25506.3	0.001546	
3812.82	0.011973	
860.556	0.059943	1s
242.940	0.207528	
79.0448	0.442977	
27.5705	0.392193	
6.49476	0.406937	2s
2.41078	0.700363	
0.469815	0.524282	3s
0.173396	0.655507	
129.088	0.028414	2p
29.6305	0.175840	
8.84715	0.467398	
2.85576	0.485545	
0.626108	0.450422	3p
0.175233	0.678482	
0.541000	1.0	3d

^3P State Total Energy -396.69879

Orbital Energies	1s	-91.43454
	2s	-8.61435
	2p	-6.48566
	3s	-0.81116
	3p	-0.37654

Total Energy at S^+ -396.34922

TABLE 8

Carbon, Scaled-Ethylene Basis Set

Exponent	Contraction Coefficient	Type	Scale Factor
0.581226	0.522342	2s	1.1088
0.181271	0.594186		
4.74919	0.112194	2p	1.1354
0.966859	0.466227		
0.226177	0.622569		

TABLE 9

Hydrogen, Scaled-Ethylene Basis Set

Exponent	Contraction Coefficient	Type	Scale Factor
6.99357	0.07048	1s	1.5540
1.05870	0.40789		
0.235235	0.64767		

TABLE 10

Hydrogen, Scaled-Methane Basis Set

Exponent	Contraction Coefficient	Type	Scale Factor
7.37812	0.07048	1s	1.6395
1.11692	0.40789		
0.24817	0.64767		

TABLE 11

Carbon Scaled-Methane Set

Exponent	Contraction Coefficient	Type	Scale Factor
0.557981	0.522342	2s	1.0645
0.174021	0.594186		
4.68331	0.112194	2p	1.1914
0.953399	0.466227		
0.223029	0.622569		

TABLE 12

Oxygen, Scaled-Vinyl-Alcohol Set

Exponent	Contraction Coefficient	Type	Scale Factor
0.967457	0.504708	2s	0.9100
0.293638	0.616734		
7.57741	0.129373	2p	0.9770
1.58602	0.481269		
0.356634	0.604484		

TABLE 13

Sulphur, Scaled Thio-Formaldehyde Basis Set

Exponent	Contraction Coefficient	Type	Scale Factor
0.412644	0.463545	3s	0.8783
0.152296	0.579568		
0.650366	0.441037	3p	1.0387
0.182022	0.664344		

TABLE 14

Phosphorus, Scaled $H_2C = P^{-H}$ Basis Set

Exponent	Contraction Coefficient	Type	Scale Factor
0.330206	0.557322	3s	0.9423
0.123458	0.609385		
0.583141	0.391025	3p	1.0980
0.168477	0.729140		

TABLE 15

Hydrogen, Scaled $H_2C = P^{-H}$ Basis Set (Hp)

Exponent	Contraction Coefficient	Type	Scale Factor
6.63118	0.07048	1s	1.4735
1.00384	0.40789		
0.223046	0.64767		

TABLE 16

Nitrogen, Scaled Vinyl Amine

Exponent	Contraction Coefficient	Type	Scale Factor
0.719093	0.513598	2s	0.9400
0.220359	0.605721		
6.25234	0.119664	2p	1.0500
1.29458	0.474629		
0.31009	0.611142		

TABLE 17

Hydrogen, Scaled Vinyl Amine (H_N)

Exponent	Contraction Coefficient	Type	Scale Factor
8.38779	0.07048	1s	1.8638
1.26976	0.40789		
0.282131	0.64767		

Appendix 3. Geometric Parameters and Symmetry Orbitals

This Appendix contains the molecular geometries and symmetry orbitals of the molecules whose electronic structure has been investigated. As in the text standard chemical nomenclature is used with some additional conventions:- the hydrogen atoms attached to a particular centre take as their numerical subscript the chemical number of the atom to which they are bonded. Where this is not unique the additional superscripts prime and asterisk are used for distinction.

The vast majority of the molecules are planar with the molecular plane being assumed to be the x-y plane; this results in those molecules which have the molecular plane as the only element of symmetry having s, p_x, p_y functions in the A' (or sigma) representation and p_z functions in the A" (pi) representation. Symmetry orbitals for such molecules are not recorded but are indicated by "Molecular Plane Only." The planar C_{2v} molecules fall into two classes (a) the C_2 axis passes through an atom (b) the C_2 axis passes through bonds only. These are indicated by "C_{2v}(Type A)" and "C_{2v} (Type B)" respectively and their symmetry orbitals will be recorded once only. Tables are arranged in the following manner:-

(a) Molecule name and point group

(b) Drawing of molecule and centre nomenclature; unique bond lengths and angles

(c) Symmetry Orbitals (detailed, or referenced to a standard set)

(d) Occupation number of each molecular representation.

Finally, "X" implies "p_x", "XX" implies "d_{x^2}" etc., and in C_{2v} planar molecules A_1 and B_2 are sigma in nature, leaving B_1 and A_2 as pi.

Ozone (C_{2v})

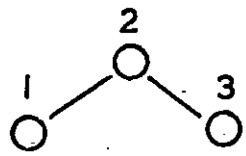

Bond Length		Bond Angle	
01-02	1.2759	01-02-03	116.75

Symmetry Orbitals:- A_1 ; 1s 01 + 03   1s 02
2s 01 + 03   2s 02
X 01 - 03   Y 01 + 03
Y 02

B_2 ; 1s 01 - 03   X 01 + 03
2s 01 - 03   X 02
Y 01 - 03

B_1 ; Z 01 + 03
A_2 ; Z 01 - 03

These are the symmetry orbitals of the type A, C_{2v} molecules

Occupation Numbers:- $6A_1$, $4B_2$, $1B_1$, $1A_2$

--- oOo ---

Ethylene Oxide (C_{2v})

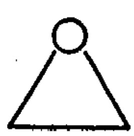

Bond Lengths		Bond Angles	
C-O	1.435	H-C-H	116.3
C-C	1.470	α	158.1
C-H	1.083		

α is the angle between the HCH plane and the C-C bond, with the CCO plane assumed perpendicular to the HCH plane.

Symmetry Orbitals: A_1 ; 1s H1 + H2 + H3 + H4
B_2 ; 1s H1 - H2 + H3 - H4
B_1 ; 1s H1 + H2 - H3 - H4
B_2 ; 1s H1 - H2 - H3 + H4

The carbon and oxygen belong to the C_{2v} (type A) set.

Occupation Numbers: $6A_1$, $3B_2$, $2B_1$, $1A_2$

--- oOo ---

Formaldehyde (C_{2v})

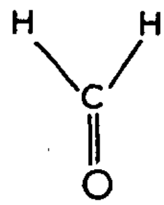

Bond Lengths		Bond Angle	
C-H	1.102	H-C-O	119.45
C-O	1.210		

Symmetry Orbitals:- C_{2v}(type A)

Occupation Numbers:- $5A_1$, $2B_2$, $1A_2$

--- oOo ---

Criegee Zwitterion (C_s)

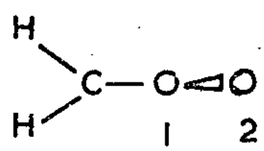

Bond Lengths		Bond Angles	
C-H	1.102	H-C-O1	119.45
C-O1	1.210	C-O1-O2	103.0
O1-O2	1.278		

The O2 atom is out of the plane of the remaining atoms.

Occupation Numbers:- 9A', 3A"

--- oOo ---

Ethylene (D_{2h})

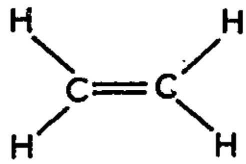

Bond Lengths		Bond Angles	
C-H	1.086	H-C-H	117.6
C-C	1.339	C-C-H	121.2

Symmetry Orbitals:-			
	A_g ;	1s C1 + C2	1s H1 + H2 + H3 + H4
		2s C1 + C2	X C1 - C2
	B_{1g};	Y C1 - C2	1s H1 - H2 - H3 + H4
	B_{2g};	Z C1 - C2	
	B_{1u};	Z C1 + C2	
	B_{2u};	Y C1 + C2	1s H1 + H2 - H3 - H4
	B_{3u};	X C1 + C2	1s H1 - H2 + H3 - H4
		1s C1 - C2	2s C1 - C2

Occupation Numbers:- $3A_g$, $2B_{3u}$, $1B_{2u}$, $1B_{1g}$, $1B_{1u}$

--- oOo ---

1,2,3-Trioxolane (C_{2v})

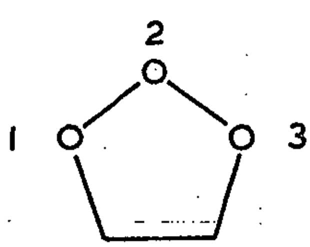

Bond Lengths		Bond Angles	
C-O	1.435	O1-O2-O3	116.8
O-O	1.278	O2-O3-O2	107.3
C-C	1.470	O3-C2-C1	104.3
C-H	1.083	H-C-H	116.3

Symmetry Orbitals:- Carbon and oxygen belong to C_{2v} (type A) while the hydrogens behave as those of ethylene oxide

Occupation Numbers:- $9A_1$, $6B_2$, $3B_1$, $2A_2$

--- oOo ---

Molozonide (C_s)

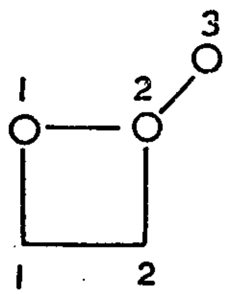

Bond Lengths		Bond Angles	
C1-O1	1.435	O1-O2-O3	116.75
O1-O2	1.278	O1-O2-C2	93.8
O2-O3	1.278	O2-C2-C1	86.2
C2-O2	1.435	H-C-H	116.3
C1-C2	1.470		
C-H	1.083		

Symmetry Orbitals:- A'(σ); 1s, 2s, X, Y of C and O

1s H1 + H3, 1s H2 + H4

A"(π); Z of C and O

1s H1 - H3, 1s H2 - H4

Occupation Numbers:- 15A', 5A"

--- oOo ---

Peroxy-epoxide (C_s)

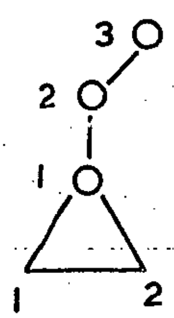

Bond Lengths		Bond Angles	
C1-O1	1.435	O1-O2-O3	116.8
O1-O2	1.278	C2-O1-O2	149.2
O2-O3	1.278	O1-C2-C1	59.2
C1-C2	1.470	H-C-H	116.3
C-H	1.083		

Symmetry Orbitals:- As for the molozonide structure.

Occupation Numbers:- 15A', 5A"

--- oOo ---

Ethylene Ozonide (C_s)

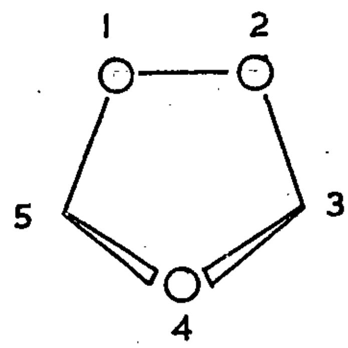

Bond Lengths		Bond Angles	
01-02	1.487	01-02-C3	103.3
02-C3	1.414	02-C3-04	104.1
C3-04	1.414	C3-04-C5	98.1
C3-H3	1.123	H3-C3-H3'	117.2

Symmetry Orbitals:-

A';	1s	01+02	1s	C3+C5	1s	04
	2s	01+02	2s	C3+C5	2s	04
	1s	H1+H2	1s	H3+H4	X	01-02
	X	C3-C5			Y	01+02
	Y	C3+C5	Y	04	Z	01+02
	Z	C3+C5	Z	04		
A";	1s	01-02	1s	C3-C5	1s	H1-H2
	2s	01-02	2s	C3-C5	1s	H3-H4
	X	01+02	X	C3+C5	X	04
	Y	01-02	Y	C3-C5	Z	01-02
	Z	C3-C5				

Occupation Numbers:- 12A', 8A"

--- oOo ---

Ethylene Ozonide (C_2)

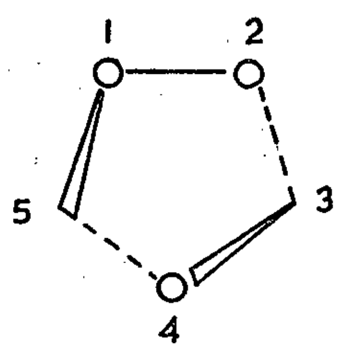

Bond Lengths		Bond Angles	
01-02	1.487	01-02-C3	99.2
02-C3	1.414	02-C3-04	105.3
C3-04	1.414	C3-04-C5	105.9
C3-H3	1.126	H3-C3-H3	112.3

Symmetry Orbitals:-

A ;	1s	01+02	1s	C3+C5	1s	04
	2s	01+02	2s	C3+C5	2s	04
	1s	H1+H4	1s	H2+H3	X	01-02
	X	C3-C5	Y	01+02	Y	C3+C5
	Y	C4	Z	01-02	Z	C3-C5

(Contd.)

Symmetry Orbitals:- B; (Contd.)

1s	O1-O2	1s	C3-C5	1s	H1-H4
2s	O1-O2	2s	C3-C5	1s	H2-H3
X	O1+O2	X	C3+C5	X	O4
Y	O1-O2	Y	C3-C5	Z	O1+O2
Z	C3+C5	Z	O4		

Ethylene Ozonide (C_2); Microwave Geometry

Bond Lengths		Bond Angles	
O1-O2	1.470	O1-O2-C3	99.2
O2-C3	1.395	O2-C3-C4	106.3
C3-O4	1.436	C3-O4-C5	102.8
C-H	1.094	H-C-H	112.9

Occupation Numbers:- 11A, 9B

--- oOo ---

1,2-Dioxetane and Epoxide-O-oxide both have C_{2v} structures with the same geometric parameters as the appropriate parts of the Staudinger molozonide and peroxyepoxide structures respectively. The symmetry orbitals of 1,2-dioxetane are of C_{2v} (type B) and are the same as the carbon atoms and hydrogen atoms of ethylene oxide. The epoxide-O-oxide has all symmetry orbitals comparable to ethylene oxide.

Occupation Numbers (1,2-dioxetane):- $7A_1$, $5B_2$, $2B_1$, $2A_2$

Occupation Numbers (epoxide-O-oxide):-$8A_1$, $4B_2$, $3B_1$, $1A_2$

--- oOo ---

Pyrrole (C_{2v})

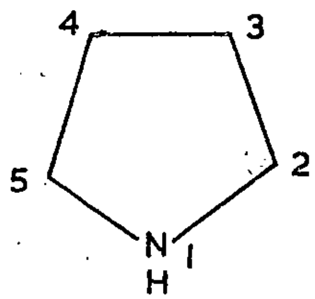

Bond Lengths		Bond Angles	
N1-C2	1.370	C5-N1-C2	119.8
C2-C3	1.382	N1-C2-C3	102.7
C3-C4	1.417	C2-C3-C4	107.4
N-H	0.99	C2-C3-H3	125.5
C1-H1	1.076	N1-C2-H2	121.5
C2-H2	1.077		

Symmetry Orbitals:- C_{2v} (type A)

Occupation:- $9A_1$, $6B_2$, $2B_1$, $1A_2$

--- oOo ---

Pyrazole (C_s)

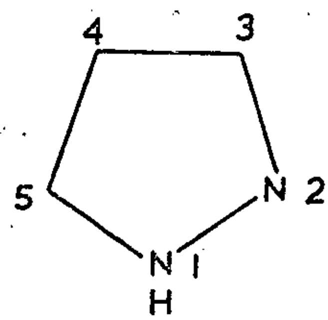

Bond Lengths		Bond Angles	
N1-N2	1.36	N1-N2-C3	107.6
N2-C3	1.34	N2-C3-C4	110.8
C3-C4	1.33	C3-C4-C5	104.7
C4-C5	1.41	C4-C5-N1	109.6
C5-N1	1.31	C5-N1-N2	107.5
N1-H1	1.10		
C3-H3	0.84		
C4-H4	0.98		
C5-H5	0.84		

Symmetry Orbitals:- Molecular Plane Only

Occupation:- 15A', 3A"

--- oOo ---

Imidazole (C_s)

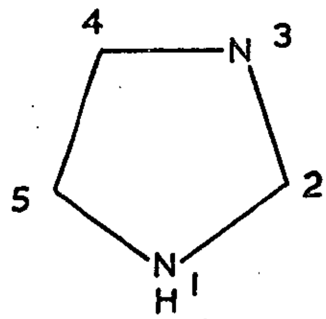

Bond Lengths		Bond Angles	
N1-C2	1.349	N1-C2-N3	111.3
C2-N3	1.326	C2-N3-C4	105.4
N3-C4	1.378	N3-C4-C5	109.8
C4-C5	1.358	C4-C5-N1	106.3
C5-N1	1.369	C5-N1-C2	107.2
N1-H1	0.99	C2-N1-H1	129.1
C2-H2	1.082	N3-C2-H2	138.2
C4-H4	0.958	N3-C4-H4	115.8
C5-H5	1.031	C4-C5-H5	136.3

Symmetry Orbitals and Occupation identical to Pyrazole.

--- oOo ---

1,2,3-Triazole (C_s)

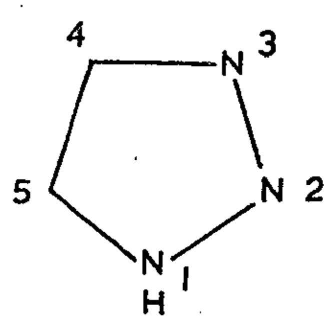

Bond Lengths		Bond Angles	
N1-N2	1.354	C5-N1-N2	110.2
N2-N3	1.280	N1-N2-N3	106.0
N3-C4	1.320	N2-N3-C4	108.5
C4-C5	1.303	N3-C4-C5	111.3
C5-N1	1.327	C4-C5-N1	104.0
H1-N1	0.99	H1-N1-N2	124.9
H4-C4	1.08	H4-C4-C5	124.3
H5-C5	1.08	H50C5-N1	128.0

Symmetry Orbitals and Occupation as for Pyrazole.

--- oOo ---

1,2,4-Triazole (C_s)

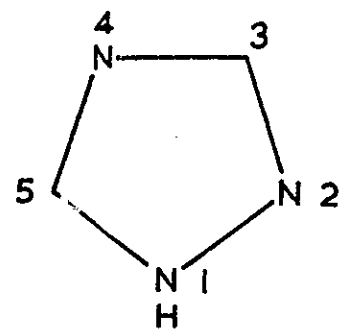

Bond Lengths		Bond Angles	
N1-N2	1.354	C5-N1-N2	110.2
N2-C3	1.319	N1-N2-C3	102.1
C3-N4	1.323	N2-C3-N4	114.6
N4-C5	1.352	C3-N4-C5	103.0
C5-N1	1.320	N4-C5-N1	110.1
N1-H1	1.03	H1-N1-N2	124.0
C5-H5	0.93	H5-C5-N1	123.0
C3-H3	0.93	H3-C3-N2	114.0

Symmetry Orbitals and Occupation as for Pyrazole

--- oOo ---

1-H Tetrazole (C_s)

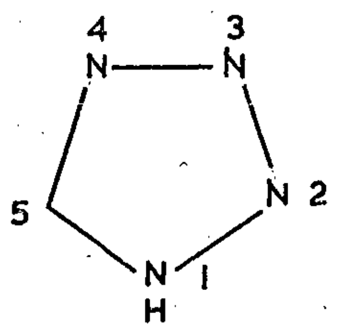

Bond Lengths		Bond Angles	
N1-N2	1.381	N1-N2-N3	107.6
N2-N3	1.255	N2-N3-N4	111.1
N3-N4	1.373	N3-N4-C5	105.0
N4-C5	1.321	N4-C5-N1	109.8
N1-H1	0.93	H1-N1-N2	126.8
C5-H5	1.03	H5-C5-N4	125.1

Symmetry Orbitals and Occupation as for Pyrazole

--- oOo ---

2H-1,2,3-Triazole (C_{2v})

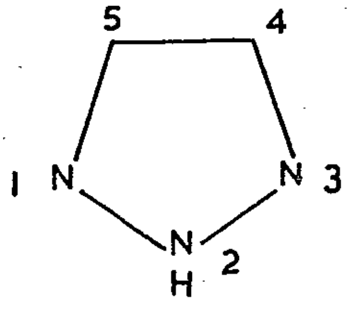

Bond Lengths		Bond Angles	
N1-N2	1.380	C5-N1-N2	106.5
N3-C4	1.320	N1-N2-N3	109.8
C4-C5	1.416	C4-C5-N1	108.6
N2-H2	0.97	H2-N2-N3	125.1
C4-H4	1.076	H4-C4-C5	125.7

Symmetry Orbitals:- C_{2v} (type A)

Occupation Numbers:- $9A_1$, $6B_2$, $2B_1$, $1A_2$

--- oOo ---

2H-Tetrazole (C_s)

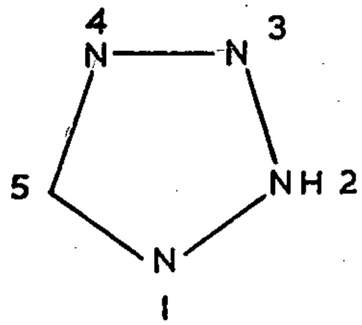

Bond Lengths		Bond Angles	
N1-N2	1.34	N1-N2-N3	114
N2-N3	1.29	N2-N3-N4	107
N3-N4	1.32	N3-N4-C5	106
N4-C5	1.35	N4-C5-N1	112
C5-N1	1.32	H2-N2-N3	124
N2-H2	0.93	H2-N2-N1	122
C5-H5	1.03	H5-C5-N4	123
		H5-C5-N1	125

Symmetry Orbitals and Occupation as for Pyrazole

--- oOo ---

1H,2H-1,2,3-Triazole (C_s)

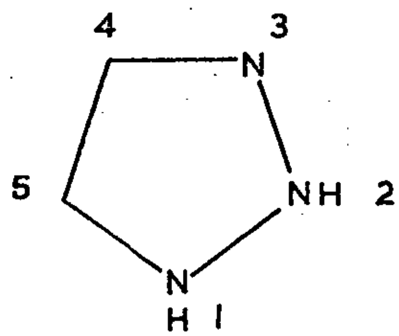

Bond Lengths		Bond Angles	
N1-N2	1.354	N1-N2-N3	106.0
N2-N3	1.280	N2-N3-C4	108.5
N3-C4	1.32	N3-C4-C5	111.3
C4-C5	1.303	C4-C5-N1	104.0
C5-N1	1.327	C5-N1-N2	110.2
N1-H1	1.01	H1-N1-N2	124.9
N2-H2	1.01	H2-N2-N3	127.0
C4-H4	1.03	H4-C4-C5	124.4
C5-H5	1.03	H5-C5-N1	128.0

Symmetry Orbitals and Occupation as for Pyrazole

--- oOo ---

1H,3H-1,2,3-Triazole (C_{2v})

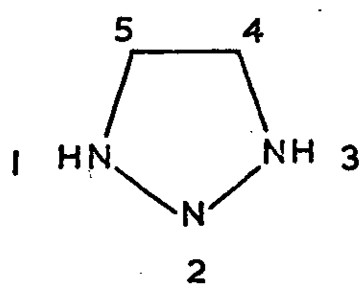

Bond Lengths		Bond Angles	
C4-C5	1.303	C4-C5-N1	107.65
C5-N1	1.3235	C5-N1-N2	109.35
N1-N2	1.300	N1-N2-N3	106.0
N1-H1	1.01	H1-N1-N2	125.33
C5-H5	1.03	H5-C5-N1	126.18

Symmetry Orbitals:- C_{2v} (type A)

Occupation Numbers:- $9A_1$, $6B_2$, $2B_1$, $1A_2$

--- oOo ---

1H,4H-1,2,4-Triazole (C_s)

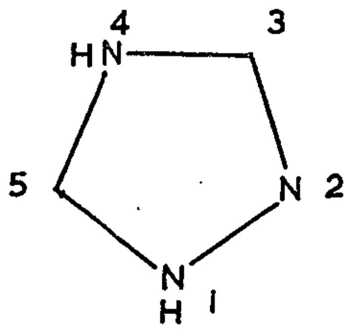

Bond Lengths		Bond Angles	
N1-N2	1.356	C5-N1-N2	110.2
N2-C3	1.316	N1-N2-C3	102.2
C3-N4	1.354	N2-C3-N4	114.66
N4-C5	1.320	C3-N4-C5	102.89
C5-N1	1.326	N4-C5-N1	110.05
N1-H1	1.03	H1-N1-N2	124.9
C3-H3	0.93	H3-C3-N4	122.67
N4-H4	1.04	H4-N4-C5	128.55
C5-H5	0.93	H5-C5-N1	124.98

Symmetry Orbitals and Occupation as for Pyrazole

--- oOo ---

1H,2H-1,2,4-Triazole (C_{2v})

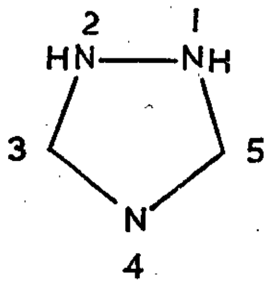

Bond Lengths		Bond Angles	
N1-N2	1.324	C5-N1-N2	106.1
N2-C3	1.327	N4-C5-N1	112.35
C3-N4	1.344	C3-N4-C5	103
		H1-N1-N2	126
		H5-C5-N1	129.5

Symmetry Orbitals:- C_{2v}(type A)

Occupation Numbers:- $9A_1$, $6B_2$, $2B_1$, $1A_2$

--- oOo ---

1H,2H-Tetrazole (C_s)

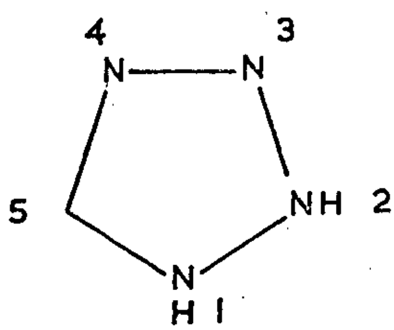

Bond Lengths		Bond Angles	
N1-N2	1.29	N1-N2-N3	112
N2-N3	1.30	N2-N3-N4	106.5
N3-N4	1.374	N3-N4-C5	107.5
N4-C5	1.36	N4-C5-N1	106
N1-H1	0.93	H1-N1-N2	126
N2-H2	0.93	H2-N2-N3	124
C5-H5	1.03	H5-C5-N1	127

Symmetry Orbitals and Occupation Numbers as for Pyrazole

--- oOo ---

1H,3H-Tetrazole (C_s)

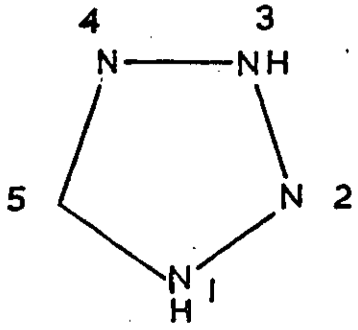

Bond Lengths		Bond Angles	
N1-N2	1.35	N1-N2-N3	103
N2-N3	1.30	N2-N3-N4	117
N3-N4	1.31	N3-N4-C5	104
N4-C5	1.376	N4-C5-N1	106
N1-H1	0.93	H1-N1-N2	125
N3-H3	0.93	H3-N3-N4	121.5
C5-H5	1.03	H5-C5-N1	127

Symmetry Orbitals and Occupation Numbers as for Pyrazole

--- oOo ---

1H,4H-Tetrazole (C_{2v})

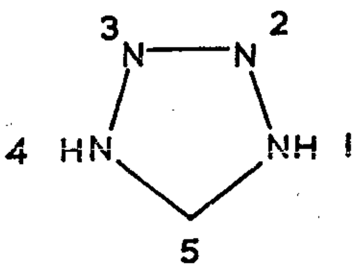

Bond Lengths		Bond Angles	
N1-N2	1.377	C5-N1-N2	105.7
N2-N3	1.255	N1-N2-N3	109.4
C5-N1	1.324	N4-C5-N1	110.9
N1-H1	0.93	H1-N1-N2	127.2
C5-H5	1.03	H5-C5-N1	124.6

Symmetry Orbitals:- C_{2v}(type A)

Occupation Numbers:- $9A_1$, $6B_2$, $2B_1$, $1A_2$

--- oOo ---

2H,3H-Tetrazole (C_{2v})

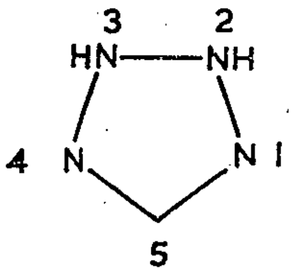

Bond Lengths		Bond Angles	
N1-N2	1.33	C5-N1-N2	103.5
N2-N3	1.29	N1-N2-N3	110.5
C5-N1	1.338	N4-C5-N1	112
N2-H2	0.93	H2-N2-N3	124.8
C5-H5	1.03	H5-C5-N1	124

Symmetry Orbitals:- C_{2v}(type A)

Occupation Numbers:- $9A_1$, $6B_2$, $2B_1$, $1A_2$

--- oOo ---

Pyridine (C_{2v})

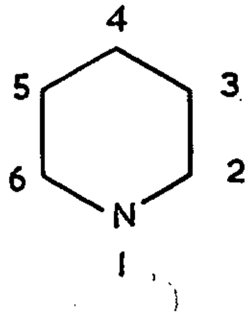

Bond Lengths		Bond Angles	
N1-C2	1.340	N1-C2-C3	116.7
C2-C3	1.390	C2-C3-C4	124.0
C3-C4	1.400	C3-C4-C5	118.6
C2-H2	1.080	C6-N1-C2	118.1
C3-H3	1.080	N1-C2-H2	121.6
C4-H4	1.080	C2-C3-H3	118.0
		C3-C4-H4	120.7

Symmetry Orbitals:- C_{2v}(type A)

Occupation Numbers:- $11A_1$, $7B_2$, $2B_1$, $1A_2$

--- oOo ---

Pyrimidine (C_{2v})

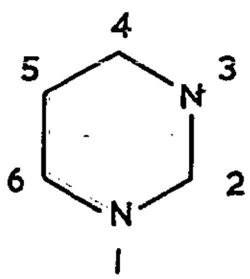

Bond Lengths		Bond Angles	
N1-C2	1.315	N1-C2-N3	116.2
N3-C4	1.337	C2-N3-C4	115.2
C4-C5	1.372	N3-C4-C5	122.6
C2-H2	1.08	C4-C5-C6	128.2
C4-H4	1.08	N1-C2-H2	115.9
C5-H5	1.08	N3-C4-H4	118.7
		C4-C5-H5	121.9

Symmetry Orbitals:- C_{2v}(type A)

Occupation Numbers:- $11A_1$, $7B_2$, $2B_1$, $1A_2$

--- oOo ---

Pyridazine (C_{2v})

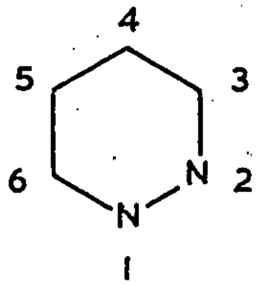

Bond Lengths		Bond Angles	
N1-N2	1.330	N1-N2-C3	119.02
N2-C3	1.353	N2-C3-C4	117.29
C3-C4	1.382	C3-C4-C5	123.69
C4-C5	1.375	N2-C3-H3	121.4
C3-H3	1.085	C3-C4-H4	118.2
C4-H4	1.080		

Symmetry Orbitals:- C_{2v} (type B)

Occupation Numbers:- $10A_1$, $8B_2$, $2B_1$, $1A_2$

--- oOo ---

1,2,3-Triazine (C_{2v})

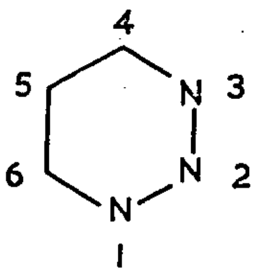

Bond Lengths		Bond Angles	
N1-N2	1.332	N1-N2-N3	123.0
N3-C4	1.350	N2-N3-C4	119.0
C4-C5	1.365	N3-C4-C5	119.5
C4-H4	1.08	C4-C5-C6	120.0
C5-H5	1.08	C4-C5-H5	120.0
		N3-C4-H4	120.3

Symmetry Orbitals:- C_{2v} (type A)

Occupation Numbers: $11A_1$, $7B_2$, $2B_1$, $1A_2$

--- oOo ---

1,2,4-Triazine (C_s)

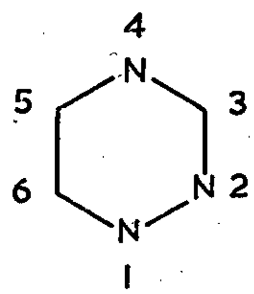

Bond Lengths		Bond Angles	
N1-N2	1.335	N1-N2-C3	119.0
N2-C3	1.352	N2-C3-N4	123.0
C3-N4	1.352	C3-N4-C5	118.2
N4-C5	1.335	N4-C5-C6	122.1
C5-C6	1.360	C5-C6-N1	119.7
C6-N1	1.354	C6-N1-N2	118.0
		N2-C3-H3	118.5
		C4-C5-H5	118.95
		N1-C6-H6	120.15

Symmetry Orbitals:- Molecular Plane Only

--- oOo ---

1,3,5-Triazine (D_{3h})

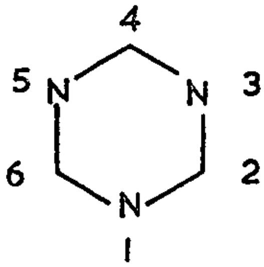

Bond Lengths		Bond Angles	
C-N	1.319	N-C-N	126.8
C-H	1.00	C-N-C	113.2
		N-C-H	116.6

Symmetry Orbitals:- A_1 ; 1s,2s N1+N3+N5, 1s,2s C2+C4+C6
1s H2+H4+H6, R1+R3+R5, R2+R4+R6

E' ; 1s,2s 2N1-N3-N5, 1s,2s 2C4-C2-C6
1s 2H4-H2-H6, 2R1-R3-R5, 2R4-R2-R6
Ts-T5, T2-T6

E' ; 1s,2s N3-N5, 1s,2s C2-C6, R3-R5
1s H2-H6, R2-R6, 2T1-T3-T5,
2T4-T2-T6

A_2' ; T1+T3+T5, T2+T4+T6

A_2'' ; N1+N3+N5, C2+C4+C6

E" ; 2N1-N3-N5, 2C4-C2-C6

E" ; N3-N5, C2-C6

--- oOo ---

1,2,3,4-Tetrazine (C_{2v})

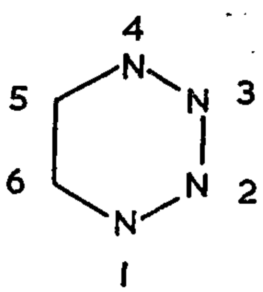

Bond Lengths		Bond Angles	
N1-N2	1.335	N1-N2-N3	122.0
N2-N3	1.331	N3-N4-C5	116.0
N4-C5	1.345	N4-C5-C6	122.0
C-H	1.08	N4-C5-H6	119.0

Symmetry Orbitals:- C_{2v} (type A)

Occupation Numbers: $10A_1$, $8B_2$, $2B_1$, $1A_2$

--- oOo ---

1,2,3,5-Tetrazine (C_{2v})

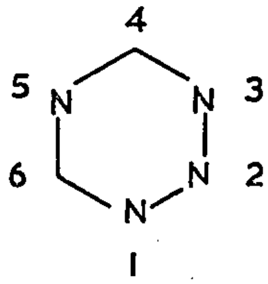

Bond Lengths		Bond Angles	
N1-N2	1.338	N1-N2-N3	123.0
N3-C4	1.350	N2-N3-C4	120.5
N4-C5	1.354	N3-C4-N5	119.7
C-H	1.08	C4-N5-C6	116.6
		N3-C4-H4	120.1

Symmetry Orbitals:- C_{2v} (type A)

Occupation Numbers:- $11A_1$, $7B_2$, $2B_1$, $1A_2$

--- oOo ---

1,2,4,5-Tetrazine (D_{2h})

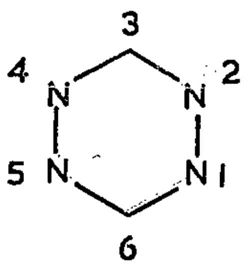

Bond Lengths		Bond Angles	
N1-N2	1.321	N2-C3-N4	127.35
N2-C3	1.334	C3-N4-N5	115.95
C-H	1.08	N2-C3-H3	116.32

Symmetry Orbitals:-

A_g ; 1s,2s N1+N2+N4+N5, 1s,2s, C3-C6,
1s H3+H6, X N1+N2-N4-N5, Y C3-C6
Y N1-N2+N5-N4

B_{1g}; 1s,2s N1-N2+N4-N5, X N1-N2-N4+N5
Y N1+N2-N4-N5, X C3-C6

B_{2u}; 1s,2s N1-N2-N4+N5, 1s,2s C3-C6,
Y C3+C6 1s H3-H6
X N1-N2+N4-N5, Y N1+N2+N4+N5

B_{3u}; 1s,2s N1+N2-N4-N5, X N1+N2+N4+N5
Y N1-N2+N4-N5, X C3+C6

B_{2g}; Z N1+N2-N4-N5

A_u ; Z N1-N2+N4-N5

B_{1u}; Z N1+N2+N4+N5, Z C3+C6

B_{3g}; Z N1-N2-N4-N5, Z C3-C6

Occupation Numbers:- $6A_g$, $5B_{2u}$, $4B_{3u}$, $2B_{1g}$, $1B_{1u}$, $1B_{3g}$, $1B_{2g}$

--- oOo ---

Pentazine (C_{2v})

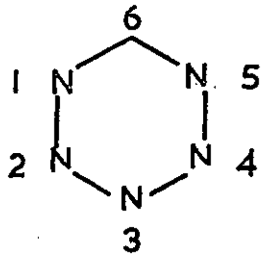

Bond Lengths		Bond Angles	
N1-N2	1.292	N1-N2-N3	120.0
N2-N3	1.292	N2-N3-N4	120.0
N1-C6	1.330	N4-N5-C6	122.9
C-H	1.08	N1-C6-N5	114.2
		N5-C6-H6	122.9

Symmetry Orbitals:- C_{2v} (type A)

Occupation Numbers:- $11A_1$, $7B_2$, $2B_1$, $1A_2$

--- oOo ---

Hexazine (D_{6h})

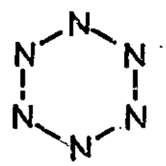

Bond Length		Bond Angle	
N-N	1.292	N-N-N	120

Symmetry Orbitals:- A_{1g}; 1s & 2s N1+N2+N3+N4+N5+N6
R1+R2+R3+R4+R5+R6

B_{1u}; 1s & 2s N1-N2+N3-N4+N5-N6
R1-R2+R3-R4+R5-R6

B_{2u}; T1-T2+T3-T4+T5-T6

E_{1u}; 1s & 2s 2N1+N2-N3-2N4-N5+N6
2R1+R2-R3-2R4-R5+R6, T3-T5-T2+T6

E_{1u}; 1s & 2s N3-N5-N2+N6
R3-R5-R2+R6,
2T1+T2-T3-T5-2T4

E_{2g}; 1s & 2s 2N1-N2-N3+2N4-N5-N6
2R1-R2-R3+2R4-R5-R6
T3-T5+T2-T6

E_{2g}; 1s & 2s N3-N5+N2-N6
R3-R5+R2-R6,

2T1-T2-T6-T3-T5+2T4

(Contd.)

A_{2u} ; Z1+Z2+Z3+Z4+Z5+Z6

E_{1g} ; 2Z1+Z2-Z3-2Z4-Z5+Z6

E_{1g} ; Z3-Z5-Z2+Z6

Occupation Numbers:- $3A_{1g}$, $3E_{2g}$, $3E_{1u}$, $2B_{1u}$, $1B_{2u}$, $1A_{2u}$, $1E_{1g}$

--- oOo ---

Pyrylium Ion (C_{2v})

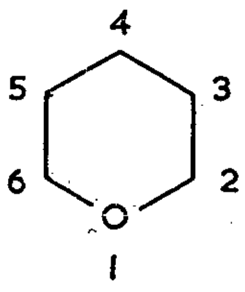

Bond Lengths		Bond Angles	
O1-C2	1.302	C6-O1-C2	121.1
C2-C3	1.401	O1-C2-C3	121.8
C3-C4	1.396	C2-C3-C4	118.5
		C3-C4-C5	118.3
		O1-C2-H2	119.1
		C2-C3-H3	120.8
		C3-C4-H4	120.9

Symmetry Orbitals:- C_{2v} (type A)

Occupation $11A_1$, $7B_2$, $2B_1$, $1A_2$

--- oOo ---

Thiopyrylium Ion (C_{2v})

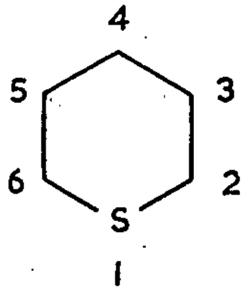

Bond Lengths		Bond Angles	
S1-C2	1.673	S1-C2-C3	123.27
C2-C3	1.403	C2-C3-C4	126.13
C3-C4	1.388	C3-C4-C5	122.5
C2-H2	1.08	C6-S1-C2	98.7
C3-H3	1.08	S1-C2-H2	118.37
C4-H4	1.08	C2-C3-H3	116.94
		C3-C4-H4	118.75

(Contd.)

Symmetry Orbitals:- C_{2v} (type A)

Symmetry Orbitals (d-Orbitals):-

A_1 ; 3s', XX-YY, 2ZZ-XX-YY

B_2 ; XY

B_1 ; YZ

A_2 ; XZ

Occupation Numbers:- $13A_1$, $8B_2$, $3B_1$, $1A_2$

--- oOo ---

1,2-Dithiolium Cation (C_{2v})

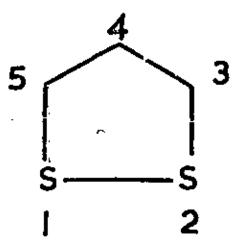

	Bond Lengths		Bond Angles
S1-S2	2.021	S1-S2-C3	95.1
S1-C5	1.673	S2-C3-C4	118.0
C4-C5	1.384	C3-C4-C5	113.7
C3-H3	0.93	S1-C5-H5	121.0
C4-H4	0.93	C5-C4-H4	123.15

Symmetry Orbitals:- C_{2v}(type A)

Symmetry Orbitals (d-Orbitals):-

A_1 ; $3s_1' + 3s_2'$, $XX_1-YY_1+XX_2-YY_2$
$2ZZ_1-XX_1-YY_1+2ZZ_2-XX_2-YY_2$
XY_1-XY_2

B_2 ; $3s_1'-3s_2'$, $XX_1-YY_1-XX_2+YY_2$
$2ZZ_1-XX_1-YY_1-2ZZ_2+XX_2+YY_2$
XY_1+XY_2

B_1 ; XZ_1-XZ_2, YZ_1+YZ_2

A_2 ; XZ_1+XZ_2, YZ_1-YZ_2

Occupation Numbers:- $12A_1$, $9B_2$, $3B_1$, $2A_2$

--- oOo ---

1,3-Dithiolium Ion (C_{2v})

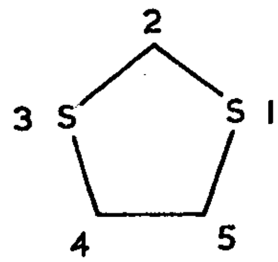

Bond Lengths		Bond Angles	
S1-C2	1.757	S1-C2-S3	114.5
S1-C5	1.743	C2-S3-C4	94.75
C4-C5	1.317	S3-C4-C5	118.0
C2-H2	0.93	S1-C2-H2	122.75
C4-H4	0.93	S1-C5-H5	121.0

Symmetry Orbitals and Occupation Numbers as for 1,2-Dithiolium Ion

--- oOo ---

Thiophene (C_{2v})

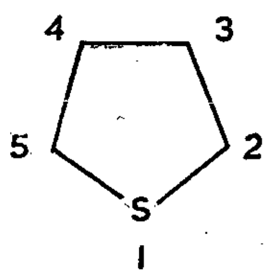

Bond Lengths		Bond Angles	
S1-C2	1.714	S1-C2-C3	$111^{\circ}28'$
C2-C3	1.370	C2-C3-C4	$112^{\circ}27'$
C3-C4	1.423	C2-S1-C5	$92^{\circ}10'$
C2-H2	1.078	S1-C2-H2	$119^{\circ}51'$
C3-H3	1.081	C4-C3-H3	$124^{\circ}16'$

Symmetry Orbitals:- C_{2v}(type A), with the d-orbitals identical to thiopyrylium

Occupation Number:- $11A_1$, $7B_2$, $3B_1$, $1A_2$

--- oOo ---

Thiophene-S-Oxides

Lengths and Angles of Ring are Identical to those of Thiophene; the S-O Length is 1.49Å in all cases

--- oOo ---

Phosphorin (C_{2v})

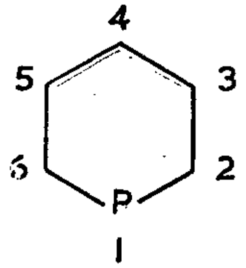

Bond Lengths		Bond Angles	
P1-C2	1.740	C6-P1-C2	102.9
C2-C3	1.403	P1-C2-C3	122.65
C3-C4	1.388	C2-C3-C4	124.65
C2-H2	1.08	C3-C4-C5	122.5
C3-H3	1.08	P1-C2-H2	118.7
C4-H4	1.08	C2-C3-H3	117.7
		C3-C4-H4	118.75

Symmetry Orbitals:- As for Thiopyrylium Ion

Occupation Numbers:- $13A_1$, $8B_2$, $3B_1$, $1A_2$

--- oOo ---

Planar Phosphole (C_{2v})

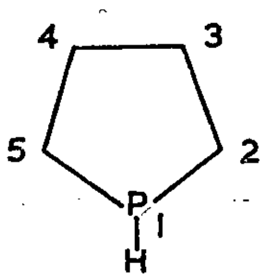

Bond Lengths		Bond Angles	
P1-C2	1.783	H1-P1-C2	134.7
C2-C3	1.343	P1-C2-H2	124.7
C3-C4	1.438	C2-C3-H3	123.0
P1-H1	1.381	C2-P1-C5	90.6
C2-H2	1.08	P1-C2-C3	110.6
C3-H3	1.08	C2-C3-C4	114.1

Symmetry Orbitals:- C_{2v}(type A), with d-Orbitals as for Thiopyrylium

Occupation Numbers:- $11A_1$, $7B_2$, $3B_1$, $1A_2$

--- oOo ---

Puckered Phosphole (C_s)

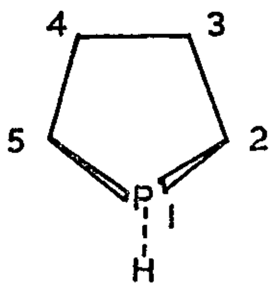

Bond Lengths		Bond Angles	
P1-C2	1.783	P1-C2-C3	110.04
C2-C3	1.343	C2-C3-C4	114.1
C3-C4	1.438	C5-P1-C2	90.6
P1-H1	1.381	C3-C2-H2	124.7
C2-H2	1.08	C2-C3-H3	123.0
C3-H3	1.08	H1-P1-C2	103.95

(Contd.)

Symmetry Orbitals:- A'; Symmetric S, Y and Z combinations

Anti-symmetric X combinations

3s', XX-YY, 2ZZ-XX-YY, YZ

A"; Anti-symmetric S, Y and Z combinations

Symmetric X combinations

XY, XZ

Occupation Numbers:- 14A', 8A"

--- oOo ---

Thiathiophthen (C_{2v})

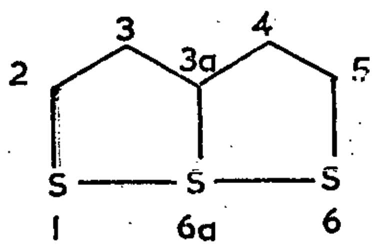

Bond Lengths		Bond Angles	
S1-C2	1.667	S1-C2-C3	120.4
C2-C3	1.368	C2-C3-C3a	118.6
C3-C3a	1.418	C2-S1-S6a	92.1
S1-S6a	2.351	C3-C3a-S6a	119.7
C3a-S6a	1.719	S1-S6a-S6	178.4
		S1-C2-H2	119.8
		C2-C3-H3	120.7

Symmetry Orbitals:- C_{2v}(type A) with d-Orbitals transforming as those of Thiopyrylium (S6a) and the Dithiolium ions (S6 and S1)

Occupation Numbers:- $19A_1$, $14B_2$, $5B_1$, $3A_2$

--- oOo ---

Thiathiophthen Isosteres

New Bond Lengths		New Bond Angles	
C2-O1	1.276	C3-C2-O1	111.25
O1-S6a	2.410	C2-O1-S6a	101.25
C2-N1	1.399	C3-C2-N1	99.0
N1-S6a	2.085	C2-N1-S6a	113.5
N1-H(N)	0.99	C2-N1-H(N)	123.2

(Contd.)

Symmetry Orbitals:- 1) O-S-O compound, C_{2v} (type A)

2) S-S-NH " , Molecular Plane Only

3) S-S-O " , " " "

Occupation Numbers:- 1) O-S-O compound, $16A_1$, $11B_2$, $4B_1$, $1A_2$

2) S-S-O and S-S-NH compounds, 30A', 7A"

--- oOo ---

Norbornadiene (C_{2v})

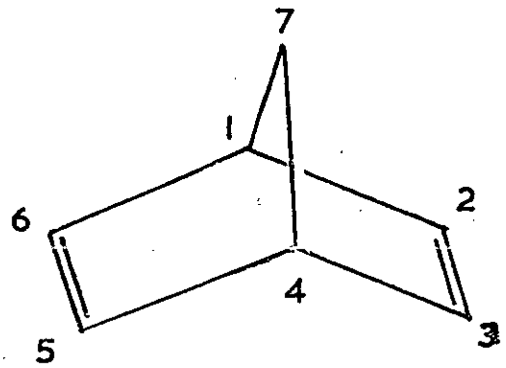

Bond Lengths		Bond Angles	
C1-C2	1.554	C1-C2-C3	106.9
C2-C3	1.366	C7-C1-C2	99.5
C1-C7	1.547	C1-C7-C4	100.3
C1-H1	0.94	C6-C1-C2	100.3
C2-H2	1.03	H7-C7-H7	109.5
C7-H7	1.03	H1-C1-C2	

Symmetry Orbitals:- A_1 ; 1s C7, 2s C7, 1s C1+C4
2s C1+C4, 1s C6+C2+C5+C3
2s C6+C2+C5+C3, 1s H7+H7'
1s H1+H4, 1s H6+H2+H5+H3
X C6-C2+C5-C3, Y C1-C4
Y C6+C2-C5-C3, Z C7
Z C1+C4, Z C6+C2+C5+C3

B_2 ; 1s C6-C2+C5-C3, 2s C6-C2+C5-C3
1s H7-H7'
1s H6-H2+H5-H3, X C7
X C1+C4, X C6+C2+C5+C3
Y C6-C2-C5+C3
Z C6-C2+C5-C3

B_1 ; 1s C1-C4, 2s C1-C4
1s C6+C2-C5-C3
2s C6+C2-C5-C3
1s H1-H4

(Contd.)

	1s	H6+H3-H5-H2
	X	C6-C3-C5+C2
	Y	C6+C3+C5+C2
	Y	C7, Z C1-C4
	Z	C6+C3-C5-C2
A_2 ;	1s	C6-C3-C5+C2
	2s	C6-C3-C5+C2
	1s	H6-H3-H5+H2
	X	C1-C4
	X	C6+C3-C5-C2
	Y	C6-C3+C5-C2
	Z	C6-C3-C5+C2

Occupation Numbers:- $10A_1$, $6B_2$, $6B_1$, $3A_2$

σ- and π- Orbitals in Norbornadiene

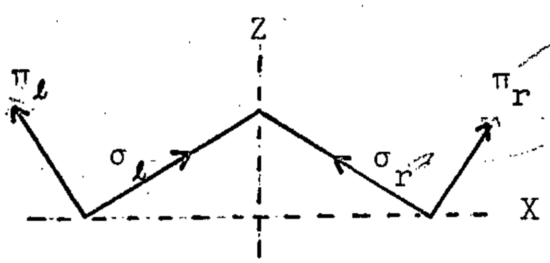

$$\pi_r = Z \sin \alpha + X \cos \alpha$$

$$\sigma_r = X \sin \alpha - Z \cos \alpha$$

$$\pi_\ell = Z \sin \alpha - X \cos \alpha$$

$$\sigma_\ell = Z \cos \alpha + X \sin \alpha$$

Appendix 4. Integrals over Gaussian-Type Functions

In this Appendix are gathered the overlap, kinetic energy, potential energy and electron repulsion integrals over gaussian type functions. An example of the integration techniques is shown for the kinetic energy integral; this is based on the work of Shavitt who demonstrates the method for an electron repulsion. The potential energy integral can be evaluated in a similar manner to the electron repulsion integral.

<u>Kinetic Energy Integrals,</u> $< aA|K|bB >$

This integral has the form

$$\int_0^\infty \exp(-ar_{1A}^2)\ (-\tfrac{1}{2}\nabla^2)\ \exp(-br_{1B}^2)\ dr_1$$

where $\nabla^2 = \dfrac{\partial^2}{\partial x^2} + \dfrac{\partial^2}{\partial y^2} + \dfrac{\partial^2}{\partial z^2}$

and a, b are the exponents centred on nuclei A and B. As written, the $-\frac{1}{2}\nabla^2$ operator applies to the second exponential term. The operator has thus to be evaluated first; dropping subscripts temporarily one obtains:-

$$\frac{\partial\phi}{\partial x} = \frac{\partial}{\partial x}\exp\ (-bx^2-by^2-bz^2)$$

$$= -2bx.\exp(-bx^2-by^2-bz^2)$$

$$\therefore\ \frac{\partial^2\phi}{\partial x^2} = -2b.\exp(-bx^2-by^2-bz^2)-2bx.(-2bx).\exp(-bx^2-by^2-bz^2)$$

$$= -2b\ \exp(-br^2) + 4b^2x^2.\exp(-br^2)$$

$$\therefore \nabla^2 = -6b\ \exp(-br^2) + 4b^2\exp(-br^2).(x^2+y^2+z^2)$$

$$\therefore -\tfrac{1}{2}\nabla^2 = 3b\ \exp(-br^2)-2b^2r^2\ \exp(-br^2)$$

$$\therefore \langle aA|K|bB\rangle = b\int_0^\infty \exp(-ar_{1A}^2).\exp(-br_{1B}^2).(3-2br_{1B}^2)dr_1$$

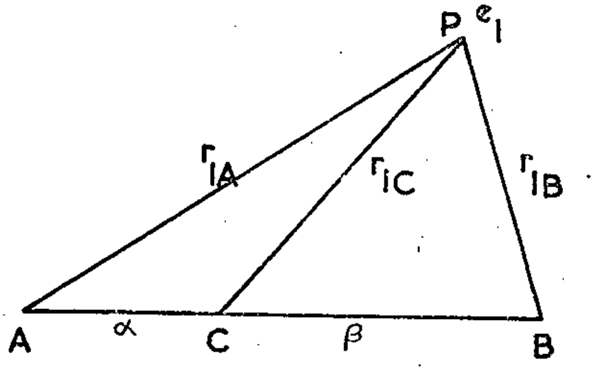

Define the point C using $C_x = \frac{aA_x + bB_x}{a + b}$ where the subscript x denotes the x co-ordinate of the relevant centre; C_y and C_z are similarly defined. Then

$$\alpha = (AC^2)^{\frac{1}{2}} = \left[(C_x-A_x)^2 + (C_y-A_y)^2+(C_z-A_z)^2\right]^{\frac{1}{2}}$$

$$= \left[\left(\frac{aA_x+bB_x}{a+b} - A_x\right)^2 + \ldots\ldots\right]^{\frac{1}{2}}$$

$$= \left[\left(\frac{b}{a+b}\right)^2 (B_x-A_x)^2 + \ldots\ldots\right]^{\frac{1}{2}}$$

$$= \frac{b}{a+b} r_{AB}$$

$$\therefore \beta = r_{AB} - \frac{b}{a+b} r_{AB} = \frac{a}{a+b} r_{AB}$$

Applying the cosine to triangles ACP, BCP one obtains (see Chapter 1)

$$\langle aA|K|bB\rangle = \exp\left(-\frac{ab}{a+b} r_{AB}^2\right)\left[3b\int_0^\infty \exp\left[-(a+b)r_{1C}^2\right] dr_1\right.$$

$$\left. -2b^2\int_0^\infty r_{1B}^2 \exp\left[-(a+b)r_{1C}^2\right] dr_1\right]$$

$$= L[3b\ I_a - 2b^2\ I_b]$$

$I_a = I_x . I_y . I_z$

where $I_x = \int_{-\infty}^{\infty} \exp\left[-(a+b)x_{1C}^2\right] dx_1 = 2\int_0^{\infty} \exp\left[-(a+b)x_{1C}^2\right] dx_1$

This substitution and limits change is valid since the function is symmetrical about the origin and will be so valid for any <u>even</u> power of x.

This is a special case of the general integral

$$\int_0^{\infty} x^{\lambda} \exp\left[-(a+b)x^2\right] dx = \tfrac{1}{2}\alpha^{-(\lambda+1)/2} \Gamma\left(\frac{\lambda+1}{2}\right)$$

$$= \left(\frac{\pi}{4(a+b)}\right)^{\frac{1}{2}} \text{ for } \lambda = 0$$

(This is the integral representation of the Gamma Function.)

$\therefore I_x = 2. \tfrac{1}{2}\left(\frac{\pi}{a+b}\right)^{\frac{1}{2}}$

$\therefore I_a = \left(\frac{\pi}{a+b}\right)^{3/2}$

To evaluate I_b one has recourse to the cosine rule again:-

$$r_{1B}^2 = r_{1C}^2 + \beta^2 - 2\beta r_{1C}\cos\theta$$

$$\therefore I_b = \int_0^{\infty} r_{1C}^2 \exp\left[-(a+b)r_{1C}^2\right] dr_1 + \beta^2 \int_0^{\infty} \exp\left[-(a+b)r_{1C}^2\right] dr_1$$

$$-2\beta \int_0^{\infty}\int_0^{2\pi} r_{1C}\cos\theta \, d\theta \, dr_1$$

$$= I_1 + I_2 - I_3$$

$$I_3 = 2\beta \int_0^{\infty} r_{1C} \int_0^{2\pi} \cos\theta \, d\theta = 2\beta \int_0^{\infty} r_{1C}\left[\sin\theta\right]_0^{2\pi} = 0$$

$$I_2 = \beta^2\left(\frac{\pi}{a+b}\right)^{3/2} = \left(\frac{a}{a+b}\right)^2\left(\frac{\pi}{a+b}\right)^{3/2} \text{ (i.e. } I_A \text{ above)}$$

$$I_1 = \iiint_{-\infty}^{+\infty} (x_{1C}^2+y_{1C}^2+z_{1C}^2) \exp\left[-(a+b)(x_{1C}^2+y_{1C}^2+z_{1C}^2)\right] dx_1 dy_1 dz_1$$

$$= 24\int_0^{\infty} x_{1C}^2 \exp\left[-(a+b)x_{1C}^2\right] dx_1 \int_0^{\infty} \exp\left[-(a+b)y_{1C}^2\right] dy_1$$

$$\int_0^{\infty} \exp\left[-(a+b)z_{1C}^2\right] dz_1$$

$$= 24.\ \frac{1}{2(a+b)} \int_0^{\infty} \exp\left[-(a+b)x_{1C}^2\right] dx_1 . \tfrac{1}{2}\left(\frac{\pi}{a+b}\right)^{\frac{1}{2}} . \tfrac{1}{2}\left(\frac{\pi}{a+b}\right)^{\frac{1}{2}}$$

where integration by parts has been carried out on the first term.

$$\therefore\ I_1 = 24.\ \frac{1}{2(a+b)}\ \tfrac{1}{2}\left(\frac{\pi}{a+b}\right)^{\frac{1}{2}} . \tfrac{1}{2}\left(\frac{\pi}{a+b}\right)^{\frac{1}{2}} \tfrac{1}{2}\left(\frac{\pi}{a+b}\right)$$

$$= \frac{3}{2(a+b)} \left(\frac{\pi}{a+b}\right)^{3/2}$$

$$\therefore\ I_b = \left(\frac{\pi}{a+b}\right)^{3/2} \left[\frac{3}{2(a+b)} + \frac{a^2}{(a+b)^2} r_{AB}^2\right]$$

$$\therefore\ < aA\,|K|\,bB >$$

$$= \left[3b - \frac{3b^2}{a+b} - \frac{2a^2b^2}{(a+b)^2} r_{AB}^2\right] \left(\frac{\pi}{a+b}\right)^{3/2} \exp\left[-\frac{\pi}{a+b} r_{AB}^2\right]$$

$$= \underline{\underline{\left(3 - \frac{2ab}{a+b} r_{AB}^2\right) \left(\frac{ab}{a+b}\right) \exp\left[-\frac{ab}{a+b} r_{AB}^2\right] . \left(\frac{\pi}{a+b}\right)^{3/2}}}$$

This can be expressed in terms of the overlap integral betwean two s-functions:-

$$<aA\,|\,K\,|\,bB> = \left(3 - \frac{2ab}{a+b} r_{AB}^2\right) \left(\frac{ab}{a+b}\right) \quad S_{ab}^{00}$$

Higher Integrals

The above integral has been evaluated for s-functions only. Extension to higher is made by Shavitt's differentiation technique:-

$$\frac{\delta}{\delta A_x} \exp\ (-ar^2_{1A}) = \exp(-az^2_{1A}-ay^2_{1A}) \frac{\delta}{\delta A_x} \exp\ (-ax^2_{1A})$$

$$= \exp\ (-az^2_{1A} - ay^2_{1A})\ \frac{\delta}{\delta A_x}\ \exp\left[-a(X_1-A_1)^2\right]$$

$$= \exp\ (-az^2_{1A}-ay^2_{1A})\ (-2a).(X_1-A_x)\ (-1)\ \exp\left[-a(X_1-A_x)^2\right]$$

$$= \exp(-ar^2_{1A}).2a.X_{1A}$$

$$\therefore\ X_{1A} \exp\ (-ar^2_{1A}) = \frac{1}{2a} \frac{\delta}{\delta A_x} \exp(-ar^2_{1A})$$

The extension to d functions by successive differentiation is obvious.

Since the differentiation is carried out over a variable which is not integrated later, it is possible to differentiate the result of an s-orbital integration, i.e., all integrals have to be analytically evaluated for s-functions only. The kinetic energy integral for a ps function would then be

$$< P|K|S > = \frac{1}{2a} \frac{\delta}{\delta A_x} < aA|K|bB >$$

$$= \frac{1}{2a}\ \frac{\delta}{\delta A_x}\ \frac{ab}{a+b}\ (3- \frac{2ab}{a+b}\ r^2_{AB})(\frac{\pi}{a+b})^{3/2} \exp[-\ \frac{ab}{a+b}\ r^2_{AB}]$$

$$= (\frac{3ab}{a+b})(A_x-B_x)(\frac{\pi}{a+b})^{3/2}\ (-\ \frac{b}{a+b})\ \exp\left[-\ \frac{ab}{a+b}\ r^2_{AB}\right]$$

$$-\ (\frac{2a^2b^2}{(a+b)^2}\ r^2_{AB})(\frac{\pi}{a+b})^{3/2}(\frac{-b}{a+b})\ (A_x-B_x)\ \exp\left[-\ \frac{ab}{a+b}\ \ r^2_{AB}\right]$$

$$-\ \frac{2ab^2}{(a+b)^2}\ (A_x-B_x)\ (\frac{\pi}{a+b})^{3/2}\ \exp\left[-\ \frac{ab}{a+b}\ r^2_{AB}\ \right]$$

$$= \exp\left[-\ \frac{ab}{a+b}\ r^2_{AB}\right]\ .\ (A_x-B_x).\ (\frac{\pi}{a+b})^{3/2}\left[-\frac{5ab^2}{(a+b)^2} + \frac{2a^2b^3}{(a+b)^3}\right]$$

Overlap Integrals

The overlap integral between s-functions has implicitly been evaluated as it is identical in mathematical treatment to $L\ I_a$ in the kinetic energy integral above. Higher integrals are obtained in the same way, i.e., by the differentiation technique.

Potential Energy Integrals

The potential energy integral is defined by

$$< aA|P|bB > = \int_0^\infty \exp(-ar_{1A}^2) \frac{1}{r_{1C}} \exp(-br_{1B}^2 \, dr_1$$

As $1/r_{1C}$ does not affect the second exponential term in the same way that a true operator like $-\frac{1}{2}\nabla^2$ does, the first stage in evaluating this integral is to "collapse" the two gaussian terms into one, as done above, i.e.

$$<aA|P|bB> = \int_0^\infty \exp\left[- \frac{ab}{a+b} r_{AB}^2\right] \cdot \frac{1}{r_{1C}} \exp\left[-(a+b) r_{1P}^2\right] dr_1$$

Shavitts substitution for $1/r_{1C}$ is used

$$\frac{1}{r_{1C}} = \frac{1}{\sqrt{\pi}} \int_0^\infty s^{-\frac{1}{2}} \exp(-sr_{1C}^2) \, ds$$

The two exponential terms are again collapsed into one and integration is carried out over r_1 and finally s giving

$$<aA|P|bB> = \frac{2\pi}{a+b} \exp\left[- \frac{ab}{a+b} r_{AB}^2\right] \int_0^1 \exp\left[-(a+b) r_{CP}^2 t^2\right] dt$$

The integral over t is known as the Incomplete Gamma Function and has to be evaluated numerically. It is the m = 0 integral of the general expression $F_m(\alpha) = \int_0^1 t^{2m} \exp(-\alpha t^2) dt$.

Electron Repulsion Integrals

This integral is defined by

$$<aA\ bB \left|\frac{1}{r_{12}}\right| cC\ dD> = \int_0^\infty \exp(-ar_{1A}^2) \exp(-br_{1B}^2) \cdot \frac{1}{r_{12}} \exp(-cr_{2C}^2)$$

$$\cdot \exp(-dr_{2D}^2) \, dr_1 dr_2$$

The terms dependent on electron 1 are collapsed as are those for electron 2; substitution for $1/r_{12}$ is then made using the same expression as for the potential energy with r_{12} replacing r_{1C}. The evaluated integral has the form

$$\frac{2\pi^{5/2}}{(a+b)(c+d)} \cdot \frac{1}{(a+b+c+d)^{\frac{1}{2}}} \exp[-\frac{ab}{a+b} r_{AB}^2 - \frac{cd}{c+d} r_{CD}^2]^* F_0(\beta)$$

where $\beta = \frac{(a+b)(c+d)}{a+b+c+d} r_{PQ}^2$ with P, Q being the "collapsed" centres for functions based on A, B and C, D respectively.

Special Formulae for s and p Integrals

One can define the overlap integrals in the following manner

$$S_{ab}^{oo} = \int_0^\infty \exp(-ar_{1A}^2)\exp(-br_{1B}^2)dr_1 = N_1N_2\left(\frac{\pi}{a+b}\right)^{3/2}\exp\left(-\frac{ab}{a+b} r_{AB}^2\right)$$

$$S_{ab}^{io} = \langle P_{ia} \quad S_b \rangle = \frac{-b}{a+b}(A_i-B_i) \quad S_{ab}^{oo}$$

$$S_{ab}^{oi} = \langle S_a \quad P_{ib} \rangle = \frac{a}{a+b}(A_i-B_i) \quad S_{ab}^{oo}$$

$$S_{ab}^{ij} = \langle P_{ia} \; P_{ib} \rangle = \frac{1}{2(a+b)}\delta_{ij} - \frac{ab}{(a+b)^2}(A_i-B_i)(A_j-B_j) \quad S_{ab}^{oo}$$

where N_1, N_2 are normalising constants, δ_{ij} is the Kronecher delta and i, j are x, y or z. Thus it can be seen that all the overlap integrals involving p-orbitals are readily evaluated from s-only integrals.

Let us now consider the kinetic energy integrals; these again can be expressed in terms of overlap integral by

$$T_{ab}^{oo} = K_{ab}^{oo} S_{ab}^{oo}$$

$$T_{ab}^{io} = K_{ab}^{io} S_{ab}^{oo} + K_{ab}^{oo} S_{ab}^{io}$$

$$T_{ab}^{oj} = K_{ab}^{oj} S_{ab}^{oo} + K_{ab}^{oo} S_{ab}^{oj}$$

$$T_{ab}^{ij} = K_{ab}^{ij} S_{ab}^{oo} + K_{ab}^{io} S_{ab}^{oj} + K_{ab}^{oj} S_{ab}^{io} + K_{ab}^{oo} S_{ab}^{ij}$$

where $K_{ab}^{oo} = \frac{3ab}{a+b} - \frac{2a^2b^2}{(a+b)^2} r_{AB}^2$

$$K^{io}_{ab} = -\frac{2ab^2}{(a+b)^2}\ (A_i - B_i)$$

$$K^{oj}_{ab} = \frac{2a^2b}{(a+b)^2}\ (A_j - B_j)$$

$$K^{ij}_{ab} = \frac{ab}{(a+b)^2}\ \delta_{ij}$$

Each term of these formulae contains either explicitly or implicitly the term S^{oo}_{ab}, which is normalised. This also applies to the following potential energy and electron repulsion integrals.

Define $L^{oo}_{c,ab} = F_o(t)$ where the argument is $(a+b)r^2_{CP}$

and $L^{io}_{c,ab} = L^{oi}_{c,ab} = (C_i - P_i)F_1(t)$

$$L^{ij}_{c,ab} = (P_i - C_i)(P_j - C_j)F_2(t) - 2\,\frac{F_1(t)}{(a+b)}\ \delta_{ij}$$

The nuclear attraction integrals may now be defined by

$$V^{oo}_{ab} = \Theta \sum_c L^{oo}_{c,ab}\ S^{oo}_{ab}$$

$$V^{io}_{ab} = \Theta \sum_c (L^{oo}_{c,ab}\ S^{io}_{ab} + L^{io}_{c,ab}\ S^{oo}_{ab})$$

$$V^{oi}_{ab} = \Theta \sum_c (S^{oj}_{ab}\ L^{oo}_{c,ab} + S^{oo}_{ab}\ L^{oj}_{c,ab})$$

$$V^{ij}_{ab} = \Theta \sum_c (S^{ij}_{ab}\ L^{oo}_{c,ab} + S^{io}_{ab}\ L^{oj}_{ab} + S^{oj}_{a,b}\ L^{io}_{ab} + S^{oo}_{ab}\ L^{ij}_{ab})$$

where $\Theta = 2\ (\frac{a+b}{\pi})^{\frac{1}{2}}$

The electron repulsion integrals are simplified by first defining a set of intermediate functions (below). In these functions the argument of the Incomplete Gamma Function is given by

$$\frac{S_1 S_2}{S_1 + S_2}\ r^2_{PQ} \text{ where } S_1 = a+b,\ S_2 = c+d \text{ and } S_4 = a+b+c+d.$$

$$G^{oooo} = F_o(t)$$

$$G^{iooo} = G^{oioo} = \frac{S_2}{S_4}(P_i-Q_i)F_1(t)$$

$$G^{ooio} = G^{oooi} = \frac{S_1}{S_4}(P_i-Q_i)F_1(t)$$

$$G^{ijoo} = \frac{S_2}{S_4}\left[\frac{S_2}{S_4}(P_i-Q_i)(P_j-Q_j)\ F_2(t) - \delta_{ij}\frac{1}{2S_1}F_1(t)\right]$$

$$G^{ooij} = \frac{S_1}{S_4}\left[\frac{S_1}{S_4}(P_i-Q_i)(P_j-Q_j)F_2(t) - \delta_{ij}\frac{1}{2S_2}F_1(t)\right]$$

$$G^{iojo} = G^{oijo} = G^{oioj} = G^{iooj}$$

$$= \frac{-1}{S_4}\left[\frac{S_1S_2}{S_4}(P_i-Q_i)(P_j-Q_j)\ F_2(t) - \tfrac{1}{2}\delta_{ij}F_1(t)\right]$$

$$G^{ijko} = G^{ijok} = \frac{S_2}{S_4}\left[\frac{S_1S_2}{S_4}(P_i-Q_i)(P_j-Q_j)(P_k-Q_k)\ F_3(t)\right.$$

$$\left. -\tfrac{1}{2}[\delta_{ij}(P_k-Q_k)+\delta_{ik}(P_j-Q_j)+\delta_{jk}(P_i-Q_i)]F_2(t)\right]$$

$$G^{oijk} = G^{iojk} = -\frac{S_1}{S_4^2}\left[(P_i-Q_i)(P_j-Q_j)(P_k-Q_k)\ F_3(t)\right.$$

$$\left. -\tfrac{1}{2}[\delta_{ij}(P_k-Q_k)+\delta_{ik}(P_j-Q_j)+\delta_{jk}(P_i-Q_i)]F_2(t)\right]$$

$$G^{ijkl} = \frac{1}{S_4^2}\left[\frac{S_1^2S_2^2}{S_4^2}(P_i-Q_i)(P_j-Q_j)(P_k-Q_k)(P_\ell-Q_\ell)\ F_4(t)\right.$$

$$-\tfrac{1}{2}\frac{S_1S_2}{S_4}[\delta_{ij}(P_k-Q_k)(P_\ell-Q_\ell)+\delta_{ik}(P_j-Q_j)(P_\ell-Q_\ell)$$

$$+\delta_{i\ell}(P_j-Q_j)(P_k-Q_k)+\delta_{ik}(P_i-Q_i)(P_\ell-Q_\ell)$$

$$+\delta_{j\ell}(P_i-Q_i)(P_k-Q_k)+\delta_{k\ell}(P_i-Q_i)(P_j-Q_j)]\ F_3(t)$$

$$\left. +\tfrac{1}{4}[\delta_{ij}\delta_{j\ell}+\delta_{ik}\delta_{j\ell}+\delta_{i\ell}\delta_{jk}]\ F_2(t)\right]$$

The electron repulsion integrals can now be defined in terms of these G-functions and the overlap functions (below) where the multiplative constant M is given by $2(\frac{S_1S_2}{\pi S_4})^{\frac{1}{2}}$

$$\langle S_a S_b | S_c S_d \rangle = M\, S_{ab}^{oo}\, S_{cd}^{oo}\, G^{oooo}$$

$$\langle P_{ia} S_b | S_c S_d \rangle = M \left[S_{ab}^{io}\, S_{cd}^{oo}\, G^{oooo} + S_{ab}^{oo}\, S_{cd}^{oo}\, G^{iooo} \right]$$

$$\langle P_{ia} S_b | P_{kc} S_d \rangle = M \left[S_{ab}^{io}\, S_{cd}^{ko}\, G^{oooo} + S_{ab}^{io}\, S_{cd}^{oo}\, G^{ooko} + S_{ab}^{oo}\, S_{cd}^{ko}\, G^{iooo} + S_{ab}^{oo}\, S_{cd}^{oo}\, G^{ioko} \right]$$

$$\langle P_{ia} P_{jb} | S_c S_d \rangle = M \left[S_{ab}^{ij}\, S_{cd}^{oo}\, G^{oooo} + S_{ab}^{io}\, S_{cd}^{oo}\, G^{ojoo} + S_{ab}^{oj}\, S_{cd}^{oo}\, G^{iooo} + S^{oo}\, S^{oo}\, G^{ijoo} \right]$$

$$\begin{aligned}\langle P_{ia} P_{jb} | P_{kc} S_d \rangle = M \Big[& S_{ab}^{ij}[S_{cd}^{ko}\, G^{oooo} + S_{cd}^{oo}\, G^{ooko}] \\ & + S_{ab}^{io}[S_{cd}^{ko}\, G^{ojoo} + S_{cd}^{oo}\, G^{ojko}] \\ & + S_{ab}^{oj}[S_{cd}^{ko}\, G^{iooo} + S_{cd}^{oo}\, G^{ioko}] \\ & + S_{ab}^{oo}[S_{cd}^{ko}\, G^{ijoo} + S_{cd}^{oo}\, G^{ijko}] \Big]\end{aligned}$$

$$\begin{aligned}\langle P_{ia} P_{jb} | P_{kc} P_{\ell d} \rangle = M \Big[& S_{ab}^{ij}[S_{cd}^{k\ell}\, G^{oooo} + S_{cd}^{ko}\, G^{ooo\ell} + S_{cd}^{o\ell}\, G^{ooko} \\ & \qquad + S_{cd}^{oo}\, G^{ook\ell}] \\ & + S_{ab}^{io}[S_{cd}^{k\ell} G^{ojoo} + S_{cd}^{ko}\, G^{ojo\ell} + S_{cd}^{o\ell}\, G^{ojko} \\ & \qquad + S_{cd}^{oo}\, G^{ojk\ell}] \\ & + S_{ab}^{oj}[S_{ab}^{k\ell}\, G^{iooo} + S_{cd}^{ko}\, G^{ioo\ell} + S_{cd}^{o\ell}\, G^{ioko} \\ & \qquad + S_{cd}^{oo}\, G^{iok\ell}] \\ & + S_{ab}^{oo}[S_{cd}^{k\ell}\, G^{ijoo} + S_{cd}^{ko}\, G^{ijo\ell} + S_{cd}^{o1}\, G^{ijko} \\ & \qquad + S_{cd}^{oo}\, G^{ijk\ell}] \Big]\end{aligned}$$

Since all integrals of all types use the overlap integrals, it is thus possible to save computer time by storing the overlap integrals. These are integrals over gaussian functions rather than over contracted functions. Contracted function integrals are obtained from appropriately weighted integrals over primitive gaussian functions.

PUBLICATIONS

Reprinted from:

CHEMICAL PHYSICS LETTERS

Volume 15, No. 3, 15 August 1972

AB INITIO MOLECULAR ORBITAL CALCULATIONS, THE ELECTRONIC STRUCTURE AND ELECTRON SPECTRUM OF NORBORNADIENE

M.H. PALMER and R.H. FINDLAY
University of Edinburgh, Department of Chemistry, Edinburgh, EH9 3JJ, UK

pp. 416 – 420

NORTH-HOLLAND PUBLISHING COMPANY — AMSTERDAM

AB INITIO MOLECULAR ORBITAL CALCULATIONS, THE ELECTRONIC STRUCTURE AND ELECTRON SPECTRUM OF NORBORNADIENE

M.H. PALMER and R.H. FINDLAY
University of Edinburgh, Department of Chemistry, Edinburgh, EH9 3JJ, UK

Received 24 January 1972
Revised manuscript received 17 March 1972

Two LCGO minimal basis (7/3/3) calculations are reported using best atom and scaled gaussian functions. The electron spectrum (ESCA) of the core and valency shell orbitals is obtained, for the title compound norbornadiene.

1. Introduction

One of the most hotly debated subjects of experimental and theoretical organic chemistry has been the existence or otherwise of non-classical carbonium ions [1]. A key compound in these studies has been norbornadiene (I) and cations derived from it. Our interest in this subject is in the application of linear combination

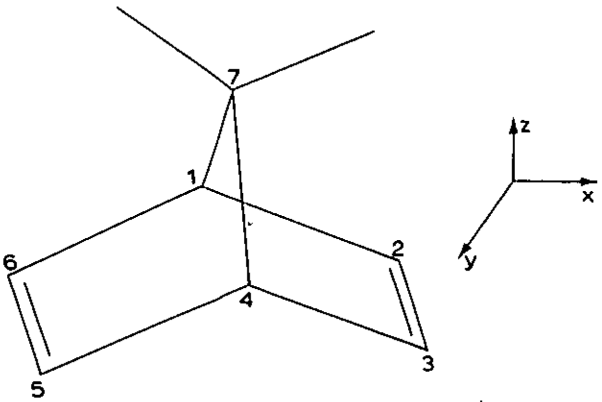

(I)

of gaussian orbital calculations (LCGO) to the diene (I) and its ions, and the use of electron spectroscopy in the study of electronic structural details. A number of semi-empirical calculations on the diene I [2, 3] and its ions [4] have been published, as has its He^{I} photoelectron spectrum [3, 5].

2. The electron spectra

2.1. *X-ray stimulation*

The valency shell orbitals were investigated in the solid state with AEI ES100 and Hewlett-Packard 5950A ESCA spectrometers and the core levels with the former instrument. The latter incorporates an X-ray monochromator thus increasing the resolving power. The 1s electron binding energy (a broad singlet at 285.3eV) was determined using chloroform (289.6 eV) and *n*-hexane (285.0 eV) as internal standards; this procedure involves only the measurement of well resolved doublets close together on the energy scale, thus overcoming any possible errors arising from charging or non-linearity of the energy scale.

In the valency shell region using the ES100 (without a monochromator) only four broad bands are visible, centred on 8.0, 13.0, 17.2 and 26.6 eV (integrated areas 1 : 5 : 9 : 3 respectively). With the HP5950A (containing a monochromator) the main peaks and associated shoulders (sh) were at 9.8 and 11.2 (sh), 14.5 (sh), and 16.8, 22.2 and 26.8 (sh), 28.5, and 33.4 eV. The approximate areas are in the ratios 1 : 1 : 1 : 3 : 2 : 2 : 3 : 2, with at least one further peak probable between those at 11.2 and 14.5 where the counts per second do not fall too near the base line. Owing to the differential cross sections of 2s and 2p electrons it is not possible to use these areas directly to determine the assignments of the eighteen molecular orbitals present in this region.

2.2. *He^I excitation*

We have also obtained the photoelectron spectrum of norbornadiene using a prototype version of the ES100 having a He^I light source. The spectrum is similar in form to those reported elsewhere with peaks and shoulders (sh) at 8.6, 9.4, 11.1 (sh) and 12.17, 13.64, 15.03 eV. Correlation of these bands with those of the X-ray spectra is fairly straightforward, see fig. 1.

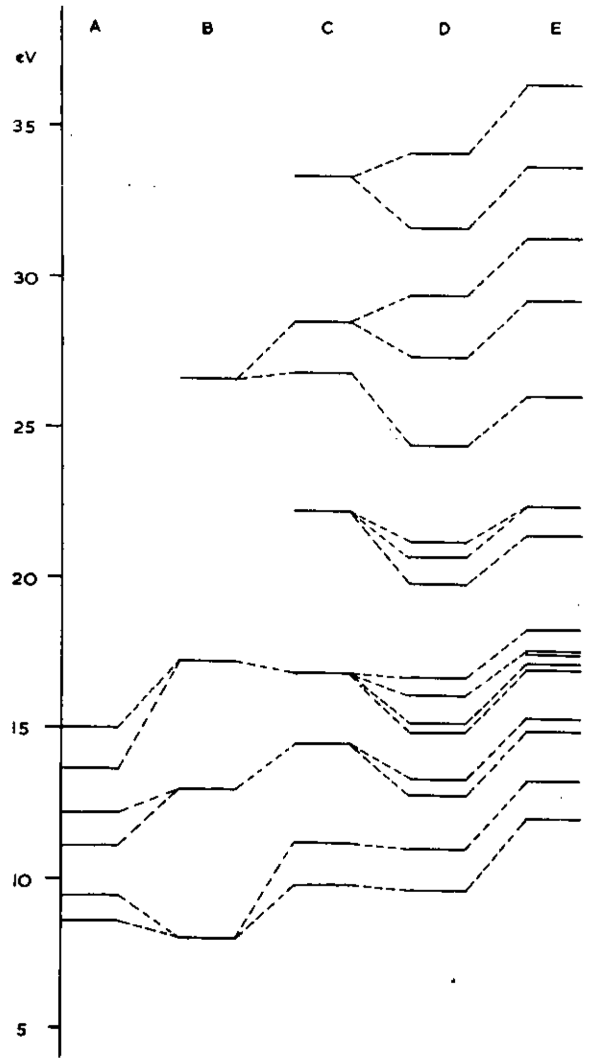

Fig. 1. Correlation diagram of ionisation potentials and orbital energies; A. He(I) on ES100; B. AlKα on ES100; C. HP5950A; D. Scaled gaussian set; E. Unscaled gaussian set.

3. The LCGO calculations

Two basis sets were used. The "best atom" set, consisted of seven s-type and three p-type (for each of x, y, z) gaussian functions and three s-type for hydrogen. These were contracted to a minimum basis of 43 functions, as described in Part I [6]. The free atom energies using these bases are carbon, −37.6104 and hydrogen, −0.4971 au to be compared with the Hartree–Fock limit of −37.6886 and −0.5000 au respectively. The second set consisted of scaled best atom functions, where the scaling was performed on methane (for C–1, C–4 and C–7) and ethylene (for C–2, C–3, C–5, C–6); the method is described in detail in Part III [7], but it will suffice to say that for fixed best atom contraction coefficients A_i the contracted functions

$$\phi_j = \sum_{i=1}^{n} A_{ij} \exp(-\alpha_{ij} r^2)$$

were scaled as in

$$\phi_j = \sum_{i=1}^{n} A_{ij} \exp(-k_{ij}\alpha_{ij} r^2)$$

for the valency shell orbitals, the optimum molecular energy being sought as a function of the scaling factors k_i. The best energies obtained (for fixed k_i for x, y and z orbitals of ethylene) are ethylene −77.83140 au and methane −40.10325 au *. As will be seen in Part III it was possible to improve upon the energy for ethylene by separate scaling of the σ- and π-components; however, this was not used in the present work where the separation of σ- and π-levels is less complete. The two sets of scaled gaussians were then used for the atoms indicated above. The calculations were performed using IBMOL-4 on an IBM360/50 for the preliminary work and an IBM370/195 for the main calculations. For this program the ratio of machine speeds is 1 : 60 respectively and the calculation on the latter took approximately 1 hour to perform. The results are shown in table 1, with the valen-

* The corresponding uncontracted total energies obtained were −77.93577 and −40.14162 au respectively.

Table 1
Calculated energies for norbornadiene

	Scaled gaussians	Unscaled gaussians
Total energy (au)	−268.18036	−267.70658
Electron–nucleus attraction (au)	−947.24069	−941.59191
Electron–electron repulsion (au)	+381.67300	+376.49740
Nucleus–nucleus repulsion (au)	+297.38793	+297.38793
Binding energy (au)	− 0.93092	− 0.45714

Orbital energies (eV) (a) Scaled gaussians

A1	B2	B1	A2
−308.00	−306.04	−308.01	−306.02
−307.57	− 31.49	−306.02	− 20.69
−306.03	− 20.67	− 27.31	− 14.81
− 34.12	− 16.06	− 19.76	
− 29.36	− 13.27 ("π")	− 16.02	
− 24.41	− 9.62 ("π")	− 15.22	
− 21.17			
− 16.53			
− 12.78			
− 11.00 ("π")			

Orbital energies (eV) (b) Unscaled gaussians

A1	B2	B1	A2
−311.96	−310.75	−311.96	−310.73
−311.37	− 33.60	−310.73	− 22.35
−310.74	− 22.33	− 29.20	− 16.91
− 36.30	− 17.54	− 21.35	
− 31.28	− 15.26 ("π")	− 17.70	
− 25.99	− 11.94 ("π")	− 17.15	
− 22.42			
− 18.23			
− 14.84			
− 13.21 ("π")			

Table 2
Orbital energies (eV) for ethylene using the 7/3/3 basis set

	$1B_{1u}$	$1B_{1g}$	$3A_g$	$1B_{2u}$	$2B_{3u}$	$2A_g$	$1B_{3u}$	$1A_g$	Total energy
Unscaled a)	−12.66	−14.96	−17.50	−18.81	−22.58	−29.79	−310.58	−310.59	−77.6893
Scaled b)	−10.64	−13.57	−15.77	−17.49	−21.14	−27.84	−305.80	−305.82	−77.8314
Photoelectron c)	−10.51	−12.38	−14.4	−15.6	−18.8	−	−279.6 d)	−279.6 d)	−

a) Using the gaussian set of ref. [1].
b) Using the optimised scaling factors $k_{2sC} = 1.1088$, $k_{2pC} = 1.1354$, $k_H = 1.5540$.
c) Ref. [12].
d) Soft X-ray emission spectrum (see text).

Table 3
Orbital energies (eV) for methane using the 7/3/3 basis set

	$(1F_2)^3$	$2A_1$	$1A_1$	Total energie (au)
Unscaled [a]	−16.33	−27.00	−309.60	−39.98584
Scaled [b]	−14.85	−25.33	−305.09	−40.10325
Scaled [c]	−14.52	−25.59	−305.02	−40.14162
Photoelectron	13.5 − 14.5 [d]	23.0 [e]	275.7 [f]	−

a) Using gaussian set of ref. [1].
b) Scale factors optimal k_{2sC} = 1.0645, k_{2pC} = 1.1196, k_H = 1.6395.
c) Uncontracted gaussian sets using scaling factors of footnote b.
d) Very broad peak with double maximum showing Jahn–Teller effects.
e) Ref. [13].
f) Soft X-ray emission spectrum, see text [9].

cy shell orbital energies for methane and ethylene, scaled and unscaled for comparison in tables 2 and 3. It is immediately clear that the scaling procedure leads to a marked increase in molecular energy and binding energy (here defined as the difference between the molecular and the best atom energy rather than the scaled atom energy). The unscaled result is probably about 0.8 au from the Hartree–Fock limit while that of the scaled one is probably about 0.25 au from the limit. Almost all of the loss comes from the contraction procedure since the difference between the total energies of the contracted and uncontracted runs for ethylene and methane using the best gaussian sets are 0.1044 and 0.0384 au respectively.

4. Discussion

The carbon 1s broad singlet has a line width at half height of 1.9 eV, to be compared with the usual width for single peaks under these conditions of about 1.4 eV. The peak, which should have a 4 : 1 : 2 weighting (olefin : bridge : ring junction), clearly has a rather smaller splitting than that calculated (about 0.6 eV); this is not unusual for LCGO calculations of this type. The peak maximum is about 21 eV above that calculated from Koopmans' theorem (to be compared with the corresponding figures of 26 and 30 eV for ethylene and methane respectively). It is of interest to determine whether the experimental value gives any indication of strain in the norbornadiene system; the only figures available for comparison are the soft X-ray *emission* spectra of Mattsen and Ehlert [8]; they obtain 276.5, 279.6 and 277.7 eV for methane, ethylene and cyclohexane respectively *. After allowing 7.3 eV (based on cyclohexane) for the experimental differences, the solid state ESCA binding energy for C_{1s} is probably near 286.9 eV; the value for norbornadiene (285.3 eV) suggests that there may be up to about 1.6 eV of strain evident here; (thermochemical) estimates of 1.07 [9] and 1.28 eV [10] have been given.

No clear separation of σ- and π-orbitals occurs in three dimensional molecules such as norbornadiene. In the present work (both calculations) we used a set of symmetry orbitals consisting of the allowed combinations of p_x, p_y and p_z without separation into the σ- and π-types with respect to the olefinic system. This decision was based upon the observation that the transformation section of IBMOL-4 becomes exceedingly long when the symmetry orbitals are complicated linear combinations. None the less it is possible to see from the eigenvectors (available upon request) that the orbitals $10A_1$, $6B_1$ and to a lesser extent $5B_1$ (owing to the methylene bridge) are largely π orbitals. These have eigenvectors for C-p_z of approximately 0.75. The ordering of the orbital energies and states is effectively identical between the two calculations, with the scaled levels being about 2 eV higher (less negative) in most cases, and thus in better agreement with experiment

* Multiplet peaks are commonplace in these carbon spectra (see also references cited in ref. [8]). Many of these lines result from transitions from outer to inner shell vacancies as well as to excited fragments. We have assumed, as did the authors, that the most abundant ion is the ion of interest here. This is only ambiguous in the case of ethylene, so that the final assignment is made by analogy with acetylene (279.4 eV).

(Koopmans' Theorem). The first two ionisation potentials are of π-type as is anticipated from the narrowness of the photoelectron lines. The calculated (scaled functions) and experimental values are in reasonably good agreement, but the predicted splitting (1.38 eV) is rather larger than experiment (0.85 eV). This in part could be due to the geometry of the palladium complex used [11] being distorted relative to the free molecule, the double bonds being forced together more in the complex. Direct comparison of the higher ionisation potentials either from the photo- or X-ray stimulated electron spectra is difficult since in neither case is there sufficient fine structure to assign the individual theoretical lines; none the less the theoretical lines can be grouped with centroids at 9.62, 11.00, 13.03, 15.8, 20.8, 24.41, 28.33, 32.8 eV and these eight points (Y) lead to a linear correlation with the X-ray values (X) given by $Y = 1.010X - 0.713$ eV with standard errors in slope and intercept of 0.038 and 0.805 eV respectively. The calculations on ethylene and norbornadiene correctly predict the latter to have the lower first ionisation potential, but because of the greater separation of the $10A_1$ and $6B_1$ levels in the latter, do not predict the second level also below that of ethylene (see above).

Acknowledgement

We are grateful to Drs. M.S. Barber (A.E.I. Scientific Apparatus Ltd.) and P. Hotellier (Hewlett Packard Ltd., Geneva) for assistance in obtaining the electron spectra recorded here. We are also grateful to the S.R.C. through the Atlas and Rutherford Laboratories for provision of IBM370/195 time.

References

[1] P.D. Bartlett, Nonclassical ions (Benjamin, New York, 1965).
[2] R. Hoffmann, E. Heilbronner and R. Gleiter, J. Am. Chem. Soc. 92 (1970) 706 (EHT).
[3] M.J.S. Dewar, N. Bodor and S.D. Worley, J. Am. Chem. Soc. 92 (1970) 19 (MINDO 2).
[4] M.J.S. Dewar and W.W. Schoeller, Tetrahedron 27 (1971) 4401. (MINDO 2).
[5] P. Bischof, J.A. Hashmall, E. Heilbronner and V. Hornung, Helv. Chim. Acta 52 (1969) 1745;
D.A. Demeo and A.J. Yencha, J. Chem. Phys. 53 (1970) 4536; D.W. Turner, C. Baker, A.D. Baker and C.R. Brundle, Molecular photoelectron spectroscopy (Wiley, New York, 1970).
[6] M.H. Palmer and A.J. Gaskell, Theoret. Chim. Acta 23 (1971) 52.
[7] M.H. Palmer and A.J. Gaskell, Theoret. Chim. Acta, to be published.
[8] R.A. Mattsen and R.C. Ehlert, J. Chem. Phys. 48 (1968) 5465, 5471.
[9] R.B. Turner, P. Goebel, B.J. Mallion, W.E. von Doering, J.F. Coburn and M. Pomerantz, J. Am. Chem. Soc. 90 (1968) 4315.
[10] P. von R. Schleyer, J.E. Williams and K.R. Blanchard, J. Am. Chem. Soc. 92 (1970) 2377.
[11] N.C. Baenziger, G.S. Richards and G.R. Boyle, Acta Cryst. 18 (1965) 924.
[12] A.D. Baker, C. Baker, C.R. Brundle and D.W. Turner, Intern. J. Mass Spectrom. Ion Phys. 1 (1968) 285.
[13] K. Hamrin, G. Johansson, U. Gelius, A. Fahlman, C. Nordling and K. Siegbahn, Chem. Phys. Letters 1 (1968) 613.

Tetrahedron Letters No. 41, pp 4165 - 4168, 1972. Pergamon Press. Printed in Great Britain.

THE ELECTRONIC STRUCTURE OF SOME SULPHUR-CONTAINING HETEROCYCLES

Michael H. Palmer and Robert H. Findlay

(Department of Chemistry, Edinburgh University, West Mains Road, Edinburgh EH9 3JJ)
(Received in UK 25 July 1972; accepted for publication 7 September 1972)

The question of whether d-orbitals play an important role in the ground state bonding of the compounds thiophene (1), 1, 3-dithiolium cation (2), 1, 2-dithiolium cation (3), thiapyrylium cation (4) and thiathiophthene (5) has aroused much controversy.[1-4] We now report a series of non-empirical calculations for these molecules.

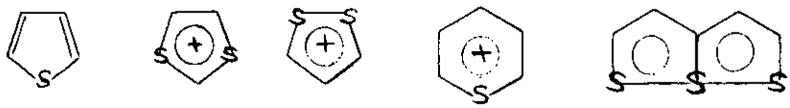

(1) (2) (3) (4) (5)

The procedure uses a linear combination of gaussian orbitals (LCGO) with 10s- and 6p-type for sulphur, 7s- and 3p-type for carbon, and 3s-type for hydrogen, which were then contracted to the normal 1s, 2s, 3s, 2p, 3p orbitals. These were then augmented with a single gaussian for each of the five 3d-orbitals where appropriate. (For computational simplicity it is conventional to use six 3d functions (x^2, y^2, z^2, xy, xz, yz) rather than the usual five. The former were then converted to the latter and an additional s-orbital (3s' orbital) by linear combinations[5]). Comparison with earlier work on furan, pyrrole and 1, 2, 5-oxadiazole[6] suggests that the results are likely to be less than 0.2% away from the Hartree-Fock limit, and that the conclusions are unlikely to be significantly changed by closer approaches. The final energies and atomic populations with and without added d-orbitals are given in Tables 1 and 2.

TABLE 1

	Total Energy (a.u.)			Binding Energy[a] (kcal/mole)		
	sp	spd	spd + 3s'	sp	spd	spd + 3s'
1	-550.0751	-550.1442	-550.1914	593	637	666
2	-908.0214	-908.1677	-908.2629	438	533	589
3	-908.1639	-908.1766	-908.2734	434	442	503
4	-588.1449	-588.2303	-588.2773	821	874	904

[a] Binding Energy = Total Energy of Molecule - Σ Total Energy of Atoms

TABLE 2

Net charges on atoms

	sp	spd	spd + 3s'		sp	spd	spd + 3s'
		(1)				(2)	
S	0.1437	0.0374	0.0275	$S_{1,3}$	0.4294	0.3130	0.3061
$C_{2,5}$	-0.2393	-0.1722	-0.1653	C_2	-0.1810	-0.1310	-0.1275
$C_{3,4}$	-0.1654	-0.1643	-0.1657	$C_{4,5}$	-0.2007	-0.0430	-0.0337
$H_{2,5}$	0.1734	0.1638	0.1632	H_2	0.2572	0.2222	0.2213
$H_{3,4}$	0.2596	0.1541	0.1541	$H_{4,5}$	0.2362	0.2350	0.2338
		(3)				(4)	
$S_{1,2}$	0.3570	0.2838	0.2789	S	0.4234	0.2928	0.2826
$C_{3,5}$	-0.1541	-0.0604	-0.0528	$C_{2,6}$	-0.1652	-0.0859	-0.0778
C_4	-0.1296	-0.1286	-0.1319	$C_{3,5}$	-0.1143-	-0.1074	-0.1094
$H_{3,5}$	0.2484	0.2324	0.7685	C_4	-0.0528	-0.0577	-0.0575
H_4	0.2272	0.2170	0.2168	$H_{2,6}$	0.2531	0.2410	0.2402
				$H_{3,5}$	0.2258	0.2215	0.2213
				H_4	0.2311	0.2266	0.2265

THIOPHENE. The total energy improvement when the five 3d-orbitals are included is 44 kcal/mole, in agreement with a slightly larger calculation by Clark,[2] who however used six 3d-functions and did not report the effect of the extra s-function implicit in his calculations. We observe that a single 3s'-function is almost as important as all five 3d-functions together. Thus inclusion of the d-orbitals represents merely a gain in variational flexibility rather than significant d-orbital participation. The d-orbitals do lead to some electron redistribution and hence improve the agreement of calculated and experimental dipole moments, which are heavily dependent upon the atomic populations. The photo-electron ionisation potentials and the molecular orbital energies are in fair agreement for the first two ionisation potentials [Experimental:-[7] 8.87 ($1a_2$), 9.52 ($2b_1$); Calculated:- 9.82 ($1a_2$), 10.25 ($2b_1$)]. The calculation including d-orbitals leads to slight improvement in the agreement.

1,3-DITHIOLIUM, 1,2-DITHIOLIUM and THIAPYRYLIUM CATIONS. For these molecules the total and orbital energies show similar trends to thiophene. We thus conclude, again, that the d-orbitals are used only to a trivial extent. Almost the whole of the positive charge on these rings is shared by the sulphur and hydrogen atoms. This appears to induce a negative charge on C-2 in the 1,3-dithiolium cation. Although this cation undergoes nucleophilic substitution at C-2 these results are not incompatible since the presence of the reagent would be expected to induce an opposite polarisation. The polarographic half-wave reduction potentials may be compared with the energy of the lowest unoccupied molecular orbital (LUMO). The LUMO energies (eV) for (2), (3), (4) are -1.47 (A_1), -0.99 (A_2), -2.66 (A_2). The experimental values[8] are -0.69V for (2) -0.12 for (3), with (4) not yet reported. Thus there is a correct prediction of sign, order and energy difference for (2) and (3). We are currently investigating the value for (4) and details will be reported later.

THIATHIOPHTHEN. The results obtained for thiathiophthen are presented in Table 3. As can be seen the approach was different, with only one d_π and one d_σ function being used. These were added to the centre sulphur atom. The effect of the d-orbitals appears to be additive and, even allowing for the different number of d-orbitals used, is much less than in the other molecules under consideration.

TABLE 3

	sp	sp + d_π	sp + d_σ	sp + d_π + d_σ
Total Energy	-1381.0944	-1381.0974	-1381.0988	-1371.1018
Binding Energy	580	582	583	585
1st I.P. ($1a_1$)	8.49	8.50	8.49	8.49
2nd I.P. ($1a_2$)	8.82	8.85	8.82	8.85

The first two ionisation potentials are also listed in Table 3. The first ionisation potential corresponds to an orbital which is predominantly the asymmetric combination of the terminal sulphur $3p_x$ atomic orbitals, ie it is the equivalent of a lone pair. Semi-empirical calculations[9,10] also lead to a similar prediction. The d-orbitals do not alter the order of the ionisation potentials and have very little effect on the magnitude. The values obtained are in reasonable agreement with the experimental[9] values of 8.11 eV and 8.27 eV. The existence of a 2-electron 3-centre π-bond has been used to explain the bonding in thiathiophthen. However, examination of the atomic orbital co-efficients does not reveal any π-orbital with sufficiently large co-efficients to justify the existence of such a bond.

REFERENCES

1 H.C. Longuet-Higgins, Trans. Faraday Soc. 1949, 45, 174.
2 D.T. Clark and D.R. Armstrong, Chem. Comm. 1970, 319.
3 R. Zahradnik and J. Koutecky, Tet. Lett. 1961, 631.
4 R. Gleiter and R. Hoffmann, Tet. 1968, 24, 5899.
5 A. Rauk and I.G. Csizmadia, Canad. J. Chem. 1968, 46, 1205.

6 A. J. Gaskell and M. H. Palmer, Theor. Chim. Acta 1972, in press.

7 P. J. Derrick, L. Asbrink, O. Edqvist, B-O. Johsson and E. Lindholm, Int. J. Mass. Spec. Ion Phys. 1971 (6), 177.

8 K. Fabian, H. Hartmann, J. Fabian, and R. Mayer, Tet. 1971, 27, 4705.

9 R. Gleiter, V. Hornung, B. Lindberg, S. Hogberg, and N. Lozac'h, Chem. Phys. Lett. 1971 (11) 401.

10 D. T. Clark and D. Kilcast, Tet. 1971, 27, 4367.

Tetrahedron. Vol. 29, pp. 2173 to 2181. Pergamon Press 1973. Printed in Great Britain

THE MOLECULAR ENERGY LEVELS OF THE AZOLES: A STUDY BY PHOTOELECTRON SPECTROSCOPY AND AB INITIO MOLECULAR ORBITAL CALCULATIONS

S. CRADOCK, R. H. FINDLAY and M. H. PALMER
Chemistry Department, University of Edinburgh, West Mains Road, Edinburgh EH9 3JJ

(*Received in the UK* 30 *January* 1973; *Accepted for publication* 9 *March* 1973)

Abstract—HeI photoelectron spectroscopy and *ab initio* calculations have been applied to the azoles, providing sets of energy levels that correlate well with each other in the upper valence shell region. Observed IPs are assigned to the three π- and to the five σ-levels that involve (principally) valence shell p orbitals. The observed vibration structure is not particularly informative as an aid to assignment since both π- and σ-levels give some bands with vibration structure. The calculations provide in addition to eigenvalues (energy levels) a set of eigenvectors, permitting analysis of the bonding characteristics of the levels, and trends apparent within the series.

The photoelectron spectrum of pyrrole has been reported by several authors;[1-3] while there is general agreement on the assignment of the two isolated bands at lowest ionisation potential (IP) to two of the π-levels, there has been no completely convincing assignment to either the third π- or the σ-levels. Lindholm[3] has arrived at a spectroscopically parameterized set of calculated energy levels for pyrrole (SPINDO) which fits the observed spectra well; our non-empirical calculations (containing no adjustable parameter beyond those necessary to specify the atom involved) suggest that this is fortuitous, since some band assignments are incorrect. One of us[2] has attempted to perform these assignments by comparison of pyrrole with furan and 1,2,5-oxadiazole, and with *ab initio* molecular orbital calculations, but the results were not entirely satisfactory. The present work attempts to extend and clarify knowledge of pyrrole (**1**) by similar calculations for the azoles (**2–6**) and by HeI photoelectron spectroscopy. Spectra for pyrrole and pyrazole (**3**) agree with those previously published, but interpretations differ in several significant points; no data on the remaining azoles have been published to date.

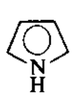
1

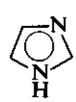
2

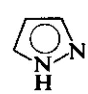
3

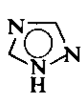
4

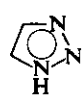
5

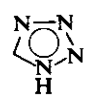
6

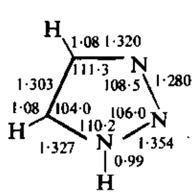

5a

INSTRUMENTAL PROCEDURES

Photoelectron spectra of gas phase samples were recorded using a Perkin Elmer PS16 spectrometer. The instrument resolution was approximately 30 meV for bands near 10 eV. Pyrrole was admitted through a volatile sample manifold, the pressure being controlled by a needlevalve; the samples **2–6** were introduced *via* a direct insertion probe in the temperature range 25–75°, the lowest temperature to give a satisfactory spectrum being used. The energy scale was calibrated by means of the sharp peaks arising from water (12·62 eV) and argon (15·75, 15·93 eV). The samples were either commercial materials or prepared by standard procedures; for high resolution gas phase infra-red spectra (Perkin Elmer 225), pyrrole was purified by distillation and by low temperature fractional crystallisation. Raman spectra were recorded on a Cary 83 spectrometer with 4880 Å (Ar^+) excitation.

CALCULATIONS

In order to provide comparability with earlier work on heteroaromatic compounds, the *ab initio* calculations used a best-atom* minimal basis set consisting of seven s-type and three p-type (for each p_x, p_y, p_z) gaussian functions

*A best atom set is defined as that set of functions of chosen size which best optimises the atom energy. For the atoms in this set of molecules the total energies obtained are $H(^1S)-0{\cdot}4970$ au, $C(^3P)-37{\cdot}6104$ au, $N(^4S)-54{\cdot}2754$ au, which may be compared with the Hartree-Fock limiting values of $-0{\cdot}5000$, $-37{\cdot}6886$, $-54{\cdot}4009$ au respectively.[5]

for carbon and nitrogen and three of s-type for hydrogen. The functions were contracted to 1s (five functions) 2s (two functions) and 2p (three functions) for carbon and nitrogen and one for hydrogen. The calculations were performed using the programme IBMOL-4 on IBM360/195, 360/50 and 370/155 computers; initially delocalised molecular orbitals were obtained, which show the degree of localisation of the 2s levels (see below). The basis integrals were then converted, by Coulson's method,[4] to hybrid orbitals about the ring atom centres, with orbitals pointing along each bond, or bisecting the exterior angle for lone pairs. Bond orbitals were obtained by taking linear combinations of the hybrid orbitals or hybrid and hydrogen 1s orbitals as appropriate in the symmetry transformation part of the programme. This transformation has no effect upon the total energies, eigenvalues or density matrix. The eigenvalues are shown in Table 3 and in graphical form in Fig. 1.

In these calculations the recent microwave structure for pyrrole[6] was used, while imidazole (2),[7] pyrazole (3)[8] and 1,2,4-triazole (4)[9] and tetrazole (6)[10] were represented by their crystal structures or the 5-amino derivative in the last case. The 1,2,3-triazole geometry was based upon general experience of lengths in heterocyclic molecules and is shown above (5a).

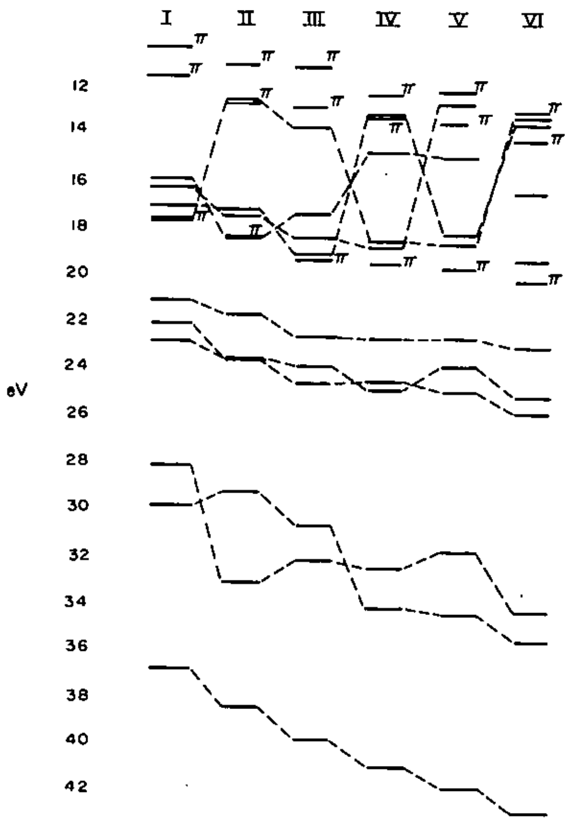

Fig 1. Correlation diagram for theoretical energy levels in the azoles 1 to 6.

CORRELATION OF EXPERIMENTAL WITH CALCULATED VALUES

In all cases the inner valency shell orbitals up to 9a′ in 2 to 6 are predominantly 2s-type as can be seen from the eigenvector matrix in delocalised orbitals. The orbitals 9a′ to 11a′ are largely sp^2 hybridised bonding orbitals from the ring atoms to each other or to the hydrogen atoms. The orbitals above 11a′ in 2 to 6 are dominated by two types of bonding: (a) solely p-orbital contributions to ring bonding and/or CH and NH bonding; (b) lone pair orbitals from 15a′ downwards. The last type, effectively sp^2 hybrid orbitals, occur in symmetric and antisymmetric combinations (14a′ and 15a′) for the triazoles, while 1,2,3,4-tetrazole shows three lone pair levels in the form of a pseudo C_3 rotation group with A_1 (13a′) and E type orbitals (14a′ and 15a′). These generalisations are amplified below but they enable us to correlate the experimental and theoretical data in two ways: (a) by direct use of Koopmans' theorem and the assumption of a linear correlation, but better by (b) using the calculated values to estimate the experimental band intensity. Thus the cross section for HeI (584 Å) stimulated emission of electrons in 2p levels is greater than that for 2s electrons; this means that the π- and other outer valency shell orbitals rich in p-orbital character (11a′) etc. should be stronger than the "lone pair" and inner valency shell orbitals which have higher s-orbital character.

The observed spectra up to about 20 eV may be separated into three distinct regions (A, B and C), Figs 3, 4 and Table 2. Region A, which extends from 8–10 eV in pyrrole, moves to higher binding energy as nitrogen atoms are substituted for CH groups, and is at 10–14 eV in tetrazole. It contains two or three more or less separated bands, some or all of which show resolved vibrational structure. Region B begins some 2 eV to higher binding energy than region A for each molecule, and contains a set of strong overlapping bands with no resolvable fine structure. It extends over about 3 eV for pyrrole, reducing gradually to about 1·5 eV for tetrazole. Region C consists of a single band of moderate intensity and no vibrational structure, with vertical I.P. 17·5–18 eV and with a downward trend from pyrrole to tetrazole. Lindholm[3,11] has observed a group [Region (D)] of bands in the range 19–26 eV for HeII irradiated cyclopentadiene, pyrrole, furan and thiophene.[11] Those of this group which are accessible to HeI are much weaker to HeI than to HeII excitation, and it is plausible on cross-section grounds, and indeed on the grounds of the calculations reported here, to assign five σ(a′) levels to the 2s orbitals in this region D. For the molecules with one or two nitrogen atoms there is comparatively little delocalisation of $2s_N$ with $2s_C$, $2p_C$ or $2p_N$; this can be understood in terms of the free atom orbital energies which in the Hartree Fock limit are $2s_N$ (^{4}S) 25·72, $2s_O$ (^{3}P) 19·20, $2p_N$ (^{4}S) 15·44, and $2p_C$ (^{3}P) 11·79 eV, respectively.[5] For

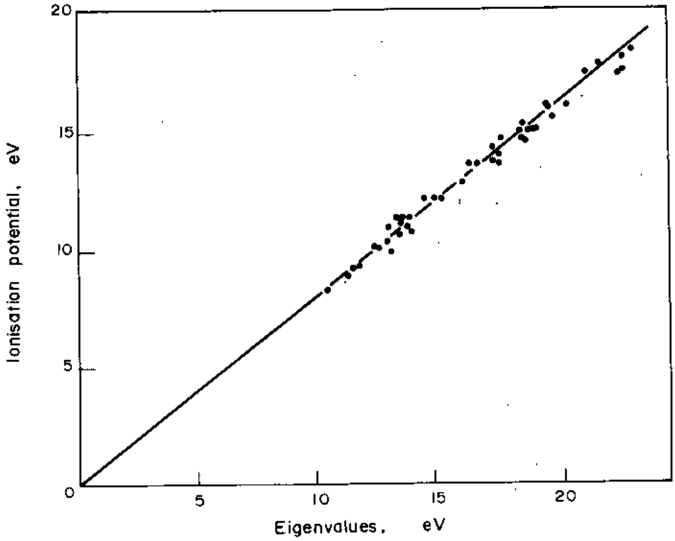

Fig 2. Correlation of observed ionisation potential and eigenvalues.

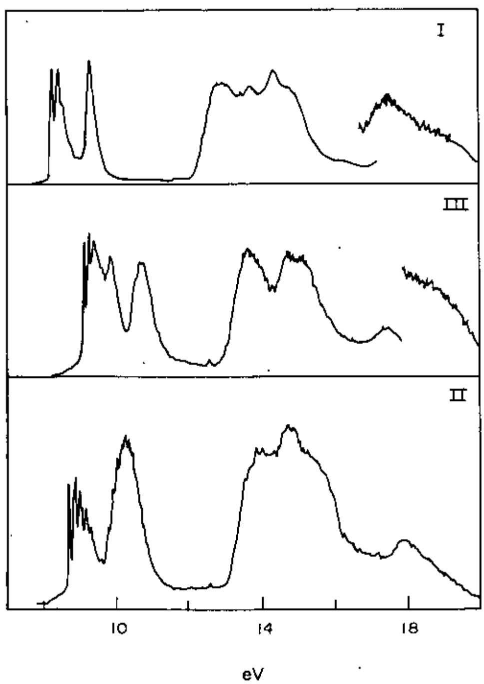

Fig 3. HeI photoelectron spectra of pyrrole (1), imidazole (2) and pyrazole (3).

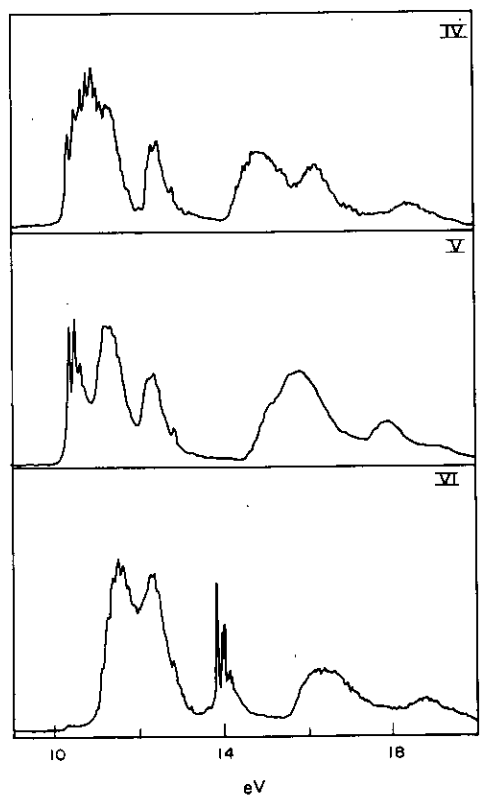

Fig 4. HeI photoelectron spectra of 1,2,4-triazole (4), 1,2,3-triazole (5) and 1,2,3,4-tetrazole (6).

molecules with three nitrogen atoms, splitting of the atomic $2s_N$ levels on molecule formation leads to the overlap of $2s_N$ and $2s_C$ levels and hence very delocalised orbitals; this is clearly observed in the 6a′–8a′ levels of 1,2,3-triazole. We may thus conclude that eight valency shell orbitals, five σ(a′) and three π(a″), remain to be assigned in the present investigation. In practice we observe 5, 6 or 7 bands so that some overlapping is occurring. Our calculations confirm the anticipated effect of substitution of CH by N in the ring, transforming one σ-level from largely ⋛C—H bonding to ⋛N: lone pair character. The binding energy of the orbital in this substitution will thus be markedly decreased, while the reverse tendency should occur with the other orbitals owing to the general effect that an increase in nuclear attraction leads to a lowering of the eigenvalues. These effects are found to occur; while pyrrole has two clearly separated bands in Region A, pyrazole has three and 1,2,4-triazole has four (two of which overlap considerably). Region B correspondingly shrinks in width and overall intensity, while Region C is unaffected except for the expected shift to higher binding energy.

The assignment of this single level in Region C to $7a_1$ in pyrrole and $11a'$ in the azoles is a key step in the overall assignment. It is based upon the observation that it is well separated from the other bands, has moderately high intensity and hence largely p-orbital character; the calculations show that a band is expected to occur in this region which derives largely from p-orbital components from the ring atoms towards the hydrogens of the α-positions with respect to the NH group. The seven outstanding bands in regions A and B combined can then be divided on experimental intensity and calculated groupings to be in the following ratios (A:B): pyrrole, 2:5; diazoles, 3:4; triazoles, 4:3; tetrazole, 5:2. Region A contains $2\pi+(n-1)\sigma$ levels, where n is the number of ring nitrogen atoms. The calculations suggest that in all the compounds studied, the $1a_2(3a'')$ π-level is the least strongly bound; assigning the first band in each spectrum to this level and the band near 18 eV to $7a_1$ ($11a'$) suggested that the ratio of observed IP to calculated eigenvalue was consistently about 0·81. The whole set of 48 points were then plotted as a graph of observed IP against calculated eigenvalue (Fig 2), using the intensity ratios of the regions A and B and assuming that the calculated orbital ordering was correct. The two sets of data correlate well, the best straight line having a slope of $0{\cdot}799\pm0{\cdot}023$, while the maximum deviation from the line is 0·6 eV and the standard deviation is 0·4 eV. Bearing in mind the uncertainties in the geometries used for some of the molecules and the limited size of basis set, this is an excellent correlation and justifies the assumption that the ordering of the energy levels is correctly calculated. The third π level ($1a''$; $1b_1$ for pyrrole) may be assigned to the *high* IP end of region B, as suggested by the calculations, rather than to the low IP end, as assigned by Lindholm for pyrrole. No distinct band appears for this level in any of the compounds in the present study.

Vibrational structure

As mentioned earlier, only bands in region A (upper π and N lone pair levels) show vibrational structure. We find two modes excited in the first band of pyrrole, and these have frequencies of $1020\pm40\ \mathrm{cm}^{-1}$ and $1370\pm40\ \mathrm{cm}^{-1}$; we assign these two modes to the skeletal stretching frequencies of A_1 symmetry which are at 1148 cm^{-1} and 1472 cm^{-1} in the ground state molecule, thus suggesting a reduction of about 10% in the frequencies for the ion. Lindholm,[12] using H Lyman α (1215 Å) excitation and higher resolution, observed four vibrational modes for this band, two of which correspond with our modes. However, we do not agree with his assignments of these bands to those at 1017 cm^{-1} and 1387 cm^{-1} in the free molecule, since it seems unlikely that removal of a bonding electron would leave the molecular vibrational frequencies essentially unchanged. Furthermore it is clear that both the published assignment[13] of the vibrational spectrum of pyrrole and Lindholm's reassignment are incorrect, since the line at 1387 cm^{-1} appears only in the spectrum of *liquid* pyrrole and not in its gas phase spectrum.

Imidazole, 1,2,4-triazole and 1,2,3,4-tetrazole also give bands containing two vibrational modes, which again appear singly and in combination; in the last case all of the combinations up to 3a+2b (where a and b are the apparent fundamentals) occur. The magnitudes of the two fundamentals, which are given in Table 2 are similar to those found in pyrrole, and we feel it is likely that they may be assigned to the two most symmetric skeletal stretching modes in each case.

In 1,2,3-triazole, as in the second band of pyrrole, only one vibrational mode appears to be excited, though a short progression appears. In pyrazole a more complex pattern appears with three or possibly four modes excited. The lowest frequency, of 660 cm^{-1}, does not correlate well with the A_1 frequencies of pyrrole, the lowest of which is at 882 cm^{-1}. We propose that an in-plane deformation mode may be involved, but in the absence of a complete assignment of the vibrational spectrum of pyrazole, this remains to be confirmed. The third band of tetrazole shows two fundamentals, and is the only band in this set of molecules to be assigned solely to a nitrogen lone pair in-plane level. The higher frequency mode has an energy (1470 cm^{-1}) very close to that expected for an unaltered skeletal stretching vibration, found for instance at 1472 cm^{-1} in the pyrrole ground state molecule.

Detailed description of the molecular orbitals

(i) *Core levels*. The orbitals $1a'$ to $5a'$ (2 to 6) and $1a_1$ to $3a_1$ with $1b_2$ and $2b_2$ (pyrrole, 1) are highly localised 1s levels (eigenvectors about 0·98). The nitrogen atom attached to hydrogen (N_1 in all cases) has the highest binding energy while a nitrogen atom in the α-(2,5-) positions is more strongly bound than one in the β-(3,4-) positions. The carbon 1s levels move smoothly to higher binding energy as more nitrogen atoms are incorporated into the rings. The separation of the levels calculated here (Table 3) is likely to be larger than experiment, and this can be largely explained by the limited size of

Table 1. Vertical ionisation potentials (eV) and assigned energy levels

1		2		3		4		5		6		Regions
8·23	$1a_2$	8·78	3a″	9·15	3a″	10·0	3a″	10·06		11·3	{3a″, 15a′, 14a′}	A
9·22	$2b_1$	10·3	{2a″, 15a′}	9·88	2a″	10·56	15a′					
				10·7	15a′	11·1	2a″	10·9	{15a′, 2a″}			
						12·15	14a′	12·1	14a′	12·1	2a″	
12·85	$9a_1$									13·63	13a′	
13·65	$6b_2$	13·7	14a′	13·6	{14a′, 13a′}							
14·3	$5b_2$	14·0	13a′			14·6	13a′	15·0	13a′			
14·7	{$8a_1$, $1b_1$}	14·7	1a″	14·7	1a″	15·1	12a′		12a′	16·1	{12a′, 1a′}	B
		15·3	12a′	15·1	12a′	16·0	1a′	15·6	1a″			
17·5	$7a_1$	17·9	11a′	17·5	11a′	18·2	11a′	17·6	11a′	18·5	11a′	C

Table 2. Vibration frequencies excited in spectra of azoles **1–6**

Azole	1		2		3	4			5		6		Suggested assignment
Band	1	2	1	2	1	1	2	3	1	2	1	3	
					82 (660)								In-plane deformation?
	126 (1020)	125 (1010)	120 (970)	100 (810)	112 (900)	130 (1050)	130 (1050)	110 (900)	131 (1060)	120 (970)	100 (810)	123 (1000)	"Breathing" vibration
	170 (1370)		163 (1320)	140 (1130)	130 (1050)	147 (1190)					145 (1170)	182 (1470)	Symetric skeletal stretch

Note. These figures represent a plausible choice of fundamentals in each case sufficient to explain the observed patterns, which include up to 12 peaks. In each case all observed peaks can be explained as combinations of the fundamentals listed. The units are meV (values in cm^{-1} in brackets).

the basis set. Gas phase measurements would be necessary for comparison since the molecules form hydrogen bonded polymers in the solid state.

The molecules **1–6** are aza-analogues of the cyclopentadienyl anion (D_{5h} symmetry), but of lower symmetry (C_{2v} for **1**, C_s for the others **2–6**). The splitting of the cyclopentadienyl anion e_1' and e_2' levels in the series **1–6** is comparatively small being typically 0·6 and 0·4 eV respectively in the orbitals $6a_1/4b_2$ and $8a_1/5b_2$ for pyrrole, 9a′–12a′ for **2–6**. However, attempts to correlate the orbitals of the azoles **2–6** directly back to the cyclopentadienyl anion by the use of radial and tangential orbitals in D_{5h} are unsuccessful; an analysis based upon the C_{2v} system of pyrrole is much more successful and is shown in Fig 1. Thus there is an apparent C_2 axis for each molecule and the linear combinations of bond orbitals are either symmetric or antisymmetric with respect to this axis; of course the correlation is only in sign of the wave function and not in the magnitudes of the eigenvectors. For example the "lone pair" orbitals in the triazoles 14a′ and 15a′, are linear combinations of approximately sp^2 hybrid orbitals centred at the tertiary nitrogens (N_A, N_B) and are of form $N_A \pm N_B$. The interaction energy in the 1,2,3-isomer is greater (2·3 eV) than in the 1,2,4-isomer (1·6 eV) owing to the closer proximity in the former case. Similarly for tetrazole (Table 4) there is a pseudo A_1 ($N_A + N_B + N_C$) type (13a′) and E ($2N_A - N_B - N_C$, $N_B - N_C$) types (14a′, 15a′). This dominance of the outmost σ-orbitals of the azoles by the nitrogen atoms both in the eigenvectors and the siting of the "C_2 axis" is apparent in the inner valency shell also. The NH σ-bond is not evident among the largely 2s levels, thus the position of the C_2 axis is determined purely by the siting of the nitrogen atoms rather than whether they are formally $\geqq$N or >NH: as an example we cite (Table 5) the orbitals 6a′ to 8a′ for pyrazole which is largely $2s_N + 2s_C$ and conform to the $A_1 + E$ of the cyclopentadienyl anion, or $4a_1 + 5a_1 + 3b_2$ for pyrrole. The only example in this group 6a′ to 8a′ where the nodal position is not determined purely by symmetry with respect to the siting of the nitrogen atoms is in 1,2,3-triazole, where the division is into bonding regions CC+NN (8a′) and CN+CN N (7a′) rather than 2CN (8a′) and CC+NNN (7a′). The two separately strongly NN bonding regions obtained are evidently more favourable than the NNN system. The large split in the pseudo degenerate pair is much larger for 1,2,3-triazole (2·71 eV) and imidazole

Table 3.1. Pyrrole (1)

Eigenvalue (eV)	Principal character	Centres/bond orbitals
a_1		
−427·9	1s	N
−311·0	1s	C_α^+
−309·8	1s	C_β^+
−36·95	2s	$N^+, (C_\alpha + C_\beta)^+$
−30·01	2s	$C_\beta^+, -N$
−22·93	2s	$C_\alpha N^+$
−21·29	$2p_{C\alpha\beta}$, $1s_H$	$C_\alpha H^+, C_\beta C_\beta$
−17·68	$2p_{C\alpha\beta}$, $2p_N$, $1s_H$	$NH, C_\alpha C_\beta^+$
−16·02	$2p_{C\beta}$, $1s_H$	$C_\beta H^+, C_\beta C_\beta$
b_2		
−311·0	1s	C_α^+
−309·8	1s	C_β^-
−28·27	$2s_{C\alpha\beta}$, $2p_N$	$C_\alpha C_\beta^- + C_\alpha N^-$
−22·23	$2s_{C\beta}$, $2p_{yC\alpha}$, $2p_{xN}$	$C_\alpha C_\beta^- - C_\alpha N^-$
−17·31	$2p_{xC}$, $1s_H$	$C_\alpha H^-$
−16·37	$2p_{xC}$, $2p_{yC\beta}$, $1s_H$	$C_\beta H^-, C_\alpha C_\beta^-$
b_1		
−17·69	$2p_{zCN}$ ("A")	$N + C_\alpha C_\beta^+$
−11·65	$2p_{zCN}$ ("E")	$-N, C_\beta C_\beta$
a_2		
−10·34	$2p_{zC}$ ("E")	$C_\alpha C^-$

Table 3.2. Imidazole (2)

Eigenvalue (eV)	Principal character	Centres/bond orbitals
a'		
−428·3	1s	N_1
−425·5	1s	N_3
−312·1	1s	C_2
−311·5	1s	C_5
−310·9	1s	C_4
−38·69	$2s_{N,C}$ ("A")	N, C
−33·31	$2s_{N,C}$ ("E")	$C_5N_1 - C_4N_3$
−29·39	$2s_{N,C}$ ("E")	$C_4C_5, N_3C_2N_1H$
−23·79	$2s_{N,C}$, $2p_{N,C}$, $1s_H$	NH, CN
−23·71	$2s_{N,C}$, $2p_{N,C}$, $1s_H$	$C_4H - C_5H$
−21·84	$2s_{N,C}$, $2p_{N,C}$, $1s_H$	$C_2H + C_5H$
−18·59	$2p_{N,C}$, $1s_H$	C_4C_5, NH
−17·60	$2p_{N,C}$, $1s_H$	$C_2N_1C_5, C_2H - C_5H$
−17·33	sp^2, $1s_H$	$C_2H - C_4H, C_2N_3C_4$
−12·83	sp^2	N_3
a''		
−18·57	$2p_z$ ("A")	N, C
−12·71	$2p_z$ ("E")	CN^-
−11·17	$2p_z$ ("E")	CC, NCN

Table 3.3. Pyrazole (3)

Eigenvalue (eV)	Principal character	Centres/bond orbitals
a'		
−429·7	1s	N_1
−426·9	1s	N_2
−312·2	1s	C_5
−311·5	1s	C_3
−310·6	1s	C_4
−39·95	2s ("A")	N, C
−32·32	2s ("E")	$N_1C_5 - N_2C_3$
−30·81	2s ("E")	$C_3C_4C_5 - N_1N_2$
−24·77	2p, $1s_H$	$NH + C_3H$
−24·07	2p, $1s_H$	$C_3H + C_5H - C_4H$
−22·79	2p, $1s_H$	$C_5N_1, C_4H + C_5H$
−19·24	2p, $1s_H$	$NH - C_3H$
−18·59	2p, $1s_H$	$C_4H - C_5H$
−17·58	2p; $1s_H$	$C_4C_5 - C_3C_4$
−13·84	sp^2	N_2
a''		
−19·15	$2p_z$ ("A")	N_1, C
−13·01	$2p_z$ ("E")	$N_2C_3C_4 - N_1C_5$
−11·32	$2p_z$ ("E")	$N_1N_2 - C_2C_3$

Table 3.4. 1,2,4-Triazole (**4**)

Eigenvalue (eV)	Principal character	Centres/bond orbitals
a′		
−429·5	1s	N_1
−427·5	1s	N_2
−426·2	1s	N_4
−313·1	1s	C_5
−312·1	1s	C_3
−41·13	2s ("A")	$N_1+N_2+N_3, C_3+C_5$
−34·40	2s ("E")	$N_1N_2-C_5N_4C_3$
−32·73	2s ("E")	$C_5N_1-C_3N_2$
−25·07	2s 2p $1s_H$	$C_5H+N_1N_2+C_3N_4$
−24·68	2s 2p $1s_H$	C_3H+NH
−22·90	2s 2p $1s_H$	$C_5H+N_1C_5N_4$
−19·02	2p	$N_2C_3N_4$
−18·76	2p	C_3H+CN
−14·92	sp^2	N_2+N_4
−13·34	sp^2	N_2-N_4
a″		
−19·72	$2p_z$ ("A")	$N_1+N_2+N_4+C_3+C_5$
−13·42	$2p_z$ ("E")	$N_1-C_3N_4$
−12·50	$2p_z$ ("E")	$C_3N_2-N_4C_5$

Table 3.5. 1,2,3-Triazole (**5**)

Eigenvalue (eV)	Principal character	Centres/bond orbitals
a′		
−429·4	1s	N_1
−428·2	1s	N_2
−427·0	1s	N_3
−312·5	1s	C_5
−311·5	1s	C_4
−42·03	2s ("A")	$N_1+N_2+N_3$
−34·69	2s	N_1-N_3
−31·98	2s	$N_2-(C_4+C_5)$
−25·18	2s 2p $1s_H$	NH, N_3C_4, C_4C_5
−24·09	2s 2p $1s_H$	$NN+CN, C_4H-C_5H$
−22·85	2p $1s_H$	CN, C_4H+C_5H
−18·85	2p $1s_H$	$C_4C_5, NH-C_5H$
−18·47	2p $1s_H$	C_4H, CN
−15·16	sp^2	N_3+N_2
−12·81	sp^2	N_3-N_2
a″		
−19·90	$2p_z$	$N_1+N_2+N_3+C_4+C_5$
−13·71	$2p_z$	$N_3C_4-N_1C_5$
−12·35	$2p_z$	$(N_1+N_2+N_3)-(C_4+C_5)$

Table 3.6. 1,2,3,4-1H-Tetrazole (**6**)

Eigenvalue (eV)	Principal character	Centres/bond orbitals
a′		
−429·7	1s	N_1
−429·0	1s	N_2
−428·0	1s	N_3
−427·0	1s	N.
−313·8	1s	C_5
−43·09	2s ("A")	$N_1+N_2+N_3+N_4, C_5$
−35·80	2s ("E")	$N_2+N_3-2N_4$
−34·55	2s ("E")	$N_1+N_2-(N_3+C_5)$
−26·08	2s 2p $1s_H$	NH
−25·35	2s 2p $1s_H$	$N_1N_2+C_5H$
−23·26	2s 2p $1s_H$	C_5H+CN
−19·56	2p	$N_1N_2N_3N_4$
−16·70	sp^2 ("A")	$N_2+N_3+N_4$
−13·73	sp^2 ("E")	N_2-N_4
−13·50	sp^2 ("E")	$2N_3-N_2-N_4$
a″		
−20·46	$2p_z$ ("A")	$N_1+N_2+N_3+N_4+C_5$
−14·47	$2p_z$ ("E")	$N_1C_5-N_2N_3N_4$
	$2p_z$ ("E")	$N_1N_2-C_5N_4$

Table 4. Tetrazole lone pair orbitals

15a′	$-0.822\,N_3+0.444\,N_4+0.424\,N_2$	"E"
14a′	$-0.763\,N_4+0.576\,N_2$	"E"
13a′	$-0.455\,N_3-0.382\,N_4-0.629\,N_2$	"A"

ised and consist of NH with C_3H in **3** and **4** for example; similarly $8a_1$ in pyrrole ($C_\beta C_\beta+C_\alpha H^+$) correlates with those 11a′ orbitals with largely transverse CH components$-C_5H$ with less C_4H in **3** and **5**, C_2H+C_5H (**2**), C_5H in **4** and **6**. Further considerations of this type lead to the complete correlation diagram shown in Fig 1. The complication is in the cases of accicental degeneracy where it is apparent that both orbitals have mixed character; this is the case with 9a′ and 10a; and 13a′ and 14a′ in imidazole and 12a′ and 13a′ in 1,2,3-triazoles. Finally the orbitals 12a′–15a′ in tetrazole cannot really be correlated directly with the same group of orbitals in the other molecules; this is especially true for the symmetric lone pair combination 13a′ and the immediately lower orbital 12a′.

Table 5. 2s Levels in pyrazole

8a′	$0.213\,N_1+0.331\,N_2-0.165\,C_3-0.398\,C_4-0.305\,C_5$	"E"
7a′	$0.424\,N_1+0.369\,N_2-0.353\,C_3+0.245\,C_5$	"E"
6a	$0.500\,N_1+0.358\,N_2+0.132\,C_3+0.096\,C_4+0.168\,C_5$	A

(3·92 eV) than for the other compounds (1·6 eV). That in imidazole may also be a consequence of the absence of NN bonds.

The centre group of valency shell σ-orbitals contains the main XH bonding levels, together with CN and CC bonding. Again the pseudo "A_1+E" system occurs, but the separation of the pseudo "E" type orbitals is more variable. The orbitals 9A′ to 13A′ ($6a_1$ to $8a_1$, $4b_2$ and $5b_2$ for pyrrole) are strongly influenced by the NH position and contain nodes through the NH (along the y-axis) or across the ring at right angles to it; the principal orbitals are correspondingly largely $(2p_y\pm2s)_{N.C}\pm1s_H$ and $(2p_x\pm2s)_{N.C}\pm1s_H$, and it is convenient to refer to this as *longitudinal* and *transverse polarisation* of the *orbitals* respectively. This does not infer polarisation in the sense of molecular charge separation as in a dipole moment, since as in pyrrole (Fig 5) transverse polarisation (for example $7a_1$) leads to a zero dipole moment vector component in the x-direction. There is some vestigial character of the radial and tangential character of the E orbitals of the cyclopentadienyl anion in $7a_1$ and $8a_1$ of pyrrole respectively, but this is still less evident in the other azoles, such that it is better to regard these as $C_\beta C_\beta+C_\alpha H^+$ and $C_\alpha C_\beta^\pm+C_\beta H^+$ bonding respectively where the superscript sign + indicates symmetric (a_1) or − sign an antisymmetric (b_2) combination (see Table 3.1). All of these orbitals contain $1s_H$ together with s and p character from the ring atoms. The longitudinal or transverse polarisation allows a direct correlation with the orbitals of pyrrole. Thus $6a_1$ in pyrrole ($NH+C_\beta H^+$) correlated with 9a′ in all azoles (except 1,2,4-triazole where it is 10a′) which are all longitudinally polarised and consist of NH with C_3H in **3** and **4** for example;

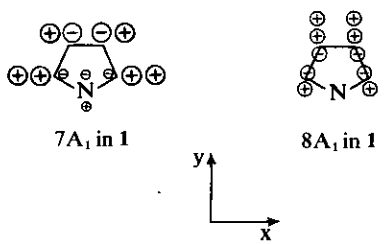

Fig 5. Transverse ($7A_1$) and longitudinal ($8A_1$) polarisation of orbitals in pyrrole.

The π orbitals similarly correlate well with the A_1+E π-levels of cyclopentadienyl (D_{5h}); the separation of the two levels at lower IP ($1b_1$ and $1a_2$ for pyrrole, 2a″ and 3a″ for the others) is almost invariant (1.5 ± 0.3 eV) throughout the set. The most strongly bound π-level is a totally symmetric combination of p_z orbitals in each case, while the others have a single node each, passing through NH or perpendicular to it respectively.

CONCLUSIONS

Leaving aside the question of whether Koopmans' theorem has validity here or elsewhere, or what form of relationship should hold between eigenvalue and photoelectron energy levels, we observe that a linear relationship between these two variables holds over the first seven observed levels and has the form $(IP)_{exptl}=0.799\,(IP)_{calc}$.

The lone pair levels are heavily localised on nitrogen, but occur as linear combinations where more than one lone pair exists. The other molecular orbitals of the valency shell are heavily delocalised but their principal components determined by the calculations assist in the correlation through the use of relative intensity, and the known different cross sections to 2s and 2p electrons.

REFERENCES

[1]A. D. Baker, D. Beteridge, N. R. Kemp and R. E. Kirby, *J. Chem. Soc.* (D), 286 (1970)
[2]M. H. Palmer and A. J. Gaskell, *Theoret. Chim. Acta* **23**, 51 (1971)
[3]P. J. Derrick, L. Åsbrink, O. Edqvist, B.-Ö. Jonsson and E. Lindholm, *Int. J. Mass Spectrom. Ion Phys.* **6**, 191 (1971)
[4]C. A. Coulson, "Valence," Oxford Univ. Press, 1961, p. 203.

[5]E. Clementi, Supplement "Tables of Atomic Functions" *IBM J. of Res. and Development* **9**, 2 (1965)
[6]D. H. Sutter and W. H. Flygare, *J. Amer. Chem. Soc.* **91**, 6895 (1969)
[7]S. Martinez-Carrera, *Acta Cryst.* **B20**, 783 (1966)
[8]H. W. W. Ehrlich, *Acta Cryst.* **B13**, 946 (1960)
[9]P. Goldstein, J. Ladell and G. Abowitz, *Acta Cryst.* **B25**, 135 (1969)
[10]K. Britts and I. L. Karle, *Acta Cryst.* **B22**, 308 (1967)
[11]P. J. Derrick, L. Åsbrink, O. Edqvist, B.-Ö. Jonsson and E. Lindholm, *Int. J. Mass Spectrom. Ion Phys.* **6**, 161, 177, 203 (1971)
[12]P. J. Derrick, L. Åsbrink, O. Edqvist and E. Lindholm, *Spectrochim. Acta* **27A**, 2525 (1971)
[13]R. C. Lord and F. A. Miller, *J. Chem. Phys.* **10**, 328 (1942)

Tetrahedron Letters No. 47, pp 4659 - 4662, 1973. Pergamon Press. Printed in Great Britain.

THE MOLECULAR ENERGY LEVELS OF THE AZINES. AB INITIO CALCULATIONS AND THE CORRELATION WITH PHOTOELECTRON SPECTROSCOPY

by M. H. Palmer, A. J. Gaskell and R. H. Findlay

Department of Chemistry, University of Edinburgh, West Mains Road, Edinburgh EH9 3JJ.

(Received in UK 27 September 1973; accepted for publication 10 October 1973)

Photoelectron spectroscopy has rapidly become the major method for investigation of molecular energy levels;[1] line assignments are generally made on the basis of chemical intuition or semiempirical molecular orbital calculations. Thus for the azines two groups of workers[2,3] have arrived at different conclusions. The present work used minimal basis set (cf. Reference 4) non-empirical calculations and leads to firm conclusions, both for the known and unknown azines. The total energies and binding energies (Table 1) show that the binding energy decreases as the value of n increases in $C_{6-n}H_{6-n}N_n$, but that 1,2,3-triazine, and 1,2,3,4- and 1,2,3,5-tetrazines should be stable in contrast to pentazine or hexazine.

Table 1

Molecule	Total Energy (a.u.)	Binding Energy[a] (kcal/mole)
Pyridine	-245.76489	-597.5
Pyrazine[b]	-261.559	-444.9
Pyridazine	-261.68003	-438.9
Pyrimidine	-261.67872	-438.0
1,2,3-Triazine	-277.59443	-279.8
1,2,4-Triazine	-277.61161	-290.6
1,3,5-Triazine	-277.54134	-246.5
1,2,3,4-Tetrazine	-293.51233	-122.6
1,2,3,5-Tetrazine	-293.54386	-142.4
1,2,4,5-Tetrazine	-293.47477	- 99.31
Pentazine	-309.39321	+ 57.4
Hexazine	-325.28963	+227.6

a) Binding Energy = Molecular Energy - Σ Atom Energies.

b) Data from Reference 5b, which used a similar basis set, is included for completeness.

The corresponding molecular orbital energies, correlated with the known experimental ionisation potentials via Koopmans' Theorem, lead to the linear relationship $IP_{lbs} = 0.785\ IP_{calc} + 0.33eV$ shown graphically in Figure 1 (the standard deviations in slope and intercept and the overall standard deviation are 0.01, 0.2 and 0.54 eV respectively); the line is effectively identical to that found for the azoles.[4] The usual semiempirical methods lead to the following results (method, slope, intercept, standard deviation in slope, standard deviation in intercept, overall standard deviation):-

(a) CNDO-2, 0.546, 3.71, 0.015, 0.34, 1.03;
(b) INDO, 0.504, 4.98, 0.022, 0.52, 1.69;
(c) Extended Huckel Method[2] 1.359, -7.49, 0.037, 0.651, 1.05. It is clear that the scatter is much worse in these methods than in the LCGO calculations. Furthermore graphical presentation of these results shows that the major groupings of the experimental spectra are only reproduced well by the non-empirical calculations (Figure 2).

For pyridine, the present work (as in previous calculations[5a,6]) gives the I.P. order $1a_2$ $2b_1$ $11a_1$ in contrast to the order from the earlier assignments.[2,3] Our ordering agrees almost completely with Lindholm's[2] Extended Huckel calculations for pyrimidine, pyridazine, 1,3,5-triazine and 1,2,4,5-tetrazine, and contrast with those of Heilbronner et al.[3]

Although the symmetry of the molecules $C_{6-n}H_{6-n}N_n$ n = 0-6 varies from D_{6h} through C_{2v} to C_s, all of the molecules show pseudo D_{6h} (e.g. C_6H_6) symmetry, in that the orbitals can be classified on the basis of their eigenvectors into the D_{6h} types. This leads to the correlation diagram (Figure 3), and allows an explanation of the apparently anomalous "lone pair" orbital

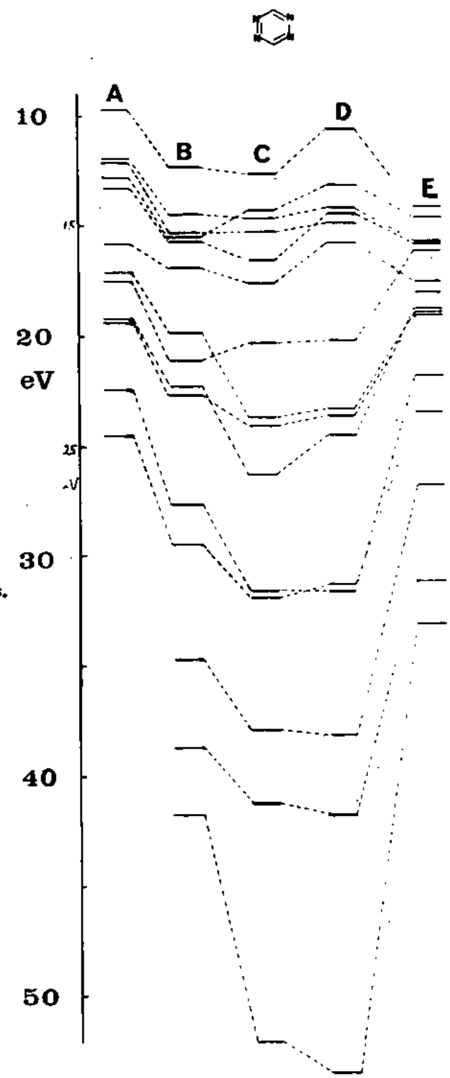

Fig. 2. Correlation of Experimental (A), LCGO (B), CNDO-2 (C), INDO (D), EHM (E) Orbital Energies for 1,2,4,5-Tetrazine.

combinations which are calculated for some of the molecules. The filling of the σ-orbitals from low to high binding energy is in the same order as benzene namely $3e_{2g}$, $3e_{1u}$, $2b_{1u}$. Thus if the lone pair orbitals at centre i are given by N_i, with the corresponding D_{6h} orbital in brackets, then for 1,2,4-triazine the calculated combinations are 18a' $(N_1-N_2+N_4)$ (e_{2g}), 17a' $(N_2 + N_4)$ (e_{2g}), 16a' $(N_1 - N_4)$ (e_{1u}); 1,2,3,4-tetrazine has $9a_1$ and $10a_1$ $(N_2 + N_3)$ (e_{1u} and e_{2g} respectively), $8b_2$ $(N_2 - N_3)$ (e_{2g}), and $7b_2$ $(N_1 - N_4)$ (e_{1u}); 1,2,3,5-tetrazine has 11a' $(N_1 + N_3) - (N_2 + N_5)$ (e_{2g}), 10a' $(N_2 - N_5)$ (b_{1u}), 9a' $(N_1 + N_2 + N_3 - N_5)$ (e_{1u}), $7b_2$ $(N_1 - N_3)$ (e_{2g}). Combinations for the remaining azines can be interpreted in similar terms.

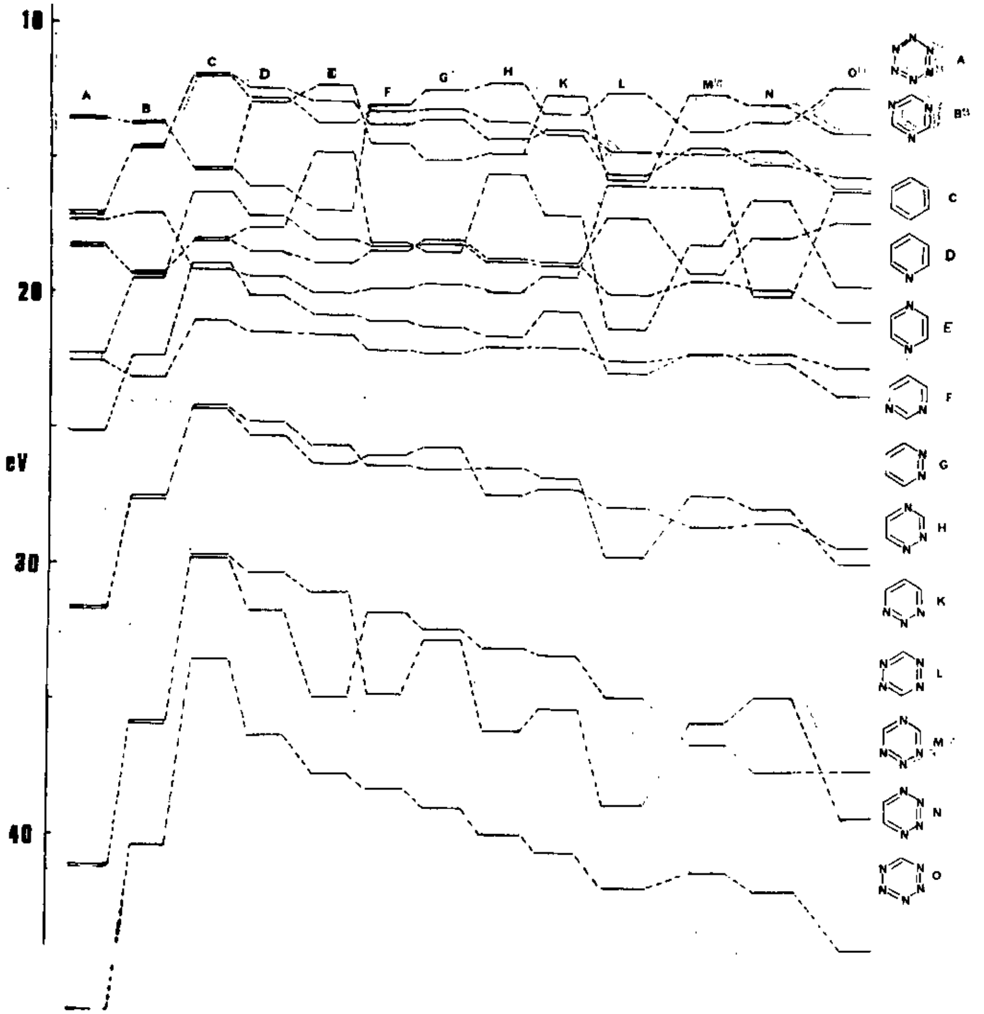

Fig. 3 Correlation of Theoretical (LCGO) Orbital Energies in the Azines.

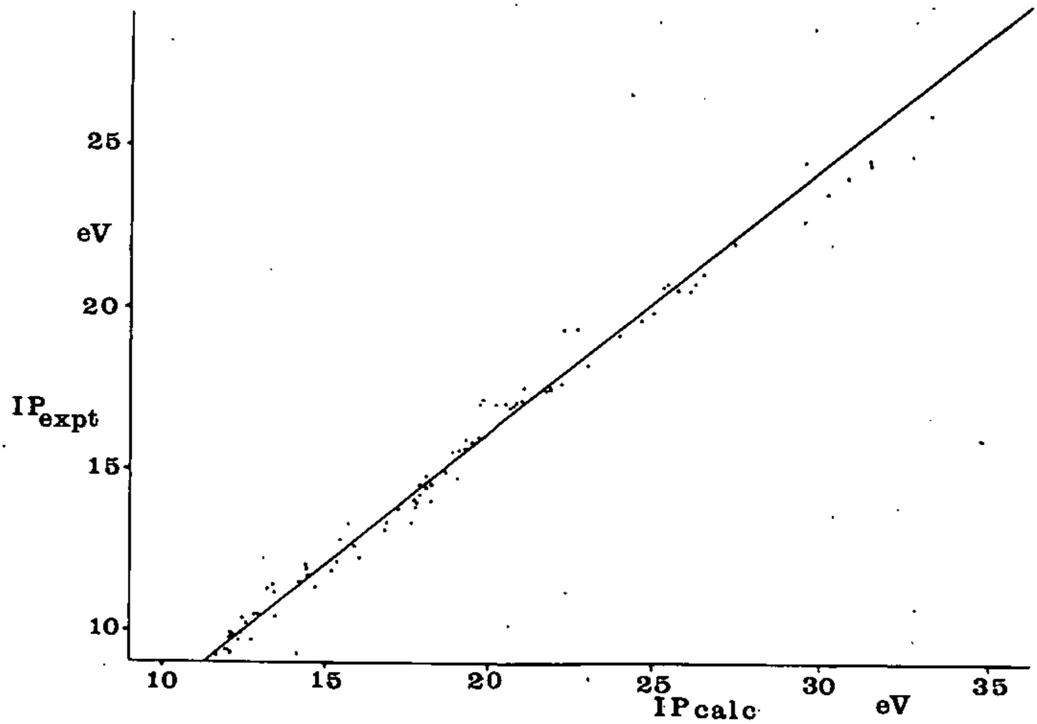

Fig. 1 Least Squares plot of Orbital Energies as Ionisation Potentials.

References

1. D.W. Turner, A.D. Baker, C. Baker, and C.R. Brundle, "High Resolution Photoelectron Spectroscopy," Wiley and Sons Ltd., England, 1970.
2. (a) B.O. Jonsson, and E. Lindholm, Int. J. Mass Spectrom. Ion Phys., 1969, 3, 385; C. Fridh, L. Asbrink, B.P. Jonsson, and E. Lindholm, Int.J.Mass Spectrom. Ion Phys., 1972, 8; (b) 85; (c) 101; (d) 215; (e) 229; (f) 485.
3. (a) R. Gleiter, E. Heilbronner, and V. Hornung, Helv.Chim.Acta, 1972, 55, 255; (b) F. Brogli, E. Heilbronner, and T. Kobayashi, Helv.Chim.Acta, 1972, 55, 274; (c) E. Heilbronner, V. Hornung, F.H. Pinkerton, and S.F. Thomas, Helv.Chim.Acta, 1972, 55, 289.
4. (a) M.H. Palmer and A.J. Gaskell, Theor.Chim.Acta (Berl.), 1971, 23, 52; (b) S. Cradock, R.H. Findlay, and M.H. Palmer, Tetrahedron, 1973, 29, 2173.
5. E. Clementi, J.Chem.Phys., 1967, 46; (a) 4731, (b) 4737.
6. J.D. Petke, J.L. Whitten, and J.A. Ryan, J.Chem.Phys., 1968, 48, 953.